EurAAP

EuCAP 2025

19TH EUROPEAN CONFERENCE ON ANTENNAS & PROPAGATION

STOCKHOLM
MARCH 30 – APRIL 4 2025

TECHNICAL PROGRAMME

2025

SESSION TRACKS

TO1	Sub-6 GHz for terrestrial networks (5G/6G)	TO5	Positioning, localization, identification & tracking
TO2	Milimetre wave and THz for terrestrial networks (5G/6G)	TO6	Biomedical and health
TO3	Aerospace, space and non-terrestrial networks	TO7	Electromagnetic modelling and simulation tools
TO4	RF sensing for automotive, security, IoT, and other applications	TO8	Fundamental research and emerging technologies/processes
SW	Scientific workshop	KIS	Keynotes & Invited speakers
IW	Industrial workshop	WG	Meeting and Working groups

EurAAP activities (at EurAAP booth)

SUNDAY, MARCH 30th

Registration (12:30-19:30)

Short courses (13:30-17:00) with a coffee break (15:00-15:30)

Room	Short course
Bergman (34)	SC01 - Advanced antenna modeling and simulation techniques
Mosig (26)	SC02 - Design of quasi-periodic surfaces for high-performance applications
Jansson (31)	SC03 - Electrodynamics of space-time systems: modern analysis techniques and applications
Munch (23)	SC06 - Advancing 5G/6G ORAN, MIMO and RIS research and development from FR2 antenna design to 5G/6G testbeds
Maxwell (C2)	SC07 - Innovative antenna design: insights through modal decomposition
Felsen (35 + 36)	SC13 - Transformations for radar cross-section (RCS) and imaging from monostatic near-field measurements

Room	Short course
Ørsted (24 + 25)	SC08 - Integral equation based synthesis of metasurfaces
Björk (33)	SC09 - Machine learning-enabled optimization and synthesis of metasurface antennas
Collin (27)	SC10 - Microwave imaging and sensing and innovative applications
Schelkunoff (C1)	SC11 - Multibeam antennas and beamforming networks
Zorn (32)	SC12 - Plane waves in anisotropic and bianisotropic media

MONDAY, MARCH 31st

	08:00–08:30	08:30–09:30	09:30–10:15	10:15–10:45	10:45–11:30	11:30–12:15	12:15–13:45	13:45–15:45	15:45–16:15	16:15–18:15	
	REGISTRATION			COFFEE BREAK	Level 5		LUNCH	Level 5	COFFEE BREAK		
ALFVÉN (A3+A4)		Opening ceremony	Petter Bedoire - SAAB		Magnus Frodigh - Ericsson	Elena Saenz - ESA		A01 - Advances in array synthesis		A02 - Developments in array analysis and design	
KILDAL (A2)								A05a - Optical, THz and subTHz antennas		A05b - Optical, THz and subTHz antennas	
HALLÉN (BAR5)								A16 - New results in reflectarrays		EuCAP 2026	
					Level 4			Level 4			
MARCUVITZ (M3)								A22 - Advanced methods in antenna design and manufacturing		A03 - Modelling for advanced antenna design	18:45-21:00
					Level 3			Level 3			
JANSSON (31)											
ZORN (32)											
BJÖRK (33)								SW2a - Measurement advancements for 5G/6G and emerging wireless standards: innovations, precision and standardisation (IET Workshop)		SW2b - Measurement advancements for 5G/6G and emerging wireless standards: innovations, precision and standardisation (IET Workshop)	
BERGMAN (34)									JOB CORNER - EURAAP BOOTH	E06 - Imaging	
FELSEN (35+36)								A24a - Antennas for sensing I		A24b - Antennas for sensing II	
					Level 2			Level 2			
SCHELKUNOFF (C1)								E04a - Optimization methods and machine learning I		E04b - Optimization methods and machine learning I	
MAXWELL (C2)								M03 - Recent advances in antenna ranges		M04 - Recent advances in near field measurements	
OLINER (C3)								A08 - Developments in reconfigurable antennas and surfaces		A17 - RIS and metasurface design	
KRAUS (C4)								E09a - Metasurfaces I		E09b - Metasurfaces I	
MUNCH (23)										A09 - Multiband and multifunctional antennas	
ØRSTED (24+25)								A11a - Advances in leaky-wave and fabry-perot cavity antennas		A11b - Advances in leaky-wave and Fabry-Perot cavity antennas	
MOSIG (26)								A14 - Mmwave antennas for space applications		AMTA meeting	
COLLIN (27)								P08a - Channel modeling approaches		P08b - Channel modeling approaches	

WELCOME RECEPTION

TUESDAY, APRIL 1st

	08:00–09:40	09:40–10:10	10:10–11:50	12:00–12:40	12:40–13:30	13:30–14:40	14:40–15:20	15:20–15:50	15:50–17:30	17:40–18:15
			Level 5							
ALFVÉN (A3+A4)	A06a – Advances in lens antennas I		A06b – Advances in lens antennas I	Sergei Tretyakov			Diego Masotti		CS35 – Emerging beam-steering technologies for 5G milimeter-wave and beyond cellular and satellite communications	EurAAP Award Ceremony
KILDAL (A2)	A13a – Antenna arrays for space applications		A13b – Antenna arrays for space applications	Almudena Suarez			Yong Mei Pan		CS3 – Physics-compliant RIS modeling	
HALLÉN (BAR5)	E01a – Electromagnetic theory		E01b – Electromagnetic theory					EurAAP DA		
			Level 4							
MARCUVITZ (M3)	CS13a – Advances in channel sounding and measurements for 6G: from cm-wave to sub-THz		CS13b – Advances in channel sounding and measurements for 6G: from cm-wave to sub-THz						CS58 – Coexistence and spectrum sharing	
			Level 3							
JANSSON (31)	SW1a – AMTA SW – Reverberation chambers for antenna measurements		SW1b – AMTA SW – Reverberation chambers for antenna measurements							
ZORN (32)	08:00 – 08:45 IW4 – European Space Agency (ESTEC) – Spaceborne antennas for earth observation missions 08:55 – 09:40 IW14 – Simr – SimOps (simulation operations) for antenna engineers: accelerating simulations and automating data handling	COFFEE BREAK	WG ECAP		LUNCH	POSTER SESSION		COFFEE BREAK	P03 – Sub-THz channel characterization	
BJÖRK (33)	SW4a – Emerging materials for applied antenna engineering: sensing and communications		SW4b – Emerging materials for applied antenna engineering: sensing and communications						IW12 Ansys – Next-gen RF and antenna engineering: simulation solutions and workflows for comprehensive systems	
BERGMAN (34)	IW1 – Altair technology – Pushing the boundaries of computational electromagnetics – advanced antenna simulation including multiphysics analysis and AI-powered optimization		SW9 – 3D-printing for high-frequency topologies: advances and challenges						CS30 – Time-domain EM – opportunities and solution	
FELSEN (35+36)	CS46a – Metamaterials for future industrial applications		CS46b – Metamaterials for future industrial applications						P09 – Propagation for radar technologies	
			Level 2							
SCHELKUNOFF (C1)	A12a – Antennas for medical application and health		A12b – Antennas for medical application and health						M02 – Bio and EM exposure	
MAXWELL (C2)	CS40a – Novel antenna measurement techniques: advancements in design and evaluation		CS40b – Novel antenna measurement techniques: advancements in design and evaluation						In Memoriam of Marco Sabbadini	
OLINER (C3)	CS24a – Small antennas: from theory to applications	MENTORING-EURAAP BOOTH	CS24b– Small antennas: from theory to applications					JOB CORNER-EURAAP BOOTH	CS16 – Characteristic modes – advanced antenna modelling and design	
KRAUS (C4)	CS67a – Joint communication and sensing: from EM modelling to application		CS67b – Joint communication and sensing: from EM modelling to application						CS59 –Advances in 3D-printing for antenna applications	
MUNCH (23)	IW5 ETS – Lindgren – Emerging 5G test methodologies to efficient and cost-effectively validate antenna performance		IW6 IMST GmbH – Design, simulation and realization of phased array antennas						IW13 Quadsat – Recent trend of drone-based measurement	
ØRSTED (24+25)	MO1a – Material and device characterization		MO1b – Material and device characterization						CS9 – Dome antennas for the next generation communication systems	
MOSIG (26)	SW5a – Stand on the IEEE antennas & propagation standards		SW5b – Stand on the IEEE antennas & propagation standards							
COLLIN (27)	P02a – Ray tracing channel simulation		P02b – Ray tracing channel simulation						15:50 – 16:35 IW10 – Keysight – Unlocking 6G potential: exploring the 6G R&D testbed and its variants and applications 16:45 – 17:30 IW11 – Keysight – Prototyping and certifying 5G NTN using realistic emulators	

18:15-20:00 RECEPTION WITH EXHIBITORS&SPONSORS-EXHIBITION AREA

Information about the Poster sessions

Level 2

- PP1 – Propagation I
- PM1 – Measurements I
- PE1 – Electromagnetics I

Level 3

- PA1 – Antennas I Sub-6GHz for terrestrial networks
- PA2 – Antennas III Aerospace, Space and non-terrestrial networks
- PA3 – Antennas II milimetre wave and THz for terrestrial networks

WEDNESDAY, APRIL 2nd

	08:00–09:40	09:40–10:10	10:10–11:50	12:00–12:40	12:40–13:30	13:30–14:40	14:40–15:20	15:20–15:50	15:50–17:30	17:40–18:50	18:50–20:00
			Level 5								
ALFVÉN (A3+A4)	A04a – Mmwave antenna technologies		A04b – Mmwave antenna technologies	Joachim Oberhammer			David R. Jackson		CS48 – Advancement of gap waveguide technology		
KILDAL (A2)	A10a – Wideband antennas		A10b – Wideband antennas	Miguel Beruete			Dirk Heberling		E07 – Frequency/polarization selective surfaces	WiAP – ECAP event	
HALLÉN (BAR5)	CS49a – Propagation for smart mobility scenarios		CS49b – Propagation for smart mobility scenarios						CS44 – High-power beam-steerable antennas and Sub-systems		WiAP ECAP reception
			Level 4								
MARCUVITZ (M3)	SW7 – EMF Exposure evaluation approaches and perspectives in 6G		SW3 – Electromagnetic technologies for life sciences: challenges and opportunities in the EurAAP community						ESoA		
			Level 3								
JANSSON (31)									WG Measurements		
ZORN (32)									Exhibitors meeting (16:00 – 17:40)		
BJÖRK (33)	08:00 - 08:45 IW8 – Dicaliant Ltd. – Phase-accurate on-board S-parameter measurements using pigtails up to 8.5 GHz 08:55 - 09:40 IW9 – Kaelus – The evolution of base station antennas from early designs to modern innovations	COFFEE BREAK	IW3 – Dassault systems and partners – SIMULIA: Advanced antenna array design and simulation		LUNCH	POSTER SESSION		COFFEE BREAK	WG Software and modeling tools		
BERGMAN (34)	PO4a – Satellite channel characterization I		PO4b – Satellite channel characterization I						WG Small antennas		
FELSEN (35+36)	CS23a – Antennas, metasurfaces, and arrays for radio astronomy		CS23b– Antennas, metasurfaces, and arrays for radio astronomy						PO5 – Channel characterization for massive MIMO		
			Level 2								
SCHELKUNOFF (C1)	CS51a – Physics assisted learning and inversion strategies for electromagnetic imaging	JOB CORNER - EURAAP BOOTH	CS51b – Physics assisted learning and inversion strategies for electromagnetic imaging					WiRS - EURAAP BOOTH	MO6 – RIS and scattering measurements		
MAXWELL (C2)			CS66 – AMTA – Special-session on advanced robotic antenna measurements						CS42 – Time-modulated electromagnetic systems for modern technological applications		
OLINER (C3)	CS25a – Advances in reconfigurable antennas for communication, localization and sensing applications		CS25b – Advances in reconfigurable antennas for communication, localization and sensing applications						EO5 – Optimization methods and machine learning II		
KRAUS (C4)	CS24a – Quantum electromagnetics – from photonics to quantum computing		CS24b – Quantum electromagnetics – from photonics to quantum computing						A18 – Terrestrial communications with sub-6GHz antennas		
MUNCH (23)	IW2 – COMSOL – Design robustness and digital twins for antenna engineering: uncertainty quantification and surrogate models with deep neural networks		WG WIAP						IW7 – TICRA – Dedicated software tool for rapid full-wave design, optimization, and analysis of phased array antennas		
ØRSTED (24+25)	CS2a – Emerging electromagnetic solutions for non-terrestrial networks		CS2b – Emerging electromagnetic solutions for non-terrestrial networks						PO6 – Propagation channel for communication, sensing and localization		
MOSIG (26)	SW6a – Innovative techniques to improve measurement accuracy		SW6b – Innovative techniques to improve measurement accuracy						CS21 – ISAP session: Recent advances in asian antennas and propagation research		
COLLIN (27)	MO5a – Recent advances in antenna measurement and over the air testing		MO5b – Recent advances in antenna measurement and over the air testing						CS11 – Metamorphose VI session on plasma in electromagnetics		

Information about the Poster sessions

Level 2

- PA4 – Antennas IV Sub-6 GHz for terrestrial networks
- PM2 – Measurements II
- PE2 – Electromagnetics II
- PP2 – Propagation II

Level 3

- PA5 – Antennas V millimetre wave and THz for terrestrial networks
- PA6 – Antennas VI sensing, localization and tracking
- PA7 – Antennas VII biomedical and health

THURSDAY, APRIL 3rd

	08:00-09:40	09:40-10:10	10:10-11:50	12:00-12:40	12:40-13:30	13:30-14:40	14:40-15:20	15:20-15:50	15:50-17:30
			Level5						
ALFVÉN (A3+A4)	CS31a – Wi-Fi 8 – Currents trends and advances in antennas, architectures, and techniques		CS31b – Wi-Fi 8 – Currents trends and advances in antennas, architectures, and techniques	Nicolas Capet			Carolina Vigano		CS4 – Advances on metasurfaces for wavefront manipulation
KILDAL (A2)	CS60a – Lens and metalens antennas: theory, design, and applications		CS60b – Lens and metalens antennas: theory, design, and applications	Rodolfo Feick			Jorge L. Salazar-Cerreño		A07 – Advances in Lens antennas II
HALLÉN (BAR5)	E02a – Computational and numerical techniques I		E02b – Computational and numerical techniques I						CS12 – Electromagnetic beams in near-field applications: from microwaves to optics
			Level 4						
MARCUVITZ (M3)	CS52a – IRACON session: Recent progress in THz channel modeling and applications		CS52b – IRACON session: Recent progress in THz channel modeling and applications						E03 – Computational and numerical techniques II
			Level 3						
BJÖRK (33)	RoE	COFFEE BREAK	SW10 – From the beginnings of electricity into antennas and radio wave propagation: A road over 3000 years		LUNCH	POSTER SESSION		COFFEE BREAK	WG Active array antennas
BERGMAN (34)	CS64a – Extremely large or distributed antenna systems in near-field environments		CS64b – Extremely large or distributed antenna systems in near-field environments						SW11 – The 1924 2.2 km electrically small Grimeton VLF antenna
FELSEN (35+36)	CS55a – Fundamental challenges and novel methodologies in the next-generation computational electromagnetics		CS55b – Fundamental challenges and novel methodologies in the next-generation computational electromagnetics						P10 – Propagation for body network and bio applications
			Level 2						
SCHELKUNOFF (C1)	CS15a – Shared-aperture antenna and antenna collocation strategies and methods for communication, radar and SATCOM	JOB CORNER-EURAAP BOOTH	CS15b – Shared-aperture antenna and antenna collocation strategies and methods for communication, radar and SATCOM					WiM-YP-EURAAP BOOTH	E10 – Metasurfaces II
MAXWELL (C2)	CS61a – AMTA – Post processing techniques in antenna measurements		CS61b – AMTA – Post processing techniques in antenna measurements						CS41 – AMTA session: Select best measurement paper candidates from AMTA authors at EuCAP – updates in 2025 on best measurement techniques
OLINER (C3)	CS5a – Vehicular antenna systems and solutions		CS5b – Vehicular antenna systems and solutions						A15 – Developments in antenna design for space applications
KRAUS (C4)	CS57a – Biomedical microwave techniques and devices: from diagnosis to treatment		CS57b – Biomedical microwave techniques and devices: from diagnosis to treatment						CS50 – Advances in 2D leaky-wave antennas
MUNCH (23)	SW8a – Sub-THz reconfigurable intelligent surfaces, RF front-ends, and channels for 6G networks		SW8b – Sub-THz reconfigurable intelligent surfaces, RF front-ends, and channels for 6G networks						WG Education
ØRSTED (24+25)	CS34a – Recent advances on propagation research and its impact on localizations		CS34b – Recent advances on propagation research and its impact on localizations						A23 – Antennas for identification and localization
MOSIG (26)	CS27a – Advanced additive manufactured dielectric resonator antennas		CS27b – Advanced additive manufactured dielectric resonator antennas						P07 – mmWave channel characterization
COLLIN (27)	In memoriam of Bertram Arbesser-Rastburg		WG Propagation						A20 – Mmwave antennas for radar and sensing applications

Information about the Poster sessions

Level 2

PE3	Electromagnetics III
PS1	Best paper awards
PP3	Propagation III

Level 3

PA10	Antennas X modeling, simulation tools, emerging technologies and processes
PA8	Antennas VIII millimetre wave and THz for terrestrial networks
PA9	Antennas IX sensing, localization and tracking

19:00-00:30 Gala dinner at Vasa museum

FRIDAY, APRIL 4th

	08:30–10:10	10:10–10:40	10:40–12:20	12:40–13:10
	Level 5		**Level 5**	
ALFVÉN (A3+A4)	CS1a – Reconfigurable intelligent surfaces for communication, sensing and computing		CS1b – Reconfigurable intelligent surfaces for communication, sensing and computing	Closing ceremony
KILDAL (A2)	CS18a – Emerging antenna technologies for satellite communications and applications		CS18b – Emerging antenna technologies for satellite communications and applications	
HALLÉN (BAR5)	CS6a – Challenges in human RF exposure assessment to legacy, 5G and 6G mobile radio technologies		CS6b – Challenges in human RF exposure assessment to legacy, 5G and 6G mobile radio technologies	
	Level 4		**Level 4**	
MARCUVITZ (M3)	CS56a – Characterization of biological tissues and tissue mimicking materials for electromagnetic medical applications	COFFEE BREAK	CS56b – Characterization of biological tissues and tissue mimicking materials for electromagnetic medical applications	
	Level 3		**Level 3**	
FELSEN (35+36)	CS7a – mm-Wave and THz antennas for radar and 6G communication		CS7b – mm-Wave and THz antennas for radar and 6G communication	
	Level 2		**Level 2**	
SCHELKUNOFF (C1)	CS54a – Compact antennas and arrays for communications and sensing		CS54b – Compact antennas and arrays for communications and sensing	
MAXWELL (C2)	CS62a – Advancements in IoT antennas: design strategies, optimization techniques, materials, physical insights, and integrating AI		CS62b – Advancements in IoT antennas: design strategies, optimization techniques, materials, physical insights, and integrating AI	
OLINER (C3)	E08a – Periodic structures and metamaterials		E08b – Periodic structures and metamaterials	
KRAUS (C4)	CS53a – Electromagnetic wave control through reflective and transmissive periodic surfaces		CS53b – Electromagnetic wave control through reflective and transmissive periodic surfaces	
MUNCH (23)	P01 – Modeling of rain effects for channel characterization			
ØRSTED (24+25)	CS43a – AMTA convened session – Trends and advances in test and measurement for 5G and beyond		CS43b – AMTA convened session – Trends and advances in test and measurement for 5G and beyond	
MOSIG (26)	P11 – Wideband channel measurements from sub-6 GHz to (sub-)THz			
COLLIN (27)	CS38a – Fast, low-invasive visualization of EM-VNF distributions around wireless communication/sensing devices: from anechoic chamber to microscope		CS38b – Fast, low-invasive visualization of EM-VNF distributions around wireless communication/sensing devices: from anechoic chamber to microscope	

Monday, March 31st

Monday - 08:30-09:30

Room: Alfvén (A2+ A3 + A4) — **Opening ceremony**

Monday - 09:30-10:15

Room: Alfvén (A2 +A3 + A4) — **Petter Bedoire - SAAB**

Technology Development in a World Shaped by Geopolitical Tensions

Chair: Mats Gustafsson (Lund University, Sweden)

For decades, Saab has developed solutions with the mission to keep people and society safe. In an era marked by heightened geopolitical tensions, development of sensor systems plays a pivotal role in shaping global security. This keynote explores how advancements in microwave and antenna technologies address emerging challenges in defence, communications, and strategic resilience. Geopolitical uncertainties demand innovative solutions for secure data transmission, surveillance, and electronic warfare capabilities, emphasizing the intersection of technology and national security. The talk highlights the evolving landscape of microwave systems, phased array antennas, and adaptive technologies tailored to mitigate risks and ensure operational readiness. The aim of the session is to inspire researchers, engineers, and policymakers to harness the transformative power of microwave and antenna innovations while navigating the complexities of a divided geopolitical environment.

Monday - 10:45-11:30

Room: Alfvén & Kildal (A2 + A3 + A4) — **Magnus Frodigh - Ericsson**

Research Challenges for 6G

Chair: Fredrik Tufvesson (Lund University, Sweden)

What will future mobile networks look like? We envision 6G networks that provide enhancements in classic performance metrics such as achievable data rates, latency and energy performance as well as new capabilities like ever-present connectivity, intelligence, AI and compute services, and sensing functionalities. These new functionalities will enable a "cyber-physical world", fusing the connected physical world of senses, actions, and experiences with the physical world's programmable digital representation. We will see new use cases such as mixed reality, Integrated Sensing And Communication (ISAC), and digital airspace i.e. connectivity above the ground. We will see new spectrum being taken into service in the cmWave range. And we will see new deployments such as Non-Terrestrial Networks (NTN) and Distributed MIMO, as well as deployments of cmWave base stations on existing 4G/5G grid. These trends demand new antenna solutions, including very large arrays, arrays with integrated filters, and antennas with high isolation between Tx and Rx. Efficient simulation tools and OTA test methods will also be needed.

Monday - 10:45-11:30

Room: Alfvén (A2+A3 + A4) — **Elena Saenz - ESA**

Recent space antenna developments and RF testing capabilities at ESA

Chair: Marianna Ivashina (Chalmers University of Technology, Sweden)

In the recent years ESA has developed several missions for different applications like Earth Observation, Science, Telecommunication, Navigation, and launchers with very challenging antenna requirements. This paper will present an overview of the latest developments, main characteristics and challenges of such antennas. Besides, the main highlights in the field of antennas extracted from the ESA 2040 technology vision will be presented. At the same time, in order to be able to test those antennas, new testing facilities are needed with state-of-the-art characteristics. This paper will present the latest developments for antenna measurements and RF material characterization.

MONDAY

T01 Sub-6 GHz for terrestrial networks (5G/6G) / / Antennas

Chairs: Maria Antonia Maisto (Università degli studi della Campania Luigi Vanvitelli, Italy), Mladen Vucic (University of Zagreb, Faculty of Electrical Engineering and Computing, Croatia)

13:45 High-Efficiency and Independent Multi-Beam Scanning in Time-Modulated Arrays with Quantized Phase Modulation Sequences

Haotian Li, Rongfang Feng and Zhongkai Zhu (University of Electronic Science and Technology of China, China)

Owing to the inherent multi-harmonic characteristics, a time-modulated antenna array (TMA) offers significant potential for multi-beam forming under a single radio-frequency (RF) channel. However, existing multi-beam TMAs face a trade-off between beamforming flexibility and hardware complexity, which poses challenges for high-efficiency and independent multi-beam scanning. To tackle this challenge, this work presents a novel quantized phase modulation scheme. By quantizing the continuous instantaneous phase statuses of traditional multi-beam modulation waveforms to 0°, 90°, 180°, and 270°, the proposed approach achieves high-precision, independent control of beam-pointing directions with significantly reduced complexity. Moreover, this approach avoids amplitude modulation of antenna elements, resulting in improved efficiency. On this basis, a radiation pattern synthesis strategy is developed to determine the quantized phase modulation sequences based on the desired number of beams and beam scanning angles. The proposed approach is validated through the synthesis of five independent beams using a 16-element isotropic linear array.

14:05 Low-Sidelobe Multibeam Synthesis for Overlapped Subarray with Non-Identical Element Excitations

Hui Zeng, Zhenhai Xu, Gongqing Yang and Xinxin Li (National University of Defense Technology, China); Shunping Xiao (National University of Denfence Technology, China)

A new overlapped subarray structure with non-identical element-level weights is proposed to reduce the sidelobe level of multi-beam patterns. Firstly, by introducing two types of weight matrices, the relationship between the element-level weights and the overlapped subarray beam pattern is analyzed, with the subarray-level weights kept constant. Subsequently, an optimization model for element-level weights is established, with the goal of minimizing the sidelobe level, and convex programming is utilized to solve this model. Through these steps, satisfactory element-level weights for multi-beam patterns can be obtained. Compared to existing uniform continuous subarrays and overlapped subarrays with identical element-level weights, the proposed subarray structure achieves a lower sidelobe level.

14:25 Optimal Near-Field Synthesis of Shaped Patterns Thorugh Realistic Arrays

Giada Maria Battaglia (Università Mediterranea di Reggio Calabria, Italy); Tommaso Isernia (University of Reggio Calabria, Italy); Maria Antonia Maisto (Università degli studi della Campania Luigi Vanvitelli, Italy); Andrea Francesco Morabito (University Mediterranea of Reggio Calabria, Italy); Roberta Palmeri (IREA-CNR, Napoli, Italy); Raffaele Solimene (Università degli studi della Campania Luigi Vanvitelli, Italy)

We present a new method for the fast design of 1-D array antennas composed of realistic elements, including mutual coupling and mounting platform effects, such to fulfill an arbitrary power mask in the near field region. The technique represents the extension of the well-known spectral factorization method, originally developed in the far-field case and relying to the exploitation of the array factor, to near-field scenarios involving realistic antennas. The proposed approach includes a feasibility criterion allowing to a-priori ascertain whether or not an array of given size can generate a field fulfilling the assigned mask and, in the affirmative case, allows finding a number of different excitation sets all corresponding to the sought power pattern.

14:45 Optimization of End-Fire Realized Gain and Side Lobe Levels in Active and Parasitic Antenna Arrays

Rozita Konstantinou (Queen's University Belfast, United Kingdom); Ihsan Kanbaz (Gazi University, Turkey); Okan Yurduseven and Michail Matthaiou (Queen's University Belfast, United Kingdom)

This work presents a comprehensive optimization strategy for both active and parasitic antenna arrays, focusing on maximizing the overall efficiency and realized gain (RG). Using a differential evolution (DE) algorithm, we optimize key parameters such as element spacing, excitation currents, and load values. By removing predefined constraints on excitation vectors, this approach achieves greater flexibility and higher RG for all the array configurations, which is validated through full-wave simulations. Using the proposed DE-based optimization technique, we show a five-element parasitic array, achieving a maximum RG of 11.42 dB. Then, the optimization is extended to include side lobe level (SLL) minimization, balancing RG and low SLLs to improve the end-fire radiation performance. The parasitic five-element array achieves a RG of 10.32 dB with a SLL of –20 dB. This approach offers promising results for 5G and beyond wireless communication systems requiring compact, high-efficiency arrays with controlled interference.

MONDAY

15:05 Phase-Only Synthesis of Pencil Beams via Sequential Quadratic Programming

Mladen Vucic (University of Zagreb, Faculty of Electrical Engineering and Computing, Croatia); Katarina Vodvarka (University of Zagreb Faculty, Croatia); Maja Jurisic Bellotti (University of Zagreb, Faculty of Electrical Engineering and Computing, Croatia)

Phase-only adjustment of antenna arrays simplifies design of their feeding networks and maximizes energy efficiency. However, optimization-based synthesis of the corresponding beam patterns leads to nonconvex problems. Various techniques for solving these problems have been considered. In this paper, we present an approach based on sequential quadratic programming. We focus on phase-only design of pencil beams with the sidelobes optimum in minimax sense. In this context, we consider beampatterns without and with null regions, having specified coefficients' magnitudes and arbitrary, even-symmetric, or odd-symmetric phases.

15:25 Steerable Collimated Vortex Wave Beam Generation by a Planar Radiating Aperture as a Phased Array Excited by Multi-Parameter Virtual Antenna Systems

Altunkan Hizal (ASELSAN, Turkey); Ramazan Cetiner (Aselsan Inc., Turkey); Seyit Koc (Middle East Technical University, Turkey); Hayrullah Yildiz (Baskent University, Turkey)

A multi-parameter virtual antenna (VA) creates collimated electromagnetic vortex wave beams with orbital angular momentum (OAM). The VA consists of a point source feed and a collimating paraboloidal reflector. The VA beams illuminate a tilted real reference aperture, called a radiating aperture (RAP) or an active phased array (PA). The square planar RAP is divided into square sub-apertures (SAP), which are then replaced by linearly polarized rectangular microstrip patch antennas excited by the VA's near field. This method is used for RAPs with 60-68 wavelength sides and steering (tilt) angles of 0 to 60 degrees. The OAM mode number (topological charge) ranges from 1 to 25. The dimensions of the SAP, 0.81-0.9 wavelengths, cause grating lobes, which are suppressed by intra-SAP sub-arrays. The numerical simulations provided verify the effectiveness of this method.

Room: Kildal (A2) — A05a - Optical, THz and subTHz antennas

T02 Millimetre wave and THz for terrestrial networks (5G/6G) / / Antennas

Chairs: Nuria LLombart (Delft University of Technology, The Netherlands), Takashi Tomura (Tokyo Institute of Technology,Japan)

13:45 Sub-Terahertz Waveguide Antennas Based on Contactless Thin Metal Sheets

Sergio Garcia-Martinez (Universidad Politécnica de Madrid, Spain); Adrián Tamayo-Domínguez and Pablo Sanchez-Olivares (Universidad Politecnica de Madrid, Spain)

This paper presents the design, manufacturing, and measurement of waveguide antennas based on a contactless multilayer structure incorporating glide-symmetric electromagnetic band gap (EBG) technology to prevent leakage. The proposed multilayer waveguide technology is analyzed by examining the stopband behavior of the EBG and the propagation constant of the waveguide's fundamental mode. The paper demonstrates the scalability and reliability of this technology by developing and testing three slotted waveguide antennas operating at W-band (75-110 GHz), G-band (140-220 GHz), and J-band (220-330 GHz). The prototypes, fabricated using laser cutting and copper plating, show low manufacturing errors, stable performance despite variations in the air gaps between layers, and high efficiency, proving the feasibility of the multilayer waveguide technology for mmWave and sub-terahertz frequency applications.

14:05 Dual-Polarized Double-Slot Lens Antenna with Low Cross-Polarization at 300GHz in 90nm SiGe BiCMOS

Alexandros Bechrakis Triantafyllos, Maria Alonso-delPino and Daniele Cavallo (Delft University of Technology, The Netherlands); Klaus Aufinger (Infineon Technologies AG, Germany); Marco Spirito and Nuria LLombart (Delft University of Technology, The Netherlands)

To fulfill the throughput requirement of future wireless systems, polarization diversity can be an important tool to boost the network's capacity. In this context, dual-polarized antennas with high isolation and low levels of cross-polarization are desirable at THz frequencies. This contribution presents a dual-polarized double-slot antenna operating at 300 GHz and implemented in a 90 nm SiGe BiCMOS process. The antenna's feeding enables integration with differential circuit topologies, avoiding the need for single-ended to differential baluns and their associated losses. Simulation results show high isolation (<-50 dB), low levels of cross-polarization (<-24 dB), good matching (<-15 dB) and reasonable radiation efficiency (>53%) in the 250-320 GHz band which has been proposed for wireless communications. These performance metrics make this antenna a suitable candidate for wireless communication systems at THz frequencies.

14:25 Single-Feed Multi-Beam W-Band Reflectarray for Ultra-Capacity Fixed Wireless Access

Daniel R. Prado, Xuekang Liu, Claudio Paoloni, Rosa Letizia and Lei Wang (Lancaster University, United Kingdom)

A quad-beam reflectarray fed by a single feed horn is designed in W-band at 105 GHz. The feed horn is designed with the goal of being manufactured in a single metallic piece by a CNC milling process. The reflectarray is circular with a periodicity of 0.857 mm and comprised of 15380 rectangular patches in a single layer of metallization. The four beams are realized by means of the superposition principle and positioned in a great circle corresponding to (□ □) = (30°, 0°). The reflectarray is simulated in HFSS modelling each element as a copper patch with a gold coating to avoid corrosion. Simulations show that more than 30 dBi of gain per beam and a gain variation of 1.1 dB are achieved in the frequency range 103 GHz-109 GHz, making suitable for future 6G ultra-capacity fixed wireless access enabled by travelling wave tubes.

14:45 Low-Loss Integration Strategy for Regularly Spaced ICs in Unconventional Phased Arrays Beyond 100 GHz

Yigit Ertugrul (Imec, Belgium); Kamil Yavuz Kapusuz (Ghent University-Imec, Belgium); Ilker Comart (Imec, Belgium); Claude Desset (IMEC, Belgium); Sofie Pollin (KU Leuven, Belgium)

This study investigates the design and synthesis of tiled planar phased arrays operating beyond 100 GHz, focusing on the impact of insertion losses between regularly placed integrated circuit (IC) ports and tiles. To address the interconnect challenge, the problem is simplified to a two-dimensional framework and formulate a novel multiobjective optimization problem aimed at minimizing insertion losses while ensuring optimal array performance across fully digital and hybrid/analog systems. The proposed framework has been successfully applied to tetromino-based (\lambda_0/2)-spaced clustered 8(\times)8 planar arrays, consisting of sixteen subarrays at 135 GHz. These arrays were integrated with four ICs, each equipped with four output ports. The effectiveness of the proposed approach has been validated through numerical full-wave simulations.

15:05 Dual-Polarized Microstrip Antenna with Cross Grid Structure Radiating Towards the Edge of the Substrate in the D-Band

Ryosuke Hasaba (Panasonic Industry Co., Ltd., Japan); Ken Takahashi (Panasonic System Networks R&D Lab. Co., Ltd., Japan); Tomoki Abe (Panasonic Industry, Japan); Tomohiro Murata, Yoichi Nakagawa and Koji Takinami (Panasonic Corporation, Japan); Hiroshi Taneda (Shinko Electric Industries, Japan); Takashi Tomura (Tokyo Institute of Technology, Japan); Issei Watanabe (National Institute of Information and Communications Technology, Japan)

This paper proposes a dual-polarized antenna for D-band applications, which radiates in the substrate end direction. The antenna's radiating elements and ground are formed using vias, via lands, and copper foil. Due to the grid structure of the radiating elements, it is possible to adjust the resonant frequencies of each polarization even under manufacturing constraints. The characteristics and operation of a single-element antenna were demonstrated through simulations. Subsequently, the gain of an 8-element array was compared between measured and calculated values, demonstrating the effectiveness of the proposed antenna.

15:25 Design of a Scanning Quasi-Optical Lens System for Radiative Near-Field Communication Links

Huasheng Zhang, Alexandros Bechrakis Triantafyllos, Nuria LLombart and Maria Alonso-delPino (Delft University of Technology, The Netherlands)

Recently, the use of radiative near-field links in high-data-rate wireless communication has gained noticeable interests. Unlike far-field links, near-field links can have negligible path loss within hundreds of meters for electrically large antennas at high frequencies. In this work, we propose a quasi-optical (QO) lens system for a 100 m near-field link at H-band. The QO system is analyzed using a field-correlation approach combined with geometrical optics and physical optics techniques. The trade-offs in designing the primary lens are discussed, and then a multi-lens QO system is designed with a compact size (aspect ratio of 1.3:1) and high coupling efficiency of 82%. Moreover, the auxiliary lens in the system can be rotated to achieve also good scanning performance for the link alignment. The scan range is in the order of 1 m with low scan loss and large scanning magnification of 20:1.

MONDAY

Room: Hallén (BAR5) | **A16 - New results in reflectarrays**

T08 Fundamental research and emerging technologies/processes / / Antennas

Chairs: Manuel Arrebola (Universidad Politécnica de Madrid, Spain), Lars Manholm (Ericsson Research, Sweden)

13:45 A New Focal Line for the East-West Arm of the Northern Cross Radio Telescope

Mirko Bercigli (IDS Ingegneria Dei Sistemi S. p. A, Italy); Davide Bianchi (IDS Ingegneria Dei Sistemi SPA, Italy); Germano Bianchi (INAF - IRA, Italy); Pietro Bolli (INAF Arcetri Astrophysical Observatory, Italy); Claudio Bortolotti and Giovanni Naldi (INAF - IRA, Italy); Andrea Orlati (INAF - Istituto di Radioastronomia, Medicina, Italy); Federico Perini (INAF - IRA, Italy); Giuseppe Pupillo (IRA - INAF, Italy); Mauro Roma and Marco Schiaffino (INAF - IRA, Italy)

The feed system of the 564 m long parabolic-cylindrical reflector of the Italian Northern Cross radio telescope operating at 408 MHz has been entirely reviewed to improve the overall performance of the antenna. As a result of a full-wave electromagnetic study, a decision has been made to replace the current illuminator consisting of 1488 half-wavelength dipoles and a corner reflector with 416 Yagi-Uda antennas. The new proposed feed system is presented in this paper and numerical results are compared to the original performance.

14:05 Design of Electromagnetic Skins Based on Multi-Faceted Reflectarrays for Millimeter-Wave Coverage Improvement

Borja Imaz-Lueje and Eduardo Martinez-de-Rioja (Universidad Rey Juan Carlos, Spain); Manuel Arrebola (Universidad Politécnica de Madrid, Spain)

In this contribution, low-profile electromagnetic skins based on reflectarray multi-faceted topologies have been designed to improve wireless communications in different 5G/6G mm-wave scenarios. The proposed structures comprise multiple panels, assembled edge-to-edge following the curve profile of different architectural elements (cylindrical corners or vaults). Working in the 28 GHz band and dual-linear polarization, the multi-faceted approach deflects the impinging beam coming from a base station to a certain direction or coverage. The results of this work demonstrate that the multifaceted approach can efficiently generate the required coverage in each scenario but increasing the integrability with the architectural elements of the environment compared to a traditional single-facet electromagnetic skin.

14:25 A Steerable 50 dBi E-Band Reflector Antenna Using a Contactless Waveguide Joint

Oskar Talcoth (Ericsson AB, Sweden); Lars Manholm (Ericsson Research, Sweden)
In this paper, the design and experimental evaluation of a steerable 50 dBi E-band reflector antenna based on a dualpolarized, all-metal, contactless waveguide joint is reported. The waveguide joint allows the hat feed of the reflector antenna to move away from the focal point thus steering the beam in the opposite direction. The antenna beam can be steered ±2.1 ◦ in one direction with limited impact on the side lobes outside ±5 ◦ in the horizontal plane.

14:45 A Phoenix Unit Cell with Linear Polarization for Weather Radar Applications

Dendani Ikram (INSA of Rennes, France & Higher School of Communications of Tunis, Tunisia); Erwan Fourn (INSA of Rennes & IETR, France); Saber Dakhli (GeePS Laboratory, CNRS & CentraleSupélec, Université Paris- Saclay, France); Fethi Choubani (Innov'Com Laboratory, SUPCOM, University of Carthage, Tunisia)
This paper presents a novel phase-shifting unit cell topology for reconfigurable reflectarray antennas, designed for weather radar applications at a resonance frequency of 10 GHz. The proposed unit cell structure comprises two concentric half square rings surrounding a half square patchs, integrated with variable capacitor. This design achieves a wide phase range of 284 degrees, making it ideal for adaptive beam-forming. Simulation results demonstrate the cell's effectiveness, highlighting its potential in advanced reflectarray antenna systems for improved, low-cost radar solutions

15:05 Field Trial with a 50 dBi E-Band Sway Compensating Reflector Antenna

Lars Manholm (Ericsson Research, Sweden); Sam Agneessens (Ericsson AB, Sweden); Piero Lauri (Ericsson Telecomunicazioni SPA, Italy); Christoffer Fougstedt (Ericsson AB, Sweden)
The ability of an E-band radio link steerable 50 dBi sway compensating reflector antenna (SCA) to compensate for mast sway has been tested in field. Two parallel links were used in the test, where one link served as the reference having standard, fixed beam reflector antennas, and the other had an SCA at one end. The monopole tower with the SCA is known for having significant solar induced sway, also called sunflower effect. The results show that the link with the SCA suffers up to 14 dB less from sway fading than the reference link and is able to maintain a link performance that is almost unaffected by sway.

15:25 Reflectarray Antenna Design Using the Deep Learning ControlNet Diffusion Model

Ruonan Chen, Cedric W. L. Lee, Peng-Khiang Tan and Theng Huat Gan (National University of Singapore, Singapore)
In this paper, we apply the ControlNet diffusion model, a generative deep learning framework that integrates both text and image inputs for enhanced conditional control, to design reflectarray antennas. This generative deep learningenabled method facilitates the design of pixelated unit cells with a high degree of freedom, enabling the generation of diverse patterns that satisfy the S-parameters requirements for reflectarray antennas. The generated unit cells cover a 2π phase range across the 9.0 GHz to 11.0 GHz. A single-layer reflectarray antenna with dimensions of 300 mm × 300 mm and a focal length of 180 mm was designed, achieving a maximum gain of 28.0 dBi at 10 GHz, an aperture efficiency of 50.3% and 1-dB bandwidth of 7.5%. The co-polarized antenna pattern has sidelobe levels of 22.2 dB and 19.4 dB in the E-plane and H-plane respectively.

MONDAY

Room: Marcuvitz (M3) | **A22 - Advanced methods in antenna design and manufacturing**

T02 Millimetre wave and THz for terrestrial networks (5G/6G) / / Antennas

Chairs: Mehdi Ahmadi-Boroujeni (Sharif University of Technology, Iran), Gino Sorbello (University of Catania, Italy)

13:45 Confocal Ellipsoidal Reflectors with Phased Array Vivaldi Antenna Source for Imaging Systems

Mohammad Hossein Koohi Ghamsari (Sharif University of Technology, Iran); Mahyar Mehri Pashaki (Sharif University of Technology, Iran & University of Surrey, United Kingdom); Mehdi Ahmadi-Boroujeni (Sharif University of Technology, Iran)
In this paper, an on-axis dual-reflector confocal ellipsoidal structure is presented for near-field imaging systems. In the proposed structure, the backscattered electromagnetic wave problem, known as the blockage effect, is reduced considerably using an elaborate design of the sub-reflector and precise alignment of the reflectors. The proposed geometry is analyzed, followed by a design example for the stand-off distance of 2 m. The blockage reduction characteristic is verified using ray-tracing simulation. Next, the scanning performance of the structure is investigated utilizing a Vivaldi phased array antenna as the source designed at the central frequency of 28 GHz. The fullwave simulations proved a field-of-view (FoV) of approximately 40 cm. Furthermore, tuning the proposed reflectors configuration stand-off distance is examined with a point source. The ray-tracing simulations showed that standoff distance can be easily changed up to tens of centimeters with just a few centimeters of source point lateral displacement.

14:05 A Screen-Printed CPW-Fed Circularly Polarized Antenna Using a Sustainable Cork Substrate

Sanjeev Kumar (Tyndall National Institute & University College Cork, Ireland); Gholamhosein Moloudian, Dinesh R. Gawade and Daniela Iacopino (Tyndall National Institute, Ireland); Brendan O'Flynn (Tyndall National Institute, Ireland); John Laurence Buckley (Tyndall National Institute & University College Cork, Ireland)

This paper presents a novel, coplanar waveguide (CPW)-fed circularly polarized (CP) monopole antenna. The antenna is fabricated using screen-printing techniques, with silver nanoparticles as the conductive material and cork used as a sustainable substrate. Circular polarization is achieved by introducing a radiating element orthogonal to the main radiating monopole element. The measurements of the fabricated antenna show a -10 dB impedance bandwidth of 183 MHz, corresponding to a fractional bandwidth (FBW) of 7.6% at 2.4 GHz. Furthermore, at 2.4 GHz, the antenna demonstrates a measured peak realized gain of -1.8 dBi and a radiation efficiency of 58%. A 3-dB axial-ratio fractional bandwidth for right-hand circular polarization (RHCP) operation at 2.4 GHz is 5.3%. The proposed antenna is well-suited for use in various 2.4 GHz wireless local area network (WLAN) technologies, such as Bluetooth and Wi-Fi, and can be integrated into items such as next-generation smart floors using sustainable materials.

14:25 Time-Switched Matching Network for Transmitting Antenna Systems

Luca Stefanini (Roma Tre University, Italy); Davide Ramaccia (RomaTre University, Italy); Andrea Alù (CUNY Advanced Science Research Center, USA); Alessandro Toscano and Filiberto Bilotti (Roma Tre University, Italy)

Antenna matching is a critical aspect of antenna design and operation. It involves ensuring that an antenna's impedance is optimally matched to the feeding transmission line it is connected to at the operative frequency of the transmitter. Traditional matching networks, constrained by the Bode-Fano limit, struggle to provide adequate bandwidth and performance across multiple frequencies. In this contribution, we propose a matching network based on the timeswitched metamaterials, a class of media whose properties changes abruptly in time. We investigate the possibility to perform frequency conversion, instead of a impedance conversion, in order to align the spectral content of the signal to the natural band of the antenna. Full-wave simulations demonstrate the system's ability to match signals across different frequencies without distorting the antenna's radiation pattern. This approach represents a potential alternative to traditional schemes that can be further exploited for applications to next-generation communication, Radar and sensing systems.

14:45 Paper-Based RFID Tag Using MXene Towards Sustainable IoT

Zahra Sarpanah Sourkouhi (The University of British Columbia, Canada); Jamal AlHourani (Drexel University, Philadelphia, USA); Alessio Mostaccio and Gaetano Marrocco (University of Rome Tor Vergata, Italy); Yury Gogotsi (Drexel University, USA); Mohammad H. Zarifi (The University of British Columbia, Canada)

The growing demand for the Internet of Things (IoT) is driving the need for advancements in wireless technologies, including radio frequency identification (RFID), across various industrial and commercial areas. Due to the rising trend in smart electronic devices, electronic waste is becoming a concern, and research studies are being urged to replace conventional materials and fabrication methods. This study introduces MXene-based RFID tags integrated onto a paper substrate, designed to operate within the European (EU) frequency band (865 to 868 MHz). The impedance of the designed standard dipole antenna was matched to the EM4152 RFID IC with 96% efficiency in power transmission coefficient at the frequency of f≈851 MHz. Approximately 600 uL Ti3C2Tx MXene solution was drop-casted to form the antenna pattern on paper, and the final tag demonstrated at least 145 cm readability in a cluttered environment.

15:05 Shaping Focused Wave Beams in the near Field by Spatially Distributed Caustic Synthesis

Santi Concetto Pavone (Università degli Studi di Catania, Italy); Federica Anfuso, Ahsan Ullah Khan and Gino Sorbello (University of Catania, Italy)

In this contribution, we introduce a technique for general focused beam synthesis based on ray-caustic shaping at microwaves and millimeter waves. Indeed, it is well-know from geometrical optics that caustics, i.e., the envelope of tangents to reflected rays, are characterized by strong field intensity, and can be profitably used to focus beams on specific spatial trajectories. In this sense, the proposed approach represents a physics-based technique to shape the focusing capabilities of an antenna, beyond more conventional nondiffractive beams.

15:25 Synthesis of Flat-Top Antenna Array Radiation Patterns Based on Pencil Beam Smoothing and Element Pattern Compensation

Goran Molnar and Marko Matijaščić (Ericsson Nikola Tesla & Research and Development Centre, Croatia)

This paper presents an analytic method for the synthesis of steerable flat-top radiation patterns using linear arrays with arbitrary antenna elements. The method is based on flattening a given pencil-beam pattern in specified direction with simultaneous compensation of the element pattern. Flattening and compensation are performed using maximum flat criterion. The application of the method is illustrated with the design of arrays with specified beamwidth and minimum sidelobe level, where the Gegenbauer pencil beam is utilized. For this application, a simple method for obtaining array's excitation coefficients is provided.

Room: Björk (33)

Scientific Workshop

SW2a - Measurement Advancements for 5G/6G and Emerging Wireless Standards: Innovations, Precision and Standardisation (IET Workshop)

13:45 An Ultra-Sensitive Online Calibration-Quality Monitoring Metric for MIMO Radar Systems

Michael Braunwarth and Johanna Geiss (Friedrich-Alexander-Universität Erlangen-Nürnberg, Germany); Erik Sippel (Friedrich-Alexander Universiät Erlangen-Nürnberg, Germany); Martin Vossiek (LHFT, Friedrich-Alexander-Universität Erlangen-Nürnberg, Germany)

The usual radar end-of-line (EOL) tests compensate for amplitude and phase imbalances and mutual coupling in multichannel MIMO radar systems. A high-quality calibration is required to provide a good cross-range imaging performance. However, harsh environmental conditions, like temperature and moisture changes, often experienced, e.g., by automotive radars, change the initially estimated system parameters and degrade the calibration and measuring quality over time. This publication proposes two new metrics that enable an easy implementable online estimation of a radar's overall calibration quality based on generated synthetic aperture radar (SAR) images. The approach exploits the effect that the calibration error power in multichannel SAR systems accumulates in a few analytically predictable positions. Utilizing this knowledge leads to a very high sensitivity of the derived metrics. The high performance of the proposed new method is demonstrated by measurements.

14:05 Electrically Small Flared Half-Loop Shaped Antenna for NB-IoT

Luca Persano (University of Grenoble Alpes & CEA-Leti, France); Marwan Jadid and Christophe Delaveaud (CEA-LETI, France); Tan-Phu Vuong, Sr. (Grenoble INP, France)

An electrically small, cuboid shaped antenna has been designed and simulated in this paper. The design with an electrical size ka of 0.24 and a maximum size of λ/13 achieves an overall radiation efficiency of 37%, a directivity of 5.83 dBi and a quality factor of 3.2 times the Chu limit. The design has been evaluated using the spherical wave expansion, and has been compared with the excited modes of well known reference antenna designs.

14:25 Cost Effective Butler Matrix-Based Digital/Hybrid Antenna Array Architecture with Element Tapering

Dagna I Wójciak, Alexander Thorburn Don, Jr., Ronnie Frith and Symon K. Podilchak (University of Edinburgh, United Kingdom)

Fully digital beamformers present complexity, power, and cost challenges, making hybrid architectures practical alternatives for sensing, radar, and communications. By replacing analogue phase shifters with an analogue beamformer, like a low-cost, passive Butler matrix (BM), costs can be reduced by about 75% when compared to a fully digital equivalent. A new architecture, builds on this by integrating BM-based subarrays with fully digital ones. Moreover, by placing digital subarrays at the centre of a larger array and where amplitude excitation can be programmable, allows for enhanced pattern control and reduced sidelobe levels (SLLs) and when compared to traditional hybrid beamformers. Despite the standard limitations of BMs, amplitude tapering still remains effective for lowering SLLs, as demonstrated achieving SLLs below -10 dB. By including such hybrid subarrays and with digital hardware as well as the appropriate beamforming algorithms, radiation performances can be enhanced while keeping costs, complexity, and power consumption manageable.

14:45 Effect of Antenna Radiation Pattern Variation on the Secrecy Key Generation in LoS Indoor Environment Under On-The-Shoulder Attack

Alessandro Santorsola (Politecnico di Bari); Giovanni Magno (Politecnico di Bari, Italy); Vincenzo Petruzzelli (Politecnico di Bari); Sabino Roberto Caporusso (BV TECH spa, Italy); Giovanna Calo (Politecnico di Bari, Italy)

The upcoming Sixth-Generation (6G) communication systems bring several challenges to systems security. The Secrecy Key Generation (SKG) is a Physical Layer Security (PLS) technique in which two trusted nodes negotiate a session key, taking advantage of the physical layer phenomena, i.e., radio propagation and/or hardware characteristics, as a source of entropy. In this contribution, we investigate the impact of the variation of the antenna radiation pattern on the SKG performance. We considered two legitimate nodes that apply the SKG to negotiate their session key, whereas a malicious node tries to eavesdrop on the communication to obtain the key by performing the on-the-shoulder attack. The results highlight how the number of antenna dipoles, the Half Power Beamwidth (HPBW) of the main lobe, and the presence of secondary lobes or minima of radiation influence the key mismatch between the legitimate nodes as well as the eavesdropper attack surface.

15:05 In-Band Full-Duplex Antenna Beamforming and Synchronization for Self-Interference Mitigation: Multi-Tile RFSoC Testbed Design and Deploym

Mustafa Ayebe (Chalmers University of Technology, Sweden); Rob Maaskant (CHALMERS, Sweden); Marianna Ivashina (Chalmers University of Technology, Sweden); Johan Malmström (Saab Surveillance, Sweden); Sten E. Gunnarson (Saab, Sweden); Henrik Holter (Ericsson AB, Sweden); Simon Westergren and Erik Johansson (Chalmers, Sweden)

This paper introduces an in-band full-duplex (IBFD) communication and sensing testbed using digital beamforming on the Xilinx ZCU216 RFSoC platform, featuring 16 DACs and 16 ADCs across four tiles. Key challenges include phase synchronization across tiles, which have independent clocks, and mitigating self-interference (SI) due to mutual coupling between closely spaced transmitting and receiving antennas. To overcome these, a Tx beamforming algorithm is used for maximum antenna gain, and an Rx beamforming approach maximizes the signal-to-self-interference ratio (SSIR). The testbed integrates two 1x5 Vivaldi antenna arrays (3-6 GHz) and implements multi-tile synchronization. Experimental results show over 80 dB SI suppression with half-wavelength separation (@6 GHz), demonstrating the testbed's potential for 6G communication and radar sensing.

MONDAY

15:25 A Differential Series-Fed Dipole Array for D-Band Sensing in Wafer Level Package Technology

Martijn de Kok, Paola Andrea Escobari Vargas and Elmine Meyer (Eindhoven University of Technology, The Netherlands); Friedrich Mueller and Tanja Braun (Fraunhofer IZM, Germany); Ad Reniers and Ulf Johannsen (Eindhoven University of Technology, The Netherlands)

This paper presents the design and characterization of a series-fed differential Antenna-in-Package (AiP) design, demonstrated as a four- and a six-element reflector-backed linear dipole array, that has been realized in a resin-based fan-out wafer level package technology. The four- and six-element designs achieve -10 dB input reflection bandwidths of 5.5 and 5.9 percent, realized gains of 14 and 15.4 dBi, and side-lobe levels of -10.7 and -12.1 dB, respectively. The realized samples were characterized through probed measurements in a state-of-the-art millimeter-wave anechoic chamber. After taking the RF-probe influence on the antenna performance into consideration, the measurements corroborated the simulated results.

Room: Schelkunoff (C1) — E04a - Optimisation methods and machine learning I

T07 Electromagnetic modelling and simulation tools / / Electromagnetics

Chairs: Harald Hultin (KTH Royal Institute of Technology & Saab AB, Sweden), Marcello Zucchi (Politecnico di Torino, Italy)

13:45 Fast, Robust and Global Optimisation for Antenna Design Using Meta Modelling

Lasse Hjuler Christiansen, Anders Eltved, Søren Hartmann, Sabine Fie Hansen, Nafsika Memeletzoglou, Edoardo Baldazzi, Oscar Borries and Min Zhou (TICRA, Denmark); Erio Gandini (ESA - European Space Agency, The Netherlands)

This paper introduces a data-driven meta-modelling framework designed to optimize challenging antenna designs, addressing the limitations of traditional gradient-based - and global search methods. The framework utilizes Bayesian Optimization (BO) and High-Order Gaussian Processes (HOGPs) to approximate black-box functions, substantially reducing the reliance on full simulations. Two case studies that 1) optimises a multi-section corrugated horn antenna and 2) balances gain and return loss in a dual-reflector system, demonstrate the framework's effectiveness in handling complex design challenges, offering a scalable and efficient tool for antenna engineers.

14:05 Wideband Side-Lobe Suppression of Tightly Coupled Arrays

Harald Hultin (KTH Royal Institute of Technology & Saab AB, Sweden); Henrik Frid (Saab, Sweden); Lars Jonsson (KTH Royal Institute of Technology, Sweden)

Tightly coupled arrays are a class of antenna arrays that are very wideband and have applications in communication and sensor systems. In both applications, low side-lobe levels are of interest. However, as tightly coupled arrays have high inter-element coupling, care must be taken when finding a suitable set of excitation coefficients. To demonstrate this, we design a tightly coupled array. Second, we extend a previously published convex optimization algorithm to account for strong inter-element coupling. This optimization algorithm solely finds excitations implementable in a simplified hardware model. The results are compared with conventional taperings, and show that our algorithm can achieve an excitation with lower reflected power compared to the conventional taperings, while maintaining similar gain and side-lobe levels.

14:25 RCS Predictions Using Geometric Deep Learning

Christoph Mäurer, Amit Mudgal and Aakash Raja (Altair Engineering, Germany)

Evaluation of Radar Cross Section (RCS) for different designs of electrically large objects like aircrafts can be very time consuming. We demonstrate how Geometric Deep Learning (GDL) could be used for fast RCS predictions. The approach learns for historical simulation data the relation between mesh geometry and the RCS results. As soon as sufficient simulation data are available for reasonable GDL prediction models, the RCS can be evaluated for new designs in real time.

14:45 Q-Factor Evaluation Accelerated by a Deep Neural Network

Stepan Bosak and Miloslav Capek (Czech Technical University in Prague, Czech Republic); Jiri Matas (Czech Technical University, Czech Republic)

Antenna inverse design has gained significant popularity, yet it often faces challenges with slow convergence to optimal solutions. This paper presents a novel deep-learning algorithm for accelerated Q-factor evaluation based on the Method-of-Moments (MoM). The proposed deep neural network directly processes triangular antenna meshes to estimate the vector of current expansion coefficients, effectively replacing the traditional impedance matrix inversion required in MoM. The Q-factor is subsequently computed. For this purpose, we introduce QfResNET, a Residual Network (ResNET) architecture featuring an upsampling convolutional network and the GELU activation function. Antennas are represented as multi-channel 2D arrays, preserving the neighborhood relationships in the antenna mesh and labeled with Q-factors derived through MoM calculations. Our results demonstrate that QfResNET achieves a speed-up of up to 957% compared to MoM. However, for coarser antenna meshes, the deep neural network does not offer a significant advantage.

MONDAY

15:05 A Super-Resolution Electromagnetic Inversion Scheme for Brain Stroke Detection

Lingqi Gao and Hakan Bagci (King Abdullah University of Science and Technology (KAUST), Saudi Arabia)

A super-resolution electromagnetic inversion scheme is proposed for brain stroke detection. The scheme operates in two stages: (i) A quantitative Gauss-Newton method with Tikhonov regularization and frequency-hopping is employed to get a low-resolution inversion result. (ii) A U-Net-based super-resolution method is used to significantly enhance the spatial resolution of the inversion result from (i). The proposed scheme is demonstrated through several numerical examples, highlighting its effectiveness in accurately reconstructing the brain's permittivity and conductivity profiles, thereby contributing to advancements in stroke diagnosis.

15:25 3D Database for Deep Learning - Application to Microwave Breast Imaging with a Planar Camera

Ambroise Diès (Sorbonne Université, Laboratoire de Génie Electrique et Electronique de Paris, France); Hélène Roussel (Sorbonne Université, CNRS, Laboratoire de Génie Electrique et Electronique de Paris, France); Nadine Joachimowicz (Sorbonne Université, CNRS Laboratoire de Génie Electrique et Electronique de Paris, France & Université Paris Cité, France)

This paper introduces a database of anthropomorphic breast models designed for machine learning applications. Its use is presented for quantitative spectral imaging of the breast using a planar microwave camera.

Room: Maxwell (C2) — M03 - Recent advances in antenna ranges

T02 Millimetre wave and THz for terrestrial networks (5G/6G) / / Measurements

Chairs: Jonas Fridén (Ericsson AB, Sweden), Sergiy Pivnenko (Antenna Systems Solutions, Denmark)

13:45 Efficient Reconstruction of the Sensitivity Map Characterizing the Equivalence of Working Volumes in Undermoded Reverberation Chambers

Anett Kenderes (Budapest University of Technology and Economics & Robert Bosch Kft. Hungary, Hungary); Péter Tamás Benkő (Robert Bosch Kft, Hungary); Szabolcs Gyimóthy (Budapest University of Technology and Economics, Hungary)

The equivalence of multiple working volumes (WV) in reverberation chambers (RCs) is investigated by the regime of state-of-the-art sensitivity analysis (SA) techniques while inspecting the effect of changing configuration parameters to the field uniformity (FU) close to the lowest usable frequency (LUF). The Sobol' indices as SA measures are evaluated at each stirrer step. For efficient calculation, different state-of-the-art surrogate modeling techniques were utilized to substitute the full-wave simulation model depending on the characteristics of the WVs. The computational expenses of the problem are further reduced by using a decreased number of stirrer steps and configurations as experimental design (ED) samples. The former is achieved by means of adaptive sampling techniques through kriging interpolation. The latter is carried out by performing convergence studies. The proposed method is able to reconstruct the sensitivity map of the configuration parameters as functions of the stirrer steps with a fewer number of samples.

14:05 A Comparative Study on Spatial Uniformity Metrics for Reverberation Chambers

Nazanin Farid and Asad Korfiatis (Eindhoven University of Technology, The Netherlands); Jonas Fridén (Ericsson AB, Sweden); Laurens A. Bronckers (Eindhoven University of Technology, The Netherlands)

Reverberation chambers are well-known for their time-efficient and flexible testing functionality. Spatial uniformity is a key characteristic of the chamber influencing measurement uncertainty. Depending on the target parameter and application, the conventional uniformity assessment method may not fully capture the effects within the chamber. Thus, the capability of the enhanced backscattering constant and the K-gamma factor to assess uniformity is investigated at millimeter-wave frequencies. Using the standard deviation of power transfer function as a reference and demonstrating its correlation with other parameters shows that the enhanced backscattering constant could be applied for uniformity assessments. Moreover, the practical importance of each parameter in its relevant application is highlighted, leading to effective methods for assessing uniformity and validating chambers for Over-the-Air tests. Given its high sensitivity to chamber configuration and antenna positioning, the K-gamma factor can complement the conventional power transfer function method, delivering additional insights and practical improvements in measurement setups.

14:25 Applying Time Gating and Stirring for Radiation Pattern Measurements in a Reverberation Chamber

Remco Heijs and Antonius Johannes van den Biggelaar (ANTENNEX, The Netherlands); A. B. (Bart) Smolders (Eindhoven University of Technology, The Netherlands)

This paper applies both stirring and time gating to measure the radiation pattern of antennas in a reverberation chamber. Time gating in highly reflective environments requires a large bandwidth but has a similar measurement time compared to measurements performed in an anechoic chamber. Mechanical stirring itself fails to isolate the line-of-sight path from the unstirred non-line-of-sight signal. This method requires a long measurement time but could be performed at a single frequency. This work shows that by combining mechanical stirring and frequency stirring over a small bandwidth, the unwanted effects of the non-line-of-sight unstirred components can be reduced while having a negligible impact on the measurement time. This work applies stirring and time gating to measure the radiation pattern in the E-plane of a standard gain horn antenna at the Ka-band. The radiation patterns are compared to full-wave simulations performed in CST and shown at 28 and 35 GHz.

14:45 Accuracy Analysis of Group Delay Variation Measurement in Anechoic Chambers

Stefano Caizzone (German Aerospace Center (DLR), Germany); Veenu Tripathi (DLR- German Aerospace Center, Germany); Wahid Elmarissi and Bernd Gabler (German Aerospace Center (DLR), Germany)

Precise GNSS antenna characterization is needed in several applications, targeting high-accuracy positioning and timing. While the characterization of phase center variations is nowadays canonically established, the measurement of group delay variations is still a matter of research for its high requirements in terms of measurement accuracy. The present paper shows an analysis of the accuracy performance achievable in anechoic chambers, estimating the uncertainty in the group delay variation produced by imperfections of the measurement system itself and assessing the impact of signal processing countermeasures.

15:05 Reaction Analysis of Quiet Zone Error Impact on Relative Gain Accuracy

Naila Rubab (Eindhoven University of Technology, The Netherlands); Antonius Johannes van den Biggelaar (ANTENNEX, The Netherlands); A. B. (Bart) Smolders and Ad Reniers (Eindhoven University of Technology, The Netherlands); Jonas Fridén (Ericsson AB, Sweden)

This paper presents an error model using the reaction integral to quantify measurement uncertainty in relative gain pattern measurements under near-plane wave conditions. By deliberately introducing errors into an ideal quiet zone, the study evaluates their impact through root mean square metrics and site acceptance standard error criteria. The investigation focuses on assessing the tightness of the upper bound on the relative gain accuracy, as determined by the root mean square error of the field across the antenna surface. Furthermore, the uncertainty in estimating quiet zone error metrics from incomplete but widely used scanning techniques is illustrated through practical examples.

15:25 Instrumental Faraday-Like Rotation and Temporal Autocorrelation for Radio Astronomical Antennas

Tobia Carozzi (Onsala Space Observatory, Chalmers University of Technology, Sweden); Paola Di Ninni (OAA - INAF, Italy)

We investigated oscillations in the frequency spectra of dual-polarized, radio astronomy antennas by applying the Fourier transform to obtain their temporal autocorrelation. The temporal autocorrelation is equivalent to the so-called delay transform of zero length baselines. Of particular interest are wideband antennas at low frequencies, which are planned for use in next generation Faraday rotation observations. We found that antennas such as the one proposed for the SKA-Low telescope, the SKALA4.1, exhibit spectral oscillations at 150 MHz and at 20 MHz that may appear as Faraday rotation. The strength of this effect tends to be stronger at lower elevations, as anticipated, but still exists even for zenith elevation, which is bore-sight. This effect is seen mainly in wideband antennas, and suggests that the additonal complexity of wideband antennas needs more attention in full polarimetric calibration than narrowband antennas more commonly used for Faraday measurement.

Room: Oliner (C3) | **A08 - Developments in reconfigurable antennas and surfaces**

T08 Fundamental research and emerging technologies/processes / / Antennas

Chairs: Arvind Kumar (Dept of ECE,. Visvesvaraya National Institute of Technology Nagpur India, India), Cody Scarborough (University of Colorado Boulder, USA)

13:45 1-Bit Circularly Polarized Transmit-Array with Orthogonal Elements in X Band

Silong Chen, Kunping Yang, Zhijing Wu and Ping Chen (Nanjing University, China)

In this paper, we present two universal layout schemes for designing a 1-bit circularly polarized (CP) transmit-array utilizing only a single phase-modulated layer. These schemes eliminate the correlation of co- and cross-polarization phase patterns caused by 1-bit phase discreteness in the CP array, effectively preventing cross-polarization beam in the same direction. As a proof of concept, a broadband CP transmit-array antenna with goodish polarization purity beams is designed in X-band around 10 GHz. Compared to a uniform element array, the staggered placement of two orthogonal 1-bit elements significantly improves the cross-polarization discrimination (XPD), achieving a 3 dB axial ratio bandwidth of 32.7%. The performance of wide-angle scanning beams up to 60° further validates the effectiveness. The proposed schemes could be used for CP reconfigurable array antennas, enabling electronic beam-steering with just a single phase-modulated functional layer.

14:05 Amplitude-Reconfigurable Unit Cell in CLAF-SIW for Beamforming Applications at mmWaves

Cleofás Segura-Gómez, Andrés Biedma-Pérez and Pablo Padilla (University of Granada, Spain); Angel Palomares-Caballero (IETR-INSA Rennes, France)

This work presents an amplitude-reconfigurable unit cell for the design of active 1D metasurfaces at the millimeter-wave frequency range. The reconfigurable unit cell consists of contactless air-filled substrate-integrated waveguide (CLAF-SIW) that feeds a SIW cavity with a ring-shaped slot as a radiating element. In order to perform the reconfiguration, two PIN diodes are placed in the ring-shaped slot. The CLAF-SIW allows reduced losses while feeding the reconfigurable SIW cavities in a progressive form as a leaky-wave antenna. The structure requires a single layer for the radiating elements and only two for the feeding layer since the radiation layer completes the CLAF-SIW. For the implementation of beamforming at 40 GHz, a method of switching OFF/ON in each reconfigurable unit cell is applied. By optimizing the state of each unit cell in the reconfigurable leaky-wave antenna, various radiation patterns can be achieved.

14:25 Liquid-Metal-Enabled Multi-Polarization Reconfigurable Antenna

Yi-Wen Wu and Yi Wang (University of Birmingham, United Kingdom)
This paper presents an antenna that can reconfigure its polarization. It is possible to obtain four different states of excitation to the antenna, leading to four different polarization states, namely: horizontal polarization, vertical polarization, left-hand circular polarization, and right-hand circular polarization. The radiating element of the antenna is a microstrip patch incorporating two feed points. The driven patch is surrounded by four parasitic elements which are used to improve the realized gain. Most of the polarization reconfigurable antennas, presented in the literature, involve reconfiguring the radiating element. In the proposed antenna, polarization-reconfiguration is achieved by a liquid metal-based reconfigurable network. For validation, a quad-polarization antenna has been designed, fabricated and measured. The simulation and measurement results are in excellent agreement. The measured peak realized gain of the single radiating element is approximately 10.0 dBic. At 3.5 GHz, the measured axial ratios (ARs) are 1.2 dB.

14:45 Network-Based Hybrid Spatial-Spectral RIS Synthesis Method

Timothy Macdonald, Ryan Montoya, Alan Brannon and Cody Scarborough (University of Colorado Boulder, USA)
A network-based technique is presented that incorporates the full-wave scattering from reconfigurable intelligent surfaces (RISs) with global periodicity. The RIS is treated as a multi-port network that connects loaded RIS ports to propagating plane waves. The scattering matrix is collected using a commercial solver in the spectral domain to alleviate the computational cost of computing the hybrid spatial-spectral scattering matrix of the RIS. Using the Neumann method, sparsity within the scattering matrix is leveraged to compute the scattered field rapidly. Further, the Gerchberg-Saxton algorithm is modified to directly synthesize load impedances distributed throughout the RIS. Beam splitting is demonstrated for an active RIS containing 9,801 unit cells where a plane wave illuminates the surface and redirects the radiation in two directions; a retroreflected component back towards the illumination, and a desired auxiliary scanned direction.

15:05 Varactor-Tunable RFID-Based Wireless Programmable Frequency Selective Surface as a Smart Shield for Implanted Medical Devices

Francesco Lestini and Gaetano Marrocco (University of Rome Tor Vergata, Italy); Cecilia Occhiuzzi (University of Roma Tor Vergata, Italy)
Modern Implantable Medical Devices (IMDs) feature wireless capabilities that enable remote monitoring and device programmability. However, this increased connectivity also introduces vulnerabilities to both cyber and physical threats, potentially endangering patient safety. This study presents a novel, miniaturized design of an epidermal Radio-Frequency Identification (RFID)-based wireless programmable Frequency Selective Surface (FSS) to shield IMDs from unauthorized users while ensuring secure communication. Compared to previous studies, the proposed design reduces power consumption using varactor diodes instead of PIN diodes. Simulation results demonstrate the effectiveness of the shield in attenuating Electromagnetic Interference (EMI) in the Medical Implant Communication Service (MICS) band by 49 dB, as well as its programmability to achieve transparency. Four dipoles surrounding the finite FSS allow for RFID-based wireless programmability. This solution represents a significant advancement in the cyber and physical protection of IMDs, being at the same time the first example of a wireless programmable FSS.

15:25 Beam Steering Antenna Using Reconfigurable Partially Reflective Surface

Ranjit Kumar Dutta, Baisakhi Bandyopadhyay and Kumar Vaibhav Srivastava (Indian Institute of Technology Kanpur, India)
This paper presents a electronically reconfigurable beam steering system. The proposed structure incorporates coaxial feed microstrip patch radiator and a reconfigurable partially reflective surface (PRS). The reconfigurable PRS is mounted over the antenna layer at a height of 27 mm. The PRS layer consists of 6 × 6 reconfigurable unit cells. To make the PRS reconfigurable, PIN diodes are used. To obtain the beam steering, the PRS layer is divided in two sections. The radiating beam can be make tilt by making the individual section ON and OFF accordingly. The complete beam steering system shares a volume of $2.4\lambda0 \times 2.4\lambda0 \times 0.49\lambda0$. The beam steering system obtains measured beam tilting upto $\pm 50^{\circ}$, with a maximum measured realized gain of 11.3 dBi at the operating frequency 5.5 GHz.

Room: Kraus (C4) | **E09a - Metasurfaces I**

T08 Fundamental research and emerging technologies/processes / / Electromagnetics

Chairs: Ariel Epstein (Technion - Israel Institute of Technology, Israel), Raúl Rodríguez-Berral (Universidad de Sevilla, Spain)

13:45 Programmable Metasurface for DOA Estimation from Mobile Objects and Wave Redirection

Nawel Meftah and Badreddine Ratni (Univ Paris Nanterre, France); Mohammed Nabil El Korso (Université Paris-Saclay, France); Shah Nawaz Burokur (LEME, France)
A method to estimate the direction of an incoming wave and to redirect it to a desired direction is proposed. The tasks are achieved by a metasurface exploited as reconfigurable intelligent surface (RIS). To estimate the direction-of-arrival (DOA), the RIS is configured as tunable parabolic reflector, making the incident waves converge to a common focal point where a receiving antenna is placed to act as a power detector. To redirect the waves, the RIS is configured as a phase-gradient reflector. Experimental measurements performed on a programmable metasurface in an anechoic chamber allow validating the proposed method

MONDAY

14:05 Maximal Operation Band of Binary Metasurfaces with Controllable Anomalous Reflection

Constantin Simovski (Aalto University, Finland)

The maximal achievable bandwidth of a reconfigurable intelligent surface implemented as a binary metasurface is considered and analytically deduced taking into account the restrictions imposed by the non-ideal angular stability of practical metasurfaces. This bandwidth is proportional to the effective inductance of the metasurface, and its maximum demands the low-index substrate of sufficient thickness.

14:25 An Efficient Array Synthesis Method for Reconfigurable Reflectarray Antennas Based on a Macroscopic Model of Metasurface

Ruiwen Shao (Southeast University, China)

A more efficient and accurate array synthesis method for reconfigurable reflectarray antenna (RRA) is proposed. A macroscopic model of digital coding metasurface that can take the mutual coupling of adjacent elements into account is utilized to replace array theory in traditional synthesis method, making the numerically calculated farfield patterns closer to full-wave simulated ones. Then, the macroscopic model is integrated with genetic algorithm (GA) to realize an efficient and accurate array synthesis method. A 32×32-element RRA is designed to verify the macroscopicmodel- genetic-algorithm (MM-GA) array synthesis method. Compared with the array-theory-genetic-algorithm (ATGA) method, our proposed MM-GA performs better in full-wave simulations. The full-wave simulated sidelobe level by MM-GA synthesis is 15.3dB, while that of AT-GA is 14.8dB, when the RRA scans to φ=90°, θ=45°.

14:45 Simple Metal-Only 1-Bit Coding Metasurface for RCS Reduction

Thomas Uguen (CNES, France); Raphael Gillard and Renaud Loison (IETR & INSA, France); Jeanne Pagès-Mounic (CNES, France); Pouliguen Philippe (DGA, France)

1-bit coding metasurfaces, which combine two basic unit cells with out-of-phase responses, have shown significant potential for achieving diffuse scattering, making them valuable for radar signature control. This paper presents a simple metal-only unit cell to design metasurfaces for radar cross-section reduction. The various steps of designing this unit cell are outlined. The recently introduced Minimum Peak Sidelobes codes in the field of coding metasurfaces, associated with the metal-only unit cell, are being utilized to validate their diffusion capabilities through electromagnetic simulations. The results are compared to those obtained with an analytical approach. To enhance performance and align more closely with the analytical approach, modifications to the unit cell are presented, which involve adding rooftops.

15:05 Bistable Beam Splitting in Nonlinear Metagratings

Naama Cohen Levi (Technion-Israel Institute of Technology, Israel); Ariel Epstein (Technion - Israel Institute of Technology, Israel)

We present an analytical model for the response of a beam-splitting metagrating (MG) comprised of thin wires loaded by nonlinear capacitors. Through rigorous formulation, we reveal that a bistable switching response may emerge in such a configuration, and identify analytically the parameters governing its formation. We show that by judicious choice of these structural and electromagnetic MG parameters, a distinct hysteresis loop may be observed, switching between high specular reflection to high split efficiency, depending on the input field intensity and history of excitation. These results, verified via full-wave simulations, lay the grounds for the development of MG-based electromagnetic switches for communication and analog computing, while establishing the foundations for analysis and synthesis of advanced nonlinear MGs in the future.

15:25 Design of a Dichroic Transmissive Huygens' Metasurface Unit-Cell Presenting Refraction Angle Duality

Georgios Kyriakou and Giampaolo Pisano (University of Rome 'La Sapienza', Italy); Luca Olmi (INAF-Arcetri Astrophysical Observatory, Italy); Francesco Piacentini (Sapienza, University of Rome, Italy)

A purely transmissive Huygens' metasurface model under plane-illumination is used to derive circuit parameters describing a constituent unit cell, such that diverse refraction angles are attained at two distinct frequency bands. Various levels of accuracy of the circuit description approaching the analytical are possible by constraining certain numbers of parameters. This theoretical study is then tested by calculating the exact formulas of the two representations for the various strategies proposed. By using simulations of a candidate unit-cell, we then examine whether such circuit parameters correspond to fine-tuned versions of the geometry of a so-called parallel `dogbone' structure. A device of this type is intended as dual-band (dichroic), dual-angle beam refractor diverting an incoming beam at different directions in two different bands without reflections.

MONDAY

13:45 Formulas for the Maximum Radiated Power Density at Broadside in Lossy Fabry-Perot Cavity Antennas

Walter Fuscaldo (Consiglio Nazionale delle Ricerche (CNR), Italy); David R. Jackson (University of Houston, USA); Alessandro Galli (Sapienza University of Rome, Italy)

The leaky-wave analysis of lossless Fabry-Perot cavity antennas (FPCAs) reveals that the maximum radiated power at broadside is reached at the leaky cutoff, i.e., when the leaky phase and attenuation constant of the fundamental TE-TM leaky-mode pair excited in the structure are equal to each other. Formulas for optimizing the cavity height to reach the leaky cutoff at the design frequency were previously provided under one of these two assumptions: i) the radiated power at broadside is dominated by the leaky-wave contribution, and ii) the structure is lossless. Here, a new formula is derived to accurately optimize the cavity height for maximum radiated power density at broadside which accounts for both dielectric and ohmic losses. The formula is based on the expression of the total pattern radiated by a lossy FPCA, and thus remains accurate even when the leaky-wave contribution does not dominate the aperture field.

14:05 A Hybrid Approach for Efficiently Illuminated Fabry-Pérot Cavity Antennas with Enhanced Bandwidth

Pablo Mateos-Ruiz (University of Malaga, Spain); Elena Abdo-Sánchez (University of Málaga & E. T. S. I. Telecomunicación, Spain); Carlos Camacho-Peñalosa (University of Málaga, Spain)

This contribution proposes a design methodology to realize Fabry-Pérot cavity antennas with enhanced aperture efficiency and bandwidth. The proposed antenna employs a tapered partially reflective surface and leverages a combined approach incorporating principles from the simplified ray model and two-dimensional leaky-wave theory. By employing a transmission line model of the PRS, unit cells are selected that simultaneously satisfy the resonance condition, present a positive reflection phase slope, and synthesize the necessary leakage factor function. A design to obtain a uniform aperture distribution is carried out. The simulation results are compared against the best design from a previous study, thus showing the improvement realized by incorporating leaky-wave theory into the antenna design process.

14:25 Unlocking Extended Nondiffractive Ranges in Leaky-Wave Bessel Beams via an Open-Stopband Mitigation Technique

Edoardo Negri (Sapienza University of Rome, Italy); Federico Giusti (University of Siena, Italy); Walter Fuscaldo (Consiglio Nazionale delle Ricerche (CNR), Italy); Enrica Martini (University of Siena, Italy); Alessandro Galli (Sapienza University of Rome, Italy)

The 'chimera' of point-to-point wireless links is to efficiently transfer the largest amount of power at the farthest distance, possibly with the slightest waste of energy, and resilience to obstacles. For this purpose, thanks to their limited-diffraction, focusing, and self-healing properties, Bessel beams are usually considered important candidates for near-field applications. However, their main limitation is usually constituted by a low-value nondiffractive range, viz. the maximum distance for which Bessel beams maintain their intriguing features. For this reason, an original, lowprofile, cost-effective, leaky-wave device able to generate an ultra-long-range Bessel beam by exploiting an openstopband mitigation technique is proposed in this work. In particular, we design a radially periodic leaky-wave Besselbeam launcher with a double-strip unit-cell configuration operating at 30 GHz. This device achieves an impressive nondiffractive range of approximately 25 m, which corresponds to 2500 vacuum wavelengths and to 50 times its aperture diameter of 50 cm.

14:45 Unit Cell Design for 3D-Printed Leaky-Wave Antennas

Patrick J Bartley (The University of Queensland, Australia); Christophe Fumeaux (University of Queensland, Australia); Nghia Nguyen (Nextwaves Industries, Vietnam); Nic Lawrence (University of Adelaide & Defence Science Technology Group, Australia)

This paper presents a simulated analysis of three unit cells for 3D-printed Dielectric Image Line (DIL) Leaky-Wave Antennas (LWAs). These unit cells, which are to be printed with the filament Preperm ABS1000 with bulk relative permittivity of 10, will be subject to multi-line parametric analysis. Predicted radiation and aperture efficiency are then assessed. Finally, preliminary results of an experimental 3D-printed antenna are demonstrated using one of the discussed unit cell designs as a validation for such antenna design.

15:05 Meander Leaky Wave Antenna with Open Stop-Band Suppression for Millimetre Wave Direction-Finding

Aritra Roy, Guido Valerio and Julien Sarrazin (Sorbonne Université, France)

A meander unit cell with a pin-based open stop band (OSB) mitigation technique is presented to design a fast frequency-beam-scanning leaky wave antenna (LWA) at millimeter-wave frequencies. The complex propagation constant of the unit cell is obtained based on an S-parameter simulation approach. The classical open stop-band issue observed is thus observed and addressed by inserting a pin inside the unit cell. A LWA is accordingly designed which exhibits impedance matching and no drop in the gain at the OSB frequency. This LWA beam seamlessly steers from -46 ◦ to 44 ◦ over a 400 MHz bandwidth only at 27.25 GHz, thereby exhibiting a scanning rate as high as 61.3 ◦ /%.

15:25 Modal Analysis of Leaky Modes Supported by Planar Metallic Corrugation

Beatrice Ambrogi (Sapienza University, Italy); Guido Valerio and Yuhuan Tong (Sorbonne Université, France); Davide Comite (Sapienza University of Rome, Italy)

Corrugated metal planar surfaces lend themselves to the realization of a wide range of radiating devices thanks to their compact and robust shape. In a homogenization regime they can support a proper surface-wave mode. At higher frequencies, i.e., when the unit cell period and the free-space wavelength are comparable, they support proper and improper leaky-wave regimes. Here, we present an original dispersive study of a corrugated allmetal plane constituted by narrow grooves. A modal dispersive analysis is carried out using a method-of-moments approach across a relatively large spectrum. An interesting modal solution is achieved, showing large variations of the attenuation constant, an open stop band at the forward/backward transition and closed stop bands. A large region just after the open stop band is achieved, where the phase constant is smaller than the attenuation constant. The structure can support the design of an all-metal planar antenna, potentially having wideband broadside radiation.

Room: Mosig (26) — A14 - Mmwave antennas for space applications

T03 Aerospace, space and non-terrestrial networks / / Antennas

Chairs: George Goussetis (Heriot-Watt University, United Kingdom), Carolina Tienda (ESA, ESTEC, Noordwijk, The Netherlands)

13:45 Hybrid Beamforming for Satellite Ground Stations in the mmWave Band

Amélia Struyf and Nédid Ismaili (Université Libre de Bruxelles, Belgium); Philippe De Doncker (ULB, Belgium); Dimitri Lederer (Université Catholique de Louvain, Belgium); François Quitin (Université libre de Bruxelles, Belgium)

One promising approach to increase data rates in satellite communication systems is using millimeter-wave (mmWave) communications. Ground stations (GSs) with mmWave antenna arrays offer high signal gains and more flexibility than traditional parabolic antennas. However, design costs of mmWave systems do not allow for fully-digital antenna arrays, where each antenna has its own Radio-Frequency (RF) chain. Instead, hybrid beamforming architectures, combining digital and analog beamforming, are preferred. In this paper, we present a low-complexity hybrid beamforming algorithm for GSs that relies on the knowledge of the satellites directions. We benchmark the rate performance of this method in a multi-satellite Multiple-Input Multiple-Output (MIMO) scenario and provide a comparison with more complex hybrid beamforming design methods. Simulation results show that the performance of the proposed geometrical algorithm approaches the performance of more complex state-of-the-art methods. Moreover, we present an experiment using mmWave Software-Defined Radios (SDRs) to validate the geometrical hybrid beamforming approach.

14:05 Integrated Design and Optimization of a Shared-Aperture Dual-Band Ku/Ka Flat Panel Antenna Array for Enhanced LEO SATCOM Performance

Hakmin Lee and Seong-Mo Moon (ETRI, Korea (South)); Sol Kim (Electronics and Telecommunications Research Institute (ETRI), Korea (South)); Junhan Lim, Jongho Yoo and Dong-pil Chang (ETRI, Korea (South))

This paper presents the design and development of a shared-aperture dual-band Ku/Ka flat panel antenna array optimized for Low Earth Orbit (LEO) satellite communications. Integrating dual-band capabilities within a compact flat panel design, the antenna achieves efficient performance across both Ku and Ka bands. A novel 2x3 array configuration employing a sequential feeding technique is introduced, enhancing circular polarization and broadening coverage. This surpasses traditional 2x2 array setups with directivity improvements and bandwidth utilization: S-parameter isolation is below -10 dB, with a bandwidth of 6.3% at 18.8-20.0 GHz for the Ku-band and 8.5% at 26.6-29.0 GHz for the Ka-band. These metrics, rigorously evaluated through simulation, demonstrate significant advancements in satellite communication efficiency.

14:25 Mechanical Beam Steering Reflectarray Antennas Using Focal Arc Geometries: Performance and Limitations

Andrés Gómez-Álvarez (Universidad de Oviedo, Spain); Manuel Arrebola (Universidad Politécnica de Madrid, Spain); Marcos R. Pino (Universidad de Oviedo, Spain)

This paper presents a parametric study on passive, mechanically steerable reflectarray (RA) antennas using a tilted focal arc configuration. The objective is to examine the trade-offs in designing compact RA systems capable of steering beams over a wide angular range while minimizing scan losses. Multiple RA designs at 29.5 GHz are evaluated, featuring varying degrees of compactness and steering ranges with highly uniform gain across the steering range. Performance is assessed in terms of gain and aperture efficiency, highlighting the effects of focal ratio and steering range on these metrics. A prototype antenna is also manufactured and measured, validating the simulation results with a demonstrated scan loss of only 0.5 dB over a 90-degree range and a maximum gain of 28.2 dBi. The findings provide insights into the design compromises required for passive, mechanically steerable RA systems, offering guidelines for optimizing such antennas for mm-Wave applications.

14:45 Preliminary Simulations of Spherical Reflectarrays in Dual Configuration for Satellite Antennas in Ka-Band

Daniel Martinez-de-Rioja (Universidad Politécnica de Madrid, Spain); Yolanda Rodriguez-Vaqueiro and Antonio Pino (University of Vigo, Spain); Eduardo Martinez-de-Rioja (Universidad Rey Juan Carlos, Spain); Jose A. Encinar (Universidad Politecnica de Madrid, Spain); Manuel Arrebola (Universidad Politécnica de Madrid, Spain); Giovanni Toso (European Space Agency, ESA ESTEC, The Netherlands)

In this contribution, the design of spherical reflectarray antennas is proposed to achieve a compromise between parabolic and spherical surfaces. The spherical surface simplifies the folding mechanism of the antenna, while the printed elements on the reflectarray surface are designed to correct the spherical aberration, improving the focusing of the spherical surface and providing the electrical performance of a parabolic reflector antenna. The focusing and scanning capabilities of spherical reflectarrays are evaluated and the implementation of spherical reflectarrays in dual antenna configurations is proposed to provide further compact antenna solutions

MONDAY

15:05 Ultralight Deployable Multi-Modular Faced Reflectarray

Borja Imaz-Lueje (Universidad Rey Juan Carlos, Spain); Carolina Tienda (ESA, ESTEC, Noordwijk, The Netherlands); Daniel Martinez-de-Rioja and Manuel Arrebola (Universidad Politécnica de Madrid, Spain)

This paper proposes a multi-modular and multi-faceted reflectarray antenna solution that reduces the weight and complexity of implementation. The antenna consists of multiple facets, not aligned among them, and following an equivalent parabolic reflector profile. The supporting structure of the antenna is stowed and deployed in several parts to accommodate the facets of the structure. Each facet consists of one or several modules with ultrathin and flexible surface that are independently deployed to conform the surface of each facet. The use of multi-faceted topologies enhances the electrical performance of the antenna compared to planar apertures and relax the accuracy constraints imposed in the reflector surface, compared to parabolic reflectors. A modular approach from mechanical and RF point of view is a more robust solution to overcome bandwidth limitations and deployment failures of large reflectarrays.

15:25 A SiGe Integrated Active Phased Array Antenna for a 183GHz Water-Vapor Radiometer

Juan M Herrera-Martín (Universidad Carlos III de Madrid, Spain); Alvaro Urain (TECNUN, Spain); David del Río (CEIT and TECNUN, Spain); Vicente González Posadas (Polytechnic University of Madrid, Spain); Iñigo Ederra (Universidad Pública de Navarra & Institute of Smart Cities, Universidad Pública de Navarra, Spain); Jorge Teniente-Vallinas (Public University of Navarra & Institute of Smart Cities, Spain); Roc Berenguer (TECNUN, Spain); Daniel Segovia-Vargas (Universidad Carlos III de Madrid, Spain)

Millimeter-wave radiometers can benefit from state-of-the-art on-chip technologies to construct a fully integrated front-end at frequencies above 100 GHz. The first step is to integrate a fully capable antenna design with a complex low-low noise amplifier in the same technology. This paper presents the integration simulation of a passive antenna array in IHP's SiGe 130 nm BiCMOS SG13G2 process and a 3-stage low-noise amplifier using the same technology. The final seamlessly integrated design proves to be a viable first building block for a future complete radiometer frontendon- a-chip for frequencies exceeding 100 GHz.

Room: Collin (27) — P08a - Channel modeling approaches

T07 Electromagnetic modelling and simulation tools / / Propagation

Chairs: François Sarrazin (Université de Rennes & IETR, France), Claude Oestges (Université catholique de Louvain, Belgium)

13:45 Statistical Analysis of Scattering Invariant Mode Wave Propagation Validated by Measurements

Oliver Csernyava and József Pávó (Budapest University of Technology and Economics, Hungary); Zsolt Badics (Tensor Research LLC, USA)

This paper investigates microwave propagation using Scattering Invariant Modes, validated through both experimental measurements and numerical simulations. The numerical model, based on finite metallic cylinder rods, is verified against measured data. A statistical analysis of the simulated results is conducted by varying the geometric parameters, including the radius and coordinates of the scattering structure. The findings reveal a threshold beyond which changes in geometry do not significantly affect the Scattering Invariant Modes excitation, demonstrating consistent low-loss propagation despite structural variations. This highlights the robustness of SIMs in dynamically changing environments.

14:05 Power-Angle Spectrum Characterization Based on Antenna Directivity Statistics in Wireless Multipath Channels Using Spherical Vector Waves

Andrés Alayón Glazunov (Linköping University, Sweden)

This paper introduces a novel method for characterizing the power-angle spectrum and antenna directivity in wireless multipath channels using spherical vector wave expansion. Based on measurements at 5.2 GHz in indoor-to-outdoor scenarios, we analyze dipole and quadrupole modes in both vertically and cross-polarized channels. We propose characterizing the direction-spread based on the corresponding antenna directivity. This offers a more detailed understanding of antenna performance influenced by spatial fading and propagation effects.

14:25 A Closed-Form Formulation for EM Wave Pathloss into Train Wagons

Nima Jamaly (Swisscom, Switzerland)

This paper presents a comprehensive analysis of EM wave pathloss into train wagons, focusing on signal penetration through windows. The formulation applies to any train type, accommodating both coated and uncoated windowpanes. A closed-form expression is derived, offering a precise calculation of the power received by an onboard antenna, based on the available electromagnetic power density at the window surface.

14:45 A Diffusion-Based Propagation Model for Path Loss Prediction in Indoor Environments

Charley Xu, Danjie Tang, Aristeidis Seretis and Costas D Sarris (University of Toronto, Canada)

Machine learning methods have been widely used to design accurate and computationally efficient propagation models. Various machine learning models have been used for this task, ranging from simple artificial neural networks to more complex deep learning structures. In most cases, these models are trained utilizing either measured or simulated data. In this paper, we introduce a new approach to propagation modeling in indoor environments, leveraging a diffusion model. Our model is trained using simulated path loss maps in many diverse indoor geometries. Then, it can efficiently extrapolate full path loss maps from a small number of path loss samples, collected by measurements or low-cost simulations. This form of path loss "inpainting" requires no re-training of the model, and is agnostic to the shape and source of the provided path loss samples.

15:05 Instantaneous DoA Estimation Using Poynting Vector and a Vector Sensor

Erik R Algarp (EPFL, Switzerland); Angelo Freni (University of Florence, Italy); Anja K. Skrivervik (EPFL, Switzerland)

The direction of arrival (DoA) estimation performance of a vector sensor using the instantaneous Poynting vector is evaluated in relation to the realized element patterns of the vector sensor. Up to six amplitudes, one amplitude per field component of the impinging wave, are measured in the vector sensor in a time instance and yield a DoA estimate via the instantaneous Poynting vector based on the direction of maximum incoming power. Proportional amplitude readings with respect to the impinging fields are necessary to correctly estimate the angular coordinates of the impinging signal, making the study of element pattern anisotropy in the vector sensor critical for the DoA estimation error.

15:25 Experimental Demonstration of Safe Beamforming Integrated with Wireless Human Sensing for Microwave Wireless Power Transfer

Kentaro Murata (Iwate University, Japan); Haruki Yamamoto (Iwate Universitiy, Japan); Naoki Honma (Iwate University, Japan)

This paper proposes the safe beamforming (BF) integrated with wireless human sensing for microwave wireless power transfer (MWPT) employing multiple cooperative MWPT stations as a radar. The proposed method first estimates the human location and width based on the channel information via a human. Subsequently, a safe BF can maximise the power density at the receiver to meet the maximum permissible exposure (MPE) within the human area. The above processes can be performed using only the RF front end; no additional optical system is required to scan the human geometric information. Experiments conducted using our multi-antenna testbed successfully demonstrated the high accuracy of human location and width estimation, with a few degrees of error in the angle of view. Consequently, the proposed BF method achieved both high received power, comparable to the achievable maximum, and human exposure below the MPE.

Monday - 16:15-18:15

Room: Alfvén (A3+A4)

A02 - Developments in Array Analysis and Design

T02 Millimetre wave and THz for terrestrial networks (5G/6G) / / Antennas

Chairs: Marianna Ivashina (Chalmers University of Technology, Sweden), Agostino Monorchio (Pisa University & CNIT, Italy)

16:15 A Stacked Patch Array for UHF Band with Dual Circular Polarization

Chiara Scarselli (University of Pisa, Italy); Agostino Monorchio (Pisa University & CNIT, Sweden)

This paper presents a design optimization of an existing receiving antenna array with dual circular polarization, specifically tailored for advanced bistatic radar systems. The proposed array operates at 412 MHz and consists of 13 stacked circular slot-patch antennas in a thinned configuration, as opposed to the 19 elements of the original design. Each radiating patch features two slots on opposite sides and is coaxially fed at two distinct points to achieve both Right-Hand and Left-Hand circular polarizations. Additionally, two dielectric substrates are positioned above the radiating patch, each topped with a parasitic passive patch to enhance gain. The results show a gain of 17 dBi and an Axial Ratio (AR) less than 3 dB within a 14° Half Power Beamwidth (HPBW), with a Side Lobe Level (SLL) equal to -13 dB. By reducing the number of elements, the design retains the required gain, offering a more efficient and cost-effective solution.

16:35 Analysis of Millimeter-Wave Array Frontend Architectures for High EIRP: Comparing Various Beamforming and Power Combining Techniques

Viktor Chernikov, Artem Vilenskiy and Marianna Ivashina (Chalmers University of Technology, Sweden)

This paper analyzes different active beamforming array antenna frontend architectures for future point-to-point communication systems. Our focus is on utilizing W-band frequencies (75-110 GHz) to develop antenna system capable of operation in different weather conditions. We use simplified scalable models of array transmitters, incorporating literature data for mmWave power amplifier (PA) designs and power combiners (i.e., output power, insertion loss) to evaluate the maximum achievable performance for each architecture. The resulting design curves, which plot the effective isotropic radiated power (EIRP) of the frontend vs. the number of combined PAs in different array architectures, help guide trade-offs in achieving the required performance with minimal energy consumption. A practical example, i.e., a 50~dBi single offset reflector antenna fed by 7-element waveguide-based focal plane array with 0.75 wavelength inter-element spacing for W-band backhauling links, is briefly discussed and used to validate the findings of the analysis.

16:55 Even/Odd Method to Speed Up the Rigorous Full-Wave Simulation of Large Phased Arrays Exploiting 90 ◦ Geometrical Symmetries for Wide Scanning Angles

Lisa Berretti and María García-Vigueras (IETR-INSA Rennes, France); Giovanni Toso (European Space Agency, ESA ESTEC, The Netherlands); Lucas Polo-López (IETR-INSA Rennes, France); Esteban Menargues (SWISSto12, Switzerland); Renaud Loison (IETR & INSA, France)

Enhancing the scanning capabilities of phased arrays and eliminating grating lobes requires small periodicities and large array dimensions. This paper proposes an efficient simulation methodology that leverages 90 ◦ symmetry and the even/odd technique to reduce computational costs. Validated on a small array and applied to a larger one with a wider field of view, the method effectively decreases simulation time by reducing the number of required elements, enabling the full-wave analysis of larger structures.

17:15 Optimized Ridge Air-Filled Substrate-Integrated Waveguides for Beyond-5G Antenna Array Systems

Sofie Lenders (Ghent University, Belgium); Samuel Rimbaut and Bram Hoflack (Universiteit Gent, Belgium); Sam Lemey (Ghent University-imec, Belgium); Hendrik Rogier (Ghent University, Belgium)

A design strategy is proposed to optimize ridge air-filled substrate-integrated-waveguides (RAFSIWs), reconciling conflicting low-loss and miniaturization requirements arising for antenna array feeding structures operating at new 6G frequencies. Through comprehensive parameter analyses, effects of the ridge dimensions on the waveguide's width miniaturization and efficiency are delineated, leading to general guidelines for identifying pareto-optimal RAFSIW cross-sections. To demonstrate, such a pareto-optimal RAFSIW is designed for operation in the 5G n257 band (26.5-29.5 GHz), including transitions to GCPW. The design is prototyped and characterized, showcasing a 1.42dB insertion loss for a 15mm length and a fractional -10dB-impedance bandwidth exceeding 30%. A width miniaturization of 63% compared to the conventional AFSIW is obtained, facilitating grating-lobe-free scanning angles of 90° over the entire n257 band, when applying this waveguide in antenna array feeding networks. Hence, the proposed RAFSIW paves the way for miniaturized low-loss millimeter-wave components to realize high-efficiency beyond-5G antenna array systems.

17:35 Phase Optimization for Transmission-Type Varactor-Based Tunable Attenuators

Yuan Yuan (The University of Adelaide, Australia); Shengjian Jammy Chen (Flinders University, Australia & The University of Adelaide, Australia); Christophe Fumeaux (University of Queensland, Australia)

A transmission-type varactor-based tunable attenuator with improved phase variation characteristics is presented. The attenuator is based on a standard 50 Ω microstrip transmission line with 9 identical varactor-loaded stubs. These stubs are equally grouped into three blocks, each with its independent DC controller. By contrast, the original attenuator has identical structure however with just one bias voltage control applied to the 9 stubs. Both attenuators can achieve a continuously tunable attenuation level up to 30 dB. By optimizing the DC bias for each subgroup of the proposed 3-block design, the phase variation across the attenuation range is predicted to be significantly reduced to 28.3 degree, from 63.2 degree of the original design. The measured results show a reasonable agreement with simulations, which demonstrate a compact transmission-type attenuator with large dynamic attenuation level, low reflection and small phase variation. The proposed tunable attenuator is suitable for seamless planar microwave circuit integration.

17:55 Ultra-Wideband Vertically Polarized Circular Array for Passive Sensing Applications

Gengming Wei and Yi He (University of Technology Sydney (UTS), Australia); Richard W Ziolkowski (University of Arizona, USA); Y. Jay Guo (University of Technology Sydney, Australia)

We present an ultra-wideband (UWB) vertically polarized long-slot circular phased array with a compact design for passive sensing applications. Unlike conventional tightly coupled cylindrical systems that require multiple circular arrays, our quasi-magnetic current sheet array uses a single circular array while achieving similar radiated field properties. A 16-element prototype demonstrates azimuthally invariant radiation capabilities. Measurements indicate that the array offers wide impedance bandwidth, high cross-polarization discrimination (XPD), and significant compactness. In its omnidirectional mode, the array achieves a 107.07% bandwidth (VSWR ≤ 2.0) with XPD better than 19.5 dB. In its directional mode, it operates over 100% bandwidth with XPD better than 20.9 dB. The prototype also exhibits excellent azimuthal out-of-roundness (better than 1.3 dB in its omnidirectional mode) and scan-invariant radiation with a maximum deviation of only 0.8 dB in its directional mode.

Room: Kildal (A2) | **A05b - Optical, THz and subTHz antennas**

T02 Millimetre wave and THz for terrestrial networks (5G/6G) / / Antennas

Chairs: Nuria LLombart (Delft University of Technology, The Netherlands), Takashi Tomura (Tokyo Institute of Technology, Japan)

16:15 Omnidirectional Reflector Antenna Using TE01 Mode Converter at 300 GHz

Shunta Ichikawa (DKK Co., Ltd., Japan); Keisuke Sato (Denki Kogyo co., Ltd., Japan); Katsumori Sasaki and Ichiro Oshima (Denki Kogyo Co., Ltd., Japan)

In this study, a horizontally polarized omnidirectional antenna at sub-THz band for 6G was developed. The antenna was designed for sub-THz band propagation experiments using an electromagnetic field simulator. It consisted of a circular horn antenna, TE10-TE01 mode converter, and parabolic reflector and was evaluated with a prototype. The proposed antenna realized a VSWR of <2 and a directivity deviation of <4 dB in range of 290 to 330 GHz.

MONDAY

16:35 Silicon-Micromachined High-Gain Multi-Beam Beam-Steering THz Graded-Index Lens Antenna Enabled by a Passive Beamforming Interposer

Alireza Madannejad, Mohammad Mehrabi Gohari and Joachim Oberhammer (KTH Royal Institute of Technology, Sweden)
This paper presents, for the first time, a novel high-gain beam-steering lens antenna operating in the 610 to 645 GHz range. The antenna, fabricated using silicon micromachining, is based on incorporating a Fresnel lens layer in combination with a frequency-dependent graded-index interposer that acts as a passive beamformer. Frequencydependent narrow beams are generated using an open waveguide feed. The prototype implemented in this paper features the generation of 8 frequency-dependent narrow beams with just two open waveguide feeds. These beams can be steered from -30° to 2° in the azimuth. The prototype achieves a measured realized gain of 32.1 dBi with low beam-steering losses of just 0.8 dB. The antenna also exhibits a high radiation efficiency of -1.25 dB. The lens antenna is very compact, measuring only 15.8 mm × 15.8 mm × 0.526 mm. This beam-steering antenna offers a promising solution for future high-gain, multi-beam THz communication systems.

16:55 Low-Profile Horn Antenna Array in Groove Gap Waveguide Technology with Glide Symmetrical Holes for 100 GHz Applications

Sebastian Diaz-Beiza (Universidad Carlos III de Madrid, Spain); Eva Rajo-Iglesias and Jose-Luis Vazquez-Roy (University Carlos III of Madrid, Spain)
This paper presents the design of an 8x8 low-profile horn antenna array operating at 100 GHz. The array is optimized for aperture efficiency and implemented using groove gap waveguide technology with glide-symmetric holes to reduce manufacturing complexity and prevent leakage. The array is built in three layers and assembled with screws, eliminating the need for strict electrical contact. The 8x8 array antenna achieves an aperture efficiency exceeding 93%, providing a directivity over 33 dBi, while maintaining sidelobe levels (SLL) below -20 dB in H-plane thanks to a non uniform excitation.

17:15 Off-Chip Double U-Shaped Slot Patch Antenna for H-Band Applications

Felix-Christopher Lutz (Technische Universität Berlin, Germany); Bersant Gashi (Fraunhofer IAF, Germany); Wilhelm Keusgen (Technische Universität Berlin, Germany)
An innovation planar single layer off-chip antenna for the use in broadband communication and sensing applications in the 220 GHz to 330 GHz frequency range is presented. The antenna employs the use of double U-shaped slots as loading for a rectangular patch to introduce coupled resonances, leading to a broadband radiation characteristic. As an off-chip design low permittivity substrates such as fused silica can be used, ensuring good radiation characteristics. An impedance transformer is added to the microstrip antenna feed line allowing to match a 50 ohm bondwire connection to the 65 ohm antenna input impedance, satisfying the condition of a reflection coefficient of less than -10 dB over the whole H-Band. Simulation and measurement show good accordance, with the antenna having a peak gain of 6.2 dBi at the centre frequency of 300 GHz. In the measurements a bandwidth of at least 13.3 % is achieved.

17:35 Design of a High-Gain Single-Feed Quad-Beam Metalens with Polarization Conversion at 0.1 THz

Xuekang Liu, Daniel R. Prado, Claudio Paoloni and Rosa Letizia (Lancaster University, United Kingdom); Lu Zhang (Swansea University, United Kingdom); Benito Sanz-Izquierdo (University of Kent, United Kingdom); Steven Shichang Gao (Chinese University of Hong Kong, China); Lei Wang (Lancaster University, United Kingdom)
This paper presents a novel 2-bit single-feed quad-beam metalens antenna for sub-THz links powered by traveling wave tubes. The metalens surface, consisting of 7692 unit cells with orthogonal slots and vias, allows precise electromagnetic wave manipulation by adjusting slot lengths to control the transmission phase. Rotating the lowerlayer slots in opposite directions creates a stable 180° phase difference, providing over 530° phase coverage. The design is fed by a custom pyramid horn with a WR-10 waveguide interface, optimized for single-unit fabrication. The superposition method was used to achieve the required phase distribution, generating four beams at φ = (0°, 90°, 180°, 270°) and θ = 15°, with a peak gain of 32.1 dBi at 105 GHz and all beams above 30.5 dBi within 102-109.5 GHz. This high-performance metalens offers a promising solution for future 6G high-capacity links.

17:55 Symmetrical 1:4 Power Divider with Out-Of-Phase Outputs Using Gapwave Guide Pins and Coupling Ridge with Iris at D-Band

Usman Shehryar and Jian Yang (Chalmers University of Technology, Sweden); Ahmed A Kishk (Concordia University, Canada); Ashraf Uz Zaman (Chalmers University of Technology, Sweden)
Paper presents a novel 1 to 4 power divider design, implemented using gap waveguide technology for equal power splitting with half out-of-phase outputs and half in-phase outputs. The design incorporates E-plane and Hplane Tees for power division. A coupling ridge and inductive iris formed by gap waveguide pins ensure efficient coupling and impedance matching, eliminating the need for traditional multi-section impedance transformers. The device operates across the 135-155 GHz band with a reflection coefficient below -15 dB, and low insertion loss of 0.05 dB. The phase imbalance is negligible (0.0005°) with equal power division of -6 dB on each of 4-ports. The simulated power divider will be incorporated and tested within high gain array's feeding network in the 140-150 GHz range. The approach to use pins for tuning and inductive iris, for matching and power splitting, ensures precise phase control, low insertion loss, and optimal impedance matching with compact size.

16:15 A Forward-Backward Matrix Pencil and Variable Projection Based Method for Reducing the Number of Elements in Shaped-Beam Pattern Linear Arrays

Ramonika Sengupta (Eindhoven University of Technology, The Netherlands); Annie Cuyt (University of Stirling, Scotland, UK); David S Prinsloo (ASTRON & Netherlands Institute for Radio Astronomy, The Netherlands); Thomas Schäfer (Satcube, Sweden); A. B. (Bart) Smolders (Eindhoven University of Technology, The Netherlands)

This paper presents a variable projection based method, used along with the forward-backward matrix pencil method, for the synthesis of linear arrays with shaped-beam patterns employing a least number of antenna elements. The forward-backward matrix pencil method has been used previously for this application. However, the array factor obtained using fewer elements may not always provide a satisfactory approximation of the true array factor, as demonstrated by some examples in this work. Therefore, we propose incorporating a variable projection iterative step to enhance the performance of the array derived from the forward-backward matrix pencil method.

16:35 Analytical Model of Parallel Plate Waveguide Feeding Structure for Connected Array Designs

Caspar M Coco Martin and Daniele Cavallo (Delft University of Technology, The Netherlands)

Connected slots are suitable elements in phased array designs to achieve ultra-wide bandwidth and wide-scanning properties. The slots can be conveniently fed by parallel plate waveguides (PPWs) to reduce the complexity of the unit cell. However, existing analytical models used for the array design cannot account for the PPW feed, which typically requires a lengthy design process with commercial antenna simulators. Here, we develop an equivalent circuit model for the PPW that includes the reactive components associated with the feed. The proposed feed model can be used in combination with the existing array model for optimization of the array unit cell together with the detailed feed structure.

16:55 Co-Simulation Methodology for the Study of Active Electronically Scanned Arrays (AESA)

Jeremy Michel (Limoges University, France & Thales Land Air Systems France, France); Cyrille Menudier (XLIM Université de Limoges, France); Guillaume Neveux (University of Limoges, France); Marc Thevenot (XLIM-UMR CNRS 7252, University of Limoges, France); Michel Stanislawiak, Faycel Fezai and Damien Pithon (Thales LAS France, France)

This paper presents an efficient simulation methodology for large active antennas derived from commercial softwares. Due to important challenges in optimizing the SWaP-C (Size, Weight, Power and Cost) for the new Radar generation, it is especially necessary to consider the nonlinearities of amplifiers and the impact of variations of the active reflection coefficients at the antenna level. In this contribution, the proposed methodolody allows for the calculation of voltages and currents in each active chain and the total radiated field. The chosen example to demonstrate the interest of this approach is an active antenna composed of 228 high power amplifiers (HPA) connected to a multilayer PCB with microstrip patches and a parasitic superstrate to improve scanning performances. This study helps to define the most suited architecture to improve the SWaP-C of Radar application.

17:15 Multipolar FFT-Based Adjoint Optimization for Designing Goal-Oriented Materials with Metallic Insertions

Jorge Cabrera (Universitat Politecnica de Valencia, Spain); Felipe Vico (Universidad Politécnica de Valencia, Spain); Eva Antonino-Daviu and Miguel Ferrando-Bataller (Universitat Politècnica de València, Spain)

In this paper, we present a fast and efficient al- gorithm for optimizing the orientation of dipoles centered in a 3D equispaced array. By using appropriate goal functions, the method enables the design of lenses with focal points at varying distances. The approach combines several numerical tools, including the Fast Fourier Transform (FFT), multipolar expansion, the quasi-Newton method (BFGS), and the adjoint method, to achieve the optimization objectives. The algorithm is capable of handling problems with a large number of degrees of freedom and diverse goal functions. In each iteration, it performs a full-wave electromagnetic simulation to compute the cost function for the current dipole orientations and calculates the gradient to guide the optimization toward improvement.

17:35 Q-Factor and Bandwidth for Multi-Port Antennas

Vojtech Neuman, Miloslav Capek and Lukas Jelinek (Czech Technical University in Prague, Czech Republic)

This paper proposes a derivation of the Q-factor valid for multi-port antennas and being inversely proportional to fractional bandwidth. The method is based on the second derivative of total efficiency and can be expanded for more general cases, such as adding dissipation losses into the system. It is shown that the new formula coincides with results known for single-port antennas. A simple case of two parallel dipoles demonstrates the most salient features of the proposed theory.

MONDAY

17:55 Revisiting Embedded Element Efficiency in Dense Arrays: Embedded Element Patterns for Enhanced Radiation Performance

Yanwen Chen and Stefano Maci (University of Siena, Italy)
Dense array antennas play a critical role in modern wireless systems, offering more degrees of freedom and greater beamforming potential. However, closely spaced elements in these arrays experience significant mutual coupling, which imposes intrinsic limits on radiation efficiency. This paper revisits the embedded element pattern (EEP) and its impact on embedded element efficiency (EEE) in dense arrays. We demonstrate that the conventional assumption of a cosineshaped EEP does not always hold for dense arrays, necessitating a re-evaluation of the efficiency limits. Through numerical simulations, we analyzed the performance of four cases of dense arrays with sub-half-wavelength element spacing. Our findings reveal that wider EEPs correspond to improved EEE, providing new insights into optimizing dense array designs.

Room: Björk (33)

Scientific Workshop

SW2b - Measurement Advancements for 5G/6G and Emerging Wireless Standards: Innovations, Precision and Standardisation (IET Workshop)

Room: Bergman (34)

E06 - Imaging

T05 Positioning, localization, identification & tracking / / Electromagnetics

Chairs: Stephen Pistorius (University of Manitoba, Canada), Daniel Sjöberg (Lund University, Sweden)

16:15 Robust Calibration for Enhanced Imaging in Near-Field D-Band MIMO Radar Systems

Lorena María Pérez-Eijo (Universidade de Vigo, Spain); Marcos Arias and Borja Gonzalez-Valdes (University of Vigo, Spain); Jose Vazquez Cabo (Universidade de Vigo, Spain); Ignacio Sardinero-Meirás (Information Processing and Telecommunications Center, Universidad Politécnica de Madrid, Spain); Jesús Grajal (Universidad Politécnica de Madrid, Spain)
This work introduces a calibration algorithm designed to improve high-precision imaging in real-time MIMO radar systems. The algorithm applies the Inverse Fourier Transform (IFFT) and advanced signal processing techniques to efficiently extract and process key data from raw measurements, focusing on critical Regions Of Interest (ROI) while filtering out unnecessary information. A robust phase correction mechanism ensures precise calibration and alignment, preventing phase errors that could otherwise lower image quality. The algorithm provides an effective balance between computational efficiency and the high accuracy required by modern MIMO radars, paving the way for further improvements in real-time imaging.

16:35 Microwave Reconstruction of Fabrication Defects in Known Objects Using Scattering Parameter Sensitivities

Alexandros Pallaris and Daniel Sjöberg (Lund University, Sweden)
This paper investigates the detection of permittivity defects in a fabricated, known object, motivated by a desire to detect errors in additively manufactured objects that may affect their electromagnetic performance. We use scattering parameter sensitivities to reconstruct the relative permittivity of a generic 2D object from microwave scattering measurements and a known reference model. To find guidelines for the implementation of a future measurement system, this reconstruction was done using different parameters such as number of antennas used, frequencies, and bandwidth. The effect of bandwidth on the limits of the reconstruction's spatial resolution was investigated, showing a resolution of approximately one tenth of a wavelength, which improves with increased bandwidth.

16:55 Real-Time Road Surface Identification Using Ultrasound, Microwave and Sub-THz Radar

Aleksandr Bystrov, Fatemeh Norouzian and Mikhail Cherniakov (University of Birmingham, United Kingdom); Marina S. Gashinova (University of Birmngham, United Kingdom)
This paper investigates the use of sonar and radar-based sensors for real-time road surface recognition in automotive systems, with the goal of improving road safety. The study demonstrates that statistical analysis of backscattered signals from actual road surfaces, when enhanced by machine learning, can significantly improve the accuracy of surface type classification. The research also shows that fusing data from multiple sensors and increasing radar signal frequency further improve classification accuracy, with an 8% to 12% increase in recognition observed in our experimental data. These findings lay a strong foundation for the development of advanced automotive systems capable of accurately recognizing road surfaces in real time during vehicle motion.

MONDAY

17:15 Distorted Iterative Step-Wise Approach for Plasma Microwave Imaging Profiling

Shaimaa Elghetany (Demostrator, Egypt); Maria Antonia Maisto and Raffaele Solimene (Università degli studi della Campania Luigi Vanvitelli, Italy); Gino Sorbello and Loreto Di Donato (University of Catania, Italy)

The inverse scattering problem (ISP) at hand involves reconstructing the dielectric profile of a slab through single-view multi-frequency scattered field data. This problem, also known as dielectric profiling, is non-linear and ill-posed. The proposed iterative method exploits both transmitted and reflected scattered field measurements and updating of the Green function and the background field at each iteration. The results shows that the proposed iterative technique is considered to be a prominent quantitative reconstruction algorithm for addressing profiling for a class of lossless plasma profiles, which cannot be reconstructed via state-of-the-art available model-based inversion approaches.

17:35 Impact of the Measurement Setup and Unknowns Modelling for Phaseless Imaging Based on Multi-Plane Acquisition

Alejandro del Hoyo Vijande (Universidad de Oviedo, Spain); Yuri Alvarez-Lopez (University of Oviedo, Spain); Jaime Laviada (Universidad de Oviedo, Spain); Fernando Las-Heras (University of Oviedo, Spain)

Phaseless imaging based on multi-plane acquisition has a high dependence on a large number of parameters such as the plane extension, sampling step, choice of basis functions, number of unknowns, etc. This contribution analyzes the parameters with highest impact in the final imaging result. For this purpose, several targets with a difference balance between metallic and empty parts have been measured on large surfaces with a high sampling density. After that, multiple configurations have been emulated to assess the impact of the different parameters.

17:55 Effective Time-Domain and Frequency-Domain Terahertz Imaging Techniques for the Analysis of Metal-Dielectric Multilayered Structures

Walter Fuscaldo (Consiglio Nazionale delle Ricerche (CNR), Italy); Tiziana Ritacco (Consiglio Nazionale delle Ricerche, Italy); Dimitrios Zografopoulos (CNR-IMM, Italy)

Terahertz imaging techniques via time-domain spectroscopy in reflection mode is typically based on the time-domain analysis of the peak-to-peak amplitude of the signal or its energy. In the frequency domain, one usually exploits the absorption frequencies of the materials employed. In this work, we show how these techniques fail in imaging (in a spectroscopic approach) a multilayered structure consisting of a metallic pattern embedded between two nominally identical lossy dielectric layers. For this purpose, alternative imaging techniques are here proposed by exploiting a simple ray-optics analysis and a Fabry–Perot interpretation of the electromagnetic interaction between the transmitted THz beam and the metal-dielectric structure.

Room: Felsen (35+36)

A24b - Antennas for sensing II

T04 RF sensing for automotive, security, IoT, and other applications / / Antennas

Chairs: Pilar Castillo-Tapia (KTH Royal Institute of Technology, Sweden), Susanne Hipp (OTH Regensburg, Germany)

16:15 A Wideband WiFi/NB-IoT On-Glass Antenna for Smart Building Applications

Muhammad Uzair (King Mongkuts University of Technology North Bangkok, Thailand); Juin Acharjee (NSHM Knowledge CAMPUS DURGAPUR, India); Akkarat Boonpoonga (KMUTNB, Thailand); Dirk Heberling (RWTH Aachen University, Germany); Suramate Chalermwisutkul (King Mongkut's University of Technology North Bangkok & The Sirindhorn International Thai-German Graduate School of Engineering, Thailand)

In this work, an on-glass antenna is proposed for IoT and smart building applications. The dielectric properties of five common glass types used in architecture were investigated. Clear glass, 3 mm thick, was selected as the substrate. The antenna is a rectangular monopole with a coplanar waveguide feed and an asymmetric ground. It was designed and simulated using Ansys HFSS, then fabricated using clear glass and copper tape. Measurements of the reflection coefficient and radiation pattern showed good agreement with simulations. The antenna exhibits a bidirectional radiation pattern, with gains of 2.8 dBi at 2.1 GHz and 3.9 dBi at 2.4 GHz. A -10 dB bandwidth of 650 MHz (29.3%) centered at 2.215 GHz was achieved. The proposed antenna shows promise for integration with architectural glass elements in smart building applications, such as smart glass doors and windows.

16:35 Enhancing IoT Network Reliability Through Antenna Diversity in Real-World Scenarios

Marco Niederberger, Yanick Schoch and Michel A Nyffenegger (OST Eastern Switzerland University of Applied Sciences Rapperswil, Switzerland); Christian Gwerder (Steinel Solutions AG, Switzerland); Hans-Dieter Lang (OST Eastern Switzerland University of Applied Sciences Rapperswil & ICOM Institute for Communication Systems, Switzerland)

Antenna diversity in Internet of Things (IoT) devices is explored to address challenges associated with fixed device orientation and interference from nearby metallic objects, which can degrade wireless network performance. Integrating multiple antennas with different polarizations can significantly enhance signal quality and network reliability. Experiments demonstrated significant improvements in link quality, with gains exceeding 30 dB in received signal strength for specific scenarios. Already the addition of a second PCB-based antenna alone, resulted in a 17 dB improvement. These findings suggest that the added complexity in hardware and software to incorporate antenna diversity could well be justified by the resulting enhancements in network stability for real-world applications.

16:55 Experimental Validation of a Full Polarimetric Channel Model with Frequency-Dependent Antenna Gain for Polarization Diversity Studies

Franziska Rasp (Graz University of Technology & Continental Automotive Technologies Regensburg, OTH Regensburg, Austria); Burak Sahinbas and Thomas Reisinger (Continental Automotive, Germany); Susanne Hipp (OTH Regensburg, Germany); Erich Leitgeb (Graz University of Technology, Austria)

Autonomous driving, child presence detection, and digital car keys rely on precise localization. Therefore, accurate simulation environments are essential for designing radio systems and optimizing their positioning algorithms. A critical aspect of developing a reliable localization system is modeling the physical radio channel, which includes the transmitting antenna, the propagation medium, and the receiving antenna. However, existing channel models often overlook important physical effects of antennas, such as frequency dependence and polarization, leading to discrepancies between simulations and real-world measurements. To address this, the paper enhances full polarimetric channel models by incorporating the frequency dependence of both antennas and propagation channels. The theoretical model is validated through Vector Network Analyzer channel sounding measurements using reference antennas. This approach provides a foundation for polarization-based post-processing, ultimately improving positioning accuracy.

17:15 High-Efficiency Waveguide Antenna with Low-Cost Materials for Radar Sensors in LRR and SRR Band

Nataliia Lupyna, Andreas Bettray, Markus Krengel, Aline Friedrich and Oliver Litschke (IMST GmbH, Germany)

This paper presents a novel antenna structure developed for operation in the 77 GHz frequency range. The proposed structure integrates an air waveguide in low cost materials such as FR4. The transmission takes place in the air and the waveguide walls are implemented with an electromagnetic band gap (EBG) structure in the printed circuit board (PCB). This new waveguide technology is used to design a slotted waveguide array. The design is optimized in terms of radiation pattern and directivity. In addition, the proposed slot antenna is modified to avoid diagonal side lobes in the 3D pattern, which is a common problem in non-uniform slot antennas. The proposed structure outperforms existing antenna technologies and opens new perspectives for the development of highly efficient antenna systems in the millimeter-wave range.

17:35 Design of an Integrated Chopper in SiGe BiCMOS for Passive Dual-Polarized Terahertz Imaging

Martijn Hoogelander, Nuria LLombart, Marco Spirito and Maria Alonso-delPino (Delft University of Technology, The Netherlands)

This paper presents a solid-state chopping solution integrated in 130nm SiGe BiCMOS for passive dual-polarized terahertz imagers. The chopper consists of an array of sub-wavelength metal patches loaded with varactors, which in turn are implemented using RFNMOS devices. By switching the gate voltage of the RFNMOS devices between 0V and 1V, the transmittivity of the chopper can be changed, hereby realizing a chopping operation. The design operates from 300GHz to 500GHz and adds only 2dB to 3dB of losses. The proposed design permits the chopping rates needed to suppress the flicker noise in solid-state detectors. With respect to classical solutions such as chopping wheels or Dicke switches, the proposed design enables the design of a terahertz imaging system that is compact, wideband and has a high spatial resolution.

17:55 C-Slotted Patch Filter Antenna with Triple Notches for Enhanced Wi-Fi Performance

Yasmine Dahmani (Apside, France); Francis Keshmiri (Huawei Technologies, France)

This paper presents a low-cost passive patch antenna with filtering capabilities for Wi-Fi applications. The antenna achieves a realized gain of over 5 dBi across all channels in the 5 GHz band. It incorporates a three-pole rejection mechanism with etched C-shaped slots on the same patch radiator. The resulting filter antenna demonstrates radiation nulls and effective band rejections in coexisting Wi-Fi bands, significantly reducing interference. Specifically, a gain reduction of at least 20 dB is achieved at critical coexisting WiFi frequencies: 4.9 GHz (closest 5G licensed band), 5.4 GHz (UNII-2B), and 5.9 GHz (CV2X).

Room: Schelkunoff (C1) — E04b - Optimisation methods and machine learning I

T07 Electromagnetic modelling and simulation tools / / Electromagnetics

Chairs: Harald Hultin (KTH Royal Institute of Technology & Saab AB, Sweden), Marcello Zucchi (Politecnico di Torino, Italy)

16:15 Modified Oracles for Quantum Selection Applied to Electromagnetic Problems

Gabriel Felipe Martinez, Alessandro Niccolai and Riccardo Enrico Zich (Politecnico di Milano, Italy)

The emergence of quantum computing has brought with it multiple applications like hybrid classic-quantum evolutionary optimization algorithms. In electromagnetics, optimization has always been present to increase the performance of complex systems. This paper presents two new oracles for the genetic algorithm with quantum selection and its newer version that uses simulated binary crossover. These algorithms are applied to two common electromagnetic optimization problems showing strong results and demonstrating the flexibility that these hybrid algorithms have by making small changes to their quantum circuits.

MONDAY

16:35 Topology Optimization of Electromagnetic 2D Structures for Antennas

Johann Brandmeier, Michael Ponschab and Philipp Gentner (Ericsson Antenna Technology Germany GmbH, Germany)
The growing demand for high-performance antennas requires a fast and efficient development of radio frequency components. Manually pushing the performance to the limit is time-consuming, and conventional optimization approaches with parameter sizing are rigid and need more flexibility. The study investigates the potential of topology optimization (TO) in radio frequency component development - a technique primarily applied in mechanics. Four different optimization algorithms are compared. They are a genetic algorithm, particle swarm optimization, a surrogate model based optimizer working with deep neural networks, and a newly developed population-based optimizer that leverages electromagnetic field strengths. Additionally, two TO approaches are tested - i.e. a fragment/pixel-based method and a normalized Gaussian network. The algorithms and approaches are compared to each other and to a benchmark structure. The test object used for the investigations is a frequency-selective surface. The genetic algorithm combined with the pixel-based approach demonstrated the fastest convergence and best performance.

16:55 Fast Quantum-Inspired Algorithm for Beamforming

Yutong Jiang (ZheJiang University, China); Shuai S. A. Yuan, Hangyu Ge and Wei E. I. Sha (Zhejiang University, China)
This paper presents a fast quantum-inspired algorithm to tackle the NP-hard beamforming problem in MIMO arrays. The proposed method achieves high-bit phase optimization with over a 1000-fold speedup compared to genetic algorithms while maintaining near-ground-state solutions. Tests on various array sizes demonstrate the algorithm's scalability, stability, and near real-time performance for small-size arrays, confirming its potential for large-scale electromagnetic optimization.

17:15 Capacity-Driven Smart Skin Loads Selection Utilizing KNN and Gradient Boosting

Aleksandr D. Kuznetsov, Albert Salmi and Jari Holopainen (Aalto University, Finland); Ville Viikari (Aalto University & School of Electrical Engineering, Finland)
In this paper, we present a method for engineering loads terminated to smart skins across multiple operating angles using k-nearest neighbors (KNN) and gradient boosting (GB) regression algorithms. Modelling the smart skin as a multiport scattering structure loaded by the passive loads, we formulate requirements for the structure following the capacity-driven approach to smart radio environment design. The load selection process is framed as a regression task, addressed through the proposed machine learning algorithms. To validate the practicality of the method, we evaluate the performance of various regressors applied to a sample scatterer, demonstrating their effectiveness under different operational constraints.

17:35 Current-Based Design of Metasurface Antennas with Tensorial Surface Impedance

Lucia Teodorani, Marcello Zucchi and Giuseppe Vecchi (Politecnico di Torino, Italy)
In this paper, a current-based algorithm for the synthesis of metasurface antennas is adapted to deal with tensorial surface impedance. The surface current is obtained through the minimization of an objective function that takes into account all constraint related to a tensorial impedance. A non-linear conjugate gradient algorithm is applied to minimize an objective function that includes both realizability and far field requirements. The proposed surface impedance distribution is then implemented through a suitable choice of anisotropic unit cells, either through local optimization or from a database of precomputed shapes. Results are shown for the case of a circular metasurface antenna radiating a linearly-polarized broadside beam.

17:55 A Pruned Neural Network in Multi-Monostatic Inversion of Two-Dimensional Metallic Scatterers

Florindo Bevilacqua, Amedeo Capozzoli, Claudio Curcio and Angelo Liseno (Università di Napoli Federico II, Italy)
We consider the application of Neural Networks (NNs) to the case of multi-monostatic inversion of twodimensional metallic scatterers. The aim is twofold. First, we want to reconstruct the support of the involved objects from the scattering data. Second, we want to demonstrate a pruning process to reduce the NN complexity without a worsening of its performance. In particular, the NN result is compared to that achieved with the standard approach of reconstructing the reflection coefficient by a Truncated Singular Value Decomposition (TSVD) scheme. The approach is validated experimentally.

Room: Maxwell (C2) — M04 - Recent advances in near field measurements

T01 Sub-6 GHz for terrestrial networks (5G/6G) / / Measurements

Chairs: Antonio Cuccaro (Università della Calabria, Italy), Thomas F. Eibert (Technical University of Munich (TUM) & Chair of High-Frequency Engineering (HFT), Germany)

16:15 Efficient Data Reduction in Near-Field Measurements by an Improved Warping Greedy Method

Mario Del Prete (University of Campania Luigi Vanvitelli, Italy); Maria Antonia Maisto (Università degli studi della Campania Luigi Vanvitelli, Italy); Antonio Cuccaro (Università della Calabria, Italy); Raffaele Solimene (Università degli studi della Campania Luigi Vanvitelli, Italy)
In this paper, a fast greedy method for data reduction in near-field antenna testing is proposed. Starting from the recent Warping Driven Greedy Method, the execution times of the latter can be further improved by considering as the initial set of points of the iterative procedure, those of the measurement aperture that do not exceed the size of the antenna. A numerical example shows that the proposed approach has the same performance as the classical one but with a lower computation burden.

MONDAY

16:35 A Proposal of Near-Field Measurement System Using Software Defined Radio for 5G Antenna Pattern Measurement

Takuma Akada, Shu Takahashi and Kazuhiro Fujimori (Okayama University, Japan); Toshiyasu Tanaka (Microwave Factory Co., Ltd., Japan)

Although 5G has been in operation for several years, the 28 GHz band has not been widely used in most countries. One reason is that the measurement environment required for development is expensive, creating a high barrier to entry. Near-field measurements are widely used to evaluate antenna patterns because they do not require a large anechoic chamber. However, it is expected that future mobile terminals and antenna systems will not have RF connectors and cannot be directly connected to a measurement instrument. Such devices require over-the-air (OTA) measurements, which are difficult to perform using conventional VNAs. In this study, we proposed a near-field measurement system using a software-defined radio (SDR) to perform OTA measurements at a lower cost and more conveniently than conventional methods. As a result, although some issues remain to be resolved, a way of realizing OTA antenna pattern measurement using an SDR has been confirmed.

16:55 Leveraging Near-Field Measurement Data to Enhance Digital Twin Accuracy

Shoaib Anwar (Microwave Vision Group, Satimo Industries, France); Evgueni Kaverine (MVG Industries, France); David Prestaux and Amazir Moknache (Ansys, France); Aurelien Lelievre (MVG Industries Technopole Best Iroise - Plouzane, France); Francesco Saccardi (Microwave Vision Italy, Italy); Nicolas Gross (MVG Industries, France); Lars Foged (Microwave Vision Italy, Italy)

This paper addresses the challenges of achieving high-fidelity digital twin models for electrically large structures, particularly in areas such as electromagnetic field scattering, antenna placement, electromagnetic compatibility, and coupling evaluations. The "Link" approach combines spherical near-field electromagnetic measurements with advanced post-processing techniques to produce a highly accurate digital twin of the radiating element. This digital twin can then be exported to any full-wave electromagnetic solver and integrated into large structures, such as the aircraft studied in this work. In this paper, we investigate and validate the accuracy of this approach by comparing the digital twin model derived from measurements to a full-wave simulation of the same antenna element using the Ansys HFSS solver. The radiation patterns, with the antenna placed in various positions on the electrically large aircraft, closely matched, confirming the effectiveness of the "Link" approach.

17:15 Radar-Based Tomographic Imaging of Inhomogeneous Structures with Filtered Backprojection Algorithm

Irwin Barengolts, Ali Al-Tayar, Manuel Funk and Kristof Dausien (Ruhr University Bochum, Germany); Dennis Pohle, Christian Schulz, Ilona Rolfes and Jan Barowski (Ruhr-Universität Bochum, Germany)

In this contribution a tomographic imaging system using a broadband frequency modulated continuous wave (FMCW) radar system operating from 126-182 GHz is presented. The system consists of two parabolic mirrors to focus the beam and investigate objects in the area of the focal point. Moreover, the setup is based on the parallel-beam geometry, containing multiple electrical translation stages and a turntable to measure from various positions and angles. The tomographic reconstruction follows a monostatic approach, analyzing reflections from a metallic plate in terms of attenuation and time shift caused by the object itself. A 3D-printed cylinder made of polylactic acid (PLA) with an eccentrically arranged hole was used to investigate the utilization of the reconstruction algorithm on inhomogeneous objects. The image processing is based on the filtered backprojection algorithm, which is mainly used for computed tomography (CT). The results show promising potential and provide the basis for further investigations.

17:35 An Automatic Focusing Technique for Inverse Source Reconstructions Based Near-Field Passive Radar Imaging

Quanfeng Wang (Technical University of Munich, Germany); Thomas F. Eibert (Technical University of Munich (TUM) & Chair of High-Frequency Engineering (HFT), Germany)

An autofocusing phase correction method for 3D near-field (NF) passive radar imaging is presented for scenarios where the direct signal is absent. Phase shifts caused by delays from measurement instrumentation and spatial propagation are compensated separately. A single-frequency inverse source solver is used to reconstruct spectral representations of equivalent surface sources for the targets of interest (TOIs) from the captured scattering fields in NF measurements. These equivalent sources are then used to generate single-frequency images, from which the phase information of the induced sources is extracted for phase correction and source localization. Normalizing the induced sources within the target region to a specific, though arbitrary reference source, compensates for the spatially invariant part of the phase shifts. Additionally, analyzing the time-domain signals of the normalized induced sources provides the time differences of arrival (TDoA) from the Tx to different anchors, enabling Tx source localization and spatially varying phase shifts correction.

17:55 Radiation Pattern Modulation Impact on Turntable Near-Field ISAR Images

Lorenzo Ciorba (University of Bern & Institute of Applied Physics, Switzerland); Tobias Plüss, Gunter Stober and Axel Murk (University of Bern, Switzerland)

The impact of the antenna radiation pattern on the quality of inverse synthetic aperture radar (ISAR) images is investigated for turntable near-field (NF) measurements. In particular, radar data are synthetically produced for a circular scan using a uniform and tapered illumination. From these radar data, ISAR images are produced using a NF processing including a compensation for path loss and the non-planar phase front of the incident wave. Results using a standard far-field (FF) ISAR processing are also reported. The produced ISAR images are compared in terms of different quality metrics, i.e., image entropy, contrast and energy. Finally, the radar cross section (RCS) of the target is extracted from the ISAR images and compared to a reference one.

MONDAY

Chairs: Luis M. Pessoa (INESC TEC & Faculty of Engineering, University of Porto, Portugal), Paola Pirinoli (Politecnico di Torino, Italy)

16:15 A mmWave Polarization-Dependent Simultaneously Transmitting and Reflecting Reconfigurable Intelligent Surface Based on a Novel Independent 1-Bit Phase-Agile Unit Cell

Bing-Jia Chen (Academia Sinica, Taiwan); Yun-Ting Tsai and Shih-Yuan Chen (National Taiwan University, Taiwan)

To overcome the main limitation of conventional reconfigurable intelligent surfaces (RISs), simultaneously transmitting and reflecting reconfigurable intelligent surface (STAR-RIS) can extend the coverage of signals to its backside to provide a more comprehensive service from all directions. This paper combines the design concepts of transmitarray and reflectarray and proposes a novel unit cell of STAR-RIS. The measured reflection loss and transmission loss are 0.43 dB and 1.26 dB, respectively. The ability to achieve independent 1-bit reconfigurability for the reflection and transmission phases is validated. A Ka-band 20x20 STAR-RIS is realized. The sidelobe levels are both lower than -10 dB for transmitting and reflecting beams. These results demonstrate the feasibility of the STAR-RIS based on the proposed 1-bit phase-agile unit cell in mmWave applications.

16:35 Transparent Smart Electromagnetic Skins for Outdoor to Indoor Communications

Michele Beccaria, Pio F. Lupinacci, Andrea Massaccesi and Paola Pirinoli (Politecnico di Torino, Italy)

In this communication, preliminary results on the design of a passive, transparent, Smart Electromagnetic Skin (SES) for outdoor-to-indoor (O2I) communications are presented. Contrary to what is already available in literature, here a dielectric-only configuration is proposed, in order to avoid the presence of metallizations that can reduce the transparency. Moreover, a glass layer is directly introduced in the unit cell, to take into account the presence of the window. Different configurations have been designed and numerically analyzed: the obtained results demonstrate the feasibility of the proposed solution and its effectiveness.

16:55 A Reconfigurable Intelligent Surface for 3.6 GHz Based on a Double Squared Slot Shaped Element

Tiago E. S. Oliveira (Universidade de Vigo, Portugal & Instituto de Telecomunicações, Portugal); João Ricardo Reis (Instituto de Telecomunicações and Polytechnic Institute of Leiria, Portugal); Iñigo Cuiñas (University of Vigo, Spain); Rafael F. S. Caldeirinha (Polytechnic Institute of Leiria & Instituto de Telecomunicações, Portugal)

In this paper, a reconfigurable intelligent surface (RIS) designed to operate at 3.6 GHz featuring a double square unit cell layout, is presented. The unit cell includes two varactor diodes, enabling reconfigurable functionality. Two RIS configurations, with dimensions of 5 × 5 and 10 × 10, each employing the proposed unit cell, are studied. Simulation results demonstrate the reconfigurability of both configurations, effectively steering incident waves toward specified angles. The 5 × 5 RIS achieved an aperture efficiency of η = 42.7% at a reflection angle of 25 ◦ , highlighting the unit cell's effectiveness. To validate the design, a prototype of the 5 × 5 fabricated. Preliminary results obtained on the prototype yield to a scanning angle region of 20 ◦ with the best performance being achieved on the frequency range from 3.5 to 3.7 GHz.

17:15 Multi-Resonant Unit Cell for Efficient Smart Electromagnetic Skins

Shahid Ayaz, Michele Beccaria and Paola Pirinoli (Politecnico di Torino, Italy)

Recently, passive Smart Electromagnetic Skins (SESs) have gained popularity for their capability to enhance the performance of a communication system without increasing its complexity. Since the focus was initially on the design of the structure at the whole, less attention was paid to the effects that the unit cell used for discretizing the surface itself has on the SES performance, just making a distinction between the use of resonant or sub-wavelength elements. Conversely, in this communication a multi-resonant unit cell is introduced and some preliminary numerical results on its application to the design of a smart skin are shown: they confirm its effectiveness and capability to improve the performance of the SES in comparison with other unit cells.

17:35 1-Bit Reconfigurable Intelligent Surface Unit Cell Based on Non-Volatile Technology at D-Band

Mohamed Elsaid Ghatas (INESC TEC, Campus Da FEUP, Portugal & University of Porto, Portugal); Sanaâ Finich (University of Porto, Portugal); Henrique M Salgado (University of Porto & INESC Porto, Portugal); Luis M. Pessoa (INESC TEC & Faculty of Engineering, University of Porto, Portugal)

Research on Programmable Electromagnetic Surfaces has gained considerable attention as an enabling technology for 6G communications, particularly at millimeter-wave and sub-THz bands. However, RISs face challenges related to the need for high-performance reconfigurable techniques that offer compact size and reduced power consumption at high frequencies. Moreover, the experimental characterization of unit cell performance using a waveguide remains a challenging issue. This paper discusses the design and performance analysis of a 1-bit reconfigurable unit cell at the Dband using non-volatile reconfigurable technology. The efficiency analysis of the unit cell was performed using periodic boundary conditions and waveguide configurations to mitigate simulation risks and validate the proposed design at the unit cell level. All simulation configurations confirmed an operational bandwidth of 25.65 GHz across the 147.8-173.45 GHz range, with a reflection loss of less than 1 dB and a phase difference within 180° ± 20°.

MONDAY

17:55 On Transmissive RIS for mm-Waves Outdoor-To-Indoor Coverage Enhancement

Silvi Kodra, Simone Del Prete, Elena Bernardi, Enrico M. Vitucci, Marina Barbiroli, Franco Fuschini and Vittorio Degli-Esposti (University of Bologna, Italy)

This paper investigates the use of large Reconfigurable Intelligent Surfaces (RIS), also known as "Smart Skins", to improve outdoor-to-indoor millimetre-wave (mmWave) propagation, taking advantage of ventilation holes commonly found, or easily realizable, in European buildings. By using a transmissive, focusing RIS, the signal could be concentrated and routed through the opening, enhancing signal penetration into the indoor space even in modern, highly insulated buildings that particularly hinder signal penetration. Using Ray tracing simulations at 27 GHz we compare scenarios with and without RIS, demonstrating significant indoor signal coverage improvements in the first case. The study highlights the use of RIS - or smart-skins - as a cost-effective solution to address the challenges of mmWave propagation in modern building designs.

Room: Kraus (C4) — E09b - Metasurfaces I

T08 Fundamental research and emerging technologies/processes / / Electromagnetics

Chairs: Ariel Epstein (Technion - Israel Institute of Technology, Israel), Raúl Rodríguez-Berral (Universidad de Sevilla, Spain)

16:15 Cavity-Excited Impedance Surfaces for Full-Space Beam Steering

Minseok Kim (Hongik University, Korea (South))

This work proposes and validates a design framework for full-space beam steering, facilitated by two-dimensional impedance surfaces driven by cavity modes. The design integrates sources directly into the cavity, enabling a compact form factor. To efficiently synthesize the surfaces, we integrate the idea of baffles with an integral equation-based method. The baffles are carefully positioned within the cavity to suppress mutual coupling along one axis, while the integral equation formulation captures coupling effects along the other. We demonstrate the system's capabilities through multiple beam-steering scenarios, achieving directivity levels comparable to ideal apertures.

16:35 A Spray-On Reconfigurable Reflectarray Element Using Polymer Dispersed Liquid Crystal

Douglas A Bowe (The University of Sheffield, United Kingdom); Matthew MJ Davies, Benedict EG Davies, Jon R Willmott and Stephen Henthorn (University of Sheffield, United Kingdom)

A multilayer aerosol jet printed (AJP) tuneable metamaterial reflectarray structure capable of 1-bit phase control between 0° and 180° effects at 30GHz is designed and simulated. The reflectarray is tuned through the input of a DC stimulus to a biasing layer that alters the permittivity of a polymer dispersed liquid crystal (PDLC) layer. Integrated biasing layers close to the PDLC are designed to provide a biasing electric field at lower voltages and with minimal effects on element performance. Numerical modelling shows a tuning bandwidth of approximately 700MHz around 30GHz, allowing 180° phase change with loss of between 0.9dB and 3.4dB.

16:55 Impact of via Placement on Reflection Coefficient in Reflective Metasurfaces

Hang Yu and Rola Saad (The University of Sheffield, United Kingdom); Edward A. Ball (University of Sheffield, United Kingdom)

This paper investigates the impact of via placement on the reflection coefficient of a reflective patch metasurface, initially designed with resonate frequency of 4.59 GHz and a reflection magnitude of -3.7 dB. Simulations were conducted for 36 different via locations within the unit cell across a frequency range of 4.60 GHz to 4.72 GHz. The results show that specific via placements can significantly reduce the reflection magnitude, with reductions up to -35 dB at 4.60 GHz. At higher frequencies, the region of maximum absorption shifts within the unit cell. Increasing the number of vias per unit cell also shifts the resonant frequency, reaching approximately 6.25 GHz with four vias. Three Surfaces was fabricated and tested at the coordinates of interest. The findings offer insights into optimizing metasurface designs for improved control over reflection coefficient.

17:15 Elevation Tilt Synthesis with Huygens Passive Metasurfaces

Michela Longhi and Stefano Vellucci (Niccolò Cusano University, Italy); Mirko Barbuto, Alessio Monti, Filiberto Bilotti and Alessandro Toscano (Roma Tre University, Italy)

This paper explores the use of passive Huygens metasurfaces (HMS) to enhance antenna performance in nextgeneration wireless communication systems. These systems demand higher efficiency, reduced costs, and simplified infrastructure. In response, smart electromagnetic environments and metasurfaces have emerged as critical technologies, enabling dynamic signal rerouting, improved coverage, and reduced signal loss, especially in the mmWave spectrum. Here, we focus on the application of cylindrical HMS coatings on wire antennas to achieve beamsteering and directivity enhancement. Building on previous works, where phase insertion was modified on the H-plane, this paper extends the concept by applying a rigorous synthesis approach to the E-plane, enabling focusing and tilt capabilities. The proposed method leverages a refined phase-gradient metasurface design, addressing limitations in existing models such as angular response and wavefront superposition, to offer improved control over antenna radiation patterns. This approach has the potential to significantly improve the performance of future wireless communication systems.

MONDAY

17:35 An Accurate Surface Susceptibility Extraction Method for Physical Representation of Electromagnetic Metasurfaces

Jordan R. Dugan, Tom Smy and Shulabh Gupta (Carleton University, Canada)
Spatially dispersive, or nonlocal, metasurfaces are an important class of metasurfaces that can be characterized with angle dependent surface susceptibilities. These surfaces have potential applications in analog computing and space compression. Conventional metasurface characterization techniques fail on spatially dispersive metasurfaces as there are an infinite number of susceptibility representations that will produce the same macroscopic scattering response for a uniform surface. In this work, we propose an updated extraction method that will yield the correct susceptibility representation and demonstrate this method by extracting the susceptibilities of a dielectric slab.

17:55 Propagation of Electromagnetic Waves Along Cylindrical Metasurface Structure

Davorin Mikulic and Marko Bosiljevac (University of Zagreb, Croatia); Christophe Craeye (Université Catholique de Louvain, Belgium); Zvonimir Sipus (University of Zagreb, Croatia)
This paper explores the design of cylindrical leaky-wave metasurface antennas, addressing the need for antennas that conform to curved cylindrical surfaces. We introduce analytical tools for efficiently extracting the properties of electromagnetic waves propagating along cylindrical metasurfaces, enabling the suppression of curvature effects in the antenna design. A comprehensive design procedure is presented, along with a detailed design example and its corresponding simulation results. Our approach provides a fast and efficient method for designing cylindrical leakywave metasurface antennas, enabling the ability to radiate in the desired direction.

Room: Munch (23) — A09 - Multiband and multifunctional antennas

T01 Sub-6 GHz for terrestrial networks (5G/6G) / / Antennas

Chairs: Hendrik Rogier (Ghent University, Belgium), Ala Sharaiha (Université de Rennes & IETR, France)

16:15 3D-Printed Dual-Polarized Magneto-Electric Dipole Antenna with Wideband High Isolation for Full-Duplex Applications

Mehmet Ahad Yurtoglu and Ramez Askar (Fraunhofer HHI, Germany)
The paper introduces a novel dual-port dual-polarized magneto-electric dipole (MED) antenna with orthogonal Gamma and inverted-Gamma shape probes, which was fabricated by means of an additive 3D metal printing process. Electromagnetic wave simulation and RF measurement report a resonance bandwidth from 3 GHz to 4 GHz at both MED's ports with respect to a standing wave ratio of less than 2. The cross-polarization isolation (XPI) between the MED's ports was also measured to be greater than 50 dB across its entire resonance bandwidth. The paper also thoroughly examines the impact of misalignments in the polarization of the MED probes on the XPI level. The broadband resonance and excellent isolation between the MED ports make it a strong candidate for a full-duplex wireless transceiver in network infrastructure.

16:35 Triple-Band, Triple-Polarization Antenna for Multiple Satellite Applications

Azat Meredov and Maximilian Holzner (Universität der Bundeswehr München, Germany); Stefan Lindenmeier (Universität der Bundeswehr, Germany)
In this paper, we present a multi-antenna system consisting of two circularly polarized GNSS antennas, two passive director elements, and a linear polarized conical monopole with an additional structure stabilizing purpose. The scarabaeus antennas in the antenna system cover the complete GNSS L5 and L1 band with high gain and both left and right-hand circular polarization. The monopole antenna at the center has a linear polarization and covers the frequencies from 1.616 GHz to 1.661 GHz by the monopole for several SeRANIS experiments.

16:55 Dual-Band Single/Dual-Beam High-Gain Patch Antenna Working in TM20 and TM21 Modes

Min Wang (Beihang University (BUAA), China); Mingyang Li and Aixin Chen (Beihang University, China)
A dual-band antenna with single/dual-beam radiation pattern is proposed. By harnessing the TM11 and TM21 modes, the antenna achieves dual-band functionality, positioning it as a promising candidate for future multiband communication systems. The TM21 mode produces split beams due to the inherent opposing magnetic currents on the antenna aperture. To address this, a unique cut is introduced on the radiating patch surface, ensuring a uniform magnetic current direction. This modification results in a single, high-gain beam at the broadside. In TM11 mode, the two pairs of opposing magnetic currents are reshaped into a single pair, generating a dual-beam radiation pattern. The lower band radiation pattern exhibits dual-beam characteristics, with beams pointing at -36° and 38°, and peak gains of 3.9 dBi and 5.5 dBi, respectively, at 2.16 GHz. In contrast, the higher band radiation pattern is a single broadside beam with a peak gain of 8.7 dBi at 2.43 GHz.

MONDAY

17:15 Low-Profile Diplexing Filtenna Using Shielded SIW Cavities for Closely Spaced Frequency Channels

Inapurapu Suryarajitha (Indian Institute of Technology, Roorkee, India); Rajib Kumar Panigrahi (Associate Professor, India); M. Kartikeyan (Indian Institute of Technology Roorkee, India)

A compact, diplexing filtenna (DF) is presented in this paper with second order filtering response for closely spaced frequency channels. The design is based on shielded half-mode substrate integrated waveguide (SD-HMSIW) and shielded quarter-mode substrate integrated waveguide (SD-QMSIW) cavities. A slot loaded SD-HMSIW cavity is used as the common radiating cavity for both frequency channels and SD-QMSIW cavities are utilized to introduce the filtering response. A prototype of the proposed design is fabricated and measured to validate the concept. The proposed DF features a peak gain of 6.2 dBi and 5.1 dBi at center frequencies of 5.35 GHz and 5.71 GHz with a fractional bandwidth (FBW) of 2.2% and 2.3%, respectively. The proposed DF achieves an inter-channel isolation better than 31 dB. This method delivers a considerable reduction in size compared to conventional cavity solutions.

17:35 Novel Dual-Band SIW-To-Metal Waveguide Transition with Integrated Filtering for Diplexing 77GHz and 130GHz Frequency Bands

Kevin Adrianus Petrus van Hastenberg (University of Technology Eindhoven & AntenneX, The Netherlands); Marianna Ivashina (Chalmers University of Technology, Sweden); A. B. (Bart) Smolders (Eindhoven University of Technology, The Netherlands); Artem Vilenskiy (Chalmers University of Technology, Sweden)

This paper presents a novel dual-band transition from a substrate-integrated waveguide (SIW) to two air-filled waveguides (WGs) operating at 77 GHz and 130 GHz, targeting applications such as automotive radar systems. The major design challenges include an increased insertion loss, limited bandwidth, and poor signal isolation. The proposed structure addresses these challenges by incorporating a diplexing mechanism to effectively combine/separate the two frequency bands, allowing them to share a common WG environment while keeping their signals distinct. The dualband transition consists of a common input/output SIW supporting both frequency bands, with individual WG ports for each specific band (77 GHz and 130 GHz). This SIW contains two slots to couple the signals from the SIW to the separate WG outputs. The diplexer consists of a filter in the 77 GHz WG, blocking the 130 GHz signals, and a below cut-off SIW and WG in the 130 GHz signal path.

17:55 Dual-Band Microstrip Leaky-Wave Antenna for Wi-Fi Applications

David Cañete Rebenaque (Polytechnic University of Cartagena, Spain); Alejandro Gil Martinez (Technical University of Cartagena Cartagena, Spain); Nuria García-Alcaraz and Astrid Algaba-Brazález (Technical University of Cartagena, Spain); Jose-Luis Gómez-Tornero (Polytechnic University of Cartagena, Spain)

We present a novel design of a frequency-scanned leaky-wave antenna with dual-band operation in the 2.4 GHz and in the 5 GHz ISM bands of the Wi-Fi wireless LAN standard. It is designed in microstrip technology, using two halfwidth microstrip leaky lines sharing a common substrate, each one tuned to radiate in a separate frequency band. A microstrip notch filter and the self-filtering response of the leaky lines are the mechanisms used to isolate the lower and upper bands, leading to a compact and simple design. This architecture allows independent tuning of each band frequencies and beamwidths.

MONDAY

Room: Ørsted (24+25) — A11b - Advances in leaky-wave and Fabry-Perot cavity antennas

T02 Millimetre wave and THz for terrestrial networks (5G/6G) / / Antennas

Chairs: David R. Jackson (University of Houston, USA), Enrica Martini (University of Siena, Italy)

16:15 A Radially Periodic TE-Polarized Leaky-Wave Bessel-Beam Launcher at Submillimeter Waves

Edoardo Negri (Sapienza University of Rome, Italy); Walter Fuscaldo (Consiglio Nazionale delle Ricerche (CNR), Italy); David González-Ovejero (Université de Rennes, France); Paolo Burghignoli and Alessandro Galli (Sapienza University of Rome, Italy)

The generation of a limited-diffractive, focusing, and self-healing field profile is crucial for the implementation of nextgeneration, near-field, wireless links. For this reason, this work presents a wideband, leaky-wave Bessel-beam launcher realized through a planar, low-profile, cost-effective grounded dielectric slab with a radially periodic metal strip grating printed on top. The proposed device, excited by a circular waveguide, can generate a transverse-electric-polarized Bessel beam at 300 GHz, reaching a nondiffractive range of 25 mm with an aperture radius of just 12.75 mm. Theoretical results, obtained through an effective and elegant leaky-wave approach, are in a remarkable agreement with full-wave simulations, corroborating the launcher design.

16:35 Techniques to Create Shaped Scanned Beams with Leaky-Wave Antennas

Jose-Luis Gómez-Tornero (Polytechnic University of Cartagena, Spain)

It is reported a comprehensive summary of the different techniques which can be used to synthesize scanned shapedbeam radiation patterns using leaky-wave antennas. The different approaches are compared in terms of design and structural complexity, as well as the flexibility to control the radiation level inside the desired angular sector and the rejection outside. The far-field radiation patterns of each approach are connected with their associated near fields to provide some physical insight on the different mechanisms.

16:55 Investigation of the Far- and Near-Field Performance of a Bull's Eye Leaky-Wave Antenna with Open-Stopband Suppression

Sadia Riaz (The University of Edinburgh, United Kingdom); Davide Comite (Sapienza University of Rome, Italy); Paolo Baccarelli (Roma Tre University, Italy); Symon K. Podilchak (University of Edinburgh, United Kingdom)

In this paper, we introduce a 2-D leaky-wave antenna design with suppressed open stopband operating both in the near- and far-field, offering enhanced performance compared to existing designs. Two configurations, a double strip (DS) and a single strip (SS) bull's-eye (BE) leaky-wave antenna structure, are analyzed and compared. The DS launcher demonstrates superior broadband performance, maintaining efficient beam collimation across a wide frequency range in the near-field and enabling continuous beam scanning in the far-field. In contrast, the SS configuration exhibits an open stopband at 19.2 GHz and no continuous radiation. Both launchers employ a coaxial TM-polarized feed mechanism to ensure optimal power transfer, and dispersion curves show identical crossover frequencies for both BE antenna implementations. However, the suppression of the open stopband combined with the wideband capability of the DS configuration, highlights the potential of this design for next-generation high-frequency communication and radars operating in the near- or far-field.

17:15 Aspects of Ray Tracing in Modeling Radiation Patterns of Leaky Wave Antennas

SMiguel Poveda-García (Technical University of Cartagena, Spain); Francisco Mesa (University of Seville, Spain); Astrid Algaba-Brazález (Technical University of Cartagena, Spain); Oscar Quevedo-Teruel (KTH Royal Institute of Technology, Sweden); Jose-Luis Gómez-Tornero (Polytechnic University of Cartagena, Spain)

In this paper, we study three key aspects that should be considered when applying ray-tracing (RT) techniques to model the radiating performance of a leaky wave antenna (LWA). These aspects are the spatial resolution of the rays, the length of the LWA aperture, and the line where physical optics is applied to derive the radiation pattern. The results of the radiation pattern obtained through RT are compared with those derived from numerical integration along the LWA aperture.
It is shown that careful consideration of these factors is necessary to accurately calculate the radiation pattern while maintaining a computationally efficient analysis. Finally, as a practical example, a structure consisting of a modulated LWA combined with a lens for broad-beam generation is analyzed and compared to full-wave simulation to show the necessity of properly setting the analysis parameters.

17:35 A 2-D Beam-Steering Leaky-Wave Antenna Array in X Band for Non-Terrestrial Networks

Trung D Ha and Nga Vu (University of Illinois at Chicago, USA); Danilo Erricolo (University of Illinois Chicago, USA); Pai-Yen Chen (University of Illinois at Chicago, USA); Chung-Tse Michael Wu (Rutgers University, USA)

This paper presents a low-profile, high-gain beam-steering leaky-wave antenna (LWA) array designed for operation in the X band for non-terrestrial networks. Specifically, the proposed array is based on a co-planar waveguide (CPW) structure with bi-directional radiation patterns in the H-plane as a result of frequency scanning. In addition, the integration of the proposed LWA array with a Butler matrix enabling beam steering in the E-plane at a fixed 8GHz frequency band is introduced. Numerical results are presented for an array of four 22-element LWAs operating at 8 GHz. The radiation patterns in both the H-plane and E-plane could be either achieved by scanning the operating frequency or switching between exciting ports, respectively. We envision that the proposed beam steering LWA array may be of great interest for next-generation wireless communication in emerging applications such as 5G/6G base stations, and satellite communication.

17:55 Flexible Antipodal Vivaldi Leaky-Wave Antennas

Francis Baccin-Smith, David F Hardy and Shulabh Gupta (Carleton University, Canada)

A novel design for a flexible bi-directional leaky-wave antenna (LWA) is proposed and experimentally verified. The design is based on differential microstrip technology and use a periodic antipodal Vivaldi array to emit side-fire radiation beams. The LWA design utilizes a single feed to achieve bi-directional radiation and was engineered for a broadside frequency of 6 GHz. The design is fabricated using a thin flexible polyethylene terephthalate (PET) sheet substrate and Kapton sheets. The fabricated antenna shows high gain, high directivity, and good reflection characteristics while being thin, flexible and lightweight. The antenna can be engineered to point high gain beams in multiple desired directions, and can be further adapted to allow for precision control of the beams in various frequency bands when mounted on both flat and conformal surfaces.

Room: Mosig (26)

Meetings and working group

AMTA Meeting

MONDAY

Chairs: François Sarrazin (Université de Rennes & IETR, France), Claude Oestges (Université catholique de Louvain, Belgium)

16:15 Phase Distribution of the Large-Scale Scattered Field from the Sea Surface

Giacomo Melloni and Torbjörn Ekman (Norwegian University of Science and Technology, Norway)
A new phase distribution model of the scattered field from the sea surface is proposed, combining Geometrical-based Stochastic Channel Modeling (GSCM) and the Effective Roughness (ER) approaches. The presented model applies to the large-scale roughness of the sea surface. Assuming the sea surface elevation follows a Normal distribution, a phase relation model is derived, capturing the statistical correlation between distinct scattering points across the surface. The phase correlation function is derived from the sea surface's autocorrelation function (ACF), highlighting the influence of sea state parameters on the resulting phase distribution. The model demonstrates a strong dependence of the phase distribution on the characteristics of sea conditions and is applicable to any surface with a correlated Normal distributed roughness profile.

16:35 Outdoor Propagation Measurements for Drone Relay Systems - Drone Altitude Characteristics of Ricean K-Factor

Yudai Ishikawa and Tetsuro Imai (Tokyo Denki University, Japan)
Currently, mobile communication system using drones as relay stations has been considered in order to further increase the transmission speed in mobile communication system, to expand the service area, and to respond to the increase of localized traffic. However, the transmission characteristics of these systems in real propagation environments have not yet been fully clarified. In this paper, we evaluate the radio wave propagation characteristics in a drone relay system by the received power characteristics, drone altitude, presence of line-of-sight, and antenna directivity, based on the results of outdoor experiments using 5.12 GHz for the drone altitude characteristics of K-factor.

16:55 Space-Time Modulated Metasurface System for Anti-Interference DoA Estimation

Jie Wu (Nanjing University of Science and Technology, China); Mengmeng Li (Nanjing University of Science and Technology & Communication Engineering, China); Xinyu Fang (Nanjing University of Science and Technology, China); Davide Ramaccia (RomaTre University, Italy); Alessandro Toscano and Filiberto Bilotti (Roma Tre University, Italy); Dazhi Ding (Nanjing University of Science and Technology, China)
In this contribution, a space-time-modulated metasurface (STM-MTS) is designed to enable anti-interference direction of arrival (DoA) estimation. The proposed system consists of a 1-bit STM-MTS, that generates a set of scattered harmonics whose components are related to the space-time modulation scheme of the metasurface and the specific incident angle, and a single receiving antenna that collects the modulated mixed signal reflected by the metasurface for performing DoA estimation. A properly designed separation procedure is presented here to extend the antiinterference feature to a metasurface-based DoA system. The metasurface is fabricated, experimentally characterized, and embedded in the DoA system, showing that the absolute errors in the DoA estimation are less than 2° within the incident range of [-50°,+50°], in both fixed and dynamic direction of arrival of the intended signal. The results demonstrate the effectiveness and accuracy of the proposed anti-interference DoA estimation system based on spacetime- modulated metasurfaces.

17:15 Significance of Extreme Reflection Angles in RIS-Assisted Wireless Networks

Ilyas Saleem (Macquaire University, Australia); Muhammad Ali Babar Abbasi (Queen's University Belfast & The Institute of Electronics, Communications and Information Technology (ECIT), United Kingdom); Subhas Chandra Mukhopadhyay (Macquarie University, Australia); Dmitry E Zelenchuk (Queen's University of Belfast, United Kingdom); Hazer Inaltekin and Syed Muzahir Abbas (Macquarie University, Australia)
This study examines the importance of the extreme reflection angles in terms of the spectral efficiency in a Reconfigurable Intelligent Surfaces (RIS) - assisted wireless communication system. The investigation considers practical RIS unit cells with a non-ideal reflection response, which is typical, especially when the extreme angles of incidence, as well as reflection, are considered. A significant disparity was found in spectral efficiency when RIS is employed to reflect signals at extreme angles, with a notable 150% - 200% increase in the required number of unit cells to maintain the same spectral efficiency compared to scenarios with normal reflection angles. This observation underscores the importance of considering reflection angles in the design and optimization of RIS hardware. The results contribute valuable insights to the understanding of RIS behaviour in practical scenarios, paving the way for enhanced spectral efficiency and improved network performance.

17:35 FR3 Radio Propagation Channel Measurements and Modelling in Outdoor Environment for 5G and 6G Wireless Networks

Jiahao Hu, Amar Al-Jzari, Yubei He and Sana Salous (Durham University, United Kingdom)
Propagation channel measurements in Line-of-sight (LoS) and None-Line-of-Sight (NLoS) scenarios were conducted at 7.6 GHz and 13.6 GHz in the FR3 frequency band in an outdoor environment at Durham University. The measurements employed omnidirectional transmitter and receiver antennas to evaluate multipath components and characterize the channel properties of these recently allocated frequency bands for International Mobile Telecommunications (IMT) [1]. The analysis covered several channel parameters, including the Power Delay Profile (PDP), Root-Mean-Square (RMS) delay spread, and the Rician K-Factor. Additionally, the path loss coefficient was estimated using both the Close-In (CI) and the Floating-Intercept (FI) models.

17:55 Ray-Tracing Based Algorithms for Indoor RIS Optimization and Coverage Enhancement

Emre Kilcioglu and Claude Oestges (Université catholique de Louvain, Belgium)
Reconfigurable Intelligent Surfaces (RISs) represent a key emerging technology in wireless communication systems, allowing for precise control over previously uncontrolled propagation environments. This paper investigates the integration and optimization of RISs to enhance coverage in indoor environments using NVIDIA's Sionna Ray-Tracing (RT) tool. The RIS is modeled as an array of reflective tiles with adjustable phase profiles. We analyze two phase profile approaches (gradient-based and distance-based) for steering reflected signals toward blind zones identified in the transmitter-only coverage map. Based on the fixed positions of the transmitter and RIS, we propose a clusteringbased algorithm to determine sub-optimal target positions, focusing on the least covered areas in the transmitter-only coverage map. Additionally, we introduce a ray-tracing-based search algorithm to provide insights into a sub-optimal RIS size. Simulation results demonstrate that the proposed methods effectively enhance signal coverage and minimize blind zones, confirming their viability for real-world implementations in RIS-assisted communications.

Monday - 18:45-21:00

Room: Blue Hall, Stockholm City Hall

Welcome Reception

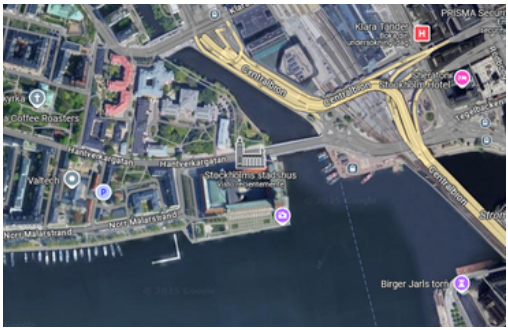

You can guide yourself to the city hall using Google Maps in the following link: https://maps.app.goo.gl/NYK99qy4GRhKZLd87

MONDAY

Tuesday - 08:00-09:40

Room: Alfvén (A3 + A4)

A06a - Advances in Lens Antennas I

T02 Millimetre wave and THz for terrestrial networks (5G/6G) / / Antennas

Chairs: Marta Martínez-Vázquez (Renesas Electronics, Germany), Eva Rajo-Iglesias (University Carlos III of Madrid, Spain)

8:00 A Sequential Geometrical Optics Technique for Field Shaping in Multi-Lens Antenna Systems

Shahab Oddin Dabironezare, Alexandra Mavropoulou and Akira Endo (Delft University of Technology, The Netherlands); Jochem Baselmans (SRON, The Netherlands); Nuria LLombart (Delft University of Technology, The Netherlands); Giorgio Carluccio (NXP Semiconductors, The Netherlands)

In this contribution, a multi-objective optimization tool with a rapid and accurate kernel based on sequential Geometrical Optics is discussed to design wide band and wide scanning compact multi-lens antenna systems for future far infrared imaging spectrometers. An example scenario was optimized using the proposed tool to demonstrate the capabilities of the method. The response of the optimized solution in terms of efficiencies and beam pattern was validated against PO solver of TICRA tools with excellent agreement.

8:20 Analysis Methodology Based on Bidirectional Forward Ray Tracing for the Optimization of Lens Phased Arrays

Ashwita Nair (Delft University of Technology, The Netherlands); Giorgio Carluccio and Waqas Syed (NXP Semiconductors, The Netherlands); Harish Nandagopal (NXP Semiconductor, The Netherlands); Maria AlonsodelPino and Daniele Cavallo (Delft University of Technology, The Netherlands); Kostas Doris (NXP Semiconductors, The Netherlands); Nuria LLombart (Delft University of Technology, The Netherlands)

In this contribution, we present the design of a fully electronic lens phased array antenna that can achieve an angular resolution in the order of 1° for continuous scanning in a moderate field of view (FoV) of 20°. The optimal antenna beam-forming weights are computed using a bi-directional ray tracing approach to include the effects of the lens feed pattern and mutual coupling. The lens elements spacing, longitudinal location and shape of the lens are optimized to minimize the side lobes and the scan loss.

8:40 Analysis and Design of a Wide Scanning Array-Fed Lens Antenna for mm-Wave Applications

Jinglin Geng, Nuria LLombart and Daniele Cavallo (Delft University of Technology, The Netherlands); Waqas Syed and Giorgio Carluccio (NXP Semiconductors, The Netherlands); Harish Nandagopal (NXP Semiconductor, The Netherlands); Kostas Doris (NXP Semiconductors, The Netherlands)

This work deals with the analysis and design of an array-fed dielectric lens antenna with large scan range. The lens is fed by an array of cavity-backed double-slot antennas. A spectral method of moments (MoM) is developed to estimate the impedance and the primary patterns of the slot array. The method is rendered computationally efficient by considering, for each slot, only two basis functions that suitably describe the magnetic current distribution. The MoM is combined with geometrical and physical optics to estimate the patterns outside the lens. Based on this approach, an array-fed lens is designed, aiming at achieving a large field of view (FoV). The complex excitation and the array placement are optimized to reduce the scan loss. Metallic reflectors are used at the array edges to enhance the scan range. The resulting design achieves a nearly flat gain>21dB within a 100 degree FoV, for a 5-wavelength lens diameter.

9:00 3D-Printed Correction Surfaces for Gain Enhancement of Metamaterial Lenses

Andrzej Dudek (AGH University Krakow, Poland); Slawomir Gruszczynski and Krzysztof Wincza (AGH University of Krakow, Poland)

This paper proposes a gain enhancement method for metamaterial lenses. The method is based on local phase difference compensation between all the rays that illuminate every single unit cell of the metamaterial lens. This local phase compensation within one unit cell is realized by adding an additional fully dielectric structure with a required geometry, so that all the rays that illuminate the lens unit cell are in phase after passing through the added structure. All added compensation structures make up a correction surface for the lens. The idea of metamaterial lenses with the correction surfaces has been validated in simulations and measurements of the metamaterial lens with and without the correction surface in K band. The measured gain enhancement resulting from the use of correction surface is up to 1.3 dB.

9:20 Metallic Elements Inside a Mismatched Luneburg Lens: Experimental Validation at V-Band

Vincent Kaschten, Dimitri Lederer and Christophe Craeye (Université Catholique de Louvain, Belgium)

We implement a cylindrical mismatched Luneburg lens on PCB at V-band, including metallic elements inside the GRIN lens. The lens has a relative dielectric permittivity of 2.2 at its edge, while the exterior medium is air. The judicious choice of dielectric substrate, and the introduction of metallic posts at carefully selected positions, both enhance the bandwidth and radiation properties of the GRIN lens antenna. Measurements confirm that this design can produce a stable fan-shaped beam over a 10 GHz bandwidth and at multiple excitation points covering a 90 degrees angular range.

8:00 A Design of A Circular-Shaped Monopulse Slotted Cavity Waveguide Array Antenna Systems

Tuan-Anh Le Trong (Viettel Group & Viettel Aerospace Institute, Vietnam); Quyet Nguyen Manh (Viettel Group, Vietnam); Son Van Hoang (Viettel Group, Vietnam & Viettel Aerospace Institute, Vietnam); Hieu Trong Dam (Viettel Aerospace Institute, Vietnam)

This paper presents the design of a circular-shaped monopulse slotted cavity waveguide array antenna system. The antenna integrates a 16×16 slotted array with a highly compact monopulse comparator. The overall dimensions of the design are 120×π×22 mm, making it one of the most compact, wideband, high-gain, and low-sidelobe designs available. Due to its circular shape, the array comprises a total of 208 radiating slots and 52 coupling slots, compared to the typical 256 and 64, respectively. The proposed design not only still keep the size but also has the great performance as the full-sized structure. Furthermore, the very compact monopulse comparator (MC) provides an extremely effective solution in applications that require a narrow or restrict configuration. The bandwidth of 15.7%, the peak gain of 30.6 dBi, the beamwidth of 5.40 and the sidelobe of 23.7 dBi are simulated and verified.

8:20 Design and Development of SWaP Optimized C-KuBand RF Front End for Futuristic EW Systems

ARP Mallika (Gov & Defence Electronics Research Laboratory, India); M Uma Ravindra (Scientist F, India); Latha Thokala (DRDO Hyderabad, India); D. Srinivas Rao (Scientist D, India); Sravani Matham, C. Vasant Kumar, G. Syamala Rao and Y. Hemalatha (DRDO, India)

This paper presents a compact RF front-end designed for Electronic Warfare (EW) systems, utilizing a state-of-the-art C-Ku band dual 16-channel Transmit-Receive (TR) plank. The system integrates 192 closely spaced T/R modules across six planks, along with bidirectional amplifiers, a master controller, calibration circuits, and RF, control, and DC-power manifolds into a single chassis, greatly improving array performance and integration. Each T/R module delivers 30 dBm of output power, enabling the system to achieve an Effective Radiated Power (ERP) of more than 62 dBm across the entire band. Leveraging Commercial Off-The-Shelf (COTS) MMICs, the system provides precise phase control and adaptive beam steering, enhancing detection and jamming capabilities. Liquid cooling manifolds are incorporated for thermal management. Optimized for Size, Weight, Power, and Cost (SWaP-C), this design is compact and suitable for airborne applications.

8:40 Initial Beamforming Analysis for Substations in the SKA-Low Radio Telescope

David B Davidson (Curtin University, Australia & Stellenbosch University, South Africa); Cathryn Trott and Maria Kovaleva (Curtin University, Australia)

This paper reports initial work on forming substation beams within the SKA-Low telescope, the lower frequency component of the Square Kilometre Array Observatory. The analysis leverages the embedded element patterns computed for a progression of SKA-Low prototype arrays over several years. The results indicate that the proposed substation layouts form beams as expected. There is detailed structure in these substation beams which can now be evaluated against the requirements for specific science cases.

9:00 Mitigation of the Antenna Carrier Impact in Dual-Polarized Phased Arrays with Electromagnetic Bandgaps for Airborne SAR Sensors

Diego Lorente, Markus Limbach and Bernd Gabler (German Aerospace Center (DLR), Germany); Hector Esteban (Universidad Politecnica de Valencia, Spain); Vicente Boria (Universidad Politécnica de Valencia, Spain)

In this work, the impact of the antenna carrier is analyzed. The resulting polarization-dependent edge diffraction effects of a flight-model L-band phased array antenna, embedded in the antenna carrier, is experimentally validated. Measurements show a pattern distortion in the horizontal polarization and a gain reduction of 1 dB in the elevation plane, in which the beam steering is performed that also corresponds with the E-plane, thus becoming this polarization more sensitive to edge diffraction effects. Further analysis is performed increasing the electrical size of the antenna carrier. A low-profile and planar solution, based on Electromagnetic Bandgaps is presented, by which the induced surface currents on the antenna carrier for the horizontal polarization are mitigated, thus reducing the impact of edge diffraction effects without interfering in the performance of the vertical polarization. Thereby, the desired radiation characteristics can be fulfilled regardless of the antenna carrier structure for both polarizations.

TUESDAY

9:20 A Modular Dual-Polarized Antenna Array with Four Interleaved 4×4 Arrays for Synthetic Aperture Radar (SAR) Applications

Alessio Tornese, Gong Chen, Peizhuo Yang and Koen Mouthaan (National University of Singapore, Singapore)
A modular, dual-polarized array with four interleaved arrays is presented for application in L-band Synthetic Aperture Radar. One array is for transmit and one is for receive in horizontal polarization and the other two arrays are for transmit and receive in vertical polarization. The design enables direct connection to RF circuitry for transmit and receive without the need for circulators or switches. Each antenna element has a dedicated channel, which is particularly advantageous for beamforming scenarios. The antenna elements, realized as printed dipoles on a substrate mounted on a ground plane, use a printed balun to enable broadband, balanced excitation. The array is simulated and measured for two cases: all receive modules terminated with a 50Ohm load and all receive modules left open-circuited. The realized gain exceeds 19dBi in the open-circuit case for both polarizations. When the RX modules are terminated with the load, the gain is reduced to 16dBi.

Room: Hallén(BAR5) **E01a - Electromagnetic theory**

T08 Fundamental research and emerging technologies/processes / / Electromagnetics

Chairs: Ioan E. Lager (Delft University of Technology, The Netherlands), Martin Norgren (KTH Royal Institute of Technology, Sweden)

8:00 Leaky-Wave Radiation from a Slot: The Time-Domain View

Ioan E. Lager and Andrea Neto (Delft University of Technology, The Netherlands); Martin Štumpf (Brno University of Technology, Czech Republic)
A time-domain model of the leaky-wave radiation from a slot is assembled via an in-depth numerical investigation. The reported numerical experiments, all making use of a strictly causal excitation, provide a practical guideline for designing leaky-lens antennas (LLAs) and, above all, cogently elucidate the causal mechanism building up the propitious electromagnetic field distribution underpinning the LLA operation.

8:20 Fast PMCHWT Solution Based on Spectral Integral Method for 2-D Scattering Problem of a Cylinder

Yiming He (The Hong Kong Polytechnic University, Hong Kong & Eastern Institute of Technology, Ningbo, China); Wen Chen (The Hong Kong Polytechnic University, Hong Kong); Qing Huo Liu (Eastern Institute of Technology, China)
Starting from surface integral equations in the 2-D case, this paper reports transform to the well-known Poggio-MillerChang-Harrington-Wu-Tsai (PMCHWT) formulations from the spatial domain into the spectral domain with a spectral integral method. With explicit formula deductions, this method provides fast solutions for a classic scattering problem of a single dielectric cylinder incident by a plane wave, efficiently eliminating interior resonance problems with high accuracy. Numerical experiments demonstrate the exponential convergence of the method and its merits going beyond the first-order method of moments.

8:40 Chebyshev Polynomial Expansion Approach to the Scattering from a Thin Tubular PEC Cylinder

Martin Norgren (KTH Royal Institute of Technology, Sweden)
The scattering from a thin PEC cylinder is solved by means of a semi-analytical method. In azimuth, the surface current is expanded into a standard Fourier series, while an expansion into Chebyshev polynomials is used in the longitudinal direction. For an, in principle, arbitrary incident electromagnetic field, the expansion coefficients are determined using a Galerkin method. The numerical part involves solving Sommerfeld type integrals in the spectral domain. Given the expansion coefficients, analytical expressions for the scattered fields are derived. Numerical results are compared with the wire antenna with midpoint delta-gap feeding, and for plane wave illumination. Extensions to cylinders with surface resistance and multiple section cylinders are presented

9:00 Evanescent TE-Polarized Bessel-Beam Launcher Using a Coplanar Loop Array

Luca Del Biondo (Michigan State University, USA); Walter Fuscaldo (Consiglio Nazionale delle Ricerche (CNR), Italy); Gianluca Lazzi (University of Southern California, USA); Mauro Ettorre (Michigan State University, Electrical and Computer Engineering, USA)
Bessel beams in the propagation regime have long been investigated for their unique properties of limited diffraction and self healing. Conversely, Bessel beams in the evanescent regime have not met the same interest in spite of their attractive features of a subwavelength, highly focused main beam and highly decaying radiation amplitude. These additional features, unachievable with propagating Bessel beams, make technologies based on evanescent Bessel beams potentially well suited for several applications. For this reason, in this work, an original device generating evanescent Bessel beams is proposed and demonstrated by full-wave simulations.

TUESDAY

9:20 Scattering Matrix Representation for Arrays of Quasi Optical Antennas Focusing in Radiative Near-Field

Andrea Neto, Nina Beschoor Plug and Nuria Llombart (Delft University of Technology, The Netherlands); Angelo Freni (Università degli studi Firenze, Italy)

We present a scattering matrix representation to be used in the efficient design of wireless links between arrays of quasi optical antennas (lenses or horns). The applicative scenario is that of high frequency (around 300 GHz) wide band communications, over very short distances where wired connection appears to be emerging as a bottle neck. In these scenarios arrays of multiple lenses have recently been proposed and it is apparent that the interaction between the lenses on both the transmitting and the receiving sides cannot be neglected. The possible applicability of simplified representations that emerge when the dimensions of the apertures are very large is assessed and discussed.

Room: Marcuvitz (M3)

CS13a - Advances in Channel Sounding and Measurements for 6G: From cm-Wave to sub-THz

T07 Electromagnetic modelling and simulation tools / Convened Session / Propagation

Chairs: Diego Andrés Dupleich (Technische Universität Ilmenau, Germany & Fraunhofer Institute for Integrated Circuits IIS, Germany), Wei Fan (Southeast University, China)

8:00 Dynamic Wideband Channel Sounding in an Urban Macrocellular Scenario at 15 GHz

Ali Kourani, Juha Tuomela, Visa Kurvi, Lauri Vähä-Savo and Katsuyuki Haneda (Aalto University, Finland)

Fifth-generation cellular networks have become a part of infrastructure of modern society to support the effective and efficient information exchange. Despite significant advancements in mobile cellular technologies, the radio frequency range between 6 GHz and millimeter-wave 26 GHz, specifically around 15 GHz, remains underexplored in cellular mobile communications. This paper describes the implementation of a channel sounder based on a software defined radio and its application to dynamic field measurements to investigate the potential and challenges associated with mobile communications at 15 GHz carrier in non-line-of-sight (NLOS) radio channel conditions. The work provides initial insights into propagation losses in NLOS conditions in this frequency band due to foliage and urban structures. Our measurements revealed a 20 dB loss due to building corner shadowing, a 10-15 dB loss from foliage blockage, and an 8-15 dB penetration loss through building windows.

8:20 Human Blockage Measurements Using Multiband CW Sounder

Sana Salous, Yubei He, Amar Al-Jzari and Jiahao Hu (Durham University, United Kingdom); Silvi Kodra (University of Bologna, Italy)

In the World Radiocommunications Conference in 2019 (WRC-19), several frequency bands including the millimeter wave (mm-Wave) bands below 100 GHz were identified for 5G technology which led to several frequency bands being approved for 5G radio systems. In WRC-23 the frequency bands were extend above 100 GHz: 140-170 GHz and 235-300 GHz for 6G technology. While these bands provide more bandwidth that enables high data rates with low latency, they tend to suffer from blockage. To estimate the path loss due to human blockage on 5G and future 6G frequency bands, measurements were conducted at 25.8 GHz, 77.5 GHz and 155 GHz using the multiband Continuous Waveform (CW) channel sounder developed at Durham University. The measurements were used to estimate the cumulative distribution functions where are also compared with various blockage models.

8:40 Variable Reference Structure for Channel Sounding in the Low Terahertz Range

Tobias Doeker, Carla E. Reinhardt, Christoph Herold and Uwe Hellrung (Technische Universität Braunschweig, Germany); Daniel Mittleman (Brown University, USA); Thomas Kürner (Technische Universität Braunschweig, Germany)

In this paper, a structure is presented that can be used as a common reference for different channel sounding systems. The structure is designed to create a defined channel impulse response with two multipath components. The delay of the second multipath component can be varied due to a variable part of the structure. Initial measurements with a correlation-based time-domain channel sounder evaluate the functional behavior of the structure. The results illustrate the expected variation of the channel impulse response for horizontal polarization. However, additional multipath components appear in the channel impulse response, and the behavior for vertical polarization deviates from theoretical predictions.

9:00 Rician Fading Models for Rough Surface Reflection at 300 GHz

Minseok Kim and Minghe Mao (Niigata University, Japan)

Compared to existing frequency bands, terahertz (THz) waves are more susceptible to diffuse scattering due to surface roughness, and this effect must be considered when predicting propagation paths using deterministic methods like ray tracing. In this study, an experimental investigation of the reflection characteristics of plasterboard-a common indoor wall material-at 300 GHz is conducted. First, this paper proposes a rough surface reflection model, incorporating both specular and diffuse components, which result in small-scale fading through interference. Rician fading models for plasterboard reflection at 300 GHz are then presented based on extensive measurements under four different conditions: bare plasterboard, paper-covered plasterboard, painted plasterboard, and painted plasterboard wall. The results reveal that the K-factor ranges from 11.06 to 26.32 dB, with the specular component being more prominent in the TE mode than in the TM mode.

9:20 4.8 GHz Band Radio Channel Measurement by Unmanned Aerial Vehicle-Based Virtual Array Channel Sounding System

Kentaro Saito (Tottori University, Japan); Sora Kojima (Tokyo Denki University, Japan)

In this paper, we propose the UAV-based virtual array channel sounding system in the 4.8 GHz band to investigate the air-to-ground (A2G) propagation channel characteristics for the design and evaluation of the mobile communication system in the sky area. In our system, the channel data are continuously measured by the receiver, which is mounted on the UAV station. The data are combined offline, and they are processed virtually as data of large array antenna for investigation of angular characteristics of the propagation channel. A great advantage of our system is to be able to configure an arbitrary virtual antenna array in the air. The experiment was conducted in an indoor workshop space in the 4.85 GHz band. The HPBW of the angular power spectrum was 3.2 deg. Future work will include conducting experiments in various radio propagation environments and analyzing more detailed channel characteristics.

Room: Jansson (31)
Scientific Workshop
SW1a - AMTA SW - Reverberation Chambers for Antenna Measurements

Room: Zorn (32)
Industrial Workshop
08:00-08:45
IW4 - European Space Agency (ESTEC) - Spaceborne Antennas for Earth Observations missions

Room: Zorn (32)
Industrial Workshop
08:55-09:40
IW14 - Simr - SimOps (Simulation Operations) for Antenna Engineers: Accelerating Simulations and Automating Data Handling

Room: Björk (33)
Scientific Workshop
SW4a - Emerging Materials for Applied Antenna Engineering: Sensing and Communications

Room: Bergman (34)
Industrial Workshop
IW1 - Altair Technology - Pushing the boundaries of Computational Electromagnetics - Advanced antenna simulation including multiphysics analysis and AI-powered optimization

Room: Felsen (35+36)
CS46a - Metamaterials for future industrial applications

T08 Fundamental research and emerging technologies/processes / Convened Session / Electromagnetics

Chairs: Matthieu Bertrand (Thales Research and Technology, France), Guido Valerio (Sorbonne Université, France)

8:00 Wideband Reflectarray Design for CubeSat Applications in X-Band

Nelson Fonseca and Michele Del Mastro (Anywaves, France); Fatemeh Sadr and Jordan Budhu (Virginia Tech, USA); Gautier Mazingue (Anywaves, France); Louis Mangenot (ANYWAVES, France); Maxime Romier (Anywaves, France); Nicolas Capet (ANYWAVES FRANCE, France)

This paper reports on the design of a reflectarray for CubeSat applications. In an effort to industrialize the concept, a wideband unit cell is selected to cover a significant part of the X-band, corresponding to identified use cases for the technology.

8:20 Multifunctional Dual-Band Metasurface-Based Transmit- and Reflect-Arrays at Sub-THz

Bilal Ouardi (CEA-LETI, France); Ronan Sauleau (Universite de Rennes, France); Antonio Clemente (CEA-Leti, France)

In this paper, we present the design of a dual-band multifunctional metasurface-based (MMS) transmit- and reflectarray (TRA) antennas for wave manipulation at sub-terahertz (sub-THz). The proposed design allows independent beam control in both transmission and reflection hemispheres. The MMS exploits 1-bit phase control of the incident wave over a wide bandwidth while maintaining remarkably low insertion and reflection losses, using only three metallic layers. Passive dual-band TRA antennas, consisting of 30×30 unit-cells (UCs), are demonstrated based on the metasurface phase modulation capability. These features make the proposed MMS a highly promising solution for next-generation sub-THz applications, offering independent full space beamforming and steering coverage.

TUESDAY

8:40 Measuring Waveguide Devices Based on Rotational Corrugations Through OMTs

Gines Garcia-Contreras (INSA Rennes, Rennes, France); Francisco Mesa (University of Seville, Spain); Juan Córcoles and Jorge A Ruiz-Cruz (Universidad Politécnica de Madrid, Spain); Oscar Quevedo-Teruel (KTH Royal Institute of Technology, Sweden)

Rotational corrugations, based on discrete rotational symmetries, allow for a frequency-dependent physical rotation of the electromagnetic fields by arbitrary angles. They are especially promising in dual-polarization applications in which, due to geometrical or manufacturing constraints, it is not possible to physically twist the system. In this work, we will briefly discuss their working principle and explore how it is possible to characterize such devices through the use of ortho-Mode transducers. Moreover, one dual-polarization-plane rotator manufactured through 3D~printing has been measured, and its performance validated in terms of rotational symmetries.

9:00 Stacked Multi-Via Mushroom-Type EBG Structures with Glide Symmetry

Ashray Ugle (Sorbonne University, France); Massimiliano Casaletti (Sorbonne Universités UPMC, France); Marta Arias Campo and Simona Bruni (IMST GmbH, Germany); Guido Valerio (Sorbonne Université, France)

In this work, the dispersion of stacked mushroom-type EBG structures exhibiting glide symmetry are investigated and compared with conventional single-via structures in the frequency range of 50-90 GHz, useful for millimetre-wave sensing. While standard single-via cells do not provide a stopband in this frequency range when stacked, a new glidesymmetric multi-via cell is shown to function as an EBG, independent of the number of layers. With the use of multimode transmission matrix method, the complex wavenumber for the unit cell is obtained. The calculation is performed by applying post-processing to the generalised S-parameters of the unit cell obtained by means of a commercial solver. The computation of the complex wavenumber is particularly advantageous, as its imaginary part facilitates the analysis of attenuation in the stopband. The stacked multi-via EBG structures with glide symmetry show promising results beneficial for the design of gap-waveguide components constructed with inexpensive multi-layer PCB technology.

9:20 Design of Dual-Polarized 3-D Slotline Reflective Metasurface to Improve Millimeter-Wave Coverage

Angel Palomares-Caballero (IETR-INSA Rennes, France); Carlos Molero and Pablo Padilla (University of Granada, Spain); María García-Vigueras (IETR-INSA Rennes, France); Raphael Gillard (IETR & INSA, France)

This paper proposes a dual-polarized slotline unit cell for designing reflective metasurface at millimeter waves. The unit cell consists of a three-dimensional (3-D) assembly of PCB layers. The metallic pattern of each PCB layer implements an orthogonal short-circuited slotlines whose length can be varied independently to control the phase in reflection of each incident polarization. The performance has been studied for normal and oblique incidences, showing high levels of co-polar and a linear phase between 37 GHz and 44 GHz. Using the proposed unit cell, a use case is presented where a reflective metasurface is needed to improve the coverage at various positions of an NLOS scenario. Two design options for the phase distribution in the metasurface are discussed. Through their radiation patterns, a comparison is performed. The advantages of using a metasurface with a broad-beam for coverage over a large bandwidth and for different angularly separated positions are demonstrated.

TUESDAY

Room: Schelkunoff (C1)

A12a - Antennas for medical application and health

T06 Biomedical and health / / Antennas

Chairs: Jari Holopainen (Aalto University, Finland), Gaetano Marrocco (University of Rome Tor Vergata, Italy)

8:00 Design and Validation of a Compact Dual-Band Bluetooth Antenna for Smartwatch Applications

Sravan Kumar Reddy Vuyyuru, Mohamed Räsänen, Jan H. S. Bergman and Jari Holopainen (Aalto University, Finland)

This paper presents the compact dual-band Nonplanar Bluetooth antenna design for smartwatches targeting 2.45/ 5.85 GHz operation. The antenna features a straightforward structure that enhances bandwidth and efficiency without external matching circuits, addressing challenges like miniaturization using inductive meander lines, performance degradation due to human-body proximity, radiation obstruction from metal bezels, and strict size constraints, all while maintaining dual-band operation. The combination of an I-shaped monopole and an inverted U-shaped stripline demonstrates dual-resonance behavior, and simulations closely align with experimental measurements conducted at the microwave lab and StarLAB facility. The gain analysis demonstrates the antenna's ability to provide a Bluetooth range of 30 meters at 2.45 GHz and 10 meters at 5.85 GHz, supporting next-generation smartwatch integration with reliable connectivity.

8:20 A Preliminary Multi-Physics Study for Intra-Cardiac Communication Based on Biventricular Model

Maoyuan Li and Takahiro Aoyagi (Institute of Science Tokyo, Japan); Ilangko Balasingham (NTNU, Norway); Ali Khaleghi (NTNU, Norway & OUS, Norway)

Wireless modules have become a crucial component of many modern implantable medical devices (IMDs), including those used for cardiac applications. In this study, we conducted a preliminary multi-physics simulation for intra-cardiac communication based on a simplified biventricular geometry. Initially, we simulated the cardiac cycle, demonstrating the deformation of the biventricular, and in one scenario, two cardiac implants were positioned within the cardiac chamber, with relative displacement observed. Based on electromagnetic simulations, we analyzed the fluctuations in coupling at different frequencies (6.78, 13.56, 433, 915, and 2400 MHz) during myocardial mechanical deformation over a simulated cardiac cycle. The method used in this study provides a paradigm for the intra-cardiac implant investigation, and the results are a major component in the link budget analysis.

8:40 Resonance-Frequency Uncertainty Due to Orientation-Specific Wearable-Antenna Bending by BodyMorphology Variations

Hendrik Rogier and Sofie Lenders (Ghent University, Belgium)

When bending wearable antennas along various body areas of a representative sample of a given human population, the distribution of their shift in resonance frequency is efficiently computed by an Amoroso-Laguerre generalized polynomial chaos expansion. The varying body morphologies of children, adults and military personnel cause an upward shift when bending textile antennas along their resonant length. This shift is slightly compensated by substrate compression occurring in case of non-stretchable patches. Moreover, this compression causes a downward shift in resonance frequency when bending the antenna along its non-resonant length.

9:00 Design of a Compact 868 MHz On-Body Matched Antenna for Relaying Biomedical Implants

Yizhen Yang (Ghent University, Belgium & IMEC, Belgium); Gunter Vermeeren (Ghent University, Belgium); Wout Joseph (Ghent University/IMEC, Belgium)

A compact 868 MHz Long Range (LoRa, 863-870~MHz) band repeater antenna is proposed for the on-body relaying of biomedical implants. The antenna is designed in close proximity to a canonical three-layer tissue model and validated with simulations using three realistic human models. The antenna achieves a 12.3% fractional bandwidth and maintains robust performance across different models with a maximum on-body gain of -8.1 dBi. Specific Absorption Rate (SAR) analysis confirms compliance with International Commission on Non-Ionizing Radiation Protection (ICNIRP) guidelines, making it suitable for on-body biomedical applications

9:20 Cylindrical Phantom Model for Characterization of Implantable Antennas

Marko Bosiljevac (University of Zagreb, Croatia); Mingxiang Gao (EPFL, Switzerland & IT'IS Foundation, Switzerland); Anja K. Skrivervik (EPFL, Switzerland); Zvonimir Sipus (University of Zagreb, Croatia)

Fundamental radiation limitations for in-body or implantable antennas provide valuable insights into the feasibility of certain systems. Previous work has shown that near-field effects and the distance from the body-to-freespace boundary are critical factors, giving good approximate formulas for the power density obtained at body interface. In this paper, we extend this analysis by examining the effect of the body curvature on the system radiation pattern and gain, by introducing a model for a cylindrical body phantom and comparing it to the planar and spherical cases. To accomplish this, we developed an analysis model based on cylindrical mode expansion of the electromagnetic fields. This analysis offered the insights needed to extract key information about EM fields radiated by the implant. Furthermore, from this analysis model, we derived simple analytical expressions that provide estimates for gain and power density reaching free space, aiding in the design of implanted antenna devices.

Room: Maxwell (C2)

CS40a - Novel Antenna Measurement Techniques: Advancements in Design and Evaluation

T08 Fundamental research and emerging technologies/processes / Convened Session / Measurements

Chairs: Dennis Lewis (Boeing, USA), Janet O'Neil (ETS-Lindgren, USA)

8:00 Time-Domain FMCW-Radar Measurement in a Reverberation Chamber

Antonius Johannes van den Biggelaar (ANTENNEX, The Netherlands); Roel X.F. Budé (Eindhoven University of Technology, The Netherlands); Anouk Hubrechsen (Eindhoven University of Technology & AntenneX B. V., The Netherlands)

This work shows preliminary results of over-the-air measurements of a 60 to 64 GHz FMCW radar module. The results are acquired in the time domain using an oscilloscope and a reverberation chamber. It is shown that this chamber is suited for measuring metrics such as the power spectral density, spectrogram, output power, ramp rate and chirp duration. The speed, accuracy, insensitivity to positioning, and not having to rely on control signals to the radar module makes this an effective approach for measuring FMCW radars.

TUESDAY

8:20 Analysis of Vehicle Body Impact on Antenna Pattern and Effective Antenna Aperture for Full Vehicle Antenna Testing

Ya Jing (Keysight Technologies, China); Rui Chen, Xin Yang and TingTing Tao (China Automotive Engineering Research Institute, China); Ziquan Bai (Keysight Technologies, China)

Measuring the performance of vehicle-mounted antennas has been a growing demand with the rapid evolution of vehicular wireless communication technologies. Because the antenna performance is impacted by its installation position and vehicle body, the large electrical size of the vehicle makes the testing of such a system challenging. One interesting question from the vehicle industry is the effective antenna aperture and acceptable test range, which can satisfy the full vehicle antenna test requirement. Following the two test range acceptance criteria proposed in the 5G Automotive Association (5GAA) Technical Report, this paper analyzes the acceptable test range and its corresponding effective antenna aperture for full vehicle antenna testing based on Electromagnetic (EM) simulation of one kind of 4G communication antenna and measurement of one real car's Global Navigation Satellite System (GNSS) antenna in a full vehicle anechoic chamber.

8:40 Localization of Defects on Large Antennas Utilizing Sparsity and Spectral Filtering

Jonas Tiede, Alexander H. Paulus and Uwe Siart (Technical University of Munich, Germany); Thomas F. Eibert (Technical University of Munich (TUM) & Chair of High-Frequency Engineering (HFT), Germany)

Reconstructed equivalent currents on the surface of an antenna under test (AUT) can indicate local defects of the antenna structure. An accurate analysis of electrically large AUTs commonly requires a large number of potentially redundant measurement samples causing prolonged acquisition times. We combine the prior knowledge of sparsely localized defects with the pronounced directivity of large antennas. Employing local basis functions, the difference of the equivalent sources of the AUT with and without defects can be expected to be sparse. Cognizant of the large directivity of the AUT, we additionally employ spectral filtering of the radiated far field in the reconstruction process. Measurement results indicate the potential to significantly reduce the required number of samples while retaining reasonably accurate diagnostic information. A reduction of the number of measurement samples from 16960 to 3000, i.e., by more than 80 percent, has been achieved with a real-world setup.

9:00 Expansion of an Incident Field by Means of Vectorial Spherical Harmonics - Analysis in Terms of Active and Reactive Powers

Anne-Laure Vergnes (Université de Toulouse & ENAC, France); Alexandre Chabory, Rémi Douvenot, Lucille Kuhler and Christophe Morlaas (ENAC, France); Nicolas Mezieres (Centre National d'Etudes Spatiales, France); Pouliguen Philippe (DGA, France)

In this article, the coefficients of the spherical expansion of an incident plane wave on an empty sphere are analyzed in terms of active and reactive powers. These coefficients derive from the expansion of the field by means of the vectorial spherical harmonics (VSH), which is the formulation commonly used in the antenna domain. This expansion leads to an infinite number of non-negligible active power normalized coefficients. On one hand, the associated active power increases with respect to the degree of the coefficient. On the other hand, the reactive power is weak when the degree is small and strong when the band-limit is reached. Therefore the use of VSH normalization may cause issues when spherical harmonics are involved on the processing of antenna radiation patterns.

9:20 Multi-Frequency Compressed Sensing for Spherical Antenna Measurements

Nicolas Mezieres (Centre National d'Etudes Spatiales, France); Laurent Le Le Coq (University of Rennes 1 & IETR, France); Gwenn Le Fur (CNES, France)

This paper focuses on a multi-frequency approach based on compressed sensing for the characterization of radiation pattern of antennas. It relies on a matrix formulation allowing to solve for the spherical wave expansion coefficients at all measured frequencies simultaneously. The proposed method is shown to be as efficient and accurate as the standard one or even leading to improvements through validation on simulation and measurement data.

Room: Oliner (C3) — CS26a - Small Antennas: From Theory to Applications

T01 Sub-6 GHz for terrestrial networks (5G/6G) / Convened Session / Antennas

Chairs: Miloslav Capek (Czech Technical University in Prague, Czech Republic), Christophe Delaveaud (CEA-LETI, France)

8:00 Electrically Small Unidirectional Mixed-Multipole Antennas: Recent Advances and Their Applications

Ming-Chun Tang, Yi-Lin Lang and Mei Li (Chongqing University, China); Richard W Ziolkowski (University of Arizona, USA)

This paper reviews recent advances in and applications of electrically small unidirectional mixed-multipole antennas (ES-UMMAs), with a focus on notable improvements in bandwidth and directivity. The bandwidth enhancement methodologies applied to ES Huygens dipole antennas (HDAs), which are the lowest order UMMAs, are based on near-field resonant parasitic (NFRP) grid-shaped elements that act as electric dipoles and interdigitated capacitor (IDC) loaded loops that act as magnetic dipoles. Directivity enhancements include the realization of a superdirective ES Huygens quadrupole antenna (ES-HQA). These innovative dipole and quadrupole designs have been demonstrated experimentally; they achieve significantly improved performance characteristics over previously reported ES-HDAs. Their recent applications include integration with and direct impedance matching to complex circuits to realize rectennas for wireless power transfer (WPT) systems. Examples include battery-less sensors such as an RFID epidermal skin temperature monitoring tag whose reading range is significantly beyond that of commercially available products.

TUESDAY

8:20 High Realized Gain Compact End-Fire Arrays: A Simple Design Solution

Alessio Tornese (National University of Singapore, Singapore); Antonio Clemente (CEA-Leti, France); Christophe Delaveaud (CEA-LETI, France)

This paper presents a compact end-fire array with a high realized gain, featuring a simple planar design that offers a cost-effective solution for RFID applications and other uses. The synthesis strategy of this supergain array utilizes the Spherical Wave Expansion (SWE) theory. An array prototype consisting of four electrical dipoles spaced at 0.21λ, englobed in a total radiansphere of kr = 2.3, has been analyzed. By applying our optimization method, we demonstrate that tailoring the element feeding leads to significantly higher directivity and improved efficiency compared to conventional compact superdirective arrays. Additionally, the prototype is matched to a standard 50 Ω impedance using a printed T-match at the feeding point. The results demonstrate a notable realized gain exceeding 10 dBi.

8:40 Impact of Reader Sensitivity on Miniaturized Chipless Tag Detection

Adrián Fernández Carnicero (EPFL, Switzerland); German Augusto Ramirez Arroyave (EPFL - École Polytechnique Fédérale de Lausanne & Universidad Nacional de Colombia, Switzerland); Anja K. Skrivervik (EPFL, Switzerland)

This work presents a magnetic near field-based RFID system in which a miniaturized RFID chipless tag of 1.65 mm2 is detected by two RFID readers (#Reader 1 and #Reader 2) of different sensitivity. The two readers are 7.5x7.5 mm2 tunable segmented square loop antennas working in UHF band. However, #Reader 2 presents a better impedance matching and a finer frequency tunability than #Reader 1. Measurements were post-processed using frequency sweep envelope (FSE) method and the RFID chipless tag was detected at a maximum distance of 6.5 mm with #Reader 1 and at 11 mm in the case of #Reader 2. In this way, it is proved that a RFID reader with higher sensitivity in frequency and magnitude allows to detect RFID chipless tags at longer distances.

9:00 The Concept of Recoverable Energy Applied to Small Antennas

Guy Vandenbosch (Katholieke Universiteit Leuven (KU Leuven), Belgium)

In this paper the concept of recoverable energy, a concept recently introduced in electromagnetics, is applied to small radiating systems. Recoverable energy has a very clear physical definition, and in many cases has proven to be equal to the mystical concept of stored energy of a system. Since recoverable energy can be completely and rigorously derived from the system impedance, it is extremely interesting to study the link between the MacLaurin series of an impedance, describing the low frequency behavior, and recoverable energy. As shown in this paper, this can be done in several ways, based on several approximating models for the low frequency system impedance.

9:20 Systematic Method to Design Filtering Patch Antennas

Riku Kormilainen (Radientum Oy, Finland); Anton Helin and Anu Lehtovuori (Aalto University, Finland); Ville Viikari (Aalto University & School of Electrical Engineering, Finland)

We introduce a novel low-profile filtering patch antenna and a method to design it. A single radiating patch is divided into several interconnected elements with each element having a connection to the antenna ground plane as well. The antenna structure is first modeled as a multi-port element and then reduced to a single-feed antenna. In practice, the interconnections between the elements are implemented with discretized components, such as lumped elements and open/short connections. One element acts as an exciter while the remaining elements are loaded reactively. The appropriate reactive loads are found by using a genetic algorithm. The method is demonstrated by designing a patch antenna having a reasonable bandwidth and filtering characteristics, both of which are comparable to other works.

Room: Kraus (C4)

CS67a - Joint Communication and Sensing: from EM modelling to application

T04 RF sensing for automotive, security, IoT, and other applications / Convened Session / Propagation

Chairs: Raffaele D'Errico (CEA, LETI & Université Grenoble-Alpes, France), Claude Oestges (Université catholique de Louvain, Belgium)

8:00 Second Order Statistics of Sub-THz Communications and Sensing Channels

Jiri Blumenstein (Munich Research Center, Huawei Technologies Duesseldorf GmbH, Munich, Germany); Tommaso Zugno and Mate Boban (Huawei Technologies Duesseldorf GmbH, Germany)

We present a ray-tracing-based study on the second-order statistics of sub-THz indoor channels in an industrial environment. The accuracy of the ray- tracing tool has been validated through several extensive measurement campaigns. We report Root mean square (RMS) delay spreads ranging from 8 ns to 55 ns and the correlation bandwidth (BW) span from 20 MHz to 120 MHz. Also, we investigate an Integrated Sensing and Communication (ISAC) scenario, where we sepa- rately evaluate the path loss of Multipath Components (MPCs) interacting with the sensed target and those that do not. We show separate statistics for Line-of-sight (LOS) and Non-line-of-sight (NLOS) channels, compare directive and omni-directional antenna setups and con- sider two different clutter densities within the scene as defined by 3GPP. The generated channel statistics can serve as a baseline for analytical and simulation-based performance evaluation of THz communications systems in industrial settings.

TUESDAY

8:20 State of the Art on Stacked Intelligent Metasurfaces: Communication, Sensing and Computing in the Wave Domain

Marco Di Renzo (CentraleSupelec-University, France)
Stacked intelligent metasurface (SIM) is an emerging technology that capitalizes on reconfigurable metasurfaces for several applications in wireless communications. SIM is considered an enabler for integrating communication, sensing and computing in a unique platform. In this paper, we offer a survey on the state of the art of SIM for wireless communications.

8:40 Multipath Component Estimation with Hybrid Beamforming mmWave Architectures

Nigus Yirga Shimuye (Universite Libre de Bruxelles, Belgium); Claude Oestges (Université catholique de Louvain, Belgium); Amélia Struyf (Université Libre de Bruxelles, Belgium); François Quitin (Université libre de Bruxelles, Belgium)
The accurate estimation of multipath components in hybrid beamforming millimeter-wave systems is challenging due to limited spatial channel information and multiple beamforming sidelobes. High-resolution antenna array algorithms like SAGE and MUSIC, which typically rely on baseband signals from individual antennas, are impractical for architectures with fewer RF chains. This paper proposes a signal model that leverages baseband signals from multiple beam-steering directions to overcome hardware limitations. By adapting the SAGE and MUSIC algorithms to exploit joint transmitter (Tx) and receiver (Rx) beam-steering direction baseband signals, we achieve effective multipath component parameter estimation. Monte Carlo simulations at 28 GHz show that both algorithms demonstrate strong performance, with the majority of absolute angular errors falling below 10 degrees. While MUSIC achieves higher precision under certain conditions, its computational time increases with finer beamsteering resolution. In contrast, SAGE offers a more computationally efficient and robust solution, with a slight tradeoff in precision.

9:00 Simultaneous Communications and Sensing with Hybrid Reconfigurable Intelligent Surfaces

Ioannis Gavras and George C. Alexandropoulos (National and Kapodistrian University of Athens, Greece)
Hybrid Reconfigurable Intelligent Surfaces (HRISs) constitute a new paradigm of truly smart metasurfaces with the additional features of signal reception and processing, which have been primarily considered for channel estimation and self-reconfiguration. In this paper, leveraging the simultaneous tunable reflection and signal absorption functionality of HRIS elements, we present a novel framework for the joint design of transmit beamforming and the HRIS parameters with the goal to maximize downlink communications, while simultaneously illuminating an area of interest for guaranteed localization coverage performance. Our simulation results verify the effectiveness of the proposed scheme and showcase the interplay of the various system parameters on the achievable Integrated Sensing and Communications (ISAC) performance.

9:20 Leveraging Beam-Level RSRP of 5G mmWave Signal for Indoor Passive Crowd Counting

Nopphon Keerativoranan and Hang Song (Institute of Science Tokyo, Japan); Hsueh Han Wu, Saurabh Verma and Daisuke Ichihashi (Rakuten Mobile, Inc, Japan); Kelvin Cheng (Rakuten Institute of Technology & Rakuten Mobile, Inc., Japan); Junichi Takada (Institute of Science Tokyo, Japan)
Crowd counting estimation are crucial for applications such as intrusion detection, event crowd control, and retail staffing optimization. Traditional visual-based systems, while effective, are limited by challenges in low-light conditions, privacy concerns, and restricted field-of-view. RF-based approaches offer a non-intrusive alternative but struggle with defining coverage zones and update rates. This work explores the use of 5G mmWave signal to address these issues, leveraging beam-level reference signal received power (RSRP) for crowd monitoring. Using a fingerprinting approach and K-nearest neighbor classifier with additional beam-level RSRP process, this work comprehensively evaluates the crowd counting performance with the crowd up to five walking individuals in indoor office. The results demonstrated the feasibility of using commercial 5G mobile communication system for passive indoor crowd counting.

Room: Munch (23)

Industrial Workshop

IW5 - ETS-Lindgren - Emerging 5G Test Methodologies to Efficiently and Cost-Effectively Validate Antenna Performance

TUESDAY

Chair: Rafael F. S. Caldeirinha (Polytechnic Institute of Leiria & Instituto de Telecomunicações, Portugal), Stephen Pistorius (University of Manitoba, Canada)

8:00 Material Characterization Using Waveguide Measurement Technique for the Development of Textile Antennas

Verena Marterer (OTH Regensburg, Germany); Franz-Xaver Muhr (Ostbayerische Technische Hochschule Regensburg, Germany); Radek Soukup (University of West Bohemia, Czech Republic); Susanne Hipp (OTH Regensburg, Germany); Tomas Blecha (University of West Bohemia, Czech Republic)

Significant advances in using conductive textiles have been made over the past two decades, particularly in knitted fabrics. The aim is to deepen understanding of how knitted structures, especially those with hybrid yarns containing fine conductive elements (microwires), interact with electromagnetic fields. To establish simulation models that align with subsequent measurements, it is crucial to determine the dielectric properties, specifically relative permittivity and loss tangent/conductivity. This research investigates whether knitted structures with hybrid yarns exhibit anisotropic permittivity, meaning different dielectric properties along orthogonal axes within the fabric plane. These properties were measured using a waveguide technique, whereby the structures were rotated by 90° to observe changes. The results demonstrate that the knitted structure exhibits metallic-like reflective behavior in one direction, while rotation leads to dielectric material characteristics. This effect is influenced by the number of conductive microwires and the materials used for these wires, such as silver-plated copper or bronze.

8:20 A Method for the Dielectric Characterization of Liquids Combining Power Laws of Absorbent-Liquid Mixtures

Sergio López-Soriano and Mohammed Ahmed Alsultan (Universitat Oberta de Catalunya, Spain); Joan MeliàSeguí (Universitat Oberta de Catalunya (FUOC), Spain); Pol Brunet (Universitat Oberta de Catalunya, Spain)

This contribution proposes a method for determining the dielectric properties of a liquid under test (LUT) from the S-Parameters measurements of a microstrip transmission line (TL). The TL is mounted on an absorbent substrate that can be filled with different LUTs. The proposed method uses the TL method for measuring the dielectric properties of the combination of the absorbent substrate and the LUT. The LUT complex permittivity is estimated by combining two mixing rules: one describing the relationship of the absorbent and a known fluid (air) with the union of both, and the other one describing the relationship of the absorbent and the LUT with the union of both. Results show that the proposed method enables the dielectric characterization of liquids achieving an average accuracy of 97.62% and 59.64% in the estimation of the LUT relative permittivity and the loss tangent, respectively, compared to the values found in the literature.

8:40 A Protocol for the Electromagnetic Characterization of Dielectrics and 2-D Materials Through Terahertz Time-Domain Spectroscopy in Reflection Mode

Walter Fuscaldo (Consiglio Nazionale delle Ricerche (CNR), Italy); Francesco Maita (IMM-CNR, Italy); Luca Maiolo and Dimitrios Zografopoulos (CNR-IMM, Italy)

Terahertz time-domain spectroscopy in reflection mode has been recently proven to be an effective technique for the nondestructive, contactless characterization of the electromagnetic properties of materials. In this work, we provide an overview of the methods that we have developed so far for characterizing the generally complex permittivity and conductivity of bulk and two-dimensional materials. Experimental results are reported for two considerably different examples such as the retrieval of the complex permittivity of a silica substrate and the sheet resistance of a thin titanium layer on a cyclo-olefin substrate.

9:00 Measurement and Modelling of Dielectric Properties of Building Materials at Sub-THz Frequencies

Valeri Mikhnev (CENTERA Labs., Institute of High Pressure Physics, Polish Academy of Sciences, Poland); Dmytro B. But (CENTERA LAboratory, Institute of High Pressure Physics PAS, Poland & V. Ye. Lashkaryov Institute of Semiconductor Physics NASU, Ukraine); Tommaso Zugno and Mate Boban (Huawei Technologies Duesseldorf GmbH, Germany); Joseph Eichinger (Huawei Technologies Duesseldorf GmbH, European Research Center (ERC), Germany); Wojciech Knap (Université Montpellier, CNRS, France)

Due to the large available bands and specific propagation characteristics, terahertz communication systems hold the promise of providing high throughput and low latency communications. For the accurate modelling of THz channels in indoor communications environments, the precise knowledge of the dielectric properties of common building materials is essential. In this paper we present a measurement setup based on state-of-the-art frequency-domain spectroscopy system. For accurate characterization of the material properties, custom beam-guide fixture and signal processing technique were developed. Preliminary tests carried out with samples of well-known dielectric materials proved a good measurement accuracy. Further, we performed measurements of glass and ceiling board samples in the frequency band of 100 to 400 GHz. Using our measurements, we extended the model in ITU recommendation by deriving custom parameters to describe the dielectric behavior of these materials. The outcomes of this study can improve the deterministic modelling of wireless channels at sub-THz frequencies.

TUESDAY

9:20 Relative Permittivity Extraction of 3D Printed Samples Using Fast-Prototyped Waveguide Standards

Saúl Santos Carvalho (Polytechnic of Leiria, Portugal & Instituto de Telecomunicações, Portugal); João Ricardo Reis (Instituto de Telecomunicações and Polytechnic Institute of Leiria, Portugal); Rafael F. S. Caldeirinha (Polytechnic Institute of Leiria & Instituto de Telecomunicações, Portugal)

This paper presents an alternative approach to extract the relative permittivity of dielectric materials utilising the waveguide method, by using fast-prototyped 3D-printed waveguide standards. The standards have been fabricated by traditional 3D printing methods and were used to measure the relative permittivity of dielectric samples at C-band (4-6 GHz) and K-band (18-20 GHz). The study evaluates standard laminates such as, FR4 and low-loss (e.g. Rogers) substrates, but also multiple 3D printed materials, comparing their dielectric properties against reference values from literature. Although measurement results obtained from several material samples show comparable relative permittivity values to those from existing literature, higher loss tangent values were observed. Such effect is sought to be associated to surface irregularities and interface mismatches of the printed waveguide standards. These findings underscore the potential of using 3D printing techniques for cost-effective dielectric property assessment while highlighting the need for careful consideration of anomalies in loss measurements.

Room: Mosig (26)

Scientific Workshop

SW5a - Stand on the IEEE Antennas & Propagation Standards

Room: Collin (27)

P02a - Ray tracing channel simulation

T07 Electromagnetic modelling and simulation tools / / Propagation

Chair: Conor Brennan (Dublin City University, Ireland), Mengting Li (Aalborg University, Denmark)

8:00 Accuracy Improvement of Ray-Tracing-Based Received Power Prediction in Office Environments

Azril Haniz and Hirokazu Sawada (National Institute of Information and Communications Technology, Japan); Takeshi Matsumura (National Institute of Information and Communications Technology (NICT), Japan & Kyoto University, Japan)

Ray-tracing (RT) generally suffers from errors in the calculated received power especially at low frequencies where objects may be on the same order or smaller than the wavelength due to the high-frequency approximation used. Previously, an algorithm to reduce this error by attenuating the calculated received power depending on the object size with respect to wavelength was proposed and evaluated in an industrial environment. In this paper, we verified that the proposed algorithm can be applied not only to factory environments but also to other environments such as office environments. The adjusted received power was compared with measured received power at 922 MHz, 4850 MHz, and 28.35 GHz bands taken in an office environment. Results show that the proposed algorithm could reduce the RMSE of received power calculated by RT from 14.1 dB, 7.5 dB, and 4.1 dB to 9.0 dB, 5.3 dB, and 3.7 dB for each frequency, respectively.

8:20 Impact of Beamforming on Electromagnetic Field Exposure with Ray-Launching Simulations

Xueyun Long, Mario Pauli and Yueheng Li (Karlsruhe Institute of Technology, Germany); Thomas Zwick (Karlsruhe Institute of Technology (KIT), Germany)

In this paper, the impact of beamforming at base stations (BSs) on electromagnetic field (EMF) exposure is assessed using a GPU-based ray-launching (RL) tool in 3D urban environments. Beamforming enables the concentration of power towards user equipment (UE), which may lead to increased EMF exposure. To address EMF safety concerns, deterministic channel simulations are conducted, enabling beamforming operations and providing reliable predictions. A newly developed least-time shooting and bouncing ray (SBR) algorithm is implemented in the RL tool. Compared to a validated ray-tracing (RT) tool, the new algorithm identifies multipaths accurately while operating hundreds of times faster. Measurements were conducted to verify the simulations, however, they fall outside the scope of this paper. Beamforming is applied to multiple BSs, with power control to minimize EMF exposure while maintaining a required data rate. The results provide insights for optimizing the trade-off between data rate, EMF exposure, and energy consumption.

8:40 Interpolation of Reflected and Diffracted Rays for Accelerated Ray Tracing Simulation

Conor Brennan (Dublin City University, Ireland); Allan Mbugua and Yun Chen (Huawei Technologies Duesseldorf GmbH, Munich Research Center, Germany); Sajjad Hussain (National University of Sciences and Technology, Pakistan)

The problem of efficiently computing an image-based ray-trace for a receiver moving along a linear trajectory in an urban area is considered. The requirement to sample channel information at the Nyquist rate or higher imposes a considerable computational burden. The proposed algorithm instead makes use of the fact that such receivers will move in and out of well-defined finite illumination regions within which reflected and diffracted rays can potentially propagate. Rather than computing an independent ray trace for each receiver location within such regions a simple model for the associated ray is created. This model is based on field information computed at a finite set of locations within the region which is then interpolated to efficiently give amplitude and phase data along the trajectory. The paper demonstrates the effectiveness of this operation within a simulated street canyon environment.

TUESDAY

9:00 Comparing Differentiable and Dynamic Ray Tracing: Introducing the Multipath Lifetime Map

Jérome Eertmans (UCLouvain, Belgium); Enrico M. Vitucci and Vittorio Degli-Esposti (University of Bologna, Italy); Laurent Jacques (University of Louvain, Belgium); Claude Oestges (Université catholique de Louvain, Belgium)

With the increasing presence of dynamic scenarios, such as Vehicle-to-Vehicle communications, radio propagation modeling tools must adapt to the rapidly changing nature of the radio channel. Recently, both Differentiable and Dynamic Ray Tracing frameworks have emerged to address these challenges. However, there is often confusion about how these approaches differ and which one should be used in specific contexts. In this paper, we provide an overview of these two techniques and a comparative analysis against two state-of-the-art tools: 3DSCAT from UniBo and Sionna from NVIDIA. To provide a more precise characterization of the scope of these methods, we introduce a novel simulation-based metric, the Multipath Lifetime Map, which enables the evaluation of spatial and temporal coherence in radio channels only based on the geometrical description of the environment. Finally, our metrics are evaluated on a classic urban street canyon scenario, yielding similar results to those obtained from measurement campaigns.

9:20 Comparative Analysis of Ray Tracing and Rayleigh Fading Models for Distributed MIMO Systems in Industrial Environments

Aymen Jaziri (SIRADEL, France); David Demmer (CEA-LETI, France); Yoann Corre (SIRADEL, France); Jean-Baptiste Doré (CEA-LETI, France); Didier Le Ruyet, Hmaied Shaiek and Pascal Chevalier (CNAM, France)

This paper presents a detailed analysis of coverage in a factory environment using realistic 3D map data to evaluate the benefits of Distributed MIMO (D-MIMO) over colocalized approach. Our study emphasizes the importance of network densification in enhancing D-MIMO performance, ensuring that User Equipment (UE) remains within range of multiple Access Points (APs). To assess MIMO capacity, we compare two propagation channel models: ray tracing and stochastic. While ray tracing provides accurate predictions by considering environmental details and consistent correlations within the MIMO response, stochastic models offer a more generalized and efficient approach. The analysis outlines the strengths and limitations of each model when applied to the simulation of the downlink (DL) and uplink (UL) singleuser capacity in various D-MIMO deployment scenarios.

Tuesday - 9:40-10:10

Room: EurAAP booth — **Mentoring at the EurAAP booth**

Tuesday - 10:10-11:50

Room: Alfvén (A3 + A4) — **A06b - Advances in Lens Antennas I**

T02 Millimetre wave and THz for terrestrial networks (5G/6G) / / Antennas

Chairs: Marta Martínez-Vázquez (Renesas Electronics, Germany), Eva Rajo-Iglesias (University Carlos III of Madrid, Spain)

10:10 Integrated Lens Antenna with Strong Illumination of the Critical Angle and the Validity of Physical Optics Approximation

Dunja Lončarević, Huasheng Zhang, Andrea Neto and Nuria LLombart (Delft University of Technology, The Netherlands)

Analysing an integrated lens antenna with strong illumination of the critical angle, this contribution investigates the validity of Physical Optics (PO) approximation that sets the transmitted field to zero beyond the critical angle. A comparative study between PO and full-wave simulations using CST Studio Suite is conducted, demonstrating that CST predicts higher directivity and gain than PO. The observed discrepancies are attributed to the neglect of the transmitted field beyond the critical angle in the PO method. Additionally, a lens prototype operating at 180 GHz was fabricated and measured. The measurement results are compared to PO predictions, revealing similar trends as in the CST comparison, particularly a noticeable difference in the main beam width and a 2 dB difference in gain. Additionally, the measured radiation patterns exhibit a clean profile with low side lobes, highlighting the design potential of integrated lenses with strongly illuminated critical angle.

10:30 A Comparative Study on Ray-Tracing and Physical-Optics Methods for the Analysis of Transmitarray Antennas

Andrea Tummolo (Université de Rennes, France); Orestis Koutsos (CEA Leti, France); Francesco Foglia Manzillo (CEA-LETI, France); Antonio Clemente (CEA-Leti, France); Ronan Sauleau (University of Rennes 1, France)

This study compares the accuracy of two semi-analytical methods based on ray tracing(RT) and physical optics(PO) for the analysis and design of transmitarrays of different sizes, considering several focal-to-diameter ratios and eight unitcells realizing a 3-bit uniform phase quantization at 30 GHz. The results, validated by full-wave simulations, demonstrate that both RT and PO yield excellent agreement in standard-profile configurations. However, the RT approach, which assumes the transmitarray to be in the far-field of the primary feed, provides a wrong evaluation of the gain of lowprofile antennas, with errors up to 1.5dB at 34 GHz. Conversely, PO accounts for near-field effects and accurately predicts the transmitarray performance even when the focal distance is comparable to the wavelength. Moreover, it is shown that the PO method enables the analysis of very large antennas with a computational time similar to that of RT (about 4 minutes for transmitarray diameters of 30 wavelengths).

10:50 Performance Enhancement of a Si Hemispherical Lens Using a Coating Layer for 300 GHz Frequency Band

Umair Rafique, Kimmo Rasilainen, Jiangcheng Chen, Marko E Leinonen and Aarno Pärssinen (University of Oulu, Finland); Ping Jack Soh (University of Oulu & Katholieke Universiteit Leuven, Finland)

To enhance the radiation characteristics of an on-chip antenna, in this paper, a silicon (Si) extended hemispherical dielectric lens antenna is designed with a coating layer for sub-terahertz (sub-THz) applications. First, to prove the concept, the coated Si lens is illuminated using a dielectric-filled WR-3.4 waveguide. From the simulations, it is observed that the designed coated lens offers better radiation characteristics compared to a non-coated lens in the frequency range of 220-330 GHz. In the second phase, an on-chip antenna is used for the lens illumination, which is designed on a high-permittivity silicon germanium (SiGe) dielectric substrate. The results show that the coated Si lens improves impedance matching and radiation performance of the on-chip antenna across the operating band, i.e., 230-360 GHz.

11:10 A Geodesic H-Plane Horn Antenna with Switchable Circular Polarization at Ka-Band

Freysteinn Vidar Vidarsson, Oskar Zetterstrom and Oscar Quevedo-Teruel (KTH Royal Institute of Technology, Sweden)

This paper presents a geodesic H-plane horn antenna with switchable circular polarization. The polarization diversity is realized by stacking two identical geodesic horn antennas and joining them at the aperture using a parallel plate waveguide septum polarizer. Depending on which of the two horns is fed, the antenna can radiate either left-hand or right-hand circular polarization. The proposed antenna operates in the Ka-band, with a center frequency of 30 GHz and a 3 dB axial ratio bandwidth of 15 %.

11:30 Spillover Mitigation Method in Rotman Lens-Based Retrodirective Arrays

Alireza Jahanbakhshi (University of Duisburg Essen, Germany); Navid Amani and Henk Wymeersch (Chalmers University of Technology, Sweden); Daniel Erni and Andreas Rennings (University of Duisburg-Essen, Germany)

This paper presents a new method to compensate for spillover loss in Rotman lens-based retrodirective arrays. The proposed approach aims to minimize the radar cross section (RCS) variation across the full field-of-view (FoV) of ±30 ◦ and the operating bandwidth of 24-24.25 GHz. By proper phase correction transmission line (TL) design at the array side and compensating for phase errors between adjacent beamports, the method significantly reduces the initial RCS variation from 25 dB to 3.2 dB over the 30 ◦ scan angle. The results demonstrate improved performance in maintaining a more uniform RCS across the entire FoV, contributing to enhanced retrodirective array functionality.

Room: Kildal (A2) | **A13b - Antenna Arrays for space applications**

T03 Aerospace, space and non-terrestrial networks / / Antennas

Chairs: David B Davidson (Curtin University, Australia & Stellenbosch University, South Africa), Dirk Heberling (RWTH Aachen University, Germany)

10:10 A Metasurface-Loaded ±80°-Scanning Phased Array Antenna with Active VSWR ≤ 2 for SATCOM Applications

Jianping Zeng, Chenhao Chu, Tzu-Yuan Huang and Hua Wang (ETH Zurich, Switzerland)

A Ku-band dual-polarized metasurface-loaded stacked patch phased array antenna is proposed. The hexagonal lattice and dual polarization are optimized to increase the directivity and system communication capacity, respectively. The metasurface realized with four symmetrical split ring unit cells introduces additional magnetic dipole modes to improve active impedance matching and broaden scanning range across all azimuth planes. A probe-direct-fed stacked patch antenna without blind vias is designed to enhance bandwidth and simplify the PCB stackup. To validate the concept, the metasurface and a 4 × 4 array are fabricated and tested. Both simulated and measured results demonstrate a ultrawide-angle scanning of ±80° and a broad bandwidth of 13.4–14.7 GHz (covering the full transmitter band for Ku-band SATCOM ground terminals) with active voltage standing wave ratio (VSWR) ≤ 2, representing a significant improvement over conventional dielectric superstrate loading.

10:30 Uniform Linear Arrays with Hybrid Beamforming: To Overlap or Not to Overlap?

Margaux Pellet, George Goussetis and Joao Mota (Heriot-Watt University, United Kingdom); Hervé Legay (Thalès Alenia Space, France); Giovanni Toso (European Space Agency, ESA ESTEC, The Netherlands); Piero Angeletti (European Space Agency, The Netherlands)

Overlapping strategies for hybrid beamformed direct radiating arrays have been studied in the past decades as a means to improve the gain of a directive beam. It is widely known that overlapping subarrays guarantees the suppression or the partial mitigation of some unwanted grating lobes. However, such techniques come with a cost, either in terms of hardware or in terms of digital complexity. Performance-wise, the overlapping strategies have also shown particular cases where the scanning improvements were not evident. This paper presents a study of the general overlapping principles in hybrid analogue-digital beamformed direct radiating arrays for the case of a GEO satellite application. This study allows to identify cases where the overlapping technique is beneficial compared to a non-overlapped array.

10:50 Analysis and Design of Large Array Antennas Using a Fast Direct Solver

Min Zhou, Martin Haulund Gæde, Søren Hartmann, Pasquale Giuseppe Nicolaci, Michael F. Palvig, Niels Vesterdal, Magnus Brandt-Møller, Asger Limkilde, Edoardo Baldazzi and Erik Jørgensen (TICRA, Denmark); Giovanni Toso (European Space Agency, ESA ESTEC, The Netherlands)

This paper presents the application of TICRA's recent full-wave analysis advancements for antenna arrays, with a particular emphasis on the use of the Fast Direct Solver (FDS). We showcase the effectiveness of this method through real-world examples, including a 10×10 spline horn array, a 218 circular horn array, and a 25×25 microstrip patch array. The results demonstrate that the FDS-based approach offers significant improvements in efficiency and memory usage compared to traditional methods.

11:10 Conformable, Foldable and Deployable Lightweight Antenna Array Using CCPF and Mylar Film

Mohammad Ameen and Koen Mouthaan (National University of Singapore, Singapore)

A highly conformable, foldable, and deployable single antenna and its 2×2 array configuration are presented. The antenna is lightweight by combining copper-cladded polyimide film (CCPF), Mylar transparent film, and polyethylene foam (PF-4) strips. A single conformable and foldable antenna (SCFA) at L-band is presented, which can be completely conformed to a cylinder with radius Rc = 40 mm. The SCFA is used to design a 2×2 array, which is completely foldable to 360 degree. The antenna provides an impedance bandwidth from 1.20-1.32 GHz (9.7%), isolation better than 20 dB between the antenna elements, and a gain of 14.1 dBi at 1.26 GHz. The antenna array is measured for the flat case and conformed to cylinders of radius 200 mm, 160 mm, and 150 mm.

11:30 Development of a Modified Yagi-Uda Antenna Operating in UHF for Communication Systems Embedded onto Nano-Satellites

Magdalena Mbuy Miko Mikue (Universidade Federal Do Pampa, Brazil); Juner M. Vieira (National Institute for Space Research (INPE), Brazil); Edson R. Schlosser and Marcos V. T. Heckler (Universidade Federal do Pampa, Brazil)

This paper presents the results of simulations performed using the Ansys HFSS software for a sequentially rotated 2x2 antenna array model, whose basic element is a modified Yagi-Uda antenna operating at 436.5 MHz. The array will be integrated onto a 2U CubeSat, with progressive phase shift of 90° between the elements to achieve right-hand circular polarization (RHCP) as the main polarization. The results obtained from the simulations yielded overall better performance in comparison to other miniaturized antenna models found in the literature.

Room: Hallén (BAR5) | **E01b - Electromagnetic theory**

T08 Fundamental research and emerging technologies/processes / / Electromagnetics

Chairs: Ioan E. Lager (Delft University of Technology, The Netherlands), Martin Norgren (KTH Royal Institute of Technology, Sweden)

10:10 The Autocorrelation of the Thermally Induced Currents in Infinite Media

Andrea Neto and Laurens F.E. Beijnen (Delft University of Technology, The Netherlands)

According to our recent modal representation, the origin of thermal radiation can be associated to the distribution of a finite number of current sources, independent one from the other (the Degrees of Freedom). Here we shown that, if one is only interested in the energy radiated, the DoF current sources can be mathematically replaced by much larger number of equivalent sources, that are unphysical, as they are imposed to be uncorrelated at any distance and are distributed all over the volume. The derivation presented here shows explicitly that even the Quantum born, Rytov currents, can be interpreted as mathematically constructed energetically equivalent currents, that have no physical meaning, and whose origin needs to be established.

10:30 Substrate Integrated Waveguide Wide-Band Notch Filter Based on Second-Order Mode Cancellation

Navid Razi (University of Wuppertal, Germany); Nooshin Feiz (Wuppertal University & APTIV, Germany); Pedram Ghasemian (Bergische Universität Wuppertal, Germany); Dennis Vollbracht (Aptiv Services Deutschland GmbH, Germany); Markus Clemens (University of Wuppertal & Chair of Electromagnetic Theory, Germany)

The paper presents a promising filtering method for the cancellation and suppression of dominant mode propagation in Substrate Integrated waveguide structures through the out-of-phase cancellation of the first and second resonance modes. This method achieves a high selectivity by using only two-step coupled resonating cavities, which enhance both stop-band and pass-band bandwidth and selectivity by employing cavities of different internal sizes. Additionally, positioning a row of inductive vias between the two cavities brings the second resonance closer to the first resonance in the stop-band region by modifying the transmission zeroes, resulting in a significant increase in the stop-band bandwidth. The proposed filter demonstrates an insertion loss of less than 0.7 dB, a return loss exceeding 20 dB, and a 6 GHz bandwidth for both pass and stop-bands

TUESDAY

10:50 On Characteristic Modes in the Presence of a Grounded Dielectric Slab

Adrian Mrochen and Leonardo Mörlein (Leibniz Universität Hannover, Germany); Dirk Manteuffel (University of Hannover, Germany)

In this work, the characteristic modes of a perfectly electrically conducting scatterer in the presence of a lossless grounded dielectric slab are investigated. The orthogonality properties of the far fields of the characteristic modes are discussed in terms of space wave and surface wave far fields. Then, the resonance behavior of the characteristic modes is examined under variation of dielectric permittivity, dielectric slab thickness and frequency. As it turns out, the far field orthogonality of lossless systems still holds true overall, but it must be distinguished between space wave and surface wave fields. Also, the resonance behavior can be systematically explained using knowledge from patch antennas and geometrical optics.

11:10 On the Implied Approximations Appearing in Simplified Emissivity for the Investigation of the Thermal Emission from Dense Media

Laurens F.E. Beijnen and Andrea Neto (Delft University of Technology, The Netherlands)

According to our recent modal representation, the origin of thermal radiation can be associated to the distribution of a finite number of current sources, independent one from the other (the Degrees of Freedom). Here we shown that, if one is only interested in the energy radiated, the DoF current sources can be mathematically replaced by much larger number of equivalent sources, that are unphysical, as they are imposed to be uncorrelated at any distance and are distributed all over the volume. The derivation presented here shows explicitly that even the Quantum born, Rytov currents, can be interpreted as mathematically constructed energetically equivalent currents, that have no physical meaning, and whose origin needs to be established

11:30 The Richmond-Marcuvitz Theory for Cascaded Impedances in Radial Lines

Giuseppe Labate and Cristina Yepes (TNO, The Netherlands); Stefania Monni (TNO Defence Security and Safety, The Netherlands); Bastiaan Florijn (TNO, The Netherlands); Giampiero Gerini (TNO - Defence, Security and Safety, The Netherlands)

Using standard Mie theory, the computational complexity increases for multilayer systems with the number of layers, limiting the factor to maximum two or three shells. Here, we break this limit for any arbitrary number of layers, by reformulating 2D Mie theory in terms of cascaded radial transmission lines. Exploiting a recursive method, developed in 1965 by Richmond [1], who expanded the fields in radial lines as unknown Bessel and Neumann functions, we first reformulate the problem as proposed by Marcuvitz in terms of Hankel functions, associating a physical meaning of traveling waves along the radial lines. In addition, we include at each interface an impedance sheet, generalizing the recursive method useful for mantle scattering cancellation. By manipulating the scattering with additional surface admittances/impedances at every boundary, a theoretical formulation is reported and validation with a commercial software for metallic cylinders cladded with several dielectric layers and impedance sheets is highlighted.

Room: Marcuvitz (M3)

CS13b - Advances in Channel Sounding and Measurements for 6G: From cm-Wave to sub-THz

T07 Electromagnetic modelling and simulation tools / Convened Session / Propagation

Chairs: Diego Andrés Dupleich (Technische Universität Ilmenau, Germany & Fraunhofer Institute for Integrated Circuits IIS, Germany), Wei Fan (Southeast University, China)

10:10 Performance and Feasibility Analysis of a Channel Sounding Based Massive MIMO Channel Model

Joonas Kokkoniemi and Chathuri Weragama (University of Oulu, Finland); Pekka Kyösti (Keysight Technologies & University of Oulu, Finland); Markku Juntti (University of Oulu, Finland)

The high millimeter wave frequencies (100 - 300 GHz) have retained their interest in the scientific community for various high data rate applications, such as front- and backhaul networks. The high path losses at these frequencies require utilization of very large antenna gains. Large arrays are a natural way to generate antenna gain and allow degrees of freedom in beamforming at the same time, as well as they allow multiple-input multiple-output (MIMO) access methods. This paper analyses a newly developed MIMO channel model for 140 GHz. The results show that as expected based on the literature, the channels are quite sparse. Interestingly, optimal power allocation uses only few of the available degrees of freedom. This is mostly attributed to the high losses in the channel. Still, the channel ranks theoretically allow large numbers parallel channels, albeit using them all would not always be energy optimal.

10:30 Building Penetration Loss Measurements and Modeling from Cm-Wave to Sub-Terahertz Bands

Minoru Inomata, Wataru Yamada and Ryotaro Taniguchi (NTT, Japan); Nobuaki Kuno, Koshiro Kitao, Takahiro Tomie and Satoshi Suyama (NTT DOCOMO, INC., Japan)

As cellular networks move toward 6G, newly exploiting the centimeter wave (cm-wave) and sub-terahertz (THz) bands, the utilization of a combination of multiple frequency bands will be necessary for achieving extremely high-speed and reliable communications. However, the building penetration loss characteristics have not been sufficiently studied in terms of the frequency dependency from the cm-wave to sub-THz bands. We therefore investigated and modeled the building penetration loss characteristics and, as the measurement results indicated a more gradual frequency dependency than the conventional ITU-R model, we opted to build the penetration loss model based on single transmission paths with the lowest transmission loss through multi-layer standard glass. Our findings showed that the RMSE value with the proposed model was improved over the conventional ITU-R model for 26.4-158 GHz bands. We also confirmed the validity of the proposed model from the cm-wave to sub-THz bands.

10:50 Measuring the RCS of Multipoint-Scattering Targets in JCAS Channel Sounding

Camillo Gentile (National Institute of Standards and Technology (NIST), USA); Jack Chuang (NIST, USA); Steve Blandino (National Institute of Standards and Technology, USA); Jelena Senic, Jihoon Bang and Samuel Berweger (NIST, USA)
This paper introduces a methodology for measuring the radar cross-section (RCS) of multipoint-scattering targets in the context of joint communication and Sensing (JCAS) applications. By leveraging the fine resolution of millimeterwave and sub-terahertz radar systems, the proposed approach estimates the location of multiple scattering points on a target and computes their respective RCS values. This enables enhanced target classification and recognition, essential for high-resolution applications such as gesture recognition, indoor localization, and biomedical sensing. A comprehensive calibration procedure ensures accurate RCS estimation by incorporating techniques such as calibration against a metal sphere, background subtraction, and super-resolution. The paper details the use of a 28.5 GHz channel sounder to illustrate the proposed method, highlighting its application in a human gesture JCAS scenario. The results demonstrate the accuracy and potential of this

11:10 Doppler Measurements Inside of Machines for ISAC at Sub-THz in Industrial Scenarios

Diego Andrés Dupleich (Technische Universität Ilmenau, Germany & Fraunhofer Institute for Integrated Circuits IIS, Germany); Jonas Gedschold (Technische Universität Ilmenau, Germany); Alexander Ebert (Fraunhofer IIS, Germany); Mate Boban (Huawei Technologies Duesseldorf GmbH, Germany); Giovanni Del Galdo (Fraunhofer Institute for Integrated Circuits IIS & Technische Universität Ilmenau, Germany)
The utilization of the sub-THz frequency range for industrial applications has gained relevance in the latest years. The free blocks of available spectrum and the need of implementing high gain radio interfaces result in high resolution systems, ideal for sensing applications as well. This contribution shows novel results on ultra wide-band measurements of Doppler and micro-Doppler at 170 GHz inside industrial machines with the objective of characterizing propagation for integrated sensing and communications. The results have shown complex patterns from the interaction of multiplepaths with different typical Doppler signatures.

11:30 On Experimental Analysis of Mono-Static 3D UAV RCS for ISAC Channel Modeling

Zhiqiang Yuan, Le Yu, Chunhui Li and Wei Fan (Southeast University, China)
Realistic modeling of the UAV radar cross section (RCS) is vital for integrated sensing and communication systems to ensure accurate sensing predictions and performance evaluation. Despite advancements in the UAV RCS research, the available experimental data remains insufficient and a realistic model has not yet been established, especially for 3D scenarios. This study presents an experimental analysis and modeling of UAV RCS. First, we conduct mono-static UAV RCS measurements in an anechoic chamber, recording RCS covering frequency band of 1.8~18.2 GHz and azimuth angles of -90 ◦ ~90 ◦ (given the symmetry of the UAV) at three UAV elevation sides {90 ◦ ,0 ◦ ,180 ◦ }. Subsequently, the measured RCS data is fitted using three well-known distributions, Rician, Gamma, and LogNormal. Our analysis reveals the superiority of the Rician distribution in modeling UAV RCS. Furthermore, a statistical assessment of the UAV RCS based on the modeling result is conducted, offering insights for predicting and evaluating the UAV sensing.

Room: Jansson (31)
Scientific Workshop
SW1b - AMTA SW - Reverberation Chambers for Antenna Measurements

Room: Zorn (32)
EurAPP Working Groups
WG ECAP

Room: Björk (33)
Scientific Workshop
SW4b - Emerging Materials for Applied Antenna Engineering: Sensing and Communications

Room: Bergman (34)
Scientific Workshop
SW9 - 3D-printing for high-frequency topologies: advances and challenges

TUESDAY

Chairs: Matthieu Bertrand (Thales Research and Technology, France), Guido Valerio (Sorbonne Université, France)

10:10 H-Band-Multilayer-Waveguide-Using-Glide-Symmetric-EBG

Jorge Martin Villar, Martin Petek and Jorge Tobon (Politecnico di Torino, Italy); Zhongxia Simon He (SINOWAVE, Sweden); Francesca Vipiana (Politecnico di Torino, Italy)
This work presents a fully metallic air-filled multilayer waveguide (MLW), that utilizes a glide symmetric unit cell as electromagnetic band-gap for improving manufacture tolerance. The proposed MLW is designed for the H-band, 220 – 330 GHz, obtaining an insertion losses below 0.4 dB. Additionally, the electromagnetic properties of the used unit cell, in particular its stopband attenuation, are investigated with the multimodal transfer matrix method, to better understand its physics.

10:30 Cost Effective PCB Gap Waveguide Based on Broken Glide Symmetry

Kaan Aktas (Politecnico di Torino, Italy & IMST GmbH, Germany); Martin Petek (Politecnico di Torino, Italy); Enrico Tolin (IMST GmbH, Germany & Politecnico di Torino, Italy); Simona Bruni (IMST GmbH, Germany); Francesca Vipiana (Politecnico di Torino, Italy)
Gap waveguides can provide a cost-effective and low-loss solution for high frequency transmission line technologies. This paper introduces a novel electromagnetic bandgap structure for a gap waveguide operating across the entire E band, targeting automotive radar applications. The proposed concept is compatible with cost-effective FR4-based printed circuit boards, utilizing substrate-integrated hole unit cells. Broken glide-symmetric geometry is adopted in the proposed approach to reach wider stopbands and greater adaptability for larger gap sizes. The final design achieves an average transmission loss of 0.1 dB/cm within the 76 – 81 GHz frequency band.

10:50 Retrieval of Effective Parameters of Periodic Structures Using a Multi-Modal Approach

Moises Tercero (KTH Royal Institute of Technology, Sweden & Thales Research and Technology, France); Francisco Mesa (University of Seville, Spain); Thi Quynh Van Hoang (Thales Research & Technology, France); Matthieu Bertrand (Thales Research and Technology, France); Oscar Quevedo-Teruel (KTH Royal Institute of Technology, Sweden)
We present an extension of the multimodal transfer matrix method applied to the homogenization of periodic structures with arbitrary geometries. Solving the eigenvalue problem of an infinite cascade of layers, a set of eigenvectors is obtained that allows us to calculate the average fields in the periodic structure. From these average fields, the effective constitutive parameters can be obtained by direct use of Maxwell's equations. For illustration purposes, we present the results of the homogenization of a high-permittivity artificial material; nevertheless, this method is general and thus capable of handling other configurations.

11:10 Exploiting Symmetries for the Analysis of Metasurfaces with a Multimodal Approach

Jesus M. Jimenez-Suarez (KTH Royal Institute of Technology, Sweden); Francisco Mesa (University of Seville, Spain); Oscar Quevedo-Teruel (KTH Royal Institute of Technology, Sweden)
We propose an efficient quasi-numerical approach to compute the dispersion diagram of periodic structures with 2-D periodicity when the primitive cell possesses internal symmetries. In this situation, symmetry planes can be imposed and the study of the unit cell can be simplified to several 1-D scenarios resulting from the boundary conditions imposed by the symmetry planes. This approach involves dealing with simpler geometries and is particularly advantageous in terms of CPU effort. Here, the underlying computational method is the multimodal transfer matrix method. This method is used to analyze a square unit cell in parallel plate waveguide whose motif is one circular hole in one plate and two square holes in the other plate.

11:30 Glide Symmetric Corrugated Waveguides Exhibiting Exceptional Points of Degeneracy

Nelson Castro (University Carlos III of Madrid, Spain); Miguel Saavedra-Melo and Filippo Capolino (University of California, Irvine, USA); Eva Rajo-Iglesias (University Carlos III of Madrid, Spain)
The presence of exceptional points of degeneracy (EPD) in rectangular waveguides loaded with glide symmetric corrugations is here studied. Two distinct yet related waveguides are analyzed, each exhibiting different orders of EPDs, allowing for the realization of both a Degenerate Band Edge (DBE) and a Stationary Inflection Point (SIP). These structures demonstrate promising potential for various applications, including solid-state amplifiers and oscillators, electron-beam amplifiers, and oscillators, and true time delay systems for beamforming.

TUESDAY

10:10 Embedded C-Dipole Antenna for the Wireless Monitoring of Abdominal Grafts

Francesca Nanni, Sergio Biondi, Francesco Mancuso, Camilla Medori, Eleonora Oddi and Gaetano Marrocco (University of Rome Tor Vergata, Italy)

Abdominal aortic aneurysms (AAAs) and related vascular conditions often require the implantation of stent grafts to prevent life-threatening complications, such as rupture or internal bleeding, yet the long-term success of these devices can be compromised by issues like endoleaks, thrombosis, and mechanical failure. This paper presents
the design and testing of a wireless RFID-based sensing device integrated into an abdominal graft for real-time monitoring. The system, which includes a miniaturized C-dipole antenna embedded between the stent's metallic rings, leverages battery-free RFID technology for remote data transmission. The proposed approach allows non-invasive, continuous monitoring of the stent graft, reducing the need for costly imaging techniques and hospital visits. The numerical simulations and preliminary tests in a liquid human body phantom show that the device allows a reliable communication link at a depth of 7 cm, and so has the potential to detect complications by leveraging on its sensing capabilities.

10:30 Gastrointestinal Segment Tracking of Ingestible Capsules Using Biodegradable Superstrates

Azar Hadi (Bogazici University, Turkey); Erdem Cil (University of Rennes 1, France); Zeliha Cansu Canbek Özdil (Yeditepe University, Turkey); Denys Nikolayev (Institut d'Électronique et des Technologies du Numérique (IETR) - UMR CNRS 6164, France); Sema Dumanli (Bogazici University, Turkey)

This work proposes the utilization of a pH-sensitive biodegradable superstrate for gastrointestinal segment tracking in the 433 MHz ISM band. The superstrate consists of three rings engineered to degrade at specific pH levels that correspond to the distinct environments of the GI tissues. This superstrate covers the outer surface of a capsule which features an integrated conformal dipole antenna. Biodegradation of each ring of the superstrate in its respective GI segment leads to the alteration of the near-field of the antenna, changing its center frequency and reflection coefficient at 434 MHz in each segment. Hence, biodegradation process links the location data to the input parameters of the antenna, enabling segment tracking within the tract. Simulation results show that a shift of at least 5 MHz can be created in the center frequency as the capsule advances along each segment. Preliminary tests using liquid gastrointestinal phantoms are also presented.

10:50 Closed-Form Approximations for RF Radiation from Implantable Medical Devices

Mingxiang Gao (EPFL, Switzerland & IT'IS Foundation, Switzerland); Zvonimir Sipus (University of Zagreb, Croatia); Myles Capstick (IT'IS Foundation, Switzerland); Niels Kuster (Foundation for Research on Information Technologies in Society, IT'IS Foundation, Switzerland); Anja K. Skrivervik (EPFL, Switzerland)

The radio frequency (RF) performance of implantable antennas is significantly affected by the lossy biological tissues surrounding the implant. This paper introduces an analytical method for assessing implantable antennas' gain and radiation patterns using planar body models, which are particularly suitable for large host bodies like the human body. The closed-form expressions derived in this method reveal that the antenna gain mainly depends on a few key parameters such as host body permittivity, implantation depth, operating frequency, and encapsulation dimensions. A case study featuring an ingestible smart capsule within an anatomical human body model demonstrates the practical application of this method, offering a streamlined approach for assessing RF performance in the early stages of implantable antenna design.

11:10 Optimized Dipole Antenna for Non-Invasive RF Sensing of Cardiac Motion

Vladislav Koloskov, Nico van den Berg and Bart R Steensma (University Medical Center Utrecht, The Netherlands)

Radio-frequency Sensing (RFS) is a novel cardiac diagnostic platform that uses radio-antennas to quantify hemodynamic parameters. Previously the technology used loop antennas that do not provide full heart coverage. Alternatively, dipole antennas can cover the region of interest with higher homogeneity. However, dipoles are strongly affected by variation in body composition and placement due to load sensitivity. In this work we propose a two antenna RFS setup that uses a folded dipole antenna design optimized for enhanced load and placement stability. Experimental studies validated the numerical simulations and optimization results, showing high sensitivity of the antenna to cardiac motion and with good agreement of the RFS signal and MRI data. The proposed design allows the use of a simple setup for accurate non-invasive monitoring of the hemodynamic parameters at home.

11:30 Metal-Free Antennas by Laser-Induced Graphene (LIG) on Poly-Ether-Ether-Ketone (PEEK) Films for Application to Cyber Prostheses

Alessio Mostaccio, Francesca Nanni, Francesca Deon and Gaetano Marrocco (University of Rome Tor Vergata, Italy)

The current trend of personalized medicine fosters additive manufacturing techniques to fabricate custom polymeric prosthetic devices. Inevitably, metal replacement requires the use of deposition techniques to integrate electronic circuits into the device, which poses challenges in terms of adhesion. The laser induction of Graphene (LIG) is a novel solution for scribing conductor-less circuits onto polymeric precursors. In this paper, we hence present the first experimental demonstration of a LIG-based implanted antenna for establishing a through-the-body telemetry link. To achieve a reliable communication performance the sheet resistance of the trace was minimized down to 4 Ohm/ sq, by finding the optimal laser parameters. Then, a first prototype of a metal-free implanted LIG tapered dipole was fabricated and tested. The antenna, deep-seated in a muscle phantom at 35 mm implantation depth, demonstrated a safe 15 dB power margin with just 5 dB loss with respect to copper.

10:10 A 39-dBi Long Slot Array at K-Band

Ahmed Alwakil (Universite de Rennes, France); Romain Greard (Planexus, France); Adham Mahmoud (Institut d'Électronique et de Télécommunications de Rennes, France); Thi Quynh Van Hoang (Thales Research & Technology, France); Matthieu Bertrand (Thales Research and Technology, France); Laurent Le Le Coq (University of Rennes 1 & IETR, France); Khalid Sayegrih (Planexus, France); Ronan Sauleau (University of Rennes 1, France); Mauro Ettorre (Michigan State University, Electrical and Computer Engineering, USA)

In this communication, we introduce a high-gain antenna at K-band, covering the frequency range 17.3-21.5 GHz. The antenna is based on a long slot array fed by a parallel corporate feeding network (CFN). The CFN is tapered to reduce side lobe levels (SLL) in the radiating plane orthogonal to the long slots across the entire frequency band (SLL < -26 dB). A pillbox coupler serves as a quasi-optical system to convert cylindrical waves from the feeding rectangular waveguide to a guided field with a tapered amplitude and linear phase front to feed the CFN. The antenna is fabricated using computer numerically controlled (CNC) milling technology in aluminum to minimize losses. The antenna has a diameter of 630 mm and a thickness of 70 mm. The antenna exhibits a minimum measured realized gain of 39.7 dBi at 17.3 GHz.

10:30 E-Band Active Transmitarray Characterization Using Selective Element Illumination

Jan H. S. Bergman, Eero Pietiläinen and Juha Ala-Laurinaho (Aalto University, Finland); Antti E. I. Lamminen (VTT Technical Research Centre of Finland, Finland); Jehki Pusa (IQM Finland Oy, Finland); Mikko Kaunisto and Jussi Säily (VTT Technical Research Centre of Finland, Finland); Ville Viikari (Aalto University & School of Electrical Engineering, Finland)

A transmitarray (TA)-characterization method utilizing selective element illumination (SEI) using a metallic mask to isolate individual elements is described. This method allows for the effective turning off of all other elements while having minimal effect on the illumination of the desired element. The impact of the mask is analyzed through the electric fields on the aperture of the TA and the measured radiation patterns with and without the mask present. Compared to other element-isolation methods, using a mask preserves more detail in the embedded element pattern (EEP), better representing the true performance of the element as a part of the TA.

10:50 Further Investigating Antenna Extrapolation Through Direct Higher Order Fitting

Yibo Wang and Zhong Chen (ETS-Lindgren, USA); Dennis Lewis (Boeing, USA); Kyle Pitz (The Boeing Company, USA)

Direct higher order fitting was introduced to process measurement data from the antenna extrapolation range. This method fits the measured response to a more complete generalized antenna response equation, which includes antenna-to-antenna multiple reflections, thus the terms responsible for the fast oscillating ripples. This approach is especially effective for moderate- and high-gain antennas, where chamber reflections are relatively small compared to multiple antenna-to-antenna reflections. The advantage of this approach lies in its simplicity, as it is a one-step process and much easier to implement than spectrum filtering. However, in the previous study, the fit between the measurement data and the generalized response equation was not ideal. In this paper, we propose a new scheme for using the direct higher order method to improve fitting accuracy, resulting in a more precise far-field gain calibration. Additionally, the improved method provides phase center information for the antenna under test, without requiring additional measurements.

11:10 An Application of CG-NUFFT to UAV-Based Amplitude-Only Near-Field Antenna Testing

Yahya Rahmat-Samii (University of California Los Angeles (UCLA) & UCLA, USA); Vincent Lee (University of California Los Angeles, USA)

Unmanned aerial vehicles (UAVs) have gained attention in antenna near-field measurements for outdoor antennas due to their ability to reduce the amount of required test equipment. The most promising UAV-based setup for these outdoor measurements is an amplitude-only approach as amplitude-only measurements are robust against positioning errors which is an inherent problem facing UAVs. Current implementations of UAV amplitude-only near-field scans utilize matrix solvers and equivalent currents to account for the non-uniform data collection when performing phase reconstruction. In this paper, the conjugate gradient non-uniform fast Fourier transform (CG-NUFFT) algorithm is utilized for phase reconstruction from non-uniform two planar amplitude-only measurements. The system is tested through simulations of a dipole-element phased array antenna with various tapering and steering angles, aiming to reconstruct the far-field patterns. UAV non-uniform positioning is also simulated by introducing deviations to the targeted uniform waypoints. Simulation results demonstrate that the CG-NUFFT algorithm accurately reconstructs far- field patterns.

TUESDAY

11:30 Numerical Investigations on Phase Recovery from Phaseless Spherical Near-Field Antenna Measurements with Probe-Based Masks

Adrien Antoine Guth (RWTH Aachen University, Germany); Sakirudeen Abdulsalaam and Holger Rauhut (LMU Munich, Germany); Dirk Heberling (RWTH Aachen University, Germany)

Phaseless spherical near-field antenna measurements tackle the challenge of deriving complex coefficients representing the radiation characteristics of an antenna under test (AUT) based on amplitude-only near-field measurements. These complex coefficients can subsequently be used to determine the AUT's far-field behavior. In this article, we address the application of probe-based masks, which have been introduced within the scope of random masks. Random masks lean on the concept of diffraction patterns, which is well-known in Mathematics. In this work, we first establish the equivalence of probe-based masks to the general definition of masks. Secondly, implementations of probe-based masks and adapted masks are shown. For this, practical patch arrays with two different numbers of elements are used, and multiple probes are generated by varying the element's excitation.

Room: Oliner (C3) — CS26b - Small Antennas: From Theory to Applications

T01 Sub-6 GHz for terrestrial networks (5G/6G) / Convened Session / Antennas

Chairs: Miloslav Capek (Czech Technical University in Prague, Czech Republic), Christophe Delaveaud (CEA-LETI, France)

10:10 Fundamental Tradeoffs Between Antenna Parameters

Mats Gustafsson (Lund University, Sweden)

Trade-offs are an inherent part of antenna design. Designers often seek to achieve large bandwidth, high efficiency, and high gain, all within a small form factor and in complex environments. Balancing these often conflicting requirements requires careful consideration to find an optimal compromise. In this paper, we provide an overview of analytical expressions that relate key antenna parameters, along with computational optimization techniques, to identify the fundamental trade-offs between these parameters.

10:30 Small Antenna Bounds in Closed Analytical Form

Laura Passalacqua, Enrica Martini and Stefano Maci (University of Siena, Italy)

This paper offers a thorough review of the theoretical limits that define the performance of electrically small antennas, synthesizing key findings from the existing literature. Classical bounds, such as those established by Harrington and Chu, are analyzed with respect to their influence on parameters like directivity, gain, bandwidth, and efficiency. Particular focus is placed on the constraints associated with achieving super-directivity and super-gain, especially in the context of practical limitations like the bandwidth (or the Q-factor).

10:50 Inverse Design with Multi-Objective Topology Optimization Based on Binary Rank-1 Perturbations

Miloslav Capek (Czech Technical University in Prague, Czech Republic); Petr Kadlec (Brno University of Technology, Czech Republic)

This contribution shows the extension of the state-of-the-art single-objective binary topology optimization technique to a multi-objective framework. This achievement significantly expands the applicability of the optimization routine since only an inefficient scalarization technique was available before. We utilize the adaptive weighting method, which forces locally optimal solutions to move as close to the Pareto front as possible. The method's efficacy is high, solving multi-objective problems at a computational cost comparable to that of the original algorithm, which solved single- objective problems. All the advantages and features of the original method are preserved. An example is presented in this paper to demonstrate the superb performance of the algorithm.

11:10 Compact Meandered Dipole Array Presenting Super-Realized Gain

Donal P Lynch (Queen's University Belfast, United Kingdom); Mengran Zhao (Queen's University Belfast, United Kingdom & Xi'an Jiaotong University, China); Aaron M Graham (Queens University Belfast, United Kingdom); Stylianos D. Asimonis (University of Patras, Greece)

This paper presents a comprehensive study of a compact two-element meandered dipole array aimed at achieving super-realized gain. An optimization was performed using a Genetic Algorithm (GA) implemented in MATLAB, targeting the maximization of the realized gain in the end-fire direction. Three primary excitation schemes were evaluated: the conventional optimization to achieve superdirectivity (signal magnitude and phase angle), phase-only optimization, and uniform excitation (characterized by equal amplitude and no phase shift). The results show that by carefully optimizing both the signal magnitudes and phase angles, the array could achieve a substantial improvement in realized gain. Phase-only optimization provided a competitive realized gain with only minor reductions compared to conventional optimization, suggesting that optimizing the signal phase alone can be an effective strategy in practical implementations.

TUESDAY

11:30 Defected Laser-Induced-Graphene (LIG) Antennas for Physical Unclonable Function Applications

Francesca Nanni and Gaetano Marrocco (University of Rome Tor Vergata, Italy)

This paper explores the development of RFID devices using Laser-Induced Graphene (LIG) to enhance security against counterfeiting and duplication attacks. By leveraging the unique properties of LIG, we introduce deliberate, hardly reproducible defects on the radiating elements of RFID antennas, creating distinct variations in the backscattered signal. These defects, generated through precise laser parameter settings, modify the surface currents and produce unique RF fingerprints detectable via multi-power interrogation. This approach preliminary lays the foundation for robust Physical Unclonable Function (PUF) manufacturing without the need for additional circuitry or cryptographic methods. The method is experimented on a family of seven RFID dipoles made of both LIG and aluminium, and the proposed preliminary results demonstrate the feasibility of using graphene RFID antennas for secure, anticounterfeiting applications.

Room: Kraus (C4)

CS67b - Joint Communication and Sensing: from EM modelling to application

T04 RF sensing for automotive, security, IoT, and other applications / Convened Session / Propagation

Chairs: Raffaele D'Errico (CEA, LETI & Université Grenoble-Alpes, France), Claude Oestges (Université catholique de Louvain, Belgium)

10:10 Millimeter-Wave Backscattering Channel Modelling for Sensing Applications in an Industrial Scenario

Frederic Munoz (CEA LETI & University of Grenoble-Alpes, France); Grégory Gougeon and Yoann Corre (SIRADEL, France); Raffaele D'Errico (CEA, LETI & Université Grenoble-Alpes, France)

Joint Communication and Sensing (JCAS) and radar-based detection in industrial scenarios face harsh propagation conditions, which pose challenges for designing and evaluating radio system performance. In this work, we introduce a wideband backscattering channel measurement campaign from 18 to 40 GHz in a machine room, using a quasimonostatic antenna setup to scan the environment. Based on the experimental data, a Ray-Tracing (RT) tool is calibrated, and the Large Scale Parameters (LSPs) are analyzed. The measured and predicted data are then used to evaluate the performance of Radio Simultaneous Localization and Mapping (SLAM) applications.

10:30 Ray-Based Simulation of Multistatic Scattering from Target Objects in ISAC

Ainur Ziganshin (Technische Universität Ilmenau, Germany); Enrico M. Vitucci (University of Bologna, Italy); Saw James Myint, Wim A. Th. Kotterman and Christian Schneider (Technische Universität Ilmenau, Germany); Vittorio Degli-Esposti (University of Bologna, Italy); Reiner S. Thomä (Technische Universität Ilmenau, Germany)

An essential task of channel modeling for vehicular communications and sensing applications is predicting scattering from traffic participants, here represented by complex-shaped curved bodies. One approach is to discretize the curved body into facets and then use Ray Tracing (RT), combined with the Uniform Theory of Diffraction, to find the scattered field. We show that more comprehensive diffraction methods are required to achieve realistic results: one of them is vertex diffraction, and its implementation in the RT framework is considered in this work. Simulations by thus augmented RT are compared with simulations by MLFMM and PO solvers for discretized spheres and a simplified car, respectively.

10:50 Realistic Evaluation of Impedance-Based RIS Modeling: Practical Insights and Applications

Ayane Lebeta Goshu (NEC Laboratories Europe, Germany); Placido Mursia and Vincenzo Sciancalepore (NEC Laboratories Europe GmbH, Germany); Marco Di Renzo (CNRS & Paris-Saclay University, France); Xavier Costa Perez (NEC Laboratories Europe, Germany)

Reconfigurable Intelligent Surfaces (RISs) have emerged as a promising technology for next-generation wireless communication, offering energy-efficient control of electromagnetic (EM) waves. While conventional RIS models based on phase shifts and amplitude adjustments have been widely studied, they overlook complex EM phenomena such as mutual coupling, which are crucial for advanced wave manipulation. Recent efforts in EM-consistent modelling have provided more accurate representations of RIS behavior, highlighting challenges like structural scattering-an unwanted signal reflection that can lead to interference. In this paper, we analyze the impact of structural scattering in RIS architectures and compare traditional and EM-consistent models through full-wave simulations, thus providing practical insights on the realistic performance of current RIS designs. Our findings reveal the limitations of current modelling approaches in mitigating this issue, underscoring the need for new optimization strategies.

11:10 Electromagnetic Scattering by Poisson Point Process Distributed PEC Cylinders

Srikumar Sandeep and Gabriele Gradoni (University of Surrey, United Kingdom)

This paper describes a fast, robust and efficient method to calculate the scattered field due to multiple PEC cylinders located at random positions excited by a plane wave. The cylinder collocation follows stochastic geometry principles while including multiple electromagnetic interactions. By using this method, we study the statistics of scattered field due to Poisson point process distributed multiple cylinder samples

TUESDAY

11:30 Beam Pattern Optimization for Integrated Sensing and Communication in UAV Applications

Juan A. Vásquez Peralvo (University of Luxembourg, Luxembourg); Gianluca Fontanesi (Nokia Bell Labs, Germany); Anna Guerra (University of Bologna, Italy); Francesco Guidi (National Research Council of Italy (CNR) - IEIIT, Italy); Nir Shlezinger (Ben-Gurion University, Israel); Alberto Zanella (National Research Council of Italy (CNR), Italy); Eva Lagunas and Symeon Chatzinotas (University of Luxembourg, Luxembourg); Davide Dardari (University of Bologna & CNIT, Italy); Petar M. Djurić (Stony Brook University, USA)

The deployment of unmanned aerial vehicles (UAVs) equipped with uniform rectangular array (URA) offers a promising solution for simultaneous communication with multiple ground base stations (GBSs) and the sensing of groundbased target. However, designing a transmit beamforming system that optimizes communication while maintaining high sensing ac- curacy is challenging. In this regard, this paper proposes a comprehensive beam pattern optimization framework tailored for integrated sensing and communication in UAV applications, where the beam is synthesized based on the required steering direction, beamwidth, side lobe suppression, and nulling in targeted areas, providing robust connectivity. This comprehensive framework integrates sensing and communication, improving system performance and connectivity in UAV applications.

Room: Munch (23)

Industrial Workshop

IW6 - IMST GmbH - Design, Simulation and Realization of Phased Array Antennas

Room: Ørsted (24+25)

M01b - Material and device characterization

T07 Electromagnetic modelling and simulation tools / / Propagation

Chairs: Rafael F. S. Caldeirinha (Polytechnic Institute of Leiria & Instituto de Telecomunicações, Portugal), Michael J Havrilla (Air Force Institute of Technology, USA)

10:10 Extraction and Analysis of the Resonance Properties of a Differential SRR-Based RF Sensor

Josephine Pichereau (Université Gustave Eiffel, France); Hakim Takhedmit (Université Gustave Eiffel & ESYCOM Lab, France); Ulrich Kuhl and Olivier Legrand (Institut de Physique de Nice, France); Leszczynski Jimmy (Gustave Eiffel University, France); Stéphane Protat (Universite Gustave Eiffel & ESYCOM Lab, France); Patrick Poulichet (ESIEE, France); Olivier Français (ESIEE Paris, France); Elodie Richalot (Université Gustave Eiffel, France)

A radio-frequency (RF) sensor dedicated to characterize a small liquid volume is presented in this paper. In order to increase its robustness in regard to the ambient factors (as temperature, humidity, moisture, etc...), a differential configuration is adopted with a reference resonator that is loaded by a sample of well-known properties, whereas the sample under test is placed on the second resonator. However, depending on the similarity between the dielectric properties of the sample under test and the reference one, the properties of both resonances can be difficult to determine. The proposed post-processing method permits to extract the resonance parameters even for a strong overlap, increasing the reliability of the measure interpretation.

10:30 Material Tensor Rotor Transformation for Geometric Algebra

Nicholas O'Gorman and Michael J Havrilla (Air Force Institute of Technology, USA)

Geometric algebra possesses many advantages and mathematical simplifications in electromagnetics. One of these advantages is the simple way that reflections and rotations can be depicted. Using geometric algebra, this paper derives a method of converting material tensors into rotors, expanding geometric algebra's usefulness in electromagnetics. The Rotors are derived by viewing the interaction between electromagnetic waves and a medium's polarization or magnetization as a description of an axial rotation on the incident field, giving a direct relationship to the materials scattering effects.

10:50 Metallization Processes for 3D Printed Rectangular Waveguides in E- and D-Band

Alexander Quint and Akanksha Bhutani (Karlsruhe Institute of Technology, Germany); Maximilian Eckl (Karlsruher Institut für Technologie (KIT), Germany); Thomas Zwick (Karlsruhe Institute of Technology (KIT), Germany); Fabian Michael Hochberg (German Aerospace Center (DLR), Germany); Andreas Frölich (Horizon Microtechnologies GmbH, Germany)

Different metallization techniques for 3D printed plastic rectangular waveguides are evaluated in E- and D-band for split block and monolithic waveguides from different base materials. The metallization techniques include physical vapor deposition, electroplating and electroless plating. The measured attenuation of the 3D printed waveguides is highly comparable to commercially fabricated metal waveguides. For split block waveguides, electroplating as a final plating step showed the lowest attenuation. For monolithic waveguides, electroless copper plating showed very good results. Further, the metallization techniques are analyzed regarding different aspects such as repeatability, resin dependence and cost.

11:10 Fabrication and Characterization of 3D Printed mmWave RF Devices

Paola Andrea Escobari Vargas (Eindhoven University of Technology, The Netherlands); Jeroen A.H.P. Sol (TNO at Holst Centre, The Netherlands); Francesca Chiappini (Chip Integration Technology Centre CITC, The Netherlands); Stefania Monni (TNO Defence Security and Safety, The Netherlands); Ad Reniers, Ulf Johannsen and Elmine Meyer (Eindhoven University of Technology, The Netherlands)

Employing a novel 3D printing technique, a ring resonator and a patch antenna array for millimeter-wave applications were successfully fabricated. Microscopic examination confirmed precise dimensional accuracy and manufacturing tolerances. Frequency domain measurements validated the design, with the antenna array achieving a -10 dB bandwidth of 1.6 GHz and a resonant frequency of 34.6 GHz. The ring resonator's first four modes accurately determined the dielectric's relative permittivity for 10-37 GHz, demonstrating the feasibility of this technology to produce high-precision RF components at millimeter-wave frequencies.

TUESDAY

11:30 Dual-Band Frequency Selective Surface Sensor for Detection and Mapping of Coating Wear

Mohammad H. Zarifi (The University of British Columbia, Canada); Vishal Balasubramanian (University of British Columbia, Canada)

Coating degradation on aircraft surfaces poses a critical challenge to structural integrity and operational safety, requiring precise detection of damages over large surface areas. Current non-destructive testing methods either lack the sensitivity to detect early-stage damage or are limited by slow, area-wise inspections that affect faster inspections. Herein, a multi-resonant FSS sensor capable of localizing coating wear by correlating resonant frequency shifts with changes in coating thickness. The FSS consists of two regions with 10x10 arrays of nested square patch resonators, designed to resonate at 4.5 GHz and 5 GHz, respectively. Each region responds independently, with minimal interference, enabling precise identification of localized wear. The developed FSS is tested by the erosive wear of a 225 µm PVC coating, resulting in resonant frequency shifts of up to 198 MHz in Region A and 231 MHz in Region B, with an average shift of 70 MHz per 75 µm of wear.

Room: Mosig (26)

Scientific Workshop

SW5b - Stand on the IEEE Antennas & Propagation Standards

Room: Collin (27)

P02b - Ray tracing channel simulation

T07 Electromagnetic modelling and simulation tools / / Propagation

Chair: Conor Brennan (Dublin City University, Ireland), Mengting Li (Aalborg University, Denmark)

10:10 Site-Specific Outdoor Propagation Assessment and Ray-Tracing Analysis for Wireless Digital Twins

Morteza Ghaderi Aram (Chalmers University of Technology, Sweden); Hao Guo (New York University, USA & Chalmers University of Technology, Sweden); Mingsheng Yin (New York University & Google LLC, USA); Tommy Svensson (Chalmers University of Technology, Sweden)

Digital twinning is becoming increasingly vital in the design and real-time control of future wireless networks by providing precise cost-effective simulations, predictive insights, and real-time data integration. This paper explores the application of digital twinning in optimizing wireless communication systems within urban environments, where building arrangements can critically impact network performances. We develop a digital twin platform to simulate and analyze how factors such as building positioning, base station placement, and antenna design influence wireless propagation. The ray-tracing software package of Matlab is compared with Remcom Wireless InSite. Using a realistic radiation pattern of a base transceiver station (BTS) antenna, ray tracing simulations for signal propagation and interactions in urban landscapes are then extensively examined. By analyzing radio heat maps alongside antenna patterns, we gain valuable insights into optimizing wireless deployment strategies. This study highlights the potential of digital twinning as a critical tool for urban planners and network engineers.

10:30 Propagation Analysis Inside Lunar Caves

Germán León (Universidad de Oviedo, Spain); Susana Loredo (University of Oviedo, Spain); Marcos Arias (University of Vigo, Spain); Lorena María Pérez-Eijo (Universidade de Vigo, Spain); Álvaro Pendás-Recondo (University of Oviedo, Spain); Alejandro Manuel Gómez-Sanjuan (University of Vigo, Spain); Erio Gandini (ESA - European Space Agency, The Netherlands); Leonardo Turchi (ESA, France)

Lunar caves, formed from cooled lava tubes, remain a major enigma in Moon exploration. As potential future habitats for human settlements, these caves will initially be explored by a network of robots. The analysis of radio wave propagation between exploratory robots is then necessary to optimize communications within these underground environments. In this work, we use a ray tracing tool to perform a preliminary analysis of radio wave behavior in these conditions. In addition, we provide an experimental validation of the proposed tool based on the measurements performed in analogous terrestrial caves. The results prove to be a good starting point to extend the analysis to other situations, such as the existence of bends or inclined ground.

10:50 Assessing the Necessity of Modeling Non-Planar Wavefronts for Large Arrays with Ray-Tracing Simulation

Zhenguo Ma (Ericsson China, China); Gerhard Steinbock (Ericsson AB, Sweden); Henrik Asplund (Ericsson Research, Ericsson AB, Sweden)

This paper utilizes a ray-tracing based channel model simulation tool to quantify wave curvature at the base station (BS) in representative Urban Macro (UMa) scenarios, to determine the necessity of integrating non-planar wavefront channel modeling into the 3GPP channel model. The study aims to evaluate the impact of non-planar wave-fronts on system performance, and analyze the importance of non-planar wavefront channel modeling in wireless communication systems. The analysis of power distribution between planar and non-planar wave-fronts in different scenarios reveals that the power contribution of non-planar wave-fronts is insignificant, indicating that it may not have a substantial impact on current communication systems. These findings underscore that the current demand for non-planar wavefront modeling in communication systems may not be urgent.

TUESDAY

11:10 Empirical and Simulated Analysis of 28 GHz Propagation in Indoor Office Environments

Gerhard Steinbock, Johan Karedal and Bengt-Erik Olsson (Ericsson AB, Sweden); Christina Larsson (Ericsson Research & Ericsson AB, Sweden)

Indoor office propagation at 28 GHz is studied using empirical measurements and ray-tracing simulations. Measurements were conducted in a typical office setting, capturing angular power profiles, pathgain, and RMS azimuth spreads for two transmitter locations and their corresponding receiver tracks. Ray-tracing simulations are conducted incorporating specular reflections, diffractions, and diffuse scattering, using a 3D office model with realistic material properties. A good alignment between the simulations and the measurements is observed. Discrepancies between simulations and measurements were typically noted for low signal to noise ratios in the measurements. This typically coincided with locations where the ray-tracing tool produced poor coverage, too. For these locations diffuse scattering and diffractions could slightly improve the performance. However, higher-order specular interactions are observed to be the dominant type of interaction. This study indicates that raytracing can aid in the design of next-generation wireless systems in complex indoor environments.

11:30 Impact of Rough Building Material Surfaces on Reflection Coefficients from 5 GHz to 260 GHz

Jean-Marc Conrat (Orange Labs, France); Jean-Christophe Cousin (Telecom ParisTech, France); Xavier Begaud (LTCI & Télécom Paris, Institut Polytechnique de Paris, France)

When an electromagnetic wave is reflected by a smooth and planar surface, its amplitude is decreased by the Fresnel reflection coefficients depending on the material permittivity, incidence angle and polarization. Recent work showed that the permittivity does not depend on the frequency from 2 to 260 GHz implying that the reflection gain is constant from 2 to 260 GHz for a given incidence angle and polarization. But Fresnel coefficients are only valid for materials with a smooth surface which is not always the case for building materials. Materials such as concrete or patterned glass may be rough or have a relief surface. This paper analyzes the reflection gain deviation from the Fresnel coefficients when material surfaces are not smooth and proposed a simplified model based on the Rayleigh-Rice or Beckmann-Kirchhoff theoretical approaches. The investigated frequencies ranged from 5 to 260 GHz.

Tuesday - 12:00-12:40

Room: Alfvén (A3+A4)

Invited Speaker

Sergei Tretyakov

Chair: Filiberto Bilotti (Roma Tre University, Italy)

Room: Kildal (A2)

Invited Speaker

Almudena Suarez

Chair: Francisco Mesa (University of Seville, Spain)

Tuesday - 13:30-14:40

Room: Poster level 3

PA1 (level 3) - Antennas I Sub-6 GHz for terrestrial networks

T01 Sub-6 GHz for terrestrial networks (5G/6G) / / Antennas

Chairs: Buon Kiong Lau (Lund University, Sweden), Miguel Poveda-García (Technical University of Cartagena, Spain)

3.24. A New Broadband Magneto-Electric Cross Dipole Sub-Array with Efficient Feed Configuration for TD LTE 4G and Sub-6GHz 5G Base Stations

Hamed Tahmasbi (K N Toosi University of Technology, Iran); Hadi Aliakbarian and Reza Asadi (K. N. Toosi University of Technology, Iran); Davood Siyar, Soroush Shafigh and Mohammad Javad Namaazi (KN Toosi University of Technology, Iran)

A new linearly dual-polarized antenna element is proposed for 5th generation base station antennas. By incorporating a parasitic element as a second layer and modifying the radiating patches with leaf-shaped corner cuts, the antenna achieves an impressive wide bandwidth of more than 58% (VSWR<2) from 2 to 4 GHz, also covering the frequency range of 2.3 to 2.7 GHz and 3.3 to 3.8 GHz with VSWR<1.6. This makes the design suitable TD LTE, and Sub-6GHz 5G applications. The antenna features a simple microstrip feed structure, offering reduced complexity compared to conventional cabling methods. Efforts were made to feed this two-element antenna to achieve maximum gain at a 6-degree angle in order to make the sub-array more efficient. The single dual-polarized element provides an average gain of 8.9 dBi, while the two-element configuration reaches an enhanced gain of 11.8 dBi. The fabrication results are in good agreement with the simulations.

3.25. A Multi-Beam Transmitarray Antenna with Scanning Loss Improvement

Zhubin Han, Yu Du and Jian-ying Li (Northwestern Polytechnical University, China)

In this paper, a multi-beam transmitarray antenna (TA) is proposed, which has the characteristics of polarization conversion and low scanning loss. The TA element adopts double-layer structure, and the two layers are orthogonal to each other. This element has selective properties for linearly polarized waves and can convert incident linear polarized (LP) waves into orthogonally LP waves. Seven waveguide antennas are used as feed antennas, and beam scanning can be realized by switching feed antennas. In addition, an optimization method of phase distribution is proposed to improve the scanning loss. And the method is verified by simulation. The maximum gain of TA is 21.79 dBi at 10 GHz, which can realize beam scanning of ±25° in the elevation plane, and the scanning loss is not more than 1.6dB.

3.26. A Single Substrate Layer Low-Profile Complementary Antenna with Broadside Pattern

Yukang Chen (Southwest Jiaotong University, China); feng Quanyuan (Southwest JiaoTong University, China); Yan Wen, Haoxuan Sheng and Yurong Sun (Southwest Jiaotong University, China)

A single substrate layer, low-profile, complementary antenna with broadside pattern is proposed, which is composed of a novel low-profile helical magnetic dipole and a traditional bowtie electric dipole. The novel helical magnetic dipole is achieved by two symmetric W-shaped substrate-integrated helix antennas (WSHAs). The traditional bowtie electric dipole is composed of a pair of bowtie patches. The current distribution and radiation characteristics of the proposed magnetic and electric dipole are simulated to demonstrate their magnetic and electric source behaviors. By integrating the two dipoles orthogonally into the single substrate, a complementary antenna with low profile height of 0.032λ0 (λ0 is the free-space wavelength corresponding to the operating frequency f0) is obtained. The simulated peak gain in the broadside direction is 3.6 dB, and the front-to-back ratios (FTBR) is 14.8 dB.

3.27. An Advanced 3-Stage Phased Array Architecture

Yuqi Wang and Quan Xue (South China University of Technology, China)

This paper presents an advanced 3-stage phased array antenna (PAA) architecture well-suited for modern hybrid and digital beamforming networks. The 3-stage PAA architecture supports flexible beamforming in vertical (V) and horizontal (H) planes under agile polarizations. It is built upon a 2-stage phased antenna element (PAE), capable of seamlessly integrating with progressive phases. It is implemented through a four-port, single-layer antenna to demonstrate these concepts. The 2-stage PAE provides flexible radiation covering 6 polarizations and 4 typical patterns in V and H planes. Building upon the PAE, a 1-by-3 small-scale PAA with specially arranged configurations is designed. This arrangement suppresses multi-path mutual coupling, ensuring optimal antenna efficiency across operating states. The 1-by-3 array can function as a subarray for larger-scale array extensions, even for planar arrays, as it accounts for potential couplings and demonstrates promising beam-steering capabilities. The advanced 3-stage PAA shows strong potential for future MIMO phased array applications.

3.28. Analysis of Dielectric Material Constraints Imposed in Lens Design

Robert Molina-Burgués (Universitat Politècnica de Catalunya, Spain.); Luis Jofre (Universitat Politecnica de Catalunya, Spain); Juan M. Rius (Universitat Politècnica de Catalunya, Spain); Jordi Romeu Robert (Politècnica de Catalunya, Spain)

This work presents a parametric analysis of how dielectric properties from specific materials impact traditional lens design, focusing on their impact on directivity, dielectric losses, gain, lens dimensions and operational frequency. Through this analysis, visual guidance is provided to assist in selecting dielectric materials suited to specific applications and constraints. Additionally, we conduct a focused analysis on a selection of real materials, chosen for their dielectric characteristics suited to typical lens antenna applications. In both analyses, we emphasize a key design trade-off that defines the achievable performance: while higher dielectric constants enhance antenna directivity, this benefit may be negated by increased dielectric losses.

3.29. Compact Design of a 4-Port MIMO Antenna-Diplexer Leveraging HMSIW Cavities

Divya Chaturvedi (Indian Institute of Information Technology, Pune, India); Tiru Ganesh (SRM University-AP, India); Arvind Kumar (Dept of ECE,. Visvesvaraya National Institute of Technology Nagpur India, India)

A novel 4-port MIMO self-diplexing antenna design is presented, utilizing half-mode substrate integrated waveguide (HMSIW) technology. This antenna operates at 4.9 GHz for WLAN and 5.8 GHz for ISM communications, achieving approximately 30 dB isolation. The half-mode topology reduces the antenna size by 50% while retaining the TE110 mode characteristics. To increase bandwidth, a rectangular slot is added in each cavity, splitting the mode into oddTE110 and even-TE110. Careful optimization of antenna parameters and the perpendicular arrangement of radiating elements ensure effective self-diplexing. A prototype is manufactured, with experimental results confirming simulations. The antenna shows peak gains of 5.2 dBi at the lower frequency and 5.9 dBi at the upper frequency, with efficiencies exceeding 94% in both bands. All MIMO-diversity parameters also met satisfactory levels.

3.30. Decoupled Patch Antennas Using Electric and Magnetic Coupling Cancellation

Jianfeng Qian (University of Birmingham, United Kingdom); Benito Sanz-Izquierdo (University of Kent, United Kingdom); Haiwei Zhang (Huawei Technologies Ltd, China)

A decoupling technique for reducing the mutual coupling between two patch antennas is introduced in this paper. The antennas under investigation are two rectangular patch antennas with an air substrate, being placed within a very small distance. The decoupling is facilitated by controlling the electric and magnetic couplings between two patch resonators, involving no extra complicated structures. Only with some minor modifications to the patch's shapes, good decoupling performance can be obtained between two patches.

TUESDAY

3.31. Design and Optimization of Vector Graphics-Based Dual-Band Planar Antenna Structures

Chandan Roy (Huawei Technologies Canada, Canada); Ming Jian (Huawei Technologies Co. LTD., Canada); Peyman Neshaastegaran (Huawei Technologies Canada, Canada); Wenyao Zhai (Huawei Technologies Canada Research Center, Canada)

This paper introduces a novel idea of patch antenna designing which can be adopted for dual-band application. Patch of antenna geometry has been designed in terms of vectors connecting two successive vertices of the patch forming an irregular shaped patch. Such an idea of designing antenna patch leverages the high dimensional variables for optimization of different antenna structures based on desired characteristics. In this work, dual-band antennas are designed for different applications. The genetic algorithm (GA) optimizer is used as a direct optimization technique with EM model of the antenna to get the optimized antenna structure for desired performance. To verify the antenna designing method mentioned above, two dual-band antennas are designed in the range of 2-4 GHz and 5-8 GHz, respectively. Return loss for both antennas at their operating frequencies are well below -10 dB which makes the proposed antennas attractive for dual-band applications at S-band and C-band, respectively.

3.32. Design of A Novel Reconfigurable Antenna with Independently Tunable Polarizations and Patterns

Yu Du, Zhubin Han, RuiZi Chen and Jian-ying Li (Northwestern Polytechnical University, China)

In this paper, a novel reconfigurable antenna with independent control of polarization (Pol) state and pattern deflection is proposed to improve communication quality and anti-interference ability. To achieve pattern deflection in the Eplane, the on-off states of diodes are utilized to provide a phase difference between the two inverted-L antennas on both sides. The tilting of patterns in the H-plane is implemented by the Yagi-like principle. The two deflection techniques are combined to achieve a tilting of patterns towards multiple azimuths for the four polarizations (x-Pol, y-Pol, and ±45°-Pol) in the half-space domain of z>0. The designed reconfigurable antenna realized four polarizations with flexible beam steering at the band from 4.04 GHz to 4.36 GHz, which can be a reliable antenna element for phased arrays possessing switchable polarizations and wide-angle scanning capability.

3.33. Edge Truncation Effect Suppression for A Tightly Coupled Antenna Array with 2:1 Bandwidth

Run-Zhi Tang and Shi-Wei Qu (University of Electronic Science and Technology of China, China)

A method for suppressing edge truncation effect in a finite tightly coupled antenna array is proposed in this paper. The tightly coupled antenna element can achieve a 2:1 bandwidth and ±60° scanning range in an infinite array. When the array is truncated in the E-plane direction, low-frequency impedance matching is significantly deteriorated during H-plane scanning. To address this issue, a pair of T-shaped metal plates, electrically connected to the dipole arms and ground plane, is loaded at the edges of the array without increasing the array sizes. Additionally, the excitation phases of edge elements are simply optimized to weaken the impact of H-plane truncation.

3.35. Element-Level Decoupled-Beamforming Empowered Wideband MIMO Phased Array Antennas

Yuqi Wang and Quan Xue (South China University of Technology, China)

This paper proposes wideband decoupled phased array antennas capable of pattern-preserved multi-beam generation and wide-angle beam-steering. Two novel element-level decoupled beamforming patch antennas with symmetrical configurations and feedings are developed, demonstrating over 25 dB port isolations across bandwidths of 28.2% and 27.3%, respectively. The antennas can produce broadside, tilted, and conical beams using the mixed-mode feeding strategy. Combining the two antenna elements in the E-plane forms arrays that exhibit superior multi-path coupling suppression, with port isolations over 22 dB across a bandwidth of 26.2%. This ensures optimal active reflection coefficients (ARCs) and prevents scanning blind spots. The compact designs feature pattern-preserved decoupling in array environments, supporting low-correlation multi-beam generation and wide-angle beam-steering capabilities. The single-layer, low-profile configuration of the proposed antennas and arrays makes them well-suited for advanced MIMO phased array applications.

3.36. Pin-Diode Based Low-Loss Multi-State Electrical Phase Shifter for Sub-6 GHz Base Station

Jun Hwa Oh (Samsung Research & Samsung Electronics Co., Korea (South)); Sang Hyuk Wi (Samsung Research, Samsung Electronics, Korea (South)); Yuntae Park (Samsung Research, Korea (South)); Taek Sun Kwon (Samsung Electronics, 34 Seongchon-gil, Seoul Korea, Korea (South))

This paper presents an electrical phase shifter (EPS) based on pin-diodes for adjusting the electrical tilt (e-tilt) angle of base station. The EPS is located in front of the array antenna at the base station and plays a role in adjusting the beam direction by changing the input phase of the antenna. The proposed EPS is a combination of loaded type and switched type EPS. The EPS test board including a bias circuit for controlling the pin-diode and a dip switch was manufactured. Measurements were performed using a VNA, and connector losses were excluded by de-embedding through loss compensation. The validity of the proposed EPS was verified by confirming that the measured values matched well with the simulation results, which is expected to be widely used in base stations requiring e-tilt in the future.

TUESDAY

3.37. QMSIW Based Self-Diplexing MIMO Antenna

Arvind Kumar (Dept of ECE,. Visvesvaraya National Institute of Technology Nagpur India, India); Divya Chaturvedi (Indian Institute of Information Technology, Pune, India); Mahesh P Abegaonkar (IIT Delhi, India); Ramesh Kumar Sonkar and Rakhesh Singh Kshetrimayum (Indian Institute of Technology Guwahati, India); Sidhartha Kumar Sahu (IIT Guwahati, India)
A compact self-diplexing multiple-input multiple-output (SD-MIMO) antenna has been designed using a quarter- mode substrate integrated waveguide (SIW) cavity for wireless communication applications. This design employs two quarter-mode (QM) SIW cavities-one circular and -one rectangular in the self-diplexing element, which allows for high isolation (>20 dB) across the operating channels without the need for additional isolation networks. This feature provides a significant advantage over traditional designs that typically require extra isolation components to maintain high isolation between closely spaced antenna elements. The measured results indicate two operating frequency bands around 4.0 GHz and 4.78 GHz, with peak gain values at resonant frequencies of 4.2 dBi and 4.1 dBi, respectively, comparable to other MIMO antenna designs.

Room: Poster level 3

PA2 (level 3) - Antennas II Millimetre wave and THz for terrestrial networks

T02 Millimetre wave and THz for terrestrial networks (5G/6G) / / Antennas

Chairs: Jose I Herranz-Herruzo (Universitat Politècnica de València & APL - iTEAM, Spain), Oskar Zetterstrom (KTH Royal Institute of Technology, Sweden)

3.38. A High Gain Pencil Beam Multilayer Antenna for 5G Communication

Haris Hashmi (National University of Sciences and Technology, Pakistan); Hidayat Ullah (College of Aeronautical Engineering, NUST, Pakistan); Mirza Shujaat Ali and Muhammad Noman (University of Glasgow, United Kingdom); Hattan F. Abutarboush (Taibah University & Communications and Electronics Engineering, Saudi Arabia); Farooq A Tahir and Qammer Abbasi (University of Glasgow, United Kingdom)
A high gain and low side lobe pencil beam 8×8 antenna array using substrate integrated waveguide (SIW) operating at 28 GHz millimeter wave spectrum is designed. The antenna array consists of multilayer structure with a microstrip feed network to feed SIW having slot. The feed network is implemented using Taylor distribution for low side lobe level in one plane and same distribution is also applied on series fed patch antenna elements to get low side lobe level in both planes. The antenna array provides a bandwidth of 1.6 GHz with a maximum gain of 20.3 dBi at 28.5 GHz. It provides side lobe level of less than -17.3 dB in both X-Z and Y-Z planes at 28.5 GHz. The simulated and measured results of the antenna array are in good agreement. The proposed antenna features low cost, high gain, and high efficiency, making it a potential candidate for 5G applications.

3.39. A Multiband High-Gain Antenna Array for Ka-Band Beyond 5G Wireless Communication

Joshua Parker, Anikó Német and Muhammad Aslam (Aberystwyth University, United Kingdom); Shaker Alkaraki (University of Nottingham, United Kingdom); Amit Kumar Mishra (National Spectrum Centre, United Kingdom); David Andrew Evans and Syeda Fizzah Jilani (Aberystwyth University, United Kingdom)
A multiband high-gain eight-element patch array incorporated with a defected-ground-structures (DGS) is presented in this paper. A substrate of Rogers RT/Duroid 5880 with a thickness of 0.4 mm is used, and the overall size of the antenna is 55 × 25 mm2. The antenna array operates at numerous frequencies of Ka-band, such as 26.7 GHz, 28.5 GHz, 32 GHz, 34 GHz and 37.8 GHz. The antenna array shows high-gain performance with 12.4 dBi at 26.7 GHz and 12.55 dBi at 34 GHz. The efficiency of the antenna array is above 60% in all the five operating bands with a peak efficiency of 90% in the 34 GHz band. The antenna prototype was fabricated using an HPC Laser Cutter (LSE110 Fibre 5Engraver model). The proposed antenna array is well-fitted for high-gain line-of-sight communication links beyond 5G/6G bands.

3. 40. A Wide-Angle Beam-Scanning Circularly Polarized Dielectric Resonator Antenna Phased Array

Qi Xuan Lai and Yongmei Pan (South China University of Technology, China); Wan Jun Yang (Guangzhou University & No, China)
In the paper, a wide-angle beam-scanning millimeter-wave (mm-wave) circularly polarized (CP) dielectric resonator antenna (DRA) phased array is proposed. The design employs a port self-decoupling method based on polarization orthogonality to achieve wide-angle impedance matching while leveraging the near-field coupling effect to broaden the active element pattern (AEP). As a result, the proposed phased array can achieve a wide-angle beam-scanning range without requiring additional structures. Simulated results indicate that the main beam of the proposed array can scan from −60° to +60° at 30 GHz, with a peak gain ranging from 12.0 to 15.0 dBic. Furthermore, the axial ratio (AR) of the beam is less than 3 dB across the entire beam-scanning range, showing good CP performance.

TUESDAY

3. 41. Asymmetrically Routed Phased Arrays as an Enabler for Analog Directional Encoding

Duccio Delfini, Nuutti Tervo, Muhammad Yasir Javed, Marko E Leinonen and Aarno Pärssinen (University of Oulu, Finland)
This paper introduces the concept of analog directional encoding as a new approach for delivering an encoded signal towards specific targets only while providing white noise to most of the other directions. The proposed method exploits the directional dependency of the group delay between each pair of adjacent antennas in series-fed asymmetrically routed phased arrays to generate "beams of correlation", which have analogous behaviors of the power beam patterns in classical analogical beam-forming methods. This strategy allows two additional security layers to the communication, consisting in the necessary knowledge of the encoding scheme and of the steering direction of the transmitter in order to correctly decode the received message. Moreover, the received message can be compared with the sent message, if it is a priori known, to estimate the angle-of-arrival of the signal.

3. 42. Design of a Compact DC-Block and Bias-Tee for 28 GHz mm-Wave Frequency Applications

Fayyadh Ahmed (University of Sheffield, United Kingdom & University of Duhok, Iraq); Amal Swileh (The University of Sheffield, United Kingdom); Salam Khamas (University of Sheffield, United Kingdom)
This paper introduces an innovative microstrip bias-tee (BT) circuit incorporating a compact U-shaped DC-block interdigital capacitor (IDC) combined with a newly developed sawtooth-shaped radial stub. The IDC design consists of two opposing U-shaped structures, with two adjacent λ/8 parallel open stubs placed transversely within the Ushaped layout. This design results in a 50% reduction in size, achieving λ/8 in length and width at a 28 GHz operating frequency, occupying a compact area of 0.8 × 0.8 mm^2. Additionally, the circuit offers a broad bandwidth of 10 GHz, ranging from 22 GHz to 32 GHz, corresponding to a percentage bandwidth of 37%. The proposed structure is modelled and optimized on a 0.406 mm RO4003C Rogers substrate using CST. Simulation results demonstrate a return loss (RL) greater than 20 dB, an insertion loss (IL) of less than 0.5 dB, and an isolation loss (IS) exceeding 25 dB over the entire frequency range.

3. 43. Four-Element Metamaterial Antenna with Wide Bandwidth for mm-Wave 5G MIMO Applications

Hlias Tzouras (' University of Patras', Greece); Stavros Koulouridis (University of Patras, Greece)
A four-port MIMO antenna with a metasurface array for mm-Wave applications is proposed. The antenna has a compact size of 20 x 20 x 7.15 mm3 and is realized with a Rogers Duroid 5880 dielectric layer 0.78 mm thick used as substrate and a Rogers RO3010 dielectric layer 1.65 mm thick used as superstrate at distance 5.5 mm above the radiation elements. Each one of the four radiation elements is composed of a square cut-at-the-corners, patch antenna. In addition, metasurface array structure is used at the same level with the radiation elements and the impedance bandwidth is improved . The performance of the antenna is investigated in terms of reflection coefficient, ECC and MEG. The proposed antenna achieves impedance bandwidth of 7.98 GHz (24.52-32.5 GHz) and the simulated values of ECC between antenna elements are lower than 0.03. Overall, the antenna is a good candidate for mm-Wave 5G MIMO Applications.

3. 44. Fully-Connected Beamforming Enabled by Hybrid Digital-Analog Modulation in 4-D Antenna Arrays

Kejin Chen and Feng Yang (University of Electronic Science and Technology of China, China); Shi Wen Yang (University of Electronic Science and Technology of china, China)
Conventional fully-connected array provides significant degrees of freedom (DoFs) in beamforming. However, the practical applicability of fully-connected array architecture is limited due to the high hardware complexity. To address this issue, this paper presents a novel approach for achieving efficient fully-connected beamforming by ingeniously integrating the digital and analog modulation of four-dimensional (4-D) antenna arrays. The proposed approach can be easily implemented in practice due to the low hardware complexity of the 4-D antenna array. In addition, the proposed approach, in addition to considering the analog time modulation, distinguishes itself from the conventional four-dimensional antenna array design method by incorporating digital modulation. The multi-channel signals can be pre-coded and weighted through the hybrid digital and analog modulation, facilitating their transmission to each antenna element for the realization of fully-connected mapping. Finally, some selected numerical results are provided to validate the effectiveness of the proposed approach.

3. 45. Glide-Symmetry Multilayer Antenna Design for Millimeter-Wave High-Altitude Platforms

Jorge Chavero-García (Universitat Politècnica de Valencia, Spain); Miguel Ferrando-Rocher (Universitat Politècnica de València & Antennas and Propagation Lab, Spain); Jose I Herranz-Herruzo (Universitat Politècnica de València & APL - iTEAM, Spain)
This paper presents a multilayer antenna design for millimeter-wave high-altitude platforms based on glide symmetry. The proposed antenna operates in the Ka-band (29-31 GHz), incorporating glide-symmetric holes along its contour to reduce field leakage. Simulations show stable impedance matching and good radiation efficiency across the operational band, suggesting that this early-stage design could suit high-altitude pseudo-satellite applications. The compact design makes it a promising candidate for integrating communication systems in demanding environments.

TUESDAY

3. 46. Investigation of SIW Transmission Loss on Synthetic Fused Substrate for D-Band Antennas

Daisuke Yamanaka and Osamu Kagaya (AGC Inc., Japan)

The use of wireless communication in the millimeter wave band, where bandwidth can be expanded, is highly anticipated against the backdrop of increasing traffic worldwide. Since attenuation is large in the millimeter wave band, a high-gain antenna is used for long-distance transmission. To form a large planar antenna, a radio frequency power supply network with low transmission loss is required. In frequency bands above 100 GHz, which are attracting attention for 6G and wireless backhauls, quartz glass, which has far superior electrical properties than existing materials, is one of the attractive materials. In this paper, an SIW (Substrate Integrated Waveguide) was designed using a synthetic fused silica substrate in the 140 GHz band, and transmission loss was measured. As a result, synthetic fused silica showed an extremely low transmission loss of 0.06 - 0.08 dB/mm, demonstrating the possibility that it can be applied to large array antennas exceeding 4096 elements.

3. 47. Low-Scattering Circularly Polarized Antenna Array with High Aperture Efficiency

Zhaosong Liu (Xidian University, China); Zhao Li and Hao Zhou (Nanjing Research Institute of Electronic Technology, China); Xun Qu (The Nanjing Research Institute of Electronics Technology, China); Ying Liu (Xidian University, China)

A low-scattering circularly polarized antenna array is proposed in this paper. The integrated antenna unit can realize circularly polarized radiation in X-band, and also acts as a polarization cancellation structure in the case of plane wave irradiation. The integrated and its mirror unit act as the artificial electromagnetic surface structure for polarization conversion. The mirrored design realizes the effect of monostatic RCS reduction based on polarization phase cancellation of reflected plane wave. The antenna units are formed into a 16-element array using sequential rotary feeding technique, which can achieve circularly polarized radiation characteristics in X-band, with 3-dB axial ratio bandwidth of 21.26% and the gain of 16.3 dBic at 10 GHz. The calculated aperture utilization factor is 74.63%. Moreover, the antenna array has in-band and out-of-band low-scattering characteristics from 7 GHz to 15 GHz.

3. 48. Monolithic Reconfigurable Patch Antenna and Antenna Arrays in V-Band

Rozenn Allanic and Denis Le Berre (Lab-STICC - UBO Brest, France); Benjamin Coquillas (Thales LAS France, France); Thomas Merlet (Thales & LAS OME, France)

This paper presents a monolithic reconfigurable antenna and antenna arrays for V-band applications. They are designed on a silicon substrate in a monolithic manufacture with distributed highly doped areas integrated in the substrate as active elements. Designing a V-band antenna with integrated active elements for tunability offers several key advantages reducing the interconnections problems, improving the antenna efficiency, and pushing over the frequency limitation with classical active components. Moreover, the proposed co-design method offers some degrees of freedom in the positioning and the shape of the doped areas improving the antenna efficiency. To demonstrate the approach, a reconfigurable V-band antenna is proposed. In the ON-state, it resonates at 60 GHz and in the OFF-state, the frequency can be chosen between 62 GHz to 74 GHz thanks to the degrees of freedom of the proposed approach. To go further, a 1x2 and a 1x4 frequency reconfigurable antenna arrays are discussed.

3. 49. Multiple Bondwires for E Band MMIC to Antenna Array Interconnections for Beamforming

Sumin David Joseph (The University of Sheffield, United Kingdom); Edward A. Ball (University of Sheffield, United Kingdom)

This paper presents an analysis of the effect of bondwire for low-cost E band interconnections from phase shifter MMIC to an off-chip antenna array for beamforming applications. A microstrip patch antenna array at 72.5 GHz is initially designed and its performance is optimized. The performance changes are evaluated with a 25 µm bondwire connecting the array to the GaAs phase shifter MMIC, showing reduced antenna gain and impaired impedance matching. To address bondwire losses, multiple bondwires are fabricated, showing that triple bondwires reduce insertion losses and improve matching. As compensation circuits require more space and are difficult to design, matching networks are challenging to incorporate. Multiple bondwires in the same pad area significantly reduce insertion losses and improve matching, providing an effective solution for maintaining performance without the need for additional compensation circuits.

3. 50. Power Splitters Design in Different Groove Gap Waveguide Realizations in Millimeter Wave Band

Álvaro Martín-Núñez (Universitat Politècnica de València & Antennas and Propagation Lab (APL), Spain); Miguel Ferrando-Rocher (Universitat Politècnica de València & Antennas and Propagation Lab, Spain); Jose I HerranzHerruzo (Universitat Politècnica de València & APL - iTEAM, Spain)

The design of 1-to-2 power splitters based on Ka-band groove gap waveguide (GGW) technology is presented. A comparison of four splitters in both the GGW and the half-mode GGW version is presented. The perfect magnetic conductor condition uses metallic pins or mushrooms on a substrate. The splitters have an operating bandwidth between 27 and 31 GHz with a matching level below −20 dB. A loss comparison between the different waveguides is shown, and the designed splitters confirm the difference in performance between the different waveguide topologies used.

TUESDAY

3. 51. The Upper Bound of Stacked Patch Antennas with Various Dielectric Laminate Combinations

Preethy Sethuraman (University of Hertfordshire, United Kingdom); Qi Luo (University of Herfordshire, United Kingdom); Yihan Ma, Baiqing Tang and Yichuang Sun (University of Hertfordshire, United Kingdom); Shichao Li and Dawei Zhou (Honor Device Company Limited, China)

A novel technique to calculate the maximum achievable bandwidth with given dielectric combination is presented in this paper. An equivalent circuit model of the stacked patch is used to study the upper bound of a stacked patch antenna's bandwidth with varied dielectric laminate combinations. The values of the lumped elements in the circuit model are extracted theoretically and used to demonstrate the maximum achievable bandwidth of a stacked patch with a given dielectric stack-up. The developed model using theoretical calculations is verified by comparing the results from EM simulations, and the performance of the tool is evaluated with various use cases. This model helps to predict the performance of the antenna before the design phase thus serving as powerful tool for antenna designers by predicting the performance before designing the antenna.

3. 52. W-Band Additively Manufactured Geodesic H-Plane Horn Antenna

Elisa Miquel-Nardi (ENSEEIHT, Université de Toulouse, INPT, Toulouse, France); Mingzheng Chen (KTH Royal Institute of Technology, Sweden); Jose Rico-Fernandez (Northern Waves AB, Sweden); Oscar Quevedo-Teruel (KTH Royal Institute of Technology, Sweden)

We present a compact geodesic H-plane horn antenna for point-to-point communications at W-band. The horn has a curved height profile with truncated corners to reduce phase errors and achieve high gain and aperture efficiency. The laser powder-bed fusion additive manufacturing technique is applied to fabricate the horn antenna in a monolithic manner. The resulting prototype has a weight of only 14 g including the flange part. In the operating band from 75 to 110 GHz, the measured reflection coefficient is below -15 dB in almost the entire band and agrees well with the expectations from the simulation. The simulation shows a realized gain of 20 dBi with an aperture efficiency of 80% and a total radiation efficiency of nearly 80%.

Room: Poster level 3

PA3 (level 3) - Antennas III Aerospace, space and non-terrestrial networks

T03 Aerospace, space and non-terrestrial networks / / Antennas

Chairs: Julien Sarrazin (Sorbonne Université, France), Moises Tercero (KTH Royal Institute of Technology, Sweden & Thales Research and Technology, France)

TUESDAY

3. 1. A Spin-Decoupled Transmissive Metasurface for Dual-Circularly Polarized Transmitarray with Independent Beam Control

Lijun Bu, Yang Cai, Sen Li and Siyu Qi (Space Engineering University, China)

In this paper, a dual-circularly polarized (CP) transmissive metasurface is proposed by utilizing shared-aperture metaatoms made of an antenna-filter-antenna (AFA) configuration, which achieve spin-decouple for left/right-handed CP waves. To realize the independent phase control capability, the element is loaded with the phase delay lines and the rotation angle of patches. By controlling the propagation phase and the geometric phase, the proposed metasurface can generate left-hand CP (LHCP) waves and right-hand CP (RHCP) waves to arbitrary directions in the far field. The simulated results show that the achieved peak gain better than 20.6 dBi at 20.4 GHz, while gain < 3 dB and axial ratio < 2 dB relative bandwidths of two orthogonal CP beams wider than 19.7% and 18.5%, respectively. These features of the proposed antenna present great application potential in wireless and space communications.

3. 2. Dual Circularly Polarized Wide-Angle Scanning Phased Array Antenna Based on Tri-Polarized Design

Yu-Bo Gao, Zhu Lianwei, YunHong Zhang and Shigang Zhou (Northwestern Polytechnical University, China)

This paper presents a dual circularly polarized phased array antenna based on the tri-polarized antenna design, consisting of dual linear polarization antenna elements (X and Y polarizations) and a Z polarization antenna element, covering the frequency range of 2.2-2.4 GHz. The dual polarization antenna elements are composed of the FSS and the magnetoelectric dipole radiation structure, while the Z polarization antenna is configured as a top-loaded monopole antenna. By optimizing the excitation amplitude and phase of the array antenna, the synthesized circularly polarized wave can achieve a very low axial ratio and minimal gain loss during wide-angle scanning. The profile height of the antenna element is 1.05λ. A 4×4 tri-polarized antenna array can achieve a beam scanning coverage of ±75°.When the beam is directed at ±75°, the axial ratio less than 1 dB and the gain loss less than 3.5 dB.

3. 3. Inmarsat Terminal Phased Array Element with Multiple Dual-Port Radiators Fed by a Beamforming Network for Satellite Communications

Zafer Toprak and Maximilian Holzner (Universität der Bundeswehr München, Germany); Stefan Lindenmeier (Universität der Bundeswehr, Germany)

A phased array antenna with a beamforming network in combination with a set of circular polarized ring antennas with different modes is presented for the reception of the Broadband Global Area Network (BGAN) operating in the L-Band. The structure is designed as an array element, which can be realized easily in a punched bent panel technique. Since an antenna diversity system is an additional use case, the measured patterns of the single elements are also provided together with the pattern of the complete phased array antenna. The complete structure is integrable in different types of vehicles, for example, flat rooftop radomes or spoilers, as a relatively small integration space is provided.

3. 4. Resonance-Forming: Achieving High Gain Metamaterial-Enhanced Magnetic Induction Communication Based on Reinforcement Learning

Yuheng Wang Chen, Guohao Liu, Jintao Wang and Zhi Sun (Tsinghua University, China)

Limited communication range is the major drawback of Magnetic Induction(MI) communication. Due to the subwavelength aperture of small antennas used in MI communication, radiated energy gathers around the antenna in the form of evanescent waves and cannot propagate away. State-of-the-art research surrounds antennas with metamaterials to radiate the evanescent waves away, resulting in increased transmission distance. However, existing Metamaterial-Enhanced Magnetic Induction((M^2I)) communication research ideally assume isotropy and periodicity of metamaterials, which leads to significant reduction of channel gain. To achieve higher channel gain and further transmission distance, in this paper we propose Resonance-Forming, a scheme based on reinforcement learning for adaptively adjusting metamaterial, to increase communication range in (M^2I) communication system. Simulation results validate that in low-loss and high-loss medium the Resonance-Formed (M^2I) communication ranges are respectively increased by 5.11 and 4.96 times than existing uniformly-tuned (M^2I) while maintaining a channel capacity of no less than 10 Kbps.

3. 5. 3D-Printed K/Ka-Band Antenna-Feed System with Built-In RF, Thermal and Mechanical Functionalities

Oscar Peverini (IEIIT-CNR, Italy); Giuseppe Addamo (CNR-IEIIT, Italy); Mauro Lumia (CNR, Italy); Giuseppe Virone (Consiglio Nazionale delle Ricerche, Italy); Flaviana Calignano (Dipartimento di Ingegneria Gestionale e della Produzione, Politecnico di Torino, Italy); Nazzareno Mandolesi (Pasquali Microwave Systems, Firenze - Università di Ferrara, Italy); Matteo Bigi (Pasquali Microwave Systems, Firenze, Italy); Giovanni Matticari (Pasquali Microwave Systems, Italy); Andrea Ferrara (Argotec, Italy); Nelson Fonseca (Anywaves, France)

This paper presents the results of an R&D activity, funded by the ARTES Advance Technology programme of the European Space Agency, aimed at integrating RF, thermal and mechanical functions in a monolithic K/Ka-band antenna-feed assembly through Additive Manufacturing (AM) for GEO High Throughput Satellites (HTS). After a tradeoff analysis between different configurations, an AM-oriented version of an asymmetric antenna-feed architecture was selected and realized by the laser-based powder bed fusion of metals (PBF-LB/M) process. The prototype was successfully tested for Radio-Frequency (RF), thermal and mechanical performances.

3. 6. Estimating the Mutual Coupling of Microstrip Patch Antennas on Large Platforms Through Ray-Tracing

Hannes Bartle (Ecole Polytechnique Federale de Lausanne, Switzerland); German Augusto Ramirez Arroyave (EPFL - École Polytechnique Fédérale de Lausanne & Universidad Nacional de Colombia, Switzerland); Anja K. Skrivervik (EPFL, Switzerland)

The mutual coupling between antennas is an important parameter in multi-antenna systems that needs to be controlled in order to ensure the performance of all involved components. While full-wave simulations are accurate in estimating the mutual coupling, they remain computationally expensive for large structures and are sometimes even impossible due to the lack of definition in early design stages of a system. This work summarizes the different coupling mechanisms between patch antennas and proposes a modified two-ray model technique in order to quickly estimate the mutual coupling. The proposed method is shown to agree well with full-wave simulations in the given scenarios and has the advantage of giving physical insight into the coupling mechanism especially with respect to polarization that then can be further utilized in developing methods to mitigate the mutual coupling.

3. 7. A Broadband Folded Marchand Balun Integrated with Tunable Phase-Shifting Function

Jiarui Fang and Qi Wu (Beihang University, China)

A balun structure with phase-shifting function is introduced in this paper. It integrates a loaded line phase shifter on a folded Marchand balun, which maintains a very compact size, hybrid functions, and low fabrication cost. Operating mechanism of this phase-shifting balun is explained through circuit theory. As an example, a phase-shifting balun that operates in the frequency range of 0.8-2 GHz is designed, which achieves a maximum phase shift of 168°. For practical verification, a back-to-back structure is fabricated, and the measurement results are in a good agreement with the fullwave ones. To demonstrate potential applications of this structure, a phased array with two broadband dipole elements is designed. The resulting array can scan up to ±60° in the frequency range of 1-1.8 GHz.

3. 8. Dielectric Radome Development for K/Ka-Band Beamforming Antenna Modules

N Nasimuddin and Bo Shi (Institute for Infocomm Research, Singapore); Francois Chin (Institue for InfoComm Research, Singapore); Xianming Qing and Terence S.P. See (Institute for Infocomm Research, Singapore)

Radome design for antenna systems requires a slight compromise between the electrical and mechanical requirements. In this paper, a common radome is designed for the receiving (K-band) and transmitting (Ka-band) beamforming antenna systems. A factor of transmission loss is used at K- and Ka-band with fixed radome distance from the antenna systems and the same radome's dielectric material constant to optimize the thickness of common radome thickness. The preliminary results of the common radome for K-/Ka-band antenna systems in which, taken as starting point of the common radome designs. The results of the K-/Ka-band phased array antenna with radome show a beam steering angle deviation of only approximately 1 degree and a gain reduction of about 1.1 dB when scanning ±45° for both bands as compared to without radome.

TUESDAY

3. 9. A Metal-Only Folded Reflectarray Utilizing Modified Split Ring Slot Elements

Hao Zhu, Jiakai Zhu, Nan Qin, Qiqi Zhou and Lu Guo (Nanjing University of Science and Technology, China)

A metal-only folded reflectarray employing modified split ring slot elements is proposed. The reflectarray comprises a polarization-conversion reflectarray integrated with a feed horn and an upper polarizer. The element enables continuous 360° phase coverage by varying the opening angle and mirroring its structure. Waves are reflected twice between the upper and lower layers of the folded array, reducing the profile by 1/2. A 625-element array has been designed and manufactured. The testing results demonstrate that the reflectarray exhibits a peak gain of 29.4 dBi with maximum aperture efficiency of 52.1%. Furthermore, the measured 3-dB gain bandwidth is 14%.

3. 10. A Differentially Fed Dual-Polarized TEM Horn Antenna with Stacked Multilayer PCB Technology

Mingjiang Teng and Qi Wu (Beihang University, China)

This contribution presents a differentially fed dual-polarized TEM horn antenna, which consists of a stacked multilayer PCB (printed circuit board) and an integrated feeding network. It is a feasible and convenient process for the TEM horn antenna in a compact size by discretely equivalenting a three-dimensional curved surface into two-dimensional planes. The simulated results show that the proposed antenna has a ultrawide differential impedance bandwidth of 98.75% (12.35-36 GHz) for |Sdd11| < -10 dB and a differential port isolation of more than 50 dB. Additionally, the radiation efficiency is more than 90% over the entire operation band and a low profile is achieved. The good performance of the proposed antenna means it can be applied in satellite communication from the Ku to Ka band and mm-wave array antenna.

3. 11. Designing Large-Element-Spacing Arrays for Diverse Modular Subarrays Through Iterative Convex Relaxation Optimization

Gongqing Yang, Hui Zeng, Zhenhai Xu and Wei Dong (National University of Defense Technology, China)

This paper introduces a novel modular subarray design method that employs large-element-spacing modular subarrays. By strategically designing the structure and placement of the basic modular units, the method effectively suppresses grating lobes caused by large inter-element spacings (exceeding half a wavelength). Traditional largeelement-spacing array designs are always non-modular, leading to inconvenience in design, manufacturing, assembly, and maintenance. The proposed modular design simplifies production and assembly while maintaining excellent pattern performance. The design outcomes are obtained through Iterative Convex Relaxation Optimization. Numerical simulations and analyses confirm the efficacy of the proposed design.

3. 12. High-Precision Geocasting for LEO Satellites Using Combined Spatial Data Focusing and Beamforming

Nédid Ismaili and Amélia Struyf (Université Libre de Bruxelles, Belgium); François Quitin (Université libre de Bruxelles, Belgium); Julien Sarrazin (Sorbonne Université, France); Philippe De Doncker (ULB, Belgium)

An application of spatial data focusing (SDF) for geocasting through low Earth orbit satellite communications is proposed. SDF is a high-precision solution to restrict data to a given zone, but lacks of power gain. In order to compensate for the huge path loss experienced during transmission, additional antennas are included to replicate the signal of the antennas implementing SDF. By doing so, the geocasting benefits from the high resolution of SDF and gain from beamforming. Simulations show the applicability of SDF to current system technologies, and open new perspectives in wireless geocasting.

3. 13. Dual-Band Circularly Polarized Asymmetric Linear Tapered Horn Antenna for Feeder of Synthetic Aperture Radar Onboard Microsatellite

Derry Permana Yusuf and Josaphat Tetuko Sri Sumantyo (Chiba University, Japan); Yuki Yoshimoto (Chiba University & Universitas Indonesia, Japan); Steven Shichang Gao (Chinese University of Hong Kong, China); Koichi Ito (Chiba University, Japan)

A novel dual-band waveguide-fed circularly polarized (CP) horn antenna is proposed for the feeder of synthetic aperture radar (SAR) onboard microsatellite. The proposed horn antenna consists of an asymmetric linearly tapered slot and a waveguide feed. The left-hand circular polarization (LHCP) design was simulated, and the 3-D-printed prototype was fabricated to validate the simulation and measured in an anechoic chamber. The measured circularly polarized (CP) antenna can achieve dual-band operations at C-/X-band with a 3 dB axial ratio bandwidth of 40% (5-6.5 GHz; 8.5-10 GHz), VSWR less than 1.4 in the operating band, and a peak gain of 13.6 dBic (5.3 GHz) and 18.5 dBic (9.4 GHz). The measured half-power beamwidth (HPBW) at C-band and X-band frequencies in the xz-plane and yz-plane are achieved at 26°/37° and 18°/23°, respectively. The proposed antenna features simpler configuration and lower manufacturing cost, making it competitive for SAR applications.

3. 14. C-Band Stretchable-Substrate-Impregnated Fabric Origami Deployable Reflectarray Antennas for Small Satellites

Takashi Tomura and Hiraku Sakamoto (Tokyo Institute of Technology, Japan); Tomohiro Fukao (Panasonic Corporation of North America, USA)

This template provides authors with most of the formatting specifications needed for preparing electronic versions of their papers. All standard paper components have been specified for three reasons: (1) ease of use when formatting individual papers, (2) automatic compliance to electronic requirements that facilitate the concurrent or later production of electronic products, and (3) conformity of style throughout conference proceedings. Margins, column widths, line spacing, and type styles are built-in; examples of the type styles are provided throughout this document and are identified in italic type, within parentheses, following the example. Some components, such as multi-leveled equations, graphics, and tables are not prescribed, although the various table text styles are provided. The formatter will need to create these components, incorporating the applicable criteria that follow.

3. 15. Low-Profile Lightweight X-Band PDHT Antenna for Earth Observation Satellite Constellations

Luca Di Palma and Davide Maiarelli (Thales Alenia Space, Italy)
This paper presents the design, manufacturing and experimental characterization of a X-band Antenna (XBA) dedicate to data download on ground for new Satellite platforms that will form constellations for Earth observation applications. It is characterized by a reduced profile and minimized mass in order to fulfil stringent accommodation requirements, typical of Low Earth Orbit (LEO) reduced-size platforms. The design is based on a planar array of patch antennas implemented on a sandwich made of composite materials.

3. 16. Frustum-Shaped Conformal Antenna Array for High-Performance A2G Data-Link in Aerial Surveillance Platforms

Arthi R (Indian Institute of Technology Madras, India); Masoom Verma (Indian Institute of Technology, Madras, India); Christopher S (IITM, India)
The data-link systems in aerial surveillance platforms require high-speed, efficient data transfer from multiple sensors to the ground station, necessitating a high-gain, wide-bandwidth antenna for optimal performance and effective multisensor data fusion (MSDF). This work proposes a different architecture for the air-to-ground (A2G) data-link antenna subsystem for an airborne surveillance platform. The design features a frustum-shaped conformal circular antenna array with eight elements and switchable beam, providing full 360° azimuth coverage and a well-formed elevation beam, achieved through the judicious choice of frustum angle. The power study highlights the benefits of the proposed system over conventional omnidirectional antennas. The design employs a switch matrix to direct the beam, reducing resource requirements and lowering costs and complexity. Additionally, the architecture offers redundancy under certain failure mode conditions, enhancing reliability. Thus, the proposed system provides an optimal solution for A2G data-link antenna subsystem for a surveillance platform.

3. 17. Analytical Computation of Conjugate Points' Location in 3D Parabolic Reflector Systems

Francesco Lisi (Heriot-Watt University, United Kingdom); Giovanni Toso (European Space Agency, ESA ESTEC, The Netherlands); Piero Angeletti (European Space Agency, The Netherlands); Julien Maurin (Thales Alenia Space, France); Hervé Legay (Thalès Alenia Space, France); George Goussetis (Heriot-Watt University, United Kingdom)
The location of conjugate points plays a crucial role in understanding and predicting certain radiation characteristics of reflector antenna systems. In this manuscript, we present an analytical approach for determining the location of conjugate points for both broadside radiation and beam scanning. In the 2D case, our methodology is based on the well-known mirror formula. Moving to the 3D case, we demonstrate that for broadside radiation, reflected rays converge to a single point. However, during beam scanning, incident rays from different planes converge to different points after reflection. These points can be analytically determined by locally approximating the reflector as either an ellipsoid or a hyperboloid. Our findings highlight the limitations of the conjugate point model for larger scan angles.

3. 18. Frontend Design with Special Waveguide Transition in K- and Ka-Band for a Hybrid Steerable Multi-Beam Satellite Antenna Array

Andreas Krause (Werner-Heisenberg-Weg 39 & University of Bundeswehr, Germany); Stefan Lindenmeier (Universität der Bundeswehr, Germany)
For a steerable multi-beam antenna array in the K and Ka-Band on a small satellite a bidirectional front end design is presented. The main concept of the antenna array consists of stacked Rotman lenses in hollow waveguide technology. This paper describes the waveguide transition from the electronic circuitry to the Rotman lens by using a coplanar waveguide with ground followed by a surface integrated waveguide SIW into a double ridged waveguide. A prototype of the frontend design including a distribution network and diplexer circuit is analyzed. The analysis shows good agreement in measurement and simulation results.

3. 19. Compact Microstrip Line to Gap Waveguide Transition Suitable for Beam Steering Antenna Applications at K-Band

Raha Roosefid (Chalmers University of Technology & Satcube AB, Sweden); Esperanza Alfonso Alós (PPhD, Sweden); Thomas Schäfer (Satcube, Sweden); Jian Yang and Ashraf Uz Zaman (Chalmers University of Technology, Sweden)
This paper presents an innovative microstrip-to-waveguide transition designed for beam steering antenna applications, ensuring efficient signal transmission in the K-band. Seamless transitions between microstrip and waveguide technologies are crucial for optimizing signal integrity in high-frequency systems, where minimizing loss and maintaining impedance matching are key to performance. Utilizing gap waveguide technology, the design integrates the substrate with the metallic waveguide, enhancing system efficiency while reducing complexity. A bone-shaped coupling slot enables effective energy transfer between the microstrip and groove gap waveguide sections, minimizing reflection loss. Additionally, a "bed-of-nails" structure is used behind the microstrip to suppress unwanted radiation, ensuring system stability and reducing cross-talk. This compact, high-efficiency transition meets the demands of modern communication systems and offers a reliable platform for future beam steering technologies. Simulations show excellent performance, with S11 below -10 dB and insertion loss under 0.45 dB across the 17.4 to 19.75 GHz range.

TUESDAY

3. 20. Design of Circularly Polarized Reflectarray in X-Band for Space Application in South America

Nathani Borondi dos Santos (Universidade Federal Do Pampa, Brazil); Juner M. Vieira (National Institute for Space Research (INPE), Brazil); Marcos V. T. Heckler and Edson R. Schlosser (Universidade Federal do Pampa, Brazil) In this paper, a circularly polarized reflectarray operating at 8.6 GHz is proposed. The desired phase distribution across the aperture is achieved using three parallel printed dipoles of varying dimensions, along with an additional pair of different dipoles placed at each corner of the unit cell. To ensure high polarization purity, all dipoles are symmetrically arranged around the central dipole. The primary feed system consists of a 2 x 2 circularly polarized microstrip antenna array, composed of four probe-fed quasi-rectangular microstrip antennas, sequentially rotated to provide effective cross-polarization decoupling. To characterize the phase response of the unit cell, the Floquet mode analysis technique was employed, with simulations conducted using Ansys HFSS. The reflectarray dimensions were designed to fit within the constraints of an 8U nano-satellite. Given this limitation, the scattering structure consists of a 12 x 12 elements, determined by the size of each unit cell.

3. 21. A Quad-Spiral Element with a Reconfigurable Direction of Radiation for Wide-Angle Steerable Vector Phased Array

Noaman Nasser (Queen Mary University of London, United Kingdom); Wen Dang (Queen Mary University of London, China); Shohreh Nourinovin, Jin Zhang and Chao Shu (Queen Mary University of London, United Kingdom); Anthony Keith Brown (University of Manchester, United Kingdom); Brian Collins and Xiaodong Chen (Queen Mary University of London, United Kingdom)
The conventional phased array suffers a large gain reduction during wide-angle beam steering and poses a significant challenge for Space Solar Power Systems (SPSS). This paper introduces a novel approach to address this issue by using the Vector Phased Array (VPA) concept, which aims to enhance beam collection efficiency (BCE) and reduce gain loss during wide-angle beam steering. A passive beam-steering Quad-Spiral antenna element was designed, demonstrating low side-lobe levels (SLLs) and a gain degradation of only 2.9 dB at steering angles up to 56°, with full 360° phi coverage. The design also exhibited low mutual coupling performance and stable radiation characteristics across multiple steering modes, making it an ideal candidate for VPA-based SPSS applications.

3. 22. Phase Synchronization Effects in Antenna Arrays with Independent Subarrays Based on Monte Carlo Simulation

Karim El Isa and Dirk Heberling (RWTH Aachen University, Germany)
The use of electrically independent subarrays in satellite antenna arrays offers advantages of greater flexibility for in-space assembly and manufacturing. However, challenges arise due to phase deviations between non-ideally synchronized subarrays and their impact on important antenna parameters. This study addresses these challenges by employing Monte Carlo simulations to evaluate the effect of phase deviations on key antenna parameters, including array factor (AF), side-lobe level (SLL), half-power beam width (HPBW), and main-beam direction. The effects of varying taper types and subarray sizes on overall performance are also examined. The results show that the amplitude taper applied on an array has no significant influence on the tolerance to phase errors. Furthermore, smaller subarrays exhibit greater resilience to phase deviations compared to larger subarrays, if the overall antenna element number is maintained. These findings provide valuable insights for designing satellite antennas intended to deliver internet connectivity to conventional devices, such as smartphones.

3. 23. Polarization Diverse Meandered Slot and Ring Antenna with Sum and Difference Beam Patterns

Mazen Almalki (University of Edinburgh & King Abdulaziz City for Science and Technology, United Kingdom); Maksim Kuznetcov (Heriot Watt University, United Kingdom); Symon K. Podilchak (University of Edinburgh, United Kingdom); Yahia Antar (Royal Military College of Canada, Canada)
A novel multi-polarization 8-port slot antenna is presented in this work, designed to generate both sum and difference beam patterns. Moreover, based on this multi-port feeding, operation with both dual-vertical and dual-horizontal linear polarizations is made possible and this can support simultaneous transmission and reception. The antenna design features a configuration of meandered slots and micostrip rings on its upper layer. This multi-layer antenna exhibits a good impedance match at 2.4 GHz, achieving a gain of approximately 6 dBi. It is capable of generating sum and difference co-polarized beam patterns by simultaneously exciting adjacent ports. The design also utilizes a shared aperture for all 8 ports, thereby reducing complexity and size requirements. The performance of the antenna was also evaluated through simultaneous port excitation with isolation values in excess of 10 dB. Applications include in-band full-duplex antenna systems which require polarization diversity as well as sum and difference beam patterns.

TUESDAY

2. 3. A Linear to Circular Polarization Converter with Angular Stability for K/Ka Applications

Zhaoran Chen, Junjie Hu and Xiayuan Yao (North China Electric Power University, China)

This paper presents a novel dual-band linear to circular polarization converter, operating at 19.6 to 20.3 GHz and 29.8 to 36.2 GHz, especially for satellite communication applications. Based on the theory of resonant circuits, the unit cell consists of two identical rectangular strips with thin split slots and is separated into four layers. This design achieves the conversion of the Linearly Polarized (LP) wave to the Right-Hand Circular Polarization (RHCP) wave at the lower band and the Left-Hand Circular Polarization (LHCP) wave at the upper band. The simulated insertion loss of the passbands is no more than 1 dB. The frequency range of the axial ratio on the threshold of 1 dB covers the operated bands, and the performance against large incident angles is also demonstrated.

2. 5. A Metasurface-Based Cross-Slot Aperture Coupled Antenna Array for Ku-Band Satellite Reception

Aral E. Zorkun, Praveen Naidu Vummadisetty, Juan A. Vásquez Peralvo and Eva Lagunas (University of Luxembourg, Luxembourg); Mehmet Abbak (SES, Luxembourg); Symeon Chatzinotas (University of Luxembourg, Luxembourg)

The demand for cost-effective, low-profile user terminals for satellite communications supporting multicast services for Geostationary Orbit (GEO) satellites, has become a key focus for many Direct-to-Home (DTH) providers where the high data rates in the downlink are required. Planar antenna arrays with increased frequency bandwidth and improved ratio using metasurfaces are considered as an effective solution for such systems. This paper presents a low-cost, aperturecoupled metasurface-enhanced patch antenna, operating within the 10.7-12.7 GHz frequency range. The antenna is designed to achieve a realized gain of at least 27 dBi across the band of interest using 32 x32 array antennas distributed in a rectangular lattice. Initially configured for linear polarization, the antenna can be upgraded to support dual or circular polarization if required.

2. 6. A Ray Tracing Based RCS Reduction Method for Complex Cavity Structures

Berk Bural and Ozlem Ozgun (Hacettepe University, Turkey)

Cavities typically exhibit high Radar Cross Section (RCS) characteristics due to their structural features that allow multiple reflection mechanisms. For stealth platforms, it is crucial to design these cavities in a manner that minimizes electromagnetic backscattering from the structure. This paper presents an approach for optimizing the thickness of radar-absorbing materials using a ray tracing algorithm to reduce the RCS of a cavity resembling an S-type intake. Following this, the optimized cavity is integrated into a simplified aircraft geometry to evaluate the overall reduction in RCS for the platform.

2. 7. Accurate Modelling of Fully Metallic Spherical Polarizers for Space Applications Through Method of Moments

Agnese Mazzinghi and Angelo Freni (University of Florence, Italy); Francisco Mesa (University of Seville, Spain); Oscar Quevedo-Teruel (KTH Royal Institute of Technology, Sweden); Jose Rico-Fernandez (Northern Waves AB, Sweden)

Additive manufacturing techniques have sparked interest in using fully metallic conformal polarizers for space applications. While proof of concepts can be designed using general-purpose design tools, more precise and specific numerical techniques are required to accurately model such structures. We suggest using an ad-hoc Method of Moments that utilizes analytical Green's functions for magnetic sources exciting a radial transmission line in the presence of a metallic sphere.

2. 8. An Efficient Compact Dual-Band Metasurface RF Energy Harvester

Raziyeh Sharifi, Anne-Claire Lepage, Kyriaki Niotaki and Xavier Begaud (LTCI & Télécom Paris, Institut Polytechnique de Paris, France)

This paper presents a dual-band metasurface-based RF energy harvester to efficiently collect the ambient radio frequency energy at 2.45 GHz and 5.2 GHz (Wi-Fi bands). The methodology to design the dual-band metasurface by employing the EM simulation software CST Studio Suite is presented. The dual-band metasurface is designed based on a proposed single-band metasurface harvester, with both unit cell designs achieving high absorption characteristics at their operating frequencies. An array of 4×5 unit cells for both the single-band and dual-band designs were fabricated to validate the concept. The first results for the single band design demonstrate a good agreement between the simulated and the measured results.

TUESDAY

2. 9. Co-Aperture 1-Bit Dynamic Reflection Metasurface for Microwave Computational Polarimetric Imaging

Mengran Zhao (Queen's University Belfast, United Kingdom & Xi'an Jiaotong University, China); Huilin Huang (Xi'an Jiaotong University, China); Aobo Li (Queen's University Belfast, United Kingdom); Shitao Zhu (Xi'an Jiaotong University, China); Okan Yurduseven (Queen's University Belfast, United Kingdom)

In this paper, a 1-bit dynamic reflection metasurface (DRM) is proposed to perform computational polarimetric imaging (CPI). The proposed DRM is composed of randomly distributed 1-bit dynamic cross-polarization converters (DCPCs) loaded with PIN diodes. A dual-polarized horn antenna (DPHA) is used as a transceiver to multiplex the proposed DRM. By altering the working states of the PIN diodes across the DRM aperture, low-correlated dual-polarized reflection patterns that can be used as measurement modes in a CPI system are firstly obtained. Then, the performance of these measurement modes are evaluated in terms of correlation coefficient and singular value analyses. Finally, a metallic bar is employed as a target to be imaged to verify the CPI capability. The imaging scene is encoded by the measurement modes, and the back-scattered data is captured by the DPHA, thereby enabling the implementation of microwave CPI. The proposed design is verified through full-wave simulations.

2. 10. Cost-Effective mm-Wave Polarization Conversion Metasurface Using a Fiber Laser Machine

Rana Muhammad Hasan Bilal (University of Pisa, Italy); Etienne Perret (Grenoble INP - LCIS, France); Simone Genovesi, Giuliano Manara and Filippo Costa (University of Pisa, Italy)

Metasurface-based devices are commonly fabricated using various techniques, including chemical etching, PCB technology, and 3D printing. In this paper, a fiber laser marker machine is used for the first time to fabricate lower millimeter-wave (mm-wave) polarization conversion metasurface (PCM) designed to operate within the Ka band (26-40 GHz). The proposed PCM consists of an array of 45°rotated dipole resonators, printed on an aluminium-backed plastic substrate. It effectively achieves cross-polarization conversion across a broad operating frequency range spanning from 21.8 to 42.5 GHz. Furthermore, the angular robustness of the proposed PCM is evaluated by varying the incident angles up to 40°. Finally, the simulated performance of the designed PCM has been validated through experimental measurements.

2. 11. Directivity Improvement of Low-Profile Electromagnetic Band Gap Resonator Antenna Using Phase Transformation Sheet

Mohammad Nasrat Zaqumi (Macquarie University, Australia); Saleem Shahid (Graz University of Technology, Austria); Fatima Ghulam (Zhejiang Normal University, China); Umair Rafique (University of Oulu, Finland); Mohsen Asadnia and Syed Muzahir Abbas (Macquarie University, Australia)

This study proposes an efficient method for directivity improvement of electromagnetic band gap (EBG) resonator antenna with enhancement of near-field phase distribution. A single dielectric layer phase transformation sheet (PTS) is designed at 11 GHz based on the operational frequency of the EBG resonator antenna. The PTS consists of two unit cells printed on both sides of a single dielectric layer to compensate for the non-uniform near-field phase distribution of the EBG resonator antenna. The proposed solution doubles the uniformity region of the phase distribution and achieves 22 percent aperture efficiency.

2. 12. Dual-Band Metasurface-Based Radome for Millimeter-Wave 5G Applications

Roman Soroka, Ana Arboleya and Eduardo Martinez-de-Rioja (Universidad Rey Juan Carlos, Spain); María Elena de Cos Gómez (Universidad de Oviedo, Spain)

This contribution presents the design of a dual-band metasurface-based radome (metaradome, MTR) for antenna protection applications in millimeter-wave 5G. The proposed MTR has two transmission bands at 28 GHz and 39 GHz. A parametric study has been carried out to characterize the frequency response of the MTR. Then, the designed MTR has been combined with a reflectarray-based Smart Electromagnetic Skin (SES) to analyze the impact of the MTR in the radiation performance of the SES: first, the MTR unit-cell has been combined with the SES unit-cell to analyze its performance; then, the complete SES has been loaded with the MTR and the radiation patterns of the structure have been computed. The simulated results confirm the potential of the proposed MTR to protect the SES without degrading its performance, and allowing for a much more compact design than a conventional half-wavelength radome.

2. 13. Electromagnetic Scattering from Cylinders: A Single-Scattering Model

Radu Barbulescu and Robbert Schulpen (Eindhoven University of Technology, The Netherlands); Gerhard Steinbock (Ericsson AB, Sweden); Martin Johansson (Ericsson Research, Sweden); A. B. (Bart) Smolders (Eindhoven University of Technology, The Netherlands)

As a new generation of wireless communications approaches, there is an increasing emphasis on leveraging the characteristics of urban wireless channels to facilitate higher data rates and improved connection quality. Modeling the propagation environment emerges as a crucial factor to ensure optimized network performance and reliable connectivity for users. State-of-the-art electromagnetic modelling techniques employ ray-tracing algorithms and scattering models of urban furniture to improve the accuracy of the computed the path gain. In this context, cylinders stand out as one of the most common 3D shapes present in urban environments. This work presents a scattering model for metallic cylinders that is based on Fresnel integrals and addresses some of the most notable issues that existing scattering models suffer from, mainly computational complexity and near-field validity. The model is applied to a single-scattering scenario and its accuracy is showcased with respect to the results of measurements performed in an anechoic chamber.

TUESDAY

2. 14. Eliminating Ghost Phantoms in Computational Microwave Imaging by Breaking Receiver Symmetry

Aobo Li (Queen's University Belfast, United Kingdom); Mengran Zhao (Queen's University Belfast, United Kingdom & Xi'an Jiaotong University, China); Muhammad Ali Babar Abbasi (Queen's University Belfast & The Institute of Electronics, Communications and Information Technology (ECIT), United Kingdom); Okan Yurduseven (Queen's University Belfast, United Kingdom)

This paper addresses the challenge of eliminating ghost phantoms in frequency-diverse computational microwave imaging (CMI) by optimizing the arrangement of receiving antennas. These ghost phantoms are primarily attributed to factors such as system inaccuracies, deficiencies in signal processing and the intricate electromagnetic phenomena present in the environment. In this work, we present that the intrinsic symmetry in the arrangement of transmitter (Tx) and receiver (Rx) components of a CMI system also substantially contributes to the occurrence of these ghost phantoms in reconstructions. We propose a solution by breaking the symmetry in the Rx configuration to reduce the ghost phantoms. We use full-wave simulations to investigate the effects of three different receiver arrangement schemes on image reconstruction: uniform, half-uniform and half-irregular, and fully irregular. The results demonstrate that breaking the symmetry of the Rx elements, particularly by adopting an irregular arrangement, significantly improves the quality of the reconstructed images.

2. 15. Evaluation of Human Body Scattering in near and Far Field by Iterative Physical Optics for mmWave Sensing Applications

Tom Malherbe (Université Grenoble Alpes & CEA Leti, France); Raffaele D'Errico (CEA, LETI & Université Grenoble- Alpes, France); Christophe Delaveaud (CEA-LETI, France); Pouliguen Philippe (DGA, France)

Milliliter-wave radar-based human body sensing requires for precise modeling of the backscattered field. This article presents an Iterative Physical Optics near-field model designed for evaluating the backscattering of lossy dielectric target. The model is first validated by millimeter wave measurement in anechoic chamber and applied to simplified human body, in order to examine the impact that proximity to the target can have on the response

2. 16. Frequency-Tunable Meta-Atom Design with Angular Stability for Reconfigurable Intelligent Surface

Wenbo Zhao, Junming Zhao, Tian Jiang, Ke Chen and Yijun Feng (Nanjing University, China)

In this paper, we develop a frequency-tunable, 2-bit, angle-stable meta-atom design for RIS-assisted wireless communication, integrating the combined control of PIN and varactor diodes. The proposed meta-atom operates within the Sub-6 GHz spectrum, encompassing the N78 and N79 communication bands. By loading metallic vias, the angular stability of the phase response of meta-atom is significantly enhanced within an incidence angle range of up to 60°. To validate the effectiveness, we simulate and analyze the far-field patterns of angle-stable and angle-dependent metasurfaces with identical size and periods. The simulation results demonstrate that angle-stable metasurface can effectively suppress the energy levels in undesired directions. Therefore, this design enhances communication quality and reduces interference with unrelated users in single-user communication scenarios, showing potential applications in next-generation wireless communication systems.

2. 17. Generation of Millimeter-Wave Circular Airy Vortex Beam with Huygens' Metalens

Mingze Hu, Yanni Wang and Xiaoyan Pang (Northwestern Polytechnical University, China); Qi Zheng (Shanghai University, China)

This paper presents a design for generating non-diffracting millimeter-wave circular Airy vortex beam using ultra-thin Huygens' metalens. The study provides a comprehensive analysis of Airy vortex beam generation through theoretical examination and full-wave numerical simulations. It has been demonstrated that by incorporating an azimuthal spiral phase component into a circular Airy beam, a circular Airy vortex beam can be produced. Then, based on the calculated phase distribution, the Huygens' metalens design is realized. Simulated results demonstrate the behavior of Airy vortex beam contrasts with conventional vortex beams. The circular Airy vortex beam displays non-diffracting properties, enabling it to maintain its narrow-divergence structure over significant distances. These unique propagation dynamics create new opportunities for high data-rate communication systems.

2. 18. Huygens' Metalens-Based Frequency-Diverse Bunching Metacavity Antenna

Mengran Zhao (Queen's University Belfast, United Kingdom & Xi'an Jiaotong University, China); Huilin Huang (Xi'an Jiaotong University, China); Aobo Li (Queen's University Belfast, United Kingdom); Shitao Zhu (Xi'an Jiaotong University, China); Okan Yurduseven (Queen's University Belfast, United Kingdom)

The performance of computational microwave imaging (CMI) is limited by the low signal-to-noise ratio of the detected signal, which stems from the restricted directivity of the transmitter. To address this challenge, this paper introduces a new solution: a Huygens' metalens (HM)-based frequency-diverse bunching metacavity antenna (FDBMA). By employing a frequency-diverse metacavity, it becomes feasible to generate low-correlated radiation patterns through a simple frequency sweep. These patterns can then serve as the measurement modes within the framework of CMI. To enhance the directivity of the radiation patterns, a two-dimensional (2D) HM is designed to fulfill the necessary transmission phase compensation requirements. The proposed HM-based FDBMA is realized by positioning the metacavity antenna at the focal point of the designed 2D HM. The performance of the proposed HM-based FDBMA is evaluated, including the reflection coefficient, correlation coefficients and singular values of the measurement modes. The proposed design is validated through full-wave simulations.

TUESDAY

2. 19. Improving the Multi-GBPS Signal Integrity Using Goubau-Inspired Hybrid Surface Wave Lines

Mahmoud Wagih (University of Glasgow, United Kingdom)
Single-wire transmission lines (SWTL) guiding conformal surface waves are attractive for low-loss broadband non-lineof-sight (NLOS) links. However, they suffer from a fundamental limitation that is an HF stop-band, between 1 and 100 MHz, unresolved across state-of-the-art implementations. Here, a loosely-coupled 2-wire surface-wave line structure is proposed, inspired by the Goubau SWTL, and is evaluated from analytical impedance calculations to practical signal integrity measurements. The line is fed using two flexible coplanar waveguide (CPW) tapered Vivaldi launchers, with an additional ground wire is incorporated. The proposed structure reduces the maximum insertion loss from over 40 dB to under 20 dB, lowering the rejection compared to standard Goubau lines, with under 0.3 dB/cm attenuation under 4.5 GHz. Digital signalling is measured up to 3.6 GBPS through eye diagrams, standard and Manchester (IEEE 802.3)- encoded, showing successful communication. The line is validated in a wearable application, showing the first multiGBPS wearable experimental demonstration.

2. 20. On the Radomization of an ETA Radar Antenna Preserving the Imaging Accuracy

María Elena de Cos Gómez (Universidad de Oviedo, Spain); Alicia Flórez Berdasco (University of Oviedo, Spain); Jaime Laviada (Universidad de Oviedo, Spain); Fernando Las-Heras (University of Oviedo, Spain)
The effect of radomization on the radiation pattern of a mm-wave antenna for an ETA system based on synthetic aperture radar (SAR) is analyzed, considering not only the magnitude but especially the phase shift across both the beamwidth and the bandwidth. Three different radomization approaches are considered, one of them metasurfacebased, for a radar antenna operating in 24.05 - 24.25 GHz frequency band. Fabricated prototypes, of the antenna alone and optimally randomized, are tested and compared in terms of electromagnetic image quality.

2. 21. Real-Time Direction of Arrival Estimation Using Space-Time Coding Method

Seyed Milad Miri (University of Tehran, Iran); Karim Mohammadpour Aghdam (University of Tehran, Belgium & KUL, Belgium)
This article presents a method for the real-time estimation of the impinging angle of monochromatic plane wave signal using space-time coding method. The proposed system operates within the Ku band and covers an elevation range of -60 to 60 degrees. It consists of a space-time modulated array and a receiver antenna positioned in the farfield region in broadside direction. The direction of arrival (DoA) estimation is achieved by comparing the frequency spectrum associated with each incident angle against a pre-established look-up table for various incoming wave angles. A simulation is performed to show how proposed method works

2. 22. Reconfigurable Omni-Metasurface Using Simultaneous Reflection and Transmission Pre-Phase Distribution for Single Beam Scanning

Zhifeng Pan and Hang Yu (Anhui University, China); Pan Li (Communication University of China, China); Yang Lixia (Jiangsu University, China)
In this paper, we propose a reconfigurable pre-phase omnidirectional metasurface (RPOM). The RPOM can achieve single-beam radiation under normally incident circularly polarized plane waves by a continuous pre-phase distribution. By dynamically controlling the state of the diodes integrated into the metasurface, the metasurface can manipulate the transmission and reflection of circularly polarized waves, and the position of the source is not restricted. The simulation results of the 12×12-element metasurface array show that the array has the beam scanning ability from 0° to 30° with an axial ratio is less than 3 dB.

2. 23. Splatter SAR Image: 3D Reconstruction Using a Single SAR Image

Juwen Chen, Shengchang Lan, Wei Fang and Zong Hua (Harbin Institute of Technology, China)
In this paper, we introduce a new method to exploring the conversion of single-view synthetic aperture radar (SAR) images to 3D object models using the Splatter SAR Image technique. The technique is based on Gaussion technology demonstrating an excellent ability to efficiently convert single-view SAR images into 3D models. We applied Gaussian Splatting to the 3D reconstruction process of single-view SAR images by training a neural network. The neural network operates in a feed-forward fashion during the testing phase. The network design is simple and uses 2D operators to map the input image to a 3D Gaussian distribution per pixel, thus generating a Gaussian ensemble that is rendered similarly to the image. This study not only successfully demonstrates the fast reconstruction capability of single-view SAR images, but also achieves better results in evaluation metrics. Ultimately, we demonstrate the significant cost and speed advantages of the method over other reconstruction techniques.

TUESDAY

2. 24. Tomographic Imaging of Meta-Shells: Noisy Scattering Data

Gregory Samelsohn (Shamoon College of Engineering, Israel)

In this contribution, we review our recent results and some new ideas concerning both direct and (mainly) inverse wave scattering by meta-shells, i.e., closed, generally semi-transparent metasurfaces. It is shown that these meta-shells can be characterized by a singular potential. In the most general case of Huygens' metasurfaces with magneto-electric coupling, the wave scattering is described by a four-parameter family of point interactions, derived previously within 1D quantum mechanics. A linear non-iterative inversion algorithm is used to recover the support of the scattering potential, and therefore, the shape of the meta-shell. A special attention is devoted to the impact of noise on the image quality. It is shown empirically that the inversion algorithm is extremely robust, as the recovery of arbitrary meta-shells is achieved even when the true signal is well below the noise floor in the scattering data.

Room: Poster level 2

PM1 (level 2) - Measurements I

T08 Fundamental research and emerging technologies/processes / / Measurements

Chairs: Nadine Joachimowicz (Sorbonne Université, CNRS Laboratoire de Génie Electrique et Electronique de Paris, France & Université Paris Cité, France), Omar Orgeira (Northern Waves AB, Sweden)

2. 25. A Prototype of Sub-THz Communication Link for Immersive 6G XR Applications

Pablo González Méndez, María Purriños Paz, Pablo Losada Sanisidro, Pablo Vilar Gómez, Brais Ares Fernández, David Zamorano and María Crego (Gradiant, Spain); Amr Abdel Nabi (i2CAT, Spain); J. Joaquín Escudero-Garzás (Centro Tecnolóxico de Telecomunicacións de Galicia - Gradiant, Spain)

Extended reality (XR) is an environment considered one of the pillars of future 6G networks for services such as holographic teleconference and immersive gaming. To make this a reality, communications networks must meet the stringent requirements of XR services. The combination of the ISAC (Integrated Sensing and Communications) paradigm with the utilization of the sub-THz band can be the basis of communications infrastructure that supports XR applications. Following this approach, this work presents the design and implementation details of a sub-Thz link prototype that simultaneously supports a data rate of 2 Gbps and radar functionalities. As commercial-off-the-shelf (COTS) equipment is the main hardware component of the prototype, the system has a reduced cost compared to other testbeds based on monolithic, commercial equipment and provides a high degree of flexibility for experimentation.

2. 26. Advanced Detection and Signal Reception System Utilizing Rydberg Atomic Dynamics for Applications

Wenjie Ding, Guoda Xie, Yingsong Li and Zhixiang Huang (Anhui University, China)

In this paper, we introduce a novel Monte Carlo wave function method (MCWFM) for simulating the transient response of Rydberg atoms under rapidly varying electric fields, aimed at high-precision electric field measurements and wireless communication reception. This approach leverages the electromagnetically induced transparency (EIT) effect and Autler-Townes (AT) splitting in Rydberg atoms, offering enhanced efficiency compared to traditional density matrix methods by focusing solely on wave function evolution, thereby reducing computational complexity. Additionally, we account for Doppler effects in AT splitting through MCWFM, providing faster results than conventional Runge-Kutta methods. This work lays a solid foundation for advancing Rydberg atom technology in the development of highcapacity, high-fidelity wireless communication systems.

2. 27. Dielectric Characterization of Fabric-Sweat Mixtures Using Microstrip Transmission Lines for Antenna-Based Sensing Applications

Mohammed Ahmed Alsultan and Sergio López-Soriano (Universitat Oberta de Catalunya, Spain); Joan MeliàSeguí (Universitat Oberta de Catalunya (FUOC), Spain)

In the realm of electronics and textile integration, fabric-based substrates for antennas, resonators, and sensors have emerged as innovative alternatives to traditional rigid printed circuit boards. Methods for measuring the dielectric properties, including relative permittivity and loss tangent, remain limited, especially in relation to fabric-liquid mixtures. To address this gap, this study uses the Transmission Line Method to characterize the dielectric properties of fabric-sweat mixtures in both euhydrated (i.e., regular hydration) and dehydrated states for RFID hydration monitoring applications. This study presents a set of experiments to compute the dielectric properties of the mixtures with three different fabric materials (jeans, cotton, and polyester), two types of sweat (euhydrated and dehydrated) and different amounts of sweat injected into the fabric. The results confirm the feasibility of measuring the relative permittivity and the loss tangent of fabric-liquid mixtures at 800-1000 MHz.

TUESDAY

2. 28. Grid-Based Measurement Density Optimization Considering Multipath Environments for Efficient Wireless Quality Assessment

Hiroaki Shimmiya, Tomoki Murakami, Yasushi Takatori and Tomoaki Ogawa (NTT Corporation, Japan)
The utilization of high frequency bands, such as millimeter-waves, is advancing to enhance the channel capacity of mobile communication systems. It is generally known that high frequency bands have strong directivity but poor penetration capabilities, necessitating the investigation of wireless quality through simulations and measurements tailored to specific environments to stabilize communication quality. This paper proposes a grid-based measurement density optimization method for efficient wireless quality assessment. This novel approach adjusts the number of measurement points per grid based on the gradient of the ratio between primary and secondary reflected path components, serving as an indicator of multipath environments. The effectiveness of the proposed method is validated through ray-tracing simulations on an actual city environment. The evaluation results demonstrate that referencing the multipath environment indicator to set the density of measurement points effectively reduces measurement costs while maintaining high interpolation accuracy.

2. 29. Impact of Operating Frequency and Substrate Materials on Microwave Sensor Sensitivity for Blood Glucose Monitoring

Amal Swileh and Rola Saad (The University of Sheffield, United Kingdom); Salam Khamas (University of Sheffield, United Kingdom)
A biosensor is designed to detect glucose concentration levels using a single metamaterial-based asymmetric double split ring resonator. The study investigates the influence of operating frequency and substrate on the sensor sensitivity. The glucose sample is placed in a small semi-circle gap within the sensor. At this location, a confined electric field enhances the sensor's sensitivity. The sensor's sensitivity has been investigated across three different frequencies of 1 GHz, 3 GHz, and 7 GHz, implemented on an FR4 substrate. Additionally, the study compares the sensor sensitivity across three different substrates; Teflon, Rogers AD350A, and FR4 at 7 GHz. The results show that the sensor operating at 7 GHz is the most sensitive to the glucose concentration levels, while the sensor incorporating Teflon substrate exhibits the highest sensitivity to glucose concentration levels.

2. 30. Improvement of the Target Support for RCS Testing with Accurate Evaluation of the Creeping Wave as a Function of Azimuth Along the Axis of Measurement

Thibault Charlet (CEA CESTA, France)
When measuring Radar Cross Section (RCS), the target support, mast or pylon is a critical element. The need of mechanical holding often results in significant scattering of this mast and electromagnetic interference due to contact with the Object Under Test (OUT). In particular, the creeping wave on the OUT is generally disturbed. The aim of this work is therefore to develop an effective target support for accurate evaluation of the creeping wave . The evolution of the mast geometry from a generic shape to an optimized one is described. Simulations of the new design are then validated by comparison with measurements of two canonical metallized OUT: a sphere and a sphere-cone. The results of measurements with the optimized target support show a significant improvement in the final RCS measurement, validated by analysis of the simulated impulse response where the creeping wave is accurately evaluated.

2. 31. Optimizing Real-Time GPU Image Processing for Industrial MIMO Radar Sensors

Josh Perske and Yannick Emonds (Fraunhofer Institute for High Frequency Physics and Radar Techniques FHR, Germany); Sabine Guetgemann (Fraunhofer FHR, Germany)
The development of a new sensor system involves a multitude of different steps from the concept phase to the finished product. A number of new challenges arise when it comes to bringing new concepts into actual application. This paper focuses on the development of a new FMCW (Frequency Modulated Continuous Wave) MIMO (Multiple Input Multiple Output) radar sensor, specifically addressing the implementation and optimization of GPU-based (Graphics Processing Unit), real-time signal processing software. Various aspects of the software design are examined that must be considered during the transition from a theoretical concept to a real-time capable product. This paper introduces a modular 32-channel MIMO system, expandable to 192 channels, currently operating at a 200Hz frame rate. While the current performance is sufficient for many applications, an outlook is provided on achieving higher measurement rates in the future to facilitate inline sorting of black plastics.

2. 32. Over-The-Horizon Surface Wave Radar: From the Maritime Target Point-Of-View

Antoine Lugand (ONERA & Sorbonne University, France); Stéphane Saillant (ONERA - The French Aerospace Lab, France); Muriel Darces (Sorbonne Universite, France)
The work presented in this paper is part of an extensive study on HF surface wave radar, carried out jointly by ONERA and Sorbonne University for almost 20 years. In this article, we focus in particular on characterizing the maritime targets to be detected by this radar. To do this, we propose to use tools, both numerical and experimental, previously developed to characterize the radar's transmitting antennas: a numerical target model using equivalent sources, and instrumentation of a drone enabling near-field measurement of the field diffracted by the target. Finally, couplings between sky waves and surface waves on the target will be analyzed, enabling us to define a new Radar Cross Section, suitable for surface wave propagation.

TUESDAY

2. 33. Permittivity Sensors Based on Conventional and Complementary Split Ring Resonators

German Augusto Ramirez Arroyave (EPFL - École Polytechnique Fédérale de Lausanne & Universidad Nacional de Colombia, Switzerland); Anja K. Skrivervik (EPFL, Switzerland)

This work presents some considerations for the use of a Split Ring Resonator (SRR) and its dual structure, the Complementary Split Ring Resonator (CSRR), as permittivity sensing elements. The analytical circuit equivalents of both resonators are reviewed in the light of multilayer transmission lines and adjusted models are derived for the resonant frequencies when superstrates with finite thickness are included, thus accounting for the finite thickness of the Material Under Test (MUT) and the possible use of a sample container with its corresponding material and thickness. Validations of the proposed analytical models are performed by means of full-wave electromagnetic simulation using a SRR loaded microstrip line and a CSRR loaded Substrate Integrated Waveguide (SIW), as dielectric permittivity sensors.

2. 34. Spatial Averaging Calculations of 5G Beam-Forming Antennas for EMF Compliance Assessments

Martin Batt (Alphawave Mobile Network Products (IXUS), South Africa); Danie Ludick (Stellenbosch University, South Africa); Kyle Lotter (Alphawave Mobile Network Products, South Africa); Matthew J Butcher (Sublight Engineering PLLC & Sublight Engineering, USA); Raynard Swanepoel and Rikus Human (Alphawave Mobile Network Products, South Africa)

When calculating whole-body spatially averaged electromagnetic field (EMF) exposure at cellular base stations utilizing massive multiple-input multiple-output (MIMO) and beam-forming technologies, the typical approach is to use the maximum gain envelope of all horizontal and vertical steering directions of the traffic beam. When considering the vertical steering capability of the antenna, calculations performed from multiple vertical beam directions at maximum gain across the spatial averaging range will result in an overconservative assessment since the traffic beams are not directed at multiple directions simultaneously with the same effective isotropic radiated power (EIRP). A more accurate approach would be to differentiate between multiple vertical tilt steering directions. By calculating the wholebody spatially averaged EMF exposure for each individual tilt or vertical steering direction, a less overly conservative compliance boundary for the beam-forming antenna may be derived.

2. 37. Validity of the Physics Behind Inversion Problems in Microwave Imaging: Born Approximation and Scattering Losses

Chloé Scotti (Aix-Marseille University & CEA DAM - LE RIPAULT, France); Max Groisil (CEA DAM Le Ripault Monts France, France); Amélie Litman (Aix-Marseille Univ, CNRS, Centrale Med, Institut Fresnel, France); Mohamed Latrach (RF-EMC Research Group, IETR-ESEO, Angers & ESEO, Graduate School of Engineering, France); Stefan Enoch (CNRS, Aix-Marseille University, France); Nicolas Mallejac (CEA, France)

A characterization method has been developed in recent years to measure in free space the complex permeability and permittivity of heterogeneous magneto-dielectric materials. It is based on the first-order Born approximation of the scattered field equation. However, previous work has shown, in a monostatic measurement context, difficulties in estimating the value of the dielectric losses of the material. This paper aims to explain the origin of this problem.

2. 38. Dosimetry Computation Based on Near-Field Measurements on a Huygens Box Surrounding the Antenna

Loide-De-Nascimento Lopes (University of Cote D'azur, France); Abdelrahman Abdallah Ijjeh and Soukaina Mifdal (Université Cote d'Azur, France); Alexandre Debard (LEAT, France); Marylène Cueille (University of Nice Sophia Antipolis CNRS, France); Jean-Lou Dubard (UCA, LEAT, France); Stephane Pannetrat (ART-Fi, France); Mohammad Bagheriasl (Art-fi, France); Laurence Richard (Art-Fi, France)

This article presents a new technique for dosimetry assessment in realistic environments based on free-space EM-fields' measurements around the antenna thanks to a RF phasor array embedded in an EM scanner. These measured EMfields are used in the simulation as a Huygens' box source to model the radiation from the EM-device. Note that in practice -except for the manufacturers of the EM device- the challenge is that we don't know the full details of the EM-device concretely. Such knowledge is necessary in any simulation process containing the device. The coupling of RF phasor near-field measurements with simulations (augmented measurements) are done by keeping a turned off simplified replica of the EM-device inside the Huygens' box to model the interactions between the human model and the EM-device (e.g., scattering and diffraction). Numerical simulations are done with the Finite Integration Technique (FIT) to test the accuracy and validity of the proposed approach.

TUESDAY

2.39. Power Delay Profile Characterization for THz Communications Link

Hirokazu Sawada and Azril Haniz (National Institute of Information and Communications Technology, Japan); Shingo Saito (National Institute for Information and Communications Technology, Japan); Keizo Inagaki (National Institute of Information and Communications Technology & Waseda University, Japan); Akifumi Kasamatsu (National Institute of Information and Communications Technology, Japan); Norihiko Sekine (National Institute for Information and Communications Technology, Japan); David Van Workum (Keysight Technologies, USA); Kenichi Inoue and Satoru Takahashi (Keysight Technologies, Japan); Suren Singh (Keysight Technologies, USA); Takeshi Matsumura (National Institute of Information and Communications Technology (NICT), Japan & Kyoto University, Japan)

The use of sub-terahertz and terahertz waves is considered as a frequency band for next-generation wireless communication systems that will enable high-speed communication of tens of Gbps or more, and it is necessary to clarify the radio wave propagation characteristics to design the physical layer of wireless systems. Previously, the authors developed a propagation loss model based on the results of measuring the propagation loss in the 232-500 GHz band in office and data center environments. In this report, we report the results of measuring the power-delay profile in a data center and an outdoor environment with wireless signal bandwidths of 2.16 GHz and 5 GHz. We also present analytical results on the rms delay spread and correlation bandwidth, which are important parameters for physical layer design, as an evaluation of the characteristics of the power-delay profile.

2. 40. Estimation of Ionospheric Scintillation Index S4 from Rate of Change of Total Electron Content Index (ROTI) in Low Latitudes

Teddy Surco Espejo, Charles Carrano and Keith Groves (Boston College, USA)

Ionospheric scintillation is one of the main error sources that degrade the satellite signals and hence can cause significant errors in positioning based on Global Navigation Satellite System (GNSS). However, specialized receivers that can generate the scintillation indices (S4 and σφ) are not available all around the world, which limits the application of these approaches. In spite of that, there are numerous inexpensive geodetic receivers that are capable of measuring the Total Electron Content (TEC) and Rate of TEC (ROTI). The ROTI is a commonly used measure of ionospheric irregularities level. Hence, the possibility of monitoring scintillation using dense networks of TEC monitors arises.

2. 41. Experimental Assessment of 5 GHz WiFi Coverage Expansion in Underground Mine Using Reconfigurable Intelligent Surface

Aurélien Surier (Université du Québec en Abitibi-Témiscamingue, Canada); Nadir Hakem (Université du Québec en Abitibi Témiscamingue, Canada); Nahi Kandil (Université du Québec en Abitibi-Temiscamingue, Canada)

We assess the 5 GHz WiFi coverage expansion in a underground mine using a reflecting Intelligent Surface with a transmitarray-like behavior allowing to bend the signal into secondary Non-light-Of-Sight orthogonal tunnels.

2. 42. Modelling Passive Spherical Reflectors to Improve Millimetre Wave Coverage in Corridors

Priya Qualtrough-Mittal (University of Auckland, New Zealand); Michael J Neve (The University of Auckland, New Zealand); Andrew C M Austin (University of Bristol, United Kingdom)

The millimetre wave frequency band presents challenges with coverage into non-line-of-sight regions, resulting in significant shadowing. This can become particularly prevalent in indoor corridor environments where there are many human obstacles. In this work, quarter-sphere reflectors have been investigated to provide additional ray paths along a corridor. Placement of a reflector in the centre or far end of the corridor provided more coverage than a reflector placed directly next to the source. Deployment of multiple reflectors improved coverage, regardless of wall placement, with use of 4 or more reflectors providing coverage to more than 95% of user locations. Furthermore, in cases where more than one reflector is deployed, contributions from multiple reflectors were received at some user locations, leading to increased received power.

2. 43. A First Quick Tool Based on Analytical Approach for the Analysis of the Performance of Microwave Sensors in Medical Applications

Antonio Cuccaro (Università della Calabria, Italy); Sandra Costanzo (University of Calabria, Italy); Raffaele Solimene (Università degli studi della Campania Luigi Vanvitelli, Italy)

In microwave medical applications, the sensor are often deployed in direct contact to human body. Under this working condition, it is hard to predict exactly the sensor behaviour and the standard methods for designing it fail. This has encouraged the use of full wave analysis for the design of the microwave sensors. However here, for sensors in waveguide technology, an approximate analytical model is derived for reflection coefficient (mat\Gamma). Numerical results predicts with analytical model are in agreement with the one performed via full wave simulations. This suggest that the proposed model can be considered as a first quick tool for design the sensor reducing the high computational cost of full wave analysis approach.

2. 44. Analysis of Clouds and Rain Losses on Terahertz Band for Non-Terrestrial Networks

Bushra Khan and Joonas Kokkoniemi (University of Oulu, Finland)

In today's world, high-speed and reliable internet access is a global necessity. Despite this, millions of users suffer on a daily basis due to limited service on airplanes and in remote areas. Microwave frequencies have long reachability, but due to the limited available bandwidth, they cannot serve a large number of users with high data rates and reliability guarantees. Therefore, this research focuses on providing high-speed internet access using millimeter wave (mmWave)/terahertz (THz) frequencies to address the aforementioned shortcomings of microwave frequencies. Our primary goal is to investigate the effects of various channel parameters on mmWave/THz frequencies, including pointto-point (P2P) path loss and atmospheric losses. The analysis reveals that airplane-to-satellite (A2S) links can achieve better signal-to-noise ratio (SNR) across the 100-1000 GHz frequency range by avoiding the adverse atmospheric effects at higher altitudes, whereas ground-to-satellite (G2S) links can still perform similarly up to 300 GHz but with higher atmospheric losses.

2. 45. Analysis of Shielding and Discontinuous Phantom Medium Effect on the Performance of Fat-Intra Body Communication System

Tarakeswar Shaw (Postdoctoral Researcher, Uppsala University, Sweden); Bappaditya Mandal (Uppsala University, Uppsala, Sweden); Robin Augustine (Uppsala University, Sweden)

This paper presents the design, optimization, and detailed analysis of a wearable fat intrabody communication (Fat-IBC) system based on resonator antennas, specifically tailored for biomedical applications. Fat-IBC uses the low dielectric loss properties of human fat tissue as a waveguide between the skin and muscle layers. This technique facilitates continuous communication among wearable, implanted, and semi-implanted biomedical devices, supporting seamless data exchange within body area networks (BAN). The proposed system employs a resonating antenna designed using a planar circular spiral with an enclosed notch, excited by a loop antenna. For the numerical simulations, a multi-layer human tissue model, comprising skin, fat, and muscle, is utilized to optimize the performance of the antenna resonator. To ensure bio-compatibility and prevent direct contact with human tissue, a polydimethylsiloxane (PDMS) coating surrounds the structure. The architecture of the system incorporates two identical antennas that act as transmitting (Tx) and receiving (Rx) elements.

2. 46. Design and Experiments of a Modified Double Folded Dipole for Superficial Hyperthermia

Jose Luis Duque Muñoz and Javier Leonardo Araque Quijano (Universidad Nacional de Colombia, Colombia); Iván Eduardo Díaz Pardo (Universidad El Bosque, Colombia)

We demonstrate the design, simulation, and validation of a folded dipole for melanoma treatment using local hyperthermia. This design gives us control over the size and shape of the thermal footprint, and its compact and lightweight design makes it easy to fabricate and integrate into complex structures. Experimental results utilizing a phantom that mimics the dielectric characteristics of human skin show that the thermal footprint is of appropriate size and shape for hyperthermia-based melanoma therapies.

2. 47. Design, Development and Testing of a Conformal 60 GHz Active Repeater for High Energy Physics Applications

Imran Aziz (Uppsala University & Mirpur University of Science and Technology, Mirpur Azad Jammu and Kashmir, Sweden); Yasin Alekajbaf, Dragos Dancila, Kristian Pelckmans, Abhinav Jain and Richard Brenner (Uppsala University, Sweden)

The Wireless Allowing Data and Power Transmission (WADAPT) proposal was formed to study the feasibility of wireless technologies in HEP experiments. A strong motivation of using wireless technology for data readout at the ATLAS detector is the absence of wires and connectors to reduce the passive material. Besides, radial wireless links can be used to build topological networks for neuromorphic tracking. However, the tracking layers at the detector are almost like a Faraday cage that doesn't allow propagation between the layers. For data readout through the layers, we have developed an active repeater board, which is passed through a 2-3 mm wide slit between the modules on the tracking layers. Measurements show a receive level of -19.5 dBm. In comparison, when the amplifier turned off, the receive level is ~-46 dBm. The results show a significant milestone towards the implementation of 60 GHz links for detector data readout.

2. 48. Enhancing Wireless Communications at 300 GHz Using RIS in an Industrial Scenario

Georg Jensen (TU Braunschweig, Germany); Bo Kum Jung (Technische Universität Braunschweig, Germany); Qi Luo (University of Herfordshire, United Kingdom); Thomas Kürner (Technische Universität Braunschweig, Germany)

This paper investigates the use of Reconfigurable Intelligent Surfaces (RIS) to enhance wireless communication in industrial environments operating at 300 GHz. The study focuses on a realistic factory scenario where pillars obstruct direct line-of-sight (LOS) communication. By strategically positioning RIS, signal coverage was improved in an area with shading effects. Ray-tracing simulations were conducted using the Simulator for Mobile Networks (SiMoNe) to evaluate the gain of the received power, especially in areas where the direct coverage of the transmitter (TX) was obstructed by obstacles. Results demonstrate that RIS significantly improves signal quality and coverage, offering a practical solution for overcoming communication barriers in complex industrial environments. The findings highlight the potential of RIS to enhance connectivity in future industrial wireless networks.

TUESDAY

2. 49. Experimental Investigation of Propagation over the Forearm at 24 GHz

Wasi Ur Rehman Khan, Max James Ammann and Hossein Raghib Hokmabadi (Technological University Dublin, Ireland); William G. Scanlon (Tyndall National Institute, Ireland); Adam Narbudowicz (Tyndall National Institute, Ireland & Wroclaw University of Science and Technology, Poland)

On-body propagation is experimentally investigated at 24 GHz using Vivaldi and Yagi antennas placed on a forearm phantom. The effect of antenna/body spacing on path loss is analyzed for normal and tangential polarizations. The results show that path loss varies significantly for tangential polarization when the antenna/body spacing changes. We also demonstrate that the two-ray propagation model is applicable to the human forearm, to identify locations with constructive and destructive interference between direct and reflected waves. This opens a possibility for channel enhancement.

2. 50. Impact of Antenna Topology and Polarization on Breast Tissue Penetration and Tumor Detection

Raquel A. Martins (Instituto de Telecomunicações/Instituto Superior Técnico, Portugal); Joao M Felicio (Instituto Superior Técnico, Portugal & Instituto Telecomunicacoes, Portugal); Jorge R. Costa (Instituto de Telecomunicações / ISCTE-IUL, Portugal); Carlos A. Fernandes (Instituto de Telecomunicacoes, Instituto Superior Tecnico, Portugal)

We present a study in which we assess the effect that different antenna topologies and polarization may have on breast penetration depth, and consequently on tumor detection. To this end, we simulate a homogeneous breast model which is scanned by different broadband antennas working in the 2-5 GHz band and aligned for vertical or horizontal polarization. The penetration depth is studied measuring the electric field frequency response which is retrieved by 625 field probes. To analyze the effect on tumor detection, we also included a 5-mm radius tumor inside the breast. Results show that the energy that enters the breast is commonly focused in line of sight of the antenna and is highly dependent on the shape of the breast. The horn antenna led to higher penetration values, followed by slot-based antenna, bowtie and Vivaldi, respectively. Vertical-oriented antennas led to better results. This effect is reflected in tumor detection.

2. 51. Numerical Modelling and Validation of 5g Signal Propagation in Complex Urban Environment

Marco Murgia, Matteo Bruno Lodi, Giacomo Muntoni, Giuseppe Mazzarella and Alessandro Fanti (University of Cagliari, Italy)

This paper presents a numerical analysis of 5G signal propagation in complex urban environments using the Dominant Path Model (DPM) within Feko WinProp software. The study evaluates the simulation of signal interactions with urban structures, such as irregular building layouts and significant elevation changes, with a focus on 5G frequencies within frequency range 1. In comparing simulation results with path loss measurements, we demonstrate that DPM effectively models signal behavior in high-complexity scenarios, offering a computationally efficient alternative to traditional raytracing methods. This approach promises to develop accurate path loss models, essential for optimizing 5G coverage planning in challenging urban environments

2. 52. On the Influence of DSD Fluctuations on the Cumulative Distributions of Rain Attenuation at Millimeter Waves

Jose M Riera, Juan Ramón Romero-Vilar, Domingo Pimienta-del-Valle and Ana Benarroch (Universidad Politécnica de Madrid, Spain)

Rain attenuation at millimeter waves is progressively more influenced by the Drop Size Distributions (DSD). This influence has been characterized in the last years with databases of DSD gathered in Madrid, Spain and other sites. The results showed that a significant variability of rain specific attenuation γ (dB/km) can be expected from DSD fluctuations. A model for the probability distribution function (pdf) of γ was proposed. From this model, the question was raised whether the cumulative distributions of γ would be affected by this variability. This paper tries to answer to this question, by comparing the complementary cumulative distribution functions (CCDF) obtained with and without considering this variability. The conclusion is that the variability has a significant effect on the CCDFs, more relevant as frequency grows and for lower time percentages. The application of these results to system planning would lead to higher link margins.

2. 53. Performance Evaluation of the ITU-R Prediction Model of the Rain Attenuation in Earth-Satellite Links

Arsim Kelmendi (The French Aerospace Lab - ONERA, France); Julien Queyrel (ONERA & Université de Toulouse, France); Laurent Castanet (ONERA, France)

High throughput satellite communication systems, need to utilize less congested high-frequency bands, such as the Ka- and Q-bands and above with a large available radio channel bandwidth. However, radio wave propagation at these frequencies is hindered by increased attenuation and impairment caused by tropospheric phenomena, particularly rainfall. It is crucial for such systems to characterize rain attenuation in the slant path for the design and setup of the satellite communication system. The statistical prediction model of rain attenuation in Earth-space paths, provided in Section 2.2.1.1 of Recommendation ITU-R P.618-14, depends on several parameters, including the rainfall rate and the rain height. In this paper is investigated the performance of rainfall rate Recommendation ITU-R P.837-7 and rain height Recommendation ITU-R P.839-4 based on the digital maps from ECMWF ERA5 database and their influence on the rain attenuation prediction model in Rec. ITU-R P.618-14.

TUESDAY

2.54. Site Diversity Reception Performance Evaluation in Cyprus at Ka- and Q-Band for High Throughput Satellite Systems

Nektarios Moraitis (National Technical University of Athens & Institute of Communications and Computers Systems, Greece); Apostolos Z. Papafragkakis and Athanasios D. Panagopoulos (National Technical University of Athens, Greece); Panayiotis Ioannides, Nikolaos Christoforou, Constantinos Agrotis and Sotirios Alexandrou (Cyprus Telecommunications Authority (Cyta), Cyprus)

This paper evaluates the benefits of site diversity reception at Ka- and Q-band in Cyprus. The analysis is based on local point rainfall rate meteorological data collected near the sites of interest. The performance of a double and the corresponding triple site diversity is presented along with their comparison. According to the simulations the adoption of double and triple site receptions enhances remarkably the outage performance at both examined frequencies. If very high availability for a satellite service is required, triple diversity is a convenient option at both frequencies without leading to enormous fade margins. Finally, it is endorsed that real rainfall rate data be leveraged for diversity performance calculations, since the simulations highlighted that ITU- R rain-maps tend to overestimate the outage time.

2. 55. Statistical Modelling of Loss on Short Paths

Richard Rudd (Plum Consulting Ltd, United Kingdom)

There is a frequent requirement in spectrum sharing studies to assess transmission loss between terminals of different systems with a wide range of mutual geometries. Existing propagation models are often tailored to a few standardised geometries, primarily those relating to wanted paths or intra-system interference. Furthermore, they are often specified for use in environments that are subjectively defined (i.e. 'urban' or 'suburban'). The wide availability of open data relating to the built environment opens the possibility of a more objective categorisation of propagation environments. This paper compares predictions from a proposed statistical model with measurements made below 3 GHz.

2. 56. Synthesis of Omnidirectional Path Loss Model Based on Directional Model and Multi-Elliptical Geometry

Jarosław Wojtuń, Cezary Ziółkowski and Jan M Kelner (Military University of Technology, Poland); Tomas Mikulasek, Radek Zavorka, Jiri Blumenstein and Petr Horky (Brno University of Technology, Czech Republic); Ales Prokes (Brno University of Technology & Sensor, Information and Communication Systems Research Centre, Czech Republic); Aniruddha Chandra (National Institute of Technology Durgapur, India); Rajeev Shukla (National Institute of Technology, India); Anirban Ghosh (SRM University Amaravati, India)

Millimeter wave (mmWave) technology offers high throughput but has a limited radio range, necessitating the use of directional antennas or beamforming systems such as massive MIMO. Path loss (PL) models using narrowbeam antennas are known as directional models, while those using omnidirectional antennas are referred to as omnidirectional models. To standardize the analysis, omnidirectional PL models for mmWave ranges have been introduced, including TR 38.901 by 3GPP, which is based on measurements from directional antennas. However, synthesizing these measurements can be complex and time-consuming. This study proposes a numerical approach to derive an omnidirectional model from directional data using multi-elliptical geometry. We assessed the effectiveness of this method against existing PL models for mmWaves that are available in the literature.

2. 57. Throughput of SatCom and Earth Observation Fade-Mitigated Links in X and Ka Bands Simulated from Synthetic Attenuation Time Series

Laurent Quibus and Mohamad Younes (Académie Militaire de Saint-Cyr Coëtquidan, France); Eric Plouhinec (Ecoles de St-Cyr Coëtquidan, France)

Thanks to the larger bandwidths, satellite systems at higher frequencies are expected to provide higher data throughputs for communications and Earth observation alike. These higher frequencies are however also linked to stronger propagation impairments of the carrier which must be accounted for in the system design. This paper presents a numerical study of military satellite link budgets when moving from X to Ka band. A first approach based on the distributions of the attenuation helps to select the appropriate modulation and coding. A second approach uses recent developments in attenuation synthetic time series to explore two strategies of fade mitigation: adaptive coding for the communication via a geostationary satellite, and site diversity for the download of data from low Earth orbit.

2. 58. Variability of Radio Signal Attenuation by Single Deciduous Tree Versus Reception Angle at 80 GHz

Jarosław Wojtuń, Cezary Ziółkowski and Jan M Kelner (Military University of Technology, Poland); Tomas Mikulasek, Radek Zavorka, Jiri Blumenstein and Petr Horky (Brno University of Technology, Czech Republic); Ales Prokes (Brno University of Technology & Sensor, Information and Communication Systems Research Centre, Czech Republic); Aniruddha Chandra (National Institute of Technology Durgapur, India); Niraj Narayan (National Institute of Technology, India); Anirban Ghosh (SRM University Amaravati, India)

Vegetation significantly affects radio signal attenuation, influenced by factors such as signal frequency, plant species, and foliage density. Existing attenuation models typically address specific scenarios, like single trees, rows of trees, or green spaces, with the ITU-R P.833 recommendation being a widely recognized standard. Most assessments for single trees focus on the primary radiation direction of the transmitting antenna. This paper introduces a novel approach to evaluating radio signal scattering by a single deciduous tree. Through measurements at 80 GHz and a bandwidth of approximately 2 GHz, we analyze how total signal attenuation varies with the reception angle relative to the transmitter-tree axis. The findings from various directional measurements contribute to a comprehensive attenuation model applicable to any reception angle and also highlight the impact of bandwidth on the received signal level.

TUESDAY

2. 59. An Integrated Design of UAV Passive Detection and Blanket Jamming Based on SDR

Yuchen Liu (Harbin Institute of Technology, China & School of Electronics and Information Engineering, China); Longwen Wu, Yaqin Zhao and Chentong Wu (Harbin Institute of Technology, China); Dongming Luo (Beijing Institute of Mechanical and Electrical Engineering, China)

Unmanned aerial vehicles (UAVs) have seen extensive development across multiple civilian sectors in recent years. However, the proliferation of UAVs has been accompanied by a lack of effective regulation, posing severe threats to low-altitude airspace security. This paper proposes an integrated scheme for passive detection and blanket jamming of UAVs based on software-defined radio (SDR). The scheme uses SDR, low-cost hardware, and GNU Radio to achieve passive detection and blanket jamming against UAV signals. By sweeping frequencies with SDR to stitch together large bandwidth spectra and employing adaptive thresholding for detection of UAV signals, the system can select different signal types, powers, and frequency bands for blanket jamming. Furthermore, it can be integrated with network server terminals to expand functionalities and meet diverse requirements. Various indicators have been tested in the laboratory and outdoor environment. The results validate the effectiveness of the passive detection and blanket jamming of UAVs.

2. 60. Angular Properties for Power from a Spatial Cluster

Torbjörn Ekman (Norwegian University of Science and Technology, Norway)

A spatial cluster of scatterers forming a link between a TX and RX behaves as a random array, passively relaying the radio signal. The statistical properties of the antenna pattern for this random array are derived in the far field. The analysis is performed for circular symmetric clusters. The average lobe width, average notch width, and the number of level crossings for the antenna pattern are derived for a Gaussian spatial cluster. Simulated cluster properties coincide with the analytical results.

Tuesday - 14:40-15:20

Room: Alfvén (A3+A4)

Invited Speaker

Diego Masotti

Chair: Guido Valerio (Sorbonne Université, France)

Room: Kildal (A2)

Invited Speaker

Yong Mei Pan

Chair: Mauro Ettorre (Michigan State University, Electrical and Computer Engineering, USA)

Tuesday - 15:50-17:30

Room: Alfvén (A3+A4)

CS35 - Emerging Beam-Steering Technologies for 5G Millimeter-wave and Beyond Cellular and Satellite Communications

T02 Millimetre wave and THz for terrestrial networks (5G/6G) / Convened Session / Antennas

Chairs: Lei Wang (Lancaster University, United Kingdom), Guangwei Yang (Northwestern Polytechnical University, China)

15:50 Low-Profile Slot-Coupled Millimeter-Wave Microstrip Antenna Arrays with Enhanced Isolation

Tianyan Lan (Sun Yat-sen University, China); DaCheng Huang (Sun Yat-sen University, China & School of Electronics and Information Technology, China); Yiming Zhang (Sun Yat-sen University, China)

In this paper, a simple decoupling technique for millimeter-wave (mmW) microstrip antenna arrays is proposed, which significantly improves the isolation without increasing the profile height. By introducing M-shaped microstrip in the feed layer of the patch antenna array, a new decoupling path is constructed and the decoupling resonance is generated. The decoupling depth is also significantly improved by slot line. Simulation results show that the proposed decoupling method achieves an isolation of 32.6 dB at 25 GHz in a 1×2 antenna array. In addition, in the 1×4 antenna array, the isolation between adjacent elements can reach 32.9 dB, and the coupling between non-adjacent elements is also reduced. In terms of beam scanning performance, the 1×4 array shows almost no drop in maximum gain and the sidelobe level (SLL) is less than -9.48 dB within ±45°.

16:10 A MMW Multi-Beam Full-Duplex 1×4 Antenna Array Based on the Butler Matrix

Xu Li, Yiming Zhang and Hu Lei (Sun Yat-sen University, China) **This paper presents a multi-beam full-duplex antenna system based on the Butler matrix. By loading a decoupling structure on the radiating layer of the antenna, the isolation between the receiving and transmitting antennas is improved. The center frequency of the antenna system is 25 GHz, and simulation results show that within the frequency range of 24 GHz to 26 GHz, the amplitude imbalance of the Butler matrix is 1 dB, and the phase imbalance is 3°. The 1×4 antenna system integrated with the decoupling structure and the Butler matrix has a beam scanning range of -67° to 67° and at the center frequency, the minimum isolation between the receiving and transmitting ports has increased from 23 dB to 31 dB. This antenna system is suitable for IAB technology**

TUESDAY

16:30 A Low-Profile Circularly Polarized Beam Steering Folded Reflectarray

Qiqi Zhou and Lu Guo (Nanjing University of Science and Technology, China)
This article introduces a low-profile circularly polarized beam-scanning folded reflectarray. The proposed antenna consists of a circular polarization selection surface (CPSS), a reflectarray and a circularly polarized horn. The CPSS reflects right hand circular polarization (RHCP) waves and transmits left hand circular polarization (LHCP) waves, while the reflectarray realizes polarization conversion. The rotation of the upper CPSS and lower reflectarray enables beam steering in both elevation and azimuth angles. The proposed circularly polarized beam-scanning folded reflectarray exhibits a maximum elevation scanning angle of 43° with good circularly polarized radiation performance.

16:50 1 Bit Reconfigurable Dual-Beam Magnetoelectric Dipole Array Antenna for Beam Steering

Rukiye Adil, Guangwei Yang, Yiwei Zhang and Zijian Xing (Northwestern Polytechnical University, China)
A 1-bit reconfigurable magnetoelectric (ME) antenna is introduced as the element of a nine-element array. By changing the feeding position, the antenna elements can radiate different electric field phases. This feature enables the array to form beams at various directions through the arrangement of elements in distinct phase states. Simulations confirm that the electric field phase difference between the two feeding states of the element is exactly 180°. The array is designed to produce beams at 0°, 15°, 30°, 45°, and 60° within 10 dB impedance bandwidth of 4.26 to 6.65 GHz with dual-beam capability. It exhibits the peak gain of 13.9 dBi and maintains a cross-polarization level below -20 dB across the frequency band. The proposed array offers the benefits of low cost and ease of control.

17:10 Wide-Angular Scanning Performance Enhancement Phased Aarray Using Phase Gradient Metasurface

Yihan Ma (University of Hertfordshire, United Kingdom); Qi Luo (University of Herfordshire, United Kingdom); Yonggang Zhou (Nanjing University of Aeronautics and Astronautics, China); Guangwei Yang (Northwestern Polytechnical University, China)
This work proposes a novel concept for improving beam scanning performance in a phased array. Theoretical analysis demonstrates that a 1D linear array integrated with a phase gradient metasurface ground can introduce additional phase delays to the corresponding image elements, enhancing array scanning performance, especially for gain improvement across the entire scanning range as well as sidelobe suppression at large scanning angles. To validate this concept, a printed 1D linear dipole array with a rectangular-shaped digital coding metasurface was designed and fabricated. The proposed phased array achieves accurate angle scanning and low sidelobe levels by adjusting the phase distribution of the metasurface ground. The proposed structure achieves a maximum gain enhancement of 2.7 dBi compared to the conventional phased array with a PEC ground, and the maximum sidelobe level is -9.6 dB when scanning at elevation angle of 60 degree.

Room: : Kildal (A2) | **CS3 - Physics-Compliant RIS Modeling**

T08 Fundamental research and emerging technologies/processes / Convened Session / Electromagnetics

Chairs: Philipp del Hougne (CNRS, Univ Rennes, France), Anthony Grbic (University of Michigan, Ann Arbor, USA)

15:50 Multiport Network Theory for Modeling and Optimizing Reconfigurable Metasurfaces

Marco Di Renzo (CentraleSupelec-University, France); Philipp del Hougne (CNRS, Univ Rennes, France)
Multiport network theory (MNT) is a powerful analytical tool for modeling and optimizing complex systems based on circuit models. We present an overview of current research on the application of MNT to the development of electromagnetically consistent models for programmable metasurfaces, with focus on reconfigurable intelligent surfaces for wireless communications.

16:10 Physics-Compliant Modeling and Scaling Laws of Multi-RIS Aided Systems

Matteo Nerini (Imperial College London, United Kingdom); Gabriele Gradoni (University of Surrey, United Kingdom); Bruno Clerckx (Imperial College London, United Kingdom)
Reconfigurable intelligent surface (RIS) is a revolutionary technology enabling the control of wireless channels and improving coverage in wireless networks. To further extend coverage, multi-RIS aided systems have been explored, where multiple RISs steer the signal toward the receiver via a multi-hop path. However, deriving a physics-compliant channel model for multi-RIS aided systems is still an open problem. In this study, we fill this gap by modeling multi-RIS aided systems through multiport network theory, and deriving the scaling law of the physics-compliant channel gain. The derived physics-compliant channel model differs from the widely used model, where the structural scattering of the RISs is neglected. Theoretical insights, validated by numerical results, show a significant discrepancy between the physics-compliant and the widely used models. This discrepancy increases with the number of RISs and decreases with the number of RIS elements, reaching 200% in a system with eight RISs with 128 elements each.

TUESDAY

16:30 Experimental Validation of Scalable Electromagnetically-Modeled RIS Through Ray Tracing and Indoor Measurements

Le Hao (Technische Universität Wien, Austria); Sravan Kumar Reddy Vuyyuru and Sergei Tretyakov (Aalto University, Finland); Risto Valkonen (Nokia Bell Labs, Finland)
This work focuses on integrating electromagnetically consistent modeling of scalable anomalous reflectors into the design and optimization of future wireless networks. A manufactured anomalous reflector sample is utilized to validate various path loss models for reconfigurable intelligent surface (RIS)-assisted links through theoretical analysis, ray tracing simulation, and measurements. A static anomalous reflector prototype is developed for testing based on a linear periodic 'supercell' design, accounting for intrinsic losses and mutual coupling of RIS unit cells, then scaled to a medium-sized square planar array. To accurately model RIS in ray tracers, the radiation patterns are imported from electromagnetic solver simulations. The measurement results agree with ray tracing simulations and validate the developed models. The proposed models and methods of RIS-link analysis are adaptable to other RISs and compatible with different ray tracers, potentially reducing the need for massive calibration measurements.

16:50 Design of Beamforming Metasurfaces Using Microwave Network Theory

Malik Almunif (University of Michigan, USA); Faris Alsolamy (University of Michigan Ann Arbor, USA); Anthony Grbic (University of Michigan, Ann Arbor, USA) The paper proposes a design technique for directly-fed beamforming metasurfaces using microwave network theory. The beamformning metasurface consists of a grid of unit cells that are connected to ports. The impedance matrix, which relates the voltage and current at the unit cell ports, is extracted from a full-wave solver to accurately model electromagnetic coupling. Reactive loads are connected to the ports and optimized using network theory to provide beam steering and shaping. This technique is validated using an aperture-coupled grid of unit cells. A design example is presented to produce a broadside Gaussian amplitude. The example is verified using Ansys HFSS with the reactive loads attached to the metasurface, demonstrating the ability to produce desired radiation patterns

17:10 Toward a Coupled-Dipole Formalism for Circuit Theory to Harmonize Physics-Compliant Models of RISParametrized Wireless Channels

Jean Tapie (CNRS, France); Sajedeh Keshmiri (ASU, USA); Mohammadreza F. Imani (Arizona State University, USA); Marco Di Renzo (CentraleSupelec-University, France); Philipp del Hougne (CNRS, Univ Rennes, France)
We present the first step of our efforts to derive a coupled-dipole formalism for circuit theory that ultimately aims to unify two disjoint thrusts on physics-compliant modeling of wireless channels parametrized by reconfigurable intelligent surfaces (RISs), one based on circuit theory and one based on coupled-dipole formalisms. Here, we formalize the relation between the notions of "port" in the former approach and "dipole" in the latter approach. We establish that, surprisingly, \textit{two} polarizability values are required to characterize a single dipole when it acts as port: an "inside polarizability" perceived from inside the system and an "outside polarizability" perceived from the transmission line attached to the port's outside interface. We provide an intuitive explanation as well as analytical evidence based on a model of the port as a very short conducting wire with a lumped impedance at its center.

Room: Hallén (BAR5)

EurAAP Delegates Assembly

EurAAP DA

Room: Marcuvitz (M3)

CS58 - Coexistence and Spectrum Sharing

T08 Fundamental research and emerging technologies/processes / Convened Session / Electromagnetics

Chairs: Nicholas Mastronarde (University at Buffalo, USA), Paolo Testolina (Northeastern University, USA)

15:50 Sensing Outage Probability of Space-Borne Passive Radiometry in Coexistence with an Active Terrestrial Network

Mohammad Koosha and Nicholas Mastronarde (University at Buffalo, USA)
The expansion of next-generation wireless communication networks is increasingly hindered by the limited availability of radio frequency spectrum. An emerging solution gaining attention involves utilizing restricted passive RF bands, which are traditionally reserved for passive radio services such as space-based remote sensing and radio astronomy. These satellites require interference-free spectrum access to gather accurate environmental data. One such restricted RF band is the L-band (1400-1427 MHz), where NASA's Soil Moisture Active Passive (SMAP) satellite operates as a passive sensor. In previous work, we employed stochastic geometry to derive the statistical properties of radio frequency interference (RFI) from large-scale terrestrial cellular networks affecting SMAP. This paper extends that work by analyzing the Sensing Outage Probability (SOP), which represents the likelihood of RFI exceeding the acceptable error threshold for a given passive remote sensing mission.

16:10 Opportunities for Antenna Technology to Facilitate SHF and EHF Coexistence and Spectrum Sharing

Michael J. Marcus (Northeastern University, USA & Marcus Spectrum Solutions LLC, USA)
Radio technology and spectrum policy both were developed in the early 20th century when frequencies were much lower and wavelengths much longer than options available today. The smaller wavelengths in SHF and EHF enable antenna approach unimaginable when international and national spectrum polices were first framed. Combined with MIMO-like multielement antenna technology, these antenna approaches can be used to control intersystem and interservice interference to enable novel spectrum sharing approaches that have no analogs in lower bands.

16:30 Challenges and Opportunities of Spectrum Coexistence for Passive Remote Sensing

Raul Diez Garcia (Telespazio S.p.A., Spain); Aravind Venkitasubramony (University of Colorado, USA); Nicholas Brendle (Ohio State University, USA); Paolo de Matthaeis (Universities Space Research Association (USRA), USA); Joel T. Johnson (Ohio State University, USA); Beau Backus (NOAA, USA)
The growing demand for radio frequency spectrum access motivates the development of efficient spectrum sharing approaches and techniques, especially those that try to coordinate the access to the electromagnetic medium to avoid interferences A general overview of cooperative spectrum sharing technologies is provided in this paper with particular focus on how they can improve the coexistence between passive remote sensing and active radio services. To that effect, some specific implementations are described. Finally, the challenges and opportunities that spectrum coexistence brings to remote sensing are identified and discussed from the point of view of engineers and scientists working in this field.

16:50 Evaluation of 3D Terrestrial and Aerial Spectrum Sharing with Massive MIMO Systems

Achiel Colpaert (IMEC, Belgium & KU Leuven, Belgium); Zhuangzhuang Cui and Sofie Pollin (KU Leuven, Belgium)
Connecting aerial and terrestrial users with a single base station (BS) is increasingly challenging due to the rising number of aerial users like unmanned aerial vehicles (UAVs). Traditional BSs, designed with down-tilted beams, focus mainly on ground users, but massive MIMO (mMIMO) systems can significantly enhance coverage in lowaltitude airspace. This paper analyzes how a mMIMO BS serves both aerial and terrestrial users in a 3D spectrumsharing scheme. Using Semi-orthogonal User Selection (SUS) and random scheduling, we assess the spectral efficiency and performance limits of these systems. Results reveal that mMIMO effectively supports more terrestrial users, influenced by channel characteristics and user scheduling strategies, providing key insights for future 3D aerialterrestrial networks

17:10 A New Paradigm: Mid-Band, Sharing-Native 6G

Monisha Ghosh (University of Notre Dame, USA)
The 6G juggernaut has started rolling, even as significant concerns remain about the success of 5G and spectrum availability for the continued expansion of wireless connectivity. Based on insights derived from extensive past research on measurements and analyses of real-world deployed 5G networks in licensed mid-band, mmWave and shared spectrum, as well as sharing studies between Wi-Fi and incumbent users in the unlicensed 6 GHz band, this paper offers an alternate vision for how next generation cellular networks need to change in order to address the actual needs of wireless connectivity today. Our conclusion is that 6G bandwidth needs in the mid-bands are better served by developing protocols that allow cellular networks to operate in shared spectrum as effectively as in exclusively licensed spectrum: we provide some recommendations on design choices for a "sharing native" 6G design

Room: Zorn (32) | **P03 - Sub-THz channel characterization**

T02 Millimetre wave and THz for terrestrial networks (5G/6G) / / Propagation

Chairs: Joonas Kokkoniemi (University of Oulu, Finland), Mathis Schmieder (Fraunhofer Institute for Telecommunications, Heinrich Hertz Institute, Germany)

15:50 Investigating Time-Varying Signal Propagation at Sub-THz Frequencies Using a VNA

Mohanad Dawood Al-Dabbagh (Physikalisch-Technische Bundesanstalt (PTB), Germany); David A. Humphreys (University of Bristol, United Kingdom & Physikalisch-Technische Bundesanstalt, Germany); Thomas Kleine-Ostmann (Physikalisch-Technische Bundesanstalt (PTB), Germany)
Vector network analyzers (VNAs) are traditionally designed to measure time-invariant networks, where each frequency point is measured individually over a specified interval, influenced by factors such as the intermediate frequency bandwidth (IFBW), dwell time, and the total number of points. This approach creates challenges for time-varying signals, as waveform changes must be captured throughout the sweep. This study explores methods to adapt VNA signal acquisition for time-varying transmissions, evaluating the feasibility and limitations of such measurements. We analyze sweep duration, test segmented waveforms, and conduct experimental verification to establish a measurement scenario. This setup enhances our understanding of time-varying measurements and to apply it for other dynamic channel-sounding systems, enabling estimation of measurement uncertainties of time-varying environment. We present the measurement setup, mathematical analysis of the scenario, and time intervals for each segment at varying velocities, considering optimized reflector positions for each frequency step.

TUESDAY

16:10 Angle-Resolved Channel Measurements at 28 and 160 GHz in Open Office Industrial-Like Environment

Mathis Schmieder (Fraunhofer Institute for Telecommunications, Heinrich Hertz Institute, Germany); Alper Schultze (Fraunhofer Institute for Telecommunications, Heinrich-Hertz-Institut, Germany); Niclas Kullig (Fraunhofer Institute for Telecommunications, Germany); Ramez Askar (Fraunhofer HHI, Germany); Michael Peter (Fraunhofer Institute for Telecommunications, Heinrich Hertz Institute, Germany); Wilhelm Keusgen (Technische Universität Berlin, Germany)

This paper presents channel measurements and modeling at 28 and 160 GHz in an industrial-style open office environment with angular information at the receiver. Channel impulse response snapshots are captured at 145 measurement positions for both frequencies and are evaluated in terms of power metrics, delay, and angular characteristics. Frequency-dependent models for path loss, delay, and angular spread of arrival and K-factor are estimated, and large-scale parameter cross-correlations are evaluated. The results show that delay and angle spread are not frequency dependent in this environment although twice as many multi-path components were identified at 28 GHz compared to 160 GHz

16:30 Spatial Characterization of Indoor Radio Channel in the D-Band at 165 GHz

Juan E. Galeote-Cazorla and Ginés Martínez-García (University of Granada, Spain); Alejandro Ramírez-Arroyo (Aalborg University, Denmark); Ana Vazquez Alejos (Universidade de Vigo, Spain); Juan Valenzuela-Valdés (Universidad de Granada, Spain)

This paper presents an experimental study of the indoor radio channel characteristics at 165 GHz in the D-band. Using wideband measurements based on sliding correlation technique (swept time delay cross-correlation, STDCC) with a pseudo-random binary sequence (PRBS) of length 223, we analyze key parameters such as the power delay profile, delay spread, and fading effects as the receiver moves along a linear path. The results indicate significant multipath propagation, with increasing delay spread corresponding to distance. Additionally, signal quality degradation metrics, including Error Vector Magnitude (EVM) and Modulation Error Ratio (MER) are evaluated. The obtained results are consistent with an indoor scenario dominated by a LOS component, with no significant presence of multipath contributions.

16:50 Sub-THz Indoor Propagation Measurements and Analysis for Conference and Lecture Room Environments at 159 GHz

Juyul Lee, Myung-Don Kim, Jae-Joon Park, Heon Kook Kwon and Byung Su Kang (ETRI, Korea (South))

Most indoor propagation studies have primarily focused on office environments. In this study, however, we investigate indoor propagation characteristics for conference and lecture room environments, which are relevant for applications such as hybrid meetings, digital classrooms, etc. Using 159-GHz rotational scanning measurements, we derive both the best directional and the synthesized omnidirectional path loss and delay spread characteristics. These results are compared with other environments, such as office and corridor ones. Our measurement data show that the path losses in the lecture room are higher than in the conference room, particularly for NLoS links. In terms of delay spread, the conference room shows similarities to office measurements, likely due to comparable dimensions. Unlike in the corridor environment, the path loss exponents for LoS and NLoS in the conference and lecture rooms are not significantly different, indicating that NLoS obstructions from pillars do not cause significant attenuation compared to corner turns.

17:10 Empirical Characterization of In-Vehicle Propagation at Different Frequency Bands

Elena Bernardi (University of Bologna, Italy); Mengting Li (Aalborg University, Denmark); Nicolò Cenni and Vittorio Degli-Esposti (University of Bologna, Italy); Fengchun Zhang (Aalborg University, Denmark); Enrico M. Vitucci (University of Bologna, Italy)

This paper presents an empirical characterization of in-vehicle radio wave propagation across multiple frequency bands, including FR1, FR2, FR3, and sub-THz. Measurements are conducted on three different car types in both line-of-sight and obstructed-line-of-sight conditions. Key propagation metrics, such as path loss, delay spread and transmission loss through different car components are evaluated in order to analyze radio channel characteristics for the purpose of designing future 6G in-vehicle sub-networks. The obtained results highlight significant differences in signal attenuation, time dispersion and scattering effects between the analyzed frequency bands, especially in obstructed-line-of-sight scenarios when the wireless nodes are located in the vicinity of vehicle components like seats and under-seat areas.

Room: Björk (33)

Industrial Workshop

IW12 - Ansys - Next-Gen RF and Antenna Engineering: Simulation Solutions and Workflows for Comprehensive Systems

TUESDAY

T07 Electromagnetic modelling and simulation tools / Convened Session / Electromagnetics

Chairs: Ioan E. Lager (Delft University of Technology, The Netherlands), Giuseppe Pettanice (University of L'Aquila, Italy)

15:50 Validation of Conceptual Progress in Time-Domain EM: Expectations & Practical Possibilities

Ioan E. Lager (Delft University of Technology, The Netherlands); Martin Štumpf (Brno University of Technology, Czech Republic)
The modalities to validate conceptual advancements are critically examined. Upon inspecting the capabilities of the existing measurement equipment, it is concluded that expecting a physical verification of frequency-domain (FD) results is fully justified. However, comprehensive direct measurements in the case of time-domain (TD) frameworks do not seem warranted, with TD theories being properly verified only via numerical experiments that offer the needed controlled environment for the relevant proofs.

16:10 FDTD Stability Analysis of Metasurface GSTCs with Normal Surface Polarizations

Keith Vi Kiet Ha, Jordan R. Dugan, Tom Smy and Shulabh Gupta (Carleton University, Canada)
Generalized Sheet Transition Conditions (GSTC) with tangential and normal susceptibility components in time domain are formulated as a state-space equation, which allows the poles of the system to be conveniently determined by simply finding the eigenvalues of the state matrix. The GSTC is then time-discretized based on trapezoidal rule, and formulated into discrete-time state-space form. The impact of the normal susceptibility component, and its associated oblique incidence on the numerical stability is discussed here by finding the numerical poles from the discrete-time state-space formulation.

16:30 Study of Harmonics in Nonlinear Ferroelectric Materials by Time-Domain Phase Field Simulations Using Open Source Finite Elements

Daniel Sjöberg (Lund University, Sweden)
Ferroelectric materials are the electric counterpart to ferromagnetic materials, displaying strong nonlinearities and hysteresis due to the alignment of permanent dipole moments. This paper demonstrates the use of phase field simulations, based on the Landau free energy approach in a multiphysics setting including polarization, electric potential, and material strain, implemented in the open source finite elements tool FEniCSx. The output of the simulation is the integrated polarization of the ferroelectric for each simulation time. It is shown that harmonics generated by the nonlinearities in the material can be found from Fourier analysis of the time series of this data, and that the strength of the harmonics depend on whether the peak applied voltage is above or below a certain threshold.

16:50 Time and Frequency Macromodeling Techniques for Electromagnetic Systems with Propagation Delays

Giuseppe Pettanice (University of L'Aquila, Italy); Domenico Spina (Vrije Universiteit Brussel, Belgium); Giulio Antonini (University of L'Aquila, Italy)
This paper presents a comprehensive analysis of the strengths and limitations of macromodeling techniques in both the frequency and time-domains, explicitly focusing on methods such as Vector Fitting (VF) and Delayed Vector Fitting (DVF) for the frequency-domain, and Piecewise Linear Fitting (PWLFIT) for the time-domain. We will demonstrate how the VF and DVF models can analyze systems through state-space representations, enabling efficient and accurate system analysis. Additionally, we will show how the PWLFIT method can be applied to convolution schemes to accelerate the convolution process. In particular, we illustrate how adopting Segment Fast Convolution (SFC) schemes further enhances computational efficiency. The work provides a detailed comparison of these techniques, highlighting their advantages and challenges.

17:10 Semi-Recursive Convolution Schemes for Macromodeling of Time-Invariant Linear Circuits

Giuseppe Pettanice, Roberto Valentini and Piergiuseppe Di Marco (University of L'Aquila, Italy); Fortunato Santucci (University of l'Aquila, Italy); Giulio Antonini (University of L'Aquila, Italy)
Time-domain macromodeling is a powerful technique for generating compact models of linear time-invariant (LTI) circuits. A common approach involves computing the port impulse response at the gates of the LTI system to evaluate convolution integrals, though this is often computationally demanding. To address this, a segment fast convolution (SFC) method has been recently introduced, leveraging piecewise constant (PWC) approximations of impulse responses to speed up the computation. This work proposes an extension of this method, which relies on a piecewise linear (PWL) approximation of the port impulse responses of LTI circuits. Additionally, a quasi-recursive algorithm for the convolution calculation is developed, which allows the reduction of the required number of operations and achieves significant speed improvements.

TUESDAY

15:50 Electromagnetic Characterization of Corner Reflectors for Calibration of SAR Technology

David Ramos Somolinos (INTA, Spain); Gema Sanchez Sanchez (Universidad Politecnica (UPM), Spain); Alicia Auñón Marugán, Nuria Gimeno Martínez, Nuria Casal, Juan Manuel Cuerda Muñoz, Borja Plaza Gallardo and David Poyatos Martínez (INTA, Spain)

Synthetic aperture radar (SAR) technology is present in a variety of Earth observation missions, like PAZ satellite, gathering information in such important fields as national defence, high resolution mapping environmental research, etc. To guarantee correct and accurate data, the SAR system must be appropriately calibrated. While there are several means to achieve this, passive elements such as corner reflectors are frequently used for the task. In this work, three calibration corner reflectors are studied: a reference steel model, an aluminium prototype manufactured according to a new geometry and a polylactic acid (PLA) model whose surface is coated with conductive nickel paint. The radar cross-section (RCS) of these reflectors is simulated using Ansys HFSS software and measured in the bistatic anechoic chamber (BIANCHA) belonging to the National Institute of Aerospace Technology (INTA). Finally, these results are compared with each other and with the theoretical RCS of the trihedrals.

16:10 A Method for End-To-End Blind Calibration of ZDR in Polarimetric Weather Radars

Xabier Lobregat, Veronica Santalla del Rio and María Vera Isasa (University of Vigo, Spain)

In the absence of a standardized method for the calibration of polarimetric parameters, there is a general consensus to use several methods, with one of them being end-to-end, particularly for differential reflectivity. This article presents a new method for the calibration of differential reflectivity. It is a blind method, meaning that it does not require knowledge of the characteristics of the observed target during calibration, and it is end-to-end. This method is based on the consistency of two estimators of the second-order moments of the voltages received by a polarimetric radar for different parameters at transmission.

16:30 A Geometry-Based ISAC Channel Model for Vehicle-To-Vehicle Scenarios

Guojin Zhang (Friedrich-Alexander-Universität Erlangen-Nürnberg, Germany); Xuesong Cai (Lund University, Sweden); Norman Franchi (Friedrich-Alexander-Universität Erlangen-Nürnberg, Germany); Maximilian Lübke (Friedrich-Alexander-Universität Erlangen-Nürnberg (FAU), Germany)

Integrated sensing and communication (ISAC) technique has recently gained significant attention in both academic and industrial sectors, as it can provide both sensing and communication functions using the same transmission and frequency spectrum. In this paper, a geometry-based statistical ISAC channel model for vehicle-to-vehicle (V2V) scenario is established, based on the ray-tracing simulation on the highway scenario at 77 GHz. An improved multipathcomponent-distance (MCD) threshold-based clustering algorithm is proposed to jointly group the paths for sensing and communication channels as clusters. These clusters are matched to the physical interaction objects in the scenarios. Based on the clustering results, cluster level parameters (i.e., intra-cluster delay, azimuth and Doppler spread) were explored. Furthermore, the clusters contributed from the same physical interaction object in both communication and sensing channels are regarded as ``sharing sensing clusters''. To investigate the correlation and differences between communication and sensing channel, shared degree (SD) metric is analyzed.

16:50 Modeling of Reflections Between Lens Antennas in the Radiative near Field

Nina Beschoor Plug (Delft University of Technology, The Netherlands); Sjoerd Bosma (NXP Semiconductors & Delft University of Technology, The Netherlands); Giorgio Carluccio (NXP Semiconductors, The Netherlands); Andrea Neto and Nuria LLombart (Delft University of Technology, The Netherlands)

To keep up with the ever-growing demand of higher data rates, it is expected that future high-frequency LoS communication systems will be developed that operate in the radiative near-field. Such systems, however, are prone to reflections between the closely-spaced radiating elements, which impact the signal-to-noise ratio, and therefore the capacity of the system. This work proposes an S-parameter based model which accurately captures the effect of the major reflections of such systems. The S-parameter model results are validated against full-wave electromagnetic simulations.

17:10 Reduction of the RCS on a Groove Gap-Waveguide Transverse Slot-Fed Patch Antenna Array Operating at 28 GHz

Sebastian Diaz-Beiza (Universidad Carlos III de Madrid, Spain); Nelson Castro and Eva Rajo-Iglesias (University Carlos III of Madrid, Spain)

This paper presents a novel antenna design combining Groove Gap Waveguide (GGWG) technology with a printed patch antenna array and with a metasurface to obtain a low Radar Cross Section (RCS). The patch array is fed through transverse slots in the GGWG, while reflection-canceling posts (RCPs) are introduced to enhance bandwidth. The metasurface minimizes the RCS for enhanced stealth capabilities. The result is a compact, efficient antenna system with improved radiation and scattering properties, verified by experimental results, suitable for radar and communication application.

T06 Biomedical and health / / Measurements

Chairs: Christian Bornkessel (Technische Universität Ilmenau, Germany), Nektarios Moraitis (National Technical University of Athens & Institute of Communications and Computers Systems, Greece)

15:50 An Improved Measurement Method for Radio Frequency Exposure from 5G NR Base Stations

Emrah Tas and Frederic Pythoud (Swiss Federal Institute of Metrology METAS, Switzerland)
In this publication, an improved measurement method is proposed for the quantification of the radio frequency exposure from 5G NR base stations in sub-6 GHz frequency range. The method is based on the code selective measurements of all resource elements in the resource grid and enables an estimation of the exposure at maximum data transmission. In particular, it allows the quantification of the ratio between traffic resource elements and synchronization resource elements. The use of this method is presented in this publication and some preliminary results of the laboratory measurements are demonstrated, which were performed using a code selective measuring receiver implementing the proposed method for analyzing the full 5G resource grid.

16:10 Assessment of Electromagnetic Exposure from 5G Mobile Radio in Public Transportation Systems

Tobias Struck (Technische Universität Ilmenau, Germany); Alena Pikushina (TU Ilmenau, Germany); Lisa-Marie Schilling, Christian Bornkessel and Matthias Hein (Technische Universität Ilmenau, Germany)
The progressive development of intelligent transportation systems implies an increasing exposure to high-frequency sources. From a radiation protection perspective, this development necessitates systematic assessment campaigns. In this paper, we present and discuss exposimetry studies of the instantaneous exposure to passengers riding two types of public transportation buses (conventional, and automated according to SAE-level 2, electrical drive). By comparison with results from outdoor measurements, the impact of signal attenuation by the bus windows become apparent. All measured exposure levels remained well below the ICNIRP reference levels, on average 0.4...0.9%. The study revealed that an increase of field exposure is not necessarily linked to the installation of additional radio sources but depends markedly on the data traffic originating from other passengers. Further investigations regarding scenarios with intense use of mobile phones revealed a total exposure ratio between 0.02% and 1.1%, indicating safe conditions in all scenarios at the present state of installations.

16:30 Conceptually New IR-Based Approach for Fast User Exposure Compliance Testing Above 6 GHz

Massinissa Ziane (Univ Rennes & IETR, France); Artem V. Boriskin (IETR, Université de Rennes 1, France); Maxim Zhadobov (University of RENNES 1, France)
This article introduces a novel method for fast absorbed power density (APD) measurement using a reflectivity-based phantom that mimics the scattering characteristics of the skin and allows for conversion of the absorbed mmWave power to heat. The mmWave-induced temperature rise in the phantom is recorded using an infrared (IR) camera and used to retrieve the APD at the air/skin interface. This new technique was validated using reference antennas (cavityfed dipole array and pyramidal horn loaded with a slot array). The results demonstrate its highly promising potential for experimental dosimetry and user exposure compliance testing of wireless devices operating above 6 GHz.

16:50 Imaging Heart Motion from Differential Scattering Parameters - an AI-Based Approach

Ettore Flavio Meliadò, Vladislav Koloskov, Nico van den Berg and Bart R Steensma (University Medical Center Utrecht, The Netherlands)
In this paper, we present a novel approach for monitoring cardiovascular mechanical function through the reconstruction of heart motion using differential scattering parameters. The proposed method, based on artificial intelligence, was trained on a hybrid dataset consisting of both measured and simulated data. This approach enables accurate 3D reconstruction of heart motion and estimation of key clinical parameters. Validation results demonstrate the effectiveness of this technique in reconstructing heart shape and size, as well as predicting stroke volume and ejection fraction from RF scattering measurements. This method offers a more accessible and cost-effective alternative for continuous cardiovascular monitoring.

17:10 Time-Series RF-EMF Predictions for Exposure Assessments Using Machine Learning Techniques

Nektarios Moraitis (National Technical University of Athens & Institute of Communications and Computers Systems, Greece); Konstantina Nikita (National Technical University of Athens, Greece)
This paper performs time-series forecasts for radio-frequency electromagnetic field (RF-EMF) exposure assessments, leveraging machine learning (ML) methods. More specifically, a deep bidirectional long short-term memory (BiLSTM) network is proposed which is trained and tested on long-term electric field time-series data collected by a monitoring station at frequencies between 100 kHz and 7 GHz. The adopted ML network performs very well during the testing phase delivering quite accurate time-series forecasts for unknown inputs. Finally, future electric field sequences are forecasted where the encountered electric field periodic patterns, which are correlated with the daily life, remain consistent.

TUESDAY

T07 Electromagnetic modelling and simulation tools / Convened Session / Electromagnetics

Chairs: Johan Lundgren (Lund University, Sweden), Dirk Manteuffel (University of Hannover, Germany)

15:50 Optimizing Characteristic Modes Using Density-Based Topology Optimization

Jonas Tucek, Miloslav Capek and Lukas Jelinek (Czech Technical University in Prague, Czech Republic)
Density formulation of topology optimization is utilized within method-of-moments formalism to manipulate the characteristic modes. The loss model is integrated into characteristic mode analysis to facilitate the optimization and efficient computation of sensitivities by the adjoint sensitivity analysis. The optimization procedure is demonstrated on a canonical example.

16:10 Using Impedance Sheets in Conjunction with Characteristic Mode Analysis as a Tool for Reflecting Intelligent Surface Design

Axel Hoffmann (Leibniz Universität Hannover, Germany); Alexander Gausmann (Leibniz University Hannover, Germany); Dirk Manteuffel (University of Hannover, Germany)
The computational efficiency advantage of an impedance sheet replacing the actual structure by an equivalent parameter in simulation is combined with the intuitivity of the Characteristic Modes Analysis. The synthesis of optimized unit cells with discrete meta-atoms is presented. An example reflecting intelligent surface design is shown. It is found that the impedance sheet optimization generalizes the unit cell optimization while decreasing computational costs.

16:30 Characteristic Modes Analysis of Resonant and Non Resonant Planar Structures on Magneto-Dielectric Substrates

Romain Alcesilas (Université Gustave Eiffel, France); Ozuem Chukwuka (University Gustave Eiffel & MC2 Technologies, France); Divitha Seetharamdoo (Univ Gustave Eiffel COSYS LEOST Univ Lille Nord de France & Univ Lille Nord de France, France)
This article presents the analysis of microstrip structures on magneto-dielectric substrates and their mutual coupling. Characteristic modes theory is used to evaluate the net modal energy stored in the near-field of the structure. It is shown that microstrip structures printed on magneto-dielectric substrate have a lower net modal stored energy than those printed on purely dielectric substrates. The coupling between microstrip resonator is analyzed using the theory of inter-modal coupling and has a slightly lower value on magneto-dielectric substrate than purely dielectric ones, with the same level of miniaturization. Hence, magneto-dielectric substrate is then a better alternative to design miniature microstrip structures with a level of mutual coupling lower than their equivalent highly-dielectric materials.

16:50 Wideband Single-Layer D-Band Patch Antenna with Parasitic Elements and Superstrate Loading

Yuyan Cao (Lund University, Sweden); Hanieh Aliakbari (Volvocars, Sweden & Lund University, Sweden); Parisa Aghdam (Ericsson AB, Sweden); Buon Kiong Lau (Lund University, Sweden)
This paper proposes a D-band patch antenna featuring four parasitic elements and a loaded superstrate layer. Inspired by a previous parasitic patch antenna design, the new structure is synthesized from scratch using characteristic mode analysis. The new design features different operating principles that enable low-cost single-layer fabrication on PCB HDI technology, while retaining wideband operation and high gain performance of the previous design. With the coupling between the active and parasitic patches limiting the bandwidth and radiation performance, a superstrate is added to improve the parasitic coupling and hence allowing a larger gap between the patches that fulfills fabrication requirements. The simulated results demonstrate that the antenna achieves 20.2% 10 dB impedance bandwidth and 9 dBi peak gain. The low cost and high performance make the design suitable for 6G applications.

17:10 S-Band Cylindrical Structural Antenna of Small Diameter with Radial Modes Using Aperture Coupled Feeding

Raphael Notter (Université de Rennes & French-German Research Institute of Saint-Louis, France); Loic Bernard (ISL & IETR, France); Ala Sharaiha (Université de Rennes & IETR, France); Sylvain Collardey (University of Rennes 1, France); Pouliguen Philippe and Paul Karmann (DGA, France)
This paper deals with the design of cylindrical structural antennas that operate using radial modes to achieve efficient and compact radiating antennas. Structural antenna are employed to make the load-bearing structures directly resonate, such as carriers used in aerospace and automotive applications. With this it is possible to get a very lowprofile antenna and benefit from a bigger resonant surface. However, a significant challenge with these antennas is the emergence of higher-order modes when the wavelength is small relative to the structure size. Radial modes are characterized by their quasi-insensitivity to the length of the cylinder, thus would be very relevant with those. A novel approach is proposed to excite these modes with aperture coupled feeding, helping to stabilize the antenna feeds and optimizing the number of exciters needed and the structural impact. A bandwidth of 3.6% and a peak gain of 5.5 dBi in the S-Band are obtained.

TUESDAY

T08 Fundamental research and emerging technologies/processes / Convened Session / Antennas

Chairs: Francisco Pizarro (Pontificia Universidad Catolica de Valparaiso, Chile), Jose Rico-Fernandez (Northern Waves AB, Sweden)

15:50 RF-Oriented 3D-Printing: New Materials, Advanced Printing Techniques, and Novel Antenna Concepts

Thi Quynh Van Hoang and Erika Vandelle (Thales Research & Technology, France); Matthieu Bertrand (Thales Research and Technology, France); Tom Malvaux and Romain Faye (Nanoe, France); Brigitte Loiseaux (Thales Research & Technology, France)

In recent years, numerous 3D-printed microwave and antenna components have been successfully demonstrated in both research and industrial context, highlighting the potential of this manufacturing technique to inspire innovative designs in wireless systems. This contribution will explore innovations in antennas and artificially engineered materials, encompassing novel materials specifically designed for RF applications, advanced printing techniques, and innovative antenna concepts.

16:10 Vivaldi Antenna Array in a Triangular Lattice with Dielectric Dome for Enhanced Beam Steering Capabilities

Omar Orgeira (Northern Waves AB, Sweden); Pilar Castillo-Tapia (KTH Royal Institute of Technology, Sweden); Jose Rico-Fernandez (Northern Waves AB, Sweden); Oscar Quevedo-Teruel (KTH Royal Institute of Technology, Sweden)

We present a combination of a multi-layer dielectric radome and a Vivaldi antenna array. The Vivaldi antenna element features dual-polarization and it can be arranged in a triangular lattice, which reduces the required number of elements. A coaxial structure is added as element feed for a better integration with the electronics. However, the array losses approximately 4 dB when scanning at 60 degrees. To overcome this, a multi-layer dielectric radome is designed. This design is done using a ray-tracing model based on geometrical optics. The final lens is able to increase the gain from 35 to 60 degrees. Both the array antenna and the dielectric lens are designed to be built using additive manufacturing.

16:30 Wideband Power Divider Design Based on Miniaturized Ridge Waveguides

Sergio Matos (ISCTE-IUL / Instituto de Telecommunicações, Portugal); Nelson Fonseca (Anywaves, France); Joao M Felicio (Instituto Superior Técnico, Portugal & Instituto Telecomunicacoes, Portugal); Carlos A. Fernandes (Instituto de Telecomunicacoes, Instituto Superior Tecnico, Portugal); Jorge R. Costa (Instituto de Telecomunicações / ISCTE-IUL, Portugal)

Beam forming networks (BFNs) are of paramount importance in communication satellite systems, subject to stringent mechanical, thermal and RF requirements. One of the fundamental constituents of these BFN are power dividers, enabling the distribution of the signal from a centralized input port to a larger array of output ports. In this work, we present a design of a wideband compact power divider transition connecting a conventional waveguide ridge (WRD180) to two smaller symmetric ridge waveguides within the same cross section envelope and along the longitudinal main direction of the waveguide. This strategy allows to save space by combining in a single element the functionalities of waveguide transition and power divider, minimizing its impact on the in-plane dimensions of the feeding network. The design follows a semi-analytical method for optimizing a smooth profile variation along the transition that is compatible with the tolerances of conventional milling techniques, and state-of-the-art metal 3D printing technologies. The developed design operates from 17.2 GHz to 33.9 GHz with return losses better than 20 dB in simulation, covering the uplink and downlink frequency bands dedicated to satellite communications in K/Ka-band.

16:50 57-71GHz Antenna Lensing for Wireless Backhaul Applications

Jeff von Loesecke (3D Fortify, Inc., USA); Philip Lambert and Henrik Ramberg (3D Fortify, USA)

This paper presents the process and results of developing a Gradient-Index (GRIN) lens for wireless backhaul at frequencies up to 71 GHz. At 50.8mm diameter, the Luneburg Lens achieved a peak gain of 30.2 dBi at 65 GHz. With strong alignment between simulations and experimental measurements, the results of this lens demonstrates commercial applicability of GRIN lensing for high-frequency applications.

17:10 A Wideband Quadraxial Feed for Compact Dual Polarised Vivaldi Antenna Elements

Teanette van der Spuy (Chalmers University of Technology, Sweden & Satcube AB, Sweden); Rob Maaskant (CHALMERS, Sweden); Lukas Nystrom (Satcube AB, Sweden); Johan Malmström (Saab Surveillance, Sweden); Henrik Holter (Ericsson AB, Sweden)

This work presents a fully metallic dual polarised Vivaldi antenna element for K/Ka-band SatCom phased arrays. The element is fed by a novel quadraxial-to-quadridge waveguide transition, which is designed for connectorless integration with a PCB-mounted beamformer IC network. The Vivaldi unit cell has an active reflection coefficient of better than -10 dB for scanning up to 60 degrees in the E-, D-, and H-planes in the K/Ka SatCom bands. A back-to-back (B2B) configuration of the quadraxial transition is 3D-printed in metal using the laser powder-bed fusion technique. A tolerance study shows how an initial gap between the quadraxial pins of approximately 30 um impacts the B2B insertion loss, while the zero-gap post-processed B2B structure features a reflection of -13 dB and the transmission coefficient of -0.7 dB, in both simulations and measurements and in both bands of interest.

TUESDAY

Room: Munch (23)

Industrial Workshop

IW13 - Quadsat - Recent trend of drone-based measurement

Room: Ørsted (24+25)

CS9 - Dome antennas for the next generation communication systems

T08 Fundamental research and emerging technologies/processes / Convened Session / Antennas

Chairs: Astrid Algaba-Brazález (Technical University of Cartagena, Spain), Maria Carolina Vigano (Viasat Antenna Systems SA, Switzerland)

15:50 Ultra-Compact Risley-Prism Design with a 3D-Printed Transmit-Array Fed by a Radial Line Slot Antenna

Sergio Matos (ISCTE-IUL / Instituto de Telecommunicações, Portugal); Nelson Fonseca (Anywaves, France); Joao M Felicio (Instituto Superior Técnico, Portugal & Instituto Telecomunicacoes, Portugal); Carlos A. Fernandes (Instituto de Telecomunicacoes, Instituto Superior Tecnico, Portugal); Jorge R. Costa (Instituto de Telecomunicações / ISCTE-IUL, Portugal)

Satellite-on-the-move systems based on mechanical beam steering can be a cost-effective alternative to phased-arrays. However, these solutions tend to be bulky for accommodating the mechanical displacements and the focal distance of the system (intrinsic to spatially fed array configurations). The Risley Prism mechanical scanning approach, based on the axial rotation of two transmit-arrays (TAs), can overcome some of these shortcomings. In particular, the profile of the lens can be dramatically reduced by integrating the primary source with the first TA ("Prims 1") into a single leaky wave antenna. In this work we present a low-cost implementation of this concept, consisting of a Radial Line Slot Antenna (RLSA) and a fully dielectric TA. This choice reduces the complexity of the system, as well as, facilitating the integration of these two components. The developed antenna has a profile of 2λ_0 (at 29 GHz) and can scan up to 48 degrees with a maximum directivity of 31 dBi.

16:10 Dielectric Lenses for the Reduction of Grating Lobes in Antenna Arrays with Large Inter-Element Spacing

Almudena Toronjo-Ruiz and Jose Rico-Fernandez (Northern Waves AB, Sweden); Pilar Castillo-Tapia (KTH Royal Institute of Technology, Sweden); Francisco Mesa (University of Seville, Spain); Núria Flores-Espinosa (KTH Royal Institute of Technology, Sweden); Astrid Algaba-Brazález (Technical University of Cartagena, Spain); Oscar Quevedo-Teruel (KTH Royal Institute of Technology, Sweden)

Implementing mm-wave antennas involves working with shorter wavelengths, which can challenge conventional design and manufacturing, especially in the context of array antennas. This may lead to prohibitive design sizes and manufacturing limitations for the arrays to prevent grating lobes from appearing. This study introduces a novel approach that combines dielectric lenses with antenna arrays that have a large inter-element spacing, aimed at reducing the occurrence of grating lobes that arise at specific scanning angles. Moreover, the proposed dielectric lens solution improves the antenna directivity in the main beam direction.

16:30 Performance Analysis of a Dielectric Dome in Circular Polarization for Beam Scanning at Low Elevation

Marc Emin (University of Rennes, France & Thales Research & Technology (TRT), France); Matthieu Bertrand (Thales Research and Technology, France); David González-Ovejero (Université de Rennes, France); Mauro Ettorre (Michigan State University, Electrical and Computer Engineering, USA); Ronan Sauleau (University of Rennes 1, France)

The use of phase-correcting domes above planar phased arrays allows to increase their field of view. However, such a dome may behave differently depending on the polarization of the incident wave. A different behavior for the transverse electric (TE) and transverse magnetic (TM) components of the incident field would prevent the use of such a dome for a circularly-polarized beam. The influence of a fully-dielectric dome is analyzed when placed above a linear array of printed patches. The dome is made of non-resonant sub-wavelength unit-cells. The impact of the dome on the polarization purity of the transmitted wave is estimated by considering the transmission behavior of the unit-cell for TE and TM polarizations. These results are confirmed by fullwave simulations. They validate the capability of such a dome to enhance the antenna field of view with a limited impact on the axial ratio of the radiated beam.

16:50 Phased Array Fed Lens Antenna for SATCOM Applications

Daniel L Faircloth (Nullspace, Inc., USA); Henrik Ramberg (3D Fortify, USA)

We present a phased array fed lens (PAFL) that utilizes a gradient index (GRIN) partial Maxwell-Fisheye (PMF) lens to provide enhanced beamsteering performance. PAAs provide critical connectivity for modern 5G and satellite communications (SATCOM) devices and can be enhanced using GRIN lens technology, made recently practical through advances in additive manufacturing. In this paper, we build upon prior work using switched beam or rastered individual elements to demonstrate improved wide field-of-view performance with a simple PAA. This mode of operation enables faster steering and finer beam scanning precision than previously presented PMF-based antennas.

TUESDAY

17:10 Metasurface Dome Antennas with Non-Locality Compensation

Joaquín García Fernández (WAVE UP SRL & University of Siena, Italy); Francesco Caminita (Wave-Up SRL, Italy); Cristian Della Giovampaola (Wave Up srl, Italy); Massimo Nannetti (Wave Up Srl, Italy); Enrica Martini and Stefano Maci (University of Siena, Italy)

Steerable antennas typically struggle to maintain optimal radiation performance at large scan angles. This field of view (FoV) limitation becomes critical for the implementation of efficient transmitters in reconfigurable intelligent surfaces (RIS) based networks. The inclusion of a static metasurface (MTS) dome in the antenna system has been previously proposed to increase the scan range. However, preceding investigations based the wide-angle matching on a predistortion calculated under the assumption of refraction locality. In this paper, we demonstrate that non-locality compensation provides an outperforming solution for the scan range expansion. Full-wave simulations are reported, demonstrating the enhanced performance of the metadome (MTD) system compared to the standalone antenna, as well as the superiority of the non-local approach over the compensation assuming locality.

Room: Collin (27) WG and meetings	16:00-17:40 Exhibitors meeting
Room: Collin (27) Industrial Workshop	15:50-15:35 IW10 - Keysight - Unlocking 6G Potential: Exploring the 6G R&D Testbed and its Variants and Applications IW11 Keysight - Prototyping and Certifying 5G NTN Using Realistic Emulators
Room: Collin (27) Industrial Workshop	16:45-17:30 IW11 - Keysight - Prototyping and certifying 5G NTN using realistic emulators.
Tuesday - 17:40-18:15	
Room: Alfvén (A3+A4)	EuRAAP Award Ceremony
Tuesday - 18:15-20:00	
Room: Exhibitor area	Reception with exhibitors and sponsors

End of Tuesday, April 1st

TUESDAY

Wednesday - 08:00-09:40

Room: Alfvén (A3 + A4)

A04a - Mmwave antenna technologies

T02 Millimetre wave and THz for terrestrial networks (5G/6G) / / Antennas

Chairs: Marko Bosiljevac (University of Zagreb, Croatia), Ahmed A Kishk (Concordia University, Canada)

8:00 Beamforming with Oversampled Time-Modulated Arrays

Marcin Wachowiak (KU Leuven, Belgium & IMEC, Belgium); Andre Bourdoux (IMEC, Belgium); Sofie Pollin (KU Leuven, Belgium)

The time-modulated array (TMA) is a simple array architecture in which each antenna is connected via a multi-throw switch. The switch acts as a modulator switching state faster than the symbol rate. The phase shifting and beamforming is achieved by a cyclic shift of the periodical modulating signal across antennas. In this paper, the TMA mode of operation is proposed to improve the resolution of a conventional phase shifter. The TMAs are analyzed under constrained switching frequency being a small multiple of the symbol rate. The presented generic signal model gives insight into the magnitude, phase and spacing of the harmonic components generated by the quantized modulating sequence. It is shown that the effective phase-shifting resolution can be improved multiplicatively by the oversampling factor (O) at the cost of introducing harmonics. Finally, the array tapering with an oversampled modulating signal is proposed. The oversampling provides $O+1$ uniformly distributed tapering amplitudes.

8:20 A Steerable 8 Element 73 GHz Transmitting Time Modulated Array

Edward A. Ball (University of Sheffield, United Kingdom); Sumin David Joseph (The University of Sheffield, United Kingdom)

The Time Modulated Array (TMA) is a type of phased array rarely seen applied, though it has advantages over other approaches. A TMA produces a set of radiated beams that are harmonically related to a set of digital control signals. In this paper the first mmWave beam steerable prototype TMA operating at 73 GHz, using bespoke GaAs integrated circuits, is presented. The beam steerable system consists of RF hardware and an FPGA controller. Laboratory radiated tests show good agreement to theoretical expectations. A beam steering of 24 degrees is reported (i.e. +/- 24 degrees total achievable range) for the TMA first harmonic beam, and 44 degrees for the second harmonic beam. The peak measured radiated array gain is -5 dBi. The maximum capable radiated power is +21.9 dBm. An increased level of integration on-chip, based on the existing architecture, could provide an array gain of +3 dBi.

8:40 Design Methodology for Lens Antenna Arrays in Radiative Near-Field Communication Links

Nina Beschoor Plug (Delft University of Technology, The Netherlands); Junyao Tan (TU Delft, The Netherlands); Sjoerd Bosma (NXP Semiconductors & Delft University of Technology, The Netherlands); Giorgio Carluccio (NXP Semiconductors, The Netherlands); Andrea Neto and Nuria LLombart (Delft University of Technology, The Netherlands)

A design methodology for high-capacity incoherent line-of-sight (LoS) communication arrays in the radiative near-field of each other is presented. Equivalent aperture current distributions of highly directive antennas are optimized to obtain noise-limited independent data streams with maximal SNIR. The current distributions are found to be equal for the transmitting and receiving arrays and are given by the Prolate Spheroidal Wave Function (PSWF) in amplitude and a quadratic phase focusing term. A 2x2 array at 270 GHz with 6λ_0 diameter elements is designed. The desired aperture current distribution is synthesized using a leaky-wave lens antenna fed by a double-iris slot and a focusing hyperbolic lens. The channel matrix model used to calculate the coupling between two apertures in the radiative near-field is validated using full wave (FW) CST simulations of the array. Good agreement is found between the proposed modeling and FW simulations.

9:00 Towards the Generation of a Skyrmionic Structured mmWave Beam

Steven Verwer, Ad Reniers, Roeland J. Dilz and Jom Luiten (Eindhoven University of Technology, The Netherlands)

Contemporary modulation methods for wireless communication are based on separable solutions. Most modulation techniques use a maximum of two degrees of freedom (DoF) such as, frequency, amplitude, phase, etc. To increase the data transfer it is necessary to combine these DoF as efficiently as possible. In this paper, we describe the feasibility of the generation of a mmWave Skyrmion structured beam. This system is already used for the light spectrum but, for the first time, we investigate its feasibility in the mmWave spectrum.

WEDNESDAY

9:20 Low-Profile Dual-Polarized SIW Slot Array Antenna for 5G Application

Amir Jafargholi and Romain Fleury (EPFL, Switzerland)

Decreasing the permittivity of a dielectric-loaded slotted waveguide antenna results in an increase in both impedance and radiation bandwidth, where the widest bandwidth can be achieved when the dielectric permittivity falls below unity. This concept is employed to resolve the inherently resonating nature of the SIW slot antenna. Employing two perpendicular slots, a dual-polarized antenna is proposed. This approach not only resolves cost and alignment challenges typically associated with multi-layer structures but also caters to the demand for broadband dual-polarized antennas, making it a promising candidate for practical applications. A 16-element phased array antenna with wide beam steering angle capabilities has been proposed. Designing a Rotman Lens for each individual polarization and employing an appropriate feed network, a low-profile structure is designed. Simulations reveal an impressive beam steering range of up to 50 degrees, accompanied by a peak gain exceeding 18 dBi.

Room: Kildal (A2) — A10a - Wideband antennas

T01 Sub-6 GHz for terrestrial networks (5G/6G) / / Antennas

Chairs: Mario Junior Mencagli (University of Delaware, USA), Petrie Meyer (Stellenbosch University, South Africa)

8:00 Design of a Wideband Circularly Polarized ARMA Antenna Using Characteristic Mode Analysis for SATCOM Applications

Samuel Lottin (University of Limoge, France); Ronan Adam (French-German Research Institute of Saint-Louis, France); Raphael Notter (Université de Rennes & French-German Research Institute of Saint-Louis, France); Edson Martinod (XLIM/OSA, France); Joel Andrieu (University of Limoges, France); Loic Bernard (ISL & IETR, France); Paul Karmann (DGA, France)

A wideband, circularly polarized (CP) agile radiating matrix antenna (ARMA) composed of single elements called pixel is proposed in this article. A pixel is a single-fed cavity-backed antenna made of a microstrip patch and a frequency selection surface (FSS) with specific shaped metasurfaces (MTS). The pixel antenna is designed for operation in the X- /Ku-band and achieve good operation bandwidth of 10.51%. This AR bandwidth is achieved thanks to the combination of the CP patch and CP FSS. The rectangular patch is used as a driving element to generate CP polarized wave. Then the rectangular MTS structure is used to enhance the CP. The compact size of a pixel makes it suitable for beam-scanning in SATCOM applications. Use in matrix of several elements, the matrix antenna achieves better than 3 dB scan loss to ±40° and offers AR below 3 dB over the entire proposed scan range.

8:20 Evaluation of Patch Antennas for Radar Systems in Ultra-Wideband Channel 9

Marta Martínez-Vázquez and Sachit Varma (Renesas Electronics, Germany)

This study provides a comprehensive performance analysis of UWB radar patch antennas tailored for channel 9 applications. The initial antenna consists of a single microstrip patch, while the second comprises a board with six microstrip patches configured in a 3x2 matrix. The antennas are fabricated using standard FR4 laminate and are aimed at radar use. These antennas exhibit a directional radiation pattern with a broad beamwidth in the azimuth plane, making them ideal for radar systems.

8:40 Filtering Equivalent Circuit Design of Broadband Microstrip Antennas

Ignacio Maria Delgado-Lozano (Universidad de Sevilla, Spain); Rafael R. Boix (University of Seville, Spain); Armando Fernández (Universidad de Sevilla, Spain); Vicente Losada (University of Sevilla, Spain)

This paper proposes a methodology to design a broadband aperture-stacked patch (ASP) microstrip antenna through the use of an equivalent circuit whose performance matches that of a third order filter. The antenna consists of two stacked patches fed through a resonant rectangular aperture by an open-ended microstrip line. The equivalent circuit proposed is made out of three coupled LC parallel resonators, and is de-embedded from the antenna response by using the least squares method. Then, the antenna dimensions are adjusted so that the response of the antenna matches that of a broadband third order filter based on the equivalent circuit of the antenna. This broadband filter is derived from a standard Chebyshev third order filter by introducing lumped element admittance inverters, and subsequently using optimization. As a result, a broadband ASP antenna has been designed at a center frequency of 5.5 GHz with a bandwidth around 44%.

9:00 Four-Coupled Feed Square-Ring Patch Antenna for Wideband 5G MIMO Small Base Station Applications

Shu-Chuan Chen (National Defense University Chung Cheng Institute of Technology, Taiwan & Chung Cheng Institute of Technology, Taiwan); Shao-Hung Cheng (Chung Cheng Institute of Technology, National Defense University, Taiwan); Yung-Lung Lee (National Defense University Chung Cheng Institute of Technology, Taiwan); Ming-Da Tsai (Chung Cheng Institute of Technology, National Defense University, Taiwan); Kuang-Hsiung Tan (National Defense University & Chung Cheng Institute of Technology, Taiwan)

This paper presents a 5G MIMO wideband antenna system featuring a four-coupled feed square-ring patch design for small base stations. The system, measuring 50 x 50 mm^2 with a height of 10 mm, consists of four identical rectangular metal rings on a 35 x 35 mm^2 FR4 substrate, 0.8 mm thick. Each antenna, sized at 19 x 13 mm^2, is rotated by 90 degrees to achieve orthogonal polarization for decoupling. With an isolation of 10 dB, ECC values below 0.09, the design supports wideband operation from 3300 MHz to 5000 MHz, making it ideal for 5G applications.

WEDNESDAY

9:20 A Wideband Dielectric Resonator Antenna

Zhe Chen, Yu-Xiang Sun, Wenhui Wu, Xue Ren and Tao Yuan (Shenzhen University, China)
This paper presents a broadband dielectric resonator antenna (DRA) with three excited modes: the fundamental TE111 mode and the higher-order TE113 and TE212 modes, which are merged to achieve a wide impedance bandwidth. To demonstrate the design, an antenna prototype was developed, fabricated, and measured, showing reasonable agreement between the measured and simulated results. The prototype achieved a wide measured 10-dB impedance bandwidth of 64.6% (5.85-11.48 GHz) with stable broadside radiation patterns throughout the band.

Room: Hallén (BAR5) — CS49a - Propagation for Smart Mobility Scenarios

T04 RF sensing for automotive, security, IoT, and other applications / Convened Session / Propagation

Chairs: Ibrahim Rashdan (German Aerospace Center (DLR), Germany), Martin Schmidhammer (German Aerospace Center (DLR), Germany)

8:00 Ray-Tracing Modelling and Performance Assessment of AGVs in Industrial 5G Networks

Jorge Elizalde (Ikerlan & BRTA, Spain); Aitor Arriola (Ikerlan & BRTA, Spain); Xabier Eguiluz (Ikerlan, Spain & BRTA, Spain); Azaitz Hierro Pastor (Ikerlan & BRTA & UPV/EHU, Spain); Eneko Iradier and Jon Montalban Sanchez (University of the Basque Country, Spain)
In this work the RF propagation at 3.5 GHz has been simulated in the Ikerlan's Digilab facility for a robotic application.

8:20 Novel Near-Field Radar Propagation Models for V2X Communication and Sensing

François De Saint Moulin (UCLouvain, Belgium); Christophe Craeye (Université Catholique de Louvain, Belgium); Luc Vandendorpe and Claude Oestges (Université catholique de Louvain, Belgium)
The increased carrier frequencies envisioned for future radar and communication systems call for adequate propagation models valid in near-field transmissions. In this paper, we propose a new radar propagation model, encompassing popular models from the literature, namely the radar equation and the Geometrical Optics (GO) approximation, used e.g. in ray-tracing tools. First, the scattered electromagnetic fields and radar cross-sections are analytically computed by modelling the radar target as an arbitrary curved rectangular plate. Secondly, when particularised to a flat plate, our new model directly highlights not only the link between the radar equation and the GO approximation, but also the limitations of those models. We finally propose a new model based on our analytical derivations, which unifies both approaches.

8:40 Time-Varying Rician K-Factor in Measured Vehicular Channels at cmWave and mmWave Bands

Faruk Pasic (TU Wien, Austria); Markus Hofer (AIT Austrian Institute of Technology, Austria); Thomas Zemen (AIT Austrian Institute of Technology GmbH, Austria); Andreas F. Molisch (University of Southern California, USA); Christoph F Mecklenbräuker (TU Wien, Austria)
Future vehicular communication systems will integrate millimeter wave (mmWave) technology to enhance data transmission rates. To investigate the propagation effects and small-scale fading differences between mmWave and conventional centimeter wave (cmWave) bands, multi-band channel measurements have to be conducted. One key parameter to characterize small-scale fading is the Rician K-factor. In this paper, we analyze the time-varying K-factor of vehicle-to-infrastructure (V2I) channels across multiple frequency bands, measured in an urban street environment. Specifically, we investigate three frequency bands with center frequencies of 3.2 GHz, 34.3 GHz and 62.35 GHz using measurement data with 155.5 MHz bandwidth and a sounding repetition rate of 31.25 µs. Furthermore, we analyze the relationship between K-factor and root-mean-square (RMS) delay spread. We show that the Ricean K-factor is similar at different frequency bands and that is correlated with the RMS delay spread.

9:00 Generation and Simulation of a Non-Stationary TDL Channel

Mahboubeh Ansari (Technical University of Braunschweig, Germany); Lennart Thielecke and Thomas Kürner (Technische Universität Braunschweig, Germany)
This paper presents the implementation and evaluation of a non-stationary tapped delay line channel model for vehicle-to-vehicle communication. The channel model is generated with parameters derived from measurement data. We analyze key properties such as the root mean square delay spread and packet error rate. To account for non-stationary behavior, a first order two state Markov chain model is employed to describe the dynamic characteristics of the channel. The close alignment between simulation results and measured data confirms the model's accuracy and provides deeper insights into the reliability and performance of vehicle-to-vehicle communication channels. These findings contribute to a more comprehensive understanding of non-stationary characteristics in vehicle-to-vehicle communication.

WEDNESDAY

9:20 Path Loss Modelling for UAV Communications in Urban Scenarios with Random Obstacles

Abdul Saboor and Zhuangzhuang Cui (KU Leuven, Belgium); Evgenii Vinogradov (Technology Innovation Institute (TII), United Arab Emirates & KU Leuven, Belgium); Sofie Pollin (KU Leuven, Belgium)

Path Loss (PL) is vital to evaluate the performance of Unmanned Aerial Vehicles (UAVs) as Aerial Base Stations (ABSs), particularly in urban environments with complex propagation due to various obstacles. Accurately modeling PL requires a generalized Probability of Line-of-Sight PLoS that can consider multiple obstructions. While the existing PLoS models mostly assume a simplified Manhattan grid with uniform building sizes and spacing, they overlook the real-world variability in building dimensions. Furthermore, such models do not consider other obstacles, such as trees and streetlights, which may also impact the performance, especially in millimeter-wave (mmWave) bands. This paper introduces a Manhattan Random Simulator (MRS) to estimate PLoS for UAV-based communications in urban areas by incorporating irregular building shapes, non-uniform spacing, and additional random obstacles to create a more realistic environment. Lastly, we present the PL differences with and without obstacles for standard urban environments and derive the empirical PL for these environments.

Room: Marcuvitz (M3)

Scientific Workshop

SW7 - EMF Exposure Evaluation Approaches and Perspectives in 6G

Room: Björk (33)

Industrial Workshop

08:00 - 08:45
IW8 - Dicaliant Ltd. - Phase-accurate on-board S-parameter measurements using pigtails up to 8.5 GHz

Room: Björk (33)

Industrial Workshop

08:55 - 09:40
IW9 - Kaelus - The evolution of base station antennas from early designs to modern innovations

Room: Bergman (34)

P04a - Satellite channel characterization I

T03 Aerospace, space and non-terrestrial networks / / Propagation

Chairs: Martin Rytir (Norwegian Defence Research Establishment (FFI), Norway), Zhiqiang Yuan (Southeast University,

8:00 Results from Simultaneous Ka- and X-Band Long-Term Satellite Propagation Measurements at Low Elevation Angle in the Arctic

Martin Rytir (Norwegian Defence Research Establishment (FFI), Norway)

Ka- and X-band are used for earth observation satellite data downlink and governmental satellite communications, with a gradual shift towards the higher frequencies. This paper presents results from three years of beacon measurements at 7.6 and 20.7 GHz at an elevation angle of 6.1° at 70 °N in Norway. For 99% of the time the results show excess attenuation levels of 0.5 dB at X-band and 2.6 dB at Ka-band. For tropospheric scintillation the 99% levels are 0.6 and 1.1 dB at X- and Ka-band, respectively. The ITU-R model predictions for rain attenuation agree well with the measurements, especially when local rain data are used. For scintillation, the ITU-R model gives higher than measured levels while a recent model developed from arctic data gives too low annual predictions but fits very well on monthly basis.

8:20 Long-Term Experimental Results of Propagation in a Q-Band Slant-Path Link

Domingo Pimienta-del-Valle and Jose M Riera (Universidad Politécnica de Madrid, Spain); Pedro Garcia-del-Pino (Universidad Politecnica de Madrid, Spain); Gustavo Siles (Universidad Privada Boliviana, Bolivia); Ana Benarroch (Universidad Politécnica de Madrid, Spain)

A better characterization of the satellite propagation channel remains of paramount importance. Specifically, assessing the impact of the atmospheric effects in a Q/V band (40/50 GHz) satellite signal is critical when designing systems operating at such high frequency bands, which are receiving increasing attention and interest in last years. A long-term propagation experiment is being carried out in Madrid, receiving the 40-GHz beacon signal of the Alphasat satellite since 2014. This paper presents the rainfall rate and attenuation results for the first completed 9 years of the experiment, as well as to compare them with several ITU-R models. Moreover, excess attenuation is also compared with a distribution obtained from synthetizing 100 years of attenuation time series with the procedure of Rec. ITU-R P.1853-2. Both Rec ITU-R P.618-14 and the synthetized series approach yield similar results, each one behaves better for a specific probability interval.

8:40 A Wavelet-Based Computation of the Field Received by a LEO Satellite in Radio Occultation

Clémence Allietta (Ecole Nationale de l'Aviation Civile, France); Rémi Douvenot (ENAC, France); Sonia Cafieri (French Civil Aviation University, France)

The propagation of an electromagnetic field from the edge of the atmosphere to a satellite in Low Elevation Orbit (LEO) involves the computation of a diffraction integral which evaluation can be computationally demanding when a direct numerical integration is performed. Previous studies have introduced efficient methods to perform this calculation, but these approaches often rely on physical assumptions that may compromise the accuracy of the results. In this paper, we present a novel approach that avoids such assumptions and efficiently computes the field received by the LEO satellite using a wavelet decomposition of the integral.

9:00 XGBoost Based Regression Forecast for ACM on Q/V-Band Satellite Links

Mirela Fetescu (Joanneum Research & Graz University of Technology, Austria); Johannes Ebert and Karin Plimon (Joanneum Research, Austria); Martin Winter (JOANNEUM RESEARCH Forschungsgesellschaft mbH, Austria); Michael Schmidt (Researcher & Joanneum Research, Austria); Franz Teschl (Graz University of Technology, Austria); Antonio Martellucci (European Space Agency, The Netherlands)

This paper presents a comparison between classical adaptive coding and modulation (ACM) with fixed modulation and coding (ModCod) margins and two machine learning (ML)-based approaches: univariate and multivariate forecasting models. Both ML approaches are based on variants of Extreme Gradient Boosting (XGBoost) to predict signal-to-noise ratio (SNR) time series, aiding ACM switching decisions. The evaluation of the ACM algorithms is conducted using two years of Q/V-band channel data recorded at the ground station in Graz, Austria, using the Alphasat TDP5 Aldo Paraboni Q/V-band payload. The results demonstrate that the multivariate forecasting model outperforms both the classical ACM algorithm and the univariate forecasting model in terms of spectral efficiency. Additionally, the multivariate model eliminates the need for direct SNR estimation by using easily measurable parameters from the modem.

9:20 Multiyear Second Order Statistics of ALPHASAT Beacon Measurements at ASI Ground Stations

Miles A. Turner, Alef Comisso, Carlo Riva and Lorenzo Luini (Politecnico di Milano, Italy); Giuseppe Codispoti (Italian Space Agency, Italy); Giorgia Parca (Agenzia Spaziale Italiana, Italy)

The Alphasat Aldo Paraboni experiment by the Italian Space Agency measures signal attenuation at 19.701 GHz and 39.402 GHz using beacon signals from a geosynchronous satellite to ground stations in Tito Scalo and Spino d'Adda, Italy. Second order statistics on data collected from 2015 to 2023 are presented, supporting the understanding that higher frequencies, as seen with the 39.4 GHz beacon, are more susceptible to atmospheric fading, exhibiting higher fade percentages, steeper fade slopes, and more frequent long- duration fades. Comparisons of the measurements statistics with Rec. ITU-R P.1623-1 models show expected discrepancies, with the ITU-R models underestimating fade percentages and counts while overestimating fade slope probabilities. These findings emphasize the importance of experimental campaigns and the opportunity to further refine predictive models.

Room: Felsen (35+36) — CS23a - Antennas, Metasurfaces, and Arrays for Radio Astronomy

T03 Aerospace, space and non-terrestrial networks / Convened Session / Antennas

Chairs: Sean V Hum (University of Toronto, Canada), David S Prinsloo (ASTRON & Netherlands Institute for Radio Astronomy, The Netherlands)

8:00 Metasurface Superconductive Line for Harmonic Filtering in Parametric Amplifiers

Jorge Cardenas (Pontificia Universidad Católica de Valparaíso, Chile); Fausto Mena (Central Development Laboratory, National Radio Astronomy Observatory, Charlottesville, USA); Francisco Pizarro (Pontificia Universidad Catolica de Valparaiso, Chile)

This work shows a glide-symmetric transmission line, based on previous studies, but this time implemented using superconductive characteristics. The design is intended to provide special filtering capabilities to suppress harmonics that stem from the parametric amplification. A parametric analysis was performed based on three setups for a proposed unit cell. A viable design was obtained to provide two stopbands, one slightly higher than the pump frequency of 10 GHz and another to suppress the harmonic at 30 GHz.

The simulations demonstrate that the proposed line exhibits a tuning capability to solve the stated problem and others thus opening the possibility of using them in superconducting circuits, particularly in traveling-wave kinetic-inductance parametric amplifiers.

8:20 Beam Prediction Method for Antenna Arrays in Radio Astronomy via Artificial Neural Networks

Maria Kovaleva and Chuyan Chen (Curtin University, Australia); David B Davidson (Curtin University, Australia & Stellenbosch University, South Africa)

With the SKA-Low construction underway, we explore the potential of using artificial neural networks to generate embedded element patterns (EEPs) at fine frequency channels. Exploiting the existing FEKO-simulated database of EEPs, we trained a prediction model that generates 512 EEPs (for 256 antennas with two polarizations) in only 1.28 sec. To perform the model evaluation, we derived specific performance metrics that are based on simulation tolerance threshold and consider the level of error that would have a potential impact on observations. High accuracy in EEP prediction is achieved, with significant improvements in computational efficiency compared to the full-wave simulations.

WEDNESDAY

8:40 Investigation of a Polarizing Surface to Assist in the Calibration of All-Sky Radio Telescopes

Oskar Zetterstrom (KTH Royal Institute of Technology, Sweden); Dominic Anstey and Eloy de Lera Acedo (University of Cambridge, United Kingdom)

Radio telescopes rely on calibration to provide high-quality images. Here, we present a polarizing metasurface that can be used to aid the calibration of all-sky radio telescopes. The metasurface is intended for the REACH telescope, which will be used to study the early epochs of the Universe. The polarizing metasurface successfully transforms the polarization of a radiation pattern of a test antenna within the frequency range 90 to 165 MHz (apart from a narrow band around 155 MHz). The dielectric losses in the metasurface are estimated to be below 2%. Future work to improve the performance of the polarizer is outlined.

9:00 Performance of Computational Tools for Wideband Quadruple-Ridged Flared Horn Analysis

Robert Lehmensiek (National Radio Astronomy Observatory, USA & Stellenbosch University, South Africa); Dirk de Villiers and Matthys M. Botha (Stellenbosch University, South Africa)

For full-wave analysis of a complex quadruple-ridged flared horn (QRFH) antenna over a wide band, the performance of a few well-known commercial computational electromagnetics tools is compared, to assess variability in results and runtimes, to be anticipated and contended with, by designers. The QRFH is designed for the Next Generation Very Large Array (ngVLA), radio astronomy instrument. The range of solvers include both differential and integral equation based methods, as well as frequency and time domain formulations. Default settings were used as much as possible, but manual meshing interventions were required. With these kept to a minimum, fair correspondence in port parameters, including measurements, is achieved. A few solvers yielded remarkably similar runtimes. The results may lend a degree of confidence to designers, in their full-wave computational tools. The results show the importance of informed solver selection and parameter settings.

9:20 Canadian-Chilean Array for Radio Transient Studies (CHARTS): Analog System Developments

Tomas Cassanelli (Universidad de Chile, Chile); Juan Mena-Parra (University of Toronto, Canada); Sebastian Manosalva (Universidad de Chile, Chile); Albert Wai Kit Lau (University of Toronto, Canada); Diego Gallardo (Universidad de Chile, Ingeniería Eléctrica, Chile); Keith Vanderlinde (University of Toronto, Canada); Liam Connor (Harvard Universisity, USA); Ricardo Finger (University of Chile, Chile); Sean V Hum (University of Toronto, Canada)

The Canadian-Chilean array for radio transient studies (CHARTS) is a 256-element interferometer to be located in Chile and set to study the universe's transient phenomena that has revolutionized the field since 2007. CHARTS will study energetic transients called fast radio bursts, super giant pulses from pulsars, and Galactic magnetar flares with a low frequency array of 300--500 MHz. Sensitivity of radio telescope is characterized by its aperture size and observing bandwidth, the latter increased in recent years by the revolution of new wideband digitizers. CHARTS will focus on the nearby and local universe FRB detection and further characterize them. Here we describe the CHARTS project and progress made in its antenna and radio frequency front end.

Room: Schelkunoff (C1)

CS51a - Physics assisted learning and inversion strategies for electromagnetic imaging

T07 Electromagnetic modelling and simulation tools / Convened Session / Electromagnetics

Chairs: Martina Teresa Bevacqua (Università Mediterranea di Reggio Calabria, Italy), Rosa Scapaticci (CNR-National Research Council of Italy, Italy)

8:00 Implementation of Projection-Based Neural Networks on Landweber-Kaczmarz for Parallel Multifrequency Contrast-Source Electromagnetic Imaging

Abdulla Desmal (Bahrain Polytechnic, Bahrain); Jawad Alsaei (University of Bahrain, Bahrain)

A multifrequency iterative neural projection framework, based on the recently proposed Contrast-Source Landweber-Kaczmarz (CSLK) scheme, is introduced for electromagnetic imaging. Unlike traditional Frequency-Hopping (FH) techniques that require sequential initialization after each frequency update, this framework updates the medium parameters for all the frequencies in parallel during each CSLK iteration. The recovered medium parameters are then fed into projection Neural Networks (NNs), and the refined parameters generated by the NNs after each iteration are passed to the next CSLK iteration step. To achieve convergence and stability, different projection NNs are assigned after each iteration, with a loss function that combines the enhanced medium discrepancies from each NN. The numerical results section demonstrates the efficiency of the proposed approach.

8:20 Inverse-Based Approaches for Fault Detection in Antenna Arrays

Sandra Costanzo and Giuseppe Di Massa (University of Calabria, Italy); Alessandro Fedeli and Andrea Randazzo (University of Genoa, Italy)

Diagnosis of faulty elements in antenna arrays is nowadays attracting a relevant attention in the scientific community. Indeed, due to the high dimensionality of the arrays and to the higher working frequencies required in new applications, proper diagnostic procedures are required. In this framework, the present paper present two new strategies, based on the matrix method and on regularization in non-conventional Lebesgue spaces, that can effectively address this task. Preliminary results are presented.

8:40 Mild Data-Driven Inversion for Microwave Nondestructive Diagnostics of Plants and Trees

Alessandro Fedeli, Claudio Estatico and Andrea Randazzo (University of Genoa, Italy)

The nondestructive diagnosis of pathologies in plants or trees has a great importance in agriculture and green management. In the context of microwave-based diagnostic techniques, a quantitative imaging method is proposed here to obtain two-dimensional reconstructions of the internal dielectric properties of trunks, starting from scattered-field measurements. The method, which aims at solving a nonlinear and ill-posed inverse problem, combines a mild data-driven approach with an inexact-Newton scheme. In particular, the goal of the data-driven methodology is to introduce prior information about the trunk structure, helping the reconstruction process. The proposed algorithm has been tested with numerical simulations involving different working frequencies and dimensions of the considered trunks.

9:00 Accelerated Machine Learning Antenna Synthesis Through Binary Metal-Vacuum Mesh Activation and Data Reuse in a MoM Framework

Fitim Maxharraj (Chalmers University of Technology, Sweden); Martin Sjödin (Ericsson Research, Sweden); Rob Maaskant (CHALMERS, Sweden); Marianna Ivashina (Chalmers University of Technology, Sweden)

We propose a novel approach to efficiently generate large datasets for antenna synthesis by addressing challenges in handling arbitrary geometrical configurations. In 30 minutes, a dataset of 3,000,000 antennas, covering a frequency range from 0.1 to 5 GHz, was generated, significantly accelerating the design process through machine learning. This was achieved by adding/removing triangular metal patches inside the antenna mesh domain through efficient manipulation of the rows and columns of a pre-calculated Method-of-Moment (MoM) matrix. Such flexibility in efficiently simulating new designs by reusing precomputed data is not available in commercial electromagnetic (EM) solvers. The generated dataset of antenna meshes is used to train a convolutional neural network (CNN). After training, the CNN accurately predicts the input impedance for arbitrary input meshes, without using an EM solver. The CNN was integrated into a genetic optimization algorithm, allowing antenna optimization in minutes instead of hours, with a mean squared error 0.0026.

9:20 Stroke Classification via Microwave Imaging Using Huygens' Principle Assisted by Deep Learning

Moein Movafagh (London South Bank University, United Kingdom); Navid Ghavami (Umbria Bioengineering Technology (UBT), United Kingdom); Mehran TaghipourGorjikolaie (School of Engineering, London South Bank University (LSBU), London, UK. & London South Bank University (LSBU), United Kingdom); Gianluigi Tiberi (London South Bank University, United Kingdom & UBT - Umbria Bioengineering Technologies, Italy); Mirco Cosottini (University of Pisa, United Kingdom); Sandra Dudley and Mohammad Ghavami (London South Bank University, United Kingdom)

The use of microwave imaging techniques for detection and classification of brain strokes is a growing field of research, motivated by the distinct dielectric properties of hemorrhagic and ischemic strokes relative to their surrounding tissues. In this work we combine our image processing algorithm based on the Huygens' principle (HP) and U-net based deep learning to produce morphological reconstructed images, allowing detection and classification of brain strokes.

WEDNESDAY

Room: Oliner (C3)

CS25a - Advances in Reconfigurable Antennas for Communication, Localization and Sensing Applications

T07 Electromagnetic modelling and simulation tools / Convened Session / Antennas

Chairs: Christophe Fumeaux (University of Queensland, Australia), Leonardo Lizzi (University of Trento, Italy)

8:00 Pattern-Reconfigurable Broadside Substrate-Integrated Waveguide Horn Antenna with a π-Shaped Structure

Sasan Ahdi Rezaeieh (The University of Queensland, Australia); Christophe Fumeaux (University of Queensland, Australia)

This paper presents a concept of a pattern-reconfigurable broadside substrate integrated waveguide (SIW) horn antenna that is loaded with a pair of protruding reflectors and a director forming a π-shaped structure. PIN diodes are used to electronically activate the reflectors and director, hence enabling beam reconfiguration utilizing different arrangements of the reflectors and the director. Simulated results are presented of an antenna operating at 9 -9.8 GHz with fractional bandwidth of 8.5%. The antenna achieves a peak gain of 11 dBi at 9.4 GHz and can be reconfigured to radiate at ±57° and 0° on elevation plane. Considering its versatility, ease of reconfiguration and reasonable operating bandwidth, this antenna concept can be used for modern communications systems, where beam reconfiguration is critical.

8:20 Dual-Band Circularly Polarized Ferrite Antenna

Jehison Leon Valdes and Laure Huitema (University of Limoges, France); Eric Arnaud (XLIM, France)
This work presents the development of a dual-band antenna operating in a right-hand circular polarization (RHCP) in GPS and Galileo frequency bands, L2 (1.227 GHz) and E6 (1.278 GHz). The antenna exploits the potential of biased ferrite materials to naturally generate a circular polarization. Ferrite material also allows the reduction of antenna dimensions due to their high permittivity. All performances in terms of impedance matching and radiation pattern are reported and the concept is validated by prototype measurements.

8:40 Ultra-Wideband Reconfigurable Tightly Coupled Array with A High Efficiency

Gengming Wei (University of Technology Sydney (UTS), Australia); Peiyuan Qin, Y. Jay Guo and Shan Huang (University of Technology Sydney, Australia); Yi He (University of Technology Sydney (UTS), Australia)
This paper presents novel investigations into an ultra-wideband (UWB) dual-polarized frequency-reconfigurable tightly-coupled dipole array (DP-FR-TCDA). The proposed array achieves efficient operating-band reconfigurability through a uniquely designed reconfigurable ground plane. This ground plane effectively transforms out-of-phase ground-plane reflections into in-phase reflections with minimal insertion loss, enabling seamless operation across two contiguous frequency bands. Simulation results demonstrate that the two reconfigurable states produce overlapping sub-bands spanning 0.42-1.45 GHz and 1.09-5.65 GHz, respectively. Collectively, these sub-bands offer an overall combined bandwidth of 13.5:1, covering 0.42-5.65 GHz with a voltage standing wave ratio (VSWR) less than 3. These characteristics render the array highly suitable for integrated sensing and communication (ISAC) applications based on UWB systems.

9:00 A Millimeter-Wave Horn Antenna with Reconfigurable Polarization

Maya Al Ajam, Youssef Tawk and Joseph Costantine (American University of Beirut, Lebanon)
This paper introduces the use of helical polarizing topologies within the aperture of millimeter-wave horn antennas to transform their linearly polarized fields into either right-hand or left-hand circularly polarized. The winding of the helix determines which circular polarization scheme is radiated. The reconfigurable polarizer concept is implemented on a prototype that includes one helix positioned at the center of the horn. The horn antenna with a single polarizer is tested and validated to operate between 26 GHz and 32 GHz.

9:20 The Impact of Excitation Technique on the Frequency Agility of Electrically Small Antennas

Abdellah Touhami, Marwan Jadid and Christophe Delaveaud (CEA-LETI, France)
This work presents a study of the impact of the excitation technique on the frequency agility performance of a capacitively loaded loop (CLL) electrically small antenna (ESA). Three excitation techniques are presented and analyzed: electric dipole based excitation, magnetic-dipole based excitation, and short-circuit based excitation. All the designs are electrically small with a maximal electrical size of ka less than 0.4. To compare the agility performances achieved by each excitation technique, the tunable bandwidth (TBW), the fractional tunable bandwidth (FTBW) and agility efficiency (AE) are used as figures of merit. The comparison reveals that the short-circuit based excitation archives the optimal performances with a TBW of 1104 MHz, a FTBW of 146.42% and an AE of 83.15 MHz/pF. Furthermore, it presents a radiation efficiency ranging from 1.5% (for a ka =0.06) to 94% (for a ka = 0.39).

Room: Kraus (C4)

CS24a - Quantum Electromagnetics - From Photonics to Quantum Computing

T08 Fundamental research and emerging technologies/processes / Convened Session / Electromagnetics

Chairs: Gabriele Gradoni (University of Surrey, United Kingdom), Zhen Peng (University of Illinois at Urbana-Champaign, USA)

8:00 Highly Directive and Wideband On-Chip Hybrid Plasmonic Leaky-Wave Nanoantenna Enhanced by Optical Transverse Periodic Slots

Maryam Khodadadi, Hamidreza Taghvaee and Ali Ali (University of Surrey, United Kingdom); Mohsen Khalily (University of Surrey & 5G Innovation Centre, Institute for Communication Systems (ICS), United Kingdom)
This paper presents a novel on-chip hybrid plasmonic leaky-wave nanoantenna, enhanced by optical transverse periodic slots, designed for the standard telecommunications wavelength of 1550 nm. By leveraging the combined advantages of hybrid plasmonic waveguides and leaky-wave mechanisms, this nanoantenna achieves superior light confinement and highly directive radiation patterns. The multi-layer structure, featuring InGaAsP, gold, and quartz, ensures minimal propagation loss and efficient mode conversion from guided to radiative modes. Simulation results demonstrate the antenna's impressive performance with a directivity of 18.5 dBi and a gain of 14.3 dBi, while maintaining a low side-lobe level and broad bandwidth. These characteristics make it highly suitable for integrated optical interconnects, beam-steering devices, and enhanced solar cells. The design is fully compatible with standard complementary metal-oxide-semiconductor (CMOS) processes, facilitating seamless integration into opto-electronic circuits. This advancement marks a significant step towards highly efficient, miniaturized optical communication systems and on-chip photonic applications.

WEDNESDAY

8:20 Quantum Algorithms for Reconfigurable Intelligent Surface Optimization: Barren Plateaus Analysis

Emanuel Colella (CNIT, Parma & Università Politecnica Delle Marche, Italy); Luca Bastianelli and Franco Moglie (Università Politecnica delle Marche, Italy); Gabriele Gradoni (University of Surrey, United Kingdom); Valter Mariani Primiani (Polytechnic University of Marche, Italy)

Wireless communication systems play a pivotal role in modern society, yet they face significant challenges such as latency and multipath fading. Reconfigurable intelligent surface (RIS) is emerged as a promising solution to manipulate electromagnetic waves to enhance transmission quality, although their optimization presents several limitations. In this study, we propose a hybrid approach utilizing the quantum approximate optimization algorithm (QAOA) to effectively configure RIS in multipath environments, addressing the shortcomings of classical methods. The computational model trained by the Sherrington-Kirkpatrick Hamiltonian, demonstrates high accuracy in identifying optimal RIS configurations across various scenarios, without running optimization at each condition. However, the analysis of barren plateaus reveals that the cost function gradient diminishes exponentially as the number of cells increases, making hard the training for large-scale systems. To mitigate these issues, we conclude by suggesting some potential strategies for future research aimed at enhancing RIS performance in practical applications.

8:40 Conditionally Built Quantum States for Radio Frequency Sensing and Imaging

Polina Kuzhir (University of Eastern Finland, Finland); Dmitri Mogilevtsev, Dmytro Vovchuk and Pavel Ginzburg (Tel Aviv University, Israel); Alexander Mikhalychev and Alex Ulyanenkov (Atomicus GmbH, Germany); Gregory Slepyan and Amir Boag (Tel Aviv University, Israel)

We discuss a conditional build-up of quantum states from weighted sets of coherent states' mixtures for radio frequency realization of fundamental quantum experiments such as Hong-Ou-Mandel interference, for imaging with sub-Poissonian states of light, and for far-field sensing/ranging with conditionally built single-photon states.

9:00 Spatiotemporal Metamaterials and Their Symmetries

Iñigo Liberal (Public University of Navarre, Spain)

Spatiotemporal metamaterials harness ultrafast modulations of the refractive index to implement synthetic motion, resulting in light-matter interactions where neither the energy nor the momentum of the electromagnetic field are conserved. Despite this fact, here we demonstrate that spatiotemporal metamaterials exhibit reduced spatiotemporal symmetries. Moreover, using Noether's theorem we demonstrate that such spatiotemporal symmetry results in the conservation of the energy-momentum. We present a numerical examples of the scattering of an electromagnetic pulse by a modulation pulse to validate our theoretical results.

9:20 Superradiance of Quantum Antennas in a Solid-State Environment: Phonon-Modified Electromagnetics

Devashish Pandey (Technical University of Denmark); Martijn Wubs (Technical University of Denmark, Denmark)

We consider sub- and superradiance of quantum emitters in a solid-state environment. This collective emission depends on the electromagnetic interaction between the emitters that can be engineered via the environment and described by the classical electromagnetic Green function. But also phonons may affect the collective emission. Phonons produce dephasing, both non-exponential fast initial dephasing and slower exponential dephasing. We compared several ways to account for both types of phonon interactions into the more standard optical master equation for an arbitrary number of quantum emitters that mutually interact via the electromagnetic field. In particular we present a concatenation method that incorporates phonon effects without adding computational complexity, suitable for arrays of emitters. Here we use it to study the effects of detunings on two-emitter spectra and on the corresponding population and entanglement dynamics.

Room: Munch (23)

Industrial Workshop

IW2 - COMSOL - Design Robustness and Digital Twins for Antenna Engineering: Uncertainty Quantification and Surrogate Models with Deep Neural Networks

WEDNESDAY

T03 Aerospace, space and non-terrestrial networks / Convened Session / Antennas

Chairs: Aakash Bansal (Loughborough University, United Kingdom), William Whittow (Loughborough University, United Kingdom)

8:00 Information Metasurface for Transparent Forwarding of Non-Terrestrial Networks

Lijie Wu, Zhenjie Qi, Wenxuan Tang, Jun Yan Dai, Qiang Cheng and Tie Jun Cui (Southeast University, China)
Information metasurfaces (IMs) have emerged as a key solution to improve the performance of non-terrestrial networks (NTNs). However, most IMs face inherent non-negligible ohmic losses from the tunable elements, which is not suitable for the transparent forwarding architecture of NTNs. To solve this problem, the amplifying and filtering information metasurface (AFIM) is proposed in this paper to enhance the in-band signal energy and filter the out-of-band signal. Additionally, it can realize a 2-bit phase control and exhibit great beam steering performance. The proposed AFIM may find potential applications for transparent forwarding of NTNs.

8:20 Conformal Corrugated Substrate Integrated Waveguides for Radio Systems in Space

Aakash Bansal and William Whittow (Loughborough University, United Kingdom)
The paper presents a comparative analysis of different foldable corrugated substrate integrated waveguide (CSIW) structures. Unlike traditional SIWs, vias in a CSIW are replaced with different forms of corrugations. The corrugated design makes the structure lightweight and foldable, hence, it can be used as transmission lines on satellite systems. The paper compares the conformal performance for CSIWs with four types of corrugations: (a) straight; (b) bent; (c) integrated-digitated capacitor; and (d) twisted. The comparative analysis demonstrates that the IDC-based CSIW offers the least transmission loss of < 0.7 dB/m and is comparable with conventional SIWs.

8:40 Optimizing Antenna Activation for Even Power Distribution in mm-Wave Multi-Beam Satellite Systems Using Genetic Algorithm

Aral E. Zorkun, Juan A. Vásquez Peralvo, Jorge Querol, Flor Ortiz, Luis Manuel Garcés-Socarrás, Jorge L González-Rios and Symeon Chatzinotas (University of Luxembourg, Luxembourg)
Recent advancements in onboard satellite communication have significantly enhanced the ability to dynamically modify the radiation pattern of a Direct Radiating Array (DRA), which is essential for both conventional communication satellites like Geostationary Orbit (GEO) and those in lower orbits such as Low Earth Orbit (LEO). This is particularly relevant for communication at 28 GHz, a key frequency in the mmWave spectrum, used for high-bandwidth satellite links and 5G communications. Critical design factors include the number of beams, beamwidth, and side lobe level for each beam. However, in multibeam scenarios, balancing these design factors can result in uneven power distribution, leading to over-saturation in centrally located antenna elements due to frequent activations. This paper introduces a Genetic Algorithm (GA)-based approach to optimize beamforming coefficients by modulating the amplitude component of the weight matrix, while imposing a constraint on activation instances per element to avoid over-saturation in the RF chain.

9:00 Mega-Antennas as a Key Enabler for Terrestrial and Non-Terrestrial Communication Network Integration

Marco Luise, Giacomo Bacci, Luca Sanguinetti and Riccardo De Gaudenzi (University of Pisa, Italy)
In recent years, integration of terrestrial and non-terrestrial (satellite-based) communication networks has been considered a fundamental goal, especially in the transition between current 5th-generation and future 6th-generation cellular networks. One of the key elements to attain such goal is the adoption of advanced architectures and technologies for the spaceborne antenna system, both in the context of large Geostationary-orbit (GEO) satellites, as well as for smaller Low-Earth Orbiting (LEO) satellites belonging to a mega-constellations. This paper reports on the latest advances of so-called mega-antennas, i.e., very large distributed arrays of simpler antennas carried by several satellites organized as a swarm or a formation, analyzing different system configuration options in terms of conventional beamforming and/or User-Centric MIMO network configuration.

9:20 Impact of Doppler Effect on Testing LEO Satellite Tracking Antenna Using Static Motion Platform

Samuel Arthur Rotenberg and George Goussetis (Heriot-Watt University, United Kingdom); Benjamin J Falkner and Harvinder Nagi (Satellite Applications Catapult, United Kingdom)
The demand for reliable satellite communication on moving platforms has grown considerably, becoming a critical topic for ensuring stable connectivity via Low Earth Orbit satellites to vehicles such as boats, airplanes, and cars. To meet these needs, a variety of ground-based technologies with tracking capabilities are being developed. Before deploying these terminals on actual vehicles, it is essential to test their performance using motion simulators, such as hexapod motion platform. Although these platforms offer significant freedom of rotation in all directions, they are limited in terms of linear translation, making it difficult to emulate the linear velocities of moving vehicles, which directly influence the Doppler effect. We investigate the impact of the Doppler effect for moving vehicles compared to static users and analyse whether the additional Doppler shift caused by vehicle motion needs to be compensated for, in addition to the natural Doppler shift from the satellite's movement.

WEDNESDAY

T01 Sub-6 GHz for terrestrial networks (5G/6G) / / Measurements

Chairs: Samel Arslanagić (Technical University of Denmark, Denmark), Matthias Hein (Technische Universität Ilmenau, Germany)

8:00 Gain and Efficiency Calibration Antennas for Low Frequency Automotive Measurement Systems

Andrea Giacomini (Microwave Vision Italy SRL, Italy); Lars Foged and Francesco Saccardi (Microwave Vision Italy, Italy); Vincenzo Schirosi (MICROWAVE VISION ITALY, Italy)

In this paper, we explore the use of scaled antenna models to develop a set of calibration monocone antennas, each mounted on a small ground plane, for automotive range calibration. The calibration antennas presented here cover the frequency range from 70 MHz to 6 GHz using only four antennas, though an even wider frequency range can be easily achieved. These scaled antennas are designed as precise replicas of their higher-frequency counterparts, enabling convenient measurements across various frequencies while preserving key characteristics such as gain, directivity, and efficiency. The use of such antennas is advantageous for automotive facility calibration, as a broad frequency band can be covered with a small number of antennas, and performance data can be derived from scaled measurements. Some design considerations has been addressed, and the scaled modeling approach, and the validation experiments conducted in a full-scale automotive measurement facility.

8:20 On the Representation of Measurement Uncertainty of Absorber Reflectivity

Marc Dirix (Emerson&Cumming Anechoic Chambers, The Netherlands); Amin Enayati (Emersun and Cumming Anechoic Chambers, Belgium)

Uncertainty evaluation and the appropriate way of its representation for absorber-reflectivity measurements have been addressed. The uncertainty evaluation has been done assuming the uncertainty factor as an equivalent error source to be added coherently to the measured reflectivity signal. In this way, the uncertainty shows its impact in an asymmetrical manner which could be much larger in the negative-value direction rather than in the positive-value direction. Moreover, this way of uncertainty evaluation helps the representation on top of the reflectivity curves in a way which is suitable for the community using the reflectivity curves to design anechoic environment. That is because, the main criterion for an absorber in the range design is that it needs to deliver a reflectivity value which is lower than a specified value, e.g. -50 dB, with a specified confidence level.

8:40 Analysis of an Optimisation-Based De-Pointing Measurement Method for LEO Satellite Terminal Characterisation

Benjamin J Falkner, Harvinder Nagi and Evangelos Mellios (Satellite Applications Catapult, United Kingdom)

The next generation on-the-move LEO satellite communication terminals require new testing methods to ensure their performance and pointing accuracy remains consistent while under motion. This paper presents and analyses a method for measuring the pointing angle of an electronically steered satellite communication user terminal in real time. The method uses an array of measurement probes around the target direction to sample the power of the antenna array pattern. A local optimiser is used to match a gaussian function to the sampled amplitudes. Analysis of this algorithm is presented to demonstrate how the range and density of the measurement array can impact the accuracy of the system for antennas of various beamwidths. The algorithm is found to provide accuracy within 0.05° for antenna beamwidths of 0.6° to 25° where the measurement array covers an angular range of ±5° around the desired pointing direction and has an element separation of 0.5°.

9:00 Trade-Offs for Beam Pattern Measurement of Pulsed Photoconductive Antennas Using a Pin-Hole Approach

Martijn D. Huiskes, Andrea Neto, Juan Bueno and Paolo Sberna (Delft University of Technology, The Netherlands)

With the maturing of time-domain spectroscopy (TDS) systems, the quality of the beams generated and received becomes more important. To asses this quality, pin-hole measurement schemes have been proposed, which demand a trade-off between the resolution of the imaged beam and the acquisition time. In this paper, we present an analysis procedure that can be used to guide the trade-off for the size of the pin-hole.

9:20 Hybrid GNSS Antenna Characterization for Automotive Scenarios

Veenu Tripathi and Stefano Caizzone (German Aerospace Center (DLR), Germany)

The accuracy of GNSS signal reception is crucial for precise navigation and geodetic positioning. Environmental interactions can cause signal distortions and multipath effects, impacting GNSS antenna group delays (GDVs) also known as code phase variations (CPVs). This paper addresses the accurate prediction of installed antenna performance in automotive scenarios. It introduces a hybrid calibration approach combining real-world data and simulations to enhance GNSS antenna performance predictions. This allows the simulation to reconstruct the effect of the mounting platform on the data of the individual antenna already measured in an anechoic chamber and thus predict the final error of the installed antenna on the platform.

WEDNESDAY

Wednesday - 10:10 - 11:50 | Job corner at the EurAAP booth

Wednesday - 10:10 - 11:50

Room: Alfvén (A3+A4) | A04b - Mmwave antenna technologies

T02 Millimetre wave and THz for terrestrial networks (5G/6G) / / Antennas

Chairs: Marko Bosiljevac (University of Zagreb, Croatia), Ahmed A Kishk (Concordia University, Canada)

10:10 Hedgehog Shell: Multibeam DRA with 2-D Beamsteering for mm-Wave Applications

Amir Mohsen Ahmadi Najafabadi (EPFL, Switzerland); German Augusto Ramirez Arroyave (EPFL - École Polytechnique Fédérale de Lausanne & Universidad Nacional de Colombia, Switzerland); Mohsen Ghorbanpoor (ETHZ, Switzerland); Alexander Vorobyov (CSEM & Center Suisse d'Electronique et de Microtechnique SA, Switzerland); Pascal Nussbaum (CSEM, Switzerland); Anja K. Skrivervik (EPFL, Switzerland)

This paper investigates a low-cost method to form a multibeam antenna with 2-D beamsteering capability. The simple feeding method employed in this solution enables the dielectric rod antennas to generate multiple beams in the intended direction simultaneously. In this manner, a multi-fixed-beam system is created without the need for a beamforming unit, which reduces the complexity of the final system architecture. Furthermore, a sensitivity analysis of the dielectric rod is performed, taking into account variations in critical design parameters and the permittivity of the rod. Different fabrication methods and low-loss materials that can be used for rod manufacturing are introduced, and the permittivity of these materials is characterized using the Nicolson-Ross-Weir (NRW) method. By doing so, our study not only presents a practical multibeam antenna formulation strategy but also reports appropriate materials and manufacturing processes that can be employed in the manufacturing of rod antennas.

10:30 Low-Cost Millimeter-Wave Patch Antenna Array in Package for 5G/6G Communication Applications

Xiao-Lan Tang (Gannan University of Science and Technology, China)

A low-cost and fully integrated stacked patch antenna in package for 5G/6G millimeter-wave communication applications is proposed in this paper. The 4-element patch antenna array and the 2x2 flip-chip attached beamforming chip are assembled on a 10-layer PCB board. The antenna array, together with millimeter wave interconnects, including the matching network using stripline, stripline-to-coaxial-vias transition structures and flip-chip package, are optimized using 3D full-wave simulation. The realized antenna in package shows more than 15% fractional bandwidth within the band of 25.9-30.3 GHz, 9.3 dBi realized gain, over 90% of total efficiency at 28 GHz and more than -45 dB cross-polarization level. Note that, larger phased antenna array (for example with 256 antenna element) implemented with embedded power dividers on multilayer PCB board may be investigated for 28 GHz base station applications.

10:50 Novel 2-D Beamsteerable Rectenna with Improved Power Receptivity for mm-Wave RF-WPT Applications

Amir Mohsen Ahmadi Najafabadi (EPFL, Switzerland); Mohsen Ghorbanpoor (ETHZ, Switzerland); Pratik V Vadher (Université de Rennes, France & University of Rennes 1, France); German Augusto Ramirez Arroyave (EPFL - École Polytechnique Fédérale de Lausanne & Universidad Nacional de Colombia, Switzerland); Alexander Vorobyov (CSEM & Center Suisse d'Electronique et de Microtechnique SA, Switzerland); Pascal Nussbaum (CSEM, Switzerland); Denys Nikolayev (Institut d'Électronique et des Technologies du Numérique (IETR) - UMR CNRS 6164, France); Hua Wang (ETH Zurich, Brazil); Anja K. Skrivervik (EPFL, Switzerland)

This paper introduces a novel 2-D beam-steerable rectenna designed for mm-wave RF wireless power transfer (RF-WPT) applications. The 2-D beamsteering capability of the proposed rectenna is achieved by integrating an on-chip 4 × 4 Butler matrix, which is co-integrated with a rectifier array in a 22 nm FD-SOI CMOS, and a leaky wave antenna array. The proposed solution incorporates dual rectifier units simultaneously to enhance the receiver's power receptivity. In this manner, the rectenna is capable of receiving power from the same direction while taking advantage of frequency diversity. This is accomplished using the novel integration scheme of the single leaky wave array antenna with two rectifier units. The proposed solution maintains the system's compactness and reduces the overall cost while offering a fully passive 2-D beam scanning for the receiver unit. These merits make the proposed solution promising for RF-WPT applications in the Internet of Things (IoT) ecosystem.

11:10 Q/V-Band Gap-Waveguide-Based Circularly-Polarized Antenna

Iñigo Leoz-Beltrán (Public University of Navarre, Spain); JuanCarlos Iriarte (Public University of Navarra & Antenna Group, Spain); Dayan Pérez-Quintana (University of Siena (UNISI) & Institute of Smart Cities (ISC), Italy); Fernando Teberio (Anteral, Spain); Miguel Beruete (Universidad Publica de Navarra, Spain); Iñigo Ederra (Universidad Pública de Navarra & Institute of Smart Cities, Universidad Pública de Navarra, Spain)

This paper presents the design of an all-metal Gap Waveguide-based antenna. The design is intended for satellite communications as it covers the Q/V-Band, comprised between 37.5 and 42.5 GHz and between 47.5 and 52.4 GHz. This antenna operates with circular polarization, featuring an Axial Ratio below 1.5 dB at both frequency bands. The design includes a transition from an standard WR waveguide to a Ridge Gap Waveguide. The simulation of the whole system shows an S11 parameter remaining below -10 dB at the bands of interest. Furthermore, this unit cell antenna achieves a maximum gain of 11.9 dB at 48.8 GHz.

WEDNESDAY

11:30 Rotman Lens-Based 2-Dimensional Retrodirective Beamformer for mmWave WPT

Sooyoung Oh and Sun K. Hong (Soongsil University, Korea (South))
With the rise of the internet of things (IoT), the demand for small wireless devices has grown in both commercial and military sectors. However, since most of the IoT enabled electronic devices are battery-powered, the need for recharging limits their operation, driving interest in wireless charging through wireless power transfer. In this paper, mmWaves retrodirective beamformer based on Rotman lens applicable to wireless power transfer is presented. The designed Rotman lens can perform 2-dimensional beamforming, which is capable of generating beams at both azimuth and elevation plane. The beamformer allows the beam steering range of (±20deg, ±10deg) with the interval of 10deg with the maximum gain of 11.8 dBi.

Room: Kildal (A2) | **A10b - Wideband antennas**

T01 Sub-6 GHz for terrestrial networks (5G/6G) / / Antennas

Chairs: Mario Junior Mencagli (University of Delaware, USA), Petrie Meyer (Stellenbosch University, South Africa)

10:10 3-20 GHz Wideband Tightly-Coupled Dual-Polarized Vivaldi Antenna Array

Niko Lindvall, Mikko Heino and Mikko Valkama (Tampere University, Finland)
Very wideband apertures are needed in positioning, sensing, spectrum monitoring, and modern spread spectrum, e.g., frequency hopping systems. Vivaldi antennas are one of the prominent choices for the aforementioned systems due to their natural wideband characteristics. Furthermore, tightly-coupled antenna arrays have been researched in the recent years to extend the lower band edge of compact arrays by taking advantage of the strong mutual coupling between the elements especially with dipole elements, but not with dual-polarized Vivaldi antennas. This paper presents a novel tightly-coupled dual-polarized antipodal Vivaldi antenna (TC-AVA) with -6 dB impedance bandwidth of 3 to 20 GHz. The tight coupling by overlapping the Vivaldi leaves is shown to extend the lower band edge from 3.75 to 3 GHz and 2.75 GHz, an improvement of 20% to 25% for both polarizations, compared with an isolated antipodal Vivaldi element.

10:30 Dispersionless Broadband Impedance Matching with Aperiodically Time-Modulated Capacitors

Mario Junior Mencagli (University of Delaware, USA); Dimitrios Sounas (Wayne State University, USA)
Impedance matching is one of the most important problems in microwave engineering. It allows maximizing the transfer of power from a source to a load. However, the bandwidth over which a certain amount of power can be transferred is fundamentally limited by the Bode-Fano bound, which applies to any passive, linear, and time-varying matching networks. By revoking the underlying assumption of time invariance, here, we show how a capacitor undergoing a realistic aperiodic time modulation allows going beyond the matching-bandwidth bound. In contrast to previous works, the proposed approach not only allows overcoming the restrictions of the Bode-Fano bound but also preserves the temporal shape of the pulse that needs to be transmitted/radiated (dispersionless). Our findings may open a new avenue in the design of electrically small antennas, resonators, and absorbers with a large operation bandwidth.

10:50 Sustainable Broadband Monopole Antennas Based on Recyclable Liquid Metals and Biodegradable 3D-Printed Dielectrics

XiaoChuan Fang, Nikolas Bruce and Mahmoud Wagih (University of Glasgow, United Kingdom)
This paper presents the first 3D-printable antenna with fully recyclable and re-usable metals, for sustainable RF communication applications. The proposed antenna consists of a fully 3D-printed substrate made from biodegradable polylactic acid (PLA). It features an asymmetric monopole that provides a maximum measured broadband operation range from 1.8 GHz to 3.2 GHz and is fed by a coplanar waveguide (CPW) structure. The conductive components (i.e., the radiator, feed line, and ground plane) are fabricated using liquid metal. A repeatable method for filling the channels with liquid metal is developed, allowing the conductive components to be fully recycled and refilled. The effectiveness of the recycling process is verified by consistent measurement results, the difference of bandwidth between which is less than 3%.

11:10 A 12:1 Ultra-Wideband High-Gain Probe for Future Direct Circular Polarization Antenna Measurements

Kerlos Atia Abdalmalak Dawoud (Universidad Carlos III de Madrid, Spain); Ahmed El Yousfi (Universidad Carlos III De Madrid, Spain); Daniel Segovia-Vargas (Universidad Carlos III de Madrid, Spain)
This paper presents a 12:1 high-gain UWB circular polarized (CP) probe for use in anechoic chamber measurements. The solution is based on a log-spiral antenna printed in a conical shape and, to the best of the authors' knowledge, has the widest band reported of direct CP solution with high gain and stable performance. It covers simultaneously several interesting frequency bands, including L-band (1.518-1.675GHz), S-band (1.97-2.69GHz), C-band (3.4GHz-7.025GHz), X-band (7.25-8.44GHz) and part of Ku-band (10.7-12GHz) which makes it the preferred probe for testing CP antennas for the various applications. With the comparison to state-of-the-art solutions (both in literature and commercial), this probe has six main attractive characteristics: stable radiation patterns, negligible sidelobe levels, high and stable gain of about 9dBi, pure CP with an axial ratio below 2dBi, easy scalability for different frequency bands, and low weight (compared to standard metallic horn probes). Additionally, studies for four fabrication techniques are investigated.

WEDNESDAY

11:30 A Compact UWB Textile Antenna Designed for WLAN and C-Band Applications

Asma Slimani (Fréres Mentouri University Constantine1, Algeria); Chemseddine Zebiri (Ferhat Abbas University of Setif, Algeria); Sarra Khacha (University of Ferhat Abbas, Algeria); Fouad Kerrour (Université Frères Mentouri Constantine 1, Algeria); Djamel Sayad (University of 20 Aout 1955 - Skikda, Algeria); Kamil Karacuha (Istanbul Technical University, Turkey); Issa Elfergani and Jonathan Rodriguez (Instituto de Telecomunicações, Portugal)

This paper presents the design and analysis of a compact ultra-wideband (UWB) textile antenna operating within the C-band, specifically at 5.8 GHz, with a wide bandwidth ranging from 4.46 GHz to 7.27 GHz. The antenna is designed on a Jeans dielectric substrate with dimensions of 16 mm × 10 mm × 0.78 mm. Its miniaturized design offers significant size reduction while achieving a high maximum gain of 4.9 dB and an impressive radiation efficiency of 99%.Our design is suitable for C-band applications, including WLAN, satellite communications, 5G networks, weather radar, fixed wireless access, and biomedical technologies like wireless body area networks (WBAN).

Room: Hallén (BAR5) — CS49b - Propagation for Smart Mobility Scenarios

T04 RF sensing for automotive, security, IoT, and other applications / Convened Session / Propagation

Chairs: Ibrahim Rashdan (German Aerospace Center (DLR), Germany), Martin Schmidhammer (German Aerospace Center (DLR), Germany)

10:10 Integration of RIS into CloudRT Simulator for Railway Tunnel Scenarios

Aline Habib (IMT Atlantique, France); Charlotte Langlais (IMT Atlantique Bretagne Pays de la Loire & Lab-STICC, France); Ammar El Falou (King Abdullah University of Science and Technology (KAUST), Saudi Arabia); Souleymane Kangoute (IMT Atlantique, France); Yiran Wang (Beijing Jiaotong University, China); Marion Berbineau (COSYS, Université Gustave Eiffel, IFSTTAR, Univ Lille & Railenium, France)

Radio communication in tunnels presents significant challenges due to the high likelihood of signal obstruction by elements like tunnel walls, ceilings, train carriages, or blocked trains. Reconfigurable Intelligent Surfaces (RIS) offer a promising and cost-effective solution to mitigate signal-blocking issues by transforming the unpredictable radio environment into a controllable one through managed reflections. This paper extends the CloudRT ray-tracing simulator to accommodate RIS technology and assesses its feasibility for railway tunnel scenarios. RIS is integrated into the CloudRT simulator as a phased antenna array acting as a virtual receiver (Rx)/ transmitter (Tx). The study then explores how various key parameters influence received power and compares two scenarios: one where a masked train obstructs the direct Tx-Rx path, and another where there is no obstruction. The results underscore the potential benefits of deploying RIS in obstructed tunnel environments.

10:30 Comparative Study of Real-Time Beamforming Techniques for Railway Communication Systems in LoS and NLoS Scenarios

Sameh Mabrouki (Universite Polytechnique Haut de France & UPHF, France); Iyad Dayoub (University Polytechnique Hauts-de-France, IEMN-DOAE CNRS, France & INSA Hauts de France, France); Marion Berbineau (COSYS, Université Gustave Eiffel, IFSTTAR, Univ Lille & Railenium, France)

This paper presents a comparative study of real-time beamforming techniques for railway communication systems in Line-of-Sight (LoS) and Non-Line-of-Sight (NLoS) scenarios. Using the 3rd Generation Partnership Project (3GPP) TR 38.901 channel model, we evaluate initial ML-aided beam prediction solutions and propose advanced models to address their limitations. We compare these models against the exhaustive selection technique, demonstrating significant improvements in beam prediction accuracy and robustness. Our findings highlight the importance of comprehensive data collection to capture real-world channel variability, ultimately enhancing railway communication efficiency.

10:50 Channel Measurement and Spatial Characteristics Analysis of mmWave Propagation in Maritime Evaporation Ducts

Boyuan Du, Jiaxin Chen and Peng Chen (Chang'an University, China)

This paper analyzes the channel characteristics and spatial propagation characteristics of millimeter waves in evaporation ducts on the sea surface through field measurements. Research has found that there is a clear correlation between the power level of the received signal and the horizontal and vertical receiving angles. The experiment used USRP X310 to analyze the received power of signals at different antenna angles, and calculated the average and standard deviation of the received power. The results indicate that beam alignment in the horizontal direction is beneficial for high-quality signal reception, while signal power decreases significantly when the horizontal direction deviates by a large angle. In addition, the decreasing trend of received power with the change of vertical angle slows down significantly, and even at an elevation angle of 60°, signals can still be higher than noise threshold, which further confirms the vertical multipath effect in the evaporation ducts.

WEDNESDAY

11:10 Characterization of Non-Wide-Sense Stationarity for Distributed Massive MIMO Channels

Yingjie Xu, Michiel Sandra, Xuesong Cai, Sara Willhammar and Fredrik Tufvesson (Lund University, Sweden)
Distributed massive multiple-input multiple-output (MIMO) communication is envisioned as one of the key paradigms of future MIMO systems. To investigate non-wide-sense stationarities (non-WSSs) in distributed massive MIMO channels, this paper first presents an indoor channel measurement campaign, where distributed arrays with a total of 128 elements were implemented. Then relying on the correlation matrix distance (CMD) method, the stationary distance and stationary frequency of the measured channels are estimated. Results show that the space non-WSS in the measured channels is significantly affected by locations of the distributed arrays. However, the impact of array locations on the measured frequency non-WSSs is marginal. Besides, even for a specific channel, the estimated stationary distances at the base station (BS) and user equipment (UE) side are different. The results provide insights from the perspective of channel non-WSS for accurate modelling of distributed massive MIMO channels and deployment of distributed antennas in practical systems.

11:30 Small-Scale Channel Characteristics of Shadowing Effect in Maritime Wireless Communication

Chengyuan Wen, Shuo Zhang, Kun Yang and Beining Xu (Zhejiang Ocean University, China)
This study examines the shadowing effects on shore- to-ship radio links caused by passing vessels in maritime en-vironments. Leveraging a month's data from the Norwegian Coastal Administration's Automatic Identification System (AIS), we concluded that the probability of shadowing effect occurrences in this region exceeds 60%, which indicates the importance of this study. Furthermore, we conducted an empirical analysis based on high-resolution channel measurements at 2.075 GHz in Trondheimfjorden, Norway. The amplitude distribution was investigated during the entire shadowing process, including obstructed line-of-sight (LOS) and non-line-of-sight (NLOS) sce- narios. Due to limitations of conventional amplitude distributions in accurately depicting this phenomenon, an innovative model - the Rician plus Lognormal distribution (RPLN) was proposed in this paper. This model effectively captures the probability density of the amplitude during different shadowing procedure phases. Its effectiveness was evaluated using the Akaike Information Criterion (AIC), where it outperformed conventional distribution models.

Room: Marcuvitz (M3)

Scientific Workshop

SW3 - Electromagnetic Technologies for Life Sciences: challenges and opportunities in the EurAAP community

Room: Björk (33)

Industrial Workshop

IW3 - DASSAULT SYSTEMES AND PARTNERS - SIMULIA: Advanced Antenna Array Design and Simulation

Room: Bergman (34)

P04b - Satellite channel characterization II

T03 Aerospace, space and non-terrestrial networks / / Propagation

Chairs: Martin Rytir (Norwegian Defence Research Establishment (FFI), Norway), Zhiqiang Yuan (Southeast University, China)

10:10 Ka-Band Tropospheric Scintillation and Simultaneous Rain Attenuation Measured over Rome with Alphasat

Stefano Barbieri (Sapienza University of Rome, Italy); Fernando Consalvi (FUB, Italy); Gianmarco Fusco (Istituto Superiore delle Comunicazione e delle Tecnologie dell'Informazione, Italy); Alef Comisso, Miles A. Turner and Carlo Riva (Politecnico di Milano, Italy); Marianna Biscarini (Sapienza University of Rome, Italy
Tropospheric turbulence can cause significant interference to satellite communications systems, particularly during precipitation events. Moreover, the rapid changes in signal amplitude caused by scintillation become more pronounced when it is raining. In this context, a better characterization of these phenomena is important for a correct optimization of the satellite link budget. This paper collects and analyses one year of rainfall measurements obtained by detecting the signal emitted by the Aldo Paraboni payload mounted on board the Alphasat satellite as an experiment to investigate the Ka-band radio propagation channel. The study focuses on the instantaneous relationship between rain attenuation and simultaneous scintillation. We found that the mean value of the rain attenuation and the corresponding mean value of the standard deviation of the scintillation are related by a power law. The characteristics of the experiment, details of how to detect rainfall events and how to process the data are also presented.

WEDNESDAY

10:30 Two-Dimensional Improvements to the Synthetic Storm Technique for Multi-Satellite Rain Attenuation Analyses

Fernando Pérez-Fontán, Vicente Pastoriza-Santos and Fernando Machado (University of Vigo, Spain); Arijit DE (Sapienza University, Rome, Italy)
In this paper we present an extension to the Synthetic Storm Technique, SST, into the two-dimensional space so that it can be more accurately used in multi-satellite, non-GEO scenarios. We call our approach the Stochastic SST, S-SST. When it comes to simulating the case where the link's ground projection and the storm's direction are not aligned, we need to make further simplifications regarding the transversal shape of the rain time series. We discuss the generation of static rain rate fields and then we extend the case to the generation of sequences thereof. Examples of application are also presented.

10:50 Modelling and Simulation of a Line-Of-Sight MIMO Channel in the Presence of Tropospheric Ducting

Bálint Horváth (Budapest University of Technology and Economics, Hungary); Lei Bao (Ericsson AB, Sweden); Mikael Coldrey (Ericsson Research & Ericsson AB, Sweden)
In this paper we present and evaluate a Parabolic Wave Equation and Numerical Weather Prediction based model of a Line-Of-Sight (LOS) MIMO link used for microwave point-to-point backhaul. The motivation with the model is to enable prediction of the link performance given meteorological data which can be used for microwave link planning purposes. The evaluation of the model is done by using long-term measurement data from a 44 km long LOS MIMO link operating at 6 GHz. We found very good agreement with the model-based simulation results and the measurement data during events with significant ducting in the troposphere.

11:10 Low Complexity Deep Learning Models for Ionospheric Layer Detection

Mirela Fetescu (Joanneum Research & Graz University of Technology, Austria); Karin Plimon (Joanneum Research, Austria); Martin Winter (JOANNEUM RESEARCH Forschungsgesellschaft mbH, Austria); Carlo Scotto (Istituto Nazionale di Geofisica e Vulcanologia, Italy); Bruno Nava (International Centre for Theoretical Physics (ICTP), Italy); Miquel Garcia-Fernandez and Sergi Sanchez (Rokubun, Spain); Johannes Ebert (Joanneum Research, Austria); Franz Teschl (Graz University of Technology, Austria); Raul Orus Perez (European Space Agency (ESA) / ESTEC, The Netherlands)
The ionosphere is a crucial region of Earth's atmosphere for radio communication and satellite navigation. Instruments like ionosondes monitor this region and produce ionograms depicting the ionospheric layers. Although automated ionogram scaling tools exist, they often require manual intervention. Recent advancements in deep learning, have shown promise in automating ionogram analysis with improved accuracy. However, challenges persist in detecting several ionospheric layers simultaneously and across diverse datasets. This paper compares a traditional U-net with a less complex Convolutional Neural Network architecture and evaluates the performance on a diverse ionogram database covering various sources, locations and periods within the solar cycle. The proposed method is compared to existing deep learning approaches and shows competitive performance in intersection over union (IoU) and recall metrics.

11:30 Modelling Specular and Non-Specular Propagation Components for Statistical Analysis of Clutter Loss in G2S Links

Francesco Capelletti and Carlo Riva (Politecnico di Milano, Italy); Vittorio Degli-Esposti and Nicolò Cenni (University of Bologna, Italy); Laura Resteghini (Huawei Technologies, European Research Center, Italy)
A comprehensive methodology is proposed for modelling specular and non-specular propagation components within the framework of statistical evaluation of clutter loss in Ground-to-Satellite (G2S) links. The approach, which is physically consistent, aims at developing an effective reflection coefficient that inherently accounts for both propagation phenomena, evaluated in the direction of the satellite. The methodology is shown through a reference study case, detailing the underlying assumptions and distinguishing between different wave polarizations. The proposed approach can be directly incorporated into a well-assessed stochastic simulator for the prediction of the clutter loss in G2S links, thereby improving its accuracy, particularly at frequencies that may be exploited by incumbent terrestrial networks.

WEDNESDAY

Chairs: Sean V Hum (University of Toronto, Canada), David S Prinsloo (ASTRON & Netherlands Institute for Radio Astronomy, The Netherlands)

10:10 Modelling Large Radio Telescope Visibilities Including Array Mutual Coupling Effects

Oscar OHara, Quentin Gueuning, Eloy de Lera Acedo, Fred Dulwich, Dominic Anstey and John Cumner (University of Cambridge, United Kingdom); Anthony Keith Brown (University of Manchester, United Kingdom); Andrew Faulkner and Yuchen Liu (University of Cambridge, United Kingdom)

Radio telescopes composed of phased arrays, called stations, produce visibilities by cross-correlating signals of beamformed antenna voltages from each station. For large telescopes with many stations, accurately modelling visibilities presents computational challenges due to the need for full-wave simulations of each antenna's electromagnetic response, including Mutual Coupling (MC) effects, and the evaluation of array patterns across many directions and frequencies. This paper leverages two in-house tools: the Fast Array Simulation Tool for rapid electromagnetic simulations and the OSKAR simulator for parallelized interferometric computations. For the first time, we analyze the impact of intra-station MC on the visibility time-delay impulse response across different station layouts, focusing on the 224 core stations of the Square Kilometre Array Low telescope. We show that MC significantly broadens the delay spread of instrument response, creating a key limitation for 21-cm science experiments while offering new insights into challenges posed by MC in large-scale radio telescopes.

10:30 A 3D Printed Quad-Ridged Flared Horn Antenna Feeder for Radio-Telescopes

Leonidas Marantis (University of Piraeus, Greece); Andreas Hofmann (University of Erlangen-Nuremberg, Germany); Vasileios Spanakis-Misirlis and Yorgos Stratakos (University of Piraeus, Greece); Danti Khouri (Golden Devices GmbH, Germany); Athanasios G. Kanatas (University of Piraeus, Greece)

This study proposes a 3D-printed, quad-ridged, dual-pol, flared horn antenna feeder to meet the demands of a modern radio-telescope. The research work presented in this paper involves both the theoretical and the customized / adapted mechanical design of the proposed horn antenna, as well as a description of the 3D-printing and coating process. The slotted waveguide approach is followed for perfectly homogeneous coating. Additional mechanical adaptions (i.e. optimized feed section, radome) are employed to provide realistic simulation results. The proposed antenna offers a dual polarization capability and an attractive radiation beam to properly illuminate a 6m mesh dish reflector. A satisfying impedance matching from 1-3 GHz is achieved in both polarizations while maintaining an excellent isolation between the two N-type ports. Reflection coefficient and radiation pattern simulation results are presented, derived from the theoretical and the adapted mechanical design, exhibiting a close agreement.

10:50 Applications of Reflectarray Technology for Radio Astronomy Interference Mitigation

Fatemeh Sadr (Virginia Tech, USA); Nan-Rong Hui (University of Toronto, Canada); Jordan Budhu (Virginia Tech, USA); Sean V Hum (University of Toronto, Canada); Steven Ellingson (Virginia Tech, USA)

High-gain reflector antennas commonly used to make observations in radio astronomy are especially susceptible to the reception of undesirable radiation through their sidelobes. One source of this radiation is megaconstellations associated with satellite based communications systems. In this paper, we present some recent advances in the application of reflectarrays for mitigation of interference from these megaconstellations. By placing a reflectarray along the rim of a reflector and thereby repurposing reflections to generate destructive interference to unwanted incoming radiation, interference can be nulled. The first example is a dual band reflectarray capable of producing a null to track interference throughout the sidelobe envelope in two frequency bands associated with Iridium and Starlink satellite systems. The second example is a proof-of-concept demonstration utilizing a C-band planar reflectarray of which the elements along its perimeter are made reconfigurable. Both examples point to the possibility of utilizing reflectarrays for radio astronomy interference mitigation.

11:10 300-800 MHz LNA-Integrated Log-Periodic Dipole Antenna for BURSTT

Chau-Ching Chiong and Chen Chien (Academia Sinica, Taiwan); Chao-Te Li (Institute of Astronomy and Astrophysics, Academia Sinica, Taiwan)

BURSTT (Bustling Universe Radio Survey Telescope in Taiwan) is an array antenna in Taiwan for detecting and localizing Fast Radio Bursts (FRBs). To increase its detection probability, system with wide field of view (FoV), wide bandwidth, and high sensitivity is required. To address these demands, a log-periodic dipole antenna covering 300 to 800 MHz is designed and fabricated. The antenna is with ~8 dB gain and beamwidth of 60- and 90-degree for E- and H-plane, respectively. Furthermore, the LNA is placed at the feed point of the antenna to maximize the system sensitivity. Improvement was confirmed by measuring on-sky system equivalent flux density (SEFD)

WEDNESDAY

11:30 Fast Multi-Dimensional Feed Optimization on Reflector Antennas Using a Reference Design

Dirk de Villiers and Mariet Venter (Stellenbosch University, South Africa)

We present a fast method for optimizing a feed antenna on a reflector system, leveraging a known reference reflector system design. The method uses the optimum feed parameters of the reference reflector, determined by a specific goal function, as the starting point of the optimization. This ensures exploration in a favorable region of the parameter space. Difference patterns between the two reflectors are utilized, in a Characteristic Basis Function Pattern (CBFP) interpolation framework, to estimate the radiation patterns of the desired reflector system within the design region, requiring a minimum amount of electromagnetic simulations. A practical example within a high-dimensional parameter space is provided to demonstrate the power of the method.

Room: Schelkunoff (C1)

CS51b - Physics assisted learning and inversion strategies for electromagnetic imaging

T07 Electromagnetic modelling and simulation tools / Convened Session / Electromagnetics

Chairs: Martina Teresa Bevacqua (Università Mediterranea di Reggio Calabria, Italy), Rosa Scapaticci (CNR-National Research Council of Italy, Italy)

10:10 Multi-Frequency Microwave Imaging Inspection for Industrial Food Quality Assessment

Calin I Maraloiu, Jorge Tobon and Marco Ricci (Politecnico di Torino, Italy); Lorenzo Crocco (CNR - National Research Council of Italy, Italy); Francesca Vipiana (Politecnico di Torino, Italy)

Progressive automation and throughput scaling are essential for the economic development and robustness of a productive food manufacturing company. Reliable scanning verification technologies must be put in place to ensure products quality and conformity. Due to the impressive yield of highspeed production lines, possible and undesirable malfunctionings may irreversibly alter the compliance of some of the fabricated samples, by contaminating them with foreign intrusions. In this paper, we propose the use of microwave imaging as a novel exploitable strategy, complementary to other well-established technologies, to sense foreign intrusions inside food products. The examined setup is made of a set of printed monopole antennas mounted on a 3D printed arch, which suits the placement on production chain conveyor belts. Foreign body reconstructions for an oil-filled jar, scanned in a fixed position, have been obtained in the frequency range 9 – 10 GHz. The impact of mathematical multi-frequency approaches is explored.

10:30 Recent Advances in Physics-Assisted Inverse Scattering

Luca Tosi (ELEDIA Research Center, Italy); Lorenzo Poli (ELEDIA Research Center, University of Trento, Italy); Paolo Rocca (University of Trento & ELEDIA Research Center, Italy); Marco Salucci (ELEDIA Research Center, Italy); Andrea Massa (University of Trento, Italy)

An innovative physics-assisted methodology for quantitative microwave inverse scattering (IS) is presented. In this context, the System-by-Design (SbD) paradigm is employed, jointly with the exploitation of space and time priors, to regularize the imaging procedure and reduce the ill-posedness of the inverse problem at hand. An illustrative example, concerned with brain stroke imaging, is reported to assess the effectiveness of the proposed method.

10:50 Optimization Strategy to Design Rotating Non-Local Meta-Deflectors for Risley-Prism Antenna Systems

Ayoub Bellouch (University Cote d'Azur, INRIA, CNRS, France); Mahmoud Elsawy (Université Côte d'Azur, Inria, CNRS, France); Stéphane Lanteri (INRIA - Sophia Antipolis, France); Erika Vandelle and Thi Quynh Van Hoang (Thales Research & Technology, France)

A new advanced optimization strategy is proposed to design high-performance rotating deflectors used in Risley-Prism concept for low-profile 2D-beam-steering-antenna system at Ka-band. This new methodology combines two important ingredients: (1) the non-local near-field effect generated by the interactions among adjacent sub-wavelength metasurfaces and (2) a Bayesian learning-based global optimization algorithm for deriving the geometrical characteristics of the constituting dielectric pillars, driven by a design objective. This optimization strategy delivers superior performance compared to the traditional global optimization algorithms and requires fewer solver calls. In this scenario, the meta-deflector is specifically designed to operate effectively for all rotation angles between 0° and 90°. The proposed solution provides remarkable performance across the entire Ka-band. Moreover, the numerical results show multiple advantages, mainly in enhancing transmission efficiency in the desired diffraction order and eliminating the cross-polarization.

11:10 Towards Uncertainty Estimation in Microwave Imaging Using Latent Space Analysis

Ben J Martin, Keeley Narendra, Colin Gilmore and Ian Jeffrey (University of Manitoba, Canada)

We present two methods using the latent space encoding of a trained data-to-image microwave imaging deep learning network to asses the certainty of network output. In Method 1, Kernel Density Estimation is applied to the latent vectors corresponding to the training set to obtain a probability density function. The value of the density function for a given test example is shown to have a relatively strong correlation with target reconstruction accuracy. In Method 2, the true absolute error in training predictions from the K nearest latent vectors in the training set to the latent vector of the test example are combined to produce an uncertainty map for the test prediction. Results demonstrate that the distribution of training examples in the latent space can provide a measure of confidence in imaging results.

WEDNESDAY

11:30 An Improved Virtual Experiments Based Linear Inversion for 2D Inverse Scattering

Martina Teresa Bevacqua (Università Mediterranea di Reggio Calabria, Italy); Tommaso Isernia (University of Reggio Calabria, Italy); Loreto Di Donato (University of Catania, Italy)

In this contribution the Virtual Experiments (VEs) paradigm as applied to inverse scattering problems, for 2D scalar field case, is addressed to show its actual possibilities and limitations. Recent analytical findings allow also to improve the imaging cabalities of a linear inverse approach based on VEs with comparable accuracy performance with respect to full non linear, and hence more computational burden, microwave imaging stretegies. A preliminary numerical test against simulated 2D geometry is given to support the proposed strategy.

Room: Maxwell (C2)

CS66 - AMTA Special-Session on Advanced Robotic Antenna Measurements

T08 Fundamental research and emerging technologies/processes / Convened Session / Measurements

Chairs: Stuart F Gregson (Queen Mary, University of London, United Kingdom), Dennis Lewis (Boeing, USA)

10:10 Ultrawideband Millimeterwave Robotic Antenna Measurements Enabled by FMCW Radar Sensors

Kristof Dausien and Tobias Körner (Ruhr University Bochum, Germany); Christian Schulz (Ruhr-Universität Bochum, Germany); Nils Pohl (Ruhr-University Bochum & Fraunhofer FHR, Germany); Ilona Rolfes and Jan Barowski (Ruhr-Universität Bochum, Germany)

In this paper ultrawideband frequency modulated continuous wave (FMCW) radar sensors in D-band are used to provide a coherent (magnitude and phase) measurement of an antenna pattern. The antenna under test (AUT) is mounted on the radar sensor using a standard waveguide flange. Due to the compactness of the sensor and its integrated signal source, it is easily moveable by robotic plattforms. Only an ethernet connection to a host PC is required, strongly simplifying cable handling on the robot. The coherent pattern measurement is enabled by performing radar echo measurements (in reflection) onto a probe antenna. A switchable load at the probe antenna feed is utilized to improve the dynamic range and to remove undesired environmental reflections by performing a differential measurement.

10:30 Use of Compressive Sensing Techniques for the Rapid Production Test of Commercial Nose-Mounted Radomes in a Robotic Antenna Measurement System

Stuart F Gregson (Queen Mary, University of London, United Kingdom); Clive Parini (Queen Mary University of London, United Kingdom)

The recent trend towards implementing antenna measurement ranges employing multi-axis robotic positioners that provide a near limitless degree of flexibility in terms of measurement types admits possibilities that go far beyond the requirements of classical antenna measurement systems. One recent example involves the use of a dual robotic antenna measurement system for the near-field test and measurement of commercial nose-mounted radomes. Such measurements typically involve extended measurement times due to the need to acquire two-dimensional near-field data to obtain the asymptotic far-fields. This paper introduces a new approach for the production test and verification of commercial nose-mounted radomes that uses a total difference based, sparse sampling technique that aims to accelerate the measurement process to drastically cut the requisite test time. The algorithm is introduced, simulated results are presented, where far-field results are obtained from as few as 2% of the points required by a classical spherical near-field measurement.

10:50 Increased Efficiency in Planar Near-Field Scanning Using Combined Multi-Robot Motion

Benjamin L Moser (National Institute of Standards and Technology, USA); Joshua Gordon (US National Institute of Standards and Technology, USA); Andrew J Petruska (Colorado School of Mines, USA)

Robotic antenna ranges are highly configurable, but traditional pose-selection methods do not utilize the collaborative motion capabilities presented by these positioners. We present methods to reduce planar scan measurement time on robotic antenna ranges with redundant actuation. The inverse kinematics problem is formulated as a general optimization problem to solve for a relative Antenna-Probe transform using all controllable joints of the positioning system. A secondary objective is introduced to minimize velocity-weighted joint excursion, and resultant poses are ordered to minimize motion time using a Travelling Salesman Problem heuristic. This approach is validated using experimental planar measurements collected at the WR62 band using the Large Antenna Positioning System robotic antenna range. Compared to traditional pose-selection, combined motion reduced required scan volume by 49.9% and motion time by 19.7% and 20.5% for standard and TSP pose ordering, respectively. A maximum pattern difference of -38.9dB was found between the transformed far-field patterns

11:10 6G OTA Measurements at Sub-THz Band Using a Compact Robotic System

Asad Husein, Kimmo Rasilainen, Juha-Pekka Mäkelä, Aarno Pärssinen and Marko E Leinonen (University of Oulu, Finland)
As development in the sub-THz band (100-300 GHz) for antenna designs, specifically towards radio systems for potential sixth generation (6G) wireless communications is progressing, accurate characterisation of these complex antennas requires more sophisticated measurement setups. Robotic scanning systems have ushered in configurability to the measurement setups; however industrial sized robots cannot be accommodated in a lab environment for R&D measurements. Compact robots will be required to conduct over-the-air (OTA) performance measurements for 6G radios. Such a measurement system is now being developed at the University of Oulu to complement our measurement capabilities. Initially, the system has been characterised to perform sub-THz far-field (FF) OTA measurements. The E-and H-plane co-polar patterns are determined using the measurement setup and compared to electromagnetic (EM) and planar near-field (NF) measurements illustrating good matching of the main and side lobes at 110-170 GHz band, thereby validating the performance of the developed robotic measurement system.

11:30 Numerical Analysis of Positioning Errors in Irregular Near-Field Antenna Measurements Using Robot-Based Systems

Henrik Jansen and Dirk Heberling (RWTH Aachen University, Germany)
Robotic positioning systems have a wide range of applications in antenna measurements due to their high flexibility and configurability. One application are spherical nearfield antenna measurements, where robotic systems enable the efficient implementation of irregular sampling grids to reduce the measurement time among others. However, the absolute positioning uncertainty of industrial robots is usually larger than the uncertainty for traditional antenna positioning systems, and is characterized in Cartesian space rather than the spherical domain. Therefore, a careful analysis of the measurement uncertainty due to the positioning errors is required. Here, a simulation framework is presented, which can be used to analyze the uncertainty for an antenna measurement due to Cartesian positioning errors. It is shown that the sampling grid type, oversampling ratio, and measurement radius affect the measurement error and uncertainty. Furthermore, a relation between the maximum positioning error and the error in the reconstructed far-field pattern is established.

Room: Oliner (C3)

CS25b - Advances in Reconfigurable Antennas for Communication, Localization and Sensing Applications

T07 Electromagnetic modelling and simulation tools / Convened Session / Antennas

Chairs: Christophe Fumeaux (University of Queensland, Australia), Leonardo Lizzi (University of Trento, Italy)

10:10 Enabling UWB Antenna Polarization Diversity Through a Switchable Feeding Network

Francesco Positano (Université Côte d'Azur, LEAT, CNRS, France); Leonardo Lizzi (University of Trento, Italy)
This paper presents the design of a switchable feeding network that enables polarization diversity in an ultra-wideband (UWB) antenna. The feeding network is built around a tunable quasi-lumped coupler and a Single-Pole Dual-Through (SPDT) switch. The integrated system, which combines the feeding network and the UWB antenna, supports four distinct polarization states: two circular and two linear.

10:30 Reconfigurable Mushroom-Based Metasurface Antenna for Continuous Beam Steering

Talha Arshed (University of Siena, Italy); Joaquín García Fernández (WAVE UP SRL & University of Siena, Italy); Francesco Caminita (Wave-Up SRL, Italy); Cristian Della Giovampaola (Wave Up srl, Italy); Stefano Maci and Enrica Martini (University of Siena, Italy)
We present reconfigurable metasurface (MTS)-based leaky wave antenna (LWA) that achieves continuous angular scanning through broadside at a fixed frequency in the millimeter-wave (mmWave) range. The proposed LWA uses a mushroom structure integrated with voltage-controlled varactors to achieve tunability. The mushroom configuration is chosen to ease the accommodation of biasing lines, which can be cumbersome at mmWave frequencies. The desired radiation pattern and suppression of the open stopband (OSB) at broadside, essential for achieving continuous beam scanning, are achieved through a proper design of the impedance modulation. Since this approach relies on a precise modeling of the equivalent impedance, we investigate two types of impedance boundary condition (IBC) models. Based on the insights provided by this study, a reconfigurable LWA is designed and numerically analyzed, demonstrating continuous beam scanning and effective OSB suppression. The results highlight the potential of impedance-based design techniques and provide valuable insights for advancing reconfigurable.

10:50 Varactor Based Reconfigurable Reflectarray Antenna at Ka-Band

Armin Fischer (Fraunhofer IIS, Germany); Christian Steinmetz (Fraunhofer Institute for Integrated Circuits (IIS), Germany); Hans Adel (Fraunhofer Institute for Integrated Circuits IIS, Germany)
This paper presents a manufactured electronically reconfigurable offset feed reflectarray antenna at 25 GHz. The reflective surface consist of 144 elements arranged in a 12 by 12 rectangular grid. Each element is constructed from two patch halves that are tuned by a varactor diode placed in between. Simulations show a phase tuning range of 315° at center frequency. As feed, an horn antenna is placed at a distance of 99mm at an offset angle of 30°. Measurement results of the prototype show a maximum scanning loss of 4.5 dB for beam steering from -60° to 60° in horizontal plane. In the opposite angular direction of the feed, the steered beams experience degradation due to the presence of specular reflections. Furthermore, a reflecting surface loss of smaller than 2 dB and an usable 3 dB-bandwidth of 12% are determined.

11:10 A Dual Channel Switched-Beam Yagi-Uda Array for mm-Wave Wireless Sensing and Communication

Ectis Velazquez, Jr, Murat Yuksel and Xun Gong (University of Central Florida, USA)
A Yagi-Uda array is proposed for dual channel mm-Wave wireless sensing and communications. The array is composed of four Yagi-Uda antenna elements, each with a driven dipole and a ground plane reflector. The array is reconfigurable and employs a switched-beam architecture which has the capability to have two signals transmitted and/or received at once. This design establishes 360 ◦ coverage in the azimuth plane with 5 dBi gain from each antenna element. When used as part of a wireless system it can enhance capabilities with simultaneous sensing and data transmission.

11:30 Physics-Informed Graph Neural Networks for the Inverse Design of GHz Reconfigurable Antenna

Cindy Pan, Naveen Verma and James C. Sturm (Princeton University, USA)
Reconfigurable antennas, as a subclass of metasurfaces, offer innovative and dynamic capabilities for wireless communication systems. Specifically, enabling radiation pattern reconfigurability allows for flexible beam steering through reverse-engineering of antenna parameters such as surface current distributions. In this work, we present a physics-informed machine learning model, leveraging fundamental physics such as Kirchhoff's current Law, to predict the switch configurations of 2-dimensional antenna arrays. We utilize a graph neural network (GNN) to effectively capture the spatial relationships between radio-frequency (RF) switches and antenna patches, closely emulating the antenna topology. Simulation results demonstrate that our approach successfully predicts switch configurations needed to generate complex far-field radiation patterns.

Room: Kraus (C4)

CS24b - Quantum Electromagnetics - From Photonics to Quantum Computing

T08 Fundamental research and emerging technologies/processes / Convened Session / Electromagnetics

Chairs: Gabriele Gradoni (University of Surrey, United Kingdom), Zhen Peng (University of Illinois at Urbana-Champaign, USA)

10:10 Quantum Theory of Light in Photonic Time Crystals

Mohammad Sajjad Mirmoosa (University of Eastern Finland, Finland); Iñigo Liberal (Public University of Navarre, Spain)
Photonic time crystals are exotic materials characterized by effective parameters that are uniform in space yet periodically vary over time. Recently, these materials have been the subject of extensive study from both theoretical and experimental perspectives. However, the quantum characteristics of light within photonic time crystals remain largely uncharted territory. In this presentation, we explore the interaction of light with these materials through the lens of quantum optics, addressing various topics ranging from mode operator transformation to the photon statistics of light in photonic time crystals.

10:30 An S-Matrix Formalism for Nonclassical Optical Response from Multiple Plasmonic Spheres

Xin Zheng (KU Leuven, Belgium); Guy Vandenbosch (Katholieke Universiteit Leuven (KU Leuven), Belgium); Xuezhi Zheng (Katholieke Universiteit Leuven, Belgium)
In this paper, we present a computational method coping with the nonclassical optical response from multiple spherical nanoparticles (NPs) each of which can have multiple non-concentric cores. Each NP can be made of dielectrics and metals. The electromagnetic (EM) properties of the metals are described by the nonlocal hydrodynamic model (NLHDM) and its variant, the generalized optical response (GNOR) model. The main equation behind the method is listed by detailing (1) the evaluation of the S-matrix for each individual NP and (2) the interactions between the NPs. Then, the proposed method is tested for a core-shell structure which is a spherical NP with two spherical cores. The obtained absorption cross sections and near field at a cut through the core-shell are compared to the ones from an in-house boundary element method (BEM) solver, where a good agreement is seen.

10:50 Plasmon Resonance Radiation Conductance Enhancement of 2-D Luneburg Lens Antenna Equipped with Conformal Graphene Strip

Iryna O. Mikhailikova (V. N. Karazin Kharkiv National University, Ukraine); Sergii V. Dukhopelnykov (Institute of Radio-Physics and Electronics NAS Ukraine, Kharkiv & Universite de Rennes 1, Ukraine); Mario Lucido (University of Cassino and Southern Lazio, Italy)
We consider the electromagnetic wave radiation characteristics of a layered cylindrical Luneburg lens equipped with a conformal strip of graphene, in the H-polarization case. The angular width of the strip is arbitrary and its surface impedance is characterized with the aid of the quantum-physics Kubo formalism. We use mathematically accurate full-wave analytical regularization technique, which is based on the hypersingular integral equation and Nystrom type discretization. This guarantees the convergence of the resulting numerical algorithm. We compute the radiation and absorption power of a microsize lens as a function of the frequency in wide range up to 20 THz. This analysis shows that a graphene strip, placed into the focal area of the Luneburg lens, enhances its radiation resistance at the resonance frequency proportionally to the quality factor of the plasmon mode of the strip.

WEDNESDAY

11:10 Symbolic-Numeric Co-Simulation of Josephson Traveling-Wave Parametric Amplifiers

Michael Haider, Yongjie Yuan, Johannes Stowasser and Lukas Seitner (Technical University of Munich, Germany); Samuel T. Elkin and Thomas E. Roth (Purdue University, USA); Christian Jirauschek (Technical University of Munich, Germany)

Analytic solutions fail to accurately predict the gain and added quantum noise in traveling-wave parametric amplifiers for large signal amplitudes. Thus, the underlying system Hamiltonian needs to be extended to include more and more modes in order to describe effects such as spectral leakage. For a sufficiently complex Hamiltonian, the procedure of deriving the Heisenberg equations of motion for each mode is tedious or even prohibitive. Therefore, we present a symbolic-numeric co-simulation approach, where the equations of motion are automatically derived from a given Hamiltonian using a modern computer algebra system. The resulting equations of motion can be solved numerically. We verified our approach using existing analytic and numeric solutions from the literature and found good agreement. Additionally, we simulate an amplifier from the literature, where the pump mode experiences substrate losses beyond the stiff pump approximation.

11:30 Quantum Phenomena in Space- and Time-Metamaterials

Andrea Alù (CUNY Advanced Science Research Center, USA)

In this talk, I will review our latest progress towards the theoretical understanding and experimental demonstration of quantum phenomena in metamaterials and metasurfaces, leveraging both spatial and temporal interfaces. I will discuss in particular two areas of recent interest in my group: the use of quantum engineered and polaritonic materials to realize giant nonlinearities at the nanoscale, demonstrating wave mixing, upconversion, limiting and entangled photon generation based on spontaneous parametric down-conversion, and the role of quantum phenomena at time interfaces for the manipulation of photon-photon interactions. Quantum has a dual role in metamaterial design, it enables the realization of new material responses at the basis of technological breakthroughs, and can provide a new playground for metamaterial phenomena.

Room: Munch (23)

EurAPP Working Groups

WG WIAP

Room: Ørsted (24+25)

CS2b - Emerging Electromagnetic Solutions for Non-Terrestrial Networks

T03 Aerospace, space and non-terrestrial networks / Convened Session / Antennas

Chairs: Aakash Bansal (Loughborough University, United Kingdom), William Whittow (Loughborough University, United Kingdom)

10:10 Hybrid Three-Hole Double-Layer EBG Structure for E-Band Waveguide-To-PCB Interfaces

Hairu Wang and Mingzheng Chen (KTH Royal Institute of Technology, Sweden); Nevena Saponjic and Maria Carolina Vigano (Viasat Antenna Systems SA, Switzerland); Oscar Quevedo-Teruel (KTH Royal Institute of Technology, Sweden)

In this paper, we present a hybrid electromagnetic bandgap (EBG) structure based on a three-hole double-layer configuration. One layer of the EBG structure is positioned on the metal, while the other is on the printed circuit board (PCB). Dispersion analyses reveal that this new compact hybrid EBG could produce a wide stopband with high in-band attenuation. To evaluate its effectiveness in mitigating signal leakage at waveguide-to-PCB interfaces and its potential application in next-generation satellite communications (SatComs), we designed two EBG structures specifically for low-Earth orbit and geosynchronous orbit SatCom hybrid array antennas within the E-band (71-86 GHz). The performance of these EBG structures is evaluated in the configuration of 4 * 4 hybrid arrays. We demonstrate that the proposed hybrid EBG structures can effectively enhance power transmission and significantly reduce mutual coupling in the waveguide-to-PCB interfaces.

10:30 Transmissive Metasurface for Satcom Applications

Muhammad Muneeb Arshad (National University of Sciences and Technology, NUST, Islamabad, Pakistan); Muhammad Noman and Mirza Shujaat Ali (University of Glasgow, United Kingdom); Hattan F. Abutarboush (Taibah University & Communications and Electronics Engineering, Saudi Arabia); Farooq A Tahir and Qammer Abbasi (University of Glasgow, United Kingdom)

Circular Dichroism (CD) in electromagnetic waves offers significant potential for advancing various scientific and technological fields. This study presents a novel approach using a C-shaped transmissive chiral metasurface, engineered to achieve exceptional efficiency in circular dichroism within the X-band frequency range. The metasurface demonstrates outstanding selectivity for Left-Hand Circularly Polarized (LHCP) and Right-Hand Circularly Polarized (RHCP) incident waves, featuring enhanced bandwidth and a strong CD of 68.3%. With a thickness of 0.8 mm and built on an FR-4 substrate, the metasurface is optimized for high selectivity toward LHCP and RHCP waves, representing a significant advancement in the study of circular dichroism. By seamlessly combining theoretical innovation with practical application, this research not only extends the boundaries of metamaterial design but also paves the way for diverse applications across various scientific disciplines, including satellite communication, stealth technology, and antenna design, etc.

10:50 Fully Metallic Dual-Band Reflectarray Antenna for Satellite Communications

Dayan Pérez-Quintana (University of Siena (UNISI) & Institute of Smart Cities (ISC), Italy); Massimo Nannetti (Wave Up Srl, Italy); Francesco Caminita (Wave-Up SRL, Italy); Giovanni Toso (European Space Agency, ESA ESTEC, The Netherlands); Enrica Martini (University of Siena, Italy)

This study presents the design of a fully metallic corrugated flat reflector for satellite communication applications. From a microscale optical perspective, the corrugated reflector is composed of a set of three-dimensional, fully metallic unit cells. The innovation of this research lies in utilizing the geometrical phase principle, which enables the unit cell to independently control the phase of the reflection coefficient across two distinct frequency bands, namely 20 GHz and 30 GHz, while ensuring high polarization purity. The proposed unit cell not only achieves complete independence between both frequencies but also exhibits low losses over a bandwidth exceeding 1 GHz. The final design was numerically analyzed with a corrugated reflector 18 wavelengths in diameter. The excellent results obtained demonstrate the validity and efficiency of the unit cell. This approach offers a promising solution for enhancing the performance of reflectarrays in advanced satellite communication systems.

11:10 A Novel Ku-Band Reflectarray Antenna Design Enabled by Stereolithography

Irsat Gulen (University of Birmingham, United Kingdom); Evangelos Vassos (University of Huddersfield, United Kingdom); Panagiotis Ioannis Theoharis (University of Wollongong, Australia); Thomas Whittaker and William Whittow (Loughborough University, United Kingdom); Alexandros Feresidis (University of Birmingham, United Kingdom)

A novel reflectarray antenna design enabled by stereolithography operating at Ku-band is presented. The proposed fully metalised 3-D unit cells feature multiple-layer cuboid elements attached to a ground plane through metallic vias. By varying the number of layers, the sizes of the elements of each layer, and the diameter of the vias, the required phase response is achieved, along with low reflection losses. Another benefit of the variable layer design is the engineered phase response over the frequency range of 13 to 17 GHz, which can lead to broad bandwidth reflectarray designs. At the centre frequency of 15 GHz, simulation in CST Microwave Studio demonstrates that the proposed reflectarray antenna achieves a directivity of approximately 25 dBi.

11:30 Hybrid Analogue-Digital Beamforming for Non Terrestrial Networks

Piero Angeletti (European Space Agency, The Netherlands); Giovanni Toso (European Space Agency, ESA ESTEC, The Netherlands); Daniele Petrolati (ESA ESTEC, European Space Agency, The Netherlands

The paper describes active array antennas and beamforming networks (BFN) exploiting a two level analogue-digital beamforming scheme to reduce the complexity of conventional active arrays based on a fully analogue or a fully digital beamforming. Fully digital BFNs represent the ideal solution for meeting the challenging reconfigurability requirements of satellite operators, however the key drawback of these solutions is related to the complexity of the digital BFN implementation, requiring often unaffordable mass and power consumption/dissipation resources. In order to combine the advantages of both analogue and digital beamforming schemes, hybrid active antennas have been introduced. Direct radiating arrays with hybrid beamforming adopt two or more levels of beamforming: one being analogue and the other one digital. While active antennas based on hybrid beamforming schemes have been significantly used for ground systems, only recently they have been considered for satellite systems

Room: Mosig (26)

Scientific Working

SW6b - Innovative Techniques to Improve Measurement Accuracy

Room: Collin (27)

M05b - Recent advances in antenna measurement and over the air testing

T01 Sub-6 GHz for terrestrial networks (5G/6G) / / Measurements

Chairs: Samel Arslanagić (Technical University of Denmark, Denmark), Matthias Hein (Technische Universität Ilmenau, Germany)

10:10 On the Use of CVRP to Diagnose Faulty Elements in Antenna Arrays

Alejandro Antón Ruiz (University of Twente, The Netherlands); John Kvarnstrand and Klas Arvidsson (Bluetest AB, Sweden); Andrés Alayón Glazunov (Linköping University, Sweden)

This paper investigates the application of Constrained-View Radiated Power (CVRP) for diagnosing phased array element failures, specifically focusing on on-off element failure. CVRP, similar to Partial Radiated Power (PRP), considers a specific Field-of-View (FoV) but normalizes it by the FoV area. The study explores CVRP's effectiveness in detecting failures in a 2x8 cosine element array under beam-steering conditions, accounting for random and depointing errors, angular resolution, and pattern rotation. Results indicate that CVRP can detect on-off failures based on angular resolution and error severity. Additionally, CVRP is effective with partial far-field patterns, making it suitable for near-field, indirect, and far-field measurement systems without requiring phase acquisition.

10:30 Impact of Multi-Probe Beamwidth on Spatial Correlation Simulation in a Large-Sized Test Zone of MIMO OTA Setup

Xiaolong Liu (China Academy of Information and Communications Technology, China); Xiaohang Yang (CAICT, China); Hao Sun (China Academy of Information and Telecommunications Technology, China); Lei Li (China Academy of Information and Communications Technology, China)

With the continuous development of new wireless communication technologies, the demand for wireless communication performance testing of large-volume devices is increasing. To address the performance testing issues for large-sized wireless communication devices, this paper presents a feasible Multiple-Input Multiple-Output (MIMO) Over-The-Air (OTA) performance testing system design and focuses on analyzing the impact of the anechoic chamber's multi-probe antenna beamwidth on the spatial correlation error within the large test zone. The closed-form expression of spatial correlation has been reformulated with the multi-probe Anechoic Chamber (MPAC) method by taking into account the radiation pattern of the probes. Based on the above expression, this paper proposes a spatial correlation simulation scheme for multi-probe antenna beamwidth parameter selection in typical frequency bands for 4G and 5G. Through extensive simulations, the requirements for the beamwidth of probe antenna across various frequencies have been ultimately determined with a test zone diameter from 0.2 to 4m.

10:50 Effect of Antenna Offsets in Elevation on the Bi-Static Radar Scattering of Bicyclists

Isabella B. Varga, Willi Hofmann and Matthias Hein (Technische Universität Ilmenau, Germany)

Automated and connected driving technologies enable a safer and more efficient road traffic, with radar sensors for environmental monitoring as one key element. Besides monostatic radar, bi-static radar sensing offers great potential for increasing the radar visibility of vulnerable road users. In this study, bi-static radar measurements of a bicyclist dummy conforming to the New Car Assessment Programme were performed in the frequency range between 2 GHz and 18 GHz. A spherical measurement system was used to illuminate the target from different bi-static angles and different elevation angles, in order to study the differences in RCS. In view of different mounting positions of radar sensors, the emphasis was on the elevation angle. The RCS-values varied by up to 23 dB compared to the antennas mounted at the same height. The results demonstrate the importance of considering the elevation angle and the need to extend current research to fully three-dimensional characterization.

11:10 Compensation of Gravity Bending of MetOp-SG On-Ground Calibration Measurements

Javier Fernández Álvarez, Jeppe Nielsen, Michael Mattes and Samel Arslanagić (Technical University of Denmark, Denmark)

The calibration of the MetOp-SG SAS instruments involves mounting very heavy antennas in a roll-over-azimuth positioner. The weight causes the antenna support structure to bend under gravity; this causes the near-field of the antenna under test (AUT) to be measured in points that are non-uniformly distributed on the measurement sphere. A method to compensate this bending was developed, based on a non-uniform 2D Fast Fourier Transform (FFT) to compute the spectrum of the non-uniformly sampled signals. The near-field in the nominal points is then interpolated from this spectrum, compensating the effect of bending. The algorithm was tested and validated using measured and simulated data of an antenna of similar characteristics as the MetOp-SG instruments, demonstrating its capacity to compensate the effects of bending with negligible error. Subsequently, the method was applied to near-field measurements of the MetOp-SG SAS FM2 campaign performed at the Technical University of Denmark (DTU) during 2022.

11:30 On the Uncertainty in Phase Center Determination for Directive Antennas

Joakim F Johansson (Retired); Per Magnusson (Beyond Gravity Sweden AB, Sweden)

The uncertainty in establishing the "phase center" location in a phase model for directive antennas has been theoretically analyzed and simulated through the Monte Carlo method. The uncertainty is shown to be substantial for antennas with a narrow beamwidth, even though an accurate phase model can be reconstructed.

Wednesday - 12:00-12:40

Room: Alfvén (A3+A4)

Invited Speaker

Joachim Oberhammer

Chair: Nelson Fonseca (Anywaves, France)

Room: Kildal (A2)

Invited Speaker

Miguel Beruete

Chair: Davide Ramaccia (RomaTre University, Italy)

WEDNESDAY

3.33. W-Band Cylindric Dielectric Resonator Antenna on LTCC

Achraf Sadeddine, Myssipsa Mehraz, Francois Gallée and Camilla Kärnfelt (IMT Atlantique Lab-STICC CNRS UMR 6285)
This article presents the design of a cylindrical dielectric resonator antenna (DRA) operating at 100 GHz, specifically optimized for the low-temperature co-fired ceramic (LTCC) manufacturing process. The antenna is designed to support the HE11 mode, validated through modal analysis of field distributions. The LTCC manufacturing process enables precise alignment and stable mechanical attachment of the resonator to the ground plane without the use of adhesives, as the layers form a solid and cohesive structure after firing. Experimental results reveal a 10.8 GHz -10 dB bandwidth with a 2.96 dBi gain obtained at 99.4 GHz, compared to a 6.43 dBi gain found in simulation. The measured bandwidth and performance demonstrate the potential of the antenna for high-frequency applications in the W band.

3.34. A Wideband Rotary Antenna Based on Gap Wavegudie Technology for mmWave Applications

Ali Farahbakhsh (Graduate University of Advanced Technology, Iran); Davood Zarifi and Michal Mrozowski (Gdansk University of Technology, Poland)
This study introduces the design of a gap waveguide-based rotary antenna capable of 360° mechanical beam-steering for wideband mmWave applications. This innovative design overcomes the typical limitations of electronically steerable antennas, such as narrow bandwidth, restricted steering range, gain reduction, and high cost and complexity. The designed rotary antenna achieves a gain of 13.8 dBi without any scan loss across the entire 360° steering range from 45 to 60 GHz. The proposed rotary antenna is a promising candidate for a variety of mmWave mechanical beam scanning systems.

3.35. Design and Analysis of Multi-Beam SIW-Based Hexagonal MIMO Antenna Using Phase and Amplitude Switching Technique

Subhadrita Ghosh and Swarnadipto Ghosh (Indian Institute of Space Science and Technology, Thiruvananthapuram, India); Aakash Bansal (Loughborough University, United Kingdom); Chinmoy Saha (Indian Institute of Space Science and Technology, India & Royal Military College of Canada, Canada); William Whittow (Loughborough University, United Kingdom)
A hexagonal multiple input multiple output (MIMO) antenna architecture based on multi-slot substrate integrated waveguide (SIW) technology is proposed for multi-direction beamforming. For high side lobe level (SLL) reduction, nonlinear statistical probability distribution function (PDF) and rotational factor are incorporated in 1 × 8 slotted SIW structure. The MIMO antenna is structured symmetrically through a multi-folding technique. The detailed characterization of multidirectional multibeams is done by even-odd port tuning technique in both phase and magnitude. An overall reduction of SLL to 15.3 dB and half power beamwidth (HPBW) < 10° makes the beam directive such that the beam scanning in mm-Wave 5G/6G, satellite communication and ground surveillance become more prominent.

3.36. Design of a Mechanically RIS Unit Cell with Prephased States at 26 GHz

Marcos Baena-Molina (University of Granada, Spain); Angel Palomares-Caballero (IETR-INSA Rennes, France); Pablo Padilla (University of Granada, Spain); Juan Valenzuela-Valdés (Universidad de Granada, Spain)
A prephased 1-bit mechanically reconfigurable unit cell for a reconfigurable intelligent surfaces (RIS) is presented. In the proposed RIS unit cell design, a geometric translation of the element has been implemented, obtaining two different pairs of RIS unit cell each with a 1-bit mechanical reconfiguration. The electromagnetic (EM) behavior is analyzed using the reflection coefficient for normal and oblique incidence, demonstrating its suitable operation in the n258 band of 5G. A 10 x 10 mechanically RIS is designed using the two pairs of unit cells and its radiation performance is compared to a conventional 1-bit RIS at 26 GHz. It is shown how a 1-bit configuration with pseudo-randomization for mechanically RIS enhances the radiation pattern performance while maintaining the simplicity of 1-bit reconfiguration.

3.37. Dispersive Analysis of Double-Corrugated Waveguides for Leaky-Wave Applications

Yuhuan Tong (Sorbonne Université, France); Davide Comite (Sapienza University of Rome, Italy); Beatrice Ambrogi (Sapienza University, Italy); Guido Valerio (Sorbonne Université, France)
This paper presents an investigation of dispersive behavior of glide-symmetric parallel-plate waveguides perturbed with the opening of slots on one plate of the waveguide, allowing for radiation of a leaky-wave mode. The radiation features can be predicted by computing the real part (phase constant) and imaginary part (attenuation constant) of the leaky-wave complex wavenumber. A periodic method-of-moment is employed to perform this calculation. We focus here on a parametric study of the attenuation in the open stopband. We perform a comparison between glide-and non-glide-symmetric waveguides, finding different levels of attenuation and stopband bandwidth. The effect of different geometrical parameter is discussed with the aim of increasing or reducing the attenuation in the stopband. The former case can have application to the design of EBGs while the latter to the design of leaky-wave antennas with continuous scanning from backward to forward or with stable radiation at broadside.

3.38. Enabling Integrated Communication and Sensing Using Reflectarray and Orbital Angular Momentum

Ali Ali, Maryam Khodadadi, Atta Ul Quddus and Gabriele Gradoni (University of Surrey, United Kingdom); Mohsen Khalily (University of Surrey & 5G Innovation Centre, Institute for Communication Systems (ICS), United Kingdom)

This paper proposes a novel Integrated Sensing and Communication (ISAC) metasurface designed to operate at 29.5 GHz. It leverages a Reflectarray Antenna (RA) capable of supporting dual functionalities-pencil beamforming for high-speed communication and Orbital Angular Momentum (OAM) beams for precise sensing. The communication aspect employs a pencil beam configuration to achieve high gain focused and directional transmission, while the OAM beam enables enhanced spatial resolution for sensing applications. Extensive simulations and lab measurements validate the superior performance of this single RA system, demonstrating improved gain and beam divergence metrics. This ISAC approach has the potential to significantly reduce system complexity and energy consumption by leveraging a passive antenna design to facilitate both communication and sensing functionalities.

3.39. Feeding Strategies for PCB Based ME Dipole Antennas at D-Band

Adnan Ali, Kimmo Rasilainen, Marko E Leinonen, Aarno Pärssinen and Nuutti Tervo (University of Oulu, Finland)

This study compares two different feed structures for dual-polarized magnetoelectric (ME) dipole antennas intended for D-band (110-170 GHz) applications. The investigated single-ended and differential feed designs are appropriate for next-generation wireless communication systems because they attain a large impedance bandwidth of 42.8%, effectively spanning the whole D-band spectrum. Although the single-ended feed structure exhibits steady gain and uniform radiation patterns throughout the band, its isolation is not ideal, with levels falling as low as -12 dB at certain frequencies. In contrast, the differential feed structure provides improved polarization purity and good isolation, but at the expense of decreased gain stability and weakened radiation patterns, especially at higher frequencies. Critical performance metrics such as S-parameters, gain, isolation, radiation efficiency, and radiation patterns are evaluated for a thorough comparison of these two feeding systems.

3.40. High-Gain Flexible Transparent Screen-Printed Quasi-Yagi Antenna for V-Band Applications

Matthieu Egels (Aix Marseille University, IM2NP, France); Anton Venouil (Aix-Marseille University (AMU), France); Chaouki Hannachi (Aix Marseille University, IM2NP, France); Philippe Pannier (IM2NP, France); Mohammed Benwadih and Christophe Serbutoviez (CEA, France)

In this paper a flexible, V-band Quasi-Yagi Uda antenna is presented. The antenna is implemented on a 100 µm thick Zeonex transparent flexible substrate using a reliable screen-printing process. The antenna design is optimized to operate over 47.2 to 48.2 GHz frequency bands for emerging V-band applications. Measurements and simulations show a good agreement. The maximum measured peak gain is 10.4 dB at 47.2 GHz and the realized gain is higher than 8 dB over the frequency band of interest. A good input impedance matching is achieved in the 46.7 to 49.2 GHz frequency band.The antenna size does not exceed 15 mm by 20 mm. To further decrease the side lobe level in the E-plane, an optimization technique on the ground plane is also proposed as part of this work. The achieved performances demonstrate the feasibility of high-gain screen-printed end-fire antennas on transparent flexible at the millimeter-wave frequency range.

3.41. Liquid Crystal Reconfigurable Leaky-Wave Antenna with Huygens' Metasurface and Gap Waveguide

Tomas Lira-Valdes (Universidad de Malaga, Spain); Pablo Mateos-Ruiz (University of Malaga, Spain); Elena Abdo-Sánchez (University of Málaga & E. T. S. I. Telecomunicación, Spain)

This work presents a reconfigurable leaky-wave antenna based on an Omega-bianisotropic Huygens' metasurface as leaky surface and gap waveguide as guiding structure. The latter is filled by a nematic liquid crystal, which is a tunable dielectric whose particles can be polarized through an external bias voltage. The gap waveguide technology allows for a non-electrical contact feature, which facilitates the connection of the required external bias voltage. The beam radiation angle can be controlled at a fixed frequency by adjusting the relative permittivity of the LC, so that electronical beam steering can be achieved. A design at 20 GHz of a leaky-wave antenna with beam scanning capabilities in the range of approximately [-10°, 10°] with the Merck GT7-29001 LC is accomplished and successfully tested through full-wave simulations.

3.42. Machine Learning Accelerated Passive Electronically Scanned Phased Array Design

James R Henderson (Queen Mary University of London & Plextek, United Kingdom); Yang Hao (Queen Mary University, United Kingdom)

This paper presents a passive approach to electronically scanned millimetre-wave phased arrays. To avoid the need for additional amplification within the phased array, low-loss phase shifters that exhibit minimal amplitude variation are required. To achieve this, specific low-resolution switched-line phase shifters have been designed to meet the phase requirements of individual elements, avoiding supporting unused phase states associated with high-resolution phase shifters. Furthermore, the phase shifters are designed for thin-film ceramic circuits using low-loss phase change material switches to select different delay lines. However, as the unselected delay lines are left disconnected, these naturally resonate at specific frequencies causing additional narrow-band attenuation. To mitigate this loss, these resonances can be adjusted by changing the delay line geometry such that they occur outside the passband. A machine learning model has been trained to predict the frequencies at which these resonances occur to accelerate the design process for different phase requirements.

WEDNESDAY

3.43. Millimeter-Wave Gap Waveguide-Based Broadband Slant-Polarized Slot Array Antenna

Davood Zarifi (Gdansk University of Technology, Poland); Ali Farahbakhsh (Graduate University of Advanced Technology, Iran); Michal Mrozowski (Gdansk University of Technology, Poland)

This research deals with the design of a broadband, slant-polarized antenna array for 26-40 GHz frequency band. The design employs gap waveguide technology to minimize unwanted energy leakage, ensuring high gain and efficiency. In this configuration, the radiating slots are angled at 45°, and a two-layer feed network, utilizing compact folded E-plane groove gap waveguide power dividers, is used to energize the slots. Key advantages of the proposed antenna array include its low profile, low loss, wide bandwidth, and suitability for millimeter-wave applications.

3.44. On Switch Network Topologies for mm-Wave Beam-Switching Antenna

Adam Narbudowicz (Tyndall National Institute, Ireland & Wroclaw University of Science and Technology, Poland); Vitalii Kirillov, Dmitry Kozlov and Senad Bulja (Tyndall National Institute, Ireland)

This work studies the effect of various switching topologies on the performance of switchable-beam Luneburg lens antenna with 16 possible beams. As the mm-Wave switching elements are costly and often exhibit significant insertion losses, this study seeks to optimize the switching network topology in order to minimize the total number of switches and total insertion loss, without significantly compromising on other design's parameters. Three different switching topologies are studied, with the newly proposed "hybrid" approach offering reduced cost and insertion loss, while preserving large bandwidth. While the study is conducted on a 16 beam antenna, the results offer scalability to antennas with larger number of beams.

3.45. Organic Substrate Based D-Band Vivaldi Antenna for End-Fire Applications

Muhammad Ibrahim, Kimmo Rasilainen, Aarno Pärssinen and Marko E Leinonen (University of Oulu, Finland)

Vivaldi antennas with relatively wide bandwidth and reasonable radiation characteristics can find the applications for D band.This paper shows the characteristics of single unit cell of Vivaldi antenna, fed by stripline, having two radiating flares with organic dielectric in between them contrary to anti-podal configuration. In addition to dual radiating fins, a hexagonal director and uniform cylindrical slots were added to enhance the directive performance of the antenna. Antenna shows a broad matching characteristics with bandwidth of 110-166 GHz, with a peak gain of 9.47 dBi at 166 GHz. Effects of thickening the substrate and excitation with 100-µm ground-signal-ground (GSG) probe pads are studied using printed circuit board (PCB) technology. Single unit shows a promising potential for the D-band antenna array applications.

3.46. The Bi-Curvature Method: A New Paradigm for Flexible 3D-Printed Curved Reflectarrays

Andrea Massaccesi, Michele Beccaria and Paola Pirinoli (Politecnico di Torino, Italy)

In this paper, some results on the design and analysis of a 3D-printable dielectric ReflectArray (RA) antenna that can be conformed to cylinders with different radii of curvature are presented. Thanks to the definition and the use of an innovative procedure, named Bi-Curvature Method (BCM), a curved reflectarray is designed in such a way that its performance remains stable even when its radius of curvature is changed. The effectiveness of the proposed technique is assessed through the numerical analysis and the experimental characterization of a prototype, manufactured with a 3D printer and using a flexible dielectric material. Both confirm the feasibility of the proposed solution and the good features of the considered configuration.

3.48. Water-Drop Luneburg Lens with Integrated Dielectric Circular Polarizer and In-House SLA Manufacturing for 5G Communications in the Ka-Band

Jorge Sanchez-Castillo and Javier Melendro-Jimenez (Universidad Politécnica de Madrid, Spain); Jorge Calatayud Maeso, Adrián Tamayo-Domínguez and Pablo Sanchez-Olivares (Universidad Politecnica de Madrid, Spain); Jose Luis Masa-Campos and José Manuel Fernández González (Universidad Politécnica de Madrid, Spain)

This work introduces a metallic Luneburg geodesic lens integrated with a plano-convex lens and an anisotropic polarizer at its aperture, designed for millimeter-wave applications in Ka-band (20-40 GHz). The proposed setup ensures high-gain performance and circular polarization over an azimuthal coverage of ±55°. The geodesic lens features 11 input ports on one end and a continuous flare on the opposite side, efficiently guiding the electromagnetic field from each port toward specific spatial directions, enabling the generation of 11 distinct azimuthal planar wavefronts at the flare's exit. The plano-convex lens at the flare's aperture helps produce a planar wavefront in the elevation plane, significantly boosting the system's overall directivity. Moreover, the anisotropic dielectric polarizer, made from dielectric slabs, converts the vertically polarized wave from the geodesic lens into a right-hand circularly polarized wave. The prototype's components are simple enough to be manufactured in the research group facilities using additive manufacturing techniques.

WEDNESDAY

3.49. Wideband and Compact Dual-Polarized Array Antenna on Square Waveguide for 5G Applications

Mehri Borhani-Kakhki (Huawei Technologies Canada Co., Canada); Hari Krishna Pothula (Huawei Technologies Canada, Canada); David Wessel (Huawei, Canada)

This paper presents a wideband and compact dual-polarized end-fire array antenna for millimeter-wave 5G applications. The antenna is designed on square waveguide technology to support two orthogonal modes for operation over 37 GHz to 42 GHz. To keep the antenna's size compact, a 4.4mm × 4.4mm square waveguide is used for the design with cut-off frequency at 34 GHz. Therefore, to cover lower band of the desired bandwidth in both polarizations, vertical and horizontal pairs of irises are employed in the feed network. In the presented design, element to element spacing is 0.65λ which makes the structure a good candidate for beam-steering applications. The designed antenna shows a return loss of less than -10dB, stable realized gain of better than 18.8dBi, and side lobe level of less than -13dB for both polarizations The designed prototype has been fabricated and the measurement results prove the accuracy of the achieved simulation results.

3.50. High Gain and Wideband mm-Wave Antenna Incorporating Metasurfaces and Conical PEC Walls

Ahmed Khairy (King Fahd University of Petroleum and Minerals, Saudi Arabia); Shaker Alkaraki (University of Nottingham, United Kingdom); Hussein Attia (King Fahd University of Petroleum and Minerals (KFUPM) & Interdisciplinary Research Center for Communication Systems and Sensing, Saudi Arabia)

This work presents a novel slotted patch antenna design featuring high gain and wide bandwidth, based on the Fabry-Perot approach. Advanced techniques are incorporated to enhance both gain and bandwidth. The proposed design utilizes a partially reflective surface (PRS), an artificial magnetic conductor (AMC), and conical PEC walls to improve gain and radiation characteristics. The conical PEC walls enhance gain and directivity by minimizing back radiation and concentrating radiated power. Additionally, it prevents side radiation leakage by reflecting it back onto the PRS. The proposed antenna achieves a maximum realized gain of 13 dB, with a wide 3-dB gain bandwidth of 27%, ranging from 28.6 GHz to 37.6 GHz. Optimized for fifth-generation (5G) high-frequency bands, the design also achieves a -10-dB bandwidth from 27 to 39 GHz.

Room: Poster level 3

PA6 (level 3) - Antennas VI Sensing, localization and tracking

T04 RF sensing for automotive, security, IoT, and other applications / / Antennas

Chairs: Miguel Ferrando-Rocher (Universitat Politècnica de València & Antennas and Propagation Lab, Spain), Aritra Roy (Sorbonne Université, France)

3.1. 77 GHz High-Gain Interleaved Series-Fed TM05-Mode Patch Array Antenna

Kuo-Sheng Chin and Yu-Liang Zhu Chen (Chang Gung University, Taiwan)

This work presents a 77 GHz TM05-mode patch array antenna with high gain and compact feed network, which can be used in automotive radar systems. The array element adopts TM05-mode patch, and slots are etched at the anti-phase current's position to increase the gain and improve the sidelobe level. A substrate integrated waveguide series-fed network with interleaved coupling slots was designed to form the six-element array. An in-phase feed design with an element spacing of 3 lambda/2 was proposed. The proposed feed network has the advantages of compact size and easy array assembly. The measured results show that the bandwidth is 73.76~78.44 GHz (6.1%) and the gain is as high as 17.5 dBi. Due to its high gain, the number of array elements and the complexity of the feed network can be reduced when large-scale arrays need to be designed.

3.2. A Dual-Band, Printed Inverted-F Antenna for Multi-Region ISM and GNSS Applications

Justin Beaurivage (Université du Québec à Trois-Rivières, Canada); Frederic Domingue (Universite du Quebec a Trois-Rivieres, Canada)

A modified printed IFA which exhibits dual-band behavior is proposed. It is intended for multi-region ISM (863-928 MHz) and multi-constellation GNSS (1559-1610 MHz) applications. The proposed design features a first, low-frequency meandered resonator and a second, high frequency straight resonator line. Two ground shorting paths allow for adjustment of the antenna's feed impedance. Two antenna variants were designed, using different substrate materials and thicknesses. The two variants were simulated, and prototypes were constructed and measured using a vector network analyzer. One prototype was manually trimmed by shortening the meandered line by 4.8 mm to achieve the intended center frequency. Of the three prototype variants, the trimmed FR408HR variant exhibited the most optimal reflection coefficient. The antenna features an omnidirectional radiation pattern. Within the intended operating bands, the antenna features a measured reflection coefficient below -7.68 dB, and simulated radiation efficiency greater than 96.4%.

3.3. A Fixed-Frequency Beam Scanning Circularly Polarized Leaky-Wave Antenna Based on Half-Mode Substrate Integrated Waveguide

Sheng-Wei Wu, Kuan-Hsun Mao and Robin Jeanty (National Taiwan University, Taiwan); Zi-Hao Fu (National Taiwn University, Taiwan); Kun-You Lin and Shih-Yuan Chen (National Taiwan University, Taiwan)

This paper presents a novel circularly polarized (CP) leaky-wave antenna utilizing a half-mode substrate integrated waveguide structure for continuous beam scanning at a fixed frequency of 10 GHz. By employing a modified unit cell equipped with two varactors, the antenna enables continuous beam scanning at a predetermined frequency from backward (−30°) to forward (+32°) directions, including broadside (0°). Simulation and experimental results demonstrate good agreement, with |S11| below −10 dB and axial ratio under 3 dB across main beam directions. The prototype antenna achieves a peak gain of 10.4 dBic at broadside and exhibits a gain variation of less than 2.6 dB during beam scanning. Its compact size and stable performance make it suitable for radar systems requiring CP beam scanning at fixed frequencies.

WEDNESDAY

3.4. A Novel Reconfigurable Antenna for Adaptive IoT Communications in Variable Environments

Wenjing Zhu (Southeast University, China); Lei Wang (Lancaster University, United Kingdom); Zhenxiang Yi (Southeast University, China)
This paper presents a novel reconfigurable antenna designed to adapt to variable environments and enhance communication reliability for the Internet of Things (IoT). The proposed antenna features a flexible reconfigurable cavity structure, allowing adjustment of impedance matching and radiation performance by modifying its height. Experimental results show that the proposed antenna effectively reduces signal degradation and enhances communication quality using its adaptive mechanism in the presence of interference. Notably, the radiation power gain of the antenna along the main lobe direction increased by 2.77 dB under ceramic interference, reducing signal attenuation by 96.52%. This innovative solution offers a low-power option for maintaining stable communication in challenging IoT scenarios where environmental interference impacts mobile device performance.

3.5. A Sustainable Screen-Printed Class-C Rectifier for Energy Harvesting and Wireless Power Transfer

Gholamhosein Moloudian (Tyndall National Institute, Ireland); Sanjeev Kumar (Tyndall National Institute & University College Cork, Ireland); Dinesh R. Gawade (Tyndall National Institute, Ireland); John Laurence Buckley (Tyndall National Institute & University College Cork, Ireland); Brendan O'Flynn (Tyndall National Institute, Ireland)
This paper presents a novel, sustainable microwave Class-C rectifier for radio frequency (RF) energy harvesting and wireless power transmission. The proposed rectifier is fabricated using screen-printing techniques, utilizing a conductive layer made of silver nanoparticle ink and a sustainable cork substrate. The proposed rectifier consists of a simple matching network, a shunt diode, a Class-C harmonic termination structure and a resistive load. The proposed rectifier is designed to operate at f = 2.4 GHz, achieving a peak power conversion efficiency (PCE) of 64% at an RF input power (P IN) level of 24 dBm and an optimal load (RL) of 160 Ω. In the latter case, a DC- DC boost converter and a supercapacitor are employed to ensure adequate DC voltage for powering Internet of Things (IoT) devices, validating the rectifier's performance. The proposed system successfully demonstrates the charging of both the DC-DC booster and the supercapacitor.

3.6. Accurate Pigtail Calibration Method Up to 8.5 GHz

Jaakko Juntunen (Dicaliant Ltd., Finland); Bailie Quinn (AntennaWare Ltd., United Kingdom)
We present a novel calibration technique for on-board measurements with so-called pigtails, which are thin flexible or semi-rigid coaxial cables with an SMA connector in one end, and an open-ended inner conductor extension in the other. We also suggest a measurement-modeling sequence that characterizes printed circuit board (PCB) properties with sufficient accuracy to model the interconnects in a matching circuit on a PCB. This allows the method to be used for basically any PCB material and thickness. We have validated the presented methods for measuring and matching antennas at UWB channels 5 to 9 at 6.25 GHz - 8.25 GHz, as well as for measuring a low-noise amplifier (LNA) at the same frequency band.

3.7. Compact, Highly Decoupled Antennas for Automotive SDARS, WiFi, and V2X Applications

Abdo Salah (Technical University of Munich, Germany); Thomas F. Eibert (Technical University of Munich (TUM) & Chair of High-Frequency Engineering (HFT), Germany)
Due to the limited space within shark-fin antennas and the introduction of new automotive applications, such as Vehicle-to-Everything (V2X) and Multiple Input Multiple Output (MIMO), achieving adequate isolation between all antennas presents a significant challenge. This paper presents a placement method designed to achieve high decoupling between three antennas for Satellite Digital Audio Radio Service (SDARS), 2.4 GHz WiFi, and V2X. The proposed configuration is compact and meets all operational requirements for each service.

3.8. Design and Fabrication of a Biocompatible Antenna for Wearable Technologies

Jamal Abounasr, Mariam El gharbi and Ignacio Gil (Universitat Politècnica de Catalunya, Spain); Raul Fernandez-Garcia (Universitat Politecnica de Catalunya, Spain)
This paper presents the design, simulation, fabrication, and measurement of a flexible antenna for wearable healthcare applications operating at 2.4 GHz. The antenna utilizes a coplanar waveguide (CPW) structure with strategically placed slots in the ground plane to enhance impedance matching and bandwidth performance. Printed on a thermoplastic polyurethane (TPU) substrate using a semi-sintering silverbased ink, the antenna maintains mechanical flexibility without compromising electrical performance. Simulations show a peak gain of 3.5 dBi and over 90% efficiency at 2.4 GHz. Specific Absorption Rate (SAR) analysis, performed with the antenna placed millimeters away from the body, indicates SAR values of 0.2 W/kg for 1g of tissue and 0.11 W/kg for 10g, both well below international safety limits. The proposed design provides high radiation efficiency, mechanical adaptability, and safe operation, making it a promising solution for wearable technology applications.

WEDNESDAY

3.9. Design of a 77-81 GHz Front End for a RADAR Level Measurement System

Christophe Granet (Lyrebird Antenna Research Pty Ltd, Australia); Sabin Karibasic (EM Solutions, Australia); Jeff Clugston (Transrail Innovation, Canada); John Ness (EM Solutions Pty Ltd, Australia)

The design, manufacture and test of a 77-81 GHz front end for a RADAR level measurement system is described. Index Terms- E-band, RADAR, horn antenna, Branch-line Coupler, PCB, PEEK.

3.10. Design of E-Band 3D-Printed WR12 Air-Filled Waveguide-Based 4x4 Butler Matrix for Beam Steering in 77 GHz Automotive Radar Systems

Jean Temga (Silicon Austria Labs, Austria & Research Insitute of Electrical Communication, Tohoku University, Austria); Saeid Karamzadeh (Silicon Austria Labs, Austria); Boro Reljic (Silicon Austria Labs (SAL), Austria); Shrief Rizkalla (Silicon Austria Labs GmbH, Austria); Wagner Christoph (Silicon Austria Labs (SAL), Austria)

This paper presents the design and simulation of a 3D-printed 4 × 4 Butler Matrix (BM) using WR12 air-filled waveguides for a linear 1 × 4 array antenna operating in the 77 GHz band. The air-filled waveguides significantly reduce insertion losses compared to dielectric and printed technologies while maintaining benefits such as compactness, ease of fabrication, and low weight. The Butler Matrix enables beam steering across four fixed elevation angles, complemented by digital beamforming (DBF) for 360 ◦ azimuth coverage, making it highly suitable for automotive radar. A miniaturized WR12 3-dB hybrid coupler with five branch lines ensures amplitude balance within 1 dB and phase difference of ±90 ◦ ± 0.5 ◦ over the 65-90 GHz range. Key components, including the 3-dB coupler, 0-dB crossover, and phase shifters, were optimized in HFSS and integrated into a compact design. The BM achieves a 32.26% relative bandwidth, with dimensions of 3.6λ0 × 9.2λ0 × 0.8λ0.

3.11. Dual-Band Patch Antenna Design for Integrated Sensing and Communications

Haoyuan He (School of Engineering, the University of Edinburgh, United Kingdom); Khalid M Alrushud (King Abdulaziz City for Science and Technology (KACST), United Kingdom); Sadia Riaz (The University of Edinburgh, United Kingdom); Symon K. Podilchak (University of Edinburgh, United Kingdom)

This paper proposes dual-band patch antenna designed for application in integrated sensing and communication systems, focusing on the 2.4 GHz and 5.8 GHz frequency bands. The 2.4 GHz band is designated for communication, while the 5.8 GHz band is employed for sensing. The primary objective of this research is to demonstrate that materials under test (MUT) can be differentiated based on the frequency shift observed in the 5.8 GHz band, with minimal impact on the 2.4 GHz communication band. The proposed antenna is a dual-band patch antenna featuring two slots in the patch, designed to operate at centre frequencies of 2.4 GHz and 5.8 GHz, as confirmed in simulations. Simulation results indicate that the dual functionality of the antenna is most effective when the size of the MUT matches the patch, and the frequency shift in the 5.8 GHz band increases with material thickness when the dielectric constant remains constant.

3.12. Highly Dispersive Ridge Gap Waveguide for mm-Wave Fast-Scanning Leaky-Wave Arrays

Marco Nieto-Perez (Universitat Politecnica de Valencia, Spain); Jose I Herranz-Herruzo (Universitat Politècnica de València & APL - iTEAM, Spain); Miguel Ferrando-Rocher (Universitat Politècnica de València & Antennas and Propagation Lab, Spain)

This communication explores the modification of a ridge-gap waveguide with the objective of attaining highly dispersive wave propagation. This new waveguide enables the design of leaky-wave arrays with a fast frequency-scanning rate. The modification entails the insertion of deep corrugations into the central ridge, which serves to enforce the slow-wave regime and augment the slope of the phase constant with respect to frequency. A design example of a linear shunt slot array based on this new waveguide has been proposed. With a relatively simple structure, a field of view of 60° is covered within 1-GHz bandwidth. These results confirm the promising properties of the proposed waveguide for the design of backward-to-forward fast-scanning all-metal leaky-wave arrays in the millimeter-wave band.

313. Multiband Broadcast Energy Harvesting Antenna

Christopher G Hynes and Rodney Vaughan (Simon Fraser University, Canada)

A broadband monocone antenna on a circular ground plane is presented for the application of multiband broadcast energy harvesting. The targeted broadcast bands include Amplitude-Modulated (AM) radio in the medium frequency range, frequency-modulated (FM) radio in the very high frequency range, and television signals in the Ultra High Frequency (UHF) range. The antenna matching in each band is facilitated by using a front-end triplex circuit. The antenna also has the potential to harvest energy from the cellular and WLAN bands. Simulation results show that better than -10 dB impedance matching is achieved across the FM and UHF bands while supporting a narrowband match across selected channels in the AM band.

WEDNESDAY

3.14. RFID Sensor for Breaks in Cold Chain Applications

Cong Danh Bui (Trinity College Dublin, Ireland & CONNECT Centre, Ireland); Adam Narbudowicz (Tyndall National Institute, Ireland & Wroclaw University of Science and Technology, Poland)

This paper presents a low-profile RFID sensor to detect disruptions in cold-chain operations. The sensor consists of a modified meander line resonator with a UCODE G2iL RFID chip positioned at its center. It is tailored to monitor the ice's presence on its surface, operating within an impedance bandwidth of 913 - 922 MHz, which is compatible with the European RFID band. The sensor's resonant frequency is sensitive to changes in permittivity, as the Material Under Test is placed atop the sensor. When ice melts into water, the overall permittivity increases, causing a reduction in the sensor's resonant frequency. If excessive water accumulates, the sensor's resonant frequency falls outside the RFID band (915 - 921 MHz), indicating a break in the cold chain. Additionally, the sensor maintains a similar E-field distribution and radiation pattern to a conventional dipole, with a maximum gain of -0.4 dBi, making it viable for practical applications.

3.15. Unwanted Hydrate Detection in Energy Sector Pipelines Considering Dual-Polarization Patch Antennas as the RF/Microwave Sensor

Maksim Kuznetcov (Heriot Watt University, United Kingdom); Konstantinos Kossenas (The University of Edinburgh, United Kingdom); Symon K. Podilchak (University of Edinburgh, United Kingdom); Martin Beveridge (Innerpath Technologies, United Kingdom)

The reported findings are directed towards the development of a gas hydrate two-port detection system utilizing antenna and microwave technology, which follows electromagnetic and dual-polarization principles, and is intended for use in oil and gas pipelines. This hydrate formation is an ongoing problem for the energy sector as it can cause unwanted and costly pipeline clogging. Results suggest that a dual-polarization antenna sensor concept, based on observed permittivity variations, can provide enhanced data collection and characterization of the materials flowing inside pipelines, and, when compared to more conventional approaches which only considers a single-port setup and single-polarization.

3.16. Wideband Highly-Transparent Broadbeam Circularly Polarized Antenna

Zengtai Zhou (Shenzhen University, China); Wei Lin (The Hong Kong Polytechnic University, Hong Kong); Wenhui Wu, Zhe Chen and Yu-Xiang Sun (Shenzhen University, China)

This paper proposes a wideband highly-transparent broadbeam circularly-polarized (CP) antenna. The antenna consists of a coplanar waveguide (CPW) T-shaped feed structure to achieve wideband performance. To generate CP, a grounded rectangular patch is placed inside the slot area. The antenna uses diamond-shaped meshes and is fabricated on a glass substrate for optical transparency (OT). Simulated results show a usable CP bandwidth of 33.61% (1.98 GHz-2.78 GHz), an OT of 73.47%, and broad CP beams of 119° are obtained.

Room: Poster level 3

PA7 (level 3) - Antennas VII Biomedical and health

T06 Biomedical and health / / Antennas

Chairs: Mingzheng Chen (KTH Royal Institute of Technology, Sweden), Denys Nikolayev (Institut d'Électronique et des Technologies du Numérique (IETR) - UMR CNRS 6164, France)

3.17. A Dual-Band Four-Port MIMO Implantable Antenna with Enhanced Isolation

Alok Chandra Joshi, Piyush Kumar Mishra and Debdeep Sarkar (Indian Institute of Science, India)

This paper presents the design and performance evaluation of a dual-band, four-port MIMO implantable antenna. The antenna demonstrates wide impedance bandwidths at the resonant frequencies of 433 MHz and 915 MHz. Port-to-port isolation is enhanced by connecting neutralization lines to the adjacent ground planes. Additionally, the antenna achieves pattern diversity due to the distinct radiation patterns of its individual elements. Link budget analysis confirms the suitability of the proposed antenna for high data rate biotelemetry applications.

3.18. Compact Dual-Band Camera-Integrated Antenna for Deep-Implanted Wireless Capsule Endoscopy

Muhammad Qamar (Queen Mary University of London, United Kingdom); Kamil Yavuz Kapusuz (Ghent University & IMEC, Belgium); Mohamed Thaha and Akram Alomainy (Queen Mary University of London, United Kingdom)

A compact camera integrated dual-band implantable antenna specifically designed for wireless capsule endoscopy (WCE) is presented first-time. The antenna operates in the Wireless Medical Telemetry Service (WMTS) band at 610 MHz and the Industrial, Scientific, and Medical (ISM) band at 2.4 GHz. Miniaturization is achieved through the use of arc-shaped slots on arc-shaped patches. The final structure has a compact volume of 92.3 mm^3. The antenna's performance is evaluated using both homogeneous small intestine phantom. Given the capsule's deep implantation, the antenna demonstrates gain values of -57 dBi at both operating band. The simulated impedance bandwidths are 8 MHz at 610 MHz and 25 MHz at 2.4 GHz while isolation between the antennas is larger than 25 dB.

3.19. Design of Fat-Intra Body Power Transfer System for Implantable Biomedical Devices

Tarakeswar Shaw (Postdoctoral Researcher, Uppsala University, Sweden); Bappaditya Mandal (Uppsala University, Uppsala, Sweden); Robin Augustine (Uppsala University, Sweden)

In this article, the design of a resonator-based fat intra-body power transfer (Fat-IBPT) system has been presented for the application of implantable medical devices (IMDs). Herein, the low-loss properties of human fat tissue sandwiched between skin and muscle are considered to act as an effective waveguide for microwave power transmission. In the proposed implantable wireless power transfer (WPT) system, both the transmitting (Tx) and receiving (Rx) resonating elements have been placed in the fat layer of the human body model. The wireless Fat-IBPT system is constructed by using two identical resonators, which act as Tx and Rx elements that have been placed in the fat tissue layer at different distances to show the power transmission. The concept of the proposed resonator-based Fat-IBPT system has been established by numerical studies. From the proposed Fat-IBPT system, maximum power transfer efficiency (PTE) of about 8.47 % has been achieved.

3.20. Enhancing Energy Harvesting for Wearable Sensors: A Circular 8-Element Array with Spatial Diversity

Nasir Ullah Khan (University G. d Annunzio Chieti-Pescara, Finland & Tampere University, Finland); Abdul Basir, Uzman Ali and Toni Björninen (Tampere University, Finland); Arcangelo Merla (University G. d'Annunzio of Chieti-Pescara, Italy)

This paper presents a receiving antenna array for self-powered battery-less system utilizing far field RF energy harvesting. The design, simulations, fabrication and testing of the proposed array is presented, composed of 8 elements circularly configured for wide angular range and diversity. The design exhibits dual band characteristics operating at ISM 2.45 and 5.8 GHz, which was fabricated on a wearable EPDM substrate. The simulations and optimization of the design was achieved in a realistic environment, a three-layered homogeneous body model consists of skin, fat and muscle. The simulated results were validated through testing the S parameters and radiation patterns of the fabricated prototype. Both the simulated and measured results show good agreement in terms of S11 surpassing −20 dB and S12 less than −20 dB. The 3D gain plots of the array confirm the omnidirectional patterns with maximum gain of 2.9 and 7.1 dBi at 2.45 and 5.8 GHz respectively.

3.21. Flexible 4-Element Array for on-Body RF Energy Harvesting Applications Using Aerosol Jet Printing

Nasir Ullah Khan (University G. d Annunzio Chieti-Pescara, Finland & Tampere University, Finland); Emanuele Mantini and Francesco Galliani (Comec Innovative srl, Italy); H. Joseph Christopher (Università Politecnica Delle Marche, Italy); Toni Björninen (Tampere University, Finland); Arcangelo Merla (University G. d'Annunzio of Chieti-Pescara, Italy)

This research focuses on the design, fabrication and testing of a compact, flexible 4-element array using Aerosol jet printing technology. The array operates at ISM-band 2.45 GHz for on-body RF energy harvesting applications (RFEH). The optimized array was printed on a flexible polyimide substrate having compact dimensions of π · 452 mm2. The simulated results of the array were validated through testing that exhibit good agreement, indicating that AJP is a precise and effective technique for printing high-resolution, conformal and flexible antennas. The design and optimization of the rectifier were performed at 2.45 GHz to ensure integration with the proposed array. The rectifier analysis demonstrated good performances, achieving output voltage of 2 V and power conversion efficiency of 69.4 % at 5 dBm input power with a 2 KΩ load. This potential marks the path for further advancements in RFEH applications.

3.22. Implant-To-Implant Communication Using Quad-Band PIFAs for Intracranial Applications

Ali and Abdul Basir (Tampere University, Finland); Nasir Ullah Khan (University G. d Annunzio Chieti-Pescara, Finland & Tampere University, Finland); Toni Björninen (Tampere University, Finland)

In this paper, we study the feasibility of implant-to-implant (I2I) communications with quad-band implantable planar inverted-F (PIFA) antennas through numerical simulations. The four frequency bands included are the Medical Device Radiocommunication Service (MedRadio) band (401-406MHz), the Wireless Medical Telemetry Service (WMTS) band (1427-1432 MHz), and the Industrial, Scientific, and Medical (ISM) bands (902.8-928 MHz and 2400-2483.5 MHz), where the antenna's reflection coefficient (|S11|) is better than −10 dB. The two implant antennas are positioned 14.8 mm deep in the CSF layer and 75 mm deep in the brain of the ellipsoid human head model. The relationship between the mutual coupling (|S21|) and the far-field gain products of the antennas is analyzed to understand the electromagnetic coupling mechanism between the antennas.

3.23. Integration of Substrateless Antenna into Skin Organoid Culture

Mohammed S. Salim (University of Kent, United Kingdom & University of Ninevah, Iraq); Benito Sanz-Izquierdo, Victorija Makarovaite and John Batchelor (University of Kent, United Kingdom)

This paper introduces the concept of integrating antennas into skin organoid cultures for biomedical applications. A passive loop resonator is incorporated into the equivalent skin organoid culture layers on a petri dish. The loop resonator consists of a mesh metallic layer, allowing skin to grow through it. This resonator is designed to couple with an external dipole placed in close proximity to the outer layer of the grown skin cells. The dielectric properties of each layer were measured and found to be consistent with those of real skin layers. The resonator, embedded in the skin culture, produces a variable response depending on the growth of the culture when coupled to the external dipole. The loop coupling antenna operates at 2.7 GHz before the addition of the equivalent organoid skin layer, shifting to approximately 900 MHz after the skin layer is incorporated.

WEDNESDAY

3.24. Modified Huygens Source for Maximum Gain of Implanted Antenna

Jiajun Li (École Polytechnique Fédérale de Lausanne, Switzerland); Zvonimir Sipus (University of Zagreb, Croatia); Anja K. Skrivervik (EPFL, Switzerland)

Implanted antennas are a key part of wireless implanted medical devices. However, their radiation efficiency and gain are severely decreased by the loss of the body tissue. It's important to maximize the power reaching free-space from the implanted antenna. Fundamental modes TE10 and TM10 are of great interest because they have a lower near-field loss compared with higher order modes. A Huygens source antenna combining first order modes is therefore of great interest. However, as in the implanted case losses are different for TE and TM modes, the optimal power distribution between the two modes will be different from the free-space case. Hence in this contribution we study the theoretical maximum gain and the corresponding optimum power distribution of a Huygens source antenna in a deep-implanted scenario. Near-field loss and ohmic loss's effect on the maximum gain is discussed in detail. The encapsulation size and implant depth, are studied in-depth.

3.25. Multi-Radar Near-Field System Employing Multi-Band Non-Interleaved Metasurface for Enhanced Bio-Sensing

Mohammad Omid Bagheri and Omar Ramahi (University of Waterloo, Canada); George Shaker (University of Waterloo & Spark Tech Labs, Canada)

This paper introduces a system that employs near-field focusing of radar interactions on human skin at various locations, with the multi-radar setup gathering data from multiple points to enhance detection capabilities. A multi-band non-interleaved metasurface is integrated into this system, improving the detection of physiological parameters, including the identification of human blood abnormalities. The methodology utilizes discrete zones of a transmissive metasurface, each composed of phase-synthesized arrays. These zones serve as low-profile impedance matching networks, optimized for specific frequencies within the 58 to 63 GHz radar range, thereby increasing efficiency through higher absorbed power density at different frequencies, which also enables varied penetration depths into skin. Analysis using a customized phantom, closely resembling human skin, demonstrates significant increases in near-field absorbed power density: over 11 dB at 60 GHz and 2 mm penetration depth, over 17 dB at 58 GHz, and 9 dB at 61 GHz at the same depth.

3.26. Non-Invasive Glucose Sensing System Using Microwave Technology for Saliva-Based Diabetes Management

Adarsh Singh and Rahul Neogy (Indian Institute of Engineering Science and Technology, Shibpur, India); Bappaditya Mandal (Uppsala University, Uppsala, Sweden); Soumyadeep Das (Queen's University of Belfast, United Kingdom); Debasis Mitra (Indian Institute of Engineering Science & Technology, Shibpur, India); Robin Augustine (Uppsala University, Sweden)

Diabetes is a global health issue that requires continuous monitoring of blood glucose levels to manage the disease and prevent complications. Traditional methods, like finger-prick tests, are invasive and inconvenient, leading many patients to avoid regular testing. This article presents a low-cost, non-invasive method for continuous glucose monitoring to address these challenges. The study presents a novel triple-ring implantable antenna designed to function as a tooth cap, which utilizes saliva to monitor glucose levels. The antenna operates across a wide frequency range from 5 GHz to 9.5 GHz, including the 5.8 GHz ISM band. The study establishes a detailed correlation between blood glucose levels (BGL), saliva glucose levels (SGL), and the dielectric properties of saliva. This relationship is used to demonstrate how resonant frequency can act as a sensing parameter for glucose levels. The findings highlight the potential of microwave-based, non-invasive sensors for effective and continuous glucose monitoring.

3.27. PEG-100 Stearate Based Emulsification for Tissue Phantom Development, Covering Relative Permittivity Values from 7 to 77

Anil Tulu, Burak Ferhat Ozcan and Sema Dumanli (Bogazici University, Turkey)

Phantoms are an essential part of the testing procedure for wearable and implantable devices. There are various ways of developing phantoms in different forms. Here PEG-100 Stearate is proposed to be used as an emulsifying agent to create a wide-band liquid phantom. The protocol to develop the phantom is detailed along with the analysis of the effect of each component on electrical properties. The protocol is demonstrated through a muscle phantom, a bone phantom and a phantom representing human average with a wide-band performance where the electrical properties are mimicked between 1 GHz and 6.7 GHz with less than 10% error.

3.28. Performance Comparison of Two Loop Antennas for Intracranial Implant-To-Implant Communications

Uzman Ali and Abdul Basir (Tampere University, Finland); Nasir Ullah Khan (University G. d Annunzio Chieti-Pescara, Finland & Tampere University, Finland); Toni Björninen (Tampere University, Finland)

We present the potential of implant-to-implant communication with loop-type implantable antennas, conducting deep implant analysis through numerical simulations. Loop antenna dimensions make it a suitable candidate for I2I communication. Antenna dimensions are 13.3 × 2.5 × 1.5 mm and 8 × 2.5 × 1.3 mm including the silicone coating, for 915 MHz and 2450 MHz loop antennas, respectively. Two loop antenna cases operating in industrial, medical, and scientific bands, 915 MHz and 2450 MHz, are investigated. For I2I analysis, antennas are positioned 14.8 mm deep in the CSF layer and 75 mm deep in the brain of the ellipsoid 7-layer head model. Both antenna models poses reflection coefficient below −10 dB. The maximum mutual coupling of implant antennas and combined gains of antennas are analyzed using the rotation antenna method. This method allows us to find the optimal alignment that maximizes the coupling and enhances communication efficiency between implant antennas.

WEDNESDAY

3.29. Scalar Field Intensity Shaping via Low Dimensional Global Optimization

Martina Teresa Bevacqua (Università Mediterranea di Reggio Calabria, Italy); Sabrina Zumbo (University of Naples Federico II & Università Mediterranea di Reggio Calabria, Italy); Umberto Pirrello (Università degli Studi Mediterranea di Reggio Calabria, Italy); Tommaso Isernia (University of Reggio Calabria, Italy)

The contribution proposes a new method to shape the field intensity based on the superposition of elementary patterns focused inside a given region of interest. The optimization of the complex superposition coefficients is pursued by global optimization. The procedure is tested against a bidimensional scenario and scalar field.

3.30. The Integration of Smart Textiles with LoRa Technology Enables Real-Time Health Monitoring

Usman Rizqi Iman (Hanyang University, Korea (South)); Abdul Basir (Tampere University, Finland); Muhammad Zada and Hyoungsuk Yoo (Hanyang University, Korea (South))

This paper presents the development of a smart textile-based LoRa system that can monitor the heartbeat and predict body temperature over long and short distances. The proposed system consists of a smart textile combined with a LoRa module and a pair of sensors. Notably, the reflection coefficient analysis of the antenna confirms triple-band operation with wide-bandwidth characteristics at 433, 610, and 915 MHz. Moreover, the numerical results reveal that the antenna is not affected by lossy human body and structural deformations. The fabricated prototype is combined with the LoRa and sensors, which monitor the Received Signal Strength Indicator (RSSI), heartbeat, and temperature data. The data transmission of temperature and heartbeat at a 915 MHz LoRa frequency demonstrates the effectiveness in enhancing health monitoring capabilities up to 250 m with RSSI -84 dBm and 433 MHz LoRa frequency up to 350 m with an RSSI of -90 dBm.

3.31. Wave Polarization and Propagation Analysis for Improved Smart Insole Antenna Design

Lorette Queguiner (Institut d'Electronique et des Technologies du numéRique (IETR) - UMR CNRS 6164, France); Andrey Mostovov (FeetMe SAS, France); Denys Nikolayev (Institut d'Électronique et des Technologies du Numérique (IETR) - UMR CNRS 6164, France)

This study investigates the impact of antenna polarization on RF signal propagation for smart insole applications. A numerical analysis was conducted to evaluate the performance of vertical and horizontal polarizations across different soil electromagnetic properties at 2.45 GHz. The results reveal that vertical polarization enables more effective signal transmission, with more than 8 dB improvement over horizontal polarization. The signal wavefront remains relatively stable over the soil for vertical polarization, making it suitable for communication between nodes. These findings provide valuable guidance for the design of future smart insole antennas.

Room: Poster level 2

PA4 (level 2) - Antennas IV Sub-6 GHz for terrestrial networks

T01 Sub-6 GHz for terrestrial networks (5G/6G) / / Antennas

Chairs: Angel Palomares-Caballero (IETR-INSA Rennes, France), Divitha Seetharamdoo (Univ Gustave Eiffel COSYS LEOST Univ Lille Nord de France & Univ Lille Nord de France, France)

2.27. A Broadband Low-Profile Multiple Folded Loop Antenna

Xiaolong Fu, Lintao Feng, Chenjiang Guo and Jun Ding (Northwestern Polytechnical University, China); Shixiong Liu (Northwestern Polytechnial University, China)

A low-profile base station antenna based on artificial magnetic conductor (AMC) is proposed in this article. The base station antenna consists of a pair of multiple folded loop antennas, a coaxial balun and a broadband AMC reflector. The reflector is composed of a metalized floor and an AMC surface. The loop antenna fed by coaxial balun with a wide impedance bandwidth of 37.45%. The impedance bandwidth of the AMC reflector is 40.71, which is basically consistent with the bandwidth of the loop antenna. Compared with the structure without AMC, the height of the antenna changes from 32mm to 19.5mm. In the whole working frequency band, the HPBW of the antenna in the H plane and the V plane is greater than 80 °, the input port impedance bandwidth is 2.12-3.5GHz, the cross-isolation is greater than 20 dB, and the antenna gain is 7.4 dBi.

2.28. A Comparative Analysis of 3D Printed Substrate and Laminate-Based Rectangular Patch Antennas at C-Band

Saúl Santos Carvalho (Polytechnic of Leiria, Portugal & Instituto de Telecomunicações, Portugal); João Ricardo Reis (Instituto de Telecomunicações and Polytechnic Institute of Leiria, Portugal); Rafael F. S. Caldeirinha (Polytechnic Institute of Leiria & Instituto de Telecomunicações, Portugal)

This paper presents a comparative study between 3D printed and laminate-based rectangular patch antennas, specifically designed to operate at 4.7 GHz. A total of five patch antennas, fabricated using additive manufacturing (AM) techniques and several materials as substrates (Nanoe Zetamix Epsilon filaments, PETG and PLA), are compared against four antenna prototypes made in well known laminate substrates (FR4, Rogers RT/duroid 5880, RO4350B, and RT/duroid 6010LM). For the 3D printed antenna prototypes, different metallisation techniques, including copper foil, silver spray, and silver cloth tape, were employed to enhance the electrical performance of the antennas. The results demonstrate that the 3D printed antennas presented reasonable results when comparing with the laminate ones, although several challenges related to manufacturing inconsistencies and material brittleness for the 3D printed antennas, particularly with the Zetamix filaments.

2.29. A Concentric Octagonal Shaped MIMO Antenna for 5G User Equipment

Abubeker Abdulkerim Yussuf (Istanbul Technical University, Turkey)
The paper presents the design of a concentric octagonal-shaped multiple-input multiple-output (MIMO) antenna for 5G User Equipment (UE) applications in the sub-6 GHz bandwidth, specifically the 5G n38 band (2.57-2.62 GHz). The antenna is designed to be simple and avoid multilayer and vias in antenna configurations, while achieving a gain of over 5 dBi and maintaining a mutual coupling of less than -25 dB. To evaluate the performance of the MIMO antenna, the article analyzes S-parameters, envelope correlation coefficient (ECC), and Total Active Reflection Coefficient (TARC). The experimental results demonstrate an ECC below 0.01, which agrees with the simulation results and shows excellent performance.

2.30. A Digitally Coded Intelligent Reflecting Surface for 6G Wireless Communication

Raju Malleboina and Debdeep Sarkar (Indian Institute of Science, India)
This paper presents the design of a 1-bit digitally coded intelligent reflecting surface based on anomalous reflection properties for sub-6 GHz 6G wireless communications. First, we designed a 1-bit digitally coded PIN-diode loaded unit cell to generate the required phase gradient of 180^o between two programming states. Using this unit-cell, a full RIS (reconfigurable intelligent surface) is synthesized as a square array having aperture size of 8lambda_0 times 8lambda_0 (where lambda_0 is the free-space wavelength at 5 GHz). We programmed the RIS for different steering directions and demonstrated the scattering performance using full-wave CST MWS solver. It is observed that the designed RIS successfully generates beams in the desired directions with an Half-power beam width of 6^o respectively, having scan-loss free steering range of 0^o-60^o.

2.31. Bifilar Helical Antenna for High Power Electromagnetic Applications

Maria M Bermudez Arboleda, Abdulla Al-Ali and Evgeny Gurnevich (TII, United Arab Emirates); Ernesto Neira Camelo (Technology Innovation Institute, United Arab Emirates); Fernando Albarracin (Directed Energy Research Center, TII, United Arab Emirates); Felix Vega and Chaouki Kasmi (Technology Innovation Institute, United Arab Emirates)
This paper introduces a bifilar helical antenna design tailored for integration with high-power electromagnetic (HPEM) sources working in differential mode. A turn-to-turn voltage hold-off of 200 kV has been engineered by replacing air with sulfur hexafluoride gas (SF6) as the antenna medium, leveraging its superior dielectric properties. The antenna features a cylindrical geometry with a compact ground structure, which effectively reduces backfire radiation and enhances overall performance. The introduced antenna presents an impressive impedance bandwidth of 47% in the UHF band and achieves a gain of 10.1 dBi at 433 MHz. These characteristics, along with the robust design and optimized performance parameters, enables the integration of the proposed antenna into compact HPEM applications.

2.32. Dual-Band MIMO Antenna Design with E-Shaped Slits for Sub 6 GHz 5G Cellular Communications

Haleh Jahanbakhsh Basherlou, Naser Ojaroudi Parchin, Libu Manjakkal and Chan Hwang See (Edinburgh Napier University, United Kingdom); Ming Shen (Aalborg University, Denmark
This study presents an 8×8 multiple-input, multiple-output (MIMO) antenna array specifically designed to meet the demands of future cellular handheld devices. The antenna features a distinctive configuration, utilizing low-profile rotated E-shaped slits that are fed by rotated L-shaped microstrip lines arranged in two rows on opposite sides of the board (four resonators on each side). The investigated MIMO antenna array offers dual-band functionality, operating efficiently at 3.5 GHz and 5 GHz. The array delivers excellent performance in key characteristics such as S-parameters, efficiency, gain levels, and radiation patterns, fulfilling the requirements of 5G technology while prioritizing optimal functionality, thus making it suitable for deployment in 5G cellular networks.

2.33. Evaluation of Base Station Antenna Arrays for In-Band Full Duplex Communications

Bing Xue and Katsuyuki Haneda (Aalto University, Finland); Clemens Icheln (Aalto University & School of Electrical Engineering, Finland)
This manuscript investigates the channel capacity of in-band full-duplex antenna arrays within a limited area by varying numbers of antenna elements. Patch and dipole antenna arrays with ±45 ◦ and 0 ◦ – 90 ◦ element configurations are compared based on their mutual coupling levels. Among them, the dipole antenna array with a ±45 ◦ element distribution is selected for calculating the channel capacities of in-band full-duplex systems with varying numbers of antenna elements, all within a limited area. The optimal element spacing is determined to be 0.5 wavelength at both 2.6 GHz and 7.5 GHz. Radiation patterns and S-parameters of the fabricated antenna array are measured at 3.6 GHz. These measured radiation patterns are then used to compute the channel capacity for in-band full-duplex operation, further supporting the study's conclusions.

WEDNESDAY

2.34. High Gain SIW-Fed Notched Spherical-Frustum Shaped Stacked DRA for B5G Application

Sidhartha Kumar Sahu (IIT Guwahati, India); Rakhesh Singh Kshetrimayum and Ramesh Kumar Sonkar (Indian Institute of Technology Guwahati, India); Arvind Kumar (Dept of ECE,. Visvesvaraya National Institute of Technology Nagpur India, India)

This paper introduces a high gain slotted Substrate Integrated Waveguide-fed Dielectric Resonator Antenna. To achieve high gain, a stacked, notched spherical-conical DRA structure is placed on the SIW. The proposed antenna exhibits a 250 MHz (5.25-5.50 GHz) bandwidth. This antenna is linearly polarized and shows a peak gain of 8.4 dBi. The antenna offers a broadside radiation pattern. The co-polarization and cross-polarization differences are above 45 dB for the H-plane and E-plane in the broadside direction. Due to this, the antenna can provide better signal quality and a higher signal-to-noise ratio (SNR). The front-to-back ratio (F/B ratio) of this antenna is 21.6 dB. The half-power beam width (HPBW) of this antenna is 51.5°. The bandwidth, gain, and radiation pattern measurement is done for the fabricated antenna prototype. High gain, broadside radiation pattern and wider beam width make it suitable for applications beyond the fifth-generation (B5G).

2.35. Improving the Field-Of-View of Beam-Steerable Waveguide Arrays by Wilkinson-Like Power Dividers Based on Radiating Magic-Ts

Miguel Angel Fuentes-Pascual (Universidad Politécnica de Valencia (UPV) & Antennas and Propagation Laboratory (APL), Spain); Jose I Herranz-Herruzo (Universitat Politècnica de València & APL - iTEAM, Spain); Miguel Ferrando-Rocher (Universitat Politècnica de València & Antennas and Propagation Lab, Spain); Alejandro Valero-Nogueira and Mariano Baquero-Escudero (Universidad Politécnica de Valencia, Spain)

This paper presents the design and analysis of a Radiating Magic-T Power Divider (RMT-PD) for phased-array applications at 30~GHz. The RMT-PD emulates a Wilkinson power divider in waveguide technology, simultaneously ensuring effective power division and isolation between output ports. A key feature of the design is its ability to circumvent the re-radiation of unwanted backward waves from array mismatch, which typically leads to secondary lobes and reduced efficiency. The RMT-PD has been tested with a resonant slot array, demonstrating improved beam steering performance, even at wider angles. While the current implementation focuses on a slot array, the design broadly applies to various waveguide-based arrays.

2.36. Mode-Tunable OAM Antenna System with Polarization Selectivity Characteristic

Hassan Naseri Gheisanab (University of Quebec, INRS, Canada); Peyman PourMohammadi (INRS, Canada); Sarosh Ahmad (Institute National de La Recherche Scientifique', Canada); Amjad Iqbal and Tayeb Denidni (INRS, Canada)

This paper presents a new Orbital Angular Momentum (OAM) antenna system with an innovative reconfigurable feeding network and dual-polarized antennas. The 2×4 feeding network generates phase gradients of 0°, 90°, and -90° at its outputs, enabling OAM modes 0, -1, and +1. By integrating a 2×2 uniform circular array with dual-polarized antennas and two copies of the proposed feeding network, the system supports six reconfigurable propagation types, ideal for smart OAM communications. Operating at 2.4 GHz, it achieves phase gradients with a maximum 4° imbalance, and input port reflection coefficients below -15 dB. All in all, the novel configuration of the feeding network, concept of combination of polarization and OAM modes, and ability to generate additional orthogonal reconfigurable beams can be highlighted as the novel parts of this paper.

2.37. Modifications on an Antipodal Vivaldi Antenna for 5G, ISM, Multiband or UWB Operation

Lidiane S Araujo, Edson R. Schlosser and Marcos Vinício Heckler (Universidade Federal do Pampa, Brazil)

In this paper, we propose a modification in the design of an Antipodal Vivaldi Antenna (AVA) to achieve applications on multi-band, mid-band, wide-band, and ultra-wide-band (UWB). Designed on a RT/duroid 5880 laminate (dielectric constant 2.2) of thickness 0.787 mm, the original antenna was conceived to meet the requirements of technologies 5G and ISM, as well as UWB applications. The modified AVA was designed by introducing notches on the inner exponential shape of the original AVA only on the top side. A parametric analysis of the notches dimensions shows how the antenna can be modified from a UWB to a narrowband, passing by a multi-band frequency behavior. Results also show that the approach presented here has almost no effect on the original electromagnetic performance such as radiation patterns and gain of the new antenna in comparison with the original AVA. Simulations were carried out with HFSS ANSYS software.

2.38. SIW Dual Mode Compact Filtenna for 6G Technology

Sara Javadi (Graz Uuniversity of Technology & CD Lab, Austria); Behrooz Rezaee (Graz University of Technology, Austria); Wolfgang Bosch (Graz University of Technology & Institute of Microwave and Photonic Engineering, Austria)

This paper introduces a compact Transverse Magnetic (TM) dual-mode Filtenna design, implemented on a printed circuit board (PCB to reduce the size compared to conventional waveguide designs, this Filtenna also allows for easier integration with other components. Non-resonating nodes (NRNs) are employed to enhance selectivity and improve out-of-band rejection. The design achieves a realized gain of 4.3 dBi, making it a promising, space-efficient filtering solution for modern communication systems. Fabrication results are provided to validate the performance of the proposed Filtenna.

WEDNESDAY

2.39. Study of the Configuration of Sub-Arrays for 2D Passive Antenna Beam-Forming for Beyond 5G Cellular Base Stations

Yuki Inoue and Masashi Yamamoto (NTT DOCOMO, INC., Japan)
Recently, installation and maintainability are issues for MMUs. Passive multiport base station antennas supporting BF (passive BF antenna) have been standardized in NGMN Alliance MIMO multiplexing and BF can be realized with the passive BF antenna according to communication conditions by using SVD and other techniques used for MMUs, alternatively, BF can be achieved by selecting from a predefined weight matrix, which reduces processing overhead. Although the number of transmit/receive chains is limited, and thus not as flexible as MMUs. This paper investigated the optimization of antenna sub-array configuration for passive antenna BF in beyond 5G cellular systems through system simulation. It is demonstrated that the passive BF antenna can mitigate inter-cell interference and enhance communication capacity.

2.40. UWB Dual- Slant Polarized Radiation Reconfigurable Slot-Loaded Antenna Array

Mahrukh Khan and Michael Brown (The College of New Jersey, USA)
This paper discusses the design of a 2x2 dual-polarized UWB slot-loaded antenna array. A novel constellation of antenna elements has been realized, such that two symmetrical slot-loaded patches face each other at 45o from the x and y-axis. The excitation of two opposite patches excites three dual beam modes simultaneously. The antenna array shows 35% impedance bandwidth and produces a dual beam with slant polarization (+/-45o) and a peak gain of 5 dBi. By controlling the phase of opposite ports, the array produces a single directional beam with a symmetrical radiation pattern, stable polarization, and peak gain of 8.5 dBi. A simple feed arrangement enables the dual polarization in the MIMO antenna array. The CMA analysis revealed the effect of the radiation characteristics of multiple modal fields on the radiation pattern of the antenna array.

2.42. A Pattern Reconfigurable H-Slot Dielectric Resonator Antenna for WI-FI Application

Yuerong Liu (University of Electronic Science and Technology of China, China); Francis Keshmiri (Huawei Technologies, France); Yuandan Dong (University of Electronic Science and Technology of China, China)
Based on an H-shaped slot excitation, a novel pattern reconfigurable dielectric resonator antenna is proposed in this paper. The electric field distribution of the main dielectric radiator can be flexible switched through the control of the PIN diodes across the H-slot. It could realize flexible switch of four directional patterns with Phi = 0/90/180/270 deg. It also features a compact size of 0.48λ0×0.48λ0×0.13λ0. To verify the working principle of the proposed DRA, it has been fabricated and measured. The measured overlapping impedance bandwidth of the proposed DRA is about 2.2-2.6 GHz (16.3%), which are wide enough for the WI-FI application (2.4-2.48 GHz). The simulated peak gain of each state exceeds 3.96/4.85 dBi, and the radiation efficiency is greater than -1.5dB (70%). The proposed antenna can be well applied for space-limited，complex and intelligent Wi-Fi application.

Room: Poster level 2

PE2 (level 2) - Electromagnetics II

T07 Electromagnetic modelling and simulation tools / / Electromagnetics

Chairs: Juan Córcoles (Universidad Politécnica de Madrid, Spain), Federico Giusti (University of Siena, Italy)

2.41. Investigating a Non-Linear Iterative Solver Ensemble Method for Microwave Imaging

Seth Cathers, Colin Gilmore and Ian Jeffrey (University of Manitoba, Canada)
We present a simple ensemble method for microwave imaging that combines four different non-linear iterative inversion solutions to the same imaging problem. The goals of this approach are (1) to improve the overall image quality and (2) potentially quantify confidence in the final microwave image of unknown targets. Results obtained with experimental data from a 2D near-field imaging system demonstrate that while overall image quality may be improved, and some regions of the variance between algorithms shows accurate areas of error/uncertainty, each imaging algorithm can fail in similar ways as they are applied to the same target data. This suggests that future work to produce ensemble results from different data (e.g., different frequencies or different transceiver configurations) could be used to improve microwave imaging results and provide estimates of error in unknown targets.

2.43. A Fast Wavelet-Based Hybrid Method to Model the RCS of Metallic Targets in Maritime Environment

Corentin Carré (Lab-STICC, France); Thomas Bonnafont (Lab-STICC, France & ENSTA Bretagne, France); Ali Khenchaf (ENSTA Bretagne & LAB-STICC UMR CNRS 6285, France)
This article focuses on a hybrid wavelet-based model to compute the radar cross section (RCS) of metallic targets in a maritime environment. The latter is based on the parabolic wave equation, solved in the wavelet domain, for the propagation to the target and the wavelet-based method of moments for the scattered field. Key advantages include its ability to account for terrain relief and refraction effects within the propagation channel, as well as providing accurate RCS calculations. Additionally, wavelet-domain compression enables a flexible trade-off between computational efficiency and precision. Numerical experiments in the VHF-band are performed to validate the method.

WEDNESDAY

2.44. Analysis of Drude-Like Plasma Scatterers via the Reduced-Basis Method for Phase-Gradient Reconfigurable Metasurfaces Design

Clara Iglesias-Tesouro (Universidad Politécnica de Madrid, Spain); Valentin de la Rubia (Universidad Politecnica de Madrid, Spain); Alessio Monti and Filiberto Bilotti (Roma Tre University, Italy)

In this work, we explore the EM response of Drude-like plasma scatterers with diverse geometries and physical configurations, aiming to design a phase-gradient reconfigurable metasurface. We use the Reduced-Basis Method (RBM) to obtain a reduced order model (ROM) of Maxwell's equations parametrized only by the plasma frequency of the considered scatterer. We take advantage of the efficiency and reliability of RBM to study the propagation of an electromagnetic (EM) wave through several types of plasma-based metasurfaces, analyzing different operating conditions and structural configurations.

2.45. Conure: Expanded Surrogate-Based Artwork Generator for RFCMOS Transformers

Habibur Rahman, Adrian M Llop Recha, Dag Wisland and Kristian G Kjelgård (University of Oslo, Norway)

This paper presents an enhanced version of Conure, a surrogate-based artwork generator designed for RFCMOS transformers. The tool now includes a graphical interface for visual artwork generation, parameter sweeps, and integrated EM simulations. Conure supports the generation of feed-forward artificial neural network-based surrogate models with reduced computational overhead. Using 65nm CMOS technology, we developed six transformer designs with ratios ranging from 1:1 to 4:3 and trained surrogate models on 105 datasets per design. Model accuracy, evaluated with mean absolute error, mean square error, and R^2 score, showed an R^2 score better than 0.9627. Notably, the models could be trained with only 10% of the dataset previously required while maintaining high accuracy. Conure significantly reduces computational time and improves efficiency in transformer-based circuit design.

2.46. Cubic B-Splines for Hardware-Accelerated Antenna Beampattern Interpolation

Joel Antoine Naviliat (Technische Universitaet Ilmenau, Germany); Sebastian Semper (Technische Universität Ilmenau, Germany); Michael Döbereiner (Fraunhofer Institute for Integrated Circuits IIS & Technische Universität Ilmenau, Germany)

For applications that require fast evaluations of an antenna's beampattern, we propose a computationally efficient interpolation technique based on cubic B-Splines. We expand the pattern into a sum of finite-support polynomial functions that allow a fixed runtime evaluation irrespective of the antenna's aperture size. Further, we show how B-Splines can be implemented efficiently on GPU hardware leveraging so-called texture memory. We outline how oversampling, i.e. decreasing the distance between adjacent B-Splines, can approximate ideal low-pass filtering. Comparison to the Effective Aperture Distribution on measured antenna calibration data shows a 10-fold speedup in runtime while attaining an accuracy of -100 dB. When used for direction estimation using antenna arrays, we show that the proposed B-Spline interpolation yields a statistically efficient estimator, as it attains the Cram´er-Rao Lower Bound.

2.47. Design of Tapered Extended Interaction Structures for Particle Acceleration and Terahertz Generation

Davide Guarnera (University of Reggio Calabria Mediterranea, Italy); Roberta Palmeri (Università Mediterranea of Reggio Calabria, Italy); Andrea Locatelli (Università degli Studi di Brescia, Italy); Giuseppe Torrisi and Giorgio Sebastiano Mauro (INFN-LNS, Italy); Bacci Alberto (INFN-Milano, National Institute for Nuclear Physics, Italy); Nunzio Salerno (University of Catania, Italy); Santi Concetto Pavone (Università degli Studi di Catania, Italy); Gino Sorbello (University of Catania, Italy)

We present design methodologies and Figures of Merit (FoM) for developing extended interaction structures intended for particle acceleration and/or terahertz generation. The proposed Physics-Based (PB) approach enables the design of structures with a continuous matching of subrelativistic electrons with electromagnetic guided waves and works by gradually adjusting the wave phase velocity along the interaction structure to match with the electron speed. Our focus is on geometries where the guided mode of the electromagnetic field and the particle beam propagate co- linearly, since this configuration offers superior scalability and performance compared to transverse illumination configurations. Moreover, only such interaction structures can work also in reverse mode for electromagnetic wave generation.

2.48. Extreme Field Confinement in All-Dielectric Metasurface Cavities

Pietro Brugnolo, Samel Arslanagić and Rasmus E. Jacobsen (Technical University of Denmark, Denmark)

Bound states in the continuum enable extreme confinement of electromagnetic energy in structures otherwise open to incoming waves. In recent years, they have been demonstrated in various photonic systems and single resonators. Presently, we investigate Fabry-Pérot resonances in a planar cavity consisting of two all-dielectric metasurfaces. The metasurfaces are characterized by their effective magnetic and electric surface impedances enabling an analytical approach. The resonance conditions are derived and two cavity designs comprised of metasurfaces of all-dielectric spheres are investigated. The analytical and numerical results obtained for the two designs are compared showing excellent agreement, with quality factors of ~1700 and ~6500, respectively. Furthermore, we show that the proposed approach can be extended to other geometries, presenting a design for a cylindrical cavity enclosed in a concentric metasurface with quality factor ~17000. The proposed metasurface cavity may be of interest for the design of filters, antennas, sensors, and nonlinear systems.

WEDNESDAY

2.49. Generalized Transition Matrix Model Using Multilevel Characteristic Basis Function Method for Electrically Large Open-Ended Cavity Problems

Inhwan Kim, Hyeong-Rae Im and Youngjae Yu (Yonsei University, Korea (South)); Hyunsoo Lee (Inha University, Korea (South)); Ic-Pyo Hong (Kongju National University, Korea (South)); Jong-Gwan Yook (Yonsei University, Korea (South))

This paper proposes an accelerated method for solving electrically large open-ended cavity problems by combining the generalized transition matrix (GTM) model with the multilevel characteristic basis function method (CBFM). The electric surface currents on the perfect electric conductor (PEC) surface are represented using characteristic basis functions (CBFs), which are precalculated through the multilevel CBFM. By reducing the number of unknowns, the computational cost for solving the problem is also reduced. This paper presents the formulation of the GTM model and multilevel CBFM, enabling efficient computation with lower computational complexity. Numerical simulation results are discussed, including comparisons with the commercial full-wave simulation, FEKO.

2.50. Groundless Eco-Friendly Water and PLA Based Artificial Magnetic Conductor

Edoardo Giusti, Pierpaolo Usai and Danilo Brizi (University of Pisa, Italy); Agostino Monorchio (Pisa University & CNIT, Sweden)

A groundless, eco-friendly, water and PLA based Artificial Magnetic Conductor (AMC) is presented in this manuscript, completely eliminating the need for metallic components. Environmental concerns are becoming a significant focus in many research fields, where the emphasis is not only on performance improvement but also on the sustainability of the devices manufacturing process. The proposed multilayer structure was designed by exploiting accurate numerical simulations. Specifically, the absence of a metallic ground is compensated by the insertion of a water-filled cavity, which improves isolation between the two AMC sides. The prototype was constructed by using commercially available PLA, printed with a standard 3D machine, and filled with distilled water in the required areas. The structure exhibits an excellent electromagnetic behavior as a Perfect Magnetic Conductor (PMC) in the 2-4 GHz band, as verified through waveguide measurements. The obtained AMC bandwidth is relatively large, being approximately 45% centered around 3.55 GHz.

2.51. Impedance Engineering of TaN-Based Resistive Metasurfaces for the Design of Wideband Absorbers

Rana Muhammad Hasan Bilal (University of Pisa, Italy); Stefano Moscato (SIAE Microelettronica, Italy); Michele Borgese (Surrey Satellite Technology Ltd, United Kingdom); Simone Genovesi, Giuliano Manara and Filippo Costa (University of Pisa, Italy)

This article presents the design and comprehensive analysis of a metasurface absorber, focusing on impedance engineering by controlling the shape of the TaN-based resistive surfaces. The proposed absorber features a design composed of square gold patches interconnected with TaN-based resistive surfaces, forming a cross-like unit cell. An analytical equivalent model based on RLC components is developed to provide insights into the impedance characteristics of the proposed absorber. Moreover, a detailed analysis on the impedance characteristics of the absorber is conducted by varying different sizes of the TaN resistive surfaces. Ultimately, this analysis shows that selecting the optimum size of TaN allows for achieving the desired value of the real component of impedance, which enables the design of a wideband absorber.

2.52. Incident-Angle-Insensitive Dual-Polarized Metacell Using Machine-Learning-Based Optimization

Peiqin Liu, Yuqing Zhou and Zhi Ning Chen, Z. N. Chen (National University of Singapore, Singapore)

In this paper, an incident-angle-insensitive, dual-polarization metacell is proposed using a machine-learning-based optimization method. The metacell is based on a three-layer dual-polarized metacell with two substrates vertically and symmetrically integrated, which enhances transmission performance across a wide range of incident angles for both TE and TM waves. A seven-layer artificial neural network (ANN) model is employed to optimize the metacell dimensions and achieve the desired performance. The input data for the ANN consists of the target transmission responses and the incident angle. The neural network predicts the geometric parameters that meet the specified performance criteria. As a result, a dual-polarized metacell is optimized to exhibit incident-angle insensitivity up to 60° for both TE and TM incident waves.

2.53. Reconstruction of Target Attributed Scattering Centers in SAR Images Based on Adaptive Termination Threshold Method

Zhishuang Lin, Shen Ren and Jinxing Li (School of Physics, Xidian University, China); Min Zhang (Xidian University, China)

An orthogonal matching pursuit (OMP) algorithm with an adaptive termination threshold is proposed for the reconstruction of target Attribute Scattering Centers (ASCs) in synthetic aperture radar image. By applying image segmentation to Synthetic Aperture Radar (SAR) images, a binary mask that distinguishes target regions from background noise is created, facilitating the computation of the signal-to-noise ratio (SNR) and the dynamic adjustment of the termination threshold. The OMP algorithm is then used for the extraction and reconstruction of the ASCs within the SAR images. Experimental validation, based on MSTAR measured data and SAR images simulated using the geometrical optics and physical optics (GO-PO) method, demonstrates the superior reconstruction performance of the proposed method, especially regarding background noise suppression. Furthermore, SAR images of identical ship targets from standard simulations have similar SNRs, allowing for a uniform termination threshold. This work corroborates the effectiveness of the presented ASCs extraction methodology.

WEDNESDAY

2.54. Simulation of SatCom Radome in Ku/Ka Bands

Lalaina Rakotondrainibe, Benoit Chaigne, Emilien Despres and Toufic Abboud (IMACS, France); Alexandre Piche (Airbus Operations, France); Romain Pons (Airbus Defence and Space, France); Olivier Verstraete (Airbus Operations SAS, France); Christophe Bernus (Airbus France, France); Muriel Jerome (Airbus Operations SAS, France); Gérard-Pascal Piau (Airbus, France); Shah Nawaz Burokur (LEME, France)

Numerical simulation of SatCom radome performance in Ku/Ka bands is a highly relevant topic, especially with the development of Flat Panel Active Antennas and Low Earth Orbit (LEO) mega-constellations. A typical SatCom radome consists of a complex stack of dielectric layers with various refractive indices and thicknesses, which may be very small compared to the wavelength. Multilayer stacks are first optimised using 1D models of infinite flat layers with far-field assumptions. SImulating 3D radome structure is very challenging for numerical methods due to the scale differences between the size of the radome, the wavelength, and layer thicknesses. This results in the resolution of very large, ill-conditioned linear systems. We have chosen a BEM H-matrix solver using DDM approach. The method has been validated numerically, and a study on a real radome shows excellent agreement with experimental measurements.

2.55. Swarm Intelligence Parametric Yield Optimization of Microwave Devices Using the Non-Linear Partial Least-Squares Polynomial Chaos Expansion Technique

Ketshabile Nfanyana, Leanne Bodenstein and Petrie Meyer (Stellenbosch University, South Africa); Ville Viikari (Aalto University & School of Electrical Engineering, Finland); Jan H. S. Bergman and Juha Ala-Laurinaho (Aalto University, Finland)

The effects of parameter geometry deviations can be mitigated at the design phase through optimization of suitably selected statistical figures of merit, such as yield. Optimization of yield is normally carried out with the use of the Monte Carlo method. This is a computationally expensive procedure due to the need of multiple full wave electromagnetic (EM) simulations. To alleviate this issue, surrogate modelling techniques are commonly used. However, common surrogate modelling techniques suffer from the curse of dimensionality. This work proposes a technique for optimization of high frequency devices, which relies on the NLPLS-PCE technique. NLPLS-PCE is incorporated in a swarm intelligence framework for the adaptive adjustment of design parameters as well as a convergence safeguard. The yield optimization method is demonstrated using a KA band Ridge waveguide filter terminated with a Vivaldi antenna.

2.56. Trust-Region-Based Multi-Branch Machine Learning-Assisted Optimization for Ultra-Wideband Antenna

Qi Wu and Weiqi Chen (Southeast University, China); Haiming Wang (Southeast University, China & Purple Mountain Laboratories, China); Xin Xu and Wei Hong (Southeast University, China); Weishuang Yin (ZTE Corporation, China)

In this paper, a trust-region-based multi-branch machine learning-assisted optimization (TRMB-MLAO) method is proposed for ultra-wideband antenna design. By introducing techniques including trust-region design space constraint strategy, multi-branch lower confidence bound acquisition function and multi-point acquisition function composition into machine learning-assisted optimization scheme, the proposed method achieves better convergence speed and antenna performance compared with conventional algorithm. An ultra-wideband antenna is introduced to validate the effectiveness of the proposed method.

2.57. Urban Path Loss Modelling: Integrating Machine Learning and Geometry Extraction

Mostafa Jassim and Thomas Kürner (Technische Universität Braunschweig, Germany)

In this study, we present a comprehensive system for path loss prediction that integrates data from both real measurement campaigns and ray tracing simulations for outdoor scenarios. By leveraging the strengths of LightGBM, a powerful gradient boosting framework, optimized through Optuna, an advanced hyperparameter optimization tool, we aim to enhance the model's accuracy and efficiency. The system pipeline encompasses several stages, including setting up scenarios, feature extraction, preprocessing, and model training, followed by thorough performance evaluation.

2.58. Variations of Complementary Split-Ring Resonators' Composite Media for In-Plane Wave Propagation

Michalis Nitas (Aristotle University of Thessaloniki, Greece); Samel Arslanagić (Technical University of Denmark, Denmark)

We present a numerical eigenmode approach for the investigation of the electromagnetic properties of complementary split-ring resonator media. Initially, we prove the necessity for metal backing of the structure, so as to support the resonant modes. Subsequently, we perform a parametric study modifying the distance between the resonators and the ground plane and observe the changes in the dispersion diagram. We finally propose a complementary resonator medium terminated partially at a ground plane, which maintains the dispersion diagram and the supported modes of the original, bulky metal-backed version.

WEDNESDAY

2.59. Enhancing Electromagnetic Skills Through Project-Based Learning in Short Courses on Wearable Antenna Design, Fabrication and Measurement

Thennarasan Sabapathy (University Malaysia Perlis, Malaysia); Manavalan Saravanan (Vel Tech Rangarajan Dr. Sagunthala R&D Institute of Science and Technology, India); Suresh Ponnan (Vel Tech Rangarajan Dr Sagunthala R&D Institute of Science and Technology, India); Muzammil Jusoh (Universiti Malaysia Perlis, Malaysia)

This paper presents importance of project-based learning approach in conducting a short course to enhance students understanding of antenna design. The main theme of the course focuses on advanced antenna design using electromagnetic (EM) simulation and use simple fabrication techniques and to measure the performance measurement using a vector network analyzer (VNA). The curriculum combines theoretical instruction with practical, hands-on activities, ensuring a comprehensive learning experience. The assessment strategy is framed to address both individual and group work, in order to increase collaboration among the student peers and to facilitates critical thinking. Student feedback was collected to evaluate the effectiveness of the course and identify areas for improvement.

2.60. High-Gain and High-Selectivity Filtering Folded Reflectarray Antenna for Millimeter-Wave Broadband Applications Using Similar Elements

Wen Fu, Gert Pedersen and Shuai Zhang (Aalborg University, Denmark)

A high-gain and high-selectivity filtering folded reflectarray antenna (FFRA) for millimeter-wave broadband applications is proposed, utilizing similar elements. First, a frequency selective surface (FSS) is designed, featuring a wide passband and high frequency selectivity. Based on this FSS, a polarization selective surface (PSS) and a reflectarray are developed. The reflectarray achieves high frequency selectivity and polarization conversion within the range of 23.6 GHz to 31.6 GHz. The proposed FFRA consists of the PSS as a subreflector, the reflectarray as the main reflector, and a horn feed antenna. It has a 3 dB relative fractional bandwidth (RFBW) of 16.88 % (25.6 GHz to 30.3 GHz) and exhibits outstanding filtering characteristics, resulting from the combined effects of the PSS and the reflectarray. The simulated realized gain reaches 24.1 dBi at 28 GHz with an aperture efficiency of 17.6 %.

Room: Poster level 2

PM2 (level 2) - Measurements II

T04 RF sensing for automotive, security, IoT, and other applications / / Measurements

Chairs: Shoaib Anwar (Microwave Vision Group, Satimo Industries, France), Lorenzo Crocco (CNR - National Research Council of Italy, Italy)

2.1. Autonomous Drone Measurement Approach for Flying Base Stations

Sotirios Tsakalidis, George Tsoulos and Georgia E. Athanasiadou (University of Peloponnese, Greece); Vassilis Tsoulos (University of Pelponnese, Greece)

The widespread use of Unmanned Aerial Vehicles (UAVs) has been the key in expanding the application domain for antenna and field measurements. This paper proposes an original system for the transmission patterns of flying basestations, using two drones. While one drone acts as a fixed radiation source with a transmitting antenna, the other conducts a survey over predefined trajectories to capture the received signal strength. The results from various flight plans-circular, cylindrical, and spherical-revealed consistent signal strength variations with max fluctuations of approximately 2.5 dB along the vertical axis, and the spherical flight providing comprehensive spatial coverage, all peaking towards the horizontal mounting pole of the transmit antenna. This work can serve as the basis for developing efficient UAV based measurement methods that will facilitate flying ad-hoc deployment and optimization of communication networks.

2.2. Design of High Frequency Resonator for Dielectric Spectroscopy

Antonio Alati (Università Della Calabria, Italy); Emilio Arnieri (University of Calabria, Italy); Giandomenico Amendola (Università della Calabria, Italy); Marco Lanuzza (University Of Calabria, Italy); Luigi Boccia (University of Calabria, Italy)

A design for a cost-effective one-port patch antenna for high-frequency (20GHz) dielectric spectroscopy is presented. The sensor comprises a microstrip input line, a quarter-wavelength transformer for impedance matching, and a patch antenna with a milled channel adjacent to its radiating element, allowing fluids to influence its resonant frequency. A circuit model explains the operating principle, showing that shifts in resonant frequency correspond to variations in the real part of the fluid's permittivity. The sensor's performance is assessed through finite element method (FEM) simulations under various material conditions. Results indicate that the sensor's response is predominantly governed by the real part of permittivity, with minimal impact from dielectric losses. Calibration using reference fluids in simulations yields a predictive model with high accuracy ($R^2 > 0.99$). Experimental validation and prototyping are planned for future work.

2.3. In-Situ Measurement of Patch-Antenna Thermal Properties Using Fibers Bragg Grating in a Semi-Anechoic Environment

Guillaume Cartesi (CEA, France); Thibault Charlet (CEA CESTA, France); Fabien Degery (CEA CESTA); Sébastien Hulin (CEA CESTA, France); Olivier Raphel (CEA, France); Yves Tugend (CEA CESTA, France); Emile Binot (CEA, France)

The performances of an antenna can be more or less sensitive to its thermal environment depending on its design. Actually, warming up of an antenna can mechanically deform all the parts constituting the antenna and also modify the electric properties of the materials used. In this paper we present the first results of the evolution of the antenna return loss under thermal stress in a semi-anechoic environment. A patch antenna was set up on a heating support localized at the center of a near-field 3D measurement facility. In particular, two fiber Bragg gratings were set up to achieve many acquisitions of the antenna temperature without disturbing its electromagnetic fields, and consequently its performances. This work highlights a great compatibility between optic fibers and antenna, which could permit to acquire its thermal properties with a high accuracy during an electromagnetic measurement.

2.4. Measurements of the Thermal Radiation Emitted from Silicon Wafers at Sub-THz Frequencies

Laurens F.E. Beijnen and Juan Bueno (Delft University of Technology, The Netherlands); Yanwen Chen (University of Siena, Italy); Paolo Sberna, Marco Spirito and Andrea Neto (Delft University of Technology, The Netherlands)

The thermal energy radiated by silicon wafers with different conductivities is characterized experimentally in the mm and sub-mm wave ranges. These samples are heated up, and the energy that they radiate thermally is captured by different horn antennas covering the frequency band between 75 and 500 GHz. The energy radiated (in the order of pW) and collected by the horn antennas is subsequently detected by zero bias Schottky diodes (ZBDs). The ZBDs have a noise equivalent power in the order of a few pW/Hz^1/2, rendering the measurements possible. The measured thermal radiated power agrees with the prediction from Planck's law for the highly doped wafers, corresponding to high conductivities. However, for low conductivities, the measurements show a descending pattern as a function of the frequency, which is not in line with expectations from Planck's law. Parallelly, we have developed a theoretical model providing a classical explanation of these results.

2.5. Non-Invasive Skin Cancer Detection: A High-Resolution Millimeter-Wave Time Reversal Approach

Fatemeh Ravanbakhsh (Islamic Azad University, Iran); Alireza Madannejad (KTH Royal Institute of Technology, Sweden); Javad Ebrahimizadeh (KU Leuven, Belgium)

This paper introduces a novel non-invasive skin cancer detection system using a high-resolution millimeter-wave time reversal imaging approach. Operating in the 2-30 GHz frequency range, the system utilizes two moving Vivaldi antennas to scan the imaging area, significantly reducing hardware complexity and cost compared to conventional systems. The system features a skin-removal technique that eliminates surface reflections, improving subsurface imaging accuracy. Through time-reversal methods, particularly the DORT algorithm, the system achieves high-resolution imaging capable of detecting both single and multiple tumors. In tests with phantoms, the system successfully identified single tumors with diameters of 5 mm and 8 mm and multiple tumors of 8 mm in close proximity. The worst-case positioning error for single tumor detection was 4 mm, and for multiple targets, 14 mm. The system also exhibited a high signal-to-clutter ratio (SCR) of up to 10.8 dB, demonstrating its effectiveness in distinguishing between benign and malignant tissues.

2.6. Resonator Measurements of Magnetic Microwave Absorbers at Cryogenic Temperatures

Alexandra J Brönnimann (University of Bern, Switzerland); Lorenzo Ciorba (University of Bern & Institute of Applied Physics, Switzerland); Tobias Plüss and Axel Murk (University of Bern, Switzerland)

This paper details a basic measurement technique of material losses using a cavity resonator. Magnetic losses can be determined using the TE011 mode of the resonant cavity. Microwave absorber materials containing ferrite and iron were tested at ambient and cryogenic temperatures. It was found that the ferrite sample generated higher loss when cooled, whereas the iron samples did not show much variation.

2.7. Skin Dosimetry Analysis Based on a Spatial Synthetic Exposure Equipment at 60 GHz

Kun Li (The University of Electro-Communications, Japan); Takashi Hikage (Hokkaido University, Japan); Hiroshi Masuda and Etsuko Ijima (Kurume University School of Medicine, Japan); Akiko Nagai (Aichi Gakuin University, Japan); Kenji Taguchi (Kitami Institute of Technology, Japan)

This study presents a millimeter wave dosimetry analysis based on a spatial synthetic exposure system for real animal experiments. The exposure system consists of two lens antennas operating at 60 GHz, creating a focused radiation beam area within 1 cm^2 at the skin surface of the exposure target. The spatially averaged absorbed power density (sAPD) at the skin surface was calculated by FDTD method using a high-resolution rat voxel model. Considering the potential misalignment of the exposure beam in realistic experiments, the deviation in sAPD caused by the location of the focal beam was analyzed. The results showed that, compared to the variation caused by the separation distance between the antenna and the skin surface, the misalignment of the synthetic beam center on the exposed area may have a larger impact on the calculated sAPD.

WEDNESDAY

2.8. Sustainable X-Band Microwave Absorber Using Tea Waste and Recycled Carbon Composites

Naveen Kumar (CHRIST University, Bangalore, India); Mohsen Koohestani (ESEO School of Engineering & IETR, University of Rennes, France); Sourav Roy and Hari Murthy (CHRIST University, Bangalore, India)

This paper introduces an innovative eco-friendly flat microwave absorber designed for X-band applications, utilizing plant waste and recycled materials, thereby contributing to a circular economy. The composite material is composed of 75% used tea powder and 25% carbon sourced from discarded batteries. The electromagnetic (EM) absorption performance of the proposed composite has been characterized, revealing enhanced absorption capabilities, averaging around 26.2% for a thickness of 5 mm, compared to a 100% tea waste configuration across the X-band frequency range. Furthermore, the results indicate that EM absorption improves with increasing frequency. The environmental advantages of this composite, including waste reduction and a minimal carbon footprint, position it as an attractive alternative to conventional RF absorbers. This sustainable solution shows promise for applications in EM interference shielding and microwave energy harvesting.

Room: Poster level 2 | **PP2 (level 2) - Propagation II**

T05 Positioning, localization, identification & tracking / / Propagation

Chairs: Nektarios Moraitis (National Technical University of Athens & Institute of Communications and Computers Systems, Greece), Ashray Ugle (Sorbonne University, France)

2.9. Array Antenna Diagnosis Using Self-Paced Learning Convolutional Neural Networks

Yinghao Zhang (South China University of Technology, China); Hao Jiang (South China University of Technology & School of Electronic and Information Engineering, China); Youpeng Bao, Shaowei Liao and Quan Xue (South China University of Technology, China)

The array antenna diagnosis is known as a computationally-cost task that requires many iterations to get the solution. In this article, a self-paced learning convolutional neural network (CNN) is proposed for array diagnosis. The proposed method is able to efficiently detect the impaired elements from the measured far-field radiation patterns. However, due to the noise in the complex electromagnetic environment, the diagnostic accuracy of the method is significantly decreased. To address the problem, the self-paced learning strategy is utilized to enable CNN to gradually learn the samples from "easy" to "difficult". As the training progresses, the CNN gradually improves its ability to learn difficult samples, becoming more adept at processing noisy samples. The proposed method is available for the planar array with mutual coupling effect. Numerical simulation are carried out to demonstrate the superiority of the proposed method by comparing with the CNN method and the compressed sensing method.

2.10. Clutter Removal in Automative Radar Using 3D Autoencoder

Insoo Choi, Juho Cha, Youngwook Kim and Wonhyo Kim (Sogang University, Korea (South))

This paper proposes utilizing a 3D autoencoder for the removal of clutter in automotive radar data. Automative radar systems, particularly rear corner radars, are an important role for detecting objects in blind spots but often suffer from clutter caused by environmental elements like buildings, guardrails, and trees. Previous approaches using 2D autoencoders have difficulty distinguishing between targets and clutter when their characteristics, such as size and power, are similar. By extending to 3D autoencoders, this method processes time-varying RD-maps, achieving superior clutter removal and real-time target detection performance by leveraging time-varying information. The 3D autoencoder was trained on simulated FMCW radar data, and to validate its performance, RD-maps measured from an actual FMCW radar were input into the trained 3D autoencoder for evaluation. The results confirmed that clutter was successfully removed even in actual environments.

2.11. Clutter Tracking Using Variational Message Passing

Anders Malthe Westerkam and Troels Pedersen (Aalborg University, Denmark)

We propose a message passing algorithm for tracking of clutter signals in MIMO radar. The method exploits basis expansion to linearise the signal model, to enable mean field approach for tracking the posterior distribution of the clutter as it evolves across time, as well as the mean and precision of the clutter map. The method shows good estimation accuracy in simulations for a scenario that adhere to the statistical model used for derivation as well as one that does not. The complexity of the method is linear in both the amount of parameters chosen and the amount of data under consideration.

2.12. Effective-Height Analysis of UWB Antenna Arrays for TDoA and PDoA Estimation

Tobias Lafer (NXP Semiconductors & Graz University of Technology, Austria); Michael Gadringer (Graz University of Technology, Austria); Ulrich Muehlmann (NXP Semiconductors, Austria); Franz Teschl and Klaus Witrisal (Graz University of Technology, Austria)

To assess antenna influences on time-difference of arrival (TDoA) and phase-difference of arrival (PDoA) measurements in ultra-wideband (UWB) radio systems, we propose extensions of effective-height-based analysis methods for standalone antennas to multi-antenna arrangements, which can be applied to simulations and measurements. Each antenna element is modelled as an LTI system, with its effective height as angle-of-arrival-dependent transfer function. The obtained effective heights consider coupling effects between the antenna elements as well as objects in their vicinity. The proposed simulation and measurement procedures were applied to a Vivaldi and a XETS antenna pair. We compare impulse responses as well as PDoA and TDoA estimates obtained from simulation and measurement to discuss influences of the measurement system as well as modelling uncertainties in the simulation.

WEDNESDAY

2.13. Efficient Array Pattern Prediction Using a Deep Learning Algorithm

Yinghao Zhang (South China University of Technology, China); Hao Jiang (South China University of Technology & School of Electronic and Information Engineering, China); Youpeng Bao, Shaowei Liao and Quan Xue (South China University of Technology, China)

In this article, a deep-learning (DL) algorithm is proposed to efficiently predict the pattern of the antenna array. By establishing the Bayesian-optimized convolutional neural network (CNN) framework, the far-field radiation pattern of the array with arbitrary given array geometry is successfully predicted. Specifically, the CNN is utilized to predict the pattern from the input array geometry and element excitations. The Bayesian optimization algorithm is used to optimize the network architecture to enhance the fitting ability of the CNN. To validate the effectiveness, the proposed algorithm is employed to predict the shaped beam patterns for both linear and planar arrays with various array geometries. Numerical results demonstrate that the proposed algorithm can predict the accurate direction pattern in ms time, and its response speed is more than 6 orders of magnitude faster than that of conventional full-wave simulation.

2.14. Enhanced High-Resolution Imaging for Non-Destructive Testing Using STDCC Radar

Luis Diogo Medina Duarte (Polytechnic University of Leiria, Portugal & Instituto de Telecomunicações, Portugal); Carlos M. Ribeiro (Instituto de Telecomunicações / Instituto Politécnico de Leiria, Portugal); Luis Nero Alves (DETI, Universidade of Aveiro, Portugal & Instituto de Telecomunicações, Portugal); Rafael F. S. Caldeirinha (Polytechnic Institute of Leiria & Instituto de Telecomunicações, Portugal)

This paper presents the first high-resolution imaging experiments for Non-Destructive Testing (NDT) using a Swept Time-Delay Cross Correlator (STDCC) radar. To achieve a high resolution inspection, a reconfigurable radar architecture, along with an agile mmWave dual-polarised transceiver, is proposed. This agile setup allowed authors the study of Synthetic Aperture Radar (SAR) technique performance on object image reconstruction for its inspection. This work focused on the radar reconfigurable parameters to enhance the imaging accuracy of the SAR technique and allow its inspection. Here, we also evaluated the effect that both co-polarisation components had on the target reconstruction. Results demonstrate the proposed radar capability and accuracy to represent and assess a given sample in terms of its physical dimensions and internal features.

2.15. Focusing on Nonlinear Targets Embedded in a Complex Environment

Antton Goicoechea (Université de Rennes 1 & IETR, France); Jakob Hüpfl and Stefan Rotter (Vienna University of Technology, Austria); Francois Sarrazin (Université de Rennes & IETR, France); Matthieu Davy (University of Rennes 1 & IETR, France)

In the microwave regime, electronic devices typically couple nonlinearly with the electromagnetic field. It is then possible to design approaches to detect and/or focus on targets based on their nonlinear interaction with an incoming wave. Here, we build up on a recent technique based on the measurement of a monochromatic scattering matrix at two different incident power. This noninvasive method has been used to focus waves on a single nonlinear target embedded in a chaotic microwave cavity. Here, we extend this work for the case of multiple targets located in a complex environment. We show that we are able to extract wavefronts that focus selectively on each of the targets. Additionally, we tune a disordered system through a reconfigurable metasurface to enhance the intensity received by a nonlinear target over a chosen wide range of frequency.

2.16. Foreground-Target Reconstruction in Computational Microwave Imaging Using a Generative Model

Jiaming Zhang, María García Fernández, Rahul Sharma, Guillermo Alvarez Narciandi and Jie Zhang (Queen's University Belfast, United Kingdom); Muhammad Ali Babar Abbasi (Queen's University Belfast & The Institute of Electronics, Communications and Information Technology (ECIT), United Kingdom); Okan Yurduseven (Queen's University Belfast, United Kingdom)

Although conventional microwave imaging techniques offer high-fidelity image reconstructions, they suffer from significant drawbacks, such as intensive hardware complexity. Computational microwave imaging (CMI)-based systems are often considered alternatives to address these challenges, but they are usually limited by the complexity of the computation layer due to the intensive computational demands for the reconstruction step. Deep learning techniques have been proposed to enhance the computation efficiency, but existing studies primarily focus on scenarios where the imaged targets are isolated. This work explores computational imaging scenarios involving targets of interest overlapping with secondary objects. This article designs a novel generative model to reconstruct the images of the foreground objects of the overlapping imaging targets. While conventional methods require manual removal of background objects for accurate foreground reconstructions in overlapped imaging, the proposed method achieves this by learning features directly from the measured signals, significantly improving the CMI computational efficiency.

WEDNESDAY

2.17. Learning Assisted Sensing Matrix Calculation in Computational Microwave Imaging

Jiaming Zhang, Rahul Sharma and Jie Zhang (Queen's University Belfast, United Kingdom); Muhammad Ali Babar Abbasi (Queen's University Belfast & The Institute of Electronics, Communications and Information Technology (ECIT), United Kingdom); Okan Yurduseven (Queen's University Belfast, United Kingdom)

While computational microwave imaging (CMI) addresses several limitations of conventional microwave imaging techniques, such as hardware complexity, it is still constrained by substantial computational resources required for image reconstruction. This paper presents a convolutional neural network (CNN)-based approach to enhance the computational efficiency of CMI. The proposed network directly computes the transfer function, or sensing matrix, from the aperture fields of antennas within a CMI system. To improve information extraction, convolutional block attention modules (CBAMs) are integrated into the architecture. Numerical results on a testing dataset demonstrate an average normalized mean squared error (NMSE) of 0.054. Compared to conventional methods, the proposed network reduces computation time by 69% in generating the sensing matrix. Overall, the network generates the sensing matrix from two different sets of aperture field distributions with high precision, achieving considerable computational savings for CMI applications.

2.18. Low-Altitude Wind Shear Speed Estimation Method Based on KL Divergence Orthogonal Projection of Matrix Information Geometry

Hai Li, Yifan Qiu, Zan Li, Jingrui Guo and Ruihua Liu (Civil Aviation University of China, China)

To address the issue of poor low-altitude wind shear speed estimation caused by an insufficient number of Independent and Identically Distributed (IID) training samples, a method for estimating low-altitude wind shear speed based on KL Divergence Orthogonal Projection (KLD-OP) of matrix information geometry is proposed in this paper. First, the method constructs a matrix manifold based on the intrinsic distribution of radar echo data. Then, the KL divergence on the manifold is employed to estimate the Clutter Covariance Matrix (CCM), which is subsequently used to partition the clutter subspace. Next, an orthogonal projection matrix is constructed for clutter suppression, and finally, the estimation of low-altitude wind shear speed is achieved. Simulation results validate the effectiveness of the KLD-OP method.

2.19. Low-Cost Bluetooth-Based Testbed for Wireless Connectivity Testing

Mateusz Groth, Jakub Lecki, Lukasz Kulas and Krzysztof Nyka (Gdansk University of Technology, Poland)

As wireless communication technologies and IoT networks expand, there is a growing need for cost-effective, flexible testbeds to evaluate new designs, algorithms, and hardware. Existing testing solutions are often expensive or are limited in scope, which opens up a gap for accessible tools that support diverse wireless experiments. This research addresses this need by developing a low-cost, multi-purpose testbed using Nordic NRF52840 dongles and Raspberry Pi Zero, capable of performing a wide range of tests. The testbed, arranged in a star topology with 36 controllable agents, collects key performance metrics such as Packet Error Rate (PER) and Received Signal Strength Indicator (RSSI) over time. Validation experiments demonstrated the system's effectiveness in measuring wireless performance under real-world conditions, including jamming. This testbed offers a scalable and affordable platform for wireless communication research, providing a valuable tool for academia and industry to develop next-generation wireless technologies.

2.20. Medium-Scale Measurement Campaign for Floating Macroplastic Detection in a Realistic Environment at X-Band Frequencies

Mario Vala (University of Lisbon, Portugal & Instituto de Telecomunicações, Portugal); Joao M Felicio (Instituto Superior Técnico, Portugal & Instituto Telecomunicacoes, Portugal); Tomás Soares da Costa (ULisboa - Instituto Superior Técnico & Instituto Telecomunicações, Portugal); Nuno R. Leonor (Polytechnic Institute of Leiria (IPL) & Instituto de Telecomunicações (IT), Leiria, Portugal); Jorge R. Costa (Instituto de Telecomunicações / ISCTE-IUL, Portugal); Paulo Marques (ISEL-IT Lisboa, Portugal); Antonio A Moreira (IST - University of Lisbon & Instituto de Telecomunicações/ Lisbon, Portugal); Sergio Matos (ISCTE-IUL / Instituto de Telecommunicações, Portugal); Rafael F. S. Caldeirinha (Polytechnic Institute of Leiria & Instituto de Telecomunicações, Portugal); Carlos A. Fernandes (Instituto de Telecomunicacoes, Instituto Superior Tecnico, Portugal); Nelson Fonseca (Anywaves, France); Peter de Maagt (European Space Agency, The Netherlands)

In this paper we assess the possibility of detecting floating plastics in a medium-scale realistic environment using microwave (MW) and RADAR technology at X-band. The measurement campaign performed in the "25 de Abril" bridge over the Tagus River allowed for distances of around 100 m between the antennas and the targets. Several different targets with sizes of 1 m2 were tested and detected. The use of objective metrics also allowed to see which of the targets presented a higher response. This is an encouraging step towards the implementation of such detection techniques onboard drones or airplanes.

WEDNESDAY

2.21. Model-Based Joint Delay-Doppler Estimation for ICAS with Sparse OFDM Resources

Marc Miranda, Sebastian Semper, Christian Schneider and Reiner S. Thomä (Technische Universität Ilmenau, Germany)
Studies have shown that OFDM waveforms are promising candidates for dual functionality radar and communication networks. However, when the transmitted OFDM frame contains sparsely and arbitrarily allocated resources, periodogram based target estimation suffers from high side-lobes and poor multi-path resolution.
We propose an iterative multi-path joint delay-Doppler estimator for OFDM waveforms with sparse and possibly unstructured Frequency-Time resources. We show through simulations that model-based methods achieve greater than Rayleigh resolution without the need for additional interpolation of the sampled channel transfer function. Furthermore, the estimation error as function of delay and Doppler separation is studied and shown to approach the CRB. To address issues of computational complexity, we simplify the exhaustive search step commonly found in Maximum-Likelihood based estimators and propose the use of Fischer-scored gradient optimization that requires only a small number of updates to enhance estimation accuracy.

2.22. Performance Bounds for Coherent Chirp Synthesis in Multiband Signals

Andreas Fuchs, Andreas Feiersinger and Klaus Witrisal (Graz University of Technology, Austria)
Radio-based position estimation is severely affected by multipath radio propagation. A sufficiently large signal bandwidth allows for a separation of the line-of-sight signal component from the multipath components and ensures, therefore, accurate positioning. This paper investigates the possibility of combining multiple, consecutively transmitted subband signals into a combined signal with a scaled-up effective bandwidth. The Cramér-Rao lower bound (CRLB) is derived for this time-of-arrival-estimation problem in order to analyze its scaling behavior. It is found that an overlap of the subband signals in the frequency domain can be exploited to increase the effective signal bandwidth. However, this method is only effective in presence of multipath propagation, it does not yield any gain in AWGN channels without multipath. Theoretical results are validated by means of computer simulations for chirp-based radio signals.

2.23. Spatial Multipath Characterization via in Situ Harmonic Transponders

Jeff Frolik (University of Vermont, USA)
Wireless communication between devices moving in complex environments is prone multipath effects. Thus measuring and characterizing the multipath caused by an environment prior to deploying a system is of interest. Standard approaches nominally require a transmitting source at one end of a link and a separate receiving setup at the other. In this work, we present an alternative in which a passive harmonic transponder is embedded in the environment to be characterized. Harmonic transponders are passive, nonlinear wireless devices that receive an interrogation signal at one frequency (f) and backscatter harmonics (typically, 2f is of interest). Using a remote interrogator (combination of transmitter and receiver), we are able, using an amplitude modulated (AM) interrogation signal, to separately determine the forward link loss at f, from the reverse link loss at 2f. Using the proposed method, we demonstrate the ability to characterize the multipath, over space, of a high-multipath reverberation chamber.

2.24. Subsurface Target Localization by Single-View/Multistatic MUSIC Algorithm

Angela Dell'Aversano (Università degli Studi della Campania L. Vanvitelli, Italy); Antonio Cuccaro (Università della Calabria, Italy); Maria Antonia Maisto (Università degli studi della Campania Luigi Vanvitelli, Italy); Rosa Scapaticci (CNR-National Research Council of Italy, Italy); Raffaele Solimene (Università degli studi della Campania Luigi Vanvitelli, Italy)
The problem of detecting and localizing point-like targets buried in a half-space medium from near scattered field measurements under a single-view/multistatic configuration is addressed. In order to beat the resolution limits achievable by classical imaging methods, a MUSIC algorithm is employed. The MUSIC algorithm is known for providing super-resolving localization when the data correlation matrix is full rank. The point is that the latter circumstance does not hold true for the case at hand. This drawback can be remedied by adopting some smoothing procedure. However, for near-field configurations common smoothing strategies cannot be exploited since the data matrix lacks the required Vandermonde structure. To cope with this issue, the MUSIC algorithm is properly complemented by a suitable pre-processing stage which allows restoring the rank of the data matrix. Then, standard MUSIC algorithm is run and the achievable performance assessed via numerical examples for a 2D scalar geometry.

2.26. Wave Propagation Analysis at 433MHz ISM Band for Wireless Sensor Networks

Saleem Shahid (Graz University of Technology, Austria); Wolfgang Bosch (Graz University of Technology & Institute of Microwave and Photonic Engineering, Austria)
Power efficiency and increased range were key considerations in the design of a wireless sensor network. A 'set and forget' strategy is desirable, particularly for low data rate applications. Zigbee and Bluetooth are two standards used for wireless connectivity at 2.4 GHz. However, due to higher path loss at these frequencies, the range of Zigbee and Bluetooth transceivers is quite limited. DASH7 protocol enabled devices operating in the 433MHz ISM band are an alternative for low data rate, long range wireless connectivity. This paper presents the link performance analysis of the DASH7 protocol on off-the-shelf Wizzi sensor kits. Experimental characterization of the link quality was carried out in environments such as tunnel-like corridors, between buildings, grass fields and straight roads. Packet Error Rate (PER), Received Signal Strength Indicator (RSSI) and link asymmetry were measured at different power levels for different separation distances between the devices.

WEDNESDAY

Wednesday - 14:40-15:20

Room: Alfvén (A3+A4)

Invited Speaker

David R. Jackson

Chair: Francisco Mesa (University of Seville, Spain)

Room: Kildal (A2)

Invited Speaker

Dirk Heberling

Chair: Lars Foged (Microwave Vision Italy, Italy)

Wednesday - 15:50-17:30

WiRS at the EurAAP booth

Wednesday - 15:50-17:30

Room: Alfvén (A3 + A4)

CS48 - Advancement of gap waveguide technology

T02 Millimetre wave and THz for terrestrial networks (5G/6G) / Convened Session / Antennas

Jose I Herranz-Herruzo (Universitat Politècnica de València & APL - iTEAM, Spain), Jian Yang (Chalmers University of Technology, Sweden)

15:50 Meandered Line Design Using Half-Mode Groove Gap Waveguide Technology for Travelling Wave Antennas

Miguel Ferrando-Rocher (Universitat Politècnica de València & Antennas and Propagation Lab, Spain); Jose I Herranz-Herruzo (Universitat Politècnica de València & APL - iTEAM, Spain); Jose-Luis Gómez-Tornero (Polytechnic University of Cartagena, Spain)

This communication presents a traveling wave antenna with frequency-dependent scanning capabilities tailored explicitly for automotive radar applications at a fixed center frequency of 24 GHz. The antenna utilizes a meandered line design based on Half-Mode Groove Gap Waveguide technology, ensuring high efficiency and a low profile despite its metallic composition. This compact and low-profile antenna exhibits fast scanning characteristics within a narrow bandwidth. Over a 5% bandwidth, it achieves scanning angles of 45 degrees (-25 degrees to +20 degrees). Although experimental validation is pending, the simulated results show a directivity close to 22 dBi with 90% radiation efficiency, indicating the need for further experimental verification.

16:10 An Antenna Array with Contactless Feeding Design Using MetaCoax Coupler

Prabhat Khanal (Chalmers University of Technology, Sweden); Alireza Bagheri (Gapwaves AB, Sweden); Xinxin Yang (Qamcom Research and Technology, Sweden); Jian Yang (Chalmers University of Technology, Sweden)

In this paper, contactless capacitively coupled PCB-to-PCB couplers, referred to as MetaCoax, are used to design a feeding layer with beamforming electronics for an 8×8 element circularly polarized antenna array. The simulated performance of the antenna array, both with and without the feeding layer, yields nearly identical results. The antenna with the feeding layer achieves a 15% bandwidth, with active reflection coefficients of ≤ −10 dB and axial ratios of ≤ 3 when scanning within a ±60° volume. This configuration results in a gain reduction of ≤ 0.4 dB compared to a directly fed antenna (i.e., one without the feeding layer).

16:30 PTD Symmetric Double Edge Line

Nelson Castro (University Carlos III of Madrid, Spain); Enrica Martini and Stefano Maci (University of Siena, Italy); Eva Rajo-Iglesias (University Carlos III of Madrid, Spain)

In this paper, we propose a novel backscattering protected PTD-symmetric waveguide in gap-waveguide technology that addresses several challenges encountered in existing designs. The new configuration comprises two edge lines excited by a single mode (either even or odd). This structure not only guarantees robust wave propagation but also simplifies excitation and facilitates integration with gap waveguides. We discuss the design of the waveguide in detail, including the metasurface and the transitions necessary for feeding the proposed structure. A simple microwave branching have been designed, showing a relative bandwidth of 27.5% with low reflection. highlighting the potential of this design for application in mm-wave components. A prototype for later experimental validation is designed and manufactured.

16:50 A 2-Layer Solution for 45° Slant Polarized Slotted Waveguide Arrays in Gapwaveguide Technology

Tom Eriksson (KTH Royal Institute of Technology, Sweden); Alireza Bagheri (Gapwaves AB, Sweden)

A 45° slant polarized radar antenna is designed using gapwaveguide technology. Using slant polarization in radar antennas is beneficial for collision avoidance applications as interference from opposing radars can be reduced. With a curved distribution network, the design complexity of the radiation layer is low allowing for easy fabrication. The element design consists of 4 slanted slots and is implemented in an array resulting in a realized co-polarized gain of 17.18 dBi averaged over the 76-81 GHz frequency band, and can scan to ±50° in the azimuth plane.

17:10 Circular Polarization Switchable Planar Array Antenna Based on Gap Waveguide Technology

Liang-Qin Luo, Yuanjun Shen, Honghuan Zhu, Lei Chen and Tianling Zhang (Xidian University, China)

A dual-band circular polarization switchable planar array based on gap waveguide (GW) technology is presented. The array consists of a dual-circularly polarized (DCP) waveguide radiator that utilizes a septum polarizer, a metal plate with pins, and a 1 to 4 power divider. The polarization of the array can be switched between right-hand circular polarization (RHCP) and left-hand circular polarization (LHCP) by moving the radiator position relative to the other two parts. The simulated results show that the proposed array antenna works in dual bands of 19-21.2 GHz and 27.5-30 GHz, with return loss better than 12 dB, an axial ratio below 3 dB, and an antenna efficiency higher than 68%.

Room: Kildal (A2)

E07 - Frequency/polarization selective surfaces

T08 Fundamental research and emerging technologies/processes / / Electromagnetics

Chairs: Francesco Foglia Manzillo (CEA-LETI, France), Agnese Mazzinghi (University of Florence, Italy)

15:50 Design and Realization of a Dual Band/Broadband Linear to Circular Polarization Converter 3D Printed Through Metalized Stereolythography

Andrea Guarriello and Etienne Girard (Thales Alenia Space, France); Charalampos Stoumpos (IETR, INSA of Rennes, Rennes, France); Frederic Veron (Thales Alenia Space, France); Laszlo Sajti (RHP-Technology GmbH, Austria); Hervé Legay (Thalès Alenia Space, France)

This paper presents the design, fabrication, and validation of a novel linear-to-circular polarization converter for dual-polarization and dual-band Ka-band satellite antennas. The converter, based on a transverse electromagnetic (TEM) cell topology, addresses previous design limitations using Stereolithography Apparatus (SLA) technology and copper cladding. The lightweight, metallic structure achieves high conductivity while minimizing mass. Simulations of the polarizer installed on a high efficiency radiating element show outstanding performances, with an axial ratio (AR) below 1 dB in the TX band (17.3-20.2 GHz), and AR below 2.2 dB in the RX band (27.5-30.5 GHz), and reflection below -17 dB in both bands. Measurements show excellent agreements in RX higher band and fair agreement in lower TX bands, which leave room for future improvements. The unit cell simulation shows dual or broad bandwidth and very low losses, making it one of the best-performing polarizing screen to date.

16:10 Efficient Frequency Selective Surface Analysis via End-To-End Model-Based Learning

Cheima Hammami (University of Carthage, Tunisia); Luc Le Magoarou (INSA Rennes, IETR, France); Lucas Polo-López (IETR-INSA Rennes, France)

This paper introduces an innovative end-to-end model-based deep learning approach for efficient electromagnetic analysis of high-dimensional frequency selective surfaces (FSS). Unlike traditional data-driven methods that require large datasets, this approach combines physical insights from equivalent circuit models with deep learning techniques to significantly reduce model complexity and enhance prediction accuracy. Compared to previously introduced model-based learning approaches, the proposed method is trained end-to-end from the physical structure of the FSS (geometric parameters) to its electromagnetic response (S-parameters). Additionally, an improvement in phase prediction accuracy through a modified loss function is presented. Comparisons with direct models, including deep neural networks (DNN) and radial basis function networks (RBFN), demonstrate the superiority of the model-based approach in terms of computational efficiency, model size, and generalization capability.

16:30 Dual-Band Single-Layer Half-Moon FSS Design for 5G FR1 Frequencies

Stephanie Maes (Ghent University, Belgium); Bram Decoster (University of Ghent, Belgium); Isabel Expósito (University of Vigo, Spain); João Ricardo Reis (Instituto de Telecomunicações and Polytechnic Institute of Leiria, Portugal); Iñigo Cuiñas (University of Vigo, Spain); Manuel García Sánchez (Universidade de Vigo, Spain); Rafael F. S. Caldeirinha (Polytechnic Institute of Leiria & Instituto de Telecomunicações, Portugal); Jo Verhaevert (Ghent University - imec, Belgium)

Frequency-selective surfaces (FSS) serve as open-space filters to block certain radio transmissions in controlled environments, with applications such as enhancing cybersecurity. This paper presents a novel unit cell design for a two-dimensional FSS, consisting of four half-moon elements, specifically optimized for 5G FR1 (Frequency Range 1) bands. We propose a single-layer FSS unit cell capable of dual-band frequency response. Full-wave electromagnetic simulations are conducted to evaluate the performance of the proposed structure, and parametric analyses are performed to derive design criteria that model the influence of key parameters on FSS behaviour. The resulting equations enable tuning of the design for other frequency bands and application-specific requirements, demonstrating the versatility of the proposed approach.

16:50 3D-Printed Multi-Band FSS with Near-Equal Fractional Pass-/Stop-Band Divisions

Xiaojing Lv, Zhen Luo and Yang Yang (University of Technology Sydney, Australia)

This paper presents a frequency-selective surface (FSS) design fabricated by 3D printing techniques and metallization processes. The double-layer spatial filter consists of concentric resonant rings within the hexagonal unit cells, which alternately generate three passbands and two stopbands with equal fractional bandwidths (FBWs). Each passband or stopband contains two transmission poles and zeros, with sharp transitions in the roll-off regions. The tunability can be achieved by reconfiguring the dielectric insertion plate with varied effective permittivities and thickness profiles.

17:10 Fast and Accurate Meshless EM Analysis of Small Defects in a MoM Scheme

Agnese Mazzinghi and Angelo Freni (University of Florence, Italy); Alessandro Mori, Mirko Bercigli and Mauro Bandinelli (IDS Ingegneria Dei Sistemi S. p. A, Italy)

Protruding rivets or minute holes are typical minor on-purpose surface defects affecting aircraft and vehicles. Although these imperfections are smaller than the wavelength of the impinging waves, they can significantly influence the electromagnetic field induced in and scattered by the vehicles. Nevertheless, the analysis of these imperfections through the method of moments poses certain challenges, particularly in terms of mesh generation and numerical simulation. This paper demonstrates that it is feasible to accurately replicate the effects of these imperfections on the field by superimposing small RWG basis function 'patches' into a smooth mesh that omits the imperfections. These patches facilitate the calculation of electric and magnetic currents via the appropriate polarizabilities.

Room: Jansson (31)

EurAPP Working Groups

WG Measurements

Room: Hallén (BAR5)

CS44 - High-power Beam-steerable Antennas and Sub-systems

T04 RF sensing for automotive, security, IoT, and other applications / Convened Session / Antennas

Chairs: Nader Behdad (University of Wisconsin-Madison, USA), Nima Ghalichechian (Georgia Institute of Technology, USA)

15:50 High Power Microwave Antennas: Beam Steering from a Directed Energy Perspective

Hannah Trock and Anna Janicek (Air Force Research Laboratory, USA)

High power antennas are a critical component in high power microwave systems. When integrating these antennas into the high power microwave systems, beam steering becomes an important part of the system's tactical utility. While low-power beam steering techniques have been widely used in the communication and radar industries, there are unique challenges system components must face when transitioning these conventional methods to high power operation such as breakdown and thermal handling. Due to these unique challenges, high power beam steering remains archaic compared to its conventional counterpart. However, beam steering techniques such as rotary joints, active electronically steered arrays, and phase shifters offer examples of what high power microwave systems hope to achieve. Recent advancements in bringing these components to high power using various high power operation techniques shows promise in achieving the level of beam steering seen in conventional applications.

16:10 A 2D Slotted Waveguide Antenna Array Fed by a Single Longitudinal Stage for High-Power Microwave Applications

Zubair Akhter (Directed Energy Research Center, Technology Innovation Institute (TII), United Arab Emirates & Kaust, Saudi Arabia); Fernando Albarracin (Directed Energy Research Center, TII, United Arab Emirates); Evgeny Gurnevich and Abdulla Al-Ali (TII, United Arab Emirates); Joey Trillo (Directed Energy Research Center, Technology Innovation Institute (TII), United Arab Emirates); Ernesto Neira Camelo (Technology Innovation Institute, United Arab Emirates); Luciano P. Oliveira (Technology Innovation Institute, United Arab Emirates & University of Campinas, Brazil); Mae Nasser AlMansoori, Felix Vega and Chaouki Kasmi (Technology Innovation Institute, United Arab Emirates)

In this paper, we present the design and characterization of a two-dimensional -2D- slotted waveguide antenna array tailored for multi-megawatt microwave generators working in S-band. The proposed antenna array leverages 72 radiating slots spanning over a six wave-guiding structure configuration that maintains a compact form factor while maximizes antenna gain. The design incorporates dielectric materials capable of withstanding high-power levels, ensuring reliable performance in demanding environments. Experimental results demonstrate a peak gain of 25.5 dBi at 3 GHz with a return loss better than -15 dB across an operational bandwidth of 2.1%. The design is verified by simulated and experimental characterization.

16:30 Vanadium Dioxide Energy Selective Surface for Nonlinear Wavefront Manipulation

Walter Royal Disharoon and Sree Adinarayana Dasari (Georgia Institute of Technology, USA); Joshua M Kovitz (Georgia Tech Research Institute, USA); Nima Ghalichechian (Georgia Institute of Technology, USA)

A novel vanadium dioxide (VO2) energy selective surface was designed, fabricated, and tested for operation in X-band. VO2 is an insulator-metal-transition phase-change material that exhibits a sharp conductivity change at a temperature of 68°C or with a large electric field. The periodic surface utilizes the nonlinear behavior of VO2 to allow low-power waves to be collected but reject nearby in-band or near-in-band interference sources. The energy selective surface enables a more robust receive chain for high sensitivity receive systems. The four-legged loaded slot energy selective surface has a 3-dB transmission bandwidth between 9.5-10.5 GHz, in the low power state, and a greater than 30-dB rejection (0.1% of power transmitted) in the high-power state. The updated octagonal design has a 3-dB transmission bandwidth between 9-11.5 GHz, and a greater than 25-dB rejection. Fabrication of the new design is ongoing, and measurement results will be presented at the conference.

WEDNESDAY

16:50 Ultra-Wideband, Electronically Reconfigurable Lens Antennas for High-Power Phased-Array Applications

Shiva Hajitabarmarznaki, Jinkai Wu, Halil Topozlu, John Booske and Nader Behdad (University of Wisconsin-Madison, USA)
This paper reviews recent advances in wideband phased-array antennas for high-average power microwave (HAPM) applications, focusing on the challenges of simultaneously achieving high-power handling, electronic beam scanning, and ultra-wide bandwidth performance. Traditional active phased arrays encounter significant challenges in meeting these demands, largely due to the high cost of transmit/receive (T/R) modules with moderate to high power-handling capabilities, as well as the thermal management challenges associated with high-average power. To overcome these limitations, passive phased-array architectures have emerged as a more effective solution. Recent research at the University of Wisconsin-Madison has led to the development of ultra-wideband, high-power-capable, electronically reconfigurable lens antennas utilizing polarization-rotation phase-shifting technology. This innovation not only enables the antennas to handle extreme power levels but also simplifies design and reduces associated costs. The potential of this technology is significant for applications in fields such as electronic warfare, high-power radar, satellite communications, and long-range wireless power transfer.

17:10 A Fully-Digital Phased Array for Not-Rotating IFF

Leopoldo Infante, Nicholas Ricciardella, Valerio Mannocchi, Massimo Angelilli, Carmine Romanucci, Francesco Giovannelli, Giampiero D'emilio, Massimiliano Refice and Alessandro Crescenzi (Leonardo S.p.A., Italy)
Recent developments in the field of radar antennas applications led to great interest in fully digital AESA (Active Electronically Scanned Array) architectures for various applications, going from telecommunications to automotive and defense. In the latter field there are several examples on primary radar but not many on secondary radar. In this paper, a fully digital IFF (Identification Friend or Foe) conformal phased array is shown, with a specific focus on the antenna design, the digital architecture and the antenna system architecture.

Room: Marcuvitz (M3)	ESoA
ESoA Board Meeting	
Wednesday - 16:10-17:40	Exhibitors meeting
Room: Zorn (32)	
Room: Björk (33)	WG Software and Modelling tools
EurAPP Working Groups	
Room: Bergman (34)	WG Small Antennas
EurAPP Working Groups	
Room: Felsen (35+36)	P05 - Channel characterization for massive MIMO

WEDNESDAY

T01 Sub-6 GHz for terrestrial networks (5G/6G) / / Propagation

Chairs: Henrik Asplund (Ericsson Research, Ericsson AB, Sweden), Raffaele D'Errico (CEA, LETI & Université Grenoble-Alpes, France)

15:50 Near-Field Extension for the 3GPP Geometry Based Stochastic Channel Model

Tommaso Zugno (Huawei Technologies Duesseldorf GmbH, Germany); Lutfi Samara (Huawei Technologies Duesseldorf GmbH, Munich Research Center & Technische Universität Braunschweig, Germany); Tommi Jamsa (Huawei Technologies & Tommi Jamsa Consulting, Germany); Mate Boban (Huawei Technologies Duesseldorf GmbH, Germany)
Most of the channel models used for the evaluation of wireless systems, including the 3GPP model, assume operations in the far-field region, where propagation can be modeled using the plane wave theory. However, trends in the evolution of wireless systems foresee an increase in the size of the antenna arrays and a prominent role of high frequency bands, thus providing motivation for an accurate modeling of wave propagation also in the near-field region. In this paper, we propose an extension of the geometry based stochastic channel model developed by 3GPP to support the modelling of wireless channels in the near-field region by using a spherical wavefront model.

16:10 Automated UWB-Based Phased Array Channel Sounding for the 28 GHz mmWave Band

Patrick Hödl (Graz, University of Technology, Austria); Klaus Witrisal (Graz University of Technology, Austria)
Localization and sensing are key features of future 5G and 6G wireless communication networks. To develop these functionalities, high-performance channel sounding is required. This work proposes an automated ultra-wideband (UWB) phased array channel sounder for the 28 GHz mmWave band. The system design and implementation of the channel sounder are presented. It is based on commercially available mmWave phased array antennas with up/down (U/D) converters as frontends and a UWB channel sounder as an intermediate frequency (IF) unit. Post-processing was applied to remove interfering measurement artifacts. The entire measurement setup was verified with an appropriate two-path model. Also, the dynamic range (DR) was checked. After verification, measurement campaigns were conducted to characterize the spatial propagation properties of an indoor laboratory. The results emphasize the need for beam steering and efficient beam management in mmWave systems to compensate for strongly varying path power levels inside a room.

16:30 Channel Measurements and Modelling for Large Antenna Arrays

Niklas Jalden (Ericsson, Sweden); Henrik Asplund (Ericsson Research, Ericsson AB, Sweden); Magnus Thurfjell (Ericsson AB, Sweden)
This paper presents Massive MIMO measurements conducted in Kista, Sweden utilizing one receiving base station antenna array with 448 ports in a typical Urban Macro deployment and 48, 4-port, transmitters located in mixed indoor and outdoor conditions. The measurement data is analyzed and compared to the 3GPP UMa channel model to provide insights on requirements for channel modelling for very large antenna arrays. In general, the UMa model, given its 20 clusters, is too sparse to jointly model both the angular and delay characteristics as seen in measurements for antenna arrays larger than what is commonly deployed today. Further, the analysis of scenarios where part of the array is blocked indicates that the power variation experienced over the array, seems to be sufficiently well captured by a simple knife edge diffraction model when applied per cluster for the dominant directions.

16:50 Mitigating Sea Surface Fading with D-MIMO: Experimental Validation

Michiel Sandra, Sara Willhammar and Anders Johansson (Lund University, Sweden)
The performance of wireless communications at sea are often limited by fading caused by reflections at the sea surface. The reliability could potentially be improved by employing multiple antennas. We have conducted massive multiple-input multiple-output (MIMO) measurements at sea in order to evaluate the performance. The measurements were conducted at 5.6 GHz with 64 dual-polarized antennas, which were distributed vertically in groups of eight antennas. We evaluated the CDF of the maximum-ratio combined channel gain for different number of antennas, and compared distributed and co-located antenna configurations. We conclude that having distributed antennas is key to reduce the channel fading by a significant amount. Additionally, optimizing antenna spacing can significantly minimize fading without requiring a large number of antennas. In our scenario, the channel fading could be reduced by 15 dB by employing only three distributed antennas, showing the potential of distributed MIMO systems to improve reliability in maritime communications.

17:10 Joint Sub-6 GHz and mm-Wave V2I MIMO Radio Channel Characterization

Pascal Pagani (CEA, LETI & Université Grenoble-Alpes, France); Pierre Laly (University of Lille, France); Eric P Simon (IEMN CNRS UMR8520, France); Valentin Picquet (University of Lille, France); Raffaele D'Errico (CEA, LETI & Université Grenoble-Alpes, France); Davy P Gaillot (University of Lille, France)
Cell-free massive MIMO and millimeter waves are two key enabling technologies envisioned for future wireless networks. In this paper, we present a novel channel measurement campaign for Vehicle-to-Infrastructure (V2I) applications in the mm-wave band at 26.5 GHz and in the sub-6 GHz band at 5.93 GHz. Measurements were jointly conducted in an urban scenario with two real-time channel sounders addressing the two bands. The results are presented in terms of Power Delay Profile, Doppler Spectral Density and path losses.

Room: Schelkunoff (C1) — M06 - RIS and scattering measurements

T08 Fundamental research and emerging technologies/processes / / Measurements

Chairs: Rob Maaskant (CHALMERS, Sweden), Dmitry E Zelenchuk (Queen's University of Belfast, United Kingdom)

15:50 Experimental Verification of Broadband mmWave RIS-Aided Communications: Codebook-Based Beam Steering and Indoor Channel Measurements

Ferhad Kasem (Queen's University Belfast, United Kingdom); Gabriel G. Machado (Ulster University, United Kingdom); Muhammad Ali Babar Abbasi (Queen's University Belfast & The Institute of Electronics, Communications and Information Technology (ECIT), United Kingdom); Simon Cotton (Queen's University, Belfast, United Kingdom); Dmitry E Zelenchuk (Queen's University of Belfast, United Kingdom)
This paper summarises the design, fabrication, and testing of a wideband Reconfigurable Intelligent Surface RIS operating within the millimeter wave spectrum of 5G and beyond communication. RIS elements are controlled by a pin diode and biased with RF chokes operating within the n257 millimeter wave 5G band. Experiments have been performed to validate the performance of the RIS in both near-field and far-field regions. It has been experimentally demonstrated that the proposed RIS is capable of reflecting incident beams at desired locations when appropriate phase profiles are applied to it.

WEDNESDAY

16:10 Measurement of Reconfigurable Intelligent Surfaces Through the Back-Scattering Method: Demonstration at 28 GHz

Iaroslav Shilinkov, Oleg Iupikov, Pavlo Krasov and Yuqing Zhu (Chalmers University of Technology, Sweden); Rob Maaskant (CHALMERS, Sweden); Marianna Ivashina (Chalmers University of Technology, Sweden)

This paper introduces a parameter extraction technique for characterizing and validating the performance of a Reconfigurable Intelligent Surface (RIS) unit cells (UCs) using an over-the-air back-scattering approach. This technique addresses the challenge of characterizing RIS UCs when physical access to ports is not available. Experiments were conducted at 28~GHz with a prototype featuring two RIS UCs. The results demonstrate that the UC port reflection coefficient as seen from the load termination can be estimated by measuring the backscattered field from the RIS. The accuracy of the estimation depends on the precision of the equivalent circuit models used for the reconfigurable PIN and varactor diodes employed as variable load terminations in the UCs. This method offers a practical solution for characterizing RIS UCs that may have highly integrated components so that over-the-air characterization becomes a necessity.

16:30 RIS with Continuous Amplitude and Phase Control: Functional Testing Method and Implementation

Pavlo Krasov, Oleg Iupikov, Artem Vilenskiy, Yuqing Zhu and Marianna Ivashina (Chalmers University of Technology, Sweden)

We present the methodology and supporting waveguide components for the rapid functional testing of a reconfigurable intelligent surface (RIS) prototype operating at 28GHz. The tested RIS features a 16 by 16 element array with independent continuous (16-bit) control over the amplitude and phase of its complex reflection coefficients. Over-the-air (OTA) functional testing is conducted using a custom-designed dual-polarized open-ended waveguide (OEWG) probe with a square cross-section and an orthomode transducer (OMT), both fabricated using 3D printing technology.

16:50 Scattered-Field Testing of Reconfigurable Intelligent Surfaces in a Bistatic Measurement System for Far-To-Far and Far-To-Near Scenarios

Chang-Lun Liao (Chunghwa Telecom Laboratories, Taiwan); You-Hua Lin (National Taiwan University of Science and Technology, Taiwan); Ike Lin (WaveFidelity Inc., Taiwan); Chang-Fa Yang (National Taiwan University of Science and Technology, Taiwan)

Reconfigurable intelligent surface (RIS) aided wireless communication systems have emerged as a key technology in B5G/6G networks. In these scenarios, the signals from the base transceiver station, usually located far from the RIS, impinges on the RIS as a local plane wave, and are then redirected by the RIS in various directions, shaping the field strength distributions over both near- and far-field regions. Therefore, establishing a reliable testing environment is essential to improve and verify the RIS. This paper presents a novel configuration that combines a compact antenna test range (CATR) with a planar near field scanner (PNFS) to form a bistatic measurement system to evaluate the scattering characteristics of the RIS. The analyses of the field distributions in both far-to-far and far-to-near scenarios obtained from the bistatic measurement system, along with near-field holographic imaging, may provide valuable measured data for predicting communication link budgets and optimizing RIS performance.

17:10 Double Directional Channel Measurements at 300 GHz in Indoor Environments Enhanced by Reconfigurable Intelligent Surfaces

Bo Kum Jung, Johannes M. Eckhardt, Varvara V. Elesina and Thomas Kürner (Technische Universität Braunschweig, Germany)

Terahertz (THz) communications is seen as one of the enabling key technologies for future wireless communications with the potential to provide extremely high data rates. One of the remaining challenges for THz communications is the bare necessity of a line-of-sight (LoS) condition to ensure the reliable and seamless operation of wireless communications. The introduction of reconfigurable intelligent surface (RIS) in THz communications is expected to overcome this intrinsic requirement and thus facilitate the provision of enhanced reliability and performance. To comprehensively understand its influence on the propagation channel, channel measurements were conducted in an indoor environment comprising a RIS using a channel sounder operating at a frequency range of 300 Gigahertz (GHz). The paper presents the results and findings of the double directional channel measurement of the THz propagation channel supported by a non-configurable passive RIS. The measurement results exhibit improved spatial diversity through the use of RIS

Room: Maxwell (C2)

CS42 - Time-modulated Electromagnetic Systems for Modern Technological Applications

T08 Fundamental research and emerging technologies/processes / Convened Session / Electromagnetics

Chairs: Antonio Alex-Amor (University of Pennsylvania, USA), Carlos Molero (University of Granada, Spain)

15:50 Time Modulations to Stabilize Non-Foster Circuits

Antonio Alex-Amor, Grigorii Ptitcyn and Nader Engheta (University of Pennsylvania, USA)

In this paper, we show how time modulations can be conveniently used to stabilize non-Foster circuits, i.e., circuits whose components violate Foster's reactance theorem. As an example, we study the stabilization of an L(t)C resonator constituted by a time-varying inductance L(t) and a time-invariant negative capacitance C<0.

16:10 Non-Sinusoidal Temporal Modulation in Circuits for Non-Reciprocity and Power Transfer

Juan Rafael Sanchez-Martinez (University of Granada, Spain); Mario Pérez-Escribano (Universidad de Málaga, Spain); Sergio Ortiz-Ruiz (University of Granada, Spain); Juan Valenzuela-Valdés (Universidad de Granada, Spain); Pablo Padilla and Carlos Molero (University of Granada, Spain)

In this paper, we demonstrate the improvement in circuit performance when time-varying circuits are modulated by non-sinusoidal waveforms. Specially we focus on triangular and rectangular modulations. By this, bandpass filters are designed and compared to conventional cases in order to exhibit the enhancement. Specially, the bandpass filters are desined to invoke non-reciprocity, an exotic and very interesting feature in time-modulated systems. A method of analysis based on the spectral domain is employed, establishing a general approach that is valid and applicable to other types of signals, as long as it is possible to obtain its decomposition in Fourier series. The results obtained from our model match those simulated using the Keysight ADS, thus validating the present approach.

16:30 A Robust Time-Domain Numerical Framework for the Spatiotemporal Variation of Graphene-Based Materials

Pablo Helio Zapata Cano (University of Granada, Spain); Stamatis A. Amanatiadis (Aristotle University of Thessaloniki & Ormylia Foundation, Greece); Juan Valenzuela-Valdés (Universidad de Granada, Spain); Zaharias D. Zaharis (Aristotle University of Thessaloniki, Greece)

Space-time metamaterials have gained considerable interest for their dynamism and potential for wave manipulation and control. Externally tunable materials such as graphene constitute an interesting alternative to come up with practical realizations of spatiotemporally modulated devices. In this work, we present a time-domain numerical framework that allows to simulate space-time modulation scenarios with graphene layers. The proposed algorithm is described and some scenarios including the periodical modulation of graphene's conductivity are discussed.

16:50 Temporal Modulation of Overlapped Sinusoidally Modulated Impedance Profiles

Oscar Senlis (Université de Rennes & CNRS, IETR, France); Mauro Ettorre (Michigan State University, Electrical and Computer Engineering, USA); Anthony Grbic (University of Michigan, Ann Arbor, USA); David González-Ovejero (Université de Rennes, France)

This paper explores the radiation characteristics of the temporal modulation of overlapping spatially modulated reactance surfaces, previously used in the context of multibeam metasurface antennas. A formal solution reminiscent of the method of Oliner and Cassedy is conducted for the fields of these structures. Results derived from this solution are then discussed in the context of the leaky wave metasurface antenna through the analysis of numerical examples. The presented analytical framework is relevant to the design of multiple beam-steering antennas.

17:10 Time-Modulated and Time-Switched Metamaterial Devices

Andrea Alù (CUNY Advanced Science Research Center, USA)

Progress in electromagnetics, photonics and material science has inspired a strong interest in material dynamics, opening new research directions in the context of time modulation, time switching and their impact on electromagnetic waves. Periodic modulations in time can induce Floquet phenomena for waves, which can unveil amplification, break reciprocity, and control wave mixing in new ways. In parallel, the field of metamaterials has been recently enhanced by incorporating time variations and switching as new degrees of freedom. In this talk, I will discuss the opportunities emerging from this synergy, hinging on giant wave-matter interactions enabled by metamaterials and on the exotic wave dynamics enabled by Floquet and parametric phenomena. I will discuss Floquet metamaterials in which nontrivial modulation dynamics, abrupt switching phenomena, and their interplay with tailored material dispersion and nontrivial material properties such as anisotropy, non-Hermiticity and nonreciprocity, introduce a plethora of novel opportunities for wave manipulation and control.

Room: Oliner (C3) — E05 - Optimisation methods and machine learning II

T07 Electromagnetic modelling and simulation tools / / Electromagnetics

Chairs: Mingzheng Chen (KTH Royal Institute of Technology, Sweden), Shengjian Jammy Chen (Flinders University, Australia & The University of Adelaide, Australia)

15:50 Image-To-Image Autoencoders for Quantifying Confidence in Machine Learning Solutions to the Inverse Scattering Problem

Julian Carneiro, Ian Jeffrey, Colin Gilmore, Ahmed Ashraf and Keeley Narendra (University of Manitoba, Canada); Tashfa Nadeem (University of Engineering and Technology, Lahore, Pakistan); Komal Sambhus (University of Mumbai, India)

An image-to-image autoencoder is used to assess, in part, the confidence of a deep-learning data-to-image architecture for solving the inverse scattering problem (ISP) for microwave imaging. The output image of the data-to-image model is passed through the autoencoder to assess if the target is in range of the common dataset used to train the image-to-image autoencoder and data-to-image model. The quality of the autoencoder reconstruction is assessed using the structural similarity between the input and output of the autoencoder. Results demonstrate that the image-to-image autoencoder may detect certain out-of-range targets, and serves as a partial tool for quantifying confidence in imaging results. Future work will seek to build data-to-image models from parts of pre-trained image-to-image autoencoders.

WEDNESDAY

16:10 Beam Forming Design of Anomalously Reflective Metasurface Based on Quantum Annealing

Yuto Kato (National Institute of Advanced Industrial Science and Technology, Japan); Michitaka Ameya (AIST, Japan); Ryutaro Shimasaki and Atsushi Sanada (Osaka University, Japan)

This paper presents a beam forming design of an anomalously reflective metasurface aimed at reflecting an incident wave into a specified angular range with uniform power distribution for coverage expansion applications of 6G communication. To address the enormous design degree of freedom of practical reflective metasurface designs, we introduce a quantum annealing (QA)-assisted design framework. We derive a formulation that can be applied to comprehensive design problems where the design parameters, reflection phases of elements constituting a metasurface, are arbitrarily discretized. To demonstrate the validity of the proposed design framework, we design a metasurface that reflects a normal incident wave to generate a reflected beam with a beamwidth of 30 degrees spanning over reflection angles from -15 degrees to 15 degrees and discuss its optimization performance.

16:30 Topology Optimization of Dualband Metallic Antennas with Minimum-Size Control

Pan Lu (Umeå University, Sweden); Eddie Wadbro (Karlstad University, Sweden); Martin Berggren and Emadeldeen Hassan (Umeå University, Sweden)

We use a density-based topology optimization approach to design dualband planar metallic antennas. The design problem is formulated based on the time-domain Maxwell's equations, solved using the finite-difference time-domain (FDTD) method. The antenna design is formulated as an optimization problem where the received and reflected energy by the antenna in two frequency bands, centered around 2.5 GHz and 5.5 GHz, are optimized. Two design examples that exhibit outstanding performance are presented. In one design case, we employ a nonlinear filtering scheme to impose size control on the optimized design and ensure manufacturability.

16:50 Unit-Cell Design Framework for Current-Based Synthesis of Metasurface Antennas

Leonardo Pollini (Politecnico di Torino & Thales DMS, Italy); Francesco Lattanzio, Marcello Zucchi and Giuseppe Vecchi (Politecnico di Torino, Italy)

The design of complex metasurfaces (MTS) is usually done in two steps: a) design of the surface impedance profile; b) realization of unit cells, often using a periodic approximation. In this communication we propose an innovative approach for the comprehensive design of the MTS down to the unit cell design. It is based on the recently introduced current-only metasurface synthesis. In the present approach, the unit cell is designed based only on the optimized equivalent current, without having recourse to surface impedance. While maximally effective in association with current-only approaches, it can also be used with approaches aiming at the design of the impedance profile, still avoiding the periodic approximation.

17:10 Evolutionary Algorithm and Surrogate-Assisted Optimisation of a Pattern Reconfigurable Antenna for Sub-6 GHz Applications

Sami H. A. Almalki (University of Sheffield, United Kingdom & Taif University, Saudi Arabia); Salam Khamas (University of Sheffield, United Kingdom)

This paper presents the optimisation of the states of PIN diodes in a design of a pattern reconfigurable antenna operating at a centre frequency of 5 GHz. The proposed design comprises a patch antenna and a parasitic surface placed above it. The parasitic surface is a 4 x 4 metallic array connected by PIN diodes. Two optimisation techniques were used to find a set of PIN configurations that yielded satisfactory performance. The first technique involved an evolutionary algorithm, namely, Improving the Strength Pareto Evolutionary Algorithm (SPEA2). The second technique used a surrogate-assisted approach. Through simulation results, it was shown that SPEA2 outperforms the surrogate-assisted approach in terms of convergence speed. Furthermore, the proposed design achieved radiation efficiency up to 73% and broadside beam steering capabilities.

Room: Kraus (C4) — A18 - Terrestrial communications with sub-6GHz antennas

T01 Sub-6 GHz for terrestrial networks (5G/6G) / / Antennas

Chairs: Leonardo Lizzi (University of Trento, Italy), Ville Viikari (Aalto University & School of Electrical Engineering, Finland)

15:50 Multi-Resonance Miniaturized Base Station Antenna Using Dual Resonance Rings and Fractal Technology

Yuhao Feng (University of Electronic Science and Technology of China, China)

This paper presents a novel broadband dual-polarized dipole antenna with ±45° polarization. The antenna employs a bent structure and fractal technology in both horizontal and vertical directions to extend the low-frequency current path, thereby broadening the bandwidth. The inclusion of dual resonance rings facilitates multi-frequency resonance, enhancing the antenna's impedance matching and subsequently increasing the bandwidth. The proposed miniaturized antenna has dimensions of only 0.29λ × 0.29λ. Simulation results demonstrate that the antenna achieves a bandwidth of 1.7-2.83 GHz (S11 < -15 dB), with polarization isolation greater than 30 dB, a gain of 8 dB, and a stable 3 dB beam width of 70° ± 1°. Additionally, the 10 dB beam width is 127° ± 2°, ensuring a stable radiation pattern within the operating frequency band. This antenna shows promise as a viable option for future base station communication systems.

WEDNESDAY

16:10 Realization of In-Band Full-Duplex Antenna Self-Decoupling Based on MultiLayer PCB Vertical Feeding and TE211 Mode Dielectric Resonator

Haoxuan Sheng (Southwest Jiaotong University, China); feng Quanyuan (Southwest JiaoTong University, China); Yan Wen, Yukang Chen and Yurong Sun (Southwest Jiaotong University, China)
This paper presents a self-decoupling in-band full-duplex (IBFD) antenna array for wireless WLAN and digital satellite communications. High isolation is achieved using the TE211 higher-order mode of the dielectric resonator antenna (DRA), eliminating the need for additional decoupling structures. The study concludes that the mechanism for achieving isolation is due to the near orthogonalization of the TE211 mode and the mode produced by spatial coupling, resulting in a very low level of mutual coupling. To adapt to multilayer PCB application scenarios, a vertical feeding structure based on substrate integrated waveguide (SIW) is designed. Short-circuited microstrip stub is placed internally and resonate with the coupling slot on the top layer. Simulation results indicate that the S21 is below -64 dB at 5.81 GHz, with a gain of 7.35 dBi. Notably, bandwidth with isolation below -40 dB reaches 4.3% (5.7-5.95-GHz) and S11 below -10 dB.

16:30 Self-Decoupled Patch Antenna Based on Weak-Field for MIMO Application

Zhangmin Wang, Quanyuan Feng and Yan Wen (Southwest Jiaotong University, China)
This paper introduces a self-decoupled patch antenna based on weak-field distribution is proposed for multi-input-multi-output (MIMO) applications. Due to the presence of weak-field, decoupling of the E-plane array can be effectively obtained. We proposed self-decoupling antenna eliminates coupling strength and improves isolation from patch to patch. The distance between the patches is 0.19λ0 (where λ0 is the center frequency wavelength in free space). The isolation of the proposed 1×2 antenna elements is more than -22 dB.

16:50 Wideband Filtering Patch Antenna Design for cmWave 6G Applications

Duy Hai Nguyen, Martin Jacob and Thomas Käubler (Ericsson, Germany)
This paper proposes a dual polarized planar patch antenna design for 6G applications in the cmWave frequency band. The design is based on low cost, low loss multilayer RF laminate enabling 92% of radiation efficiency. In addition, a wide impedance bandwidth of 21% is achieved using differential L-probe feeds. By implementing additional shorting pins to the feed, the antenna also exhibits good out-of-band rejection from 24.25 to 27.5 GHz, which is currently deployed for mmWave wireless communication systems.

17:10 Switched-Beam Smart Antenna for Wi-Fi 8 Solutions in FTTR Applications

Francis Keshmiri (Huawei Technologies, France)
Fiber-to-the-room (FTTR) is a new in-premises indoor network technology relying on the optical fiber backhauling to deliver Wi-Fi connectivity in each room with a Quality of Service (QoS) superior than traditional Wi-Fi systems. This paper presents a high-gain switched-beam antenna with a cost-effective design for multi-Access Points (Multi-APs) solution, mainly for FTTR, to improve Wi-Fi 8 indoor coverage and reliability. The antenna spatial switchable pattern diversity is optimized for Wi-Fi sub-6 GHz range of 5.15 to 5.87 GHz and with cost-effective standard FR4 substrate. It reduces EM Interferences (EMI) between APs by reducing radiation in unnecessary directions, at least 20 dB, which also improves FTTR power consumption, compared to conventional multi-AP antennas. We optimized the antenna's radiation performance in CST Microwave Studio, then prototyped and measured it in an anechoic chamber. Experimental qualifications of the fabricated antenna and the feeding systems accordingly demonstrate good agreement with simulated antenna characteristics. Each of four generated beams illuminates one-quarter of the room, with realized Gain of approximately 5 dBi, Envelope Correlation Coefficient of 25 dB, ensuring that each MIMO stream can operate independently. The overlapped high-gain beams into the entire room space minimizes the combined Gain and allow transmit power to have sufficiently high level while complying with the regulated limits of Effective Isotropic Radiated Power (EIRP). Further studies are ongoing to present advantages of beam-switch antennas and the spatial division of the radiation pattern in the rooms to improve Wi-Fi coverage and throughput for a FTTR Wi-Fi user. This approach aims to reduce the dependency of such performance on each AP installation and location in the room, compared to the first generation of FTTR without switch-beam features.

Room: Munch (23)

Industrial Workshop

IW7 - TICRA - Dedicated software tool for rapid full-wave design, optimisation, and analysis of phased array antennas

WEDNESDAY

15:50 Orthogonal Time Frequency Space Based 5G Broadcast - Secondary Synchronization Signal

Jonas von Beöczy (Technische Universität Braunschweig, Germany)

Recent advancements in Long Term Evolution (LTE)-based 5G Terrestrial Broadcast have enhanced physical layer performance, particularly for large-area coverage. Built on the LTE standard, it utilizes Orthogonal Frequency Division Multiplexing (OFDM), well-suited for multipath environments. Traditional LTE unicast restricts the cell radius to approximately 5 km, but modified OFDM numerologies are required for High Power High Tower (HPHT) configurations to extend coverage. However, stability issues persist in high-speed vehicular reception. Orthogonal Time Frequency Space (OTFS) modulation, resistant to Doppler shifts, offers a promising alternative. This paper investigates synchronization strategies for extending LTE-based 5G Terrestrial Broadcast using OTFS modulation, focusing on Secondary Synchronization Signal (SSS) detection. A method to map the SSS into an OTFS frame is proposed, facilitating correlation-based synchronization. Simulation results demonstrate the robustness of the approach, and future research directions are outlined.

16:10 Self-Interference Cancellation for Software-Defined Radar Using Coupling Properties of Channels

Siyu Xia, Xiao Ma and Qi Wu (Beihang University, China)

This paper presents a new software-defined radar with multiple frequency continuous waves (MFCW) and a self-interference cancellation algorithm. The presented radar is implemented as a highly reconfigurable system that is made of a USRP X310, two patch antennas and the GNU Radio software. Most of the radar operations can be configured and controlled by the software. The transmitter and receiver channels are in one radio-frequency frontend of the USRP X310, thus releasing the remaining channels for other purposes. The radar is experimentally evaluated in indoor scenarios, operating at a frequency of 4.25 GHz while transmitting MFCW signals within a narrow bandwidth. Experimental results demonstrate that the implemented algorithm enables the SDRadar to effectively measure short-range targets.

16:30 DECT-2020 NR Link Distance Performance in Varying Environments: Models and Measurements

Md Mohaiminul Haque and Joonas Säe (Tampere University, Finland); Juho Pirskanen (Wirepas Oy, Finland); Mikko Valkama (Tampere University, Finland)

Digital Enhanced Cordless Telecommunications 2020 New Radio (DECT-2020 NR) has garnered recognition as an alternative for cellular 5G technology in the internet of things industry. This paper presents a study centered around the analysis of the link distance performance in varying environments for DECT-2020 NR. The study extensively examines and analyzes received signal strength indicator and resulting path loss values in comparison with theoretical models, as well as packet success rates (SR) and signal-to-noise ratio against varying distances. The measurements show that with an SR of over 90%, an antenna height of 1.5 m, indoor link distances with a single device-to-device connection with 0 dBm transmission (TX) power can reach over 60 m in non-line-of-sight (NLOS) areas and up to 190 m in LOS areas with smaller −8 dBm TX power. Similarly, for outdoor use cases, link distances of over 600 m can be reached with +19 dBm TX power.

16:50 Experimental Analysis of Multi-AP Diversity for Reliable Industrial Communications

Dreyelian Morejon Betancourt (University of the Basque Country, Spain); Jesús Ramón Pérez (University of Cantabria, Spain); Iñaki Eizmendi and Pablo Angueira (University of the Basque Country, Spain); Rafael Torres (Universidad de Cantabria, Spain)

This paper presents the results of a measurement campaign carried out in an industrial-like environment to evaluate the benefits of a multi-Access Point (AP) architecture in enhancing the performance of wireless communications such environments. The signal levels received by a moving receiver along four trajectories from four transmitters are recorded. The microdiversity is studied by computing the autocorrelation function and the macrodiversity by the cross correlation function of the signal level variation along the trajectories. The tests were performed at the 6 GHz band, a strong candidate for industrial wireless communication in the near future. The results show that microdiversity does not bring relevant benefits for distances below 10 cm, while high macrodiversity is obtained using several AP. These results lead to the conclusion that for small-size devices the use of multiple AP (macrodiversity) significantly outperforms microdiversity (multiple antennas at the receiver side).

17:10 Indoor Localization with Passive RFID System Based on Phase Difference of Displacement

Utku Kumbul (IMEC, The Netherlands); Alireza Sheikh (IMEC Nederland, The Netherlands); Amirashkan Farsaei (IMEC, The Netherlands); Guido Dolmans (IMEC the Netherlands, The Netherlands)

The radio frequency identification (RFID) system is investigated for indoor localization. The phase difference between the relative displacement of the tag is used to estimate the range towards each anchor. The updated range information at each anchor is then used to compute the coordinates of the tag using analytical multilateration positioning. The localization performance of this multilateration method is demonstrated experimentally and compared with maximum likelihood positioning, which serves as an upper bound for localization performance. The experiments show that the passive RFID system with analytical multilateration positioning can achieve localization errors between 0.06 m and 0.18 m for the chosen trajectory.

WEDNESDAY

15:50 A Millimeter-Wave Wideband Single-Layer Substrate-Integrated Dielectric Resonator Antenna and Its Beam-Scanning Phased Array

Xue-Ying Wang and Yongmei Pan (South China University of Technology, China)
A millimeter-wave wideband single-layer substrate-integrated dielectric resonator antenna (SIDRA) and its beam-scanning phased array are investigated in this paper. Unlike traditional SIDRA, the proposed design employs a coplanar feeding structure based on slot-to-CPW transition, achieving the goal of integrating all key components of the antenna into a single-layer substrate. Thanks to the interaction of the DR with the coupling slot, a new mode emerged with a boresight radiation pattern, namely antiphase TEy211 mode. The metallic via walls around the dielectric resonator (DR) not only isolate it from the substrate but also shift the frequency of the antiphase TEy211 mode down to merge with fundamental TEy111 mode to achieve bandwidth expansion. Based on this novel single-layer SIDRA element, an H-plane eight-element linear phased array is further designed with a scanning range greater than ±53° across the entire frequency band and a gain fluctuation of 3-dB.

16:10 Wide-Angle Scanning and High-Isolation Millimeter Wave Antenna Arrays Based on Metasurfaces

Yuqi He (The Hong Kong Polytechnic University, Hong Kong); Luyu Zhao (Anhui University, China); Wei Lin (The Hong Kong Polytechnic University, Hong Kong)
This paper presents two metasurface-based design approaches for millimeter-wave (mm-Wave) antenna arrays to simultaneously achieve wide-angle beam scanning and high-isolation between array elements. One approach is to use an electromagnetic bandgap ground (EBGG) instead of the metallic ground of a conventional microstrip patch antenna array. Another method is to place a high dielectric constant layer (HDL)-mimic metasurface above patch antenna array. Both approaches effectively enlarge the beamwidth of element pattern and reduce the coupling between array elements. Thus, wide-angle scanning and decoupling performances are realized simultaneously. To prove the design concept, two distinct prototype examples are demonstrated to explain the design guidelines and considerations. The developed metasurface-based design methods exhibit universality, low cost, and easy integration. They are ideal design approach for mm-Wave antenna arrays in mobile terminals that require wide-angle beam scanning and high isolation.

16:30 Dual-Polarization and Low Scan-Loss Multi-Beam Lens Antenna Fed by Semicircular Parallel-Plate Horn Antenna with Separated Phase Centers

Shota Takada, Yoshiki Sugimoto, Kunio Sakakibara, Takanori Narita and Nobuyoshi Kikuma (Nagoya Institute of Technology, Japan)
We propose a wide-angle beam-scanning multibeam lens antenna with dual-polarization capability. Due to an astigmatism of the lens, focal points of the lens are separated in the beam-scanning plane and its orthogonal plane. This separation causes scan-loss. This issue is solved in both polarizations simultaneously by designing the semicircular wall radiuses of the horn antennas. The beam-scanning performance of the proposed antenna is evaluated by electromagnetic simulation in this paper.

16:50 Conformal Transmitarray: Design Principles and Performance Enhancement

Lizhao Song, Peiyuan Qin and Y. Jay Guo (University of Technology Sydney, Australia)
Conformal transmitarrays, adapting their shapes to curved surfaces, offer significant advantages for applications in aeronautics, vehicular systems, and satellite communications where aerodynamic or structural constraints limit the use of traditional flat arrays. For the ease of practical implementation, we investigate conformal transmitarrays based on ultra-thin elements. This paper provides a comprehensive overview of design principles and performance enhancement strategies for conformal transmitarrays. Specifically, we explore versatile element synthesis methodologies, including multi-layer frequency selective surfaces (M-FSS), Huygens metasurfaces, and true-time-delay lines, to facilitate the implementation of conformal transmitarrays and improve its radiation properties in terms of aperture efficiency and operating bandwidth. Measurement results of different conformal prototypes are provided to demonstrate the targeted functionalities.

17:10 A Modular Shared-Aperture Circularly Polarized Phased Array Antenna at K/Ka-Band on LTCC

Xianming Qing, Xinyi Tang, Bo Shi and N Nasimuddin (Institute for Infocomm Research, Singapore); Yijun Zhou (I2R, Singapore); Luo Bin and Wenjiang Wang (Institute for Infocomm Research, Singapore); Francois Chin (Institue for InfoComm Research, Singapore)
A patent pending modular interleaved shared-aperture circularly polarized phased array antenna at K/Ka-band is presented for satellite-on-the-move (SOTM) systems. Based on a basic antenna array module with 8 Tx and 4 Rx antenna elements, a larger antenna array can be easily configured for higher gain. An antenna array with 128 Tx and 64 Rx elements on low temperature co-fired ceramic (LTCC) is designed to cover frequencies of 17.7 GHz-21.2 GHz for downlink (Rx) and 27.5-31.0 GHz for uplink (Tx) with boresight gain of 25 dBic (Tx) and 21 dBic (Rx), as well as beam steering range of ±45deg with scan loss of 3 dB, respectively

WEDNESDAY

15:50 Functional Metasurfaces Furnished with Gaseous Plasma Layer and Plasma-Like Structure

Francisco Pizarro (Pontificia Universidad Catolica de Valparaiso, Chile); José Álvarez-Vidal (Pontificia Universidad Católica de Valparaíso, Chile); Itami Go and Osamu Sakai (The University of Shiga Prefecture, Japan)

This article presents a waffle iron filter (WIF) operating on the X-band that integrates a plasma discharge and metasurface for reconfiguration purposes, and a plasma-like structure based on a metallic plate array (MPA) that supports spoof surface plasmon polariton on the W-band. The WIF uses a glide symmetry structure in order to implement a split block that allows to the filter to serve as electrodes and generate the discharge, that in this case serve as a power limiter. The MPA produces a high Q-factor in its resonance frequency, while this same resonance is shifted depending on the incident angle of the impinging wave an its polarization.

16:10 Reconfigurable Transmissive Meta-Gratings Using Cylindrical Plasma Discharges

Mohammad Alijani and Alessio Monti (Roma Tre University, Italy); Stefano Vellucci (Niccolò Cusano University, Italy); Mirko Barbuto, Alessandro Toscano and Filiberto Bilotti (Roma Tre University, Italy)

In this study, we propose an innovative single-layer reconfigurable diffraction meta-gratings based on plasma technology. The meta-grating consists of a set of cylindrical plasma discharges, modelled through a free-electron permittivity with variable plasma frequency, enclosed within a high-refractive-index dielectric shell. Our findings show that, by adjusting the plasma frequencies of the discharges, it is possible to steer the direction of the main transmission lobe mode from -56° to 56°. This result is obtained through an advanced scattering engineering enabled by the combination of the negative permittivity response of plasma with high-refractive-index shell. This tunability not only enables substantial directional control in transmission mode but also ensures low reflection, achieving improved power efficiency through the structure.

16:30 A Reconfigurable Metasurface Based on Plasma Cylinders

Jiaruo Yan (Foundation for Research and Technology - Hellas (FORTH), Greece); Ioannis Katsantonis (Institute of Electronic Structure and Laser, Switzerland); Ioannis Draganidis (Foundation for Research and Technology - Hellas (FORTH), Greece); Konstantinos Kourtzanidis (Centre for Research and Technology Hellas, Greece); Alessio Monti (Roma Tre University, Italy); Stefano Vellucci (Niccolò Cusano University, Italy); Mirko Barbuto and Filiberto Bilotti (Roma Tre University, Italy); Maria Kafesaki (Ujniversity of Crete, Greece)

Reconfigurable metasurfaces enabling real-time wavefront control hold great potential for advancing future communication technologies. In this work, we rely on the unique tunability of plasma to design and numerically demonstrate metasurfaces composed of plasma cylinder arrays. Our analytical findings on the scattering properties of a single cylinder provide guiding insights for achieving a generalized Kerker condition below plasma frequency, where both electric dipole and quadrupole moments are excited and balanced, leading to a Huygens response exhibited by the cylinder array. This is validated through numerical simulations of an infinite array of identical cylinders, which show high transmission while covering a wide range of phases. Building on these results, we design, optimize, and demonstrate a phase gradient metasurface utilizing plasma cylinders with tunable plasma properties. The analysis is further expanded to be applied to coated plasma cylinders, with discussions on both frequency tunability and dynamically controllable beam steering capabilities.

16:50 Analytical Modelling of the Interaction Between an Intense Electromagnetic Pulse and a Spherical Plasma Discharge

Maëva Juste (CEA, France & Université de Toulouse - UPS INPT CNRS, France); Gerjan Hagelaar (Université de Toulouse - UPS INPT CNRS, France); Romain Pascaud (ISAE-SUPAERO, Université de Toulouse, France); Thierry Callegari (Université de Toulouse - UPS INPT CNRS, France); Rémi Maisonny, Stéphane Vauchamp and Clovis Pouant (CEA, France)

In this paper, an analytical model of the interaction between an intense electromagnetic pulse (EMP) and a spherical plasma discharge is presented. The study aims to provide a physical description of the nonlinear behavior of a plasma-based antenna subjected to an EMP during experimental illuminations. This model emphasizes the critical role of the significant energy absorbed by individual electrons from an EMP. It also shows the prominence of radiation, particularly within the electron density range of the antenna. Finally, this model offers valuable insights into the underlying physical mechanisms.

17:10 Time Interfaces in Nanoplasma-Switched Wire Media

Mikhail S. Sidorenko, Sergei Tretyakov and Constantin Simovski (Aalto University, Finland)

In this work, we consider instantaneous transitions of an infinitely extended uniaxial dielectric into a wire medium (WM) of continuous infinitely long conducting wires. Due to the strong spatial dispersion in the WM the known (Morgenthaler's) theory of temporal discontinuities is not applicable. We solve this problem analytically in time domain. We show that a transverse electromagnetic (TM) plane wave transforms into four waves: a pair of TM waves and a pair of transverse electromagnetic waves. This way, the power flow splits into two different directions, with one of them along the wires. Such a transition can possibly be achieved by nanoplasma discharges in the gaps of the split wires, initiated by an external voltage source applied to the wire and transforming the split wires forming the uniaxial dielectric into continuous ones.

WEDNESDAY

Wednesday - 17:40-18:50

Room: Kildal (A2)

Early Career and the Women in Antennas and Propagation WG

WiAP - ECAP event

Wednesday - 18:50-20:00

Room: Hallén (BAR5)

Early Career and the Women in Antennas and Propagation WG

WiAP ECAP reception

End of Wednesday, April 2nd

WEDNESDAY

Thursday - 8:00 - 9:40

Room: Alfvén (A3+A4)

CS31a - Wi-Fi 8 - Currents Trends and Advances in Antennas, Architectures, and Techniques

T01 Sub-6 GHz for terrestrial networks (5G/6G) / Convened Session / Antennas

Chairs: Francis Keshmiri (Huawei Technologies, France), Andrea Massa (University of Trento, Italy)

8:00 Loop Antenna for Wi-Fi 6/6E Application

Amir Jafargholi and Romain Fleury (EPFL, Switzerland)
This paper introduces a horizontally polarized, low-profile loop antenna. The antenna features a printed circular segmented loop loaded with capacitor varactors. By adjusting the capacitive varactors, the antenna has a broadband impedance bandwidth with a directive radiation pattern. The antenna's symmetrical design is fed by multiple coaxial cables, allowing electronic steering of the antenna beam in the azimuth plane by tuning the varactor diodes when it works in directive mode. Simulation shows an impedance bandwidth of 2.1 GHz (|S11|<-10 dB) cover from 5.0 to 7.1 GHz. The maximum radiation efficiency of 95% provides the realized gain of 2.5 dBi, making these antennas suitable for Wi-Fi 6/6E applications.

8:20 Localizing Radiation for Radiation Pattern Manipulation of Monopole Antennas with Finite-Sized Ground Planes

Zhi Ning Chen, Z. N. Chen (National University of Singapore, Singapore); Bo Zhang (NUS, Singapore); Huiwen Sheng (National University of Singapore, Singapore)
The radiation patterns of antennas, formed by monopoles and finite-sized ground planes, significantly impact the coverage and quality of wireless communications. This paper proposes a concept to manipulate the radiation patterns of the antennas by forming new ground plane's boundaries to effectively localize the radiation. The concept is proposed based on the analysis of radiation pattern distortion. Two design methods are presented to implement the concept in two antenna systems: a two-antenna system for WLAN with a rectangular ground plane and a four-antenna system for WLAN with a square ground plane. In both cases, the asymmetrical radiation configurations severely distort radiation patterns of the antennas. By integrating metasurfaces and metarings, the distorted radiations are significantly mitigated by localizing the radiation to a symmetrical region. The techniques based on the proposed concept also shows enhanced port isolation.

8:40 Metasurface-Based Surface Wave Communications for Smart Radio Environment

Talha Arshed, Xenofon Mitsalas, Stefano Maci and Enrica Martini (University of Siena, Italy)
This paper presents a novel communication paradigm based on the use of surface waves (SWs) to enhance signal propagation in smart radio environments (SRE), particularly for indoor millimeter-wave (mmWave) communication. Metasurfaces (MTSs) represent the enabling technology for the proposed approach, allowing for the implementation of the following functionalities: conversion of wireless signal into SW, guiding of SWs thoughout the indoor environment, including obstacles and sharp bends, and re-radiation of the signal towards the intended users. Simple and effective design algorithms are introduced for the implementation of all these functionalities. Moreover, it is shown how the proposed MTSs can be synthetized through microstrip patch technology, offering a cost-effective and practical solution for indoor deployment. Full-wave simulations demonstrate the high performance the proposed MTS design, achieving efficient space wave-to-SW conversion and minimal diffraction losses. This work opens new possibilities for enhancing indoor wireless system using surface wave communication.

9:00 On the Integration of SEME Solutions in the FTTR Vision

Arianna Benoni and Marco Salucci (ELEDIA Research Center, Italy); Andrea Massa (University of Trento, Italy)
Fiber-to-the-Room (FTTR) is an innovative in-premise networking solution based on optical fiber communication offering gigabit speeds, high reliability, and low latency throughout the entire space. However, deploying optical fiber is not always straightforward, particularly in older or historical buildings. This work proposes integrating the Smart Electromagnetic Environment (SEME) paradigm with the FTTR framework to enhance wireless coverage and address such indoor Wi-Fi deployment challenges.

9:20 Smart Electromagnetic Skin Synthesis for Advanced Near-Field Coverage in Indoor mm-Wave Wireless Communications

Sergio Menéndez Feito (University of Oviedo, Spain); Álvaro F. Vaquero and Marcos R. Pino (Universidad de Oviedo, Spain); Manuel Arrebola (Universidad Politécnica de Madrid, Spain)
This paper presents the near-field modeling, synthesis, and experimental validation of a passive reflectarray-based Reconfigurable Intelligent Surface (SES/RIS) to improve near-field (NF) coverage in millimeter-wave 5G networks, specifically within the 27.20-28 GHz band. Unlike traditional approaches, the proposed SES generates a shaped beam in dual-linear polarization (dual-LP) to cover blind zones in indoor environments. A NF synthesis technique controls the volumetric shape of the radiated field in the Fresnel zone of the SES, and measurements confirm the capability of the system to deliver a mostly uniform field distribution over a 20° × 20° area at 12 m distance, meeting the 3 dB ripple requirement across an 800 MHz bandwidth. The paper also compares results obtained using NF and far-field (FF) synthesis methods. The SES is an affordable, lightweight solution that is easy to fabricate and install, offering a practical approach to enhance 5G coverage in challenging indoor scenarios

THURSDAY

8:00 The Proxy Sources Method for the Numerical Analysis of Small Lens Antennas

Riccardo Ozzola and Andrea Neto (Delft University of Technology, The Netherlands); Erik Speksnijder and Cesare Tadolini (TU Delft, The Netherlands)

This contributions presents a novel technique to ease multi-scale simulations involving a feed radiating close to dielectric bodies, e.g., dielectric lenses. Three independent wave phenomena are found inside the lens: the reactance of the feed, an outwardly propagating wave in a dielectric half-space, and the reflections arising from the lens boundaries, and these three can be calculated separately. While the former two can be easily calculated numerically or even semi-analytically, the reflections from the lens require a full wave simulation of the entire system. To this aim, a feed with coarser details and the same interaction with the lens is then synthesized. This allows us to estimate the reflection from the lens efficiently and calculate the total input impedance.

8:20 Ultra-Wideband Geodesic Lens Antenna for Point-To-Point Communications

Laia Costa-Cid (KTH, Sweden); Pilar Castillo-Tapia (KTH Royal Institute of Technology, Sweden); Cristina Yepes (TNO, The Netherlands); Oscar Quevedo-Teruel (KTH Royal Institute of Technology, Sweden)

Here, we present the design of an ultra-wideband geodesic generalized Luneburg lens antenna, operating in the 10-40 GHz frequency band. This is the widest band ever reported in the literature for a geodesic lens antenna. The most innovative aspects of the design are (i) the feed, which is based on coaxial-to-ridge transition, and (ii) the broadband implementation of a compact array of flares which increases the directivity in the E-plane. The challenges in the design are related to the matching of the feeding to the lens, as well as keeping a good matching of the array of flares without excessively increasing the longitudinal size of the antenna and avoiding grating lobes in the E-plane. The antenna features a maximum directivity of 25 dB. Given the fully metallic nature of the antenna, we expect a high radiation efficiency in the measurements.

8:40 2-D Ray-Tracing Approach for the Design of 3-D Dome Arrays Considering Mutual Coupling

Maria Pubill-Font (University of Technology Sydney (UTS), Australia); Francisco Mesa (University of Seville, Spain); Astrid Algaba-Brazález (Technical University of Cartagena, Spain); Can Ding (University of Technology Sydney (UTS), Australia); Oscar Quevedo-Teruel (KTH Royal Institute of Technology, Sweden)

The integration of lenses with array antennas (referred to as dome arrays) in future communication systems offers numerous benefits, including improved radiation efficiency, adaptability in different use cases, and reduced energy consumption. This article elaborates upon using a novel two-dimensional ray-tracing technique for rapid and accurate numerical evaluation of the far-field radiation properties of three-dimensional multilayer dome arrays. Moreover, we also investigate how to account in our model for the effect of mutual coupling in dome arrays. The accuracy of the method is validated by comparing the simulated radiation patterns from the proposed ray-tracing model with results generated by widely used full-wave simulation tools like CST.

9:00 Experimental Validation of D-Band Active Antenna with Quasi-Optic and Analogue Beam Reconfiguration

Marta Arias Campo, Simona Bruni and Andreas Lauer (IMST GmbH, Germany); Michael Wleklinski (IMST, Germany); Uwe Gollor, Nora Pedrayes Nuñez, Wolfgang Wischmann, Aline Friedrich, Christos Oikonomopoulos-Zachos and Oliver Litschke (IMST GmbH, Germany); Christoph Herold and Andrea Malignaggi (IHP, Germany); Nicolò Moroni (IHP GmbH, Germany); Karthik Krishnegowda (IHP GmbH, Innovations for High Performance Microelectronics, Germany); Corrado Carta (IHP - Leibniz Institut für Innovative Mikroelektronik, Germany & Technische Universität Berlin, Germany); Wilhelm Keusgen (Technische Universität Berlin, Germany)

In this work, the experimental validation of a hybrid quasi-optic and analogue beam reconfiguration is presented at 140 GHz. A prototype consisting on two 4-channel D-band transceiver MMICs, forming a 2x4 active phased array, and a plastic lens is used to proof the beamforming concept. The agreement between simulated and measured results at 140 GHz is excellent. Potential for beam reconfigurability in two planes is validated, as well as enhanced scanning performance, thanks to the optimized phase shift in the feeding phased array.

9:20 A Compact and High-Gain Dielectric Lens Combining Luneburg and Planar GRIN Designs

Jose-Manuel Poyanco (Universidad Técnica Federico Santa María, Chile); Francisco Pizarro (Pontificia Universidad Catolica de Valparaiso, Chile); Eva Rajo-Iglesias (University Carlos III of Madrid, Spain)

In this paper, we present a novel dual-function dielectric lens that combines the characteristics of both a Luneburg lens and a GRIN (Gradient-Index) planar lens. By taking advantage of the design flexibility of GRIN lenses, we achieve a unique refractive index distribution that allows the lens to operate simultaneously as a 2.5D Luneburg lens and as a planar GRIN lens in orthogonal planes. The design methodology involves optimizing the focal length and thickness of the lens using a Mean Square Error (MSE) approach to minimize the differences between the refractive index profiles of both lenses. Simulations and analysis show excellent overlap between the two lenses' refractive index distributions, providing high directivity in two planes in the whole Ka-band. The proposed lens is compact, operates at millimeter-wave frequencies, and is ideal for applications requiring high gain in two orthogonal directions.

THURSDAY

T07 Electromagnetic modelling and simulation tools / / Electromagnetics

Chairs: Christophe Craeye (Université Catholique de Louvain, Belgium), Jesús Rubio (University of Extremadura, Spain)

8:00 Mutual Coupling Analysis of Arrays of Antennas with Overlapping Minimum Spheres Based Exclusively on Addition Theorems

Jesús Rubio, Rafael Gómez Alcalá and Yolanda Campos-Roca (University of Extremadura, Spain)

Mutual coupling in antenna arrays is calculated in the case of elements with overlapping minimum spheres. Taking the Generalized Scattering Matrix of an isolated element as the starting point, mutual coupling is calculated exclusively through the application of addition theorems for spherical vector waves. To this aim, the addition theorems are used not only to relate the scattered field of one element in the array to the incident field on another one, as usual, but also to change the coordinate origin of the incident or scattered field. This approach is compared with that based on the transformation between spherical and plane vector waves, showing similar precision.

8:20 Geometrical Optics Considerations for 3D Simulations of Array Antennas with Dielectric Lenses

Núria Flores-Espinosa and Pilar Castillo-Tapia (KTH Royal Institute of Technology, Sweden); Francisco Mesa (University of Seville, Spain); Oscar Quevedo-Teruel (KTH Royal Institute of Technology, Sweden)

The combination of arrays with dielectric lenses is an attractive solution to improve the antenna performance for millimeter wave applications. The design and optimization of these lenses present significant challenges. This is primarily due to the computational intensity of simulating them with full-wave software packages, especially since an extra simulation is required to determine the nonlinear phase distribution of the array. A potential solution to accelerate the design process is the implementation of a ray tracing (RT) method. To address the limitations of our earlier in-house 2D RT model, we are currently upgrading it to a 3D version. In this context, we outline the steps involved in geometry creation and geometrical optics within the model. The geometrical optics include both reverse RT (for phase distribution retrieval) and direct RT (for radiation pattern calculation). Our results show a good agreement with the theory.

8:40 Evaluation of Combined Availability Prediction Methods for Multicarrier Microwave Links

Antons Bezdels (SAF Tehnika, Latvia); Emmanuel Alejandro Merchan-Cruz (Transport and Telecommunication Institute, Latvia)

While the availability prediction methods for a single carrier link are well-known, the method for estimating the availability of the multicarrier system`s combined throughput needs to be developed. The original research forming the basis for this article uses experimental data, obtained by performance monitoring of a multicarrier test link over a period of 6 months, for actual combined availability estimation. The purpose of this article is to compare the obtained results with software simulation output based on ITU recommendations, as well as to evaluate the theoretical approach to combined availability calculation of a multicarrier link. The results showed a correlation between experimental and theoretical approaches, as well as between different algorithms of ITU-based theoretical approach, which will be discussed herein.

9:00 Application of Extended Multi-Branch Basis Functions in Non-Conformal Meshes

Manuel Parejo (EM3WORKS, Spain); Víctor Martín (Universidad Rey Juan Carlos, Spain); Luis Landesa (Universidad de Extremadura, Spain); Jose M. Taboada (University of Extremadura, Spain)

Accurate solution of real-life electromagnetic problems via surface integral equations commonly requires handling a large number of unknowns and multi-scale features. In this context, generating computer-aided design and mesh models in separate subdomains and then connecting them to analyze the entire problem without concern for mesh conformity is highly advantageous. Focusing on single-trace solutions, we can find some existing solutions for non-conformal mesh problems as the Multi-Branch basis functions, limited by their need for partial node conformity, or the Integral Equation Discontinuous Galerkin method, which does not require partial node conformity, however the calculation of the stabilization parameter complicates its application to realistic problems. This work introduces a new approach, the Extended Multi-Branch basis functions, which combines the advantages of both methods: it does not require partial node conformity and eliminates the stabilization parameter calculation, thus streamlining the analysis process for non-conformal meshes.

9:20 Self-Correcting Interpolation Technique for Multi-Source Electromagnetic Scattering Problems

Antonio Gomez-Rodriguez (EM3WORKS, Spain & Universidad de Extremadura, Spain); Luis Landesa (Universidad de Extremadura, Spain); Víctor Martín (Universidad Rey Juan Carlos, Spain); Jose M. Taboada (University of Extremadura, Spain); Fernando Obelleiro (University of Vigo, Spain)

In this paper, we propose a novel approach able to minimize the total number of solutions required for a set of incident excitations. The method of moment is applied to a reduced sample of the excitations and an algebraic interpolation procedure is then applied to obtain the currents solution for the rest of directions. Importantly, the new currents solutions are obtained without the need for solving the matrix systems. This interpolation method is based on the projection of the new excitation vectors onto the reduced sample vector space. Next, an a priori error estimation technique is also applied to enhance both efficiency and accuracy. Additionally, a self-correction procedure is proposed to improve the accuracy of the solution of the initial reduced sample, so that they can be solved with a low accuracy.

THURSDAY

T07 Electromagnetic modelling and simulation tools / Convened Session / Propagation

Chairs: Pekka Kyösti (Keysight Technologies & University of Oulu, Finland), Yejian Lyu (Shanghai Jiao Tong University, China)

8:00 Pathloss Measurements and Models at 300 GHz in an Industrial Environment

Lucas Cândido Ribeiro (TU Braunschweig, Germany); Thomas Kürner (Technische Universität Braunschweig, Germany)
Pathloss measurements at 300 GHz were performed in an industrial environment and large-scale propagation parameters were extracted. For the channel modelling, the close-in (CI) and floating-intercept (FI) models were considered. In this particular measurement campaign, the floating-intercept model has shown to be in better agreement with the measured data. Moreover, the models have shown how sensitive THz systems are to minor inaccuracies in antenna alignment, when horn antennas are used.

8:20 Beam-Steered Sub-THz Channel Measurements in D-Band in an Industrial Environment

Alper Schultze (Fraunhofer Institute for Telecommunications, Heinrich-Hertz-Institut, Germany); Mathis Schmieder (Fraunhofer Institute for Telecommunications, Heinrich Hertz Institute, Germany); Ramez Askar (Fraunhofer HHI, Germany); Michael Peter (Fraunhofer Institute for Telecommunications, Heinrich Hertz Institute, Germany); Wilhelm Keusgen (Technische Universität Berlin, Germany); Taro Eichler (Rohde & Schwarz, Germany)
This paper presents results of a channel measurement campaign carried out in a production hall of Rohde & Schwarz in Memmingen, Germany. The channel measurements were performed with a novel time-domain correlative channel sounder operating in the D-Band at a carrier frequency of 160 GHz. The channel measurements were performed and analyzed with respect to the topic of beam-steering and macro-diversity gains. It was found out that a macro-diversity gain of 3.2 dB for line-of-sight and 5.7 dB for non-line-of-sight is achieved.

8:40 Characterization of Indoor Sub-THz Channels at 154 and 300 GHz

Minghe Mao (Niigata University, Japan); Masato Yomoda (University of Niigata, Japan); Minseok Kim (Niigata University, Japan)
In this paper, double-directional (D-D) channel measurements under two typical indoor scenarios using an in-house developed 150/300 GHz dual-band channel sounder are reported. The measurement data are firstly processed to obtain the path loss (PL) model parameters for both omnidirectional PL and best-beam PL by fitting with the close-in and floating intercept models. Subsequently, large scale parameters are extracted and analyzed. The results demonstrate that even though the higher frequency band exhibits more significant sparsity the non-line-of-sight multipath components are still available to be used to enhance the ominidirectional path gain of the sub-THz channel.

9:00 Detection and Identification of Overlapping Cards Using Terahertz Imaging

Yasutaka Murakami (UEC, Japan); Yoshiki Sugimoto (Nagoya Institute of Technology, Japan); Hideya So (Shonan Institute of Technology, Japan); Tomoki Murakam (NTT Corporation, Japan)
Recent advancements in terahertz technology have generated significant interest in sensing and imaging and sensing applications within the 300 GHz band. This paper focuses on the detection and identification of overlapping cards utilized in competitive trading card games. We propose a novel method for identifying the overlapping cards through the use of terahertz waves. Specifically, electromagnetic waves are emitted toward the overlapping cards with identifiers. By employing the correlation coefficient between the obtained electromagnetic field distribution and a dataset analyzed in advance, the proposed method estimates both of the position and height of the overlapping cards.

9:20 Centimeter-Level Geometry Reconstruction and Material Identification in 300 GHz Monostatic Sensing

Zitong Fang (Shanghai Jiao Tong University, China); Ziming Yu (Huawei Technologies CO., LTD, China); Chong Han (Shanghai Jiao Tong University, China)
THz ISAC technology is envisioned to achieve high communication performance alongside advanced sensing abilities. For various applications of ISAC, accurate environment reconstruction including geometry reconstruction and material identification is critical. This paper presents a highly precise geometry reconstruction algorithm and material identification scheme for a monostatic sensing case in a typical indoor scenario. Experiments are conducted in the frequency range from 290 GHz to 310 GHz. A joint delay and angle SAGE-based algorithm is implemented to estimate MPC parameters and the indoor geometry is reconstructed based on the extracted parameters, reaching an accuracy of 1.75 cm. Additionally, a material database using THz-TDS is established, capturing reflection losses of over 200 common material samples. The measured reflection losses of wall and window frame are accurately identified as cement and steel, respectively. Our results demonstrate the centimeter-level geometry reconstruction and material identification for practical THz ISAC scenarios.

Room: Björk (33)

EurAAP Reviews of Electromagnetics Meeting

RoE

THURSDAY

8:00 Near-Field Localization with Extremely Large Scale Antenna Arrays in the Presence of Mutual Coupling

Zohreh Ebadi and Amir Masoud Molaei (Queen's University Belfast, United Kingdom); George C. Alexandropoulos (University of Athens & University of Illinois Chicago, Greece); Muhammad Ali Babar Abbasi (Queen's University Belfast & The Institute of Electronics, Communications and Information Technology (ECIT), United Kingdom); Simon Cotton (Queen's University, Belfast, United Kingdom); Anvar Tukmanov (BT, United Kingdom); Okan Yurduseven (Queen's University Belfast, United Kingdom)

Extremely large scale antenna arrays (ELAAs) will be a key technology in 6G wireless communication systems. Due to the large near-field region of ELAAs, sources can easily fall within this area. Hence, a near-field localization algorithm that accounts for the mutual coupling (MC) is essential for proper 6G wireless communication systems design. Recently, an iterative method based on an oblique projection operator (IMOP) has been presented. However, IMOP's computational load can still be high. We address this issue by using one sub-array of ELAA which holds far-field assumptions to estimate the direction of arrival (DOA). The DOA estimation relies on an one-dimensional (1D) MUSIC-based algorithm. Then, the MC coefficients are calculated using the estimated DOAs. Finally, another 1D MUSIC step is used to estimate the ranges corresponding to the estimated DOA and MC coefficients. Our studies verify the superiority of the proposed near-field source localization in the presence of MC.

8:20 Electromagnetic Wave Modulation for Holographic Metasurface

Xinyu Zhang and Yuchen Gao (Xidian University, China); Qi Luo (University of Herfordshire, United Kingdom); Tao Hong (Xidian University, China)

In this paper, an innovative method for designing planar and conformal holographic metasurface (HM) to modulate electromagnetic waves in desired directions is proposed. The designed holographic metasurfaces can precisely control the scattering waves, effectively enhancing the directionality of the beam. The holographic metasurfaces achieve scattering wave deflections in the range of ±60° at 10 GHz under incident plane waves with x- and y- polarization at arbitrary angles. Prototypes of the designed conformal holographic metasurfaces with different states are fabricated and measured, and the simulation and measurement results are in good agreement. The designed holographic metasurfaces have polarization insensitivity and adaptability to cylindrical platforms, which has big potential to be deployed for the smart radio environment to support wireless power transfer and wireless communications.

8:40 Degrees of Freedom for Communication Between Volumes in Canonical Environments

Mats Gustafsson (Lund University, Sweden)

The number of degrees of freedom (NDoF) is a crucial metric for evaluating the potential of wireless communication systems. NDoF can be computed numerically for regions of arbitrary shapes and diverse propagation environments, while analytical results provide complementary insights that enhance our understanding of the underlying physical principles. In this work, we extend recent analytical expressions for asymptotic NDoF, originally developed for free-space scenarios, to more complex environments such as ground planes.

9:00 Design and Implementation of Scalable 6.5 GHz Reconfigurable Intelligent Surface for Wi-Fi 6E

Nuno Paulino and Francisco M Ribeiro (INESC TEC, Portugal & University of Porto, Portugal); Luís Outeiro, Pedro A. Lopes and Sofia Inacio (INESC TEC, Portugal); Luis M. Pessoa (INESC TEC & Faculty of Engineering, University of Porto, Portugal)

Wi-Fi 6E will enable dense communications with low latency and high throughput, meeting the demands of ever growing network traffic and supporting emergent services such as ultra HD or multi-video streaming, and augmented or virtual reality. However, the 6 GHz band suffers from higher path loss and signal attenuation, and poor performance in NLoS conditions. Reconfigurable Intelligent Surfaces (RISs) can address these challenges by providing low-cost directional communications with increased spectral and energy efficiency. However, RIS designs for the WiFi-6E range are under-explored in literature. We present the implementation of an 8x8 RIS tuned for 6.5 GHz designed for scalability. We characterize the response of the unit cell, and evaluate the RIS in an anechoic chamber, measuring the far field radiation patterns for several digital beamsteering configurations in a horizontal plane, demonstrating effective signal steering.

9:20 Impact Analysis of Realistic Antennas on the Performance Metrics of Electromagnetic Degree of Freedom and Channel Capacity in Nearfield Environments

Abubakar Hamza (Aalborg University, Denmark); Zhinong Ying (Sony Coporation, Sweden); Shuai Zhang (Aalborg University, Denmark)

This paper presents a comprehensive analysis of the impact of realistic antenna configurations on key performance metrics in near-field MIMO wireless communication environments. The study focuses on the Electromagnetic Degree of Freedom (EDOF) and channel capacity, comparing four antenna types: isotropic, dipole, patch, and plane wave models. A MIMO system with a 16x16 planar array for the base station at 3GHz and a 4x4x4 cubic array for the User Equipment (UE) is simulated. The analysis considers both linear and circular UE movement patterns and examines antenna spacings ranging from 0.25λ to 2.00λ. A detailed electromagnetic (EM) channel model based on the dyadic Green's function is employed, incorporating mutual coupling effects for accurate performance estimation in both near-field and far-field regimes. The results reveal significant variations in EDOF and capacity across different antenna configurations and movement patterns.

THURSDAY

T07 Electromagnetic modelling and simulation tools / Convened Session / Electromagnetics

Chairs: Zhen Peng (University of Illinois at Urbana-Champaign, USA), Francesca Vipiana (Politecnico di Torino, Italy)

8:00 A Time-Domain Thin-Sheet Volume Integral Equation for Non-Dispersive Bi-Isotropic Media

Sebastian Celis Sierra (King Abdullah University of Science and Technology (KAUST), Saudi Arabia); Ran Zhao (University of Electronic Science and Technology of China (UESTC), Saudi Arabia); Meruyert Khamitova and Hakan Bagci (King Abdullah University of Science and Technology (KAUST), Saudi Arabia)

Thin-sheet approximation is used to convert the time-domain volume integral equation for non-dispersive bi-isotropic media into a surface integral equation. This surface equation is discretized in space using Rao-Wilton-Glisson (RWG) basis functions for the tangential components of the electric and magnetic fluxes and pulse basis functions for their normal components (relative to the surface of the thin sheet). In time, shifted Lagrange polynomials are used for discretization. Applying Galerkin testing in space and point matching time yields a matrix system. This matrix system is solved for the unknown basis expansion coefficients at each time step via time-marching. Numerical results demonstrate the accuracy of the proposed method. Future work includes extending this solver to dispersive bi-anisotropic media and use it in the simulation of metasurface represented by generalized sheet transition conditions.

8:20 Low Complexity Fast Direct Solution for Multiscale Problems with Nested Equivalence Source Approximation

Yuhan Zuo (Nanjing University of Science and Technology, China); Mengmeng Li (Nanjing University of Science and Technology & Communication Engineering, China); Francesca Vipiana (Politecnico di Torino, Italy); Dazhi Ding (Nanjing University of Science and Technology, China)

We propose a multi-level low complexity fast direct solution of electric field integral equations (EFIEs). Far coupling submatrices are compressed by a kernel-independent method with nested equivalence source approximation (NESA). In this work, equivalence sources are constructed at upper levels while skeletons are selected via the adaptive cross approximation (ACA) at the bottom level to further accelerate the computation. To factorize and inverse the system matrix, an elimination matrix is introduced to each group to reduce the far blocks dimension. Then, an LU factorization is performed to reduce the near blocks dimension. This process is repeated recursively from the bottom level to the top. The inverse of the system matrix is then represented as a multiplication of a series of matrices arising from the factorization process. Numerical results verify the accuracy and the linear complexity of our proposed method.

8:40 Investigations on Normal Systems for Low-Frequency Stabilized Equivalent Electric Surface Current Reconstructions

Mohammad Mirmohammadsadeghi and Bernd Hofmann (Technical University of Munich, Germany); Thomas F. Eibert (Technical University of Munich (TUM) & Chair of High-Frequency Engineering (HFT), Germany); Simon B Adrian (Universität Rostock, Germany)

To reconstruct equivalent electric surface currents from irregularly distributed observations of the fields radiated by a device under test (DUT), we investigate a low-frequency stabilized formulation based on a quasi-Helmholtz decomposition: Rao-Wilton Glisson (RWG) basis functions are employed for the equivalent surface currents, dipoles as probe antennas, and the relation between probes and sources is established via integral operators. Since, in general, a rectangular linear system of equations (LSE) is obtained, we analyze both the normal-residual system of equations (NRE) and the normal-error system of equations (NEE) for an iterative solution with a generalized minimum residual (GMRES) solver. Specifically, our analysis shows that a self-adaptive normalization scheme is needed in both cases, where the scheme itself can remain the same.

9:00 A Preconditioner for the Fast Analysis of Arbitrarily-Shaped Reflective Intelligent Surfaces

Jean Cavillot (Université Catholique de Louvain (UCL), Belgium); Christophe Craeye (Université Catholique de Louvain, Belgium)

Analyzing a reflective metasurface (MTS) is usually simplified by considering the MTS as a continuous sheet of impedance. Thanks to this approach, we avoid the need to describe the fine geometry of the MTS with numerous elementary basis functions. Considering the MTS at the sheet impedance level allows to analyze the structure by solving a linear system of equations with a reduced number of unknowns and, when iterative solvers are used, the convergence is usually very good for conventional highly capacitive MTS. However, the condition number of the system and hence the convergence of the solver dramatically deteriorate when considering impedance ranges spanning both capacitive and inductive domains. In this paper, we present an efficient preconditioner which significantly improves the convergence of the GMRES iterative solver when applied to both inductive and capacitive MTSs . We also show that the method can be easily extended to MTSs with arbitrary shapes.

THURSDAY

9:20 Simplified Analytic Expressions for the Line Integrals over Pair of Arbitrarily Oriented Triangular Facets in the d'Alembertian Representation of Green's Function

Elizabeth Bleszynski (Monopole Resesarch, USA); Marek Bleszynski (Monopole Resaearch, USA); Thomas Jaroszewicz (Monopole Research, USA)

We present new simplified analytic evaluation, in the static limit, of matrix elements of electromagnetic operators for the RWG basis functions located on non-coplanar planes. Our method employs the previously reported d'Alembertian representation of Green's function such that a certain d'Alembert-type operator, when acting on ax suitably constructed auxiliary function reproduces the Green function. Integration by parts allows then converting four-fold surface integrals to double integrals of the auxiliary function (which turns out to be an expression involving only elementary functions) over perimeters of the triangles. Here we describe our ongoing work on reducing the latter double integral to analytical form by carring out the integration in a nonacrtesian frame of reference with axes colinear with a pair of edges. A comparison of the prediction of the present approach, in terms of their accuracy and efficiency, will be given in the presentation.

Room: Schelkunoff (C1)

CS15a - Shared-Aperture Antenna and Antenna Collocation Strategies and Methods for Communication, Radar and SATCOM

T01 Sub-6 GHz for terrestrial networks (5G/6G) / Convened Session / Antennas

Chair: Can Ding (University of Technology Sydney (UTS), Australia), Adam Narbudowicz (Tyndall National Institute, Ireland & WroclawUniversity of Science and Technology, Poland)

8:00 Varactor-Based Polarization Convertable Cube Antenna

Dongho Kim, Yewon Kim and Soo-Jeong Kim (Sejong University, Korea (South))

This paper introduces a novel method for controlling linear polarization in a Fabry-Perot cavity (FPC) antenna. An efficient polarization conversion is achieved in a single cube antenna by utilizing varactor diodes on artificial magnetic conductor (AMC) sidewalls. Our design effectively enhances power efficiency by protecting the varactors from exposure to high conduction currents. Experimental results demonstrate a realized gain of at least 5.68 dBi and an aperture efficiency of 59 % at 8.5 GHz. The agreement between the simulation and measured data validates the polarization conversion with relatively high aperture efficiency.

8:20 A X-/Ka-Band Circularly Polarized Shared-Aperture Phased Array Antenna

Lu-Yang Ji, Shigang Zhou and Jian-ying Li (Northwestern Polytechnical University, China)

A circularly polarized (CP) X-/Ka-band shared-aperture phased array is proposed in this paper. Its unit cell consists of one X-band element and 3 × 3 Ka-band elements. The Ka-band element is a rectangular dielectric resonator antenna (DRA) with a metasurface etched on the top side. The X-band element is a dual-feed magneto-electric dipole antenna with dual CP capabilities. By hollowing out the center and the sides of the dipole antenna, 3 × 3 Ka-band elements can effectively share the same aperture with the X-band element. A shared-aperture array prototype was fabricated and measured for performance verification. The results show that the proposed array can achieve an impedance bandwidth from 7 GHz to 8.5 GHz for the X-band and from 26 GHz to 28 GHz for the Ka-band. It can realize ±45° beam scanning with an axial ratio (AR) variation less than 5 dB for both bands.

8:40 Low-Profile Electromagnetic Transparent Antenna with FSS as Radiator

Ya Nan Wang, Chu-Ting Song and Qing-Xin Chu (South China University of Technology, China)

A novel electromagnetic (EM) transparent base-station antenna, utilizing frequency selective surface (FSS) as radiator, is proposed. The utilization of FSS bestows the proposed antenna with EM transparent characteristics in the C-band (CB) of 3.3-3.8 GHz, wider working bandwidth covering low band (LB) of 0.69-1 GHz, and low-profile height. A dual-band antenna array, comprising the proposed LB and CB antennas, is constructed and assessed. This array with lower profile height of 0.15λ_L, λ_L representing the wavelength at the lowest working frequency, demonstrates a remarkable EM transparency, a good impedance matching, and a high cross-band isolation.

9:00 A Dual-Band Dual-Linearly Polarized Shared Aperture Antenna Based on Magneto-Electric Dipole Antenna and Dielectric Resonant Antenna

Yinfeng Xia (Harbin Engineering University, China); Yingsong Li (Anhui University, China); Wei Xue (Harbin Engineering University, China); Shengyuan Luo (Anhui University, China)

A dual-band dual-linearly polarized shared aperture is presented and discussed herein, which is devised based on magneto-electric (ME) dipole and dielectric resonant multiple-input-multiple-output (MIMO) antenna array. The created ME dipole excited by double ports created a dual-linear polarization and -10-dB fractional bandwidth of 51.1% from 1.94 GHz to 3.27 GHz. The MIMO array (consisting of 12 elements) based-on dielectric-resonant-antenna (DRA) loaded around the ME antenna gets dual polarization and -10-dB fractional bandwidth of 3.6% from 4.12 GHz to 4.27 GHz, which is not affected the performance of ME antenna. Moreover, the constructed antenna achieves a peak gain of 9.65 dBi and 7.56 dBi operating both bands, respectively.

9:20 Scalar and Tensor Holographic Time Reversal Mirror with Consideration of Obstacles

Jihwan Lee (Pohang University of Science and Technology (POSTECH), Korea (South)); Sirous Bahrami (Pohang University of Science and Technology, Korea (South)); Wonbin Hong (Pohang University of Science and Technology (POSTECH), Korea (South))

This paper proposes a new class of Holographic Time Reversal Mirror (HTRM) by defining scalar and tensor holographic time reversal impedance modulation. In the Scalar Holographic Time Reversal Mirror (SHTRM) mode, we set the object wave as a point source and introduce time reversal operation modulation, enabling theoretical calculation of the electric field. To validate the HTRM, the SHTRM is fabricated for near-field beam focusing. The Tensor Holographic Time Reversal Mirror (THTRM) is derived from the SHTRM by extending this concept using electric dipole sources with orthogonal polarization components for the object wave, allowing for the recording and reconstruction of beams. Two models of THTRM demonstrating arbitrary polarization control are designed with linear and circular polarization for near-field beam focusing verification purpose. Using dipole recording techniques, the HTRM is validated with a dielectric prism, which scatters the phase difference of the object wave on the hologram.

Room: Maxwell (C2) — CS61a - AMTA Post Processing Techniques in Antenna Measurements

T07 Electromagnetic modelling and simulation tools / Convened Session / Measurements

Chair: Francesco Saccardi (Microwave Vision Italy, Italy), Anouk Hubrechsen (Eindhoven University of Technology & AntenneX B. V., The Netherlands)

8:00 Inverse Source Solutions and Antenna Field Transformations Above Lossy Dielectric Halfspace via Exact Sommerfeld Integral Representation of the Green's Functions

Thomas F. Eibert (Technical University of Munich (TUM) & Chair of High-Frequency Engineering (HFT), Germany); Raimund Mauermayer (Mercedes Benz, Germany)

Automotive near-field (NF) antenna measurements above a dielectric, possibly lossy halfspace enable an accurate characterization of the antenna radiation especially for frequencies below around 300 MHz, where mutual interactions between the automobile with integrated antenna and the ground become relevant. In order to correctly consider these effects, an inverse source solver with exact Sommerfeld integral representation of the pertinent Green's functions is presented. The Sommerfeld integrals are numerically evaluated for a mixed-potential integral representation of the fields with real-axis integration and quasistatic image extraction. As such, the inverse source operator is pre-computed as a system matrix, in order to allow for an efficient iterative solution of the inverse source problem and the related antenna field transformation. The accuracy of the approach is demonstrated for hemispherical observation data of a backlight broadcast antenna on a metallic car body.

8:20 Near-Field Focusing Operators for Planar Multi-Static Microwave Imaging Using Back-Projection in the Spatial Domain

Matthias M. Saurer (Technical University of Munich, Germany); Marius Brinkmann (Rohde & Schwarz GmbH & Co. KG, Germany); Han Na and Quanfeng Wang (Technical University of Munich, Germany); Thomas F. Eibert (Technical University of Munich (TUM) & Chair of High-Frequency Engineering (HFT), Germany)

Based on a plane-wave expansion of the observation data in quasi-planar multi-static scattering scenarios, an improved formalism for image creation utilizing back-projection in the spatial domain is derived. The underlying integral expressions for different focusing operators are derived analytically leading to magnitude correction factors, which are mostly relevant for reconstructing microwave images when the distance from the scattering object to the aperture plane is small. It is shown that the derived imaging procedure is superior to the traditional backprojection only compensating the phase delay of the measurement signals and validate our findings based on simulated as well as measured data. Since the derived focusing operators correspond to a low-pass filtering of the spatial images, the resulting modified multi-static back-projection algorithms effectively suppress imaging artifacts as well.

8:40 Application of the Reduced-Order Model to Planar near-Field Antenna Measurements

Valentin Morin (IETR & Thales DMS, France); Samuel Corre (IETR, France); Renaud Loison (IETR & INSA, France); Laurent Le Le Coq (University of Rennes 1 & IETR, France); Eric Estebe (Thales DMS France, France)

The antenna characterization from planar Near-Field (NF) measurements is commonly realized by using the classical Near-Field to Far-Field Transform (NFFFT) technique of Plane Wave Expansion (PWE). Truncation effects are induced by this approach due to the finite size of the measurement scan surface, which is an issue for wide angular range beam steering applications. To overcome these limitations, an equivalent model of the Antenna Under Test (AUT) based on a distribution of infinitesimal dipoles and coupled with a Reduced-Order Model (ROM) of the problem, is proposed. The powerful ability of the ROM in determining the number of samples needed for accurate NF measurements is detailed. Moreover, the use of non-conventional measurement geometry to limit the truncation effects for strong beam tilts is studied. The analysis of our approach on simulated NF data shows that, compared to the PWE technique, only 20% of samples are needed to achieve an accurate characterization.

9:00 Post-Processing for Installed-Performance Testing of Automotive Antennas for Satellite Communications

Muhammad Ehtisham Asghar, Christian Bornkessel, Umais Tayyab, Tobias Nowack and Matthias Hein (Technische Universität Ilmenau, Germany)

Advanced post-processing of automotive antenna measurements is crucial, particularly for antennas installed in locations like rear spoilers, offset from the phase center of the measurement facility. Conventional nearfield-to-far-field transformations, like spherical-wave expansion, assume the antenna phase center is within the minimum measurement sphere. As operational frequencies increase, the minimum sphere shrinks for fixed angular resolution systems, and when antenna is outside this region, transformation errors occur, leading to inaccuracies in radiation patterns and total radiated power estimates. To address these issues, we applied the Translated Spherical Wave Expansion method, which compensates for phase-center offsets, improving installed-performance testing. A case study comparing measurements in different test facilities, including the Gantry arm-based extension of the Virtual Road Simulation and Test Area at TU Ilmenau, demonstrates the effectiveness of TSWE, particularly for embedded automotive antennas designed for non-terrestrial links at 5.9 GHz. The results show significant error reduction, closely aligning with reference measurements.

9:20 3-D Probe Positioning Errors Compensation in a Non-Redundant Spherical NF-FF Transformation

Francesco D'Agostino, Flaminio Ferrara, Claudio Gennarelli, Rocco Guerriero and Massimo Migliozzi (University of Salerno, Italy); Luigi Pascarella (Università di Salerno, Italy)

An effective two-steps technique to compensate known 3-D mispositioning errors, affecting the near-field (NF) measurements in a non-redundant spherical NF-far-field (NF-FF) transformation technique for quasi-planar antennas, is here developed. In the first step, a phase correction technique called spherical wave correction is applied to compensate the phase shifts originated by the deviations from the measurement sphere. In the second step, an iterative procedure is exploited to restore the NF samples at their exact locations from those determined at the previous step. Once the NF samples are retrieved at their exact position, an optimal sampling interpolation formula is employed to get the input NF data needed to perform the classical spherical NF- FF transformation technique. The effectiveness and the reliability of the approach are numerically assessed.

Room: Oliner (C3) — CS5a - Vehicular Antenna Systems and Solutions

T04 RF sensing for automotive, security, IoT, and other applications / Convened Session / Antennas

Chairs: Wonbin Hong (Pohang University of Science and Technology (POSTECH), Korea (South)), Christian Lötbäck (Volvo Car Corporation, Sweden)

THURSDAY

8:00 Optimizing Wireless BMS Communication with Multilayer Broadband Antenna Technology

Chisang You, Senghoon Han, Jung Hun Oh, Youngkuk Kwak, Sungki Jung, Wonseok Choi, Gihyoung Kwon, Ighyun Cho, Junghwan Choi and Shin Cho (LG Innotek, Korea (South))

This paper presents a novel antenna and its module designed for a wireless Battery Management System (wBMS). The proposed antenna module is mounted on the main printed circuit board (PCB) using surface mount technology (SMT) and enclosed within a mechanical cover case. The antenna features a coupled feeding mechanism with two radiating elements, implemented both on the surface and within the substrate layers to ensure optimal performance in the battery pack structure. This multilayer antenna provides a bandwidth exceeding 400 MHz, with an average path loss of 46.95 dB between the Battery Management Unit (BMU) and multiple nodes, even under external noise conditions of 30 dB and in the presence of coolant. Additionally, the system achieved a Packet Delivery Ratio (PDR) of 100% with a bridge network and 96% without, confirming the antenna's stable performance throughout the system.

8:20 Frequency-Independent and High Gain Comb Antenna for Radar Application

Seongjung Kim (Samsung Electronics, Korea (South))

In this work, we propose a frequency independent and high gain comb antenna for radar applications. This antenna exhibits a highly directive radiation pattern that remains consistent over a wide frequency range while also providing a broad impedance bandwidth. Three techniques contribute to pattern consistency and high gain in this antenna design. First, the stepped feeding line (SFL) enables frequency-independent directive radiation properties. Second, high gain is achieved through the use of Y-shaped elements (YEs) instead of conventional comb monopoles, along with the incorporation of parasitic elements (PEs). The operating frequency of the proposed antenna ranges from 76 to 81 GHz, achieving a broadside realized gain of 13.4 to 15.6 dBi, with a copper surface roughness of 1 um.

8:40 Low Transmission Loss Solder Ball Waveguide and Transmission Line to Waveguide Transition Using Loop Antenna Structure in PCB

Seungyoon Jung (Samsung Electronics, Korea (South))

This paper proposes Solder Ball Waveguide (SBW) and its transition (transmission line to waveguide) for low-loss signal transmission that can be applied to 77 GHz automotive radar application. The SBW was implemented using two PCB substrate ground planes, with solder balls placed in the space between them, to form a waveguide. The structure of the transition was designed in the form of a loop antenna in cavity using vias and stripline within the substrate. For smooth impedance matching between the cavity and the waveguide, and stepped ground structure was implemented using conductive vias. To evaluate the performance of the proposed SBW, HFSS simulation was conducted at 77 GHz band. The proposed SBW including the transition showed the extremely low insertion loss per unit length at copper roughness of 0 um and 1 um, with values of 0.01 dB/mm and 0.018 dB/mm, respectively.

9:00 On Channel Gain Performance of Car Roof-Glass Embedded 5G Antenna

Hanieh Aliakbari (Volvocars, Sweden & Lund University, Sweden); Christian Lötbäck and Xiaotian Li (Volvo Car Corporation, Sweden); Buon Kiong Lau (Lund University, Sweden)

5G antennas for vehicular connectivity are often mounted on the car roof to optimize signal reception. The trend of replacing metal roof with glass in modern cars opens an opportunity for embedding the 5G antennas inside the glass roof. In this work, we compare the channel gains of reference dipole, and loop antennas positioned at the roof center. Then, by considering the requirements of glass integration and the channel gain performance, a nontransparent wideband monopole antenna with an extended feedline is designed to be embedded inside a real glass roof. To recover the optical transparency of the roof glass while retaining the wideband performance, the metal conductor is replaced with non-uniform metal mesh structure. The proposed semi-transparent wideband monopole antenna covers both 5G and legacy bands. Within the operating frequency range from 617 MHz to 5 GHz, the channel gain and radiation efficiency are above -4.5 dB and 37%, respectively.

9:20 Traveling Wave Antenna-On-Display Featuring Simultaneous 2-D Phase and Frequency Beam Scanning for Integrated Sensing and Communication

Dongseop Lee and Wonbin Hong (Pohang University of Science and Technology (POSTECH), Korea (South))

This paper reports the first traveling wave antenna (TWA) concept for integrated sensing and communication (ISAC) applications. The frequency-dependent beam steering capability of the TWA enables dynamic spatial scanning for ISAC. However, TWA features a large physical footprint due to the vast number of unit cells and termination requirements. To mitigate such size constraints, this antenna is further realized within the display panel denoted as traveling wave antenna-on-display (TWAoD). The exemplified optically invisible antenna array achieves two-dimensional simultaneous phase scanning (PS)/frequency scanning (FS) mode. Denoted as PS/FS mode, this function is crucial for ISAC. Experimental results show that the design achieves high gain and dual mode capability for radar and communication at 24 and 28 GHz, respectively. By addressing core limitations of current ISAC antennas, this solution establishes a new concept for compact, high-performance solutions providing a scalable approach for modern mobile, automotive, other pragmatic and emerging scenarios.

Room: Kraus (C4)

CS57a - Biomedical Microwave Techniques and Devices: from Diagnosis to Treatment

T06 Biomedical and health / Convened Session / Propagation

Chairs: Raquel C. Conceição (Instituto de Biofísica e Engenharia Biomédica, Faculdade de Ciências, Universidade de Lisboa, Portugal), Daniela M. Godinho (Instituto de Biofísica e Engenharia Biomédica - Faculdade de Ciências - Universidade de Lisboa, Portugal)

8:00 Surface-Wave Skin Characterization with a Flexible Vivaldi Antenna

Milad Mokhtari and Milica Popović (McGill University, Canada)

This paper presents a study on characterizing skin lesions using surface waves generated by a pair of flexible Vivaldi antennas. Aimed at improving early-stage skin cancer diagnosis, the antennas operate in the 3–6 GHz range, creating surface waves that propagate along the tissue-air interface, making them sensitive to changes in the skin's dielectric properties. By analyzing the phase difference in scattering parameters (S_{21}), variations in permittivity due to lesions are detected. Full-wave simulations were performed using ANSYS Electronics on a simplified skin model, demonstrating that both tumor size and dielectric contrast affect the measured phase difference, enabling the characterization of skin lesions. This method offers a promising, non-invasive, low-cost tool for skin cancer screening. It could enable portable diagnostics and easily integrate into clinical settings, with potential to improve patient treatment and survival rates through earlier detection.

8:20 A Numerical Assessment of Enhanced Microwave Hyperthermia Using Au Nanoparticles

Iman Farhat and Julian Bonello (University of Malta, Malta); Francesco Rossi and Nguyen TK Thanh (University College London, United Kingdom); Charles Sammut and Lourdes Farrugia (University of Malta, Malta)

Microwave hyperthermia has emerged as an increasingly recognised therapeutic approach for addressing various challenging medical conditions. This study conducts a comparative analysis between a three-layered phantom with and without the inclusion of gold nanoparticles in the tumour region. The investigation explores the use of nanoparticles for enhancing hyperthermia generation, their activation source, characteristics and implementation from an electromagnetic numerical analysis perspective.

8:40 Interpretable Machine Learning for Tumour Detection in Microwave Breast Imaging Using Image-Extracted Features

Tyson Reimer, Gabrielle Fontaine and Stephen Pistorius (University of Manitoba, Canada)

Recent advancements in machine learning and microwave imaging techniques have shown significant potential in automating tumour detection. Three classification algorithms were trained using features extracted from radar-based breast images. A logistic regression classifier demonstrated the best detection accuracy. Radar images were reconstructed using conventional delay-and-sum (DAS) and delay-multiply-and-sum (DMAS) beamformers, as well as an optimization-based radar reconstruction technique employing varying levels of enhanced physics modelling. Our results show that incorporating enhanced physics modelling improves tumour classification accuracy. This work applied a robust methodology that ensures diversity and separation between training and testing sets through the use of proper machine learning methods. By utilizing appropriate techniques, we can more accurately assess the algorithm's real-world applications.

9:00 Assessment of Extending a Two-Port Calibration to a Multi-Port Microwave Scanner

Martina Gugliermino, David O. Rodriguez-Duarte, Cristina Origlia and Jorge A. Tobon Vasquez (Politecnico di Torino, Italy); Rosa Scapaticci (CNR-National Research Council of Italy, Italy); Lorenzo Crocco (CNR - National Research Council of Italy, Italy); Francesca Vipiana (Politecnico di Torino, Italy)

This work evaluates a sub-calibration method for a multi-port microwave imaging scanner. This decreases the complexity of a conventional full n-port calibration, albeit inserting uncertainties. The approach involves a combined 2-port full standard calibration along with a multi-port extension. It addresses systematic errors and reduces the impact of losses and phase shifts introduced by the multiplexing component of a microwave scanner, normally interfacing the 2-port transceiving stage with the multiple radiating elements. The analysis examines the calibration assumptions and validates them on a microwave scanner utilizing a 2-port vector network analyzer and a 2 × 22 solid-state switching matrix. Repeatability and stability tests confirm the calibration's reliability, effectiveness, and permissible effect on the imaging retrieval capabilities.

9:20 Evaluation of a Medical Microwave Imaging Device for Breast Diagnosis - First Volunteer Study

Daniela M. Godinho (Instituto de Biofísica e Engenharia Biomédica - Faculdade de Ciências - Universidade de Lisboa, Portugal); Mónica Alfaiate (NOVA University of Lisbon, Portugal); Raquel C. Conceição (Instituto de Biofísica e Engenharia Biomédica, Faculdade de Ciências, Universidade de Lisboa, Portugal)

This paper presents the first volunteer study with three healthy female volunteers using our breast radar-based microwave imaging prototype. We compare the differences in image quality when varying values of complex permittivity value are used for image reconstruction. We observed a more focused image was obtained when considering higher relative permittivity in the image reconstruction for the volunteer with lower age and lower Body Mass Index (BMI) when compared to older volunteers with higher BMI.

Room: Munch (23)

Scientific Workshop

SW8a - Sub-THz Reconfigurable Intelligent Surfaces, RF Front-Ends, and Channels for 6G Networks

Room: Ørsted (24+25)

CS34a - Recent Advances on Propagation Research and Its Impact on Localizations

T05 Positioning, localization, identification & tracking / Convened Session / Propagation

Chairs: Christian Gentner (German Aerospace Center (DLR), Germany), Wei Wang (Chang'an University, China)

8:00 Indoor MIMO Channel Measurements of the near-Field to Far-Field Transition in FR3

Richard Prüller, Robert Langwieser and Markus Rupp (TU Wien, Austria)

This paper presents an in-depth study of the near-field (NF) to far-field (FF) transition in MIMO systems from 6 GHz to 24 GHz, which largely coincides with the frequency range 3 (FR3) . A high-resolution dataset is contributed, derived from a channel sounding campaign conducted using a virtual uniform linear array (ULA) in an indoor environment. To observe the NF to FF transition we varied the ULA size while maintaining a fixed distance between the transmitter and receiver. Our findings confirm that the Fraunhofer distance provides a reliable indicator for the onset of FF conditions, offering new insights into optimizing MIMO performance for future wireless communication networks. The dataset and analysis serve as a valuable resource for further exploration of NF propagation and can be used as a study item itself or to validate NF capable channel models.

8:20 Near-Field Tracking for Reconfigurable Intelligent Surface Aided Systems Harnessing the NLoS Paths

Lingzhi Xia and Rui Wang (Tongji University, China); Xiaojun Yuan and Boyu Teng (University of Electronic Science and Technology of China, China); José Rodríguez-Piñeiro (Tongji University, China)

In this paper, the near-field tracking problem harnessing the non-line-of-sight (NLoS) paths is investigated for reconfigurable intelligent surface (RIS)-aided systems. In order to reduce the complexity of the position estimation, the near-field signal model, where the virtual line-of-sight (VLoS) paths and NLoS paths coexist, is constructed by employing the subarray far-field model. A probability transition model for the tracking problem is established, as well as the corresponding factor graph. Then, a low complexity near-field tracking algorithm based on message passing is developed to jointly estimate the UE's and scatterers' positions in each time slot. Numerical results show that the mean square error (MSE) of the proposed algorithm performs close to the misspecified Cramér-Rao Lower Bound (MCRLB), and validate the performance gain of harnessing the NLoS paths.

8:40 Bistatic Radio SLAM with Offline Shape Estimation

Peter Iwer Hoedt Karstensen (Technical University of Denmark, Denmark); Ossi Kaltiokallio, Elizaveta Rastorgueva-Foi, Jukka Talvitie and Mikko Valkama (Tampere University, Finland)

The geometric connection between the propagation environment and millimeter wave signals can be leveraged for simultaneous localization and mapping (SLAM) in 5G and beyond networks. Conventional solutions either solve the SLAM problem for a single user equipment location or rely on Bayesian filtering techniques in which the environmental landmarks are modeled using a point object model. In this paper, we devise a labeled multi-model probability hypothesis density (PHD) filter which is able to track two different types of objects. In addition, we propose an offline shape estimation algorithm which utilizes labels of the PHD filter and the measurements for estimating the shape of reflecting surfaces and small scattering objects. The proposed method is validated using ray-tracing data as well as real-world 60 GHz experimental data. The results indicate that the proposed method outperforms a state-of-the-art benchmark algorithm and the offline shape estimation algorithm improves the extracted map of the environment.

9:00 Reflection Point Localization Without Prior Environmental Knowledge

Martin Schmidhammer, Benjamin Siebler, Christian Gentner and Stephan Sand (German Aerospace Center (DLR), Germany)

We present a novel measurement-driven ray tracing approach for estimating the locations of reflection points (RPs) caused by single-bounce reflections. This approach requires no prior environmental information, like floor plans. Instead, it formulates an optimization problem that aligns the parameters of an empirical fading model with time-series data of user-induced power changes. The effectiveness of the proposed method is demonstrated through its application to ultra-wideband measurement data collected in an indoor environment. Our results show that the proposed approach achieves highly accurate RP location estimates, with minimal deviations from the true signal propagation paths. A qualitative comparison between the modeled power changes and the actual measured time-series data reveals a strong agreement, which underlines the robustness and applicability of the proposed method. This validation confirms that the approach effectively estimates both the model parameters and the RPs location, offering a reliable solution for scenarios where prior environmental information is unavailable.

9:20 An ARMA-KEST Algorithm for Ranging in Diffuse Multipath Environmen

Yue Lyu, Bingjie Xue and Wei Wang (Chang'an University, China)

In order to achieve more accurate estimation and tracking of high-resolution multipath parameters in the diffuse multipath component (DMC) environments. In this paper, based on the combination of the autoregressive moving average (ARMA) filter-based space-alternating generalized expectation-maximization (SAGE) channel parameter estimation algorithm and the Kalman filter, an enhanced super-resolution tracking algorithm which represents an enhancement of the Kalman-enhanced super resolution tracking (KEST) algorithm, i.e., ARMA-KEST algorithm. is used to achieve a highly accurate estimation and stable tracking of the channel parameters. The parameters of different paths are obtained by tracking through air-to-ground (A2G) measured data, and the power and Rice factors are analysed for different paths. The proposed algorithm provides a more accurate parameter basis for the design and performance evaluation of A2G wireless positioning systems.

Room: Mosig (26) — CS27a - Advanced additive manufactured dielectric resonator antennas

T08 Fundamental research and emerging technologies/processes / Convened Session / Antennas

Chairs: Fabien Ferrero (Université Cote d'Azur, CNRS, LEAT & CREMANT, France), Erika Vandelle (Thales Research & Technology, France)

8:00 3D-Printed DRA with Parasitic Elements to Achieve Circular Polarization

Andrea Avila-Saavedra (Pontificia Universidad Católica de Valparaíso, Chile); Henrik Ramberg and Philip Lambert (3D Fortify, USA); Francisco Pizarro (Pontificia Universidad Catolica de Valparaiso, Chile)

This article presents a 3D-printed rectangular dielectric resonator antenna (RDRA) that incorporates parasitic elements to achieve left-hand circular polarization (LHCP) in a higher-order mode, operating at 5.8 GHz. The antenna is fabricated using a high-permittivity alumina resin through a Digital Light Processing (DLP) 3D printer, which ensures precise structural integrity and material consistency. Simulation results demonstrate that the antenna achieves LHCP at the designated operational frequency, with a notable maximum gain of approximately 7.6 dB. Additionally, the 3 dB axial ratio bandwidth, is well-suited for applications such as unmanned aerial vehicles (UAVs), sensors, and other wireless communication systems. The integration of 3D printing technology further allows for rapid prototyping and customization of the antenna design, making it an attractive option for a variety of high-performance applications where conventional manufacturing techniques might fall short in terms of complexity, cost, or scalability.

8:20 3D Printable Inhomogeneous Dielectric Resonator Antenna with Cardioid Shaped Pattern

Audric Boiteau (ENAC, France & University of Toulouse, France); Christophe Morlaas (ENAC, France); Romain Pascaud (ISAE-SUPAERO, Université de Toulouse, France); Alexandre Chabory (ENAC, France); Vincent Laquerbe (CNES, France); Pouliguen Philippe (DGA, France)

This paper presents the design and simulation of rectangular dielectric resonator antennas (DRAs) that radiate linear polarization with a cardioid-shaped pattern at 2.45 GHz, without the use of a ground plane. The antenna structure allows the balanced excitation of TE and quasi-TM modes by coaxial probe feeding, resulting in orthogonal electric and magnetic dipolar contributions. Material inhomogeneity is introduced within the scope of additive manufactory possibilities, by the means of separate regions with homogeneous permittivity, in order to control resonant frequencies and quality factors of modes in spectral proximity. The proposed DRAs are numerically analyzed with eigenmode and far-field simulations using Ansys HFSS.

8:40 On the Interest of Using Bravais Lattices for the Synthesis of Effective Permittivity - Application to the Structuration of Dielectric Resonator Antennas with Additive Manufacturing

Marc Thevenot (XLIM-UMR CNRS 7252, University of Limoges, France); Cyrille Menudier (XLIM Université de Limoges, France); Nicolas Delhote (XLIM - UMR CNRS, University of Limoges, France); Olivier Tantot (XLIM - University of Limoges, France)

Dielectric Resonator Antennas (DRA) have been widely investigated in the literature, especially for their high radiation efficiency and a relative easiness to feed them with different techniques. Depending on the application, a wide range of dielectric material can be used. However, for reasons of process reliability, it can be interesting to work with the same raw material and to set its effective permittivity by adjusting a filling ratio between air medium and the raw material. Additive manufacturing is an ideal technology to create this kind of DRAs. In this contribution, a reliable homogenization technique based on Bravais crystalline lattice is proposed. It is used to synthesize the shape of the material to be built with the additive manufacturing process, without any full-wave simulation. After showing validation on measured test vehicles, examples of DRAs are presented.

9:00 A 3D-Printable High-Permittivity Ceramic Material for Lightweight Dielectric Resonator Antennas

Erika Vandelle (Thales Research & Technology, France); Chems-Eddine Naimi (Thales Research and Technology, France); Thi Quynh Van Hoang (Thales Research & Technology, France); Tom Malvaux and Guillaume Calan (Nanoe, France)

This paper presents a new 3D-printable titanium oxide (TiO2) based composite, compatible to Fused Deposition Modeling (FDM) technique, for microwave applications. After sintering, a dielectric constant of 80.7 +/- 2.2 and a loss tangent of 4.6.10-3 +/- 0.2.10^-3 were measured on the 3D filament at 5 GHz. The additive manufacturing of this material with sub-wavelength structuration enables the generation of high permittivity effective media with considerably reduced densities. In this paper, a frequency analysis of the effective permittivity is given for gyroid unit-cells with three low filling ratios of 20, 30 and 40% using the Plane Wave Expansion Method (PWEM). Finally, a very lightweight antenna of 15g operating in S band is presented. Although the sintering procedure still needs some optimization to further enhance the results, a mass reduction close to 3.3 was obtained with the antenna in TiO2 compared to its counterpart in zirconia.

9:20 Hybrid Additive Manufacturing of a Planar Dielectric Resonator Antenna Array at K-Band

Simon P Hehenberger (DLR- German Aerospace Center & TU Delft, Germany); Stefano Caizzone (German Aerospace Center (DLR), Germany); Alexander Yarovoy (TU Delft, The Netherlands)

The feasibility of using hybrid additive manufacturing (AM) to produce low-cost, phased array antennas for SatCom applications is investigated in this work. A 4x2 planar array comprised of dielectric resonator antennas (DRAs) operating in the fundamental mode within the K-band SatCom downlink band (17.7-21.2 GHz) has been designed, fabricated and measured. The impact of print settings on the material properties is assessed and incorporated into the antenna design process. Manufactured prototypes of the single element and the planar array geometry are experimentally verified in terms of their scattering parameters and far-field radiation patterns. The potential of combining hybrid AM and DRA technologies for future mmWave phased array developments is highlighted by the presented results.

Room: Collin (27) | **In memoriam of Bertram Arbesser-Rastburg**

THURSDAY

10:10 Review on the New Antenna Evolution for Next Generation WiFi-7/8 Systems

Yuandan Dong and Jiawen You (University of Electronic Science and Technology of China, China); Francis Keshmiri (Huawei Technologies, France)

This article reviews the reconfigurable antenna, beamforming array, millimeter-wave antenna, and miniaturized MIMO antennas which have attracted extensive attention in WiFi-7/8 systems. The share aperture antenna and packaged array are described. The methodologies for pattern reconfigurable antennas, miniaturized MIMO antennas, and full-plane coverage pattern diversity antennas are illustrated. Furthermore, a comparative analysis is conducted on the methods of miniaturized phased arrays, digital intelligent arrays, and nulling forming arrays based on diversity antennas. The fundamental principles and current research hotspots of these technologies are highlighted. The anticipated development path of future beam-controllable antennas is also discussed.

10:30 Low-Profile Wi-Fi Antenna with Reconfigurable Metasurface for FTTR Applications

Cristian Della Giovampaola (Wave Up srl, Italy); Francis Keshmiri (Huawei Technologies, France); Francesco Caminita (Wave-Up SRL, Italy); Yan Zeng (Huawei Technologies, China); Stefano Maci (University of Siena, Italy)

This works describes a novel, low-profile, reconfigurable two-port antenna suitable for Wi-Fi in the framework of FTTR scenarios. A total of six beams can be generated by means of a Metasurface located on top of the main radiator, and including PIN diodes as reconfigurable elements., in order to ensure proper coverage across half hemisphere. The two antenna ports and their uncorrelated beams are able to manage independent data streams for improving MIMO system capabilities. Prototype testing showed that the desired coverage was achieved with a minimal number of reconfigurable elements, which makes this technology suitable for high-performance, low-cost, low-profile devices.

10:50 Compact Horizontally Polarized Dual-Beam Antenna with Large Tilted Beam Angle for FTTR Applications

Chuyue Chen (Shenzhen University, China); Xulin Xu (ShenZhen University, China); Long Zhang (Shenzhen University, China); Francis Keshmiri (Huawei Technologies, France)

This paper proposes a horizontally polarized dual-beam antenna with a large tilted beam angle. The antenna consists of a horizontally placed dipole pair, two directors positioned on both sides of the dipole pair, an etched feeding network, and a slotted ground made from a low-cost FR4 substrate. A symmetrical feeding network is employed to provide out-of-phase excitation to the dipole pair, enabling the antenna to achieve a specific dual-beam pattern. Additionally, the directivity is enhanced by the incorporation of directors. The proposed antenna operates within a bandwidth of 5.1 to 6 GHz, with a gain between 7.5 to 8.9 dBi. With its compact size, low cost, high efficiency, and dual-tilted beam feature, the proposed antenna is well-suited for a variety of wireless networks, especially in Fiber-to-the-Room (FTTR) applications.

11:10 Accurate Prediction of the Transmission Coefficient for Surface Wave Gliding Around a Wedge

Xenofon Mitsalas, Talha Arshed, Enrica Martini and Stefano Maci (University of Siena, Italy)

A novel methodology to predict accurately the diffraction coefficients by modulated metasurfaces (MTS) forming a wedge, is presented herein. The wedge geometry of the MTS is designed to support H- polarized surface waves (SW), while its impedance faces include an angle of π/2. This work aims in proposing an elegant procedure of investigating the transmission coefficient in the framework of Sommerfeld-Maliuzhinets method. The adopted formulation enables the physical interpretation of solution in terms of field components.

11:30 Experimental Comparison Between Omnidirectional and Sectorial Antenna in a 1x8 MIMO Configuration

Cyril Buey (Orange Labs - La Turbie, France); Philippe Ratajczak (Orange Innovation, France); Fabien Ferrero (Université Cote d'Azur, CNRS, LEAT & CREMANT, France)

This work presents a comparison between Omnidirecitonal and Sectorial Antenna in a MIMO communication. A compact omnidirectional radiating element is designed and integrated in a set-top box. By adding a reflector, the radiating element can be converted to a sectorial pattern. Eight radiating element are used in a Over The Air test-bed to calculate the SNR performance in a Non-line of Sight scenario. The sectorial patern provide a higher performance communication results compared with the omnidirectional pattern.

THURSDAY

Chairs: Pilar Castillo-Tapia (KTH Royal Institute of Technology, Sweden), Cristina Yepes (TNO, The Netherlands)

10:10 Design of a Contactless AF-SIW Horn Antenna with Compact Size and Enhanced Directivity

Andrés Biedma-Pérez and Cleofás Segura-Gómez (University of Granada, Spain); Angel Palomares-Caballero (IETR-INSA Rennes, France); Juan Valenzuela-Valdés (Universidad de Granada, Spain); Pablo Padilla (University of Granada, Spain)
This work introduces a contactless air-filled substrate integrated waveguide (CLAF-SIW) horn antenna, enhanced by a metasurface along the flare of the horn. CLAF-SIW structures efficiently manage propagation zones for integrating metasurfaces, reducing phase errors at the aperture. The metasurface uses substrate integrated hole (SIH) unit cells with a parallel plate waveguide (PPW) patch. By adjusting the hollow size around the metal patch, the equivalent refractive index of the propagating mode is tuned. The antenna achieves comparable directivity to optimally sized horns, with a 41% reduction in length. Simulations show an impedance bandwidth below -10 dB from 32.8 to 49.7 GHz and directivity above 12 dBi.

10:30 Beamforming with Perfectly-Matched Metamaterials

Shrey Thakkar and Jorge Ruiz-García (University of Michigan, USA); Luke J Szymanski (MIT Lincoln Laboratory, Lexington, USA); Gurkan Gok (Raytheon Technologies Research Center, USA); Anthony Grbic (University of Michigan, Ann Arbor, USA)
This work reports an inverse design method for perfectly-matched metamaterials (PMMs) with multi-input multi-output (MIMO) functionality. PMMs are inhomogeneous, anisotropic 2-D metamaterials composed of unit cells that remain impedance-matched to each other and the surrounding medium. These reflectionless devices rely on refractive effects to perform field transformations, exhibiting true time delay behavior and broadband operation. The paper improves on a previously reported inverse design method on two fronts. First, the objective function is modified to match desired voltage magnitudes and phase profiles. Importantly, the objective function allows phase profiles to have an arbitrary phase offset instead of absolute phase values. Second, an absorbing boundary condition is imposed on all boundaries of the computational domain. As an example, a compact and broadband beamformer is presented. The device transforms the field of a point source to the far-field radiation pattern of a Dolph-Tchebyshev array of the same size, with -20dB sidelobe level.

10:50 Direct Inversion of the Regularized Ray Congruence Equation for a GRIN Deflector

Serena Assefa Asfaw (Università degli Studi di Siena, Italy); Enrica Martini and Stefano Maci (University of Siena, Italy)
This paper develops an analytical framework for designing a Graded-Index (GRIN) deflector, emphasizing a novel formulation of the regularized ray congruence (RRC) equation to achieve a closed-form solution for the refractive index profile. By deriving a new form of the integral equation, which exhibits a regularized kernel, the method facilitates the inversion of the equation in terms of the graded-index n(x). This approach enables the refractive index profile to be explicitly defined based on geometric parameters without resorting to optimization algorithms.

11:10 A Multifocal GRIN Lens Antenna Design Through the Fast Sweeping Method

Ilir Gashi, Stefano Maci and Matteo Albani (University of Siena, Italy)
The analysis of inhomogeneous lens antennas is typically done using ray tracing algorithms, which, despite being efficient, present challenges in lens design. These algorithms struggle to handle complex factors like multipath ray trajectories, complicating the design process. In this paper, we propose a novel geometrical optics (GO) analysis tool that utilizes the Fast Sweeping Method, enabling rapid computation of the Eikonal and transport equations on a rectangular grid. This method allows for the efficient retrieval of phase and amplitude distributions. We then developed a general optimization tool to determine the refractive index based on a specified target field at the lens output. To illustrate its effectiveness, we designed a wideband multifocal lens antenna operating in the Ku-band, capable of scanning ±30 degrees in the vertical plane with low scan losses. The optimization tool is versatile and can be applied to design a wide range of inhomogeneous lens antennas

11:30 Low-Profile Virtual Quasi-Optical Systems

Ethan Neitzke and Woohyung Jeon (Michigan State University, USA); Mauro Ettorre (Michigan State University, Electrical and Computer Engineering, USA)
Quasi-optical systems are used to feed in phase and amplitude radiating systems and arrays. Generally, they are based on integrated lenses or vertical metallic walls between the metallic plates of a guiding waveguide structure. This work shows the possibility of realizing reflecting optics by virtual magnetic walls. Such walls do not require any physical contact between parallel metallic plates in the structure with a clear advantage for systems requiring mechanical movements.

THURSDAY

10:10 A Method of Moments Approach for the Simulation of Truncated RIS

Adam Abazi (UCLouvain, Belgium); Jean Cavillot (Université Catholique de Louvain (UCL), Belgium); Christophe Craeye (Université Catholique de Louvain, Belgium)

A Method of Moments (MoM) approach for truncated Reflective Intelligent Surface (RIS) is proposed. The response of the truncated RIS is obtained as the sum of a term that includes only the grounded slab and a term with the response of the metallization on the same slab. The first term is truncated to the dimensions of the finite RIS based on a Physical Optics (PO) approximation. This approach is validated analytically and numerically in the case of a finite metallic plate on the grounded substrate. Besides, a design methodology for RIS made of printed parallel strips is developed assuming a structure infinite in one direction and is validated using a full 3D MoM code for a RIS finite in both directions.

10:30 Efficient S-Parameter and Far-Field Calculation of Symmetrical Multi-Port Antennas

Tim Hahn (Leibniz University Hannover, Germany); Dirk Manteuffel (University of Hannover, Germany)

A methodology for the efficient calculation of S-parameters as well as far-fields of symmetrical multi-port antennas is shown. The methodology exploits the symmetry of the antenna structure to determine the scattering matrix as well as far-fields of the antenna with attached feeding network. Using this procedure, only ports within the fundamental region have to be excited. This way, a reduction of the simulation time corresponding to the group order of the symmetry group of the antenna is achieved. Further, the coupling of the antenna ports can be predicted using a cascaded scattering matrix approach.

10:50 A Numerical Verification of Analytical Solution for the Mixed Fourier Transform Equation

Martin Petek (Politecnico di Torino, Italy); Denis Tihon (Université Catholique de Louvain, Belgium); Jorge A. Tobon Vasquez (Politecnico di Torino, Italy); Christophe Craeye (Université Catholique de Louvain, Belgium); Francesca Vipiana (Politecnico di Torino, Italy)

Analysis of 2D-periodic structures is often carried out with the Method of Moments, which is capable to obtain simultaneously the phase velocity and attenuation constant of surface- or leaky-waves (i.e. eigenmodes). However, to find the eigenmodes associated with a given geometry, many samples of the impedance matrix are needed, whose evaluation can be computationally expensive. To overcome the computational burden, efficient interpolation procedures have been proposed, which are based on the decomposition of the impedance matrix into Floquet modes and the proper extraction of some of them. However, the evaluation of a given Floquet mode with the reaction integral can be difficult when the integration regions of the source and test basis functions overlap along the z-axis. In this work, we deal with this difficult case: we propose a fully analytical solution and validate it numerically. Our work paves the way for fast interpolation procedures to arbitrary structures.

11:10 Recent Developments in Large-Scale Array Analysis for Radio Astronomy Applications

André S Conradie, Pierre I. Cilliers and Matthys M. Botha (Stellenbosch University, South Africa)

This paper presents an efficient local solution-based solver with nested cross approximation (NCA) matrix compression for the analysis of large disjoint antenna arrays. Preliminary results demonstrate runtime improvements of about an order of magnitude over the multilevel fast multipole method (MLFMM) in the commercial FEKO software suite, for the computation of embedded element patterns (EEPs) in a large antenna array above an infinite perfect electrical conductor (PEC) ground plane. The solver is ideally suited to parallelisation.

11:30 Practical Design Techniques for Time-Varying Transmission Lines with Nonlinear Capacitance

Aiganym Abzaliyeva and Bakhtiyar Orazbayev (Nazarbayev University, Kazakhstan)

This work provides a comprehensive framework for developing and implementing time-varying transmission lines (TVTLs) with capacitance modulation. It includes a multifaceted approach for designing varactor-loaded TVTLs to achieve the desired transmission by optimizing the scattering matrix using Mathematica and Advanced Design System (ADS). This approach obtains critical design parameters such as microstrip line width and length, slab thickness, and stub length. Moreover, the system's dynamic behavior under modulation is precisely modeled and analyzed in Finite-Difference Time-Domain (FDTD) simulations, demonstrating the frequency conversion and parametric amplification in TVTL. Finally, we experimentally confirmed the analytical and simulation results, focusing on presenting the frequency conversion of frequencies 0.25 and 0.5 GHz. The results show excellent alignment with theoretical predictions, significantly shortening the design process and underscoring the effectiveness of our methodology. The proposed method will be used to design and fabricate the TVTL-based parametric amplifiers to demonstrate nonreciprocal and non-Hermitian phenomena.

T07 Electromagnetic modelling and simulation tools / Convened Session / Propagation

Chairs: Pekka Kyösti (Keysight Technologies & University of Oulu, Finland), Yejian Lyu (Shanghai Jiao Tong University, China)

10:10 T-RIS and R-RIS Experimental Characterization in the Sub-THz Band

Bo Kum Jung and Varvara V. Elesina (Technische Universität Braunschweig, Germany); Sergio Matos (ISCTE-IUL / Instituto de Telecomunicações, Portugal); Orestis Koutsos (CEA Leti, France); Antonio Clemente (CEA-Leti, France); Thomas Kürner (Technische Universität Braunschweig, Germany); Raffaele D'Errico (CEA, LETI & Université Grenoble-Alpes, France)

Sub-terahertz (sub-THz) communications is expected to be a key element for future wireless communications enabling extremely high data transmission rate. Its performance can be further emphasized by the use of reconfigurable intelligent surface (RIS), which provides the beamforming possibility of electromagnetic (EM) waves in a desired direction. The channel measurement is a fundamental element in understanding the characteristics of the propagation channel. To emulate a system composed of transmissive RIS (T-RIS) and reflective RIS (R-RIS), an electrically large transmit-array and reflect-array were designed. The paper presents the results of the single directional channel measurement of the sub-THz channel composing a concatenation of non-reconfigurable T-RIS and R-RIS. The results presented in this paper demonstrate the feasibility and scalability of establishing a sub-THz link by concatenating multiple RIS units for future applications.

10:30 Validation of Ray-Tracing Tool Utilizing Multi-Band Measurements in Industrial Scenarios Up to THz Frequencies

Damir Sitdikov (Technische Universität Ilmenau, Germany); Diego Andrés Dupleich (Technische Universität Ilmenau, Germany & Fraunhofer Institute for Integrated Circuits IIS, Germany); Alexander Ebert (Technische Universität Ilmenau, Germany); Mate Boban (Huawei Technologies Duesseldorf GmbH, Germany); Giovanni Del Galdo (Fraunhofer Institute for Integrated Circuits IIS & Technische Universität Ilmenau, Germany)

In this work, we introduce a thorough comparison between ray tracing (RT) simulations and multi-band measurements in a complex scenario such as an industrial environment. The RT model was generated from precise 3D laser scans in a small machinery room. A 3D model was recreated and processed using commercial and non-commercial software. Simultaneously, double-directional dual-polarized ultra-wideband measurements at 6 GHz, mmWave, sub-THz, and THz were also carried out for calibration and validation purposes. The RT simulations were conducted in the open-source tool for physical channel modeling Sionna. Afterwards, the measurement set-up was emulated by embedding the measurement bandwidth and antenna patterns into the RT simulations for a fair comparison. The results show a good agreement on the location of the dominant scatterers.

10:50 Stochastic Analysis of THz Band Satellite Channels' Quality

Joonas Kokkoniemi (University of Oulu, Finland)

The satellite networks are among the most promising platform to achieve true global connectivity. The millimeter wave and THz frequencies on the other hand provide large data rates needed particularly in backhaul and fronthaul networks. This paper looks into the stochastic performance of +100 GHz channels in satellite uplink and downlink cases. It is shown that while SNRs can be quite good, there are still great challenges to go around very large losses and the large outage probabilities that those cause. This is particularly the case when we add on the channel losses possible rain and cloud losses, antenna misalignment losses, or any other losses that can occur in the satellite channels.

11:10 Experimental Analysis and Modeling of Scattering Characteristics with Multiple Azimuth Angles in Sub-THz Band

Yunxiao Deng, Pan Tang, Zhaowei Chang and Jianhua Zhang (Beijing University of Posts and Telecommunications, China)

The terahertz (THz) band, with its abundant spectrum resources, is regarded as a promising candidate band for future communication systems. As the frequency increases, surfaces that are smooth at low frequencies become rough for THz waves, making scattering more dominant for wave propagation. To investigate the THz scattering characteristics across multiple azimuth angles in three-dimensional space, extensive scattering measurements are conducted in three-dimensional space from 110 to 140 GHz. These measurements cover scattering from various material samples at zenith angles ranging from 5° to 80° and azimuth angles from -30° to 30°. Then, the scattering intensity distribution at different azimuth angles and its variation with frequency are analyzed based on the measurement data. Finally, a statistical model is proposed to describe the scattering intensity distribution and its frequency dependence. The model shows agreement with the measurements across surfaces with varying roughness.

11:30 Terahertz Channel Modeling Considering Near-To-Far Field Transition: Benefits & Challenges

Priyangshu Sen (SUNY Polytechnic Institute, USA); Sherif Badran (Northeastern University, USA); Josep M Jornet (Northeastern University & Institute for the Wireless Internet of Things, USA); Arjun Singh (SUNY Polytechnic Institute, USA)

Terahertz band (0.1-10 THz) communication is set to play a pivotal role in the advancement of subsequent generations of wireless technology by facilitating high data rates, ultra-secure transmission, high-resolution sensing, and low latency links, among others. Nevertheless, the issues of low transmission power and high path loss necessitate large-aperture, high-gain antennas, which can result in a considerably expanded near-field operational region. The distinctive mechanism of wave propagation within this region, as well as its transition to the far-field area, necessitates a comprehensive reevaluation of channel modeling. In this paper, we discuss the effects of antennas on path loss models and channel metrics while operating in both the near and far-field regions. We present a detailed analysis of near-field propagation mechanisms, illustrating that an antenna-agnostic channel model is not feasible. Furthermore, we discuss the potential benefits and challenges associated with these regions.

THURSDAY

Room: Bergman (34)

CS64b Extremely large or distributed antenna systems in near-field environments

T08 Fundamental research and emerging technologies/processes / Convened Session / Antennas

Chair: George C. Alexandropoulos (University of Athens & University of Illinois Chicago, Greece)

10:10 Experimental Study on the Effect of Synchronization Accuracy for Near-Field RF Wireless Power Transfer in Multi-Antenna Systems

Gilles Callebaut, Jarne Van Mulders and Bert Cox (KU Leuven, Belgium); Benjamin J. B. Deutschmann (Graz University of Technology, Austria); Geoffrey Ottoy (KU Leuven & Technology Campus Ghent, Belgium); Lieven De Strycker and Liesbet Van der Perre (KU Leuven, Belgium)

Wireless power transfer (WPT) technologies hold promise for enhancing device autonomy, particularly for energy-limited IoT systems. This paper presents experimental results on coherent and non-coherent transmit diversity approaches for WPT, tested in the near field using the Techtile testbed. We demonstrate that a fully synchronized beamfocusing system achieves a 14 dB gain over non-coherent transmission, consistent with the theoretical 14.9 dB gain for a 31-element array. Additionally, phase alignment errors below 20° result in less than 1 dB of gain loss, while errors exceeding 40° lead to losses over 3 dB. These findings suggest that phase coherency requirements for WPT can be relaxed, and that scaling the number of antennas is a promising strategy for improving power transfer efficiency.

10:30 Near-Field Beam Shaping Through Cooperative RIS for Wireless Communications and Sensing

Álvaro F. Vaquero (Universidad de Oviedo, Spain); Sergio Menéndez Feito (University of Oviedo, Spain); Manuel Arrebola (Universidad Politécnica de Madrid, Spain)

This work introduces an analysis of the use of multiple RIS to generate coverage in mm-Wave bands in the near-field region. Within the Smart EM environment paradigm, different RIS can be employed to cover the same area, collaboratively enhancing the signal received by the user. If the signals are incoherent, the coverage from each RIS can be treated independently. However, with coherent signals, combining all the RIS can create unwanted interference patterns in the coverage. A near-field model is introduced to calculate the resulting coverage from multiple RIS in arbitrary positions and orientations. Additionally, the relative phase between RISs is proposed as a control variable, enabling the reduction of interference in the region of interest. Numerical examples are presented to demonstrate the importance of this analysis in scenarios for near-field focusing and beam shaping, highlighting key parameters in the use of collaborative RIS.

10:50 Near-Field Evaluation of an Radiated-Two-Stage-Based Millimeter-Wave 5G New-Radio Multiple-Input-Multiple-Output Over-The-Air Test System

Yunsong Gui (National Physical Laboratory (UK), United Kingdom); Tian Hong Loh (UK, National Physical Laboratory, United Kingdom); Jonathan Borrill (Anritsu Corporation, Sweden)

The paper presents a preliminary near-field evaluation of a radiated-two-stage (RTS)-based mm-wave 5G new-radio (NR) MIMO OTA test system. The aim is to verify whether the RTS method is applicable in near-field for the frequency range 2 (FR2). In this paper, a software-defined-radio-based user equipment emulator has been developed, which contains a fully functioning baseband processing unit compliant to the 5G NR physical layer protocol. At the transmitting end, a base station emulator (BSE) from Anritsu has been incorporated with a channel emulator (CE). A controlling program to coordinate all different functional blocks in the testbed have also been developed. Some key factors which can significantly influence the performance of the RTS such as the ATF have been carefully studied through performing actual measurement campaign in a fully anechoic chamber. Finally, the performance evaluation of the RTS method in the near field is presented through the preliminary measurement results.

11:10 Indoor Channel Characterization with Extremely Large Reconfigurable Intelligent Surfaces at 300 GHz

Fábio Martinho Cardoso (Iscte - Instituto Universitário de Lisboa & Instituto de Telecomunicações, Portugal); Sergio Matos (ISCTE-IUL / Instituto de Telecommunicações, Portugal); Luis M. Pessoa (INESC TEC & Faculty of Engineering, University of Porto, Portugal); George C. Alexandropoulos (University of Athens & University of Illinois Chicago, Greece)

The technology of Reconfigurable Intelligent Surfaces (RISs) is lately being considered as a boosting component for various indoor wireless applications, enabling wave propagation control and coverage extension. However, the incorporation of extremely large RISs, as recently being considered for ultra-high capacity industrial environments at subTHz frequencies, imposes certain challenges for indoor channel characterization. In particular, such RISs contribute additional multipath components and their large sizes with respect to the signal wavelength lead to near-field propagation. To this end, ray tracing approaches become quite cumbersome and need to be rerun for different RIS unit cell designs. In this paper, we present a novel approach for the incorporation of RISs in indoor multipath environments towards their efficient channel characterization. An 100x100 passive RIS design with 2-bit resolution unit cells operating at 300 GHz is presented, whose radar cross-section patterns are obtained via full-wave simulations. It is showcased that the RIS behavior can be conveniently approximated by a three-ray model, which cane be efficiently incorporated within ray tracing tools, and that the far-field approximation is valid for even very small distances.

THURSDAY

11:30 Experimental Modeling of Power Attenuation Factor for Characterizing Spatial Non-Stationary in XL-MIMO Channels

Jie Meng, Pan Tang and Haiyang Miao (Beijing University of Posts and Telecommunications, China); Lei Tian (Beijing University of Posts and Telecommunications & Wireless Technology Innovation Institute, China); Jianhua Zhang (Beijing University of Posts and Telecommunications, China)

Extremely large-scale Multiple-Input Multiple-Output (XL-MIMO) is envisioned as a promising technology for sixth-generation (6G) communication, with the deployment of extremely large-scale antenna arrays at both the transmitter and receiver in XL-MIMO channels resulting in spatial non-stationary (SnS) characteristics. Although numerous channel measurements and models have been proposed focusing on the SnS characteristics of XL-MIMO channels, few low-complexity channel models characterize the characteristics. This paper proposes a low-complexity experimental model based on the power attenuation factor to characterize SnS. In this paper, channel measurements are conducted at 13 GHz in an indoor office. Analysis of the measurement data reveals significant fluctuations in cluster power along the antenna elements due to SnS. The power attenuation factor is used to model the power variations of clusters caused by SnS. The modeling method effectively captures the SnS characteristics. It provides important references for the XL-MIMO channel modeling research and standardization work

Room: Felsen (35+36)

CS55b - Fundamental challenges and novel methodologies in the next-generation computational electromagnetics

T07 Electromagnetic modelling and simulation tools / Convened Session / Electromagnetics

Chairs: Zhen Peng (University of Illinois at Urbana-Champaign, USA), Francesca Vipiana (Politecnico di Torino, Italy)

10:10 Analytical Strategy to Obtain FSS Equivalent Networks with Frequency-Dependent Elements

Raúl Rodríguez-Berral (Universidad de Sevilla, Spain); Francisco Mesa (University of Seville, Spain); Francisco Medina (University of Sevilla, Spain)

This contribution proposes a strategy to compute frequency-dependent values of the elements of an equivalent circuit network for the wideband co-pol and cross-pol response of metallic frequency-selective surfaces. In the framework of a formulation developed in previous works by the authors, which provide relatively simple semi-analytical expressions for the elements in a Foster-like network, a systematic procedure based on a power series expansion is proposed. This allows introducing the frequency dependence into the elements while keeping the overall analytical nature of the formulation. The results provided by the equivalent network are validated by proper comparison with those obtained from a custom implementation of the method of moments.

10:30 Influence of MoM Test Integral Accuracy on the Solution of Field Integral Equations

Javier Rivero (Politecnico di Torino, Italy); Víctor Martín (Universidad Rey Juan Carlos, Spain); Donald Wilton (University of Houston, USA); William Johnson (Private Consultant, USA); Francesca Vipiana (Politecnico di Torino, Italy)

The usual procedure to evaluate the outer reaction integral that appears in the method of moments is integrated with Gauss quadrature schemes. However, standard Gauss quadrature schemes often struggle with near-singular test integrals, leading to inaccuracies that degrade the solved current vector. We show that even a few inaccurate impedance matrix elements can significantly affect the overall solution.

10:50 3D Adjoint Optimization for Designing Inhomogeneous Dielectric Materials with Specified Performance Objectives

Luis Jiménez (Universitat Politecnica de Valencia, Spain); Felipe Vico and Marta Cabedo-Fabrés (Universidad Politécnica de Valencia, Spain); Miguel Ferrando-Bataller (Universitat Politècnica de València, Spain)

In this work, we present an adjoint-based optimization method for the 3D volume integral equation aimed at optimizing inhomogeneous dielectric materials. The material is discretized into voxels, with the permittivity (ε) in each voxel adjusted to maximize a specified objective function. Using this approach, we design flat, inhomogeneous lenses with tailored focal lengths, lenses that achieve distinct focal points at different frequencies, and lenses that split the power between two focal points. The optimization is formulated using the 3D acoustic wave equation and validated against full-wave electromagnetic simulations using commercial solvers.

THURSDAY

11:10 Multitrace Huygens Encapsulation for Interoperability in Electromagnetic Design

Víctor Martín (Universidad Rey Juan Carlos, Spain); Antonio Gomez-Rodriguez (EM3WORKS, Spain & Universidad de Extremadura, Spain); Manuel Parejo (EM3WORKS, Spain); Luis Landesa (Universidad de Extremadura, Spain); Marta G. Araújo (Universidade de Vigo, Spain); Fernando Obelleiro (University of Vigo, Spain); Jose M. Taboada (University of Extremadura, Spain)

Computational electromagnetics (CEM) has become essential in aerospace and naval engineering, particularly for analyzing electromagnetic interference (EMI) and compatibility (EMC) in defense applications involving complex platforms. As hyper-sensorization trends emerge, the need for enhanced CEM methods becomes evident to manage electromagnetically dense environments while meeting strict EMC/EMI and radiation hazard (RADHAZ) requirements. Confidentiality concerns pose challenges in information sharing among international partners, complicating the design of subsystems. This work proposes an EPA-based domain decomposition scheme that encapsulates electromagnetic interactions of large-scale platforms using small-scale Huygens' surfaces. The method significantly improves efficiency and accuracy in the design of antennas and sensors onboard platforms without requiring detailed geometric knowledge. Additionally, it allows assessment of antennas' contributions to radar cross-section (RCS) while maintaining safety and confidentiality standards. Integrated with advanced techniques based on the domain decomposition method and multitrace (MT) formulations, this approach also ensures robust modeling of near-field interactions among encapsulated objects.

11:30 Photon Splatting: Real-Time Neural Representation for Predicting 3D Indoor Radio Channels

Ge Cao (University of Illinois at Urbana-Champaign, USA); Qi Jian Lim (University of Illinois Urbana-Champaign, USA); Gabriele Gradoni (University of Surrey, United Kingdom); Zhen Peng (University of Illinois at Urbana-Champaign, USA)

Modeling radio wave propagation in complex indoor environments is essential for next-generation (NextG) wireless applications such as immersive computing, and wireless digital twins, which require reliable, real-time predictions to optimize connectivity and ensure seamless performance. However, traditional ray-tracing algorithms are computationally prohibitive for these applications. In this paper, we propose Photon Splatting, a novel neural representation inspired by photon mapping and Gaussian splatting, which delivers real-time predictions of channel impulse responses. Moreover, our framework accurately captures dynamic changes in transmitter and receiver locations and operates seamlessly with unseen antenna patterns, all without requiring retraining. We validate the work on both indoor room datasets and large-scale stadiums, demonstrating its scalability and robust performance, with prediction times in the order of milliseconds. This work bridges the gap between accuracy and real-time adaptability, offering a powerful tool for NextG wireless that demands high-speed, precise propagation modeling.

Room: Schelkunoff (C1)

CS15b - Shared-Aperture Antenna and Antenna Collocation Strategies and Methods for Communication, Radar and SATCOM

T01 Sub-6 GHz for terrestrial networks (5G/6G) / Convened Session / Antennas

Chair: Can Ding (University of Technology Sydney (UTS), Australia), Alessio Monti (Roma Tre University, Italy)

10:10 Suppression of Cross-Band Resonance Coupling in Dual-Band Shared-Aperture Antenna Array

Shangyi Sun (University of Technology Sydney, Australia); Can Ding (University of Technology Sydney (UTS), Australia); Haihan Sun (University of Wisconsin-Madison); Y. Jay Guo (University of Technology Sydney, Australia)

In dual-band antenna arrays, radiation patterns of low band (LB) antenna working in wide band might occur severe distortions and gain reduction with presence of adjacent high band (HB) antennas. Differing from the scattering from the LB antenna causing distortions in HB patterns and the coupling resulting in cross-band isolation degradation, this interference attributes to resonance coupling. To move resonance frequency point out of the target LB 0.69-1.00 GHz (36.7%), parallel resonance shifters are added between HB baluns and ground. Radiation patterns and realized gain within the LB are restored when the shifter-loaded HB antennas are present. In addition, this parallel structure has no adverse effect on the radiation and wideband matching of the HB antennas over 1.63-2.83 GHz (53.8%). A prototype of dual-band antenna array is fabricated, and measured results show good consistency with the simulated ones.

10:30 Radiation and Scattering Control of Antennas Through Self-Tuning Metasurfaces with Frequency- and Time-Domain Selective Properties

Stefano Vellucci (Niccolò Cusano University, Italy); Alessio Monti and Mirko Barbuto (Roma Tre University, Italy); Hiroki Wakatsuchi (Nitech, Japan); Alessandro Toscano and Filiberto Bilotti (Roma Tre University, Italy)

This paper presents a novel approach to enhancing the adaptability of wireless communication systems through the integration of self-reconfigurable metasurfaces with frequency- and time-domain selective properties. As wireless technologies such as IoT, 5G, and beyond 5G evolve, the demand for efficient use of frequency resources increases. Traditional antenna systems, with fixed-frequency responses, struggle to meet the dynamic needs of these environments. To address this, we introduce self-tuning metasurfaces that autonomously adjust their radiation and scattering characteristics based on the frequency and temporal properties of incoming signals. These metasurfaces, integrated with nonlinear circuits, offer significant improvements in applications like beam-steering, selective scattering, and filtering. We demonstrate this through three antenna configurations: a filtering aperture antenna, an invisible antenna with selective cloaking, and a beam-steering metasurface array. Our results show that this technology holds great promise for next-generation communication systems by enabling more flexible, efficient, and adaptable antenna designs.

THURSDAY

10:50 A Shared-Aperture Decoupling Network (SADN) for Dual-Band Differentially-Fed Antenna (DFA) Array

Xichen Wang (Beijing Institute of Technology, China); Can Ding (University of Technology Sydney (UTS), Australia); Li Shiyong, Guoqiang Zhao and Houjun Sun (Beijing Institute of Technology, China)

This paper proposes a dual-band shared-aperture decoupling network (SADN) to suppress mutual coupling in a dual-band antenna array. The array consists of two high-band (HB) patches and two low-band (LB) patches, all fed differentially. The SADN addresses both in-band coupling between the two HB antennas and between the two LB antennas, as well as cross-band coupling between the LB and HB antennas. The SADN can adapt to multi-band DFA arrays with different frequency ratios. To validate the design principle, a dual-band DFA array operating at 18.5 GHz and 28 GHz with a frequency ratio of 1:1.51 was designed, fabricated, and tested. The fractional bandwidths of the two bands are 5.4% and 10.1%, respectively. Within both bands, the isolation between any ports exceeds 26 dB. Compared to the case without the SADN, significant isolation improvements ranging from 15 dB to 45 dB have been achieved

11:10 A Novel Dual-Band Share Aperture Array Scheme with Sharing Feeding Ports for Bease Station Application

Shengyuan Luo, Luyu Zhao and Yingsong Li (Anhui University, China); Wei Lin (The Hong Kong Polytechnic University, Hong Kong)

A novel share aperture dual-band array scheme is proposed in paper. Different from the traditional share aperture scheme, the low band antenna is integrated into the high band antenna to form a co-designed LB/HB array that shares common feeding ports. The 3×3 high-band array and a staggered low-band array is integrated into overall one. The share aperture array has working bands of 3.2-3.7 GHz and 4.9-5.54 GHz, respectively. The isolation of the array is 13.65 dB, respectively. The proposed array has a merit that the low-band antennas and high-band antennas have common feeding ports, and the radiation performance of HB array do not affected by LB radiators.

11:30 Dual Band Dual Polarisation Shared Aperture Ka Rx/Tx Phased Array for Ultra High Throughput Satellites

Etienne Girard, Jean-Philippe Fraysse and Andrea Guarriello (Thales Alenia Space, France); Hervé Legay (Thalès Alenia Space, France)

A dual-band, Ka Tx/Rx shared aperture phased array is presented, with a frequency ratio 1.5:1 between the sub-bands. The radiators are in waveguide technology, and an innovative concept is proposed that permits to manage different lattice constraints at both sub-bands.

Room: Maxwell (C2) — CS61b - AMTA Post Processing Techniques in Antenna Measurements

T07 Electromagnetic modelling and simulation tools / Convened Session / Measurements

Chair: Francesco Saccardi (Microwave Vision Italy, Italy), Anouk Hubrechsen (Eindhoven University of Technology & AntenneX B. V., The Netherlands)

10:10 Advanced In-Situ Antenna Measurement System Employing a Robotic Arm and Composite Planar Surfaces

Celia Fontá Romero (Universidad Politécnica de Madrid, Spain & Universidad Rey Juan Carlos, Spain); Ana Arboleya (Universidad Rey Juan Carlos, Spain); Fernando Rodríguez Varela (Universidad Rey Juan Carlos de Madrid, Spain); Eduardo Martinez-de-Rioja (Universidad Rey Juan Carlos, Spain); Manuel Sierra-Castañer (Universidad Politécnica de Madrid, Spain)

This paper presents an in-situ antenna measurement system based on a small robotic arm mounted on a mobile platform. To overcome the limitations of the robot's size on the measurement surface, a new technique that assembles a large measurement plane from smaller individual ones is introduced. These smaller planes are acquired by manually repositioning the robot to different locations, where it automatically performs the plane measurements. An optical tracking system (OTS) ensures accurate positioning, and an automated calibration process compensates for any misalignments caused by the manual movements. The proposed system and technique are experimentally validated through measurements of an X-band antenna, showing good agreement with reference results

10:30 Dipole and Quadrupole Modes in Spherical Wave Expansions for Derivative Probes

Olav Breinbjerg (ElMaReCo, Denmark)

We investigate spherical wave expansions for fundamental electric and magnetic dipole and quadrupole configurations as well as for derivative probes. This investigation is aimed at developing solution procedures for the transmission formula for spherical near-field antenna measurements employing derivative probes for sampling of both the field/ signal and a field/signal spatial derivative

10:50 Compressed Sensing Based Spherical Mode Filtering Reflection Suppression for Far-Field Testing in Complex Electromagnetic Environments

Stuart F Gregson and Rostyslav Dubrovka (Queen Mary, University of London, United Kingdom); Clive Parini (Queen Mary University of London, United Kingdom)

This paper presents the first investigation of a two-dimensional, compressed sensing based spherical mode filtering reflection suppression technique for far-field antenna measurements when applied in a complex electromagnetic environment, e.g. when the test antenna is in the presence of a an electrically large parasitically coupled scatterer. Such scatterers inevitably influence measurement results including radiation pattern, cross-polarisation level, gain, directivity, etc., and are of particular concern when testing in a far-field mode; and especially so when testing outside. Through a massive numerical simulation which utilised a proprietary full-wave, three-dimensional, computational electromagnetic solver, the viability of this new processing technique has been verified, with preliminary results showing that the technique is valid even under such complex scattering conditions.

11:10 Redundancy in Near-Field Antenna Measurements: A Constrained SVO Approach

Amedeo Capozzoli, Claudio Curcio and Angelo Liseno (Università di Napoli Federico II, Italy)

The work deals with redundancy in near-field measurements and its relation with the Signal to Noise Ratio available on the data. To this end, a constrained version of the Singular Value Optimization (SVO) approach is introduced. The performance of constrained SVO is analyzed numerically for a 1D, scalar radiation problem.

11:30 3D Radiation Pattern Reconstruction of Millimeterwave Wireless Device with Phaseless Near-Field Measurements

Myssipsa Mehraz (IMT Atlantique & LabSticc Laboratory, France); Francois Gallée (IMT Atlantique, France); Shoaib Anwar (Microwave Vision Group, Satimo Industries, France)

This paper explores the application of the Iterative Fourier Transform (IFT) algorithm for reconstructing antenna radiation patterns using phaseless near-field measurements. A detailed comparison between two variants of the IFT algorithm is conducted to evaluate their convergence efficiency and accuracy in phase retrieval. The selected IFT variant was validated through measurements of a 96 GHz horn antenna. We studied key phaseless measurement parameters to ensure proper control over their impact on the algorithm, as well as to optimize and accelerate measurement times according to specific needs. It was demonstrated that the IFT algorithm is robust even when the defined aperture size exceeds the actual antenna size and can also be used to approximate the true antenna size. After algorithm validation, we applied it to an integrated antenna array within a 60 GHz Wi-Fi module to characterize its radiation pattern.

Room: Oliner (C3) — CS5b Vehicular Antenna Systems and Solutions

T04 RF sensing for automotive, security, IoT, and other applications / Convened Session / Antennas

Chairs: Wonbin Hong (Pohang University of Science and Technology (POSTECH), Korea (South)), Christian Lötbäck (Volvo Car Corporation, Sweden)

10:10 Channel Emulation for OTA Test Based on a Simulated Channel in a V2V Drive Scenario

Kristian Karlsson (RISE Research Institutes of Sweden, Sweden); Aleksei Fedorov (Lund University, Sweden); Nikita Lyamin (Volvo Car Corporation, Sweden); Fredrik Tufvesson (Lund University, Sweden)

This paper introduces a novel approach for transitioning from high-granularity Ray-Tracing (RT) channel simulations to channel emulation, accompanied by an over-the-air test. The RT simulation is performed on a Vehicle-to-Vehicle (V2V) communication drive scenario generating basis for channel emulation in a channel emulator. The channel simulation, and the accompanying channel emulation, also enables inclusion of 3D radiation patterns of both transmitting as well as receiving antennas in the V2V setup. Validation procedures are executed to verify the proposed method, which finally is used on a set of real radio units and the experimental results are presented.

10:30 Study of a Hybrid Solver Method for Vehicle-Installed Antenna Simulation

Yi Feng (Scania CV AB, Sweden)

Radiation performance simulation of vehicle-installed antennas is highly demanding in terms of computational resources because the vehicle is an electrically very large structure and the vehicle versus antenna has a very large structure ratio. A hybrid solver method has been developed in CST Studio Suite to increase the computation efficiency by separately solving the vehicle and the antenna and then coupling the two solvers. In this paper we studied the computation accuracy and efficiency of cabin roof-installed cellular antennas using this hybrid solver method. The results demonstrated that the hybrid solver method with the uni-directional coupling type chosen is able to provide very close results to those obtained using the traditional full-wave single solver method and yet reduced 70% of the computation time.

THURSDAY

10:50 Design and Evaluation of a Q-Band 4-Element DBF Antenna as Part of Direct Digital RF Transmitter Antenna Modules for On-Board SATCOM Systems

Welday Gerezgiher Berhe, Koki Furuuchi, Tomoyuki Furuichi, Satoshi Tsukamoto and Noriharu Suematsu (Tohoku University, Japan)

This paper presents the design, fabrication, and evaluation of a circularly polarized Q-band 4×1 digital beamforming (DBF) array antenna for SATCOM applications. Single beam forming and multi beam forming radiation pattern of the fabricated Q-band array antenna was measured to assess its performance. Conventional analog phased antenna array (PAA) method and DBF method were employed for single beam measurements at 40GHz. Simultaneous multi beam forming measurement at 40GHz and 40.5GHz was also conducted. Measured main polarization gain pattern results closely align with the simulated values, validating the antenna's design. Also, good axial ratio (AR) values across the main lobe are obtained, showing a good polarization purity. Moreover, the array antenna demonstrated for simultaneous multi beam forming at 0° and -30°, as well as 0° and +30° main beam direction combinations. The measurement results confirmed the potential of the fabricated antenna array for advanced beam steering applications like SATCOM systems.

11:10 A Modular Series-Fed Phased Antenna Array for Satellite Reception on Moving Vehicles

Aqeela Saghir (LINKS Foundation, Italy & Frederick University, Cyprus); Rossella Gaffoglio, Giuseppe Musacchio Adorisio and Giuseppe Franco (Fondazione LINKS, Italy); Giorgio Giordanengo (LINKS Foundation, Italy)

Flat panel phased arrays are compact and versatile solutions finding extensive applications in satellite communications thanks to their beam scanning capabilities and high performance. This paper presents a series-fed phased array antenna for GEO satellite reception on moving vehicles in the Ku band, designed with a modular approach. Each module is composed of 8 rows of 16 radiating elements fed through series striplines to achieve simple layout, high gain, and reduced costs. Simulated performance of a solution consisting of two mirrored modules of 8x16 elements (8x32 elements in total) shows a gain from 25 to 27 dB in more than 16% of the Ku band. The antenna was designed and fabricated to perform 1D electronic steering in a hybrid 2D-scanning electronic/mechanical configuration.

11:30 Overview of Polarimetry in Application to Automotive Radar: Array Design, Calibration and Target Feature Extraction Concepts

Changxu Zhao and Yanki Aslan (Delft University of Technology, The Netherlands); Alexander Yarovoy (TU Delft, The Netherlands)

An overview of polarimetric sensing and its growing application in automotive radar systems is presented. While polarimetric techniques are extensively used in fields like weather monitoring and target imaging, their integration into automotive radar presents unique challenges, particularly in calibration and measurement accuracy across wide scanning angles. This paper reviews key polarimetric principles and their use in different applications, with a focus on current automotive radar implementations, and the calibration challenges posed by off-broadside measurements. Future research directions for improving polarimetric accuracy in dynamic automotive environments are also discussed.

Room: Kraus (C4)

CS57b - Biomedical Microwave Techniques and Devices: from Diagnosis to Treatment

T06 Biomedical and health / Convened Session / Propagation

Chairs: Raquel C. Conceição (Instituto de Biofísica e Engenharia Biomédica, Faculdade de Ciências, Universidade de Lisboa, Portugal), Daniela M. Godinho (Instituto de Biofísica e Engenharia Biomédica - Faculdade de Ciências - Universidade de Lisboa, Portugal)

10:10 Permittivity Estimation for Patient-Specific Head Model via DBIM

Darko Ninković, Anja R Kovačević and Branko Kolundzija (University of Belgrade, Serbia); Rosa Scapaticci (CNR-National Research Council of Italy, Italy); Lorenzo Crocco (CNR - National Research Council of Italy, Italy); Marija Stevanovic (University of Belgrade, Serbia)

In this paper, we present a method for generating a patient-specific head model comprising four homogenous tissues. This model is meant to provide a convenient starting point for the initialization of quantitative microwave imaging algorithms. First, an approximate distribution of the head permittivity is rapidly estimated using a linear inverse scattering model based on the Born approximation, regularized with polynomial basis functions for the contrast. Segmentation of the obtained images is used to generate a four-domain 3D phantom comprising a thin surface layer mimicking skin and fat tissue covering the skull, the skull, the brain, and the soft tissue. The parameters of the four tissues are estimated using a properly cast distorted Born iterative inversion approach. The quality of the obtained model was assessed by comparing the scattering parameters of the original and the generated model.

10:30 Towards Co-Registration of MR Images with MW System via Qualitative Inverse Scattering

Martina Teresa Bevacqua (Università Mediterranea di Reggio Calabria, Italy); Michele Ambrosanio (University of Naples Parthenope, Italy); Joe LoVetri (University of Manitoba, Canada); Vito Pascazio (Università di Napoli Parthenope, Italy); Tommaso Isernia (University of Reggio Calabria, Italy)

The paper proposes a new procedure to co-register a magnetic resonance image with a microwave system. The procedure allows the extraction of prior information from MRI images to be used in biomedical microwave imaging and hyperthermia treatment planning. The tests are performed against microwave experimental data collected at the Electromagnetic Imaging Laboratory of the University of Manitoba

10:50 Electromagnetic Characterization and Biocompatibility Assessment of Magnetic Materials for Biomedical Applications

Matteo Bruno Lodi (University of Cagliari, Italy); Gennaro Bellizzi (University of Naples Federico II, Italy); Annalaura Paulis and Nicole Grandi (University of Cagliari, Italy); Roberta Palmeri (Università Mediterranea of Reggio Calabria, Italy); Ehsan Akbari Sekehravani (Institute for the Electromagnetic Sensing of the Environment, CNR, Italy); Lorenzo Crocco (CNR - National Research Council of Italy, Italy); Alessandro Fanti (University of Cagliari, Italy); Rosa Scapaticci (CNR-National Research Council of Italy, Italy)

Magneto-dielectric composite materials are gaining a huge attention in many biomedical applications, both for therapy and diagnosis. A typical example is represented by magnetic scaffolds (MaS), which are composed of a biomaterial matrix, loaded with magnetic nanoparticles. Such a kind of device can be stimulated by an external magnetic field and induce specific biological responses. However, the literature about magneto-dielectric materials has a prevalent material science perspective, thus lacking a rigorous electromagnetic engineering perspective. Therefore, an effective translation of MaS as an electromagnetically-controlled device for the applications is waiting for a dedicated study. This contribution aims at take a step forward in this direction, providing a study on the biocompatibility assessment and electromagnetic characterization, in terms of relative permittivity and permeability, of a magneto-dielectric material, namely Poly-Lactic Acid loaded with iron particles (Fe-PLA), which is not used in biomedical field, yet

11:10 Understanding the Performance of Microwave Hydration Assessment with Layered Planar Models

Xiaoru Liu and Declan O'Loughlin (Trinity College Dublin, Ireland)

Microwave hydration monitoring has been proposed and tested experimentally in volunteer studies with at least two different prototype systems. However, there are differences between the systems both in terms of technical design, but also in the use of either the transmission loss or the time-of-flight differences to estimate the hydration status of the volunteer. In this work, a simplified planar model is used to estimate the best case sensitivity of microwave hydration monitoring to changes in the hydration status. Using this model, a change of 0.5 dB in transmission amplitude and 0.89 % to 0.99 % change in time-of- arrival is calculated for each 1 % change in muscle permittivity which correlates well with the literature. These results suggest that also simplified, planar models are useful for understanding microwave transmission through the arm.

11:30 Wireless Real-Time Monitoring of Ablation Using a Wearable Antenna

Ahmet Bilir, Mehmet Emre Korkmaz and Sema Dumanli (Bogazici University, Turkey)

Accurate monitoring of the ablated area size is crucial in microwave ablation therapy to prevent insufficient or excessive tissue ablation. In this paper, we utilize the changes in the electrical properties of tissues during ablation to achieve real-time monitoring. The proposed system comprises a microwave applicator, designed as a coaxial slot antenna, and an on-body antenna. As the ablation progresses, the rising temperature alters the electrical properties of the tissues surrounding the applicator, which in turn affects the transmission coefficient between the applicator and the on-body antenna. The effectiveness of this method is validated through recursive thermal and electromagnetic simulations in a hepatic tumor scenario. The results demonstrate that while the reflection coefficient of the applicator converges after a certain point, the phase of the transmission coefficient continues to change, offering a promising method for tracking the size of the ablated area.

Room: Munch (23)

Scientific Workshop

SW8b Sub-THz Reconfigurable Intelligent Surfaces, RF Front-Ends, and Channels for 6G Networks

Room: Ørsted (24+25)

CS34b Recent Advances on Propagation Research and Its Impact on Localizations

T05 Positioning, localization, identification & tracking / Convened Session / Propagation

Chairs: Christian Gentner (German Aerospace Center (DLR), Germany), Wei Wang (Chang'an University, China)

10:10 Mitigating the Effects of Irregular Reflection Beam Patterns Through Data Association in RIS-Aided mmWave Positioning

Hyowon Kim (Chungnam National University, Korea (South)); Benoit Denis (CEA-Leti Minatec, France); Moustafa Rahal (University of Surrey, United Kingdom); Taghrid Mazloum (CEA- LETI, France); Raffaele D'Errico (CEA, LETI & Université Grenoble-Alpes, France); Henk Wymeersch (Chalmers University of Technology, Sweden)

Despite promising potential for boosting or even simply enabling the localization capabilities of future wireless communication networks, low-complexity reflective Reconfigurable Intelligent Surfaces (RISs) have recently been shown to suffer from practical limitations, such as irregular beam patterns and grating lobes caused by element-wise phase quantization or hardware impairments. The latter phenomena can introduce geometric ambiguities in the RIS-aided positioning problem, when estimating the RIS Angle of Departure (AoD) through beam sweeping based on downlink received power. In this context, our paper introduces an algorithmic framework that combines user position estimation and data association between radio observations and underlying channel model parameters, while still requiring the same basic RIS hardware and UE channel estimation capabilities. Validations based on field measurements centered around 28GHz are provided in a reference indoor environment for different bandwidths, showing the relevance of the proposed solution in terms of both position accuracy and geometric disambiguation.

10:30 REDTS: RLS-Enhanced Doppler Target Separation for Automotive FMCW Radar Systems

Wanting Zhong, José Rodríguez-Piñeiro, Xuefeng Yin and Pengqi Zhu (Tongji University, China); Carlos A. Gutiérrez (Universidad Autonoma de San Luis Potosi, Mexico); Gang Li (SINPRO Intelligent Technology Co. Ltd., China); Yang Zhang (RadioSky Communication Technology Co. Ltd., China)

This paper proposes an advanced interference suppression and target separation technique for automotive Frequency Modulated Continuous Wave (FMCW) radar systems. By employing Recursive least squares (RLS) adaptive filters, the method effectively separates moving and stationary targets while suppressing interference from various sources, such as FMCW, Range Division Multiple Access (RDMA), and Code Division Multiple Access (CDMA) signals. The approach, named RLS-Enhanced Doppler Target Separation (REDTS), uses Doppler frequency differences to isolate targets with different motion states and processes these signals in continuous time, ensuring high accuracy and real-time performance in complex environments. Simulations and real-world measurements demonstrate the method robustness, exhibiting significant improvements in target detection accuracy even when trained for different scenarios than the ones tested. Our interference suppression proposal enhances the reliability of automotive radar systems, allowing for efficient target separation with minimal computational overhead

10:50 Radio Sensing in Electric Railways for Future 5G: An Smart Railways Use Case

Juan Moreno García-Loygorri (Universidad Politecnica de Madrid, Spain); Julián Martín Jarillo, Mario Rodríguez González and Sonsoles García-Albertos (Metro de Madrid, Spain); Antonio Perez Yuste (Universidad Politecnica de Madrid, Spain); Carlos Rodríguez Sánchez (Metro de Madrid S.A., Spain)

Electric railways and Intelligent Transportation Systems (ITS) are a key use case for both current and future mobile communication systems, such as 5G and 6G, respectively. 5G sensing is mostly about spectrum sensing, whereas 6G is focused on a more advanced paradigm: Integrated Sensing and Communications (ISAC). In this paper, we provide some results from a low-cost OFDM-based spectrum sensing system designed to detect electric arcs and sparks generated by the pantograph-catenary contact on a subway train in real-world conditions. The results from the sensing system are validated using a video camera installed on top of the train. This paper describes both the testbed setup and the results obtained specifically related to radio sensing. This work is part of the Metro de Madrid SPARC Project, which focuses on innovative sensing solutions for pantographs.

11:10 Doppler Analysis and Modeling of V2V Channel at 6 GHz in Typical Urban Scenarios

Yufeng Qin (Beijing University of Posts Telecommunications, China); Pan Tang (Beijing University of Posts and Telecommunications, China); Lei Tian (Beijing University of Posts and Telecommunications & Wireless Technology Innovation Institute, China); Peijie Liu (Beijing University of Posts and Telecommunications, China); WeiRang Zuo (Beijing University of Posts and Telecommunications, Singapore); Qi Wei and Jianhua Zhang (Beijing University of Posts and Telecommunications, China)

This paper conducts a measurement campaign for the vehicle-to-vehicle (V2V) channel at 6 GHz in urban scenarios and analyzes its Doppler characteristics. Firstly, the distribution and variation of the Doppler shift of the multipath components are examined from the Doppler power spectrum (DPS). Secondly, the variation of the mean Doppler shift is described. The mean Doppler shift in the head-on driving scenario is found to have the greatest fluctuation, while the Doppler frequency shift in the overtaking is the most stable. Then, the Doppler spread (DOPS) is calculated and analyzed. The Doppler spread varies across different scenarios, and within the same environment, it also shows significant differences due to varying speeds. Finally, a normal distribution model for the Doppler spread is established. This work contributes to modeling the V2V channel in the urban environment.

11:30 Modeling of V2V Channels During Overtaking Maneuvers with Realistic 3D Mobility Patterns

Carlos A. Gutiérrez (Universidad Autonoma de San Luis Potosi, Mexico); Raúl Fabián-Rodríguez (Universidad Autónoma de San Luis Potosí, Mexico); Jorge D. Cárdenas (UASLP, Mexico); José Rodríguez-Piñeiro (Tongji University, China)

This paper presents a new three-dimensional (3D) geometry-based statistical model (GBSM) of vehicle-to-vehicle (V2V) channels for the analysis of overtaking maneuvers. The 3D trajectories of the two vehicles involved in the maneuver are described by high-order polynomials. The coefficients of such polynomials are computed from real-world mobility patterns recorded in a measurement experiment conducted in a high-speed highway. The high-order polynomial trajectories allow a realistic characterization of the channel response at multiple observation time intervals from start to end of an overtaking. This differs from other GBSM for V2V channels in the state of the art, which consider linear or quadratic models that conform to rapidly changing mobility patterns only within a short-length window. Owing to its flexibility, the 3D GBSM of V2V channels presented in this paper can be used as a baseline for the design of V2V channel simulators with realistic mobility patterns.

THURSDAY

T08 Fundamental research and emerging technologies/processes / Convened Session / Antennas

Chairs: Fabien Ferrero (Université Cote d'Azur, CNRS, LEAT & CREMANT, France), Erika Vandelle (Thales Research & Technology, France)

10:10 3-D-Printed Wideband Dual-Frequency Dielectric Resonator Antennas with Luneburg Lens for Beam Switching Capability

Jean Marc Ribero (Université Côte d'Azur & CNRS, LEAT, France); Fabien Ferrero (Université Cote d'Azur, CNRS, LEAT & CREMANT, France); Hugo Bernadac (Laboratoire d'Electronique, Antennes et Télécommunications (LEAT) & CNRS, France)

This paper presents a bi-band antenna for beam switching capability. There are two structures nested one inside the other with different permittivities, they are fed by microstrip line and slot. One structure is five dielectric resonators antennas aligned on the same axis working on the X-band which is encapsulated in a Dielectric lens for the X-band beam-steering working on the L-band.

10:30 Additively Manufactured Embedded Dielectric Resonator Antennas for 6G Applications

Payam Nayeri (California Polytechnic State University, USA); Henrik Ramberg and Philip Lambert (3D Fortify, USA)

We present a new approach for designing embedded multi-band dielectric resonator antennas (DRAs) by exploiting the capability of modern additive manufacturing to create heterogeneous dielectric materials. To demonstrate the feasibility of our proposed approach, we present a dual-band DRA operating at 6G mid-band frequencies, and we show that the proposed embedded DRA achieves dual-band coverage with desirable boresight beam at both frequency bands. Moreover, while in this design we only used one small DRA embedded in a larger DRA, our proposed approach can be easily expanded to create multi-band or broadband DRAs by utilizing multiple embedded DRAs.

10:50 Additive Manufacturing for Controlled Permittivity Ceramic - from Dielectric Characterization to Dielectric Resonator Antenna Measurement

Thomas Lavie (IETR, France); Laurent Le Gendre and Matthew Julian (University of Rennes, France); Ratiba Benzerga (IETR - Université de Rennes 1, France); Ala Sharaiha (Université de Rennes & IETR, France); Francois Chevire and Claire Le Paven (University of Rennes, France)

This work focuses on the additive manufacturing of ceramic resonators with controlled permittivity using a tailor-made gyroid structure. The effective characteristics of the materials are measured and compared to existing models, and finally used to design and fabricate dielectric resonator antennas. Results show that the effective permittivity can be controlled on a wide range and that the antennas fabricated with these structures have the same performances than those fabricated from bulk material but for half the weight.

11:10 A Study of a Dielectric Resonator Antenna with 3D-Printed Conductive Parasitic Elements

Jakub Przepiorowski (Technological University Dublin & Antenna and High Frequency Research Centre, Ireland); Irina Munina (Trinity College Dublin, Ireland); Patrick McEvoy (Technological University Dublin, Ireland); Daniel Trimble (Trinity College Dublin, Ireland); Max James Ammann (Technological University Dublin, Ireland)

A fully 3D-printed dielectric resonator antenna (DRA) with right-hand circular polarization, fed by a cross-shaped aperture is presented. The DRA utilities parasitic conductive elements to improve the circular polarization. The antenna operates in the S-band (2-3GHz). The effects of the conductive element parameters on axial ratio and gain are examined as well as the effect of using a 3D-printed conductive material versus copper for fabrication. The two prototypes are then fabricated. The microstrip line, dielectric substrate, ground plane with the aperture slot, and conductive walls are all 3D-printed in a single process using fused deposition modeling technology.

11:30 3D-Printed Wideband Embedded-Stacked Quarter-Mode Dielectric Resonator Antenna

Giacomo Muntoni, Matteo Bruno Lodi, Alessandro Fanti and Giuseppe Mazzarella (University of Cagliari, Italy)

A wideband embedded-stacked Quarter Mode Dielectric Resonator Antenna (QMDRA), obtained by exploiting the magnetic field symmetry of the fundamental TM010 mode of a standard cylindrical DRA, is presented in this paper. By placing virtual magnetic wall along the magnetic field symmetry axis, the antenna dimension has been reduced by 75%. A desirable wideband behavior has been obtained taking advantage of the embedded-stacked DRA layout. The proposed antenna extensively covers the entire European UWB (6-8.5 GHz) and it is intended for 3D-printing fabrication.

Room: Collin (27) WG Propagation

EurAPP Working Groups

Thursday - 12:00-12:40

Room: Alfvén (A3+A4) Nicolas Capet

Invited Speaker

Chair: Marta Martínez-Vázquez (Renesas Electronics, Germany)

Room: Kildal (A2)

Invited Speaker

Rodolfo Feick

Chair: Thomas Kürner (Technische Universität Braunschweig, Germany)

Thursday - 13:30-14:40

Room: Poster level 3

PA10 - Antennas X Modelling, simulation tools, emerging technologies and processes

T08 Fundamental research and emerging technologies/processes / / Antennas

Chairs: Davide Comite (Sapienza University of Rome, Italy), Lars Jonsson (KTH Royal Institute of Technology, Sweden)

3.1. A Compact Planar Antenna Based on Matryoshka-Like Geometry

Alfrêdo Gomes Neto (Federal Institute of Paraíba & Grupo de Telecomunicações e Eletromagnetismo Aplicado - GTEMA, Brazil); Elayne Cristina Lino Donato (Federal Institute of Paraiba - IFPB, Brazil); Marcus Vinicius Rocha Cohen (Federal Institute of Paraiba, Brazil); Rebeca Parente Miranda and Rafhaella Lima Henrique (Federal Institute of Paraíba, Brazil); Jefferson Costa Silva (Instituto Federal da Paraíba & IFPB, Brazil)

This paper introduces a compact antenna, MTK-LA. The MTK-LA is composed of a matryoshka-like geometry and a partial ground plane. The matryoshka-like geometry is described, including initial design equations. The initial dimensions of the partial ground plane are suggested, and a parametric analysis is presented. To verify the expected characteristics, a prototype operating at 312 MHz was designed, fabricated and characterized, verifying a good agreement between numerical and measured results. One of the most interesting features observed was the reduced dimensions, achieving an overall dimension of 0.052λ0×0.052λ0. Despite the MTK-LA being especially attractive for low frequency (dozens of MHz) applications, it can be designed for higher frequency applications.

3.2. A Voxelisation Tool for the Electromagnetic Simulation of Metal Composite Materials

Saúl Santos Carvalho (Polytechnic of Leiria, Portugal & Instituto de Telecomunicações, Portugal); João Ricardo Reis (Instituto de Telecomunicações and Polytechnic Institute of Leiria, Portugal); Rafael F. S. Caldeirinha (Polytechnic Institute of Leiria & Instituto de Telecomunicações, Portugal)

This paper presents a novel voxelisation tool designed for the electromagnetic simulation of metal composite materials, specifically in the context of 3D printed metal composite horn antennas. The tool addresses the limitations of traditional electromagnetic simulators, which struggle to accurately model hybrid structures composed of metal and dielectric components. The study employs two types of metal composite filaments, such as copper and brass-filled PLA, during the simulation of horn antennas across different fabrication stages: green, brown, and sintered. Through detailed material modelling and voxelisation techniques, the tool allows for realistic simulations that reflect the complex interactions of electromagnetic waves within these composite materials. Preliminary results indicate that while the green stage antennas exhibit poor radiative performance, significant improvements are anticipated post-debinding and sintering, suggesting a viable path forward for the development of efficient metal composite antenna

3.3. Design and Optimization of Low Profile Mechanical Steerable Antenna for User Terminals

Pasquale Giuseppe Nicolaci and Min Zhou (TICRA, Denmark)

This paper presents the preliminary design of a passive quasi-periodic structure-based antenna for user terminal application, and it works in the Ka band, 19.0-20.9 GHz. Using QUPES software and a direct optimization approach, the antenna steers the beam by mechanically rotating two identical transmitarrays. The transmitarray unit cells employ phase rotation, enabling a wide phase range with low insertion losses. Direct optimization refines both the primary patch array and the transmitarrays, achieving the desired radiation pattern with reduced sidelobe levels. This method provides efficient beam steering with improved sidelobe performance and cross-polarization control.

3.4. Far-Field Accuracy and Embedded Element Pattern Approximations in Hexomino Subarrays

Lars Jonsson and Ahmad Emadeddin (KTH Royal Institute of Technology, Sweden); Harald Hultin (KTH Royal Institute of Technology & Saab AB, Sweden); Lucas Åkerstedt (KTH Royal Institute of Technology, Sweden)

Large array antennas, constructed from disjoint irregular subarrays, where each subarray port is digitally controlled, are of growing interest for communication and sensor applications. This paper investigates two different 28x30 antenna arrays, both operating as isophoric arrays (equal amplitude excitation), designed to support pencil beams across a large scan window. We focus on how various embedded element pattern approximations influence the optimization outcomes in terms of hexomino-based subarrays and their effect on the peak sidelobe level (pSLL). Our analysis shows that commonly used embedded pattern approximations can cause peak sidelobe level deviations of up to 1.4 dB. Additionally, we demonstrate properties of a simplified and fast cost function to asses the pSLL in these arrays.

THURSDAY

3.5. Metasurface-Loaded Magnetic Small Antennas on a MWPT System

Felipe Machado de Freitas (Ecole Centrale Lyon, France & CEFET-MG, Brazil); Icaro V Soares (IETR, France & Université de Rennes 1, France); Arnaud Breard (Ecole Centrale Lyon, France); Christian Vollaire (Ampere Lab, France); Loris Pace (Ecole Centrale de Lyon, France); Sandro Trindade Mordente Gonçalves (CEFETMG, Brazil)
This work proposes a resonant metamaterial structure coupled to a small loop for increasing efficiency in a magnetic wireless power transfer (MWPT) system. A circuit model of the metamaterial arrangement and the methodology for evaluating the system efficiency are presented. The results demonstrate that, with the use of the metasurface, the quality factor of the loops was improved by 2 times, leading to a remarkable increase in the MWPT efficiency 10 times in comparison with a loop loaded for a lumped capacitor and a loop loaded for a metasurface. These results underscore the performance enhancement for electrically small magnetic WPT systems with the novel strategy proposed in this paper, suggesting that its application can provide substantial gains in small magnetic wireless power transfer systems.

3.6. Modelling of Quasi-Optical Systems: Application to Skin Spectroscopy

Gregory Gaudin, Daniel Bourreau, Alain Peden and Clément Henry (IMT Atlantique, France)
This work presents a simulation pipeline for modelling quasi-optical systems and demonstrates its potential as a transfer function for permittivity extraction at terahertz (THz) and sub-terahertz (sub-THz) frequencies. The simulated transfer function is validated against oblique reflection measurements and compared to the conventional plane wave approximation. Numerical results also show the application of this simulation tool to the modelling of a skin continuous-wave (CW) spectrometer.

3.7. Radiation Pattern Shaping of Partially Reactively Loaded Antenna Array Using Iterative Approach

Samuel Travnicek, Jan Kracek and Pavel Hazdra (Czech Technical University in Prague, Czech Republic)
An iterative approach for the shaping of the whole radiation pattern at a single frequency using a partially reactively loaded antenna array is presented. The approach is applicable to a generic array with a fixed arrangement and takes into account the interaction between ports of the array. The array is characterized by an impedance matrix and a set of radiation patterns which are calculated just once by a full-wave simulation. The excitation of the excited ports and the loads of the reactively loaded ports are determined to approximate a given radiation pattern by an array radiation pattern. The approach is validated through several examples of a circular array of quarter-wavelength monopoles.

3.8. Design X-Band Isolation Structures for Effective Antenna Decoupling

Young Jin Song, Dohyeon Kim and Sun K. Hong (Soongsil University, Korea (South))
The high isolation level between antennas is essential for maintaining signal integrity and preventing interference, especially in high-power systems where poor isolation can lead to significant performance degradation. The mutual coupling between antennas stems from various factors, with the presence of a metallic ground plane being one of the major contributors. The ground plane induces unwanted surface wave propagation and reflections, leading to signal distortion and reduced isolation. In this paper, we present a novel design that combines corrugations and a double split-ring resonator (DSRR) array to enhance isolation between two antennas separated by a metallic ground plane in the X-band. The corrugation suppresses surface wave propagation between the antennas, while the DSRR array, positioned near the excited antenna, functions as a reflector to reduce mutual coupling. The feasibility of the proposed structure is confirmed through numerical simulations, which demonstrate an average 33.4 dB isolation improvement across the X-band.

3.9. A 4 × 4 Millimeter-Wave Antenna Based on a Higher Order Mode in a Sub-Mode Microwave SIW Structure for Recent 5G Applications

Saqer S Alja'afreh (American International University, Jordan); Amjaad T Altakhaineh (Pioneers International Academy, Jordan); Chaoyun Song (King's College London, United Kingdom)
A single structure and multi-port antenna for 5G millimeter wave applications is proposed. It is constructed by exploiting the higher-order modes of a fraction-mode microwave SIW cavity at 28 GHz, mainly QMSIW. Such properties give the single cavity a MIMO capability. Firstly, two perpendicular T-shaped microstrip ports (Port 1 and Port 2) are installed to excite TE205 higher-order mode of the QMSIW cavity at 28 GHz. To extend the MIMO capability, a 4×4 MIMO QMSIW antenna is created by adding two extra coaxial feeding ports (Port 3 and Port 4), the higher-order modes of the cavity are reused by leveraging two orthogonal inverted L-shaped slots, each slot is excited using coaxial cables at 28 GHz. The proposed antenna exhibited a wide -10 dB impedance and >11dB isolation based on the simulation environment without using decoupling structures. Finally, this work represents a promising solution for future multi-port single antenna, MIMO applications

THURSDAY

3.10. A Solar Cell Integrated Antenna for On-The-Move IoT Applications

Ahmed Ali (University of Technology, Sydney, Australia); Khushboo Singh (University of Technology Sydney, Australia & Macquarie University, Australia); Dushmantha Thalakotuna (Macquarie University, Australia); Karu Esselle (University of Technology Sydney, Australia)

This paper presents a solar cell integrated antenna for IoT devices providing dual functionality. A fat dipole antenna is adapted to be used with a solar cell-based reflector. The dipole elements are made from Copper Indium Gallium Selenide solar cells. Both the dipole antenna and the reflector are composed of solar cells, allowing the design to capture sunlight from two directions. Additionally, the solar cell-based reflector significantly enhances the gain of the dipole antenna. The proposed design is well-suited for applications where the position of the solar cells relative to sunlight continuously varies. The antenna system achieves a -10 dB impedance bandwidth of 54.4%, with a maximum gain of 7.19 dBi.

3.11. Design and Fabrication Methods for a Biconical Antenna at 28 GHz

Juha Tuomela, Bing Xue and Katsuyuki Haneda (Aalto University, Finland); Clemens Icheln (Aalto University & School of Electrical Engineering, Finland)

This paper investigates the design and fabrication of a low-cost biconical antenna for wireless channel characteristic studies at mmW bands. The proposed antenna consists of a plastic base with two cone indentations, covered with a conductive material. The simulated antenna has a −10 dB impedance bandwidth of 21 to 33 GHz. The effects of the metal's thickness, roughness, and conductivity on the antenna's radiations are studied before fabrication. Finally, the metal coating of the antenna is fabricated with 3 different methods, and it is found that using a hand- painted silver paint surface is comparable to an industrially painted copper paint surface with 1.3 dBi realised gain and 1.4 dB gain variation in the H-plane at 28 GHz. Copper tape produced much worse results and was found only suitable for some applications that do not need high performance.

3.12. Design of Beamforming Conformal Antenna Array Based on Partially Reflecting Surfaces

Vivek Kumar (Université catholique de Louvain (UCLouvain), Belgium & ICTEAM, Belgium); Christophe Craeye (Université Catholique de Louvain, Belgium)

A conformal array using Partially Reflecting Surfaces (PRSs) for satellite communication is proposed. The beamforming algorithm is formulated using phase correction as well as amplitude weighting proportional to the level of embedded patterns in the direction of the scan. The pattern is effectively scanned within the field of view defined by the angular width of a facet. A fluctuation in maximum gain of less than 1 dB has been achieved, with a sidelobe level of −8.17 dB, though further research is needed to improve the sidelobe level.

3.13. Design of Wideband High Gain Reflectarray Antennas for High Speed Reliable V2X Communication Links

Mustafa Khalid Taher Al-Nuaimi (Foshan University, China & School of Eelectronic Information Engineering, China); Guan-Long Huang (Foshan University, China); Xiaoming Chen (Xi'an Jiaotong University, China); Wei Lin (The Hong Kong Polytechnic University, Hong Kong)

This article introduces a novel circularly polarized (CP) wideband high gain reflectarray antenna (WHG-RA) designed to cater to the requirements of future Vehicle-to-Everything (V2X) communication links. The WHG-RA offers an exceptional gain bandwidth spanning from 12 to 32 GHz, encompassing crucial V2X frequency bands, including vehicle-to-satellite (V2S) Ku/Ka downlinks and uplinks frequencies (12.25-12.75, 14.0-14.5, 19.6-21.2, and 29.4-31.0 GHz), the 24.25-26.65 GHz range designated for vehicle-to-vehicle (V2V) short-range radars, and all 5G millimeter-wave spectrums, such as n258 (24.25-27.5 GHz) and n257 (26.5-29.5 GHz), intended for vehicle-to-network (V2N) links. The design of the wideband unit cell within the WHG-RA is rooted in a rotational technique grounded in geometric phase theory and has multiple resonances. As a proof-of-concept, we have created a 180 × 180 mm^2 planar WHG-RA consisting of 900 unit cells, which has been fabricated and rigorously tested across the 12 - 32 GHz frequency range. Both simulation and measurement res

3.14. Dynamic Theory for Three-Coil Wireless Power Transfer Systems

Nam Ha-Van, Sergei Tretyakov and Constantin Simovski (Aalto University, Finland)

In this paper, we present a comprehensive dynamic theory for mid-range wireless power transfer (WPT) systems that include three coils (3C-WPTS). We analyze the power transfer efficiency (PTE) in comparison with the corresponding two-coil WPT system (2C-WPTS) and a conventional short-range model of the 3C-WPTS. We study and explore the physical mechanism that enables the radiation suppression in 3C-WPTS. Our theoretical findings provide insight into possible PTE enhancements for multi-coil WPT over longer distances.

THURSDAY

3.15. Efficient Endfire Superdirective Arrays of Printed Dipoles Loaded with CSRRs

Monica Wasfy William (Queens University, Canada); Yahia M. M Antar (Royal Military College of Canada, Canada); Alois Freundorfer (Queens University, Canada)

This paper discusses implementation of efficient arrays using highly directive dipoles loaded with complementary split ring resonators (CSRRs) for mm-wave applications. A Yagi-like excitation setup is proposed to overcome matching the high input impedance of the used loaded dipole element. As a result, directivity reaches 9.7 dB with radiation efficiency of 91% at 29.88 GHz for an array of three closely spaced elements. Moreover, the 3dB directivity bandwidth is improved from 313 MHz to 642 MHz using an asymmetric dipole element and up to 1001 MHz using a modified CSRR with multiple parallel radiating current strips.

3.16. Miniaturized Ultra-Wideband Omnidirectional Whip Antenna with Improved Gain

Yurong Sun (Southwest Jiaotong University, China); feng Quanyuan (Southwest JiaoTong University, China); Yan Wen, Yukang Chen and Haoxuan Sheng (Southwest Jiaotong University, China)

This paper introduces a novel miniaturized ultra-wideband omnidirectional whip antenna with enhanced gain performance. The antenna is fed by a tapered coplanar waveguide (CPW), and its radiating element is modeled after a double-ridged horn antenna. To improve the impedance matching at low frequencies, distributed resistors are loaded at the end of the patch. Through electric field distribution analysis, two pairs of parasitic elliptical patches and slots are strategically added to the back of the antenna, significantly improving gain at higher frequencies. The antenna achieves dual-band operation, with 131.6% (0.68-3.3GHz) ultra-wideband at the low frequency and more than 22.2% (4.8-6GHz) bandwidth at the high frequency. The radiation pattern demonstrates excellent horizontal omnidirectional characteristics, with minimal 3dB gain fluctuation across the effective frequency band. Additionally, the overall size of the antenna is only 0.06λlow×0.25λlow×0.001λlow, which makes it well-suited for mobile communications, satellite communication, Internet of Things (IoT) and so on.

3.17. Preliminary Investigation of Scattering Matrix Method as Inverse Design Tool for Metagratings

Renat Abdullin and Giada Maria Battaglia (Università Mediterranea di Reggio Calabria, Italy); Andrea Francesco Morabito (University Mediterranea of Reggio Calabria, Italy); Tommaso Isernia (University of Reggio Calabria, Italy); Lorenzo Crocco (CNR - National Research Council of Italy, Italy); Roberta Palmeri (Università Mediterranea of Reggio Calabria, Italy)

This paper presents a preliminary investigation of the Scattering Matrix Method (SMM) for use in the inverse design of metasurfaces aimed at achieving anomalous reflection. We focus on optimizing the dimensions of cylindrical scatterers uniformly arranged near a planar perfectly conducting surface to control the scattered field and suppress specular reflection. The optimal configuration is achieved through the combined use of global optimization via Very Fast Annealing and local optimization using the Nonlinear Programming Solver. Due to the fact that mutual interaction matrices remain constant at each iteration, this approach significantly reduces computation time without compromising accuracy. The obtained results have been verified using commercial electromagnetic software.

3.18. Q/V-Band MIMO Antenna Array for 6G Satellite-Based Communication Networks

Anikó Német (Aberystwyth University, United Kingdom); Shaker Alkaraki (University of Nottingham, United Kingdom); Muhammad Aslam, David Andrew Evans and Syeda Fizzah Jilani (Aberystwyth University, United Kingdom)

In this paper a wideband coplanar waveguide (CPW) fed multiple-input multiple-output (MIMO) antenna array is designed for beyond 5G and upcoming 6G satellite-based communication systems. The antenna is developed on Rogers RO4003C substrate, and a 4-element orthogonal MIMO is presented. The designed antenna presents a bandwidth of 9.9 GHz, ranging from 42.7-52.6 GHz. A peak realized gain of 10.19 dBi is observed at 43.8 GHz. The transmission coefficients are below -20 dB showing good isolation. The obtained envelop correlation coefficient (ECC) is below 0.0012, i.e. much less than the acceptable upper limit of 0.5. The presented antenna shows excellent performance and is well-suited for Q/V-band satellite-based communication systems and wireless applications.

3.19. RFID Integrated Circuits as Network Controllers

Francesco Lestini (University of Rome Tor Vergata, Italy); Alessandro Di Carlofelice and Piero Tognolatti (University of L'Aquila, Italy); Gaetano Marrocco (University of Rome Tor Vergata, Italy); Cecilia Occhiuzzi (University of Roma Tor Vergata, Italy)

This paper presents a novel approach for controlling reconfigurable antennas using passive Radio Frequency IDentification (RFID) Integrated Circuits (ICs) physically connected to the RF power generator through transmission lines. Selective activation of each IC enables signal path management in a passive and low-cost way. The feasibility of the idea is demonstrated by designing and testing a custom PCB equipped with 4 RFID ICs. Measurement results show the successful equal distribution of the input power among the ICs and their ability to dynamically control the signal routing. Each IC provides two programmable output voltage levels, 0 V and 1.8 V, enabling N-bit reconfigurability within the guided structure, where N corresponds to the number of ICs. The proposed architecture significantly reduces the system's cost, power consumption, and complexity compared to traditional reconfiguration mechanisms, where external controllers and power supplies are required.

THURSDAY

3.20. Split Sleeve-Based Cross-Band Decoupling Between Adjacent Dipoles

Liying Nie, Jiayi Li and Xinlei Zheng (Hefei University of Technology, China)

Balun is usually applied for dipole antennas to obtain balance currents on arms. However, more serious coupling may be caused by balun for two dipoles operating at adjacent frequency bands. The coupling mechanism between two dipoles with adjacent frequency bands are analyzed in this paper. Finally, a sleeve-based cross-band decoupling method is proposed to increase the cross-band isolation. Enhanced total efficiency of high-band dipole can be also observed.

3.21. Ultra-Broadband Overmoded Waveguide Junction with High Gain Aperture for the W- and D-Band

Manuel Funk, Irwin Barengolts and Kristof Dausien (Ruhr University Bochum, Germany); Jan Barowski, Ilona Rolfes and Christian Schulz (Ruhr-Universität Bochum, Germany)

Recent advancements in integration technologies show a consistent trend towards higher frequency ranges and bandwidths. Benefits include smaller footprints and higher range resolutions. Thus, it is beneficial to utilize higher frequency bands and bandwidths, particularly for imaging techniques such as synthetic aperture radar (SAR) or tomography. Therefore, the D-band is now being used more frequently in addition to the W-band. This paper presents a waveguide junction that can be used to guide electromagnetic waves in the frequency range from 70-170 GHz. A slot card is used to mechanically switch between the W- and D-band. Additionally, the design incorporates a high-gain antenna, which is used for both frequency bands. This is indispensable for material characterization, as no mechanical adjustment is required to align two antennas. The waveguide junction achieves good results in terms of matching and transmission properties and the mechanical components exhibit very high reproducibility.

3.22. Wideband Circularly Polarized Reflectionless Filtenna

Adnan Nadeem (Frederick University, Cyprus); Nosherwan Shoaib (National University of Sciences and Technology (NUST), Pakistan); Dimitra Psychogiou (University College Cork and Tyndall National Institute, Ireland); Photos Vryonides and Symeon Nikolaou (Frederick Research Center & Frederick University, Cyprus)

The manuscript presents the implementation of a reflectionless wideband filtenna, with circular polariazation and high gain characteristics from 1 to 2.5 GHz. The front-end consists of a reflectionless filter which consists of a two-stage λg/4 coupled line at the center frequency, f0= 1.75 GHz and a stepped impedance open-circuited stub in parallel. Cascaded with the microstrip filter a balun is used to feed a self-complementary log spiral antenna. The balun consists of two sections: a microstrip line on the input side and a parallel stripline on the output side, connected to the antenna feed point. The transition between the two sections is achieved using a Chebyshev tapering geometry. For the implementation of the wideband antenna, a cavity-backed logarithmic spiral antenna with non-uniform widths was used.

3.23. Low Loss Printable Dielectrics for mmWave Components

David Panusch (Friedrich Alexander Universität Erlangen Nürnberg); Manuel Romeis (Friedrich Alexander Universität Erlangen Nürnberg, Germany); Gerald Gold (FAU Erlangen-Nürnberg, Germany)

In this paper, a comprehensive list of materials in combination with various additive manufacture (AM) approaches is provided to facilitate the optimal selection of low-loss dielectric materials. As a case study for those AM low loss materials an additively manufactured dielectric tripole rod antenna with integrated multimode power divider is presented. The demonstrator itself has a bandwidth of B20dB ~4.7 GHz at a center frequency of fc = 75 GHz.

Room: Poster level 3 | **PA8 - Antennas VIII Millimetre wave and THz for terrestrial networks**

T02 Millimetre wave and THz for terrestrial networks (5G/6G) / / Antennas

Chairs: Guido Valerio (Sorbonne Université, France), Hairu Wang (KTH Royal Institute of Technology, Sweden)

3.44. A 60 GHz Circularly Polarized Multilayer 16-Element Antenna Array

Hoda Farhat, Youssef Tawk and Joseph Costantine (American University of Beirut, Lebanon); Ali Ramadan (Fahad Bin Sultan University, Saudi Arabia)

This paper presents an antenna array that achieves circularly polarized radiation within the span of frequencies between 57.24 GHz and 64.8 GHz with a realized gain of 14.2 dBic. The presented array is composed of 16 radiating elements that are stacked on a multilayer dielectric topology to achieve compact size and enable the appropriate phase distribution between the radiating elements. Each radiating element is further composed of four sub-elements that are series-fed with sequential rotation through an aperture-coupled feeding technique. The antenna array is fabricated and tested to prove its validity in terms of impedance matching, realized circularly polarized gain, and axial ratio bandwidth.

3.45. A Low-Profile Phased Array Antenna with Circular Polarization for Mobile Satellite Communications

Haleh Jahanbakhsh Basherlou, Naser Ojaroudi Parchin, Libu Manjakkal and Chan Hwang See (Edinburgh Napier University, United Kingdom); Ming Shen (Aalborg University, Denmark)

This study discusses the design and key characteristics of a compact circular-polarized (CP) phased array suitable for use in wireless platforms. It details a single element featuring a truncated patch antenna with a stepped slot and coaxial feed on an FR4 substrate. The array is designed for operation at 20 GHz, specifically for mobile satellite (MSAT) communications. Each element is excited through a coaxial feeding method with the inner conductor extending directly to the radiation patch. The configurations of 1×8 and 8×8 phased array versions of this CP patch antenna, both equipped with beam-steering capabilities, are thoroughly examined in the paper. Encouraging findings have been unearthed in relation to S-parameters, radiations, and antenna gains, affirming the viability of the suggested compact design and its suitability for various applications ranging from mini base stations to mobile satellites.

3.46. A Novel Modular Heatsink Antenna Array with Beam Scanning and Cooling Benefits

Feza Turgay Çelik (Delft University of Technology, The Netherlands); Alexander Yarovoy (TU Delft, The Netherlands); Yanki Aslan (Delft University of Technology, The Netherlands)

An antenna array with dual-functionality - electromagnetic radiation and thermal cooling - is proposed. An iterative array design procedure is developed to improve cooling, mutual coupling, side lobe levels, and gain levels in dual-functional antenna arrays with adaptive beam steering. Heatsink-attached patch elements are combined with complementary split ring resonator (CSRR) structures in between the elements, resulting in a novel modular heatsink antenna array. Based on the proposed design, the beam scanning performances of four-element and eight-element linear arrays at 26 GHz are studied. A conventional shorted patch antenna array is used for benchmarking. Through thermal and electromagnetic simulations, it is demonstrated that the proposed antenna array decreases the maximal array temperature by more than 40 C as compared to the benchmark. Moreover, the new design resolves the pattern performance degradation problems in heatsink arrays, while approaching to the electromagnetic performance of the benchmarked array.

3.47. Analysis of Reconfigurable Reflective Unit Cells in Waveguide Environment for Ka and D Band

Sanaá Finich (University of Porto, Portugal); Mohamed Elsaid Ghatas (INESC TEC, Campus Da FEUP, Portugal & University of Porto, Portugal); Sofia Inacio (FEUP, Portugal); Henrique M Salgado (University of Porto & INESC Porto, Portugal); Luis M. Pessoa (INESC TEC & Faculty of Engineering, University of Porto, Portugal)

A comparative analysis of Ka and D-band unit cells is presented using a Waveguide Simulator and infinite array models with a Floquet port. Initially, a single-unit cell design is employed with a tapered transition section. Subsequently, a 1 × 2-unit cell is designed and integrated into standard rectangular waveguides WR34 and WR7. For the Ka-band, the results obtained from both models exhibit excellent agreement in terms of magnitude and phase. In the D-band, the 1 × 2- unit cell demonstrated low loss for both techniques, and the phase responses were reasonably accurate with differences of less than 40 degrees. At such high frequencies (145-175 GHz), the Waveguide Simulator offers a viable solution for assessing the behavior of the unit cell without the need for a full array.

3.48. Channel Coupling Between Filters in Gap Waveguide Antenna Arrays

Jack Duncan Fourie, Petrie Meyer and Werner Steyn (Stellenbosch University, South Africa)

Gap waveguides provide an attractive alternative to conventional waveguides at millimetre wave frequencies and above. The isolation between adjacent channels in an antenna array is limited by the number of physical rows of gap waveguide pins in the system. Filter resonators couple strongly into adjacent channels and can effect the performance of antenna arrays they are integrated into. This paper presents the analysis of the effects of integrating a third order filter into a gap waveguide antenna array with the degradation of the farfield performance both with and without beam steering investigated.

3.49. Design and Implementation of an Integrated Phased Array with Stripline Series Feed in K-Band

Aqeela Saghir (LINKS Foundation, Italy & Frederick University, Cyprus); Giuseppe Musacchio Adorisio and Giuseppe Franco (Fondazione LINKS, Italy); Davide Bianchi (IDS Ingegneria Dei Sistemi SPA, Italy); Giorgio Giordanengo (LINKS Foundation, Italy)

This article discusses the design and realization of a stripline series feed aperture coupled phased array. The feeding of the antenna using the stripline technology is discussed. Simulation results of a single row of 48 elements having traveling wave feed tapering ratio of 1:5 are presented. These results covers the band from 19.5 to 20.5 GHz with a realized gain and side lobe level of 22.4dB and 18.7dB at 20GHz and a beamwidth of about 2.5°. A realized array of 64x48 elements is shown. Electronic steering in one direction (i.e., elevation) can be achieved by mounting phase shifters on the lowest layer, which is connected to the series feed through a coplanar waveguide and a via transition.

THURSDAY

3.50. Design, Fabrication and Verification of a Millimeter Wave Butler Matrix Antenna

Marcus Lindbergh (Umeå University, Sweden); Jonas Starck (Abracon LLC, Sweden); Claes Beckman (KTH Royal Institute of Technology, Sweden)

The design, fabrication and verification of a Butler matrix beamforming network connected to a four-antenna element patch array implemented at 26GHz on a four-layer printed circuit board is designed, fabricated and verified. In order to avoid crossover, the chosen solution is built by using two cascaded 90-degree hybrids, forming a 4-port, which gives the high isolation. The results from testing agreed well with simulations, indicating that the chosen circuit design based on a four layer PCB board made from Rogers RT-duroid 5880, a Butler network design with no crossover and probe fed patches, is robust and well suited for 5G massive MIMO antenna applications covering 1GHz in the 26GHz band.

3.51. High Gain and High Aperture Efficiency Wideband Dielectric Lens Antenna

Wenyi Teng (China); Kaixu Wang (Harbin Institution of Technology, China); Hang Wong (City University of Hong Kong, China)

This paper presents the design of a high-gain, high-aperture-efficiency dielectric lens antenna with an integrated anti-reflection layer for millimeter-wave applications. The proposed lens profile is meticulously analyzed and optimized to achieve uniform phase distribution across the entire aperture, resulting in high aperture efficiency and enhanced gain. In comparison to traditional elliptical lens antennas with high aperture efficiency, the proposed design introduces an additional refractive surface, significantly reducing the height and insertion loss of the lens antenna. Measurements confirm the superior performance of the proposed lens antenna, achieving a peak gain of 29.8 dBi and a maximum measured aperture efficiency of 68%. The antenna exhibits an impedance bandwidth from 23.8 GHz to 40 GHz, within which S11 remains below −10 dB. Furthermore, the aperture efficiency exceeds 50% across the frequency range from 23.8 GHz to 38 GHz.

3.52. JT-CoMP to Improve Coverage of 5G mmWave Networks in UMa and UMi Environments

Mohamad Younes and Laurent Quibus (Académie Militaire de Saint-Cyr Coëtquidan, France); Eric Plouhinec (Ecoles de St-Cyr Coëtquidan, France)

The adoption of mmWave frequencies offers a promising solution for exploiting underused spectrum and achieving very high transmission rates. However, these frequencies face major challenges, including higher signal loss and increased sensitivity to blocking. To overcome these limitations, the Joint Transmission Coordinated Multi-Point (JT-CoMP) technique improves communication quality, particularly for users located at cell boundaries, thereby enhancing network reliability. This article focuses on improving the coverage of 5G mmWave networks via JT-CoMP in Urban Micro (UMi)-Street Canyon and Urban Macro (UMa) environments. It incorporates parameters often overlooked in previous studies, such as line-of-sight and non-line-of-sight configurations, including Path Loss, LOS probability and Shadow Fading models, specifically tailored to mmWave frequencies in these environments. In addition, the analysis takes into account key factors such as three-dimensional distances, BreakPoint distances, Inter-Site Distances, as well as Inter-Cell Interference, providing a comprehensive assessment of 5G mmWave networks performance in dense UMi and UMa environments.

THURSDAY

Room: Poster level 3 | **PA9 - Antennas IX Sensing, localization and tracking**

T04 RF sensing for automotive, security, IoT, and other applications / / Antenna

Chairs: Sema Dumanli (Bogazici University, Turkey), Francisco Mesa (University of Seville, Spain)

3.24. Centimeter-Wave Electronically Scanned Array for Future 6G Applications

Mohamed Mamdouh M. Ali (Assiut University, Egypt); Mostafa O. Shady (Scientific Microwave Corporation, Canada); Syed Muhammad Sifat (Toronto Metropolitan University, Canada); Khelifa Hettak (University of Quebec in Outaouais, Canada); Larbi Talbi (University of Quebec - Outaouais, Canada); Ke Wu (Polytechnique Montréal, Canada)

This work presents an electronically controlled reconfigurable scanned array utilizing reflective phase shifters, designed for future 6G applications. Operating within the centimeter-wave (cmWave) frequency band (13-17 GHz), the electronically scanned array (ESA) demonstrates excellent performance. The system comprises a 2 × 2 horn antenna array interconnected with four digitally controlled variable reflect-type phase shifters, each constructed using a 90 ◦ hybrid coupler with a movable short-circuit. Additionally, the assembly includes E-H feeding networks, facilitating uniform signal distribution to the antenna array. Simulation results of the complete ESA exhibit outstanding performance, showcasing continuous main-lobe scanning in elevation and azimuth planes. The proposed ESA achieves a matching level below -15 dB with a stable gain of 14 ± 2 dBi over the operating bandwidth.

3.25. Circularly Polarized Conical Array for ADS-B Applications in LEO Satellites

Javier Vera-Sánchez (Universitat Politecnica de Valencia, Spain); Álvaro Martín-Núñez (Universitat Politècnica de València & Antennas and Propagation Lab (APL), Spain); Miguel Ferrando-Rocher (Universitat Politècnica de València & Antennas and Propagation Lab, Spain); Miguel Ferrando-Bataller (Universitat Politècnica de València, Spain)

This paper presents the design of a dual-layer conical antenna array tailored for Automatic Dependent Surveillance-Broadcast (ADS-B) applications intended for integration into Low Earth Orbit (LEO) satellites. The proposed antenna system comprises two vertically stacked layers, each comprising six magneto-electric dipole antennas arranged in a circular configuration. Each antenna element covers a sector of ±30° in azimuth, providing comprehensive coverage for real-time aircraft tracking over wide geographical regions. The antennas in the upper layer are positioned slightly farther apart due to the conical geometry, optimizing the radiation pattern and minimizing mutual coupling between layers. The array operates within the L-band spectrum (960-1164 MHz), making it suitable for ADS-B communication in remote areas with limited ground station coverage, such as oceans and deserts.

3.26. Differential RCS of a Set of Coupled Dipoles Using a Circuit Network Model: Application in RFID

Benoit Poussot, Shermila Mostarshedi, Jithin Mudakkarappilli Sudersanan and Aiman Mughal (University Gustave Eiffel, France); Jean-Marc Laheurte (Université Gustave Eiffel & ESYCOM Lab, France)

This study presents an N-port circuit model for N coupled RFID tags, including the coupling effects. The RFID tags are replaced by loaded dipoles. The backscattering properties of a surrounded dipole are particularly of interest in the reverse link, notably the re-radiated power and the differential radar cross section. The backscattering properties of a single dipole are compared to those of surrounded dipoles through a deterministic configuration and the impact of coupling and orientation is quantified for each dipole. A statistical analysis is presented to highlight the influence of the surface density of the dipoles on the reverse link observable.

3.27. Direction-Of-Arrival Estimation on Linear Phased Arrays Using Various Sum-Difference Patterns

Yu-Feng Chen and Wen-Jiao Liao (National Taiwan University of Science and Technology, Taiwan); Hsi-Tseng Chou (National Taiwan University, Taiwan)

This paper presents a study pertinent to the direction-of-arrival estimation in terms of received signal strengths using a beam-scanning array antenna. To improve the estimation accuracy, both beam and null scanning are employed, which is equivalent to adopt the sum-difference approach in conventional tracking radars. The implemented receiving array system comprises a series-fed patch array, a beam forming IC, an RF power detector and an Arduino board to relay control commands and to receive RF power levels. In this work, different null synthesis profiles are attempted to optimize the accuracy in estimating the incidence direction, to reject false detections coming from side lobes, and to harness the ability in discriminating multiple. Both simulations and measurements were conducted to verify the proposed method.

3.28. Wideband Pattern Reconfigurable Antenna Applied to Angle-Of-Arrival Estimation

Jeen-Sheen Row and Yu-Jie Lin (National Changhua University of Education, Taiwan)

A design for wideband pattern reconfigurable antennas is reported. The antenna is composed of three planar structures where the top and bottom layers are metallic plates and the middle layer is a microstrip circular array. The radiating elements of the array are activated with a SP4T circuit, and four switched beams are generated in the horizontal plane. The experimental results demonstrate that the proposed reconfigurable antenna has an impedance bandwidth of 50 %, and it can provide stable steerable beams within the bandwidth; besides, a maximum gain of 8.3 dBi is also achieved. Simulation results for the constructed prototype integrated with related circuits are also given, and they validate the measured data. Based on the prototype, an angle-of-arrival estimation system is developed. The system can be operated from 4 to 6 GHz, and an estimation mean error of less than 1.5° is achieved over 360° within the operation bandwidth.

3.29. An Integrated On-Chip SiGe Antenna in Dual 79GHz and 140GHz Bands for Automotive Sensing Applications

Juan Marcos-Miguel (Universidad Carlos III, Spain); Juan M Herrera-Martín (Universidad Carlos III de Madrid, Spain); Vicente González Posadas (Polytechnic University of Madrid, Spain); Daniel Segovia-Vargas (Universidad Carlos III de Madrid, Spain)

Sensing capabilities and specifically high resolution radars are fundamental in the development of increasingly autonomous vehicles. However, these kind of sensors require high bandwidths, pushing their development towards mmWave, which present complications in the integration of chips and antennas. In this paper, a dual-band, on-chip, integrated antenna is presented to operate in the 79 GHz and 140 GHz range, crucial for current and upcoming automotive sensing applications. First, an ideal design is implemented in IHP's SiGe 130nm technology, then the design is optimized taking into consideration specific design rules of the technology to yield a fully manufacturable modular antenna.

THURSDAY

3.30. 2-D LTCC Van Atta Arrays with Frequency-Domain Encoding for Millimeter Wave Chipless RFID

Benedykt Sikorski, Kamil Trzebiatowski, Lukasz Kulas and Krzysztof Nyka (Gdansk University of Technology, Poland)

The millimeter wave two-dimensional Van Atta arrays, designed for data encoding in chipless RFID systems, are presented in this paper. The arrays, fabricated using LTCC technology, are optimized for the 24 GHz band. Frequency-domain data encoding is achieved using microstrip resonators integrated with the lines of the array feed network, which selectively attenuates signal transmission at frequencies determined by their lengths. The fabricated chipless RFID tags, with dimensions of 24 x 24 mm, feature an information encoding capacity of up to 2 bits and an RCS level of up to -28 dBsm. To the best of the authors' knowledge, this is the first time that practical realization of 2-D Van Atta arrays integrated with resonant circuits for data encoding have been presented.

3.31. A Multi-Beam Planar Leaky-Wave Antenna for W Band Radar Systems

Goksel Turan, Gokhan Cinar and Hayrettin Odabasi (Eskisehir Osmangazi University, Turkey)

This article presents a multi-beam planar leaky-wave antenna designed for W-band radar systems. T-shaped and thin angled-ended slots are introduced into the circular series-fed patch array structure to enhance impedance matching and enable multi-beam functionality. The antenna operates in the 78.5 GHz to 88 GHz range, achieving a bandwidth of 11.4%, an average gain of 12 dBi, and an efficiency of 80% or higher. It provides total beam scanning of 63° across the ranges of −78° to −44°, −15° to −1°, and 27° to 42°, utilizing triple main beams. To the best of the authors' knowledge, this is the first study of a planar multi-beam leaky-wave antenna for W-band applications. The antenna's planar design, simplicity, high efficiency, and multibeam capability make it an excellent candidate for SAR imaging in airborne applications and automotive radar systems operating in the W-band.

3.32. A Sustainable and Low-Waste Temperature Sensor Based on 3D Liquid Metal and Carbon/Polymer-Loaded Lossy Transmission Lines

XiaoChuan Fang, Benjamin King and Mahmoud Wagih (University of Glasgow, United Kingdom)

We present a simple, low-waste RF temperature sensor based on liquid metal and a polydimethylsiloxane-carbon fiber (PDMS-CF) composite in a variable-attenuation coplanar waveguide (CPW) architecture. The sensor consists of a 3D-printed and liquid metal-filled CPW, and a PDMS-CF sensing element on the signal line. The PDMS-CF sensing element measures 10 mm × 3mm and is loaded on the CPW's signal line. The PDMS-CF element acts as a lossy transmission line, and the resulting transmission coefficient has an average sensitivity of 0.21 dB/°C at 50 MHz This sensitivity is greater than most of amplitude-based temperature sensor. The liquid metal and the PLA used for 3D printing are recyclable and biodegradable, respectively, with the PDMS-CF sensing element fully re-usable; the proposed RF sensor shows how chipless antenna-based sensors can be realized sustainably.

3.35. Conical Beam Compact Antenna for Manholes for IoT Applications in Smart Cities

Harsh Verdhan Singh (Mid Sweden University, Sundsvall, Sweden); Artem Pozniakov (Mid Sweden University, Sweden); T r Suresh Kumar (Vellore Institute of Technology, India); Zachariah C Alex (Vellore Institute of Technology (VIT) University, India); Johan Sidén (Mid-Sweden University, Sweden)

This paper presents a multilayered antenna solution designed for integration into manhole covers. The proposed antenna features a multilayered structure with no air gaps, ensuring mechanical feasibility in this environment. An aperture is created in the manhole cover to accommodate the antenna, which is fed by a coaxial feed at the center of the structure. The design provides an omnidirectional conical beam radiation pattern, enabling extended coverage. The antenna operates at 860 MHz, with a bandwidth ranging from 850 MHz to 870 MHz, making it suitable for LoRa-based IoT applications.

3.36. Design of a Square Ring Patch Antenna with Metallized Grid for Monopolar Radiation Applications

Luis Inclan-Sanchez (University Carlos III of Madrid, Spain)

This paper proposes the design of a semi-transparent square ring patch antenna that exhibits a monopolar radiation pattern. All metallic elements of the antenna are implemented using metallized grids, allowing most visible light to pass through the structure. The antenna operates without a substrate to significantly reduce losses and consists of a radiating layer formed by a square ring, fed by a central patch with a coaxial probe, and a ground plane. Both layers are short-circuited by four shorting walls made with grids, enabling the excitation of two conical radiation modes that, when coupled, result in wideband operation for the antenna. The antenna achieves monopolar radiation patterns over a bandwidth of 35%, with gains exceeding 4.5 dBi and transparency levels ranging from 65% to 80%, depending on the grid and ground plane size. This proposed solution is designed for 3D printing of components and integration into vehicle windows or roofs.

3.37. Directional Antennas Using Ecofriendly Materials and 3D Printing

Eryk Wojtczak, Weronika Kalista and Luiza Leszkowska (Gdansk University of Technology, Poland); Mateusz Rzymowski (Gdansk University of Technology & WiComm Center of Excellence, Poland); Krzysztof Nyka and Lukasz Kulas (Gdansk University of Technology, Poland)

This paper presents the designs and fabrication of lens antennas made of environmentally friendly materials. The specific goal of the work was to present ecological solutions used in 3D printing. Therefore, a study of the distribution of samples of four selected filaments in selected environments was conducted. It was investigated whether the selected compostable filaments are suitable to produce dielectric lenses. The tested lens antennas are intended for communication in V2X applications at 5.9 GHz. In the project, care was taken to achieve a balance between the weight and size of the lenses while aiming at highest possible gain. A patch antenna was designed, and several lenses were evaluated to select final four lenses that can provide a compromise between acceptable antenna electrical parameters and sustainability of the antenna prototypes. During the tests, it was proven that one of the two selected filaments, despite the manufacturer's assurances, is not compostable.

THURSDAY

3.38. Electroplating for Flexible Antennas by Using Laser-Induced Graphene Masks

Alessio Mostaccio, Francesco Mancuso and Gaetano Marrocco (University of Rome Tor Vergata, Italy)

Laser-Induced Graphene (LIG) is a simple and low-cost technique to pattern metal-free circuits and antennas on conformal objects. Despite its wide applicability, the high ohmic losses of the conductor currently hinder some applications requiring reliable radiation performances. In this paper, we present a preliminary experimental demonstration of a LIG-based electroplating technique for antennas, to combine the ease of manufacture of the LIG with the superior conductivity of metallic nanoparticles. Preliminary results show that with deposition times of 40 minutes, sheet resistances as low as 30 mOhm/sq can be achieved. The process is demonstrated with a typical IoT flexible dipole at 900 MHz whose radiation gain is just 1 dB less than a full-aluminum counterpart.

3.39. Experimental Analysis of UHF RFID Tags Mounted on PET Liquid Containers Subjected to External Forces

Pol Brunet, Sergio López-Soriano and Mohammed Ahmed Alsultan (Universitat Oberta de Catalunya, Spain); Joan Melià-Seguí (Universitat Oberta de Catalunya (FUOC), Spain)

This contribution presents a battery-free UHF RFID tag design for sensing applications using fluids. A container made of polyethylene terephthalate (PET) is used as the antenna substrate and then filled with a mixture of three fluids: air, water and oil. A vibration detection RFID sensor is implemented exploiting the changes in the tag antenna input impedance produced by the variations in the state of the fluids within the PET container. The variations are captured by a self-tuning integrated circuit (IC). The method is initially tested using a microstrip transmission line (TL) and an RFID tag. The devices are evaluated through an experiment where the liquid container is shaken to mix the fluids. The results of both experiments are presented and discussed in this study. The experimental results demonstrate that the sensor is capable of detecting continuous changes in the state of fluids during the relaxation process following an initial stimulus.

3.40. Millimeter Wave Rectifiers: A Review of Technology and Performance

Yibo Wang (LTCI & Télécom Paris & Institut Polytechnique de Paris, France); Kyriaki Niotaki, Anne-Claire Lepage and Xavier Begaud (LTCI & Télécom Paris, Institut Polytechnique de Paris, France)

Rectifiers operating at the millimeter wave (mmWave) frequencies have recently attracted interest for a wide range of applications, including wireless power transmission and energy harvesting. This work presents an overview of the rectifiers operating in the mmWave band, and more specifically from 24 GHz to 94 GHz. It also highlights the main mmWave rectifier's design challenges along with some novel techniques used to optimize their performance.

3.41. On the Design, Fabrication and Characterization of a Miniaturized and Optically Transparent CSRRs-Loaded Antenna Operating in C-Band for a Dual Optical-RF Purpose

Maxime Hodoul (University of Rennes, France); Loic Bernard (ISL & IETR, France); Mohamed Himdi (Université de Rennes, France); Quentin Simon Simon (Universite de Rennes 1, France); Stéphane Méric (Institut National Des Sciences Appliquées (INSA Rennes), France & IETR, France); Ronan Adam (French-German Research Institute of Saint-Louis, France); Xavier Castel (IETR-Université de Rennes 1, France)

A miniaturized and optically transparent CSRRs-loaded (Circular Split Ring Resonator) antenna operating in C-band is presented. Two miniaturization techniques were used to get a highly miniaturized microstrip antenna. By combining high-permittivity substrate with CSRRs-loaded ground plane, a reduction size over 70% was then obtained. The antenna dimension equals 0.1λ at fr =5.3 GHz with a −3.9dBi simulated gain. Optical transparency is achieved by printing a micrometric mesh metal films with pitch of 300µm and metal strip width of 10µm on both sides of sapphire substrate. Homemade prototypes were fabricated and characterized at microwaves: the operating frequency and radiation pattern were measured experimentally. Snapshots from an endoscopic camera were taken behind the transparent antenna as proof of concept. A new dual optical-RF application has therefore been developed

3.42. Rim-Integrated Bluetooth Antenna for Smartwatches with Full-Metallic Structure

Ali Kourani, Sihan Shao, Mohamed Räsänen and Jan H. S. Bergman (Aalto University, Finland); Rasmus Luomaniemi (Radientum Oy, Finland); Jari Holopainen (Aalto University, Finland)

The integration of smart technology into wearable devices has been rapidly evolving, leading to the proliferation of smartwatches, fitness trackers, smart jewelry, and other connected accessories that blend functionality with everyday use. As these devices become increasingly compact, efficient, and sophisticated, the design of internal components, such as antennas, plays a critical role in optimizing performance. This paper explores the design, manufacturing, and prototype measurements of a Bluetooth antenna integrated into the metallic rim of a smartwatch. By embedding the antenna within the structural elements of the device, we address challenges related to space constraints, complicated metallic structure inside the smartwatch influencing the antenna pattern, and overall device aesthetics. The measured prototype showed a −10 dB impedance bandwidth over the 2.38-2.65 GHz frequency range, which encompasses 2.4-2.5 GHz range of interest, when measured on a human tissue phantom, with a total efficiency of 30%.

THURSDAY

3.43. Design of a Flexible Force-Sensing Antenna for Biomedical Monitoring

Alice Champion (University of Southampton, United Kingdom & University of Southampton, United Kingdom); Irfan Ullah, Stephen Beeby and Russel Torah (University of Southampton, United Kingdom) We present a proximity-coupled meandered patch antenna implemented in a multilayer substrate for biomedical monitoring applications. The antenna's resonant frequency shifts to lower bands at a rate of 40.77 MHz/N when force is applied perpendicular to the radiating patch. Remote interrogation at a distance of 17 cm in an anechoic chamber demonstrated that the high-gain horn antenna detects this frequency shift when masses are applied to the radiating patch. These findings suggest that the proposed antenna sensor is suitable for force sensing in wearable healthcare.

Room: Poster level 2 | **PE3 - Electromagnetics III**

T08 Fundamental research and emerging technologies/processes / / Electromagnetics

Chairs: Edoardo Negri (Sapienza University of Rome, Italy), Roberta Palmeri (Università Mediterranea of Reggio Calabria, Italy)

2.49. 4-18 GHz Reconfigurable Rasorber with Grating Lobe Suppression Using Absorptive Honeycombs

Hao Jiang (South China University of Technology & School of Electronic and Information Engineering, China); Mei Qian, Yinghao Zhang and Quan Xue (South China University of Technology, China)
This paper presents a reconfigurable rasorber covering the 4-18 GHz range, utilizing absorptive honeycombs to effectively suppress grating lobes. Building on a previous threelayer frequency selective rasorber (FSR) operating in the 1-7 GHz band, we introduce a dual-layer honeycomb structure with tunable dielectric properties achieved through carbon fiber doping. The proposed configuration exhibits low-pass and high-stop transmission characteristics, efficiently absorbing high-frequency waves while maintaining low-frequency bandpass window. Compared to earlier designs constrained by p-i-n diode operating frequency limitations in radar applications, the new configuration offers improved absorption performance and broader frequency coverage, making it suitable for advanced electromagnetic (EM) interference suppression and radar cross-section reduction.

2.50. A Conformal Dual Frequency Wireless Power Transfer System Based on Magneto-Inductive Waveguides

Alessandro Luigi Dellabate and Danilo Brizi (University of Pisa, Italy); Agostino Monorchio (Pisa University & CNIT, Sweden)
This paper presents a numerical analysis of a conformal dual frequency Wireless Power Transfer system based on magneto-inductive waves. By exploiting accurate numerical simulations, we conceived an arrangement consisting of a single actively fed RF transmitter linked through two magneto-inductive waveguides to the corresponding receivers. The selected working frequencies, 13.56 MHz and 40.68 MHz, lie within the ISM available bands, making the system suitable for biomedical applications, as power transmission to implantable devices, and for consumers devices. Maximum efficiencies of 1.45% and 12.5% are achieved at 13.56 MHz and 40.68 MHz, respectively. Moreover, the proposed system requires a single layer of elements, allowing a more compact and potentially conformal realization of power transmitting devices with respect to traditional WPT systems based on external drivers. Additionally, the absence of cables and connectors linking the transmitting coil with the receivers enables wireless signal propagation even with large and arbitrarily complex separating paths.

2.51. A Dual-Polarized Wideband Frequency-Selective Rasorber in Absorption-Transmission Configuration for S-C Bands

Francesca Pascarella and Danilo Brizi (University of Pisa, Italy); Agostino Monorchio (Pisa University & CNIT, Sweden)
This paper presents a passive dual-polarized Frequency Selective Rasorber (FSR) in an Absorption Transmission configuration, covering S and C bands. The proposed FSR consists of an absorbing resistive Frequency Selective Surface (FSS) operating together with a wideband transmitting lossless FSS. The absorbing FSS includes two lossy layers, which are perpendicularly positioned on the respective side of a dielectric substrate to cover both TE and TM polarizations, featuring a meandered square spiral arm unit cell, loaded with opportune resistors. The wideband bandpass filter is designed by placing a dielectric substrate between two lossless FSS layers. The proposed FSR achieves a -3 dB transmission band ranging from 2.9 to 7.05 GHz, with a minimum insertion loss of -0.75 dB. The -10 dB absorption band spans from 1.55 to 2.9 GHz. The structure shows stable performance for oblique incidences up to 30° and a considerably reduced overall thickness, i.e. 31 mm (i.e., $\lambda L/5$).

2.52. A Study on the Reduction of Frequency Points in Muscle Rupture Microwave Imaging

Andreas Fhager and Laura Guerrero Orozco (Chalmers University of Technology, Sweden); Lars Peterson (Sahlgrenska Academy, Sweden)
Injuries in the hamstring muscles are among the most common injuries in sports. We have identified a need for new low-cost diagnostic tools to facilitate accurate diagnostics for a wide range of injured athletes and the general public. Therefore we are developing a microwave-based imaging system for muscle rupture detection based on frequency domain transmission measurements. In this paper, we have investigated the effect of the number of frequencies on the image accuracy in a delay multiply and sum algorithm. Experimental data show that a significant reduction is possible without severely sacrificing image accuracy. A reduction from 260 frequencies to about 20 increases the relative squared error by less than 1%. This is a significant result that paves the path for the development of affordable and compact systems that can be made available widely.

THURSDAY

2.53. An Ultra-Wideband Lightweight Absorber Based on Paper-Based Composites

Hao Jiang (South China University of Technology & School of Electronic and Information Engineering, China); Mei Qian, Yinghao Zhang and Quan Xue (South China University of Technology, China)
This work presents a novel absorber that showcases lightweight and ultra-wideband absorption properties. The absorber is fabricated using paper-based composites (PBCs) embedded with carbon fibers (CFs) through advanced papermaking processes. These PBCs exhibit high-frequency absorption characteristics. To improve low-frequency absorption, the permittivity of the PBCs is extracted, and an equivalent circuit model (ECM) is developed to identify the optimal architectural design for the absorber. A planar impedance layer with a hexagonal single-loop structure is employed to induce low-frequency resonant modes. The resulting device, consisting of PBCs and the impedance layer, displays multimode resonances and exhibits a broad −10-dB reflection band ranging from 2-18 GHz (160%). Experimental results demonstrate the superior performance of our design, including low density (50.7 kg/m3) and wide bandwidth under dual polarization.

2.54. Analysis and Design of Fully Dielectric Scattering Surface with Additive Manufacturing

Mehmet Emre Eralp (Middle East Technical University & Accelerate Simulation Technologies, Turkey); Ozgur Eris and Ozlem Aydin Civi (Middle East Technical University, Turkey)
This paper presents a low-profile dielectric checkerboard scattering surface designed to provide wideband RCS reduction without the use of metallic patterns. The surface is fabricated from a single 3D-printed material, where the dielectric constant is controlled by adjusting the infill ratio. This approach offers a practical, cost-effective, and scalable solution for RCS reduction by eliminating the need for complex designs and multiple materials. Simulations demonstrate a better than 10 dB monostatic RCS reduction compared to a PEC plate over a broad bandwidth of 78%, covering the frequency range from 10 GHz to 22.9 GHz, with strong performance across the Ku band.

2.55. Comparison of Optimization Approaches to Design Reactively Loaded Antenna Arrays

Albert Salmi (Aalto University, Finland); Miloslav Capek and Lukas Jelinek (Czech Technical University in Prague, Czech Republic); Anu Lehtovuori (Aalto University, Finland); Olli Pekonen, Jussi Rahola and Mikko Honkala (Optenni Ltd, Finland); Ville Viikari (Aalto University & School of Electrical Engineering, Finland)
This paper compares methods to design sparse grating-lobe-free reactively-loaded antenna arrays using different optimization approaches. Three approaches are based on optimization on a Riemannian manifold, and one utilizes the Optenni Lab software. In addition, we compute the fundamental bounds of the optimization problems using semi-definite relaxation. Demonstrations with a connected patch-diamond antenna array show that the scan loss is minimized when the reactive loads are optimized by maximizing the antenna array's minimum main beam gain within the beam-steering sector.

2.56. Design and Development of Ultra-Wideband Conformal Artificial Magnetic Conductor Metasurface for RCS Reduction

Baisakhi Bandyopadhyay and Abhishek Mishra (Indian Institute of Technology Kanpur, India); Mondeep Saikia (Queen's University Belfast, United Kingdom); Kumar Vaibhav Srivastava (Indian Institute of Technology Kanpur, India)
This work describes the design and development of an ultra-wideband conformal artificial magnetic conductor (AMC) metasurface for radar cross-section (RCS) reduction applications. The design comprises a single AMC unit cell and a single dielectric unit cell, absent of any metallic configuration on the top. The uniqueness of the proposed framework resides in the design of a singular AMC unit cell to produce a checkerboard pattern for ultra-wideband RCS reduction. The unit cell dimensions are 0.12λL in periodicity and 0.084λL in thickness, relative to the lowest frequency. The proposed configuration offers an ultra-wide bandwidth ranging from 2 GHz to 8.7 GHz, resulting in a fractional bandwidth of 125%. Furthermore, the proposed structure provides an angular stability of 50 ◦ . A thin substrate is selected for the design of the proposed metasurface which provides a conformability of 30 ◦ . The structure is fabricated and experimentally validated, yielding a favorable correlation with the simulated outcomes.

2.57. Experimental Verification of Liquid Crystal-Based Reconfigurable Intelligent Surface for 6G Communications

Youngtaek Hong, Byeongyong Park and Ilnam Cho (LG Electronics, Korea (South))
Experimental verification of liquid crystal (LC)-based reconfigurable intelligent surface (RIS) for 6G communications is presented. Two different type of LC-based RIS unit cells are proposed and the beamforming performance of the fabricated 7×7 array prototype is analyzed. In the fabrication, LC mixture GT7-29001 from Merck KGaA is used to obtain wide variation range of dielectric constant with low loss characteristics. The measured phase difference of the fabricated RIS prototype is more than 240 degrees within the 1 GHz bandwidth (9.5-10.5 GHz). To verify the beamforming performance, the bias voltage configurations of the fabricated prototype to focus the beam in the 30° and 45° directions were analyzed. The measured S21 values at 10 GHz are increased by 11.1 dB and 7.7 dB for 30° and 45° beamforming, respectively.

THURSDAY

2.58. Machine Learning-Based Antenna Optimization with Multi-Fidelity EM Analysis and Dimensionality Reduction by Global Sensitivity Analysis

Slawomir Koziel and Anna Pietrenko-Dabrowska (Gdansk University of Technology, Poland)

This work introduces a novel technique for cost-efficient antenna optimization. Our approach employs computational intelligence tools, including machine learning (ML) and bio-inspired algorithms. The ML process is conducted within a dimensionality-constrained parameter space established through global sensitivity analysis (GSA). The underlying surrogate model is kriging interpolation, whereas candidate designs are generated using the particle swarm optimizer (PSO). Further enhancement of the computational efficacy is obtained by employing multi-fidelity electromagnetic (EM) models, with majority of operations executed at low-fidelity antenna representation and final (gradient-based) tuning performed using the high-fidelity model. Extensive numerical experiments demonstrate the superiority of the introduced approach over several benchmark procedures regarding reliability, computational efficiency, and repeatability of results.

2.59. Textile Embroidery FSS for Security Applications

İbrahim Üner (Pamukkale University, Turkey); Sultan Can (Ankara University, Turkey)

This study presents the design and development of a flexible and lightweight Frequency Selective Surface (FSS) based on woven fabric, functioning as a band-stop filter with a center frequency of 3.9 GHz. FSS, composed of periodic arrays of conductive elements. The woven fabric, a plain weave of cotton fibers, measured 0.6 mm in thickness and 300 g/m^2. The conductive yarn preferred for the design was Shieldex Statex 117 d/f17-2 ply. Design topology validated by fabrications and measurements having the results showing resonance at approximately -50 dB at 3.91 GHz in simulations, -36 dB at 3.83 GHz for the copper tape sample, and -20.09 dB at 3.82 GHz for the embroidered FSS. The study highlights the potential of textile-based FSS in modern communication and defense applications, offering flexibility, durability, and ease of integration advantages.

2.60. Three-Dimensional Complex Permittivity Prediction from Spatio-Temporal Electric Field Distributions

Rahul Sharma and Okan Yurduseven (Queen's University Belfast, United Kingdom)

Quantitative imaging is a critical task in various applications, including medical diagnostics, non-destructive evaluation and material characterisation. This work addresses the problem of three-dimensional (3D) permittivity profile reconstruction of a region of interest (RoI) by leveraging a deep learning model. This is performed by training the model to establish a mapping between the spatio-temporal electric field data and the corresponding permittivity profile of the RoI. The deep learning model is designed to handle the time-varying electric field data efficiently, using a combination of convolutional layers to extract spatial features and Long Short-Term Memory (LSTM) networks, to model temporal dependencies. The effectiveness of this approach is demonstrated through comprehensive validations in different scenarios, offering a powerful tool for quantitative permittivity prediction in a wide range of applications.

Room: Poster level 2 | **PP3 - Propagation III**

T08 Fundamental research and emerging technologies/processes / / Propagation

Chairs: Tanguy Lopez (Sorbonne Université, France), Sergio Matos (ISCTE-IUL / Instituto de Telecommunicações, Portugal)

2.35. A Generative Model for Outdoor Propagation Prediction Using Generative Adversarial Networks

Miyuki Hirose (Kyushu Institute of Technology, Japan); Satoshi Iwasaki (KOZO KEIKAKU Inc., Japan)

This paper introduces a novel Generative Adversarial Network (GAN)-based model to predict outdoor propagation from building height and transmitter-receiver positioning data. Our model uses inputs such as building height, transmitter coordinates, and receiver coordinates to generate signal strength predictions at various receiver points. The GAN consists of a generator that synthesizes signal strength based on geographical data and a discriminator that distinguishes real from generated signal strength. We demonstrate the effectiveness of this method through experiments with simulated data, showing that the GAN model can predict signal strength with high accuracy. This approach demonstrates a simple and reliable new propagation prediction method for outdoor propagation in complex environments.

2.36. Channel Measurements Involving Passive RIS at 300 GHz

Lorenz H. W. Loeser (Technische Universität Braunschweig, Germany); Sergio Matos (ISCTE-IUL / Instituto de Telecommunicações, Portugal); Thomas Kürner (Technische Universität Braunschweig, Germany)

The ever growing demand for data rates motivates the exploration of the low terahertz (THz) frequency bands for mobile communications due to the large available bandwidths. To mitigate the reliance on line-of-sight (LOS), the concept of reflective intelligent surfaces (RIS) has emerged as a promising technology. By reshaping the electromagnetic environment, RIS modifies the channel, necessitating new approaches to model key parameters such as the path gain. This paper proposes the bistatic radar equation as a simple yet accurate model to predict the path gain of a link that includes a RIS, even below the Fraunhofer distance. Channel measurements at 300 GHz, incorporating a passive RIS, support the validity of this approach.

THURSDAY

2.38. Efficient Analytical Model for VED Radiation in a Lossy Half-Space: Validation by an FEM Solver

Hocine Anis Belaid (Univ Gustave Eiffel, CNRS, ESYCOM, France); Shermila Mostarshedi and Benoit Poussot (University Gustave Eiffel, France); Stéphane Protat (Université Marne La Vallée, France); Jean-Marc Laheurte (Université Gustave Eiffel & ESYCOM Lab, France)

The theoretical background of a vertical electric dipole embedded in a lossy half-space and the Sommerfeld integrals are presented. The asymptotic electromagnetic field expressions are given by using the Modified Saddle Point Method. Two commercial simulators with two different solvers are used for validation, Altair FEKO and Ansys HFSS. The efficiency of the analytical method is highlighted by introducing a parametric study.

2.39. Evaluation of Rain Rate Integration Time Conversion Models for Attenuation Prediction

José E. Silva (Universidade de Aveiro, Portugal); Armando Rocha (University of Aveiro, Portugal & Instituto de Telecomunicações, Portugal); Susana Mota (University of Aveiro & Institute of Telecommunications, Portugal) The estimation of atmospheric attenuation due to rain normally requires statistics of the rainfall rate measured with an integration time of 1 minute which is only available in a few locations. However, there are models for obtaining these statistics from available rain data measured with an integration time of up to 30 minutes or more. In this paper, these models are preliminary evaluated using two years of a rainfall rate database collected almost uninterruptedly over 8 years. The ITU-R P.618-14 attenuation model is applied using rain rate statistics measured with a 1-minute integration time and, also, estimates from various rain rate integration time conversion models. The results are compared with Ka and Q band beacon measured attenuation statistics for the same period and the errors of the predictions are, as well, estimated.

2.40. Experimental Performance Validation of Fisher Information-Optimized Multicarrier Waveforms for Sub-THz Channel Sounding

Jonas Gedschold and Sebastian Semper (Technische Universität Ilmenau, Germany); Alexander Ebert (Fraunhofer Institute for Integrated Circuits IIS & Technische Universität Ilmenau, Germany); Giovanni Del Galdo (Fraunhofer Institute for Integrated Circuits IIS & Technische Universität Ilmenau, Germany); Reiner S. Thomä (Technische Universität Ilmenau, Germany)

This paper describes an experimental performance validation of Fisher information-based waveform designs for channel sounding and high-resolution propagation parameter estimation. These waveform designs require prior knowledge about the propagation parameters which can be estimated from a preceding measurement. We describe a setup to implement this intermediate parameter estimation and waveform optimization step. A subsequent performance validation via the empirical MSE derived from measurement-based Monte Carlo trials is also presented. This paper builds upon a previous simulation-based study that found that the CRB for delay estimation improves using the optimized waveforms equivalent to an increase in SNR of 4 dB. This finding can be reproduced for the delay MSE with the presented experiments. An additional insight is that the accuracy of the intermediate estimates does not significantly impact the MSE, as long as the SNR is sufficient to detect the required paths reliably.

2.41. Impact of Propagation Environment on Cooperative Spectrum Sensing with Direct Conversion Receiver

Felipe Forza (Inatel, Brazil); Pedro Marcio Raposo Pereira (National Institute of Telecommunications, Brazil); Felipe Augusto Pereira de Figueiredo (INATEL, Brazil); Hugerles S. Silva (University of Brasilia, Brazil); Rausley Adriano Amaral de Souza (National Institute of Telecommunications (INATEL), Brazil & The University of Sydney, Australia)

This article analyzes the performance of an eigenvalue-based cooperative spectrum sensing cognitive radio (CR) system under the joint influence of short- alpha-mu model and long-term (Gamma model) fading phenomena, path loss (power-law decay), and mobility (random way-point). Each CR adopts a direct conversion receiver. The performance is evaluated under both slow- and fast-fading channels. The results demonstrate that the shadowing parameter and the path loss exponent significantly influence the spectrum sensing performance. Furthermore, the coverage analysis under various channel conditions indicates that the severity of shadowing significantly impacts system coverage capabilities. Less severe shadowing allows for greater coverage without compromising performance. Additionally, increasing the channel severity necessitates more CRs to maintain the desired performance, whereas less severe channels allow for effective performance with fewer CRs. It is revealed that the mobility scenario requires fewer cooperating CRs to achieve specified performance targets than the static scenario.

2.42. Indoor Channel Propagation Measurements and Statistical Modeling for FR3 Mid-Band Spectrum at 12-18 GHz

Demos Serghiou, Tim Brown, Ashwin Thelappilly Joy and Gabriele Gradoni (University of Surrey, United Kingdom); Mohsen Khalily (University of Surrey & 5G Innovation Centre, Institute for Communication Systems (ICS), United Kingdom); Rahim Tafazolli (University of Surrey, United Kingdom)

New spectrum allocations in the FR3 band that ranges between 7-24 GHz, are being considered for future 5G and 6G cellular deployments. This paper presents indoor Line- of-Sight (LoS) path loss measurements and angular scattering measurements using directional horn antennas for the FR3 mid-band spectrum between 12-18 GHz. The LoS path loss statistics con- firm the Friis transmission model, showing path loss exponents that are close to those of free space while delay spreads are shown to decrease over distance. The angular statistics derived from empirical measurements show that significant multipath components can be detected at a wide range of reflection angles indicating that further work is required in the characterization of different building structures with features comparable in size to the wavelength that may form frequency selective scattering, for modeling accurately future cellular communications within this band.

THURSDAY

2.43. Influence of Fire Whirls on Radiowave Propagation

Stefânia Faria (Instituto de Telecomunicações, Portugal); Mario Vala (University of Lisbon, Portugal & Instituto de Telecomunicações, Portugal); Joao M Felicio (Instituto Superior Técnico, Portugal & Instituto Telecomunicacoes, Portugal); Carlos Salema (I.S.T. - Technical U. Lisbon / IT Lisbon, Portugal); Rafael F. S. Caldeirinha (Polytechnic Institute of Leiria & Instituto de Telecomunicações, Portugal); Nuno R. Leonor (Polytechnic Institute of Leiria (IPL) & Instituto de Telecomunicações (IT), Leiria, Portugal); Carlos A. Fernandes (Instituto de Telecomunicacoes, Instituto Superior Tecnico, Portugal)

This paper presents the findings of an extensive measurement campaign conducted to assess the fire impact on signal propagation using a vortex generator. Pine needles and bushes were used as fuel, with approximately 4~kg of each material burned during the experiments. The ignition was initiated with a blowtorch, and the combustion process occurred in the presence of swirling wind to generated high and steady flames. Temperature and fuel mass consumption data were recorded, as well as the s-parameters in both transmission and reflection modes. The perturbations introduced by fire were analysed from 600~MHz to 8~GHz, considering both frequency and spatial domain assessments. At specific frequencies, the magnitude of the frequency response exhibited varying levels of reduction across the band for different species. In the spatial domain, the amplitude reduction of the reflected component at the metallic wall reached up to 0.27~dB and 0.36~dB, for pine needles and bush tests, respectively.

2.44. Monitoring Plastic Accumulations in a River Environment Using Machine Learning on Sentinel-1 SAR Data

Tomás Soares da Costa (ULisboa - Instituto Superior Técnico & Instituto Telecomunicações, Portugal); Joao M Felicio (ULisboa - Instituto Superior Técnico & Instituto Telecomunicações, Portugal); Sergio Matos (ISCTE-IUL / Instituto de Telecommunicações, Portugal); Jorge R. Costa (Instituto de Telecomunicações / ISCTE-IUL, Portugal); Carlos A. Fernandes (Instituto de Telecomunicacoes, Instituto Superior Tecnico, Portugal); Nelson Fonseca (Anywaves, France)

Plastic litter is a growing environmental issue. Microwave (MW) technology has the potential for an all-time and weather remote detection of floating macroplastics via satellites or airborne platforms. However, none of the early studies in the existing literature has addressed MW sensor requirements or the application of Machine Learning (ML) for automated monitoring with readily available data. In this study, we employ a supervised learning workflow to monitor, in a preliminary phase, floating macroplastic accumulation in a river environment utilizing polarimetric Sentinel-1 (S-1) SAR data. The combination of co-polarization (VV) and cross-polarization (VH), specifically VV-VH and VV+VH, resulted in detection accuracies exceeding 90%, without overfitting. Analysis of scattering behavior revealed that both VV and VH backscatter were sensitive to plastic patch size, with a linear relationship. This differs from the low-intensity scattering of river water. The findings highlight the importance of dual polarization for effective MW-based plastic monitoring missions.

2.45. Outdoor-To-Indoor (O2I) Propagation Loss Model Based on the New Parameter: Compound Power (CP)

Young Chul Lee and Khairunnisa Aziding (Mokpo National Maritime University, Korea (South))

In this work, we propose a novel outdoor-to-Indoor (O2I) propagation loss model centered on the new Compound Power (CP) parameter, which encapsulates the combined effects of diffraction, reflection, and penetration, specifically in non-line-of-sight (NLoS) scenarios. The model is rigorously developed through analytical derivations and experimentally validated using a unique measurement setup, proving that the inclusion of clutter, such as nearby large structures, has a substantial impact on building entry loss (BEL). By accurately accounting for both the building and its surrounding environment, the model significantly improves indoor power predictions, offering a comprehensive approach to O2I propagation in real-world, cluttered environments.

2.46. Spherical and Plane Waves Propagation Through a Realistic Turbulent Marine Layer

Rémi Douvenot and Victor Darchy (ENAC, France); Stéphane Jamme (ISAE-SUPAERO, France); Helene Galiègue (ENAC, Université de Toulouse, France)

In this paper, the impact of a realistic turbulent medium obtained from fluid mechanics equations on radiowave propagation is studied. The realistic medium contains more structured variations of refractive index than the one usually generated from Gaussian-like spectra. The impact on propagation is illustrated by comparing the effect on sources presenting both a spherical and a plane wavefront. These results highlight the impact of the localised atmospheric structure that could reveal an underestimation of the turbulence impact when obtained via the commonly used Gaussian-like spectra.

2.47. Study of Adaptative V-Band Channels Allowing Broadcast and Point to Point Communications in the WiNoC Concept

Bryan Treguer and Pierre-Marie Martin (University of Brest, France); Rozenn Allanic (Lab-STICC - UBO Brest, France); Thierry Le Gouguec (University of Brest, France); Cedric Quendo (Lab-STICC - UBO Brest, France) This paper proposes to design V-band adaptive channels for WiNOC communications. In the aim of optimizing point-to-point or broadcast communications considering a parallel plate propagation media, reflectors are introduced and simulated on a high-resistivity silicon substrate (HR-Si) surrounded by a low-resistivity silicon (LR-Si) layer obtained by doping. Polarizations of the reflectors improves the propagation channel characteristics for slot antennas located 45° apart. Another transition method is then used: CPW-SIW transitions allow point-to-point or broadcast transmissions, depending on the reflector's resistivity. In simulation, transmission levels of -4.8 dB with a bandwidth equal to 21 GHz are achieved, making it possible to reach data rates of 18 Gbit/s.

THURSDAY

2.48. Wireless Industrial Channel Characterization Through Machine Learning and Ray Tracing Simulations

Mohammad Hossein zadeh, Marina Barbiroli, Enrico M. Vitucci, Vittorio Degli-Esposti and Franco Fuschini (University of Bologna, Italy)
This paper investigates the performance of both a machine learning-based wireless propagation model and an empirical formula in an industrial environment. The study examines a configuration with the transmitter placed at the center of the ceiling, considering key propagation parameters, including path loss, shadowing, and delay spread. The machine learning model and the empirical formula applied for predicting propagation parameters demonstrate accurate results. While the empirical formula is simpler to apply, the machine learning model consistently outperforms the empirical approach in terms of predictive accuracy, making it a more effective solution for real-time wireless network optimization. Furthermore, a comparison with previous work, where transmitters were wall-mounted, reveals significant improvements in communication performance with the new configuration, as expected. The previous study was limited by not considering different transmitter heights due to associated computational effort, which is addressed in this study. The results show remarkable enhancements in the propagation parameters.

Room: Poster level 2 | **PS1 - Best Paper Awards**

Thursday - 14:40-15:20

Room: Alfvén (A3+A4)
Invited Speaker
Carolina Vigano
Chair: Oscar Quevedo-Teruel (KTH Royal Institute of Technology, Sweden)

Room: Kildal (A2)
Invited Speaker
Jorge L. Salazar-Cerreño
Chair: Davide Comite (Sapienza University of Rome, Italy)

Thursday - 15:50-17:30

Room: Alfvén (A3+A4) | **CS4 - Advances on metasurfaces for wavefront manipulation**

T08 Fundamental research and emerging technologies/processes / Convened Session / Electromagnetics

Chairs: Shah Nawaz Burokur (LEME, France), André de Lustrac (C2N, Université Paris-Saclay, France)

15:50 Spurious Transmission Dips in Waveguides Implemented with Glide-Symmetric Holey EBG

Mingzheng Chen and Oskar Zetterstrom (KTH Royal Institute of Technology, Sweden); Francisco Mesa (University of Seville, Spain); Oscar Quevedo-Teruel (KTH Royal Institute of Technology, Sweden)
Glide-symmetric holey electromagnetic bandgap (EBG) structures have found wide applications in high-frequency gap waveguide components because of their demonstrated wide stopband and easy manufacturing. However, potential dips in the transmission through the gap waveguide at certain frequencies limit the effective bandwidth. Here, we perform a Bloch analysis of the unit cell, a rectangular waveguide segment implemented with the glide-symmetric holey EBG, using a multimodal transfer matrix method. We find two main spurious dips in the transmission coefficient in the recommended operating frequency band of the investigated WR-15 standard rectangular waveguide. The first transmission dip is found to correspond to the coupling of the waveguide mode and the edge mode formed in the air gap between the waveguide and the EBG holes. The second transmission dip is caused by a small open stopband in the waveguide mode.

16:10 Time-Modulated Metasurfaces for Stealth at VHF-UHF Frequencies

Thomas Lepetit (ONERA-DEMR, France); Shah Nawaz Burokur (LEME, France); Tanguy Lopez (ONERA & LEME, France); Badreddine Ratni (Univ Paris Nanterre, France)
Radar absorbent materials (RAM) have a 10dB matching bandwidth that is intrinsically limited by thickness. This is a critical issue at large wavelengths (λ~1m), which has spurred research in many directions including time-modulated metasurfaces. We highlight an efficient simulation model to design such metasurfaces and demonstrate its benefits with the example of a Doppler cloak. Finally, we underline the necessity of measuring the impact of such metasurfaces on radar signal processing.

THURSDAY

16:30 Broadband Electromagnetic Susceptibility Modeling of Artificial Magnetic Conductors

Oscar Céspedes Vicente and Christophe Caloz (KU Leuven, Belgium)
An artificial magnetic conductor (AMC) is an patterned surface that mimics the behavior of a perfect magnetic conductor (PMC), reflecting electromagnetic waves without phase reversal, hence compensating for the inexistence of magnetic charges. However, the modeling of AMCs has been so far restricted to rudimentary RLC or transmission-line network approximations. This work introduces an advanced electromagnetic theory of AMCs based on spatially dispersive metasurfaces with multipolar responses. Additionally, it highlights the critical role of the electric linear quadrupole response, even at relatively low frequencies. These insights pave the way for more accurate simulations, optimizations and innovative AMC designs.

16:50 Investigation Toward Activating Nonreciprocal Metasurfaces

Kazuhiro Takahagi (University of Sheffield & Acquisition, Technology and Logistics Agency, Ministry of Defence, United Kingdom); Alan Tennant (University of Sheffield, United Kingdom)
Nonreciprocal metasurfaces, which spatially control electromagnetic waves depending on their propagation direction, are a critical element in achieving more advanced wave control. Several methods to realize nonreciprocity in metasurfaces include using circuit elements such as amplifiers or employing magnetic materials. In this report, we present the design and evaluation of a simple structure that combines magnetic materials and PIN diodes to control nonreciprocity. The results demonstrate that nonreciprocal characteristics with more than 10 dB of isolation in the 6 GHz band can be controlled by switching the PIN diode on and off.

17:10 Bandwidth Enhancement of Topological Insulator Metasurfaces

Vinothan Vaheesan and Miguel Navarro-Cía (University of Birmingham, United Kingdom); Kevin Mitchell (QinetiQ, United Kingdom); Alexandros Feresidis (University of Birmingham, United Kingdom) In this paper, we investigate a photonic topological insulator metasurface utilising electromagnetic duality. Using strong magneto-electric cross-coupling, a complementary two-layer structure can open a band gap. The non-trivial band gap enables strong topological protection of bound surface waves, over a large bandwidth of mm-wave frequencies. We investigate the direct relationship between bandwidth and inter-layer separation of the two-layer structure, showing that by reducing the separation from 1mm to 200µm the fractional bandwidth is increased from 39.81% to 53.77%. In this study, we also investigate the effect of the number of unit cells on either side of the interface and its effect on transmission. We observe that topological protection is maintained from 5- to 2-cell width on either side of the interface, but below 2-cell the structure suffers from high losses in the band gap frequencies. We also note a negligible change in S12 and S21 for 5-cell to 2-cell width.

Room: Kildal (A2) | **A07 Advances in Lens Antennas II**

T02 Millimetre wave and THz for terrestrial networks (5G/6G) / / Antennas

Chairs: Nelson Fonseca (Anywaves, France), Martin Schneider (University of Bremen, Germany)

15:50 A Phase Correcting Surface Based on a D-Band Transmitarray Antenna Using Hybrid-PCB-CMOS Technology

Awanish Kumar (CEA-LETI & University Grenoble Alpes, France); Jose Luis Gonzalez Jimenez (Université Grenoble-Alpes/CEA-Leti, France); Luca Lucci (CEA Leti, France); Alexandre Siligaris (Cea, Leti, Minatec, France); Antonio Clemente (CEA-Leti, France)
This papers presents a high-gain, wideband antenna for D-Band applications, designed using a hybrid-PCB-CMOS packaging technology and optimized through an in-house numerical tool. The proposed transmitarray consists of 400 unit cells with 1-bit phase quantization, arranged in a regular square lattice and illuminated by a horn antenna as the focal source. Simulations and analytically calculations demonstrate that the proposed antenna system achieves a peak gain of 19.5 dBi, with an absolute bandwidth of 30 GHz, corresponding to a fractional bandwidth of 26.7%. The accuracy of the numerical model is validated by simulating the antenna using HFSS, where full-wave simulation results closely match with the analytical predictions, confirming the efficacy of the design process. Additionally, we are extending this technology by integrating CMOS switches into the unit cells to implement a 1-bit reconfigurable transmitarray antenna for beam-scanning applications. This work contributes to the development antenna technologies for future 6G networks.

16:10 A Precise Ray-Path Analysis for GRIN Lens Synthesis with Enhanced Multi-Beam Radiations

Lizhao Song and Peiyuan Qin (University of Technology Sydney, Australia); Stefano Maci (University of Siena, Italy); Y. Jay Guo (University of Technology Sydney, Australia)
This paper presents a novel synthesis method for gradient-index (GRIN) lenses, aimed at supporting multiple beams with multiple focal points. Detailed numerical analyses of ray-path errors in the previously developed multi-beam synthesis method are provided. It is shown that the previous approach has limitations in designing lenses with arbitrary dimensions due to its assumption of linear, parallel ray paths within the lens. To overcome these limitations, a more accurate synthesis method is proposed, offering general formulas applicable to versatile lens profiles. To demonstrate the superiority of the new method, lens configurations from both synthesis approaches were investigated. The results indicate that the new method delivers more stable gains for all beams across a wide frequency band. Experimental validation was performed using a 3D-printed lens with seven independent beams, covering a wide angular range of ±44°, with measured gain drops less than 2.93 dB across the 12.3-19 GHz range.

16:30 Flat Lens Concept Using Multi-Axis Machining for D-Band Core-Shell Lens-In-Package Integration

Nick van Rooijen, Maria Alonso-delPino and Nuria LLombart (Delft University of Technology, The Netherlands)
This work introduces a novel electrically-small flat-lens design based on an earlier presented spherical core-shell lens concept. Holes are conformally machined inside a dielectric host material, creating two artificial dielectric layers. One layer is used for anti-reflection purposes, whereas the other is used to convert the spherical interface to a flat interface, to improve ease-of-integration. The designed core lens is very compact, with height of only 2.2mm and diameter of 6mm, small enough to fit in many integrated circuit packages. The design was simulated and compared to the spherical core lens, with only negligible performance degradation in pattern quality and return loss.

16:50 High-Gain Dielectric Lens Antenna Fed by Circular Dielectric Waveguide for Applications in D-Band

Abhijit Pal, Debrina Dutta and Martin Schneider (University of Bremen, Germany)
This paper illustrates the design of a high-gain dielectric lens antenna that is fed by a circular dielectric waveguide (CDWG) in the frequency range of 115-130 GHz. A 1.75 mm diameter CDWG is used to feed the lens antenna. The paper analyses the different parameters of the lens antenna and how the gain is effected by the individual parameters. Two lenses made up of different materials, High Density Polyethylene (HDPE) and Polytetrafluorethylen (PTFE), are fabricated and measured. The matching is measured with a calibrated VNA and all antennas have a return loss greater than 17 dB throughout the design range. The gain measurements are taken using a three-antenna gain method with the help of two D-band pyramidal horn antennas. A measured gain between 20.5 and 22.5 dBi is observed for all the lens antennas. A good accordance to simulation is also observed.

17:10 On the Design of a Single Layer Wide-Scanning Lens with PCB Integrated Segmented Focal Array at 26.125 GHz

Dunja Lončarević, Huasheng Zhang, Andrea Neto and Nuria LLombart (Delft University of Technology, The Netherlands)
This paper presents the design of a low-cost, highly directive single-layer lens antenna capable of multibeam wide-angle scanning, featuring a segmented focal array (FA) and a PCB-integrated dual-polarized leaky wave (LW) feed. The design starts by analyzing an extended hemispherical lens. HDPE is chosen as the lens material due to its significantly lower ohmic losses compared to higher permittivity materials for a lens with a large diameter. The lens scanning performance with a curved FA is evaluated, and a dual-polarized leaky wave antenna is selected as the feed. This achieves low reflection and minimal inter-element coupling for a 3 dB beam overlap spacing. To simplify fabrication, the curved FA is replaced with a segmented FA of five panels, meeting the design goals.

Room: Hallén (BAR5)

CS12 Electromagnetic beams in near-field applications: from microwaves to optics

T08 Fundamental research and emerging technologies/processes / Convened Session / Antennas

Chairs: Walter Fuscaldo (Consiglio Nazionale delle Ricerche (CNR), Italy), Santi Concetto Pavone (Università degli Studi di Catania, Italy)

15:50 Transition from Near-Field to Far-Field Region in Nondiffractive Beams

Stella Ventucci and Edoardo Negri (Sapienza University of Rome, Italy); Walter Fuscaldo (Consiglio Nazionale delle Ricerche (CNR), Italy); Paolo Burghignoli and Alessandro Galli (Sapienza University of Rome, Italy)
The generation of nondiffractive beams has been widely investigated in recent years due to their intriguing properties in terms of focusing, limited diffraction, and self-healing features. However, the behavior of such beams as they transition from the near-field to the far-field region has been overlooked. For this reason, the evolution of a Bessel-beam distribution from near- to far-field distances from the aperture plane has been investigated in this work. In particular, a resonant Bessel-beam launcher is here studied through a leaky-wave approach, providing the first fully vectorial analysis of a Bessel-beam near- to far-field transition.

16:10 Metasurface Antennas Radiating Quasi-Bessel Beams for Near-Field Applications

Ravel C M Pimenta (Aix-Marseille Université, France); Konstantinos D. Paschaloudis (Université de Rennes, CNRS, IETR, France); Matthieu Bertrand (Thales Research and Technology, France); David González-Ovejero (Université de Rennes, France); Gabriel Soriano (Aix-Marseille University, France); Myriam Zerrad (Aix-Marseille Université, France); Claude Amra (CNRS & Aix Marseille University, France); Mauro Ettorre (Michigan State University, Electrical and Computer Engineering, USA)
In this work, we present two distinct metasurface antenna designs operating at 30 GHz, aimed at generating quasi-Bessel beams with non-diffractive ranges reaching up to several hundred wavelengths. The first antenna is a meta-axicon transmitter, consisting of a horn antenna coupled with a 3D-printed dielectric metasurface. The second design involves a printed metasurface launcher, excited by a coaxial pin. Numerical simulations of both configurations demonstrate highly efficient beam generation and beam integrity over significant propagation distances.

THURSDAY

16:30 Optimal Apertures for Wireless Links in the Radiative near Field

Faris Alsolamy (University of Michigan Ann Arbor, USA); Anthony Grbic (University of Michigan, Ann Arbor, USA)
Traditional beams, such as Gaussian and Bessel beams, are commonly used in the design of wireless links in the near field. However, these beams are generally suboptimal for linking apertures at such standoff distances. To overcome this limitation, we propose the use of engineered quasi-bound states in the continuum (quasi-BICs) to design wireless links in the near field. We theoretically show that these quasi-BICs are optimal. A general design procedure is presented, starting with the identification of quasi-BICs for a given wireless link, and concluding with the design of a metasurface antenna that can transmit and receive the identified quasi-BICs. A design example at 30 GHz is presented to illustrate the design procedure.

16:50 From Gaussian to High-Order Laguerre-Gauss Beam Shaping in GRIN Multimode Fiber

Wasyhun A. Gemechu (Sapienza University of Rome, Italy); Mario Ferraro (University of Calabria, Italy); Daniele Modotto (Università di Brescia, Brescia, Italy); Umberto Minoni (Università di Brescia, Italy); Fabrizio Frezza, Stefan Wabnitz and Fabio Mangini (Sapienza University of Rome, Italy)
We present our findings on the direct conversion of a Gaussian-like laser beam, which was initially injected into the cladding of a graded-index multimode fiber, into a high-order Laguerre-Gauss mode within the core of the fiber

17:10 Design of an Inhomogeneous Lens for Bessel Beam Generation at Ka-Band

Ilir Gashi and Matteo Albani (University of Siena, Italy); Ronan Sauleau (University of Rennes 1, France); David González-Ovejero (Université de Rennes, France)
This paper presents the design of a Bessel beam launcher that integrates a Marié transducer with a telescopic lens at Ka-band frequencies. The Marié transducer, fed by a WR-28 rectangular waveguide, converts rectangular waveguide transverse electric (TE) TE10 mode into a circular waveguide TE01 mode at its output. A telescopic lens, designed to magnify the impinging field, is then placed atop the transducer to extend the non-diffractive range. The combined setup is described in detail, and full-wave simulation results demonstrate the effectiveness of the proposed design. The launcher achieves a fractional bandwidth of 25% and a non diffractive range of 200 mm, providing a reliable solution for near-field communication systems.

Room: Marcuvitz (M3) | **E03 - Computational and numerical techniques II**

T07 Electromagnetic modelling and simulation tools / / Electromagnetics

Chairs: Matthys M. Botha (Stellenbosch University, South Africa), Dirk Manteuffel (University of Hannover, Germany)

15:50 Deembedding and Optimization of a Decoupling Structure Using a Modal Coupling Matrix

Leonardo Mörlein (Leibniz Universität Hannover, Germany); Philipp Gentner (Ericsson Antenna Technology Germany GmbH, Germany); Dirk Manteuffel (University of Hannover, Germany)
A workflow to optimize a decoupling structure that is placed between the transmit and receive subarray of a monostatic sensing array is presented. A modal coupling model based on generalized scattering matrices in terms of characteristic modes is used to deembedd the decoupling elements from their environment. Based on this model, an iterative workflow for the optimization of the elements is derived. To represent the degrees of freedom during the design of the decoupling elements, the modal scattering behavior of the decoupling elements is synthetically modified in the model. The manopt toolbox is used to find the optimal configuration of the decoupling elements using an approximate model and full-wave simulations are only used sparingly to obtain accurate results, which reduces the simulation time to find optimal results. The finally obtained decoupling structure shows a reduction of the coupling by 17 dB.

16:10 Impedance Calculations for Wire Antenna Modelling with Macro Basis Functions

William Dommisse and Matthys M. Botha (Stellenbosch University, South Africa); Thomas Rylander (Chalmers University of Technology, Sweden)
This paper concerns the accurate calculation of wire port impedance using the method of moments (MoM) together with a macro basis function (MBF) discretisation scheme tailored to wire current modelling. The MBFs incorporate circumferential current components and variations, aiming to achieve accuracy comparable to that of general surface MoM modelling while requiring fewer degrees of freedom. The excitation is modelled using a magnetic frill source, consistent with the MBF framework. Results for a monopole antenna show that the frill functions well together with the MBFs and that it yields more stable impedance calculations than the widely-used delta-gap source.

16:30 Modeling and Analyses of Transparent Antennas on Vehicles

Ozgur Eris (Middle East Technical University, Turkey); Mehmet Emre Eralp (Middle East Technical University & Accelerate Simulation Technologies, Turkey); Lale Alatan (METU, Turkey); Ozlem Aydin Civi and Ozgur Ergul (Middle East Technical University, Turkey)

This paper presents accurate and efficient analyses of transparent antennas near platforms. Various numerical electromagnetic simulation tools are investigated during analyses of antennas mounted on platforms. The simulation environment developed in this work utilizes the equivalent source (ES) representations, and employs surface integral equation-based solutions accelerated by multilevel fast multipole algorithm to model interactions between antennas and vehicles, focusing on the impact of placements. The tool demonstrates remarkable performance compared to commercial tools and enables realistic simulations of transparent antennas on actual vehicle windshields. This facilitates more effective performance assessments and optimizations of antenna orientations and placements.

16:50 Dynamic Ray-Tracing for RF Propagation and Scattering in Hypersonic Plasmas

Andrea Scarabosio (LINKS Foundation, Italy); Salvatore Esposito, Domenic D Ambrosio and Giuseppe Vecchi (Politecnico di Torino, Italy)

Hypersonic flight regime is conventionally defined for Mach>5; in these conditions, the flying object becomes enveloped in a plasma. We present an update of our hybrid scheme \cite{ScarabosioTAP2022} for radio frequency propagation in complex media as a plasma. As an inhomogeneous media, the typical hypersonic plasma induces strong refraction but also complete reflection at the boundary with negative refractive index regions. The EM field presents caustics and the degree of inhomogeneity often exceed the condition of smooth varying media, a basic assumption in the asymptotic analysis. These physical features decrease the accuracy and applicability of standard ray-tracing methods. We extend our model using paraxial ray theory to improve caustics detection and phase shift correction. We also introduce special boundary layers or interfaces to approximately cope with extreme inhomogeneous regions. We show that the new algorithm provides higher fidelity results by comparing with full-wave calculations in presence of hypersonic plasma backgrounds

17:10 Hybrid Method for Optimizing Radiation of Implantable Antennas in Diverse Scenarios

Jakub Liška and Lukas Jelinek (Czech Technical University in Prague, Czech Republic); Mingxiang Gao (EPFL, Switzerland & IT'IS Foundation, Switzerland); Miloslav Capek (Czech Technical University in Prague, Czech Republic); Anja K. Skrivervik (EPFL, Switzerland)

This paper presents a combination of three computational methods in a hybrid approach designed to model the radiation of antennas within arbitrarily shaped capsules implanted in a host body. A surface method of moments is employed to represent the radiation source, offering the advantage of a low number of unknowns, as well as enabling performance limitation evaluation and topology optimization. The volumetric method of moments is then applied to model the antenna's surroundings, including its encapsulation. To reduce the use of the more computationally demanding volumetric method of moments, a vector spherical vector wave expansion is used to describe the host body, minimizing computational complexity.

Room: Björk (33)

EurAPP Working Groups

WG Active Array Antennas

Room: Bergman (34)

Scientific Workshop

SW11 The 1924 2.2 km electrically small Grimeton VLF antenna

Room: Felsen (35+36)

P10 - Propagation for body network and bio applications

T06 Biomedical and health / / Propagation

Chairs: Hadeel Elayan (Northeastern University, USA), Declan O'Loughlin (Trinity College Dublin, Ireland)

15:50 Optimization of the Monitoring Procedure for Determining the Ablation Zone in Ex-Vivo Bovine Liver

Mohamed Lamhamdi (University of Applied Science RheinMain, Germany); Ali Esmaeili (RheinMain University of Appilied Science, Germany); Georg Rose (OVGU, Germany); Holger Maune (University of Magdeburg, Germany); Andreas Brensing (Hochschule RheinMain, Germany); Bernd Schweizer and Mohamed El Hadidy (RheinMain University of Applied Sciences, Germany); Dana Jabali and David-Jonas Bader (Hochschule RheinMain, Germany)

This work presents optimization studies for a novel microwave ablation zone monitoring concept based on phase-shift measurements. Several ablations are carried out on ex-vivo bovine liver with a power of 50 W and an ablation time of 10 minutes. The previous research status was that the ablation zone with the novel method could be predicted reproducibly, but with a mean deviation of 70.2% and a standard deviation of 4.1%. The results from this work show that the ablation zone can now be predicted with a mean deviation of 16.8% and a standard deviation of 5.6%.

16:10 Near-Field Intra-Body Optical Communication: Leveraging the Power of Bessel Beam

Hadeel Elayan (Northeastern University, USA); Josep M Jornet (Northeastern University & Institute for the Wireless Internet of Things, USA)

This work explores the use of Bessel beams as a solution for near-field optical intra-body communication. Bessel beams possess unique non-diffracting and self-healing properties, making them superior to traditional Gaussian beams in maintaining intensity through complex biological environments. In this paper, we introduce the concept of near-field intra-body optical communication and the conditions under which it occurs. We propose a system that employs optical nanoantenna arrays to generate Bessel beams at a wavelength of 1550 nm, which falls within the biological transparency window. The system model, along with the corresponding mathematical formulation, is presented in detail. Our results offer a comparison of the propagation characteristics of Bessel and Gaussian beams in intra-body contexts, emphasizing the impact of near-field effects in enhancing spatial resolution at the sub-cellular level.

16:30 Assessment of the Representativeness of Numerical Subjects for the WBAN Indoor Channel Modeling

Badre Youssef (Thales & Télécom ParisTech-Institut Mines-Télécom LTCI, France); Christophe Roblin (Telecom Paris - Institut Polytechnique de Paris & LTCI - Institut Mines-Télécom, France)

WBAN peculiarities can be summed up in two points: firstly, the high number of sources of variability, i.e. the subject, the antennas, the frequency; secondly the strong electromagnetic disturbance of the human body. Concerning the subject, there are two aspects that can be considered: the morphology and the dynamic. When this source of variability is considered in the channel modeling, the problem is the difficulty of obtaining a representative statistical sample. One solution would be to use numerical subject models. The purpose of this article is to assess the representativeness of this approach in the context of WBAN channel modeling, by comparing key channel parameters (the mean Path Loss of the on-body cluster (PL)^On and the surrounded antenna pattern) obtained from simulations results for different numerical subjects and experimentations performed with a whole body phantom. The results obtained are satisfactory, and validate the use of this approach.

16:50 Heat Focusing in Head and Neck Hyperthermia Considering Vessels Blood Flow

Maryam Firuzalizadeh (Politecnico di Torino, Italy); Rossella Gaffoglio (Fondazione LINKS, Italy); Giorgio Giordanengo and Marco Righero (LINKS Foundation, Italy); Marcello Zucchi (Politecnico di Torino, Italy); Giuseppe Musacchio Adorisio (Fondazione LINKS, Italy); Aurora Bellone, Alberto Vallan, Guido Perrone and Giuseppe Vecchi (Politecnico di Torino, Italy)

This paper investigates how blood flow in major vessels affects temperature distribution during hyperthermia treatments in the head and neck (H&N) region. To do this, we used an in-silico model and a physical phantom of the neck region where a silicon tube with flowing water was introduced to simulate the presence of the two jugular veins and two carotid arteries. The results show that temperature variations of more than 5°C can affect temperature simulations when the effect of blood flow is not considered. The achieved results were confirmed by temperature measurements performed using the physical phantom and a full-operating mock-up reproducing an hyperthermia treatment in the neck region.

17:10 A Preliminary Study on the Impact of Model Complexity in Classification in Breast Microwave Imaging

Ana Catarina Pelicano (Instituto de Biofísica e Engenharia Biomédica, Fac. Ciências Un. Lisboa & FCiencias ID, Portugal); Nuno Araújo (Centro de Física Teórica e Computacional, Fac. Ciências Un. Lisboa, Portugal); Daniela M. Godinho (Instituto de Biofísica e Engenharia Biomédica - Faculdade de Ciências - Universidade de Lisboa, Portugal); Raquel C. Conceição (Instituto de Biofísica e Engenharia Biomédica, Faculdade de Ciências, Universidade de Lisboa, Portugal)

This study investigates the capability of microwave signals to classify benign and malignant breast tumours. The novelty of this study lies in the anatomically and dielectrically accurate breast tissue models - including tumours - used in the simulations, in multiple scenarios with different tissue types (fat, fibroglandular, skin, and muscle) and varying heterogeneity. Principal Components Analysis (PCA) was applied as a Feature Extraction Method (FEM), and Support Vector Machines (SVM) for the classification. Key metrics including accuracy, sensitivity, specificity, F1 score, and Matthews Correlation Coefficient (MCC), assessed each antenna's diagnostic capability and the combined performance across all antennas. Results suggested that combining classifications from all antennas via majority voting improved accuracy, while tumour classification was unaffected by tissue heterogeneity. Increasing model complexity did not impact SVM performance except when muscle tissue was added, slightly reducing the diagnostic performance.

THURSDAY

15:50 Efficient Incorporation of Normal Susceptibilities into Implicit IE-GSTC Metasurface Forward Solver

Mario Phaneuf and Puyan Mojabi (University of Manitoba, Canada)
The generalized sheet transition conditions (GSTCs) are combined with integral equations (IE) in order to efficiently compute the scattering response of metasurfaces that exhibit both tangential and normal polarization responses. To this end, a particular form of IE-GSTC method, known as the implicit IE-GSTC solver, is employed and augmented to incorporate both tangential and normal susceptibilities. This augmented solver offers two key benefits. First, it maintains the same computational complexity as the equivalent solver that only considers the tangential polarization response. Second, it establishes a mapping between metasurface models with tangential and normal susceptibilities and non-local metasurface models solely characterized by tangential properties. This offers valuable insights into the behavior and design of non-local metasurface structures.

16:10 Modelling Fully-Dielectric Metamaterial at 90GHz for Applications in the Sub-THz Band

Miguel Angel Balmaseda-Marquez and Carlos Molero (University of Granada, Spain); Angel Palomares-Caballero (IETR-INSA Rennes, France); Guido Valerio (Sorbonne Université, France); Pablo Padilla (University of Granada, Spain); Juan Valenzuela-Valdés (Universidad de Granada, Spain)
This study introduces a novel semi-analytical circuit model for the comprehensive characterization of dielectric unit cells comprising T-shaped blocks, providing an alternative to conventional methods like the effective medium theory. By employing a fitting strategy, the model offers an in-depth understanding of the unit cell properties. The proposed semi-analytical approach exhibits very good agreement with the scattering parameters derived from full-wave simulations. Moreover, by varying the dielectric material, the model accurately captures the diverse behaviors of unit cells with different permittivities and electrical dimensions. As a practical application, transmitarrays designed to generate orbital angular momentum (OAM) waves were fabricated using 3D printing. Simulated results show favorable performance across multiple OAM modes at 85 GHz.

16:30 High Performance Metasurface for Multi-Directional Beam Steering in mm-Wave Frequency Applications

Jibran Zahoor ahmad Pandit (Univ Gustave Eiffel, France); Mohammed Kalaagi (Institut de Recherche Technologique Railenium, Famars, France & Railenium, France); Divitha Seetharamdoo (Univ Gustave Eiffel COSYS LEOST Univ Lille Nord de France & Univ Lille Nord de France, France); Caroline Maye (Univ Gustave Eiffel, France)
In this paper, we propose a highly efficient multi-directional beam steering (MDBS) metasurface for the 28 GHz mm- Wave band, designed using a high periodicity supercell (5.76λ) and surface impedance modulation (SIM). The MDBS metasurface follows the generalized phase law of reflection and achieves eleven distinct beam steering directions with high reflection efficiencies of 98.26% for TE mode and 93.04% for TM mode. The design is polarization-independent and functions for various incident angles simultaneously, making it a robust solution for extending 5G coverage in non-line-of-sight (NLoS) scenarios. The performance of the proposed metasurface is validated through both full-wave simulations and experimental measurements, demonstrating its capability as an efficient, compact, and scalable solution for next-generation mm-Wave communication systems.

16:50 Evaluating the Bessel Characteristics of a Curved Beam in Near- and Far-Field Regions

Narimane awada Mislmani (University of Gustave Eiffel & IFSTTAR-LEOST, France); Divitha Seetharamdoo (Univ Gustave Eiffel COSYS LEOST Univ Lille Nord de France & Univ Lille Nord de France, France)
This paper presents a curved beam generated by a metasurface operating in the ITS-G5 frequency band, categorized as a hybrid Bessel beam. The beam is designed to improve communication in complex metallic environments, such as toll stations. Therefore, evaluating its properties is essential to confirm its classification as a non-diffractive beam, known for resistance to diffraction and self-healing capabilities, both of which are demonstrated here. Near- and far-field analyses confirm the ability of the metasurface to efficiently bend electromagnetic waves, providing enhanced connectivity solutions for automated vehicle communication systems in challenging environments.

17:10 Approaching Fundamental Limits on Bandwidth-To-Thickness Ratio for Electrically Thin Absorbers Through Dispersion Engineering

Pardha Sourya Nayani, Morteza Moradi and Younes Radi (Syracuse University, USA)
Electrically thin layers for perfect electromagnetic wave absorption are essential in applications from radio to optical frequencies, such as stealth and energy harvesting. There is a growing demand for thinner layers with higher absorption bandwidths, but an upper theoretical limit exists for the bandwidth-to-thickness ratio in passive, linear time-invariant (LTI) metal-backed absorbers. Current designs, regardless of frequency or thickness, fall short of this limit and fail to fully utilize the potential of LTI systems. Here, we introduce a new concept for designing passive ultra-thin metal-backed absorbers that can enable absorbing layers with the highest bandwidth-to-thickness ratio ever reported in the literature and can be several-fold higher compared to the absorbers designed based on conventional approaches. Absorbers designed on proposed concept can achieve bandwidth-to-thickness ratio approaching this theoretical limit. Using the proposed concept, we have designed and experimentally validated an absorber that demonstrates excellent agreement with the theoretical framework presented.

THURSDAY

T07 Electromagnetic modelling and simulation tools / Convened Session / Measurements

Chairs: Olav Breinbjerg (ElMaReCo, Denmark), Janet O'Neil (ETS-Lindgren, USA)

15:50 Applications of Iterative Matrix Inversion in near to Far Field Transformation Algorithms

Manuel Sierra-Castañer (Universidad Politécnica de Madrid, Spain); Fernando Rodríguez Varela (Universidad Rey Juan Carlos de Madrid, Spain); Belén Galocha Iragüen (Universidad Politécnica de Madrid, Spain)

Near-field to far-field transformations constitute a powerful antenna characterization technique for antenna measurement. In this paper applications for near-field to far-field transformations are introduced. In all these cases, iterative matrix inversion is used to retrieve the antenna spherical wave expansion, instead of the FFT based classical solution. This technique is more time consuming, but thanks to the development of the computing capabilities their advantages can be exploited, allowing some degrees of freedom in the resolution of the electromagnetic problem. The examples and applications shown in this paper are the following ones: the first technique is a multilevel spherical wave expansion that allows to reduce the processing time and process measurements in irregular grids. The second one is a technique used for reducing the number of measurement points for specific antennas with some symmetries. The third application allows the reduction of measurement samples for offset-mounted antennas, applied to automotive scenarios.

16:10 Advancements in Compressed Sensing for Antenna Far-Field Gain Calibration in an Extrapolation Range

Zhong Chen and Yibo Wang (ETS-Lindgren, USA); Jason Coder (National Institute of Standards and Technology, USA)

In this study, we apply Compressed Sensing (CS) for extrapolation calibration of high-gain aperture antennas. In earlier work, we successfully applied CS to dipole antennas. Dipoles show significant components related to chamber reflections but lack the third-order component observed in horn antennas, which arises from strong multipath interactions. This third-order component leads to sparser k-space data, making them well-suited for CS recovery. CS effectively recovers key spectral coefficients while dramatically reducing the amount of data required. Horn antennas also exhibit stronger near-field effects compared to dipoles, resulting in significant curvature in the response even after normalization by 1/r. This can lead to pronounced edge effects after filtering. We introduce a novel normalization process that detrends the raw data, effectively reducing edge artifacts. Our method demonstrates that CS can achieve accurate far-field gain extrapolation using as little as 8% of the original data, significantly reducing test time while maintaining calibration accuracy.

16:30 2019-2022 ESA-EurAAP Facility Comparison Campaign with the DTU-ESA mm-VAST Antenna - Reference Pattern at 19.76 GHz

Javier Fernández Álvarez, Jeppe Nielsen, Samel Arslanagić and Michael Mattes (Technical University of Denmark, Denmark); Ines Barbary (ESA-ESTEC, The Netherlands); Luis Rolo (European Space Agency, ESTEC, The Netherlands)

The 2019-2022 ESA-EurAAP Facility Comparison Campaign with the DTU-ESA mm-VAST antenna has involved 10 European institutions and 11 spherical near-field and compact range measurement facilities. The mm-VAST antenna, specifically designed as a reference antenna, is employed in three operational configurations at 19.76 GHz, 37.80 GHz, and 48.16 GHz, including both linear and circular polarization. This work presents the final results of the campaign for the first studied configuration, at 19.76 GHz and linear polarization. The presented results comprise the measurements received during the course campaign, as well as a comparison in terms of several metrics. From these measurements, an aggregated pattern is created as a weighted average of the received measurements. This averaged pattern is considered the new reference pattern of the mm-VAST in the 19.76 GHz configuration.

16:50 Partial Characterization of Aperture Antennas in Planar Near-Field Scanning

Amedeo Capozzoli, Claudio Curcio and Angelo Liseno (Università di Napoli Federico II, Italy)

In the framework of the near-field antenna characterization, in some applications, it can be of interest to retrieve the Far-Field pattern just along some cuts. A Partial Characterization method is a technique able to reconstruct the pattern along the cut of interest starting from a proper set of near-field data. A Partial Characterization method has been proposed. The approach is able to determine the optimal distribution of the near-field samples needed for the characterization. In this paper the method is presented and its main characteristics analyzed. Furthermore, experimental results are reported to show the performance of the approach against real data.

17:10 Synthesis and Validation of Wideband Excitation Coefficients in Plane Wave Generator Systems

Francesco Saccardi (Microwave Vision Italy, Italy); Andrea Giacomini (Microwave Vision Italy SRL, Italy); Vincenzo Schirosi (MICROWAVE VISION ITALY, Italy); Lars Foged (Microwave Vision Italy, Italy); Nicolas Gross (MVG Industries, France); Shoaib Anwar (Microwave Vision Group, Satimo Industries, France); Evgueni Kaverine (MVG Industries, France); Edward Szpindor (MVG-Orbit/FR, Inc, USA); Tom Mckeown (MVG Orbit Advanced Technologies Inc., USA)

Plane Wave Generators are arrays of elements arranged and excited to approximate a plane wave, creating far-field conditions within a Quiet Zone in the near-field proximity of the array. Thanks to its compact design, the PWG offers closer approximation to far-field conditions compared to equivalently sized Compact Antenna Test Range systems. However, the discrete sampling by the array elements of the PWG's radiating aperture constitutes a limit to the obtainable electrical size of the QZ. Consequently, PWGs are commonly used in lower-frequency measurement applications, such as UHF/VHF. Although PWGs have recently attracted significant attention, including wideband testing, the array excitation has typically been addressed at discrete frequencies. In this paper, we focus on the synthesis of excitation coefficients valid across a decade bandwidth, enabling the system to support wideband signal testing. The wideband coefficients are experimentally validated on a low-frequency PWG array, demonstrating the system's capability for effective wideband measurements.

Room: Oliner (C3) — A15 Developments in Antenna Design for space applications

T03 Aerospace, space and non-terrestrial networks / / Antennas

Chairs: Arvind Kumar (Dept of ECE,. Visvesvaraya National Institute of Technology Nagpur India, India), Sergio Matos (ISCTE-IUL / Instituto de Telecomunicações, Portugal)

15:50 Design of a Dual-Band Dual-Polarized Choke-Ring Horn Antenna for TT&C Applications in Ka-Band

Charalampos Stoumpos, Nelson Fonseca, Grégory Branger, Quentin Lamotte and Maxime Romier (Anywaves, France); Nicolas Capet (ANYWAVES FRANCE, France)

The design of a dual-band dual-polarized choke-ring horn antenna for Low Earth Orbit (LEO) Telemetry, Tracking and Control (TT&C) satellite applications in Ka-band is reported here. The antenna comprises an input circular waveguide as the primary feed where two topologies are explored with quad- and hexa-ridged cross-sections. The optimization has been performed using commercially available software. The obtained simulation results of the latter solution indicate a significant improvement on the RF performance. A preliminary design of the proposed dual-band dual-polarized excitation network is also presented and discussed. The detailed design of the complete antenna is on-going in the frame of an ESA funded activity and preliminary results will be presented during the conference.

16:10 A Planar Lens Antenna for Conical Scanning at Ka-Band, Using a Feeding Array with Optimized Amplitude and Phase Coefficients

Alexandra Mavropoulou (Delft University of Technology, The Netherlands); Aurélien Neuhart (European Space Agency (ESA-ESTEC), The Netherlands); Erio Gandini (ESA - European Space Agency, The Netherlands)

Conical scanning instruments on-board Earth observation satellites typically rely on mechanical spinning of the entire radiating architecture to acquire the conical beam sweep, significantly increasing their mass and risk of failure. In this work, a planar lens, illuminated by a passive array successively excited along a focal ring, is proposed as an alternative solution that eliminates the mechanical movement of the radiating aperture. The amplitude and phase coefficients of the array elements are optimized to correct for aberrations introduced due to the rotational symmetry of the primary component. To demonstrate the antenna concept, an array-fed planar lens, with a primary diameter of 30 cm is designed to operate at Ka-band (35.5 GHz) for conical scanning towards θ=25deg., demonstrating an aperture efficiency of 57%, with side-lobe level of -19 dB and dielectric and conduction losses of 0.5 dB.

16:30 A Mechanical and RF Performance Trade-Off for a Deployable Conical Log Spiral Antenna for Spacecrafts

Lewis Raymond Williams (University of Oslo, Norway); Lars Erling Bråten (Norwegian Defence Research Establishment (FFI), Norway); Karina Hoel (FFI & University of Oslo, Norway); Bendik Sagsveen (FFI, Norway)

A parametric study on a constant conductor diameter conical log spiral antenna has been performed, providing data for a mechanical and radio frequency (RF) performance trade-off. The antenna is a deployable spring intended for use on spacecraft which will be compressed for launch and released once in orbit. The results show that with a decrease in antenna cone angle the directivity, axial ratio and front-to-back ratio are improved. The antenna impedance increased with decreased cone angle. A lower cone angle results in a larger exerted force upon the spacecraft during antenna deployment. Truncating the tips of the spirals in order to remove the stiffest portion of the spring results in a significant reduction of RF performance and bandwidth, it is thus not recommended as a viable solution.

THURSDAY

16:50 Scan Limitations of Open-Ended Ridged Waveguide Phased Array Antennas for Satellite Communication

Sören Harms (Thales Alenia Space, France & Eindhoven University of Technology, TNO Defense, Safety and Security, The Netherlands); Jean-Philippe Fraysse (Thales Alenia Space, France); Stefania Monni (TNO Defence Security and Safety, The Netherlands); Alessandro Garufo (TNO Defense Safety and Security, The Netherlands); Ulf Johannsen (Eindhoven University of Technology, The Netherlands)

Open-ended ridged waveguide phased array antennas (PAAs) are promising candidates for future low Earth orbit satellite communications. This paper analyzes the scan limitations regarding the active reflection coefficient (ARC) and the axial ratio (AR) of circular and hexagonal waveguide elements with three and six ridges for Ka-band satellite downlink applications. For the hexagonal waveguide element with six ridges, it is shown that the degradation of the ARC and the AR at high scan angles and frequencies can be related to the onset of higher Floquet modes, resulting in single-mode scan blindness associated with one of the two orthogonal fundamental modes of the waveguide that generate the circular polarization. Reducing the element periodicity to delay the onset of higher-order Floquet modes overcomes the single-mode scan blindness and meets the Ka-band satellite downlink AR requirements.

17:10 A Dual-Polarized Leaky Lens Antenna for Wideband Spectro-Polarimetric Observations

Shahab Oddin Dabironezare, Leon Olde Scholtenhuis and Louis Hendrik Marting (Delft University of Technology, The Netherlands); Alejandro Pascual Laguna (Centro de Astrobiología - CSIC, Spain); Jochem Baselmans and Kenichi Karatsu (SRON, The Netherlands)

In this contribution a dual polarized leaky lens antenna is designed for polarization sensitive Cosmic Microwave Background observations. The lens antenna can separate the incident radiation in two orthogonal polarizations with at least 15dB of polarization purity over an octave of bandwidth (135-270GHz). The proposed structure is connected by microstrip lines to two separate on-chip low resolution filter banks. Each filter is terminated into a Microwave Kinetic Inductance Detector to form a highly sensitive on-chip spectropolarimeter. The antenna feed, the lens element, and its wide band anti-reflection corrugations are discussed here. Cryogenic experimental verifications of the optical coupling and the complex beam patterns of the lens antenna is on-going.

Room: Kraus (C4) — CS50 - Advances in 2-D Leaky-Wave Antennas

T02 Millimetre wave and THz for terrestrial networks (5G/6G) / Convened Session / Antennas

Chairs: Paolo Baccarelli (Roma Tre University, Italy), Davide Comite (Sapienza University of Rome, Italy)

15:50 Multimodal Transfer Matrix Method to Calculate the Dispersion Diagram of Open Structures

Sergio Garcia-Martinez (Universidad Politécnica de Madrid, Spain); Federico Giusti (University of Siena, Italy); Francisco Mesa (University of Seville, Spain); Adrián Tamayo-Domínguez and Pablo Sanchez-Olivares (Universidad Politecnica de Madrid, Spain); Oscar Quevedo-Teruel (KTH Royal Institute of Technology, Sweden)

We demonstrate that the multimodal transfer-matrix method (MMTMM) can be used to compute the dispersion diagram of general 1-D open periodic structures. To prove this, we analyze corrugated metallic surfaces and strip gratings as benchmark structures that are often utilized in leaky-wave antennas. This method provides a means of obtaining the complex wavenumber of proper and improper leaky modes based on the multimodal transfer-matrix of a single unit cell, which can be obtained using commercial software. The MMTMM results are verified using the ad hoc method of moments for both structures. The applicability and reliability of the proposed method are demonstrated by the convergence of results when varying the number of modes employed in the MMTMM and the simulation parameters. The MMTMM has proved to be an accurate and reliable means for obtaining the leakage constant in general open periodic structures, avoiding the necessity of developing specific ad hoc methods.

16:10 Dielectric Leaky Wave Antenna for near Field Focusing

Nelson Castro (University Carlos III of Madrid, Spain); Francisco Pizarro (Pontificia Universidad Catolica de Valparaiso, Chile); Eva Rajo-Iglesias (University Carlos III of Madrid, Spain)

The use of a fully dielectric 3D-printed leaky wave antenna for near-field focusing is proposed. The design utilizes the advantages inherent to the manufacturing technique to achieve near-field focusing. Inspired by the well-known bull eye antenna, this version employs a substrate with embedded rings with variable permittivity to achieve radiation. The antenna's operational principle is validated through full-wave simulations.

16:30 Application of Frequency-Scanned Bull's-Eye Leaky-Wave for Conical Direction Finding

Alejandro Gil Martinez (Technical University of Cartagena Cartagena, Spain); Davide Comite (Sapienza University of Rome, Italy); Jose-Luis Gómez-Tornero (Polytechnic University of Cartagena, Spain)

We demonstrate the application of a 2-D Bull's-Eye (BE) leaky-wave antenna (LWA) for conical direction finding using the frequency scanning mechanism. In contrast to other 2-D LWAs of uniform or quasi-uniform nature, such as Fabry-Perot Antennas (FPAs), the BE-LWA has a periodic nature and therefore its radiation mechanism is based on a higher-order space harmonic. As a result, both the backward-scanning and forward-scanning bands can be used to increase the direction finding performance. This is demonstrated with theoretical results using a printed-circuit BE LWA operating in the frequency band from 14 GHz to 32 GHz.

16:50 Self-Dual Modulated Metasurface Apertures for Dual-Polarized Antennas

Marceau Bouchez (University of Rennes, France); Stefano Maci (University of Siena, Italy); David González-Ovejero (Université de Rennes, France)

This paper reports a new structure that enables dual-polarized radiation using aperture antennas made of modulated metasurface planes. The desired dual-polarized radiation is achieved by exciting two orthogonally polarized and phase-matched modes within a self-dual impedance plane. To accomplish this, we tailor the dispersion characteristics of the first two higher-order transverse magnetic (TM) and transverse electric (TE) modes in the dielectric slab. The paper explores the dual-polarization radiation properties for both one-dimensional reactance modulation, for frequency scanning, and two-dimensional concentric modulations that yield a broadside beam. The latter exhibits a relatively broad bandwidth with a good aperture efficiency. Additionally, key fabrication considerations are briefly addressed.

17:10 Active Standing Wave Antenna Oscillator at Exceptional Point with Discrete Nonlinear Gain

Filippo Capolino (University of California, Irvine, USA); Alireza Nikzamir (University of California Irvine, USA)

Within a periodically loaded waveguide made of discrete nonlinear gain and radiating elements, an oscillator array tends to operate at an exceptional point of degeneracy (EPD). Relying on the concept of EPDs, we show that there is a great synchronization regime with a stable oscillation frequency, leading to a notable increase in distributed radiating power. The system consistently maintains a steady-state degenerate mode of oscillation, even with nonuniform small-signal nonlinear gain or array admittance values along the array. Importantly, we show the independence of the oscillation frequency with array length, and compare it with conventional one-dimensional cavity resonance. Furthermore, our demonstration highlights that nonuniform gain across the structure yields consistent oscillation frequency and uniform power radiation from the arrays. These findings hold significant implications for high-power radiating arrays incorporating distributed active elements.

Room: Munch (23)

EurAPP Working Groups

WG Education

Room: Ørsted (24+25)

A23 Antennas for identification and localization

T04 RF sensing for automotive, security, IoT, and other applications / / Antennas

Chairs: Stefan Lindenmeier (Universität der Bundeswehr, Germany), Adam Narbudowicz (Tyndall National Institute, Ireland & Wroclaw University of Science and Technology, Poland)

15:50 Agile Target Localization via Time-Modulation

Tommaso Tiberi (University of Bologna, Italy); Lorenzo Bastia and Enrico Fazzini (Università di Bologna, Italy); Alessandra Costanzo (DEI, University of Bologna, Italy); Diego Masotti (University of Bologna, Italy)

This work proposes a novel method for target localization based on Time-Modulated Arrays. The real-time control of the unparalleled multi-harmonic patterns is of strategic importance and allows to build a unique correspondence between observation direction and harmonics power levels. Two localization algorithms based on the power ratio between the first-order harmonic and the carrier frequency are presented. A radial multi-spoke array at 2.45 GHz has been used as time-modulated radiator for this purpose. The numerical analysis is supported by measurements results that validate the effectiveness of the time modulated array technology for localization purposes.

16:10 Double Director Frame for Easy Beam Forming of Circular Polarized Dual L-Band Antennas

Maximilian Holzner and Azat Meredov (Universität der Bundeswehr München, Germany); Stefan Lindenmeier (Universität der Bundeswehr, Germany)

In this paper a passive double director frame for tilting the main beam direction of a circular polarized GNSS antenna is presented. By adding a dual-band capable simple metal frame as a module to an already existing circular polarized dual band antenna it can be used to operate in several beam forming operations. This enables the easy adaption of the antenna to various mounting positions on a car, airplane or on a satellite. It is shown, that an elevation tilt of 20 degrees and more of the main beam direction can be realized under the condition of correct adjustment in dimensions and positioning.

16:30 Millimeter-Wave Dual-Beam Scanning by Source Polarization Rotation for High-Power Applications

Mostafa O. Shady (Scientific Microwave Corporation, Canada); Mohamed Mamdouh M. Ali (Assiut University, Egypt); Khelifa Hettak (University of Quebec in Outaouais, Canada); Larbi Talbi (University of Quebec - Outaouais, Canada); Ahmed A Kishk (Concordia University, Canada)

A novel millimeter-wave (mmWave) dual-beam antenna system with azimuthal scanning capability through polarization rotation suited for high-power applications is presented. The antenna and feed network are designed using metallic waveguide technology to handle high power levels. A circular waveguide antenna, differentially fed through a 4-port junction, enables beam scanning in multiple directions. Quadrature hybrid couplers are integrated to introduce the necessary phase shift between inputs, ensuring complete angular coverage. The proposed compact structure operates efficiently across the 28-32 GHz band, achieving a good impedance match and an average gain of 5 dBi.

16:50 Practical Considerations of a Multi-Port Leaky-Wave Antenna Array for Direction Finding

David F Hardy, Keigan MacDonell and Shulabh Gupta (Carleton University, Canada)
An array of multi-port leaky-wave antennas (LWAs) for direction finding (DF) in the X-band is proposed based on a printed double-stub configuration. A (mathbf{3\times1}) array of two-port LWAs operating at 8 GHz is designed to achieve a coverage sector of about (mathbf{40\degree}) as an illustrative example. Using the beam-scanning property of periodic LWAs, the period of each antenna in the array is selected in such a way to be able to accurately estimate the angle of arrival (AoA) across this range. Full-wave simulations in Ansys HFSS are presented using a microstrip LWA on a FR4 substrate to demonstrate the direction finding capability. A received signal strength indicator (RSSI) approach is taken whereby the relative power measured at each port is compared with the radiation patterns of each antenna in the array to estimate the AoA. Practical considerations of the excitation source and power detector ICs are finally discussed.

17:10 Study of Virtual Spherical Modes for Multi-Target Angle of Arrival Estimation

Linta Antony (Trinity College Dublin, Ireland); Adam Narbudowicz (Tyndall National Institute, Ireland & Wroclaw University of Science and Technology, Poland)
Antennas capable of selectively synthesizing desired spherical modes offer a compact alternative to classical phased arrays, offering beamforming from a limited volume. This property makes them a good candidate for size- and weight-constrained platforms. In this paper we study the application of sparse sensing to such antennas, which allows the generation of additional virtual spherical modes for the receiver antenna. This expanding the system's degrees of freedom (DoF) and improving the accuracy of angle of arrival (AoA) estimation. By selecting optimized subsets of the original spherical modes, one can produce the same virtual mode set while reducing redundancy, leading to more efficient and accurate multi-target detection. The proposed approach demonstrates that compact multiport antennas can maintain high-resolution performance, offering an effective solution for AoA estimation in size-constrained applications.

Room: Mosig (26) — P07 mmWave channel characterization

T02 Millimetre wave and THz for terrestrial networks (5G/6G) / / Propagation

Chairs: Henrik Asplund (Ericsson Research, Ericsson AB, Sweden), Nektarios Moraitis (National Technical University of Athens & Institute of Communications and Computers Systems, Greece)

15:50 Ku-, Ka- and Q-Band Propagation Experiment in French Indies

Jean-Pascal Monvoisin (Office national d'études et de recherches aérospatiales, France); Laurent Castanet (ONERA, France); Laurent Féral (Office national d'études et de recherches aérospatiales, France)
Since January 2021 Office National d'Etudes et de Recherches Aérospatiales (ONERA) and Centre National d'Etudes Spatiales (CNES) are conducting a propagation experiment at Ku-, Ka- and Q-bands in Pointe-à-Pitre (French Indies) with the beacons of the Eutelsat GEO satellite E65WA. In this paper, first statistical results of this still on-going campaign are presented. More specifically, the annual and monthly experimental Complementary Cumulative Distribution Functions (CCDF) of rain attenuation at the three frequencies and of the rainfall rate are evaluated. Monthly rainfall amount is also presented. Comparisons with ITU-R Recommendations ITU-R P.618-14 (rain attenuation) and P.837-7 (rainfall rate) are also given.

16:10 Comparative Path Loss Measurements in Multiple Frequency Bands Between 0.8-37 GHz

Henrik Asplund (Ericsson Research, Ericsson AB, Sweden); Satyam Dwivedi (Ericsson Research, Sweden); Niklas Jalden (Ericsson, Sweden)
This paper describes a comprehensive set of path loss measurements that cover a wide range of frequencies in three different scenarios. It was found that the excess loss beyond free space path loss increases monotonically with frequency but at different rates in the three scenarios. The negligible increase of excess path loss with increasing frequency in the urban macrocell and urban microcell scenarios matches well with established channel models. However, in the suburban macrocell scenario the excess loss was found to increase more strongly with frequency up to 10 GHz but remained constant for frequencies above 10 GHz. This behavior may be due to frequency-dependent diffraction mechanisms playing a more pronounced role at lower frequencies in this scenario, while reflections and diffuse scattering with weak or no frequency dependence becoming the prominent propagation mechanism above 10 GHz.

16:30 Characterization of Millimeter Wave Propagation in Agricultural Environments

Carlos Julian Furnieles Chipagra, Julian Andres Castro Pardo, Diana Sofia Lopez Cardenas, Javier Enrique Arévalo Peña and Javier Leonardo Araque Quijano (Universidad Nacional de Colombia, Colombia)
This study describes the characterization of path losses in a tomato greenhouse at 60.48 GHz. The results show considerable losses due to the presence of vegetative strata and are compared with established propagation models, successfully describing the path loss behavior. These findings aim to support the deployment of 5G networks in agriculture, promoting fields like agro-IoT.

16:50 Mid-Band Propagation Measurements in Industrial Environments

Juha-Matti Johannes Runtti and Usman Tahir Virk (Keysight Technologies Finland Oy, Finland); Pekka Kyösti (Keysight Technologies & University of Oulu, Finland); Lassi Hentila (Keysight Technologies, Finland); Jukka Kyröläinen (Keysight Technologies Finland oy, Finland); Fengchun Zhang (Aalborg University, Denmark)

6G radio access architecture is envisioned to contain a network of short-range in-X subnetworks with enhanced capabilities to provide efficient and reliable wireless connectivity. Short-range communications in industrial environments are actively researched at the so-called mid-bands or FR3, e.g., in the EU SNS JU 6G-SHINE project. In this paper, we analyze omnidirectional radio channel measurements at 10-12 GHz frequency band to estimate large-scale channel characteristics including power-delay profile, delay spread, K-factor, and pathloss for 254 radio links measured in the Industrial Production Lab at Aalborg University, Denmark. Moreover, we perform a comparison of estimated parameters with those of the 3GPP Indoor Factory channel model.

17:10 Indoor Corridor Channel Measurements and Characterization in the Upper Mid-Band

Nektarios Moraitis (National Technical University of Athens & Institute of Communications and Computers Systems, Greece); Alexandros Rogaris, Ileana Popescu and Konstantina Nikita (National Technical University of Athens, Greece)

This paper presents a preliminary characterization of the indoor channel in the upper mid-band. Narrowband measurements are launched in corridors taking into consideration line-of-sight (LOS) and non-line-of-sight (NLOS) propagation scenarios at diverse frequencies between 7 and 20 GHz. The path loss, the shadow fading, and the K-factor properties of the channel are measured and assessed. According to the results, the measured path loss can be accurately forecasted by the Close-In (CI) empirical model. Simple linear relationships are delivered, tailored to characterize the path loss exponent, the shadow fading and the K-factor variation versus frequency. The latter parameter degrades linearly versus frequency exhibiting negative values in NLOS scenarios and at frequencies above 8 GHz.

Room: Collin (27) — A20 Mmwave antennas for radar and sensing applications

T05 Positioning, localization, identification & tracking / / Antennas

Chairs: Daniele Cavallo (Delft University of Technology, The Netherlands), Stefania Monni (TNO Defence Security and Safety, The Netherlands)

15:50 Liquid Crystal-Based Beam-Steering Antenna for 77GHz Automotive Radar Application

Rossella Gaffoglio (Fondazione LINKS, Italy); Giorgio Giordanengo (LINKS Foundation, Italy); Lucia Teodorani and Giuseppe Vecchi (Politecnico di Torino, Italy)

Leaky wave antennas (LWAs) are promising solutions for the next-generation of automotive radar systems at millimeter waves. This paper presents the design of a fixed-frequency 1D-scanning periodic LWA, based on the liquid crystal (LC) technology. This solution employs a substrate-integrated waveguide (SIW) structure and is designed to create a 2D compact array configuration. To decouple the planes of the SIW and allow the tuning of the LC layer, two thin cuts are introduced in the upper plane of the unit cell. The proposed structure allows the DC bias of the LC layer, and, at the same time, the lateral confinement of the RF field. Simulation of the 2D array structure obtained via alignment of the designed 1D-scanning LWA shows a steering range of 30° from broadside to backwards at 77 GHz, which results in an overall steering of 60° feeding the antenna at both ends.

16:10 A Slant-Polarized Coaxial Slot Array Antenna Based on Gap Waveguide MLW Technology for E-Band Applications

Reza Gheybi Zarnagh (University of Twente, The Netherlands); Abolfazl Haddadi (Gapwaves AB, Gothenburg, Sweden); Coen van de Ven (University of Twente & Gapwaves AB, Sweden); Andrés Alayón Glazunov (Linköping University, Sweden)

This paper presents the design of a coaxial slot array antenna based on gap waveguide multilayer waveguide (MLW) technology for E-Band applications. The proposed array consists of two subarrays in a 2 × 4 configuration, with each element designed to generate 45 ◦ slant polarization. The design features a five-layer structure, which enables slant polarization by progressively rotating the electric field orientation by 45 ◦ through intermediate cavities. The antenna achieves an impedance bandwidth of S11 < −10 dB from 75.8–81.8 GHz. With 8 radiating slots, the maximum achieved gain is 14.7 dBi.

16:30 Experimental Validation of 3D Printed GRIN Lens for mmWave Automotive Radar

Coen van de Ven (University of Twente & Gapwaves AB, Sweden); Abolfazl Haddadi (Gapwaves AB, Gothenburg, Sweden); Andrés Alayón Glazunov (Linköping University, Sweden)

This paper presents the experimental validation of a 3D-printed Gradient Index (GRIN) lens designed for automotive radar applications. Building on prior work that introduced the core lensing elements, this study utilizes a more cost-effective extrusion 3D printing method than the expensive stereolithography process. By employing a smaller unit cell design, simulation time was significantly reduced, enabling a global optimization routine. As a result, the half-power beam width (HPBW) was successfully increased from 50 deg to 139 deg by integrating the GRIN lens, demonstrating its potential to enhance radar performance.

16:50 Prototype of a 64-Element Phased Array Transmitter with Wide Axial Ratio Bandwidth and Beam-Width

Mei Qian (South China University of Technology, China); Hao Jiang (South China University of Technology & School of Electronic and Information Engineering, China); Shaowei Liao and Quan Xue (South China University of Technology, China)

This paper presents the design and implementation of a 64-element phased array transmitter, offering wide axial ratio (AR) bandwidth and beam-width. The radiating elements feature a symmetric arc-shaped feed structure, providing dual circular polarization to the antenna. The inclusion of a dual-layer metasurface structure on the top layer enhances the impedance bandwidth, ensuring compliance with communication standards (27.5-31 GHz), while notably expanding the 3-dB AR bandwidth and beam-width. Sixteen 8-channel beamforming integrated circuits (BFICs) enable independent control of amplitude and phase for the transmitter. Both simulation and experimental results validate the system's performance, demonstrating wideangle scanning capability, high cross-polarization discrimination, and a wide AR bandwidth (27.5-31 GHz) with a beamwidth of ±50°.

17:10 Dual-Polarized Low-Sidelobe Array Antenna Consisting of Power-Weighted Networks and Series-Fed Subarrays

Xin Cheng (Xi'An Jiaotong University, China); Xiaobo Liu, Jinlin Liu and Xiaoming Chen (Xi'an Jiaotong University, China)

A dual-polarized low sidelobe level monopulse array antenna consisting of two types of series-fed resonant slot antenna subarrays and partially corporate-fed networks has been designed. The optimized vertical polarization subarray exhibits significantly improved impedance bandwidth. Amplitude tapering between individual elements of the subarray, in conjunction with power-weighted feed networks, suppressed the sidelobe levels in both the xoz and yoz planes. Measurements indicate that the -10 dB impedance bandwidth at each port exceeds 10%, the sidelobe levels are below -19 dB, and the relative null-depths are less than -37 dB.

Thursday - 19:00-23:55

Place: Vasa Museum

Social Events

Conference Dinner at the Vasa Museum

You can guide yourself to the city hall using Google Maps in the following link: https://maps.app.goo.gl/Gn3eEBJuLoJ1XtMBA

End of Thursday, April 3rd

THURSDAY

Friday - 08:30-10:10

Room: Alfvén (A3+A4)

CS1a - Reconfigurable Intelligent Surfaces for Communication, Sensing and Computing

T08 Fundamental research and emerging technologies/processes / Convened Session / Electromagnetics

Chairs: Mohsen Khalily (University of Surrey & 5G Innovation Centre, Institute for Communication Systems (ICS), United Kingdom), Okan Yurduseven (Queen's University Belfast, United Kingdom)

8:30 Energy-Efficient Encoding by Measurement-Based Power Consumption Model for RIS-Assisted Communication Systems

Jian Sang, Xiao Li and Wankai Tang (Southeast University, China); Ertugrul Basar (Koc University, Turkey); Shi Jin (Southeast University, China)

Reconfigurable intelligent surfaces (RISs) with the capability of nearly passive beamforming, have recently sparked considerable interests. This paper presents an energy-efficient discrete phase encoding method for RIS-assisted communications, which utilizes a measurement-based RIS power consumption model and considers a trade-off between the power consumption and beamforming gain. Firstly, based on the beamforming gain and power consumption models, an energy-efficient encoding optimization problem under a quality-of-service constraint is formulated for RIS-assisted systems. Subsequently, inspired by the uniform phase quantization (UPQ), the non-uniform phase quantization (NUPQ) is proposed and explained. Following the guideline of NUPQ, a phase encoding method is proposed with a linear complexity, to effectively improve the RIS energy efficiency. The simulation results verify the more favorable performance of the proposed method in terms of the RIS power consumption and energy efficiency. Furthermore, a field trial at 35 GHz validates the application performance of the proposed method in real environment.

8:50 Demonstration of mm-Wave Smart Electromagnetic Skin for NOMA Communication in Near-Field

Álvaro Pendás-Recondo and Sergio Menéndez Feito (University of Oviedo, Spain); Álvaro F. Vaquero, Jesús López-Fernández, Rafael González Ayestarán and Marcos R. Pino (Universidad de Oviedo, Spain); Manuel Arrebola (Universidad Politécnica de Madrid, Spain)

In this work, we demonstrate the practical application of a passive Smart Electromagnetic Skin (SES) in a mmWave communication context. In the indoor scenario considered, a Base Station (BS) serves two users in the same time and frequency slot using Non-Orthogonal Multiple Access (NOMA) as the multiplexing strategy. One user is in the Line-of-Sight (LOS) of the BS, while the other is in its blind zone and receives coverage from the SES. The BS and SES operate at a central frequency of 24.45 GHz with a bandwidth of 400 MHz. The design and prototyping of the communication testbed are based on Software-Defined Radio (SDR). Provided results are based on channel power and over-the-air Symbol Error Rate (SER) measurements for various NOMA strategies and user positioning.

9:10 Optically Transparent Metasurface for Orbital Angular Momentum Beam Generation

Aakash Bansal and William Whittow (Loughborough University, United Kingdom)

This paper presents the design for an optically transparent transmissive 1-bit metasurface to generate an orbital angular momentum (OAM) beam of mode 1. A transparent acrylic sheet was used as the substrate along with a low sheet resistance (≈2.4 Ω/□) Indium Tin Oxide (ITO) film as a conductor. Their dielectric and conductor properties were characterized using split post and single post dielectric resonator, respectively. A 15 × 15 metasurface was designed in simulation, which when fed with a generic horn antenna to produce an OAM beam of mode 1 at 10.5 GHz in the boresight direction.

9:30 ML-Assisted RIS for ISAC Systems: Initial Results in the 6G Study Band

Tung Duy Phan, Quoc Duy Nguyen, Niklas Takanen, Nhan Nguyen and Markku Juntti (University of Oulu, Finland); Ping Jack Soh (University of Oulu & Katholieke Universiteit Leuven, Finland)

Integrated sensing and communication (ISAC) is essential for 6G networks to tackle spectrum congestion and meet rising demands for sensing and communication. While reconfigurable intelligent surfaces (RIS) improve ISAC performance, accurate channel state information (CSI) remains a challenge. This paper proposes a machine learning (ML) approach to estimate the angle of arrival (AoA) in RIS-aided systems. By training an ML model with 6G band data, RIS can predict AoA in different scenarios. For limited scanning, prediction errors are below 1 ◦ with 83.5% scanning reduction, and with added sensors, errors drop to 0.8 ◦ , offering practical insights for balancing AoA accuracy and system complexity.

9:50 Design and Optimization of Surface-Wave Enhanced Reflecting Metasurfaces Featuring Beamforming and Polarization Control

Tianke Qiu, Jean Louis Keyrouz, Vasileios G. Ataloglou and George V. Eleftheriades (University of Toronto, Canada)
Electromagnetic metasurfaces (MTSs) are typically modeled as passive, lossless, and purely reactive homogenized impedance sheets on dielectric substrates. In this paper, we present an overview of designing reflecting MTSs using the method of moments (MoM) with gradient-based optimization. The proposed MTSs consist of printed metallic patterns placed over a grounded dielectric slab, with the patterns modeled by impedance sheets, and the impedance values optimized through gradient-descent to achieve specific far-field (FF) power patterns or beamforming objectives. This beamforming/beamshaping capability is enabled utilizing auxiliary surface waves, without the need of any explicit gain or loss. Full-wave simulations of realistic copper structures are presented to validate the proposed design procedure, with measurements preformed for an one dimensional (1D) MTS. An example of a 2D MTS featuring polarization control is also presented.

Room: Kildal (A2)

CS18a - Emerging antenna technologies for satellite communications and applications

T03 Aerospace, space and non-terrestrial networks / Convened Session / Antennas

Chairs: Antonio Clemente (CEA-Leti, France), Thi Quynh Van Hoang (Thales Research & Technology, France)

8:30 Quasi-Optical Beamformer for Space Applications

Léonin Lassauce (Planexus, France); Jean-Philippe Fraysse (Thales Alenia Space, France); Romain Contreres (CNES, France); Mauro Ettorre (Michigan State University, Electrical and Computer Engineering, USA)
A new quasi-optical beamformer has been developed using multi-layer printed circuit board (PCB) technology for downlink Ka-band applications in LEO Satcom. This paper presents the design and experimental validation. The beamformer effectively controls phase and amplitude to feed a linear array of 28 elements, producing 23 independent beams across a ±56 ◦ field of view. It provides low side lobe levels and achieves beam crossovers better than 3.9 dB within the 17.3–20.2 GHz band. Additionally, it ensures non-dispersive scanning in the band. The input beam ports exhibit reflection coefficients better than −10 dB across the entire band, with cross couplings below −19 dB and total insertion losses of 12.5 dB for the beamformer.

8:50 Evaluation of the Beam-Scanning Performance of Curved Transmitarrays

Álvaro F. Vaquero (Universidad de Oviedo, Spain); Sergio Matos (ISCTE-IUL / Instituto de Telecomunicações, Portugal); André Arraiano (Instituto Telecomunicações, Instituto Superior Técnico, Portugal); Manuel Arrebola (Universidad Politécnica de Madrid, Spain); Joao M Felicio (Instituto de Telecomunicações, Instituto Superior Tecnico, Portugal); Jorge R. Costa (Instituto de Telecomunicações / ISCTE-IUL, Portugal); Carlos A. Fernandes (Instituto de Telecomunicacoes, Instituto Superior Tecnico, Portugal); Nelson Fonseca (3SPACE Innovation, Paris, France)
This work presents mechanical wide-angle beam steering antennas based on transmitarrays for mm-Wave communication systems. Elevation steering is achieved by translating the feeder, while azimuth scanning is done by rotating the transmitarray 360°. Traditional methods use planar surfaces and advanced techniques to enhance scan range. This study introduces a convex curved surface to improve performance by reducing scan loss at high tilt angles, achieving nearly 80° of scanning. It examines bifocal phase correction for curved surfaces and compares it with planar designs, emphasizing the benefits of the curved shape. A manufactured bifocal design demonstrates effective scan performance with minimal loss and sidelobe levels, showing that curved surfaces enhance performance beyond what analytical phase correction can achieve on planar surfaces.

9:10 Folded Transmitarray Antenna for Satcom Receivers at K-Band

Orestis Koutsos and Jorick Milbrandt (CEA Leti, France); Francesco Foglia Manzillo (CEA-LETI, France); Antonio Clemente (CEA-Leti, France)
This paper presents the design of a folded, reconfigurable transmitarray antenna operating at K-band. The chosen unit-cell is a 2-bit structure composed of linearly polarized patches and four p-i-n diodes. The antenna achieves switchable circular polarization by employing a random sequential rotation scheme of vertically and horizontally polarized patches in transmission. To reduce the focal distance by a factor of approximately 3 compared to standard illumination, a broadband reflecting polarization converter is integrated into the system. A 24×24-element transmitarray was designed and analyzed using an in-house simulation tool. The antenna achieves a peak gain of 24.5 dBiC, with scan losses of less than 5 dB across a scan range of ±60 degrees. Finally, the accuracy of the design methodology was validated through comparisons with full-wave simulations, based on a simplified fixed-beam folded transmitarray design.

FRIDAY

9:30 Low-Profile Risley Scanner Using Dielectric Nonlocal Metasurfaces for Ka-Band SATCOM Applications

Thi Quynh Van Hoang and Erika Vandelle (Thales Research & Technology, France); Ayoub Bellouch (University Cote d'Azur, INRIA, CNRS, France); Mahmoud Elsawy (Université Côte d'Azur, Inria, CNRS, France); Stéphane Lanteri (INRIA - Sophia Antipolis, France); Brigitte Loiseaux (Thales Research & Technology, France)

2D beam steering is a crucial requirement for wireless communication systems in many modern and emerging applications that involve moving platforms. The mechanical scanning technique using two independently rotating deflectors, known as the Risley-prism concept, has emerged as a promising solution for cost-effective applications. Conventionally, both upper and lower deflectors are based on local metasurfaces, in which the deflection function is designed using a phase transformation generated by locally varying the dimensions of the patterns in each unit cell. In this contribution, a new design approach is applied by exploiting dielectric nonlocal metasurfaces, considering the interactions among adjacent subwavelength elements to shape the overall effective far-field response. Simulation results of a finite structure of 260 mm diameter, operating at Ka-band, are presented, demonstrating the potential of this new design approach.

9:50 Bifocal Reflectarray with Wide Angle Beam Steering for Next Generation of Satellite Communication Systems

Serena Assefa Asfaw (Università degli Studi di Siena, Italy); Dayan Pérez-Quintana (University of Siena (UNISI) & Institute of Smart Cities (ISC), Italy); Gabriele Minatti (Wave Up S. r. l., Italy); Francesco Caminita (Wave-Up SRL, Italy); Enrica Martini (University of Siena, Italy); Giovanni Toso (European Space Agency, ESA ESTEC, The Netherlands); Stefano Maci (University of Siena, Italy)

In this work, we present a single reflector antenna operating in the Ka-band with dual switchable linear polarization, capable of mechanically steering 37 beams within an angular range of ±40°, providing a minimum gain of 40 dBi. Beam steering is achieved by rotating a bifocal reflector with a custom-designed curvature profile, whose surface is a metasurface controlling the local phase of the reflection coefficient. By jointly designing the phase profile and the metasurface curvature, the reflector achieves two exact foci and good scanning performance at all intermediate angles. The metasurface is a corrugated surface composed of cross-shaped pillars arranged in a curved lattice with rhomboidal cells, capable of handling two orthogonal polarizations independently. This allows continuous steering of the high-gain beam cluster within ±40° without significantly degrading antenna performance.

Room: Hallén (BAR5)

CS6a - Challenges in Human RF Exposure Assessment to legacy, 5G and 6G Mobile Radio Technologies

T06 Biomedical and health / Convened Session / Propagation

Chairs: Wout Joseph (Ghent University/IMEC, Belgium), Lisa-Marie Schilling (Technische Universität Ilmenau, Germany)

8:30 Digital Twin-Based EMF Compliance Assessment of Base Station Sites

Davide Colombi, Jens Eilers Bischoff, Marije Ljolje, Nivaldo Curcio and Christer Törnevik (Ericsson AB, Sweden)

The trend in digitalization, where the boundaries between the physical and digital worlds are becoming thinner, will transform the way electromagnetic field (EMF) compliance assessments of base station sites are conducted. This study shows, through real implementations and practical examples, how data-driven solutions, exceptional computation capabilities and visualization tools can be used to improve the efficiency of base station evaluations with respect to EMF regulatory requirements.

8:50 Deduction of Extrapolation Factors in Realistic Scenarios for In-Situ Assessment of 5G Base Stations

Alvaro Villaescusa-Tebar (Universitat Politècnica de València, Spain); Jorge Roche Peris (iTEAM Research Intitute, Universitat Politècnica de València, Spain); Concepcion Garcia-Pardo (Universitat Politècnica de València & Institute of Telecommunications and Multimedia Applications (iTEAM), Spain)

Accurate assessment of electromagnetic field (EMF) exposure in 5G networks presents challenges due to beamforming and advanced technologies. Traditional frequency-selective methods provide actual exposure values but cannot distinguish beams or cells. Code-selective techniques differentiate cells and beams, but require complex extrapolation processes based on unavailable network parameters like beamforming patterns. This study investigates extrapolation factors like Fextbeam in realistic indoor and outdoor 5G environments, using frequency-selective and code-selective measurements. Measurements under different traffic conditions evaluated the effect of beam patterns and power. Results showed higher variability in extrapolated values due to differences in antenna radiation patterns. Outdoor environments exhibited more stable values, indicating the critical role of antenna patterns, especially indoors.

9:10 Combining Near-Field over the Air (OTA) Measurements with Advanced Post-Processing Link Approach to Evaluate Specific Absorption Rate (SAR) for a Commercial Smart Phone

Shoaib Anwar (Microwave Vision Group, Satimo Industries, France); Aurelien Lelievre (MVG Industries Technopole Best Iroise - Plouzane, France); Brice Frotte (MVG Industries, France); Francesco Saccardi (Microwave Vision Italy, Italy); Zain Haider and Nicolas Gross (MVG Industries, France); Lars Foged (Microwave Vision Italy, Italy)

This paper extends the Link approach to measure SAR for a commercial smartphone. A 10MHz bandwidth LTE signal communication between a commercial smartphone and a Radio Communication Tester (RCT) was studied in this work. The E-field distribution and SAR values derived from the Link approach were compared to results from the same Device Under Test (DUT) measured with a traditional SAR measurement system (single probe with a robot and phantom). The SAR value measured with 5mm separation between the DUT and the phantom are within 2.8% (or 0.12 dB) for 10g SAR. Using the SAR data at different separation distances, the SAR value at 0mm (contact position between DUT and Phantom) is evaluated using extrapolation from the Link approach. The 10g SAR results at 0mm are within 2.7% (or 0.11 dB) between the reference measurement and proposed Link approach.

9:30 Assessment of Mobile Radio Exposure with Digital Twins

Lisa-Marie Schilling and Christian Bornkessel (Technische Universität Ilmenau, Germany); Anna-Malin Schiffarth, Thanh Tam Julian Ta and Dirk Heberling (RWTH Aachen University, Germany); Matthias Hein (Technische Universität Ilmenau, Germany)

The advancement of mobile communication technologies necessitates the assessment of RF exposure. Numerical field simulations based on ray tracing enable a virtual assessment through digital twins. The fidelity of the simulation results depends on the accuracy of the environmental model in terms of its geometrical and electromagnetic features. Beside the propagation modeling, it is crucial to model the base station antennas as well. To reproduce the behavior of the antennas as mounted, the installed-performance radiation patterns need to be considered. We performed a systematic study of a 4G/5G mobile system with high-precision map data. The simulated field data were compared with free-space calculations and measurements. Overall, we found promising agreement between all three assessment methods. One instance revealed higher synthetic field values compared to the measured data, indicating deviations of the installed base station antenna pattern from the manufacturer specifications. Our results prove the feasibility of virtual field exposure assessment.

9:50 Systematic Numerical Evaluation of Whole Body Mass Averaged Specific Absorption Rate in Anatomical Mouse and Rat Models at Frequencies Up to 60 GHz

Rene Hirtl and Johannes Kainz (Seibersdorf Laboratories, Austria); Pia Schneeweiß (Seibersdorf Labor GmbH, Austria); Gernot Schmid (Seibersdorf Laboratories, Austria)

For investigating possible adverse health effects of radio frequency electromagnetic fields on biological systems, experimental animal studies are mandatory. A recently published systematic review found a lack in the dosimetric characterization of exposure setups in a significant number of published studies. Hence, drawn conclusions from such studies might be inadequate, since evaluated exposure probably differs significantly from actual exposure. It is considered useful to provide dosimetric data for mice and rats with state-of-the-art methods, including a broad range of animal models, frequencies and incident field orientations and polarizations. Results of this systematic numerical evaluation of mass averaged whole body specific absorption rates (wbSAR) in anatomical rodent models show a broad range depending on weight and size of the animal model, as well as on frequency and incident field orientation. It can be shown that horizontally aligned incident fields result in higher variation of wbSAR, compared to vertically aligned incident fields.

Room: Marcuvitz (M3)

CS56a - Characterisation of biological tissues and tissue mimicking materials for electromagnetic medical applications

T06 Biomedical and health / Convened Session / Measurements

Chairs: Iman Farhat (University of Malta, Malta), Daniela M. Godinho (Instituto de Biofísica e Engenharia Biomédica - Faculdade de Ciências - Universidade de Lisboa, Portugal)

8:30 Evaluation of a Monitoring Systems for Determining Ablation Zone Sizes Using Phase-Shift Measurements

Mohamed Lamhamdi (University of Applied Science RheinMain, Germany); Georg Rose (OVGU, Germany); Andreas Brensing (Hochschule RheinMain, Germany); Bernd Schweizer and Mohamed El Hadidy (RheinMain University of Applied Sciences, Germany); Holger Maune (University of Magdeburg, Germany); Rojda Swed (Medical Engineering, Germany); Ali Esmaeili (RheinMain University of Appilied Science, Germany); David-Jonas Bader (Hochschule RheinMain, Germany)

This work presents a method to determine the extent of the ablation zone in microwave liver ablation (MWA) by analyzing the phase shift between transmitted and received microwaves. A comparison is made between a theoretical model, simulation, and phantom experiment, all using two-layer models. The first layer represents ablated liver tissue (relative permittivity 12.4), and the second layer represents non-ablated tissue (relative permittivity 40). In simulations, these values are set by software, while in the experiment, two different polyethylene glycol (PEG) solutions are used. A custom transmitter (slot-applicator) emits microwaves at 10 dBm and 2.45 GHz, while a receiver (bowtie-dip antenna) detects changes. The ablation zone's radial extent is varied from 5 to 20 mm in both the simulation and experiment. Phase-shift measurements in the experiment are done using a software-defined radio (SDR) system. Results show a maximum deviation of 4.7% from theory in simulations and 22% in phantom experiments.

FRIDAY

8:50 Surface-Wave Estimate of Skin Tissue Permittivity

Shangyang Shang, Milad Mokhtari and Milica Popović (McGill University, Canada)

Microwave technologies have recently attracted attention as a viable tool for skin cancer diagnoses. In the research thereof, tissue characterization is essential. The commonly used dielectric probes are an evolved and advanced tool, which relies on electromagnetic wave reflection. Surface waves, researched in this work, hold promise for the design of low-profile sensing elements. We propose a theoretical model in this study that measures permittivity contrasts between tissues by analyzing the phase shift between two sensors. Simulations conducted using two patch antennas as sensors produced encouraging results, accurately estimating the permittivity contrasts across three models. Oil-gelatin skin phantoms were used for experimental validation. We report results that encourage us to explore microwave-range surface waves further towards a non-invasive dielectric characterization of the skin tissues.

9:10 ECOSURF SA-9: A Biodegradable Alternative to Triton X-100 for Tissue Phantoms

Adrián Fernández Carnicero (EPFL, Switzerland); Sujith Raman (University of Twente, The Netherlands); Anja K. Skrivervik (EPFL, Switzerland)

Tissue phantoms are materials designed to mimic the dielectric properties of biological tissues. This work proposes eco-friendly tissue phantoms of cartilage, cerebrospinal fluid and stomach in the frequency range between 0.4 and 6 GHz. For reaching this purpose, Triton X-100, a non-ionic surfactant is replaced by ECOSURF SA-9 seed oil-based non-ionic surfactant. Whereas Triton X-100 is very toxic to aquatic life, causes eye damage and sky irritation and is not biodegradable, ECOSURF SA-9 is a biodegradable and low risk non-ionic surfactant with similar dielectric properties to Triton X-100. The proposed phantoms are prepared and measured using both non-ionic surfactants, obtaining a good agreement between them. Therefore, it is shown that ECOSURF SA-9 is a safer and eco-friendlier alternative to Triton X-100 that permits to obtain biodegradable, safe, low cost, ease-to-prepare and time-stable phantoms.

9:30 Preliminary Study of the Mechanical Properties of Biological Tissue During Microwave Hyperthermia

Maria C. T. Gonçalves (Instituto de Biofísica e Engenharia Biomédica, Faculdade de Ciências, Universidade de Lisboa, Portugal); Emily Porter (McGill University, Canada & RI-MUHC, Canada); Raquel C. Conceição (Instituto de Biofísica e Engenharia Biomédica, Faculdade de Ciências, Universidade de Lisboa, Portugal)

Hyperthermia refers to heating tissue between 40°C and 45°C. In oncology, it is used as an adjuvant therapy to enhance the effects of radiotherapy and chemotherapy. Heat also induces conformational changes in proteins, which alter the tissue's stiffness. In this work, we measure the mechanical properties of ex vivo chicken breast samples during heating and simulate the effect of gravity and thermal deformation on tissue heated for 60 min. We compare these effects - in a smaller and larger region - to the reference state (the mechanical properties are constant, and there is no thermal deformation). We conclude that the displacement of the heated areas between the two states (reference and after 60 min of hyperthermia) is 0.70 mm and 6.45mm for the geometry with smaller and larger heated regions, respectively. Future work should address the impact of blood flow on the temperature distribution of tissues treated with hyperthermia.

9:50 On the Development of Breast-Like Tissue-Mimicking Phantoms

Simona Di Meo, Anna Maria Sergi, Alessia Cannatà and Giulia Matrone (University of Pavia, Italy); Andrea Martinez Lozano and Julia Arias Rodriguez (University Miguel Hernández of Elche, Spain); Jose Maria Sabater (Miguel Hernandez University, Spain); Roberto Gutierrez Mazon and Hector Garcia Martinez (University Miguel Hernàndez of Elche, Spain); Ernesto Ávila Navarro (Miguel Hernández University, Spain); Carolina Blanco Angulo (University Miguel Hernàndez of Elche, Spain); Marco Pasian (University of Pavia, Italy)

In this paper, a simple, low-cost and reproducible procedure for the production of phantoms to emulate the dielectric (up to 40 GHz) and morphological characteristics of the breast is presented. The presented results show that the procedure does not alter the dielectric properties of the samples under test and allows for the fabrication of phantoms with increasing complex internal structures close to the real-world scenario. These phantoms are suitable for use in the evaluation of innovative biomedical microwave and millimeter-wave prototypes.

FRIDAY

8:30 A Tensor-Based Holographic Multi-Feed Antenna Synthesis for MIMO Radar Applications

Thomas Frey (University Ulm - Institute of Microwave Engineering, Germany); Jens Österle, Maximilian Döring and Christian Waldschmidt (University of Ulm, Germany); Tobias Chaloun (Hensoldt Sensors GmbH, Germany & University of Ulm, Institute of Microwave Engineering, Germany)

A novel hologram synthesis method using the full impedance tensor for multi-feed holographic-based leaky wave antennas (HLWAs) is presented. Since, the unit cells (UCs) are shared across all feeds, all sub-holograms need to be combined into a shared holographic aperture. The shared impedance tensor is determined by minimizing the error relative to all sub-tensors for every UC. Based on the full tensorial multi-feed synthesis, a HLWA having two feeding points is fabricated on a fused silica wafer for an operational frequency of 160 GHz. The far field measurements show an antenna gain of 31.0 dBi and 31.4 dBi, corresponding to an aperture efficiency of 35 % and 38 %. The high gain and narrow beam of each feed make the antenna well-suited for an integration into a long-range MIMO radar. A polarization purity of less than 27 dB and a side-lobe level below -20.0 dB were measured at 160 GHz.

8:50 Dual Polarized Planar Array of Metallic Magnetoelectric Dipoles

Oludayo Sokunbi and Ahmed A Kishk (Concordia University, Canada)

A more effective method of designing a large finite array using a metallic magnetoelectric (ME-dipole) element is proposed. The extracted mutual admittance matrix of a small array is extrapolated to predict the mutual admittance matrix and input impedance of a large array, including the mutual coupling effect. This information is used to design a frequency- dependent feed network of a 4×4 dual-polarized metallic ME- dipole antenna. The ME-dipole used is air-filled, without a dielectric substrate, to improve the total efficiency. Also, the 4×4 metallic ME-dipole element array used is designed to exhibit 26-41 (44.7%) GHz ultra-wide impedance bandwidth without a cavity, unlike other air-filled ME-dipole, 26 dBi peak gain and 90% total efficiency. The 4×4 antenna array exhibits less than 40 dB isolation between the two polarizations within the working bandwidth without needing any external decoupling mechanism.

9:10 An Inverted-L Slot Antenna for Sub-THz Communications

Alberto Hernández-Escobar (Universidad de Málaga, Spain); Takashi Tomura (Institute of Science Tokyo, Japan)

This paper presents the design and analysis of an inverted-L slot radiating element for sub-THz mobile communications in the 151.5-164 GHz frequency range. The proposed structure addresses the manufacturing limitations of the previously developed inverted-L monopole. By leveraging the duality between the monopole and slot radiators, a half-isotropic radiation pattern is achieved, enhancing beam coverage for phased array applications. A compact and robust design for planar technology is also proposed. Simulations confirm the radiating element's performance, with a broad impedance matching and a stable radiation pattern across the target frequency band, and acceptable efficiency despite fabrication constraints. The proposed element is suitable for high-coverage, high-gain arrays in sub-THz communication systems.

9:30 An Additively Manufactured 300 GHz Dielectric Rod Antenna Packaging for Sub-THz Radar Camera Applications

Leonhard Hahn (Friedrich-Alexander Universität Erlangen-Nürnberg & Institute of Microwaves and Photonics, Germany); Tobias Bader (Friedrich-Alexander-Universität Erlangen Nürnberg, Germany); Tim Pfahler and Maximilian Glossner (Friedrich-Alexander-Universität Erlangen-Nürnberg, Germany); Martin Vossiek (LHFT, Friedrich-Alexander-Universität Erlangen-Nürnberg, Germany)

This paper presents a novel, 3D-printed dielectric packaging approach for application as sub-THz antenna-in-package (AiP) solution. The application of a dielectric AiP to an on-chip antenna results in a considerable enhancement in gain and efficiency when compared to non-packaged antennas. In comparison to more complex LTCC- or glass-based packaging solutions, the proposed dielectric AiP requires only a single material that can be produced at a low cost and with minimal effort through the use of 3D printing. Due to the homogeneity of the package, system complexity is significantly reduced. The AiP approach is benchmarked against conventional dielectric rod antennas, which were also fabricated and characterized as part of this work. This is essential for radar camera systems, whose low gain on-chip antennas are usually insufficient. The package approach also provides increased chip protection, as well as costeffective manufacturing and greatly simplified assembly.

9:50 A 95-110GHz Fully Metallic Four-Beam Passive Array Antenna with High Gain and High Efficiency

Xin Xu, Dongze Zheng, Qi Wu and Wei Hong (Southeast University, China); Xiaohe Cheng and Yuan Yao (Beijing University of Posts and Telecommunications, China)

This work reports the design of a 100GHz-band fully metallic waveguide multibeam antenna fed by E-plane groove gap waveguide (GGW) Butler Matrix. The E-plane property of the Butler matrix helps in its direct interconnection with the H-plane horns without any E- to H-plane waveguide transformer. The design concept has been verified by prototyping and it has been demonstrated that the proposed multibeam antenna can work over 95-110 GHz with peak gain of 16.6 dBi, peak efficiency of 89%, and beam coverage of −46°~46°.

T04 RF sensing for automotive, security, IoT, and other applications / Convened Session / Antennas

Chairs: Ping Jack Soh (University of Oulu & Katholieke Universiteit Leuven, Finland), Abel Zandamela (Technological University Dublin, Ireland)

8:30 Electrically Small Reflective Tag for Precise Water Level Monitoring

Cong Danh Bui (Trinity College Dublin, Ireland & CONNECT Centre, Ireland); Adam Narbudowicz (Tyndall National Institute, Ireland & Wroclaw University of Science and Technology, Poland)

This paper proposes a compact, low-profile, chipless RF sensor for detecting water level. The system features a Vivaldi antenna (interrogator) and a meander line resonator within a small container filled with liquid (tag). The resonant frequency of the tag shifts drastically from 0.71 GHz to 1.89 GHz when just 1 mm of the meander line begins to submerge. As more water is added to the container, the resonant peaks typically decrease due to the increasing effective permittivity inside the container. Additionally, water alters the resonant mode of the meander line resonator by loading and distorting the electric field distribution on the conductive surface with a high-permittivity medium. As a result, a fundamental mode and three higher-order resonating modes can be found as more water is added. Based on this behavior, the water's level can be determined with the resonant peak, the electric field distribution, and its Q-factor if required.

8:50 Analysis and Design of Compact High-Isolation Multi-Port Diversity Antenna

Tran-Hien Bui and Christophe Fumeaux (University of Queensland, Australia); Sasan Ahdi Rezaeieh (The University of Queensland, Australia); Son Xuat Ta and Nguyen Khac Kiem (Hanoi University of Science and Technology, Vietnam); Nghia Nguyen (Nextwaves Industries, Vietnam)

A compact high-isolation multi-port diversity antenna is presented in this paper. The design is a combination of a compact tripolarized antenna and four dipoles etched at four corners of the same ground plane. The feeding configuration is first analyzed to clarify the condition for high isolation of the tripolarized antenna. In the next step, the pattern and polarization orthogonality principle will be applied to add more ports into the antenna structure, allowing the design of a multiport antenna with isolation better than 22 dB. The proposed multi-port antenna provides an overlapped operation bandwidth of 2.39–2.52 (5.3%) while still retaining a compact size and low profile with an overall dimension of (0.8×0.8×0.1)λ3 L where λL is the free-space wavelength at the lowest operating frequency

9:10 Advanced Beam Reconfiguration in Horn Antennas Through Origami-Based Design

Meng-Hsuan Lin, Chia-Chen Lin, Sheng-Min Lin and Chia-Chan Chang (National Chung-Cheng University, Taiwan); Shih-Cheng Lin, Janne-Wha Wu and Sheng-Fuh Chang (National Chung Cheng University, Taiwan)

This paper introduces a novel horn antenna design that utilizes an origami-inspired, fan-fold aperture to enable advanced beam reconfiguration capabilities. The proposed antenna integrates a conventional H-plane sectoral horn with a shape-transforming origami structure, allowing for dynamic adjustments in beam shape, gain, and direction without the need for additional circuitry. Experimental results demonstrate that both double-sided and single-sided flaring configurations provide effective control over the radiation characteristics, with measured gains up to 8.8 dBi and beam steering up to 11°. This design offers potential applications in communication and radar systems, enhancing performance while maintaining simplicity and low fabrication costs

9:30 Tunable Dual-Band Loop Antennas with Simple Parametric Control for Brain Implant Applications

Abdul Basir, Baqir Kazmi, Uzman Ali and Toni Björninen (Tampere University, Finland)

This paper presents a scalable antenna design with only five geometric parameters, optimized for dual-mode operation at 402 & 2450 MHz and 915 & 2450 MHz. The antenna structure simplifies the optimization process by utilizing a limited set of design variables, making it more cost- and time-effective. The antenna length shows an inverse relationship with resonance, while the thickness of the top dielectric layer directly influences the lower frequency bands (402 and 915 MHz) and inversely affects the 2450 MHz band. The slot length exclusively controls the 2450 MHz band, while the feed position and antenna width independently adjust the impedance for the lower and higher bands, respectively. The proposed antennas achieve impedance bandwidths of 2.5%, 2.2%, and 4%, with peak gains of -33.2, -24.4, and -29.3 dBi at 402, 915, and 2450 MHz, respectively. These characteristics make them ideal candidates for efficient fabrication with minimal measurement errors.

9:50 Compact 20 MHz Balun for Miniature Antennas Using CRLH Transmission Lines

Romain Alcesilas (Université Gustave Eiffel, France); Divitha Seetharamdoo (Univ Gustave Eiffel COSYS LEOST Univ Lille Nord de France & Univ Lille Nord de France, France)

This article presents the design of a highly miniaturized 5.1 cm x 4.8 cm balun designed to operate at the center frequency of 20 MHz. Two branches are formed by splitting the input signal, one with a positive phase-shift and the other with a negative one. Complementary Right-Left-Handed Transmission (CRLH) is proposed as unit cell of the line to generate the positive and negative phase-shifts. Lumped inductors are added to further reduce the footprint of the structure. This results in a very compact balun (around 300 times smaller than the wavelength) presenting a balanced property with an insertion loss ranging from -5 dB to -7 dB on the two branches and a phase difference of 180° between the two differential ports in the 15-25 MHz frequency band.

FRIDAY

T04 RF sensing for automotive, security, IoT, and other applications / Convened Session / Antennas

Chairs: Jaume Anguera (Ignion & Universitat Ramon Llull, Spain), Martijn van Beurden (Eindhoven University of Technology, The Netherlands)

8:30 Direction-Of-Arrival Estimation by Metasurface Assisted by Deep Learning for IoT Systems

Nawel Meftah and Badreddine Ratni (Univ Paris Nanterre, France); Mohammed Nabil El Korso (Université Paris-Saclay, France); Shah Nawaz Burokur (LEME, France)

We propose to merge reconfigurable intelligent surface (RIS) and deep learning concepts to build a platform capable of estimating the direction-of-arrival (DOA) of incoming signals rapidly and accurately. The RIS is exploited as an electronically scanned virtual parabolic reflector with a coarse scanning step of 5°. A radio-frequency (RF) power detector placed at the focal point records the power levels of the incoming signals for each scan step and the data is fed into a pre-trained multilayer neural network to deduce the arriving angle with a precision less than 1°. Measurements are performed to validate the approach.

8:50 A Multi-Mode Multi-Port Antenna for WiFi Communication and Direction Finding of IoT Devices

Alexander Gausmann (Leibniz University Hannover, Germany); Dirk Manteuffel (University of Hannover, Germany)

In this paper, a Multi-Mode Multi-Port antenna for WiFi communication and direction of arrival estimation is presented. Four independent and decoupled antenna ports are realized using a square patch with a slotted ring. The matching is achieved by using a capacitive load to compensate the inductive nature of the probe feed. Thereby, the antenna system is easily integrable into the plastic chassis of an IoT device. WiFi communication, with MIMO options, can be achieved using different antenna ports. In addition, the direction-of-arrival estimation, using all four antenna ports, is accurate with a root mean square error of 20 ◦ in Θ-polarization.

9:10 Decoupling Analysis of Wideband 6G Mobile Antennas for IoT Applications

Harri Varheenmaa, Pasi Ylä-Oijala and Anu Lehtovuori (Aalto University, Finland); Ville Viikari (Aalto University & School of Electrical Engineering, Finland)

Wideband and compact sixth-generation (6G) antenna design is proposed for Internet-of-Things (IoT) applications. The antenna is placed on the metal rim of a smartphone and it covers a wide range of FR3 frequency bands, from 7.1 GHz to 13.2 GHz. Special emphasis is on the analysis and reducing coupling between two nearby located antenna elements. With an adequately designed decoupling element, a slot on the metal rim, coupling is significantly reduced, remaining below -20 dB on a wide frequency range. This allows placing antennas very close to each other, squeezing the size of a multiple antenna design, and enables efficient implementation of high-order multiple-input multiple-output (MIMO) systems.

9:30 Physical Limitations on Substructure Characteristic Modes

Johan Lundgren and Mats Gustafsson (Lund University, Sweden)

Characteristic modes (CM) and substructure CM are widely used techniques in antenna design and analysis. In this paper, we demonstrate how the slope of characteristic eigenvalue traces is fundamentally constrained for all possible designs that fit within a specified design region. The derivation is based on reformulating the frequency derivative of the CM eigenvalues as an optimization problem over the current distribution within the design region. The results reveal that the slope of the eigenvalues is constrained in a manner analogous to antenna Q-factors for CM, though it differs slightly for substructure CM.

9:50 Simulation and Analysis of a Reconfigurable Electrically Small Antenna System for Compact Wearable Devices

Niklas Takanen and Kimmo Rasilainen (University of Oulu, Finland); Juha Katajisto (Bittium Oy, Finland); Aarno Pärssinen (University of Oulu, Finland); Ping Jack Soh (University of Oulu & Katholieke Universiteit Leuven, Finland)

This work analyses a reconfigurable electrically small antenna (ESA) system operating in a limited design space at multiple 5G-NR bands (901-933 MHz and 1.635-2.1 GHz) in a switchable form under an area constraint of 63.2×25 mm^2 (0.19×0.07λ^2). First, the area constraints and operating frequencies are analysed using the Chu-Harrington limit, followed by a study of the surface currents of the ESA and chassis using characteristic mode analysis. Then, a matching circuit is designed and integrated to enable both aperture tuning and input matching of the antenna. Simulations results indicated a single band operation at 901-923 MHz (2.4 BW%) in configuration 1, and a dual band operation at 914-933 MHz (2 BW%) and at 1.635-2.1 GHz (12.4 BW%) in configuration 2. Finally, specific absorption rate is of the ESA is studied, indicating levels of 0.2-0.4 W/kg (averaged over 1 g of tissue).

FRIDAY

Chairs: Antonio Alex-Amor (University of Pennsylvania, USA), Rola Saad (The University of Sheffield, United Kingdom)

8:30 Systematic and Accurate Method to Model Dielectric Stratifications in Artificial Dielectric Layers

Roderick Giosevan Tapia Barroso and Daniele Cavallo (Delft University of Technology, The Netherlands)
We present a systematic approach to include the effects of dielectric slabs in artificial dielectric layers (ADLs). Typical implementations of ADLs consist of layers of subwavelength metal patches supported by either dielectric slabs or thin dielectric films bonded onto foam spacers. The presence of dielectrics in the proximity of the metal layers affects the equivalent layer capacitance and thus must be accurately taken into account for the modeling and design of the ADLs. The proposed procedure allows to derive an analytical expression for the effective permittivity of each capacitive layer that depends on the dielectric layers in the vicinity of the metal. The equivalent layer capacitance can be then included in the ADL equivalent transmission line model, which can be used, for instance, for the design of matching structures in ultra-wideband arrays.

8:50 High Q- Resonant Energy Selective Surface Based on Plasma

Krushna Kanth Varikuntla (Queen's University Belfast, United Kingdom); Muhammad Ali Babar Abbasi (Queen's University Belfast & The Institute of Electronics, Communications and Information Technology (ECIT), United Kingdom); Okan Yurduseven (Queen's University Belfast, United Kingdom)
In this paper, a plasma-based Energy selective surface (ESS) is proposed for high-power microwave (HPM) threat protection. The proposed design leverages the formation of plasma, generated by the induced electric field from HPM, to selectively absorb electromagnetic (EM) energy. The structure incorporates a high-efficiency frequency selective surface (FSS), implemented using substrate integrated waveguide (SIW) technology, and gas discharge tubes (GDTs). Two design variants are presented, one optimized for broadband performance and the other for narrowband operation. The selective energy absorption is achieved by creating plasma within the GDTs, positioned on the top layer of the unit cell. Simulation results demonstrate excellent isolation performance as the incoming power increases, with an insertion loss (IL) exceeding 10 dB in both unit cell designs across the targeted frequency band. This design presents significant potential for applications requiring dynamic control over electromagnetic wave propagation in high-power environments.

9:10 An Equivalent Circuit Model for a Dual Polarised Interdigital Reflective Surface Design

Rola Saad (The University of Sheffield, United Kingdom); Kenneth Lee Ford (University of Sheffield, United Kingdom)
A novel design approach is presented for realizing a compact, lightweight, single-band, single-layer, dual-polarized reflective surface, utilizing an accurate and adaptable equivalent circuit model. The proposed model is validated through numerical analysis and experimental measurements. A reflective surface, with a thickness of 0.032λ operating at 1.5 GHz with a unit cell periodicity of 0.13λ, is presented to demonstrate the approach. The surface is integrated with a wideband antenna and provides a low-profile, high-performance system, demonstrating significant potential for applications requiring compactness and dual polarization properties. This approach offers a practical solution for modern RF and microwave systems.

9:30 A Thin and Lightweight Ultrawideband Electromagnetic Wave Absorber with an Impedance Graded Microstructure

Byeongjin Park, Suk Jin Kwon and Sang Bok Lee (Korea Institute of Materials Science, Korea (South)); MinJeong Kwon (Korea Institute of Materials Science, Korea (South) & Pusan National University, Korea (South)); Hyein Jung (KIMS, Korea (South))
This article presents a thin and lightweight ultrawideband electromagnetic wave absorber designed for mmWave frequency bands. The absorber is fabricated using electrospinning of a polyvinylidene fluoride (PVDF) and single-walled carbon nanotube (CNT) composite. By varying the ratio of PVDF to CNT during fabrication, a multilayered microstructure with graded electrical conductivity and electromagnetic impedance is achieved. This structure minimizes reflection and maximizes electromagnetic wave absorption, achieving over 90% absorption of incident waves across the entire V and W bands with a thickness of just 0.32 mm. Furthermore, the porous microstructure of the composite contributes to its low density of 0.304 g/cm3.

9:50 Spatial Dispersion Engineering Using Cascaded Local Metasurfaces

Jordan R. Dugan, Tom Smy and Shulabh Gupta (Carleton University, Canada)
Spatially dispersive or nonlocal metasurfaces have gained much attention in the literature due to their promising applications in wave based computing. These surfaces can be characterized with surface susceptibilities that vary as a function of the transverse wavevector. Recently a method has been proposed that generates the nonlocal susceptibilities required to achieve some desired angular scattering response. However, the physical realization of these susceptibilities remains an open problem. In this work, we demonstrate a simple method to realize a spatially dispersive response using cascading non-spatially dispersive metasurfaces. This reduces the problem of realizing a spatially dispersive surface to the much more familiar problem of realizing a non-spatially dispersive surface.

FRIDAY

8:30 Composite Vortex Theory: Applications to Reflecting and Transmitting Metasurfaces

Mirko Barbuto and Alessio Monti (Roma Tre University, Italy); Stefano Vellucci (Niccolò Cusano University, Italy); Andrea Alù (CUNY Advanced Science Research Center, USA); Filiberto Bilotti (ROMA TRE University, Italy); Alessandro Toscano (Roma Tre University, Italy)

This contribution introduces the Composite Vortex Theory (CVT) and its application to simplified reconfiguration strategies for reflective and transmissive metasurfaces. By exploiting the unique properties of vortex fields, CVT enables efficient electromagnetic wave control with minimal structural changes to the metasurface. The proposed reconfiguration strategies simplify the design and implementation of metasurfaces for applications such as beam steering and wavefront shaping, offering a flexible and efficient solution for next-generation electromagnetic devices.

8:50 Phase-Only Synthesis of a Reflecting Surface for Enhancing Coverages in Urban Scenarios

Shahid Ayaz and Michele Beccaria (Politecnico di Torino, Italy); Amedeo Capozzoli, Claudio Curcio and Giuseppe D'ambrosio (Università di Napoli Federico II, Italy); Angelo Freni (Università degli studi Firenze, Italy); Angelo Liseno (Università di Napoli Federico II, Italy); Paola Pirinoli (Politecnico di Torino, Italy)

A Phase-Only power pattern synthesis of a flat reflecting surface is presented to scatter a beam with a flat-top shaped pattern in one cut and a cosecant pattern in the other one. Far-field illumination is assumed and the reflecting surface is appointed to reflect the impinging wave into a non-specular direction. Also by comparisons with CST studio suite simulations, the results show how, in a realistic urban scenario, the algorithm is capable to effectively enforce the design specifications.

9:10 Closed-Form Solution for the Scattering Coefficients in the Canonical Problem of Anomalous Reflection

Federico Giusti, Polina Terekhina, Enrica Martini, Stefano Maci and Matteo Albani (University of Siena, Italy)

Metasurfaces (MTSs) enable efficient manipulation of electromagnetic radiation. In practice, control over reflection direction is possibly the most useful. In past years, significant progress has been made in designing anomalous reflectors, leading to the development of various geometries and synthesis approaches, ranging from analytical models to optimization-based methods. In this paper, we derive a closed-form solution for the complex reflection coefficients of all propagating and evanescent Floquet modes (FMs) in the canonical problem of anomalous reflection based on a homogenized impenetrable impedance MTS with a tangent-like profile. Our findings reveal that the phase of the reflected FMs is influenced by the spatial discretization of the MTS. This insight is crucial for the practical applications of anomalous reflectors, as real-world MTSs are implemented using physical elements discretizing the homogenized impedance profile. We believe that our study is particularly interesting for researchers working on metasurfaces, communication technologies, and reconfigurable intelligent surfaces.

9:30 New Architectures and Concepts in Electromagnetic Wave Control Through EM Skins

Marco Salucci (ELEDIA Research Center, Italy); Giacomo Oliveri (University of Trento & ELEDIA Research Center, Italy); Francesco Zardi (ELEDIA Research Center, Italy); Aaron A Salas-Sanchez and Andrea Massa (University of Trento, Italy)

Currently, electromagnetic (EM) skins are the subject of a remarkably wide and active research effort thanks to their great potential in terms of wave control capability, design flexibility, and cost-effectiveness. This work aims to provide a review of emerging architectures and methodologies for the design, control, and planning of EM skins, as well as highlight open challenges and future trends.

9:50 Reconfigurable Metasurface Antenna-Based Mills-Cross Compressive Aperture for Computational Microwave Imaging

Guillermo Alvarez Narciandi and María García Fernández (Queen's University Belfast, United Kingdom); Mohsen Khalily (University of Surrey & 5G Innovation Centre, Institute for Communication Systems (ICS), United Kingdom); Okan Yurduseven (Queen's University Belfast, United Kingdom)

Reconfigurable metasurface-based antennas are gaining increasing attention for radar imaging applications. Especially, they play a major role in computational imaging (CI) systems at microwave frequencies, as they provide high-flexibility to generate the required spatially diverse patterns. In this contribution, the usage of reconfigurable antennas is analyzed in the framework of a hybrid microwave imaging system, aiming at exploiting the advantages of both CI and synthetic aperture radar (SAR) paradigms. Experimental results show that the combination of both approaches yields a reduced hardware complexity (as only two 1D single-fed antennas are employed to synthesize a full 2D aperture), a significant increase in the data acquisition speed (as CI enables to drastically decrease the number of measurements required compared to a conventional SAR-based system) and an enhanced target to clutter ratio (thanks to the combination of a reduced number of measurement positions and several reconfiguration states of the antennas).

FRIDAY

8:30 Rainfall Rate Data Analysis and Site Diversity Statistics in Cyprus Using Synthetic Storm Technique

Apostolos Z. Papafragkakis (National Technical University of Athens, Greece); Nektarios Moraitis (National Technical University of Athens & Institute of Communications and Computers Systems, Greece); Athanasios D. Panagopoulos (National Technical University of Athens, Greece); Panayiotis Ioannides, Nikolaos Christoforou, Constantinos Agrotis and Sotirios Alexandrou (Cyprus Telecommunications Authority (Cyta), Cyprus)

This paper examines the statistical performance of site diversity mitigation technique in Cyprus, based on measured rainfall data, collected in two locations in Cyprus, through the application of the synthetic storm technique (SST). Firstly, the long-term rain attenuation exceedance probability is calculated and assessed at Ka- and Q-bands and at various elevation angles, and then the joint-exceedance probability of hypothetical diversity downlink scenarios is presented. Finally, the number of switches as well as the required fade margins given a specific outage for various Selection Combining (SC) scenarios is also provided. The results indicate the crucial role of the elevation angle and frequency in propagation problems. For very low elevation angles or operating carriers at Q-band the number of switches is increased and lead to higher margins. However, a proper SC diversity when adopted can compensate the demands effectively.

8:50 Effect of the Spatial Distribution of Rain on mmWave Link Attenuation

Elizabeth Verdugo (Consiglio Nazionale delle Ricerche, Italy & PUC RIO, Brazil); Lorenzo Luini and Carlo Riva (Politecnico di Milano, Italy); Laura Resteghini (Huawei Technologies, European Research Center, Italy); Roberto Nebuloni (Ieiit - Cnr, Italy)

Millimeter-wave wireless links are being investigated for applications such as front/backhauling in future 6G networks, due to the large spectrum available especially in the D-band (130- 174 GHz). This study reports the preliminary results gathered from a rare experimental set-up featuring an array of disdrometers deployed along the 800 m propagation path of two E-band and D-band links. The disdrometers capture the microphysics and the spatial distribution of rainfall over the path and allow an accurate prediction of rainfall attenuation, which has a huge impact on the link budget of these systems. First results indicate that the measured attenuation at both E-band (73 GHz) and D-band can be significantly higher than the predicted attenuation, the difference increasing with rainfall intensity.

9:10 Comparison of the Height of the 0°C Isotherm with Several ERA5 Cloud Parameters

Ana Benarroch (Universidad Politécnica de Madrid, Spain); Gustavo Siles (Universidad Privada Boliviana, Bolivia); Jose M Riera (Universidad Politécnica de Madrid, Spain)

The 0°C isotherm height is used in rain attenuation prediction models to calculate the rain height, as proposed in ITU-R Recommendations. In previous studies, the 0°C isotherm obtained for Madrid was compared with the 0° isotherm height provided by ERA5.. In this paper, the comparison is extended to several ERA5 cloud parameters: cloud base height, total cloud liquid water content and total cloud ice water content. The results presented here include the monthly average, histograms of each parameter and binned scatter plots of pairs of parameters.

9:30 Electromagnetic Intersystem Interference Due to Hydrometeor Scattering: Development of a Microphysical Model

Enrico Polo, Michele D'Amico and Carlo Riva (Politecnico di Milano, Italy); Antonio Martellucci (European Space Agency, The Netherlands); Lorenzo Luini (Politecnico di Milano, Italy)

This paper presents a physically-based model to investigate the bistatic radio intersystem interference caused by hydrometeor scattering. The precipitation phenomena are reproduced accounting for both the rainfall process, through the MultiEXCELL model, and the melting layer extending above the rain height. For the latter, the adopted approach accounts for altitude-dependent variations of the physical parameters, based on the thermal equation governing the melting process of the ice particles. The interference is evaluated through the bistatic radar equation (BRE), relating the transmitted power with the interfering one. The microphysical properties of the precipitation particles are analyzed to accurately reproduce their scattering and dissipative properties. The model is validated against the ITU-R DBSG3 database, comparing the scattering coupling contribution of rain to the one induced by the melting layer.

9:50 Modelling of Rain Clutter Based on Empirical Data for Automotive Radar Validation

Sonakshi Gupta (TU Ilmenau, Germany); Isabella B. Varga, Matthias Hein and Thomas Dallmann (Technische Universität Ilmenau, Germany)

Simulation of precipitation for automotive radar validation requires suitable rain-clutter models to test radars against various weather conditions. Although there have been developments in the investigation of attenuation due to rain, rain back-scattering needs to be explored more. However, the analytical modelling is challenging. Even if the raindrops are considered perfect conducting spheres, the Rayleigh approximation cannot be used to calculate RCS since rain droplets are comparable to automotive radar wavelengths. Therefore, reflectivity measurements at different rain rates were conducted in an indoor rain facility. Based on the measured data, reflectivity from rain back-scattering for automotive radars is modelled using an empirical approach. The results indicate that reflectivity can be modelled using a gamma distribution parameterized by rain rate.

FRIDAY

8:30 Spatial Deconvolution Method Based on Power-Only Measured Data for Antenna Pattern Reconstruction in Nonanechoic Chamber

Fengchun Zhang (Aalborg University, Denmark); Wei Fan (Southeast University, China); Gert Pedersen (Aalborg University, Denmark); Heng Wang (School of Artificial Intelligence, China)

Anechoic environment with a clean far-field line-of-sight (LOS) path is required for the accurate antenna radiation pattern measurement. However, such propagation environment might be too demanding in practice. Therefore, there is a strong need for effective echo suppression methods to recover the true antenna pattern in non-anechoic environment. In this paper, a recent proposed amplitude-only echo suppression method is discussed for antenna measurement in the non-anechoic environment. Compared to the conventional complex-signal-based methods, the power-only spatial deconvolution method only requires phaseless data. Furthermore, this method can either exploit spatial scalar response at a single-frequency or wideband scalar response at a single spatial location, or joint spatial wideband scalar response. It is a phaseless antenna pattern reconstruction method, and it presents excellent multipath identification capability and enables high measurement efficiency. The feasibility and advantages of the power-only spatial deconvolution method are comprehensively demonstrated by the numerical and experimental validations.

8:50 A Broad-Band All Textile Based Absorber Using Carbon Ink

Amit Kumar Baghel (Universidade de Aveiro, Portugal & IT AVEIRO, Portugal); Pedro Pinho (UA - Universidade de Aveiro & IT - Instituto de Telecomunicações, Portugal); Nuno Borges Carvalho (Universidade de Aveiro, Portugal & InstitutodeTelecomunicacoes, Portugal)

In this paper, the authors propose a novel method to achieve broadband absorption from 0.8 to 24 GHz using highly resistive carbon ink applied to polyester fabric. The carbon ink's conductivity, expressed in terms of sheet resistance, is optimized at 400 (\Omega/\text{sq/mil}) to ensure that the reflection coefficient (S_{11}) remains below -10 dB across the entire frequency band. The pattern is printed on polyester fabric due to its low loss tangent ((\tan\delta = 0.0045)), allowing for minimal energy dissipation in the material. The design, being fabricated on polyester, also provides conformality. Owing to the four-fold symmetry of the structure, the absorption is polarization-insensitive, and the broadband absorption is maintained for incident angles (\leq 45^\circ). The proposed absorber's bandwidth is compared to previously reported designs, demonstrating a significant improvement in absorption bandwidth.

9:10 In-Situ Measurement Comparison of Cell-Wide and Directional EMF Power Control Features Using Air Interface Load Generator for 5G Massive MIMO

Bo Xu, Carla Di Paola and Christer Törnevik (Ericsson AB, Sweden)

Different software features to monitor and control the time-averaged transmitted power or the equivalent isotropic radiated power (EIRP) of radio base stations (RBSs) have been developed, enabling mobile network operators to establish the electromagnetic field (EMF) compliance boundary of the RBSs based on the actual maximum EMF exposure condition. In this paper, the performance of the Ericsson cell-wide EMF power control feature, which controls the time-averaged power of the cell, and the corresponding directional EMF power control feature, which controls the time-averaged EIRP by mapping the actual EIRP in eight azimuthal segments of the cell, are compared through in-situ measurements using the software feature called Air Interface Load Generator for a 5G massive multiple-input multiple-output (MIMO) RBS. In the controlled testing environment, the directional feature results in less or no power back-off for full-buffer downlink transmission compared to the cell-wide feature.

9:30 Spectrum Monitoring System Deployment Site Analysis Using Realistic Radiation Patterns

Joseph Mruk (MITRE, USA); Thao Nguyen and M. Keith Forsyth (National Institute of Standards and Technology, USA); Duncan A McGillivray (National Institute of Standards and Technology & National Advanced Spectrum and Communications Test Network, USA); Daniel Kuester (National Institute of Standards and Technology, USA)

Spectrum monitoring systems are becoming increasingly necessary to facilitate spectrum sharing opportunities in congested frequency bands. Shared spectrum approaches allow for more commercial use of the limited frequency allocations while protecting legacy government users from interference within the United States. Spectrum monitoring systems allow for stakeholders gain insight into how the spectrum is used over time. The location of these systems, ideally, will be able to measure aggregate emissions from all users within the dynamic range of the measurement sensor. This paper describes a computational modeling methodology to predict aggregated power at perspective sensor locations from commercial cellular deployments leveraging the irregular terrain model (ITM) and omnidirectional and directional antenna patterns that may be leveraged for generating design requirements and fielding spectrum monitoring systems.

FRIDAY

9:50 Dynamic Power Measurement Techniques in OTA Environment for Millimeter Wave Wireless Applications

Walid El Hajj (Intel Corporation, France); Juan Antonio Del Real (Maury Microwave, France); Nawfal Asrih (Intel Corporation, France)

This paper assesses the time varying power measurement complexities of mmW wireless systems in dynamic scenarios, focusing on advanced radiated power measurement techniques. An important feature typically used in wireless device to mitigate challenges related to human exposure regulatory compliance is Time Average Specific Absorption Rate (TAS) or Time average Power Density (TAPD) at higher frequencies (above 6 GHz). This feature is a good illustration of dynamic scenarios. While TAS measurement is performed in conducted setup at low frequencies, it becomes more challenging, when going higher in frequency (mmW) where in the majority of cases there is no direct access to the antenna port. In this paper multiple radiated OTA systems of power time varying measurement solutions will be presented. The results are illustrated by measurement for one system type and for all systems in final paper.

Room: Mosig (26) — P11 - Wideband channel measurements from sub-6 GHz to (sub-)THz

T07 Electromagnetic modelling and simulation tools / / Propagation

Chairs: Diego Andrés Dupleich (Technische Universität Ilmenau, Germany & Fraunhofer Institute for Integrated Circuits IIS, Germany), Fredrik Tufvesson (Lund University, Sweden)

8:30 Enabling Vehicular mmWave Communication Links Using cmWave Information

Markus Hofer (AIT Austrian Institute of Technology, Austria); Faruk Pasic (TU Wien, Austria); Benjamin Rainer (AIT Austrian Institute of Technology GmbH, Austria); Jiri Blumenstein (Brno University of Technology, Czech Republic); Ales Prokes (Brno University of Technology & Sensor, Information and Communication Systems Research Centre, Czech Republic); Christoph F Mecklenbräuker (TU Wien, Austria); Andreas F. Molisch (University of Southern California, USA); Thomas Zemen (AIT Austrian Institute of Technology GmbH, Austria)

Future connected cooperative automated mobility can benefit from high-data-rate wireless communication links between vehicles to exchange LIDAR and/or RADAR data. The millimeter wave (mmWave) frequency range offers large bandwidth for rapid sensor data exchange but suffers from higher signal attenuation compared to the centimeter wave (cmWave) band. In this paper we obtain cmWave and mmWave multipath component (MPC) parameters by combining a single omni-directional antenna that is used as virtual array with the CLEAN algorithm. The cmWave MPC information enables low-overhead mmWave beamforming by means of an antenna array. Empirical multi-band measurement data (3.2 GHz, 34.3 GHz, and 62.35 GHz) shows that considering the 5 strongest MPCs, a signal-to-noise ratio of up to 25 dB for a V2I scenario can be achieved.

8:50 Delay-Synchronous Wideband Channel Sounding Using Off-The-Shelf Multi-Antenna WiFi Devices

Koji Yamamoto (Kyoto Institute of Technology, Japan); Katsuyuki Haneda (Aalto University, Finland)

WiFi sensing with IEEE 802.11ax is based on estimates of channel state information, which, if processed properly, can also be used for wideband channel sounding with a bandwidth of up to 160MHz. However, achieving delay-synchronous channel sounding remains challenging due to factors such as uncertainty in symbol reception timing, resulting in impulse responses that are discontinuous across acquisitions. We propose and validate a delay-synchronous channel sounding framework by remoting one of the antennas with coaxial cables and calibration based on a reference antenna with a known over-the-air propagation distance to the transmitter. Experiments with commodity off-the-shelf devices confirmed that the impulse response becomes continuous across successive acquisitions and provide the absolute delay. The impulse response has a noise level at -115dBm, indicating the maximum pathloss value that can be measured with the devices, allowing successfully detection of long-delayed multipaths up to 135m propagation distance in a reverberant 30-m-long corridor.

9:10 Channel Measurements and Analysis for Terahertz Monostatic Sensing

Yejian Lyu (Shanghai Jiao Tong University, China); Zeyu Huang (TU Wien, Austria); Ziming Yu (Huawei Technologies CO., LTD, China); Chong Han (Shanghai Jiao Tong University, China)

Terahertz (THz) integrated sensing and communication (ISAC) aims to incorporate new functionalities within communication systems, such as positioning and sensing. This paper presents a THz measurement campaign focused on monostatic sensing. Channel measurements with a center frequency of 300 GHz and a bandwidth of 20 GHz, using a vector network analyzer (VNA)-based channel sounder, are carried out in a laboratory setting at 14 transceiver (TRx) locations, where the transmitter (Tx) and receiver (Rx) are co-located to mimic monostatic sensor. A directional scanning sounding (DSS) scheme is applied to capture spatial sensing channel profiles. An element-wise space-alternating generalized expectation-maximization (SAGE) algorithm estimates the multipath component (MPC) amplitudes and delays. Then, channel characteristics such as the back-scattering coefficient, delay spread, and angular spread are calculated and analyzed. The findings from this work provide valuable insights to inform the design and deployment of future THz ISAC systems.

FRIDAY

9:30 Ray-Tracing-Assisted High-Resolution Parameter Estimation for Dynamic Millimeter-Wave Channels

Ali Al-ameri (Lund University, Sweden); Gerhard Steinbock (Ericsson AB, Sweden); Juan D Sanchez, Fredrik Tufvesson and Xuesong Cai (Lund University, Sweden)

An accurate description of the wireless channel is essential to the development of modern wireless systems. In order to mathematically model the propagation channel, one important prior step often done is high-resolution parameter estimation. The estimation accuracy of this step has a significant impact on how well the channel models can represent reality. In this paper, we address this by improving the estimation performance of the well-known space-alternating generalized expectation maximization algorithm by using ray tracing estimation results in its initialization step. By using the proposed method to estimate multi-path components from raw measurement data gathered from an outdoor measurement campaign, we show that the resulting algorithm gives an improvement in estimation accuracy and lowers computational complexity.

9:50 VNA-Based Channel Sounder System Between 330 GHz and 500 GHz for LOS Indoor Scenario

Muhammad Qamar (Queen Mary University of London, United Kingdom); Lawrence WG Carslake (National Physical Laboratory UK, United Kingdom); Tian Hong Loh (UK, National Physical Laboratory, United Kingdom); Akram Alomainy (Queen Mary University of London, United Kingdom)

This paper presents a Vector Network Analyzer (VNA)-based phase-compensated channel sounder, operating in the 330-500 GHz frequency range, utilizing radio-over-fiber (RoF) technology to support long-range phase-coherent measurements. A novel phase compensation scheme is introduced to mitigate phase variations caused by optical fiber, enabling its use in multi-channel and long-range measurements. The system's performance is validated in a line-of-sight (LOS) indoor lab environment. Additionally, a link budget analysis with optical fiber lengths of up to 600 m and preliminary indoor radio channel sounding assessments have been conducted to evaluate the sounder's functionality.

Room: Collin (27)

CS38a - Fast, low-invasive visualization of EM-VNF distributions around wireless communication/sensing devices: from anechoic chamber to microscope

T08 Fundamental research and emerging technologies/processes / Convened Session / Measurements

Chairs: Jean-Charles Bolomey (Supelec Université de Paris Sud XI, France), Manuel Sierra-Castañer (Universidad Politécnica de Madrid, Spain)

8:30 Fast, Low-Invasive Visualization of EM-Very-Near-Field Distributions Around Wireless Communication/ Sensing Devices: From Anechoic Chamber to Microscope

Jean-Charles Bolomey (Université Paris-Saclay, France); Manuel Sierra-Castañer (Universidad Politécnica de Madrid, Spain.)

While fast visualization of EM field distribution is satisfactorily obtained by numerical modelling, it still constitutes a key challenge for measurements in a wide spectrum of demanding applications spreading from the early design and prototyping of antenna modules to final on-line fabrication and compliance testing of mass-produced connected devices. But recently, the rapidity of measurement has been improved thanks to several modalities exploiting either various interaction mechanisms between EM waves with adequate sensitive materials or the combination of standard Near-Field (NF) measurements with optimized sampling strategies and advanced wavefront post-processing techniques to retrieve Very-Near-Field (VNF) distributions. The aim of this paper is to provide an overview of these modalities to identify their current fields of applications and to envision their future development. As such, it is expected to offer an opportunity for comparing their performance tradeoff capabilities, in terms of rapidity, sensitivity, invasiveness and spatial resolution.

8:50 Measurement of Very-Near-Field Distribution of Onboard Antenna Using Scanning Optic-Induced Plasma Scattering Technology

Ning Leng (Beihang University, China); Liao Ma (Ningxia University, China); Zhanjian Liang and Ming Bai (Beihang University, China)

Very-near-field distribution is valuable for evaluating antenna performance. For radio frequency (RF) onboard antennas, the very near field generally includes the responses from both the antenna and other components, making it more complex to measure. In this paper, we realize a very-near-field measurement method using scanning optic-induced scattering (SOPS) technology. The SOPS method utilized a silicon wafer attached to the onboard antenna surface. A laser spot illuminates and scans across the silicon wafer surface, where the generated optic-induce plasma scatters the incident wave. A receiving antenna was applied to capture the scattered signals, allowing for the imaging of the high-resolution very-near-field distribution. A Ku-band onboard transmitting antenna module and a commercial radar were measured through coherent measurement and non-coherent measurement. Near-field distributions of different distances were observed. The proposed method can achieve flexible and efficient very-near-field measurement, which is promising in the electromagnetic field characterization of the onboard antenna.

FRIDAY

9:10 Immersive EMC Mapping System with Augmented Reality Visualization Headset Compatible with Lab Equipment

Jean Rioult (Université Gustave Eiffel, France); Nicolas Bremard and Samuel Degrande (University Lille, France); Guillaume Willefert (Luxondes, France)
To measure EM radiation sources, specialists mainly use professional and calibrated autonomous field meters or field sensors coupled with specific spectrum analyzers for EMC measurements. Recently, the company Luxondes has developed a new concept of EMC 3D Scanner using augmented reality called EM-Scanphone. This is well suited for near-field planar measurements but is not effective enough for large areas. In this paper, we will present a new augmented reality mapping system with a Hololens type headset that will allow measurements to be taken in large volumes but also to recover in 3 dimensions the environment and the object under test.

9:30 Revision of Diagnosis Techniques: Holographic and Equivalent Currents Reconstructions

Manuel Sierra-Castañer (Universidad Politécnica de Madrid, Spain); Francesco Saccardi and Lars Foged (Microwave Vision Italy, Italy)
This overview paper, included in the convened session "Fast, low-invasive visualization of EM-Very-Near Field distributions around wireless communication/sensing devices: from anechoic chamber to microscope", revises the reconstruction techniques used in antenna design and antenna measurements. Among them, the two classical approaches are presented: holographic techniques and equivalent currents, showing later some applications and examples. These techniques are a very powerful tool for being able to afford the design of very large antennas and for the reduction of uncertainty in some antenna measurement problems.

9:50 Functional Test of a Communication System by Fast Visualization of the Very-Near-Field Radiation Using Infrared Thermography

Adrien Laffont, Stéphane Fauré, Ricardo Carrizales and Ptolemy Lawson (Anyfields, France)
This paper presents the functional test of a communication system based on infrared thermography measurements. This non-intrusive method allows to measure, in a few dozen seconds, the very-near-field radiated by the antennas integrated in the system under test. More particularly, the measurements are carried out on a Wi-Fi communication system operating in the 2.4 GHz and 5 GHz bands. Coupling between the radiation of one subsystem and the other subsystem is identified by visualizing the radiated field close to the system surface.

Friday - 10:40-12:20

Room: Alfvén (A3+A4)

CS1b - Reconfigurable Intelligent Surfaces for Communication, Sensing and Computing

T08 Fundamental research and emerging technologies/processes / Convened Session / Electromagnetics

Chairs: Mohsen Khalily (University of Surrey & 5G Innovation Centre, Institute for Communication Systems (ICS), United Kingdom), Okan Yurduseven (Queen's University Belfast, United Kingdom)

10:40 STAR-RIS for Integrated Communication, Computing, and Sensing

Zahra Rahimian Omam (University of Surrey, United Kingdom); AmirMasood Bagheri and Shadi Danesh (5GIC & 6GIC, Institute for Communication Systems (ICS), University of Surrey, United Kingdom); Seyed Ehsan Hosseininejad (University of Surrey, United Kingdom); Okan Yurduseven (Queen's University Belfast, United Kingdom); Mohsen Khalily (University of Surrey & 5G Innovation Centre, Institute for Communication Systems (ICS), United Kingdom)
This paper presents a dual-functional Simultaneous Transmission and Reflection Reconfigurable Intelligent Surface (STAR-RIS) that integrates communication via reflection and computation/sensing via transmission within a single aperture. When an incoming wave impinges on the STAR-RIS, part of it is reflected for communication, while the transmitted portion, shaped by a lens phase profile, performs Fourier transformations in the k-domain enabling computational tasks. A coding metasurface approach is used to create a linear phase gradient in the reflection space and a lens phase profile in the transmission space. This enables tailored beam patterns for reflection and computational tasks, such as Fourier transforms, for accurate angle-of-arrival estimation and sensing applications. To validate the concept, a STAR-RIS with side-by-side reflection and transmission arrays is designed, fabricated, and tested at 26 GHz.

FRIDAY

11:00 Capacity Maximization for MIMO Channels Assisted by Beyond-Diagonal RIS

Emil Björnson (KTH Royal Institute of Technology, Sweden); Özlem Tuğfe Demir (TOBB University of Economics and Technology, Turkey)

Reconfigurable intelligent surfaces (RISs) can improve the capacity of wireless communication links by passively beamforming the impinging signals in desired directions. This feature has been demonstrated both analytically and experimentally for conventional RISs, consisting of independently reflecting elements. To further enhance reconfigurability, a new architecture called beyond-diagonal RIS (BD-RIS) has been proposed. It allows for controllable signal flows between RIS elements, resulting in a non-diagonal reflection matrix, unlike the conventional RIS architecture. Previous studies on BD-RIS-assisted communications have predominantly considered single-antenna transmitters/receivers. One recent work provides an iterative capacity-improving algorithm for multiple-input multiple- output (MIMO) setups but without providing geometrical insights.

In this paper, we derive the first closed-form capacity-maximizing BD-RIS reflection matrix for a MIMO channel. We describe how this solution pairs together propagation paths, how it behaves when the signal-to-noise ratio is high, and what capacity is achievable with ideal semi-unitary channel matrices. The analytical results are corroborated numerically

11:20 Dual Dielectric Metasurface for Simultaneous Sensing and Reconfigurable Reflections

Mahesh Birari (EpsilonR, United Kingdom); Deepak Singh Nagarkoti (Texas Instruments, USA); Anestis Katsounaros (Space Innovation Solutions, Greece); Hruday Kumar Reddy Mudireddy (Texas Instruments, USA); Jagannath Malik (Indian Institute of Technology Patna, India & IIT PATNA, India); George C. Alexandropoulos (University of Athens & University of Illinois Chicago, Greece)

This paper presents a novel dual-functional hybrid Reconfigurable Intelligent Surface (RIS) for simultaneous sensing and reconfigurable reflections. We design a novel hybrid unit cell featuring dual elements, which share the same phase center, to support both intended functionalities, with the antenna being miniaturized via a high dielectric material approach. The hybrid unit cell has a size of one eighth of the wavelength forming the foundation of an innovative metasurface that incorporates a sub-wavelength reflecting array of split-ring unit cells integrated with a load-tuning matrix. In particular, two interleaved sensing arrays of half-wavelength spacing, orthogonal polarization, and quarter-wavelength offset are embedded within the proposed dual-functional RIS, each tasked to sense the channel parameters towards one of the end nodes wishing to profit from the surface's reconfigurable reflections. Our full-wave simulations, indicatively centered around the frequency of 5.5GHz, showcase the promising performance of both designed hybrid unit cells and reflective split-ring ones.

11:40 Degrees of Freedom of Holographic MIMO - Fundamental Theory and Analytical Methods

Juan Carlos Ruiz-Sicilia and Marco Di Renzo (Université Paris-Saclay, CNRS, CentraleSupélec, Laboratoire des Signaux et Systèmes, 91192 Gif-sur-Yvette, France); Mérouane Debbah (Khalifa University of Science and Technology, France); Vincenzo Sciancalepore and Placido Mursia (NEC Laboratories Europe GmbH, Germany)

Holographic multiple-input multiple-output (MIMO) is envisioned as one of the most promising technology enablers for future sixth-generation (6G) networks. The use of electrically large holographic surface (HoloS) antennas has the potential to significantly boost the spatial multiplexing gain by increasing the number of degrees of freedom (DoF), even in line-of-sight (LoS) channels. In this context, the research community has shown a growing interest in characterizing the fundamental limits of this technology. In this paper, we compare the two analytical methods commonly used in the literature for this purpose: the cut-set integral and the self-adjoint operator. We provide a detailed description of both methods and discuss their benefits and limitations.

12:00 Wave-Controlled RIS: Biasing RIS Elements Using Standing Waves with Single Frequency

Benjamin C Bradshaw (University of California Irvine, USA); Miguel Saavedra-Melo and Filippo Capolino (University of California, Irvine, USA)

This paper investigates the capabilities of operating a wave-controlled reconfigurable intelligent surfaces (RIS) system using a single standing wave along its biasing transmission line (TL) to minimize computational demands. A model and scattered radiation pattern are developed for this setup, and a theoretical implementation is tested. Results show single-beam steering, though limitations arise from symmetries in the reflected phase pattern from each element.

T03 Aerospace, space and non-terrestrial networks / Convened Session / Antennas

Chairs: Antonio Clemente (CEA-Leti, France), Thi Quynh Van Hoang (Thales Research & Technology, France)

10:40 High-Gain Tapered Long Slot Array in PCB Technology Integrated with PCB Based Dual-Band LP-To-CP Converter for SatCom Applications

Romain Greard (Planexus, France); Ahmed Alwakil (Universite de Rennes, France); Adham Mahmoud (Institut d'Électronique et de Télécommunications de Rennes, France); Laurent Le Le Coq (University of Rennes 1 & IETR, France); Khalid Sayegrih (Planexus, France); Ronan Sauleau (University of Rennes 1, France); Mauro Ettorre (Michigan State University, Electrical and Computer Engineering, USA)

In this communication, we presents a circularly polarized radiating antenna covering the frequency band [17-31 GHz] for K-/Ka-band satellite. The antenna is composed of two parts, a high gain linearly-polarized (LP) antenna and a dual-band linear-to-circular polarization converter (PC). The LP antenna's radiating aperture is an array of long slots. The polarization converter converts linearly polarized waves into circularly-polarized waves at (17-22)GHz and (28.6-30) GHz frequency bands with opposite handedness. The antenna and the polarization converter are fabricated in printed circuit board (PCB) technology.The radiation patterns are shown for the LP antenna. The PC is mounted over the antenna aperture with 10 mm separating air-gap. The reflection coefficient measurements for the antenna with and without the polarization converter are presented for 0-60 degrees scanning angles.

11:00 Feed Assembly Development for INCUS 1.6 m Mesh Reflector Antenna

Paolo Focardi (Jet Propulsion Laboratory & California Institute of Technology, USA); Gaurangi Gupta (NASA Jet Propulsion Laboratory, Caltech, USA); Alessio Mancini (NASA Jet Propulsion Laboratory, USA)

INCUS (INvestigation of Convective UpdraftS) is a NASA Earth Science mission scheduled to launch in 2026. The goal of the mission is to study in detail how water vapor and droplets move inside tropical storms and thunderstorms and understand their effects on weather and climate models. To carry out this study, the mission will use three almost identical SmallSats, each equipped with a Raincube heritage Ka-Band radar. The deployable mesh reflector antenna is a new 1.6 m design provided by Tendeg, which is fed using a seven-horn feed assembly to generate overlapping secondary beams. This paper discusses the approach used to design and fabricate the feed assembly and presents the measured and calculated RF performance parameters.

11:20 Dual Band Risley Prism Antenna for Satellite-On-The-Move Applications

Sergio Matos (ISCTE-IUL / Instituto de Telecomunicações, Portugal); Juan Córcoles (Universidad Politécnica de Madrid, Spain); Joao M Felicio (Instituto Superior Técnico, Portugal & Instituto Telecomunicacoes, Portugal); Jorge R. Costa (Instituto de Telecomunicações / ISCTE-IUL, Portugal); Nelson Fonseca (Anywaves, France); Carlos A. Fernandes (Instituto de Telecomunicacoes, Instituto Superior Tecnico, Portugal)

The development of the next generation of K/Ka band ground communication systems relies on cost-effective, compact terminals that provide high gain and wide-angle beam coverage while controlling the pointing direction in two widely separated frequency bands (20/30 GHz). The authors have been working on dual-band mechanical beam steering solutions based on a single aperture, eliminating the need of having separate Rx and Tx modules. In our previous works, the 2D beam steering control resulted from in-plane movements (rotation/translation) of a single aperture. A renewed interest has emerged on an alternative scanning solution based on the Risley Prism configuration (independent axial rotation of two TAs). However, until now the focus has been on single-band solutions. In this work we present a dual-band Risley Prism antenna, enabled by an ultra-thin dual-band TA design. A dedicated in-house full-wave solver was used for a more efficient search of the unit-cell solutions space, which allows reducing 70% of the TA thickness comparing with our previous designs. Full-wave simulations show that the TA has a maximum directivity of 23.8 dBi @ 19.5 GHz and 27.3 dBi at 30 GHz and can scan up to 47 degrees in elevation with scan loss below 2.6 dB.

11:40 A Ku/Ka-Band Shared Aperture Connected Array for Satcom Applications

Alexander J van Katwijk (Delft University of Technology, The Netherlands); Giovanni Toso (European Space Agency, ESA ESTEC, The Netherlands); Daniele Cavallo (Delft University of Technology, The Netherlands)

The design of a dual-polarized broadband array that simultaneously covers the Ku- and Ka-satellite communication transmit bands is presented. The array element is a connected slot backed by a ground plane and loaded with artificial dielectric layers. Two versions of the designs are described: one employing a perforated dielectric substrate, achieving ±60° maximum scanning, and another using a solid substrate without perforations, achieving a lower scan range (±30°). Based on the second design, a 32x32 prototype array is manufactured and tested, showing good agreement with performance predicted by simulations.

FRIDAY

12:00 K/Ka-Band Shared-Aperture Dual-Circularly Polarized Lens Array Antenna for Geostationary Satellite Communications

Mingzheng Chen and Oskar Zetterstrom (KTH Royal Institute of Technology, Sweden); Teanette van der Spuy (Chalmers University of Technology, Sweden & Satcube AB, Sweden); Lukas Nystrom (Satcube AB, Sweden); Oscar Quevedo-Teruel (KTH Royal Institute of Technology, Sweden)

We present a low-loss shared-aperture dual circularly polarized 4*4 lens array antenna for full-duplex geostationary satellite communications in the K/Ka-band. The proposed array has a periodicity of approximately 2 wavelengths in the Ka-band and 1.5 wavelengths in the K-band, with the resulting grating lobes suppressed by highly directive array element patterns. Two separate sequential rotation feed networks (for the K and Ka-bands) are implemented using a combination of H-plane ridged waveguides and E-plane rectangular waveguides. The feed works for the two bands are stacked. The performance of the proposed lens array is validated using full-wave simulations in CST.

Room: Hallén (BAR5)

CS6b - Challenges in Human RF Exposure Assessment to legacy, 5G and 6G Mobile Radio Technologies

T06 Biomedical and health / Convened Session / Propagation

Chairs: Wout Joseph (Ghent University/IMEC, Belgium), Lisa-Marie Schilling (Technische Universität Ilmenau, Germany)

10:40 Evaluation of Spatiotemporal Dynamics of Adaptive Antennas Using a Low-Cost Sensor Network

Jürg Fröhlich and Marco Zahner (Fields at Work GmbH, Switzerland); Dominik Haas and Toni Ziegler (Grolimund & Partner AG, Switzerland)

Spatiotemporal dynamics of the immissions of adaptive antennas are assessed using a novel design of a sensor network in two different measurement scenarios. One tracks the horizontal dynamics by placing the sensor network on and between buildings around a base station antenna located on a university campus. The second configuration consists of two vertically arranged rows of 5 sensors on the front of a building facing the base station antenna. Measurements during daily operation and during forced download initiated by smartphones reveal the beam dynamics and the distribution of the electrical field strength generated by the base station. This measurement setup may be used to systematically evaluate the emissions under daily usage and serves as a base station exposure assessment tool for adaptive 5G antennas.

11:00 Development of a Model to Estimate Future Exposure with Increased Utilization of Mobile Radio Base Stations

Anna-Malin Schiffarth and Thanh Tam Julian Ta (RWTH Aachen University, Germany); Christian Bornkessel, Lisa-Marie Schilling and Matthias Hein (Technische Universität Ilmenau, Germany); Dirk Heberling (RWTH Aachen University, Germany)

With the development of mobile networks a change of instantaneous exposure can be anticipated. First steps for modelling the instantaneous exposure due to future utilization of the mobile radio bands were taken here by recording the instantaneous exposure to all LTE and 5G bands at two base stations at varying utilization levels, while the network operator simultaneously monitored the resource blocks in use. In order to calculate the change in exposure due to traffic, the exposure measured per data rate and per measurement point was normalized to the exposure of the signaling. This so found power-related difference factor demonstrates a linear correlation with the resource blocks utilized across all LTE bands. This seems to imply that the expected future exposure can be calculated on the basis of the signaling exposure. However, the findings for 5G suggest that a linear dependency due to beamforming cannot be derived in this way.

11:20 Holographic Phase Retrieval of RF-EMFs for Human Exposure Assessment Using Fine 3D Electric Field Measurements in a Real Environment from a Beamforming 28 GHz Antenna

Robin Wydaeghe (Ghent University & IMEC, Belgium); Olivier Caytan, Sergei Shikhantsov, Emmeric Tanghe, Gunter Vermeeren and Hendrik Rogier (Ghent University, Belgium); Sam Lemey (Ghent University-imec, Belgium); Piet Demeester (Ghent University - iMinds, Belgium); Wout Joseph (Ghent University/IMEC, Belgium)

With the increasing frequencies for 5G and 6G technology, accurate assessment of Radio-Frequency Electromagnetic Fields (RF-EMFs) on humans is crucial for compliance with safety guidelines. Matching measurement results with simulations is challenging due to the loss of phase information and the need for high-fidelity digital twins of complex environments. In this paper, we propose a novel holographic phase retrieval method based on fundamental electromagnetics, utilizing the Gerchberg-Saxton algorithm, to reconstruct the full vector electric and magnetic fields in real environments from phaseless measurements. The exposure can be computed using a Huygens' box method. We conducted fine-grained 3D electric field measurements using a calibrated probe in a real environment illuminated by a beamforming 28~GHz antenna. We validate the feasibility of our method with a proof-of-concept at 3.5~GHz. The results demonstrate interference patterns and suggest that, with further refinement, the proposed approach can be effective for human exposure assessment in realistic scenarios.

FRIDAY

11:40 Up-Link Personnal Exposimeter DEVIN5G: RF Performance Validation

Serge Bories (CEA, France); David Dassonville (Cea Leti Minatec, France); Taghrid Mazloum (CEA- LETI, France); Prince Ramahefa-Andry and Saifeddine Aloui (CEA, France)

DEVIN5G is a miniature personal Up-Link (UL) exposimeter attached to the user mobile cover. It is able to quantify the impact of 5G specificities on the UL exposure from the mobile or handled EMF source. DEVIN is dedicated to i) measure the transmitted (Tx) power emitted by the mobile phones and ii) identify the mobile phone usage, including its relative position with respect to the human body. With 5G roll off, this new version of the in-situ exposimeter has been released supporting seven UL cellular (from 717 MHz to 3500 MHz) and two Wi-Fi bands (whom WiFi6E standard). Moreover, it is able to detect Tx scheme of antenna switching, where the phone may emit signals using multiple antennas. The RF performance validation is discussed in this paper.

12:00 Realistic EMF Exposure Estimation from Low Density Sensor Network by Finite & Infinite Neural Networks

M. Mallik (Insa-Lyon, CITI Lab & CITI Lab, France); Laurent Clavier (Institut Mines-Telecom, IMT Nord Europe, France); Davy P Gaillot (University of Lille, France)

Understanding the spatial and temporal patterns of environmental exposure to radio-frequency electromagnetic fields (RF-EMF) is essential for conducting risk assessments. These assessments aim to explore potential connections between RF-EMF exposure and its effects on human health, as well as on wildlife and plant life. Existing research has used different machine learning tools for EMF exposure estimation; however, a comparative analysis of these techniques is required to better understand their performance for real-world datasets. In this work, we present both finite and infinite-width convolutional network-based methods to estimate and assess EMF exposure levels from 70 real-world sensors in Lille, France. A comparative analysis has been conducted to analyze the performance of the methods' execution time and estimation accuracy. To improve estimation accuracy for higher-resolution grids, we utilized a preconditioned gradient descent method. Root Mean Square Error(RMSE) is used as the evaluation criterion for comparing the performance of these deep learning models.

Room: Marcuvitz (M3)

CS56b - Characterisation of biological tissues and tissue mimicking materials for electromagnetic medical applications

T06 Biomedical and health / Convened Session / Measurements

Chairs: Iman Farhat (University of Malta, Malta), Daniela M. Godinho (Instituto de Biofísica e Engenharia Biomédica - Faculdade de Ciências - Universidade de Lisboa, Portugal)

10:40 Design and Characterization of an Anthropomorphic Mammary Phantom for Electromagnetic Sensing

E Fernandez-Aranzamendi (Universidad Carlos III de Madrid, Spain & Universidad Católica San Pablo, Peru); Patricia Castillo (Universidad Católica San Pablo, Peru); Sandra Santiago-Mesas (Universidad Carlos III de Madrid, Spain); Nilton Achayhua, Ebert G San Roman Castillo and Romel Gordillo (Universidad Católica San Pablo, Peru); Daniel Segovia Vargas (Universidad Carlos III de Madrid, Spain)

This article presents the fabrication of an anthropomorphic and rectangular breast phantom, designed for use in electromagnetic technologies. The process includes the precise digitization of the breast shape using the HandySCAN 3D - SILVER scanner, the optimization of the layered design with ANSYS-HFSS, and the utilization of real databases from previous research containing dielectric properties of breast tissues and types of tumors. A comparison is made of the best materials for 3D printing, selecting one that offers characteristics of flexibility, temperature resistance, low permittivity, and liquid resistance, allowing for the fabrication of a breast structure that can be filled with dielectric liquids. The aim is to realistically replicate the non-homogeneous characteristics of breast tissue, based on information extracted from the database. The result is a digitally and physically manufactured breast phantom, with realistic and non-homogeneous dielectric properties, validated for in-vivo and ex-vivo measurements.

11:00 Multiple Backgrounds in Data-to-Image Deep Learning Schemes for Microwave Imaging

Ben J Martin, Colin Gilmore and Ian Jeffrey (University of Manitoba, Canada)

We present a form of dataset augmentation for microwave imaging deep learning schemes that leverages the relationship between the assumed background medium and the physics of the underlying scattering problem. Given a synthetically collected training set we can adopt any of the targets in the set as a background medium by simply adjusting the data accordingly without any additional forward solutions to the scattering problem. Choosing different targets as backgrounds expands the training set size. Results from a trained data-to-image network on such a multi-background augmented dataset demonstrate that we can reproduce the same target relative to many different backgrounds, providing a path towards uncertainty quantification and/or local model explainability.

11:20 Novel Dielectric Spectroscopy Approach with the Open-Ended Coaxial Probe for Materials with Uneven Surface in Biomedical Applications

Klementina Vidjak (University of Split, Croatia); Fabiana Capitanio (Sapienza, University of Rome, Italy); Marta Cavagnaro (Sapienza University of Rome, Italy)

Since the turn of the century numerous studies have focused on characterizing the dielectric properties of biological tissues. Despite this progress, significant gaps persist in our understanding of certain tissue types, and data variability across different studies remains a concern. A widely adopted method for microwave characterization is the open-ended coaxial probe technique. This approach permits the use of different probe types, facilitating measurements across a broad frequency range. Nonetheless, a key drawback of this technique is that the size of the sensing volume changes with the probe diameter and it is often hard to achieve good contact between the investigated sample and the probe aperture. The aim of this work was to develop a new methodology for measuring properties of materials with irregular surfaces utilizing open probe technique. To this end, the samples are immersed in well-known background materials and their properties are then extracted from measured bulk properties.

11:40 Dielectric Characterisation of Fat Equivalent Mixtures at Radiative Hyperthermia Frequencies

Flavia Liporace, Marco Di Cristofano and Marta Cavagnaro (Sapienza University of Rome, Italy)

This work describes the realisation of mixtures which can be used to produce phantoms representing fat tissue at oncological radiative hyperthermia (HT) frequencies. HT applicators must be validated through the application of the EMF field on phantoms representative of human biological tissues. Accordingly, phantoms should be developed that well represent the response of the human body to the application of the EMF. The electromagnetic power absorbed by the tissues depends on their dielectric properties (relative permittivity εr and electric conductivity σ [S/m]) and is related to the temperature increase induced in the body by the bioheat transfer equation. In this study simple materials are used to realize the fat-equivalent tissue. To identify the optimal compositions to represent the fat tissue at various hyperthermia frequencies, experimental procedures are performed for the characterisation of the dielectric properties of the realised mixtures.

12:00 A Differential Approach for Estimating Microwave Propagation Speed in Breast Tissue Without Breast Compression or Contrast Agents

Fatimah Eashour and Stephen Pistorius (University of Manitoba, Canada)

This work investigates using differential transmission coefficient measurements to estimate the propagation speed in the breast without contact or matching liquid. Transmission measurements of the breast in air often include undesired contributions from leaky waves, and existing systems for estimating the dielectric permittivity of breast tissues require direct contact. Leaky waves propagate along the surface of the breast but lose energy by radiating into air. The differential method eliminates the need for breast contact by assuming that the leaky waves are identical for both the left and right breasts of an individual. The results demonstrate that sufficient contribution of the signal transmitted through the breast tissue could be extracted to estimate the signal propagation speed. Estimating the average speed through the breast using transmission measurements improves the performance of beamforming algorithms.

FRIDAY

Room: Felsen (35+36)

CS7b - mm-Wave and THz Antennas for Radar and 6G Communication

T02 Millimetre wave and THz for terrestrial networks (5G/6G) / Convened Session / Antennas

Chairs: Akanksha Bhutani (Karlsruhe Institute of Technology, Germany), Qi Wu (Southeast University, China)

10:40 Evaluation of 3D-Printed E-Band Waveguide Antennas

Maximilian Eckl (Karlsruher Institut für Technologie (KIT), Germany); Alexander Quint and Mario Pauli (Karlsruhe Institute of Technology, Germany); Thomas Zwick (Karlsruhe Institute of Technology (KIT), Germany); Akanksha Bhutani (Karlsruhe Institute of Technology, Germany)

An antenna manufacturing concept, combining resin three dimensional (3D) printing and metallization via electroless copper deposition (ECD) is presented. The capability of the process to produce complex antenna structures is demonstrated. A corrugated horn antenna, a straight horn antenna and various slotted waveguide antennas (SWA) are inspected. Antennas with losses of less than 1 dB as compared to simulation results were achieved.

11:00 Design of a THz Multi-Beamforming Network Based on FOWLP for High-Speed Chip-To-Chip Wireless Communications

Yin Qiang Li (University of Electronic Science and Technology of China, China); Ya Fei Wu (UESTC, China); Yang Chai (Hong Kong Polytechnic University, Hong Kong); Yu Jian Cheng (UESTC, China)

This paper proposes a multi-beamforming network (MBFN) operating at a THz frequency of 220 GHz. The network comprises seven substrate integrated waveguide (SIW), a parallel plate waveguide (PPW), and a phase shifter array consisting of 17 parallel SIWs. Simulation results indicate that feeding different ports can generate four distinct phase distributions sequentially. Partial data testing was conducted on a GSG probe station, and there was good agreement between the test and simulation. Benefiting from the fan-out wafer-level package (FOWLP), this network is well-suited for integrating with array antennas. It holds the potential for controlling beam reconstruction of packaged array antennas, enabling rapid multi-target switching in inter-chip THz wireless communication.

11:20 Silicon-Based, Dual-Polarized Aperture-Coupled mmWave On-Chip Antenna Arrays

Seung Yoon Lee, Sree Adinarayana Dasari, Walter Royal Disharoon, David L West and Nima Ghalichechian (Georgia Institute of Technology, USA)

We report V-band dual-polarized aperture-coupled on-chip antennas where the radiating patch is patterned on the Si substrate instead of the dielectric interconnect layers, eliminating the need for lossy thru-Si vias or wirebonds for interconnection. An asymmetric cross-shaped slot is employed to minimize coupling between the feeds for each polarization. The −10 dB impedance bandwidths for Port 1 (P1) and Port 2 (P2) are 59.2-60.35 and 59.4-61.0 GHz, respectively. The realized gain of the patch antenna at P1 is 3.86 dBi with a directivity of 5.94 dBi, while P2 has a realized gain of 4.15 dBi and a directivity of 5.82 dBi at 60 GHz, indicating efficiencies of 62% and 68%, respectively. We have achieved maximum port-to-port coupling of −18.4 dBi for both polarizations. The proposed on-chip antennas and arrays offer the potential for monolithic integration with radio frequency (RF) circuitry for V-band system-on-chip (SoC) applications that demand high data throughput.

11:40 Dual-Band Slot Array Antenna for W-Band Application Based on Gap Waveguide

Mu Fang (Chalmers University of Technology & Chalmers, Sweden); Ashraf Uz Zaman and Jian Yang (Chalmers University of Technology, Sweden); David Santiago, Ivan Arregui and Miguel Laso (Public University of Navarre, Spain); Ahmed A Kishk (Concordia University, Canada)

A co-aperture dual-band linearly polarized slot array utilizing ridge gap waveguide (RGW) technology has been developed to operate within the 74 - 78 GHz and 102 - 106 GHz frequency ranges. The subarray features two sets of longitudinal slots positioned on the broad wall of the single waveguide channel, allowing for dual-band radiation through a planar aperture. Furthermore, two bandpass filters (BPFs) are placed on either side of the subarray, enabling independent feeding and filtering characteristics for the dual bands. A subarray column of several slot elements has been designed and simulated to demonstrate the dual-band concept. The subarray can produce high-gain beams when expanded into a planar array configuration.

12:00 Design and Characterization of 6G D-Band Antenna Arrays with Waveguide-To-Stripline Transitions

Thi Huyen Le and Ivan Ndip (Fraunhofer IZM, Germany); Jens Schneider (Fraunhofer Institute for Reliability and Microintegration IZM, Germany); Ali Khalil, Hendrik Mohrmann, Mathias Junginger and Christian Ranzinger (CONTAG AG, Germany); Martin Schneider-Ramelow (Fraunhofer IZM & TU Berlin, Germany)

In this work, we presented the development of a wideband and high gain 1x8 aperture-coupled U-slot antenna array, which will be integrated in Antenna-in-Package (AiP) modules for 6G D-Band applications. The antenna array was designed and simulated on a PCB-based multi-layered stack-up. Aperture-coupled feeds were used to excite the array elements. To improve the antenna bandwidth a multi-resonance method, whereby U-shaped slots are designed in in the patches was applied. This yielded a large impedance bandwidth of 24 GHz and high peak gain of 14.1 dBi. For measurement-based characterization of the designed antenna array, a D-band waveguide-to-stripline transition was designed and integrated onto the antenna board. Finally, the proposed antenna array was fabricated and measured. Very good correlation between simulated and measured results was obtained.

FRIDAY

Room: Schelkunoff (C1)

CS54b - Compact Antennas and Arrays for Communications and Sensing

T04 RF sensing for automotive, security, IoT, and other applications / Convened Session / Antennas

Chairs: Ping Jack Soh (University of Oulu & Katholieke Universiteit Leuven, Finland), Abel Zandamela (Technological University Dublin, Ireland)

10:40 Compact Superdirective Electronically-Beam- Switchable Antenna Array for 5G Indoor Gateway

Abdellah Touhami (CEA-LETI, France); Ala Sharaiha (Université de Rennes & IETR, France); Sylvain Collardey (University of Rennes 1, France)

This paper presents the design of a compact, multi-band and efficient superdirective array-based antenna structure with beamforming capability in the azimuthal plane for a future 5G wireless home gateway. The antenna architecture is designed to operate in the 5G sub-6GHz spectrum between [758-3800 MHz] with a compact form factor of 131×175×175 〖mm〗^3. Furthermore, the optimized structure enables the beam steering in the four main directions of the horizontal plane for different frequency bands between 750 and 3800 MHz.

11:00 Profile-Reduced S/X-Band Shared-Aperture Antenna Array with Frequency-Selective Surfaces

Mohamed Räsänen and Juha Ala-Laurinaho (Aalto University, Finland); José Manuel Fernández González (Universidad Politécnica de Madrid, Spain); Alfonso Tomas-Muriel Barrado (Group of Radio-Frequency, Circuits, Antennas, and Systems (RFCAS), Spain); Andrea Di Giovanni (SENER Aerospacial, Spain); Ville Viikari (Aalto University & School of Electrical Engineering, Finland)

Shared aperture antennas (SAAs) are becoming more popular due to their desirable traits such as miniaturization and cost reduction. However, incorporating a high frequency ratio in an SAA typically results in increased PCB fabrication costs or additional manufacturing complexity. In this work, we present the design concept and simulation results of a circularly polarized SAA with a profile of tenth of a wavelength at the lowest frequency. The SAA simulations indicate a −10-dB active reflection coefficient bandwidth of 292 MHz for the S-band and −9-dB total active reflection coefficient bandwidth of 1.071 GHz within a +/− 40 ° 3D beam steering range for the X-band. The S-band element is realized with an inter-band filtering dipole that is co-located in the same plane as the 4x4 X-band array that utilizes slot antennas as radiating elements.

11:20 Compact Dual-Polarized Multibeam Switch Integrated Antenna System for 5G mm-Wave Applications

Firas Abdul Ghani (Sabanci University, Turkey); Amir Mohsen Ahmadi Najafabadi (EPFL, Switzerland); Ibrahim Tekin (Sabanci University, Turkey)

In this paper, a novel microstrip, single-layer, Lshaped series fed antenna array, with 12 elements operating at 28 GHz, is proposed. The antenna can switch its beam in 8 different directions covering 4 different azimuthal Φ cuts; which is accomplished using a passive beamforming network. Switching is achieved by using two 3 dB/90 ◦ couplers. Each coupler is controlled by Ultra-CMOS single-pole double-throw (SPDT) switch IC that. The antenna has an average measured realized gain of 6 dBi at 28 GHz, with an absolute steering angle between 4 ◦ to 24 ◦ . The low cost and simplified design of the antenna, allows for its compact size of 48 × 49.5 mm2 while also being suitable for 5G user equipment and high data rates applications.

11:40 3D-Printed Dual Dielectric Resonator Antennas for Localization in UWB Anchor Nodes

Hossein Raghib Hokmabadi (TUDublin AHFR, Ireland); Jakub Przepiorowski (AHFR Technological University Dublin, Ireland); Khatereh Nadali (TuDublin, Ireland); Sam Lemey (Ghent University, Belgium); Max James Ammann (Technological University Dublin, Ireland)

This paper investigates the performance of 3D-printed dielectric resonator antennas on small anchor nodes for angle-of-arrival indoor positioning systems. A small aperture-coupled DRA, supporting channels 5 to 11 (6.2 - 8.5 GHz), is proposed for use in a 1x2 array and evaluated when mounted on a 77 × 52 mm anchor node PCB. This study assesses the performance of small DRA antennas, complying with IEEE 802.15.4z-2020. The proposed antenna prototype achieves an average gain of 5 dBi across the bands of interest. The results validate the introduction of 3D-printed DRA antennas in AoA applications based on UWB.

12:00 Unit Cell Design for a Low-Profile Dual-Frequency Dual-Sense Circularly Polarized Folded Transmitarray

Zhongliang Lu and Changjiang Zha (Jiangxi University of Science and Technology, China); Qi Luo (University of Herfordshire, United Kingdom); Baiqing Tang (University of Hertfordshire, United Kingdom); Yuan-Ming Cai (Xidian University, China)

This paper presents a unit cell suitable for a dual-band, dual-sense circularly polarized (CP) transmitarray. To achieve dual-band operation, two types of patches are designed and interleaved to form a 2×2 array, serving as the unit cell for the transmitarray. Electromagnetic (EM) simulations under periodic boundary conditions are performed to optimize the unit cell's performance. The simulation results demonstrate that the 2×2 array can convert CP waves with opposite senses: the low-frequency patch transmits right-handed circularly polarized (RHCP) waves at 10.05 GHz, while the high-frequency patch transmits left-handed circularly polarized (LHCP) waves at 12.65GHz. Moreover, the developed transmitarray element maintains stable CP performance at oblique incidence angles up to 42 degrees, making it well-suited for folded transmitarray designs.

Room: Maxwell (C2)

CS62b - Advancements in IoT Antennas: Design strategies, Optimization Techniques, Materials, Physical Insights, and Integrating AI

T04 RF sensing for automotive, security, IoT, and other applications / Convened Session / Antennas

Chairs: Jaume Anguera (Ignion & Universitat Ramon Llull, Spain), Martijn van Beurden (Eindhoven University of Technology, The Netherlands)

10:40 Design of a Miniature, Low Mutual Coupling, Two-Element Microstrip Array Antenna

Hubregt J. Visser (Imec the Netherlands, The Netherlands)

To create wideband microstrip patch antennas, use can be made of a thick, grounded substrate. Such a substrate leads to a strong surface wave excitation. By tuning the dimensions of the finite grounded substrate and the patch positions in a two-element array antenna, mutual coupling may be reduced through having direct and reflected surface wave contributions add in anti-phase. A simple geometrical optics formulation proves to lead to satisfactory results that can be easily improved by fine-tuning the substrate dimensions.

FRIDAY

11:00 A Multimode Antenna Design with Polarization Diversity

Kai Zhang (Xi'an University of Technology, China); Ping Jack Soh (University of Oulu & Katholieke Universiteit Leuven, Finland); Mingjun Wang (Xi'an University of Technology & Shaanxi Civil-Military Integration Key Laboratory of Intelligence Collaborative Networks, China); Sen Yan (Xi'an Jiaotong University, China)

In this article, a multimode antenna with polarization diversity is designed for smartwatch applications. The antenna structure consists of a circular watch frame and a circuit mainboard. Two ports are used to excite the antenna in odd and even modes, and polarization-diversity resonances are achieved. Additionally, a circular current is excited on one port to realize low-frequency multimode operation. Furthermore, high-order modes are excited by introducing slots in the circuit board, enabling multiband and multimode operation. The port 1 is working at 2.45 GHz, 4.1 GHz, and 5.8 GHz. And Port 2 works at 0.82 GHz 2.45 GHz, 4.1 GHz. and 5.8 for ISM band. The proposed antenna exhibits stable radiation patterns and high port isolation across multiple frequency bands, making it a promising candidate for next-generation smartwatch devices.

11:20 Adaptive Frequency Sampling for Fast and Accurate Simulation of the Active Reflection Coefficient

Lucas Åkerstedt and Lars Jonsson (KTH Royal Institute of Technology, Sweden)

The Active Reflection Coefficient (ARC) is a key factor in designing electrically small array antennas, as it accounts for the antenna's performance in a use-case. Accurate modeling of the ARC requires the complete set of scattering parameters, which requires a full-wave simulation. In this paper, we investigate how to accelerate full-wave frequency domain simulations by using the Loewner framework with adaptive frequency sampling, to accurately model the ARC. Here we compare interpolation on the ARC data directly with interpolation on the scattering parameters from which the corresponding ARC is determined, and interpolation on the scattering parameters, but with adaptive frequency sampling according to the estimated ARC error. The three strategies are tested on two cases, one 2x2 IoT array, and one 10x10 BoR Array. In both antenna cases, the latter strategy for accurately modeling the ARC yields the most accurate model for the least number of interpolation points used

11:40 Frequency Agile Omnidirectional Alford Loop: An Implementation Perspective Overview

Francesco Positano (Université Côte d'Azur, LEAT, CNRS, France); Leonardo Lizzi (University of Trento, Italy); Fabien Ferrero (Université Cote d'Azur, CNRS, LEAT & CREMANT, France); Robert Staraj (University Cote d'Azur, CNRS, LEAT, France

compact circular Alford Loop antenna design is proposed to work at 400 MHz and 440 MHz UHF bands for satellite-based IoT applications. The frequency reconfiguration mechanism is based on PIN-diode switching. The design of a matching circuit to allow the diodes DC bias over the RF structure is presented, with a focus on practical discrete Surface mounted components. Measured results on a prototype of the antenna agrees with simulations, confirming the horizontally polarization and frequency switch by simply applying DC bias over the antenna's SMA connector. The compactness and radiation characteristics of this antenna make it a good candidate for new generation of low-cost IoT satellite-based communication's ground station.

12:00 Organic Ground Planes for Wireless Devices Embedding Antenna Boosters

Jaume Anguera (Ignion & Universitat Ramon Llull, Spain); Inés Ripoll (Universitat Ramon LLull, Spain); Gerard Massana (Universitat Ramon Llull, Spain); Aurora Andújar (Ignion, Spain)

The growing presence of Internet of Things (IoT) devices demands energy-efficient solutions to extend battery life and mitigate environmental impact. This research examines the potential of incorporating Aloe Vera as a ground plane in IoT device design to improve antenna performance while reducing the carbon footprint. Utilizing Antenna Booster technology, which enables device miniaturization without compromising efficiency, the study assesses the feasibility of using an organic Aloe Vera ground plane without diminishing performance. Both simulations and experimental results demonstrate that integrating Aloe Vera as an extension of the ground plane enhances antenna efficiency by 3 dB. These results underscore the promise of natural materials like Aloe Vera in fostering sustainable advancements in IoT device performance, setting the stage for eco-friendly wireless communication systems.

Room: Oliner (C3) | **E08b - Periodic structures and metamaterials**

T08 Fundamental research and emerging technologies/processes / / Electromagnetics

Chairs: Tanguy Lopez (Sorbonne Université, France), Rola Saad (The University of Sheffield, United Kingdom)

10:40 A Numerical Study on 3D Printed Triply Periodic Minimal Surfaces Lattices for Microwaves Shielding

Matteo Bruno Lodi, Giacomo Muntoni, Andrea Melis, Alessandro Fanti and Giuseppe Mazzarella (University of Cagliari, Italy)

3D printing has already changed the antennas and microwave (MW) devices paradigms. Being enabled to prototype innovative geometries the designers are looking for identifying new topologies useful for several MW applications. Among the underestimated topologies that can hold a great potential for MW devices, implicit surfaces such as triply periodic minimal surfaces were recently proposed. In this work we will numerically investigate 3D printed TPMS in the MW range, focusing on the Primitive surface to investigate the role of cell-porosity, assumed to vary between 20% and 80%, and studying bare PLA and on a copper-loaded PLA, analyzed in a frequency range from 1-20 GHz. 3D printed TPMS lattices with 20% and 40% porosities could be useful for shielding in the X- and K-bands for both PLA and copper-loaded PLA. The PLA maximum shielding effectiveness is 15 dB, whilst the metal-filled TPMS structure can reaches shielding effectiveness of maximum 60 dB.

FRIDAY

11:00 Modeling of Open Dielectric Structures with Glide and Broken Mirror Symmetries

Dubravko Tomić (University of Zagreb, Croatia); Francisco Mesa (University of Seville, Spain); Zvonimir Sipus (University of Zagreb, Croatia)
The increased interest in exploiting the higher symmetries in the design of microwave components necessitates the development of efficient and reliable analysis methods. Analysis of dispersion properties of open structures with commercial solvers is a non-trivial problem that requires a physical insight in distinguishing between guided modes and spurious solutions. This paper presents an analytical model based on Rigorous Coupled Wave Analysis and derives the dispersion equation, which accounts for presence of glide or broken mirror symmetries.

11:20 Overcoming the Passivity Bounds in Communications Systems with Spacetime Modulations

Salvador Moreno-Rodríguez (University of Granada, Spain); Antonio Alex-Amor (University of Pennsylvania, USA); Mario Pérez-Escribano (Universidad de Málaga, Spain); Juan Valenzuela-Valdés (Universidad de Granada, Spain); Carlos Molero and Pablo Padilla (University of Granada, Spain)
In this paper, we exploit the extra degrees of freedom associated with including time as a design variable to create communication scenarios beyond the physical bounds of passive structures. We particularize the results to a time-modulated diffractive one-dimensional grating. By tuning the temporal modulation, we show that two different scenarios can lead to the same output angles but with different output frequencies or incidence angles. These results illustrate the potential of these metastructures as diffractive beamformers and frequency mixers.

11:40 Modal Analysis of a Double-Layer Line Waveguide Inside and Outside the Homogenization Regime

Mikhail Madji (Sapienza University of Rome, Italy); Paolo Baccarelli, Alessio Monti, Filiberto Bilotti and Alessandro Toscano (Roma Tre University, Italy); Paolo Burghignoli (Sapienza University of Rome, Italy)
The dispersion features of the line wave supported by a double-layer line-wave waveguide with a cross section exhibiting central symmetry are determined through full-wave simulations of a truncated structure and a numerical post-processing fitting procedure. Within the low-frequency homogenization regime, in which the unit cell of the constituent metasurfaces is a small fraction of the free-space wavelength, the phase constant of the line wave is thus retrieved rigorously. The adopted approach has been also extended to higher frequencies beyond the homogenization limit, where higher order space harmonics become non-negligible, the line wave is thus to be regarded as a Bloch mode of a periodic structure, and the associated stopband regimes are shown to emerge

12:00 Accurate Calculation of Tensor Surface Impedance Using Scattering Analysis

Karthik P B and Uday Khankhoje (Indian Institute of Technology Madras, India)
In this work, we present a scattering analysis ap- proach for accurate calculations of tensor surface impedance that is highly time efficient than using eigenmode analysis. While previous work has shown this method for the case of scalar impedance, our work generalizes the approach for tensor impedance. Extensive numerical simulations are shown for both scalar and tensor impedance in support of the efficacy and accuracy of our results. We observe that the results obtained using eigenmode analysis with finer simulation settings which is computationally expensive converge to the results obtained using our method with scattering analysis.

Room: Kraus (C4)

CS53b - Electromagnetic wave control through reflective and transmissive periodic surfaces

T08 Fundamental research and emerging technologies/processes / Convened Session / Electromagnetics

Chairs: Manuel Arrebola (Universidad Politécnica de Madrid, Spain), Álvaro F. Vaquero (Universidad de Oviedo, Spain)

10:40 Design of a Dual-Band Polarization Selective Surface

Francisco J. Hidalgo and Rafael R. Boix (University of Seville, Spain); Miguel Camacho (Universidad de Sevilla, Spain); Juan Córcoles (Universidad Politécnica de Madrid, Spain)
This paper introduces a procedure to design dual-band polarization selective surfaces (PSS). In the lower band, the PSS enables the transmission of the polarization along the x axis while rejecting the orthogonal polarization y. In the upper band, the opposite holds. In a first step, the adjustment of the dimensions of the PSS is separately carried out in each band by using third order filtering equivalent circuits. In a second step, a joint optimization is implemented that polishes the PSS response in both bands. A final design is presented in which the lower band has a center frequency of 7 GHz with a bandwidth of 20%, and the upper band has a center frequency of 12.6 GHz with a bandwidth of 31%, the minimum isolation between polarizations being 20 dB. The response of the PSS in both bands is kept stable for incidence angles up to 30 degrees.

FRIDAY

11:00 Adaptative Optimization of Advanced Electromagnetic Surfaces in Near-Field

Álvaro F. Vaquero and Marcos R. Pino (Universidad de Oviedo, Spain); Manuel Arrebola (Universidad Politécnica de Madrid, Spain)

This work presents two complementary techniques for synthesizing Spatially Fed Array antennas within the framework of the Intersection Approach. The first technique introduces a methodology to address highly complex synthesis problems, particularly for optimizing antennas that require complex near-field shaped patterns. The second technique offers an acceleration of the gradient computation in optimization algorithms, reducing the computation times and making near-field synthesis more manageable. Both techniques are integrated within the Intersection Approach algorithm and demonstrated with the synthesis of a metalens antenna. The presented example achieves a uniform near-field pattern over a relatively large area, starting from a focused near-field focused spot.

11:20 Design and Characterization of a Transmitarray for Near-Field Focusing at Sub-THz

Marie Defives (CEA-Leti University Grenoble-Alpes Grenoble, France); Ronan Sauleau (University of Rennes 1, France); Orestis Koutsos (CEA Leti, France); Mathieu Caillet (CEA-LETI, France); Antonio Clemente (CEA-Leti, France)

This paper presents the design and experimental characterization of a transmitarray antenna shaping the near-field in the sub-THz band, specifically around 300 GHz. The prototype features a pyramidal horn illuminating a 60 × 60 anisotropic unit-cell array with 3-bit phase quantization (45° resolution). Fabricated using standard PCB technology, the phase profile is synthesized using a Fourier Transform-based numerical approach, incorporating the impinging electromagnetic field on the array, along with the full-wave simulated radiation patterns and scattering parameters of the unit-cells. Near-field behavior is analyzed using a planar scanner, measuring the focusing and axial electric field distribution. Experimental results show good agreement with the model, matching focus distance, spot size, and propagation behavior.

11:40 Design of Simultaneously Transmitting and Reflecting Bianisotropic Metasurfaces

Alessio Berto (CEA & Sorbonne Université, France); Francesco Foglia Manzillo (CEA-LETI, France); Guido Valerio (Sorbonne Université, France)

This article presents a rigorous procedure for the design of space-fed omega-type bianisotropic metasurfaces enabling independent beam-forming in transmission and reflection. It is first demonstrated that, when illuminated by a normally incident plane wave, the metasurface can generate refracted and reflected fields with equal amplitudes and apply independent phase shifts to each. Semi-analytical solutions for the surface parameters are derived. Then, a preliminary design of 32 unit-cells is presented, achieving a 2-bit and 3-bit uniform phase quantization in transmission and reflection, respectively. The cells comprise three stacked sheet impedances, spaced by two dielectric slabs. Two metasurfaces are synthesized using the designed cells to individually control the scan angles of the transmitted and reflected beams. The radiation characteristics are numerically evaluated and validate the design.

12:00 Design of Wideband Metasurface-Based Linear to Circular Polarizers

Ahmed Alwakil (Universite de Rennes, France); Romain Contreres (CNES, France); Ronan Sauleau (University of Rennes 1, France); Mauro Ettorre (Michigan State University, Electrical and Computer Engineering, USA)

We provide a new theoretical method to compute the required sheet admittance of the metasurfaces (MSs) used to implement a wideband linear-to-circular polarization converter (LP-to-CP), which consists of three cascaded MSs, separated by dielectric slabs. Each MS is modeled as a shunt load while the slabs are represented by transmission lines. The presented method is based on reactance Foster theorem and image technique of filter design. This method is applied to a three-sheet PCB based LP-to-CP optimized for normal incidence at Ka-band for SATCOM applications. The resulted LP-to-CP yields ideal axial ratio with perfect matching. The method is validated by full wave simulation where the derived sheet admittances of the ideal LP-to-CP are realized by lumped LC tanks found using pole-zero placement technique, then verified by full wave simulations. It is shown that this realization give satisfactory results in terms of axial ratio and transmission coefficients of the transmitted field.

Room: Ørsted (24+25)

CS43b - AMTA Convened Session - Trends and Advances in Test and Measurement for 5G and Beyond

T08 Fundamental research and emerging technologies/processes / Convened Session / Measurements

Chairs: Tian Hong Loh (UK, National Physical Laboratory, United Kingdom), Janet O'Neil (ETS-Lindgren, USA)

10:40 Impact of Hardware Impairments on Data-Rates in an Over-The-Air mm-Wave Testbed

Koen Buisman (University of Surrey, United Kingdom & Chalmers University of Technology, Sweden); Thomas Eriksson (Chalmers University of Technology, Sweden)

In the era of 5G and emerging 6G technology, there's an increasing demand for advanced communication systems. Innovative testbeds are crucial for rapid development of hard- ware and algorithms, maximizing performance. Estimation of the capacity potential of mm-wave transceiver arrays is essential to maximise performance, however hardware impairments limit performance. Moreover, rapid experimentation is essential for identifying and addressing potential bottlenecks due to hardware impairments. We investigate the impact of hardware impairments on obtainable signal-to-noise ratios and datarates in a mm-wave testbed using Over-The-Air measurements only. The method is tested using the Chalmers mm-wave testbed MATE at 29.4 GHz.

FRIDAY

11:00 Measurement of an Antenna Array with a Waveguide Simulator

Matti Kuosmanen (Aalto University & Saab Finland Oy, Finland); Jan H. S. Bergman, Juha Ala-Laurinaho and Jari Holopainen (Aalto University, Finland); Ville Viikari (Aalto University & School of Electrical Engineering, Finland)

The waveguide (WG) simulator method is a well-known method for measuring antenna arrays. In the WG simulator, a few antenna elements are placed in a WG and they behave like they would be in an infinite antenna array. The benefits of a WG simulator are remarkable: only a small number of antenna elements must be fabricated, the active impedance of the array can be obtained with a single S-parameter measurement, and the antenna efficiency can be easily measured. This paper briefly revisits the idea and theory behind the WG-simulator method and applies it to a practical antenna array. The measurement results are compared to unit-cell simulation results. Significant correspondence was obtained confirming the applicability of the method for modern antenna arrays.

11:20 Comparison on Convergence of Measurements in Reverberation Chamber for Different Channel Bandwidths

John Kvarnstrand and Rutger van Boeijen (Bluetest AB, Sweden)

Reverberation chambers are used to measure mobile devices on various standards from 2G onwards to 5G. Theoretical work has been performed to access the impact of the signal bandwidth on the rate of conversion in a reverberation chamber measurement, but a quantitative analysis across standards is missing. A device is used to measure TRP and TIS for 2G, WCDMA, LTE and 5G in a Bluetest RTS65 to show the rate of convergence and the sampled values are mapped to the expected distributions. Consistent with theoretical predictions, measurements show that a higher signal bandwidth leads to a faster rate of convergence in reverberation chamber tests.

11:40 Numerical Validation of a Model of Antenna-Related Losses Within Reverberation Chambers

Francois Sarrazin (Université de Rennes & IETR, France); Julien de Rosny (CNRS, ESPCI Paris, PSL Research University, France)

Reverberation Chambers (RCs) has become a common tool to perform electromagnetic testings. The contribution of antennas to the overall RC quality factor is of particular interest both to predict the amount of losses brought by antennas during measurements, as well as to perform noninvasive antenna characterisation. In this communication, we present a recently-proposed model, based on antenna scattering-matrix theory, which take into account both the structural and the antenna modes as well as the complex interactions between the two. In particular, we show, numerically, that it is possible to retrieve both the radiation efficiency and the input impedance, from the evaluation of the antenna contribution to the RC quality factor for a set of different loads.

12:00 Decentralized Coordination for Collaborative Beamforming in Mobile Wireless Networks

Jeffrey Nanzer (Michigan State University, USA)

Research and development in mobile wireless networks has progressed to the point where coordinated operations are viable. Coordination at the wavelength level, while the most challenging, provides the greatest benefits with opportunities like distributed collaborative beamforming. Achieving distributed wireless coordination that wavelength level is a difficult challenge that has seen significant interest in recent years. In this paper, a decentralized approach to wireless wavelength-level coordination is discussed. Based on consensus averaging, the approach relies only on information gathered locally at each node in the array, and on local decision rules; no master node or global control is required. The approach is described, and recent examples of decentralized coordination of spatio-electrical states such as frequency, time, and location, are discussed.

Room: Collin (27)

CS38b - Fast, low-invasive visualization of EM-VNF distributions around wireless communication/sensing devices: from anechoic chamber to microscope

T08 Fundamental research and emerging technologies/processes / Convened Session / Measurements

Chairs: Jean-Charles Bolomey (Supelec Université de Paris Sud XI, France), Manuel Sierra-Castañer (Universidad Politécnica de Madrid, Spain)

10:40 Scan Blindness Effect for Free Electron Beam Fed Infrared Diffraction Radiation Antenna Grating

Dariia O. Herasymova (Institute of Radio-Physics and Electronics NASU, Ukraine); Sergii V. Dukhopelnykov (Institute of Radio-Physics and Electronics NAS Ukraine, Kharkiv & Universite de Rennes 1, Ukraine)

The effect of scan blindness is known in the large phased array antennas. It is caused by the excitation of the ultrahigh-Q lattice modes of the array as a periodic open resonator. We consider, in a full-wave manner, the electron beam diffraction radiation in the presence of finite grating made of many graphene-coated circular dielectric nanowires. We assume a constant velocity for the modulated in density electron beam and take its field as the incident one. To characterize the graphene, we employ quantum-theory Kubo formalism and resistive sheet boundary conditions. Then, the electromagnetic boundary value problem of wave scattering is cast to a Fredholm second-kind matrix equation for the current azimuth harmonics in local coordinates, using the separation of variables and the cylindrical functions addition theorem. This method has a guaranteed convergence and enables precise control over numerical accuracy. Potential applications of the investigated effect are also described

FRIDAY

11:00 Design of a near Field Measurement System for Bistatic Measurements in CATR

Maximilian Kanz (Leibniz University Hannover, Germany); Axel Hoffmann (Leibniz Universität Hannover, Germany); Dirk Manteuffel (University of Hannover, Germany)

Bistatic measurements are required to obtain the reflection patterns from scatterers. This paper provides a design guideline for a near field measurement system to enable bistatic measurements in compact antenna test ranges. The measurement concept and the dimensioning of the system are discussed. In addition, a near field to far field transformation for calculating the reflection pattern is presented. Measurement results are presented to verify the proposed approach.

11:20 Impact of Metasurface Element Designs on Infrared-Based Antenna Near-Field Measurements

Ben A. P. Nel (Lund University, Sweden); Anja K. Skrivervik (EPFL, Switzerland); Johan Lundgren and Mats Gustafsson (Lund University, Sweden)

The measurement of electromagnetic fields near a radiating device is often required in compliance testing. In this paper, the measurement of placing the radiating device near a metasurface designed to induce heat from radio frequency fields is considered. This heat distribution on the surface can be imaged with an infrared camera. A metasurface is placed between the infrared camera and the device in this measurement setup. The metasurface design is essential as it must respond to the source field in a way that is interpretable by the infrared camera. Thus three possible metasurface designs are examined. The sensitivity of these metasurface designs to two orthogonal linear polarizations is investigated. Further, the power dissipated on the metasurface and how it compares to the field from the source is studied. The paper finds that the metasurface element's dissipated power correlates better with the incident power density than with the electric energy density.

11:40 Fluorescence Thermography for High-Resolution Characterization of Transmitarray Antenna in X Band

Daniel Prost (ONERA - The French Aerospace Lab, France); Jean-Francois Bobo (Cnrs, France); Raphael Flor (Anyfields, European Union); Stéphane Fauré (Anyfields, France)

Rapid advances in microwave technologies require accurate measurement and visualization of electromagnetic (EM) fields, particularly to optimize emerging communication systems. This work explores the application of fluorescence thermography for non-intrusive, high-resolution characterization of electromagnetic fields, focusing on an X-band Transmitting Array (TA) antenna. Using thermosensitive films coated with rhodamine B (RhB), this method enables detailed mapping of the field near the antenna, offering significant advantages over traditional probe-based methods. Our experimental results demonstrate efficient field focusing, distinct regions of high intensity and suppression of sidelobes, which corresponds well with theoretical expectations and previous research on TA antennas. The ability to visualize entire field distributions with high spatial fidelity is crucial for optimizing antenna performance for applications in satellite communications and 5G networks. Fluorescence thermography could be a powerful tool for antenna designers, enabling them to understand complex field interactions without disturbing the reactive environment.

12:00 Digital-Twin Technology Solution for Chip-Package-PCB-Antenna Systems

Sidina Wane (eV-Technologies, France); Wissam Saabe (AMCAD Engineering, France); Thanh Vinh Dinh and Damienne Bajon (eV-Technologies, France); Tony Gasseling (AMCAD, France)

A new Digital-Twin technology platform is introduced for enabling Chip-Package-PCB-Antenna co-design, co-simulation and system-level verification. The platform, based on noise and correlation-aware progressive workflow of behavioral modeling and simulation, integrating VISION software developed by AMCAD engineering hosts an innovative SPICE compatible broadband representation of antenna elements. The ability of the platform to account for dynamic impedance loading of antennas by multi-harmonic (MH) nonlinear RF electronics is demonstrated using hybrid 3D heterogeneous technologies.

Friday - 12:40- 13:10

Room: Alfvén (A3 + A4) **Closing ceremony**

End of Friday, April 4th

FRIDAY

EurAAP

EuCAP 2026

20TH EUROPEAN CONFERENCE ON ANTENNAS & PROPAGATION

DUBLIN, IRELAND
APRIL 19 – 24, 2026

NEXT YEAR EDITION

2026